

UNIVERSITÉ DU QUÉBEC
INSTITUT NATIONAL DE LA RECHERCHE SCIENTIFIQUE
ARMAND FRAPPIER SANTÉ BIOTECHNOLOGIE

**Development of Biopolymer Based Diffusion Systems by
Encapsulating Plant Derived Essential Oils (EOs) -Application
in Stored Food Products**

Par

Tofa BEGUM

*Thèse présentée pour l'obtention du grade de
Philosophiae doctor (Ph. D.) en biologie*

Jury d'évaluation

Président du jury et examinateur interne	Prof. Steven Laplante, Ph.D. INRS-Armand Frappier Health Biotechnology
Examineur externe 1	Prof. Valérie Orsat, Ph.D. McGill University
Examineur externe 2	Prof. George Szatmari, Ph.D. University of Montreal
Directeur de recherche	Prof. Monique Lacroix, Ph.D. INRS-Armand Frappier Health Biotechnology
Co-Directeur de recherche	Peter A. Follett, Ph.D. United States Department of Agriculture, Agricultural Research Service

© Droits réservés de Tofa Begum, 2023

Acknowledgment

I would like to thank and remember some people in the completion of this doctoral dissertation whose cordial help and support made it possible to complete. Words cannot express my gratitude to them and this endeavor would not have been possible without their support. The person whom I remember with the heartiest gratitude is my thesis supervisor, Prof. Monique Lacroix, who allowed me to work on this research. I am deeply indebted to her for helping me to boost up my knowledge, research skills and understanding during the research project. She is the witness of my ups and downs and she is that person who helped me to keep up my patience. Her enormous support and encouragement reached me to a place where I am finally able to complete my thesis with full confidence. I would like to express my deepest appreciation to her for mentoring me so nicely throughout this research work.

I would like to express my sincere thanks to Dr. Peter Follett who was my co-supervisor. This person amazingly helped me with his deep knowledge and experiences during my Ph.D. His precise instructions and suggestions helped me to take the right decision several times when I was disoriented. I am deeply grateful and honored for his guidance and motivation during my research. Many thanks to my committee members, Dr. Steven Laplante, Dr. Valérie Orsat and Dr. George Szatmari for their input into the dissertation and suggestions to refine my work.

I would like to give special thanks to Dr. Maherani Behnoush, Dr. Leila Bagheri, Dr. Shiv Shankar, Dr. Zahra Allahdad, Stephane Salmieri, Dr. Ruhul A. Khan, Dr. Lana Moskovchenk, Dr. Vincent Herve and Dr. Lily Jaiswal for their valuable advice and inspiration during my Ph.D. In my entire journey, I met colleagues, trainees and past students, I would like to recognize them. I would like to thank all the staffs and members of the INRS-Armand Frappier Health Biotechnology Center who cordially helped and supported me throughout the whole research. Now, I would like to give big thanks to all the library staff, especially Michele Courcelles. They helped sincerely by providing learning resources.

Behind any success story, the role of the family is inevitable. I am extremely grateful to my beloved husband (Muhammad Mainul Islam), he is always with me and inspires me to cheer up my dreams. I am grateful to my parents and siblings for their inspiration and support. Their belief helped me to keep my confidence high. My special thanks to my friends Yosra Ben Fadhel, Dr. Farah Hossain, Jumana Mahmud for their cordial support.

Finally, I am thankful to all my well-wishers and my deepest gratitude and thanks to Almighty for making me able to complete this research with sound health and mind.

Contents

Acknowledgement	ii
List of Tables	ix
List of Supplementary Data Tables	xi
List of Figures	xiii
List of Abbreviations	xvi
Résumé	xvii
Abstract	xix
Chapter 1	1
Literature Review	1
1.1. Introduction	2
1.2. Level of food contamination	5
1.3. Bacteria, fungi and insect as potent biohazards	6
1.4. Active agents	8
1.4.1. Essential oils (EOs) and plant extracts (PEs)	8
1.4.2. Metal nanoparticles	11
1.4.3. Application of active compounds in foods and their limitations	12
1.5. Possible strategies to alleviate the limitations	16
1.6. Active packaging	18
1.6.1. Chitosan (CH)	19
1.6.2. Poly lactic acid (PLA)	23
1.6.3. Poly (hydroxy butyrate adipate terephthalate) (PBAT)	26
1.7. Cellulose Nanocrystals (CNCs) as reinforcing agent	28
1.8. Food irradiation technology	30
Food model 1 : Yogurt	32
Food model 2 : Rice	33
1.9. Problem, Hypotheses and Objectives	34
1.9.1. Problematic	34
1.9.2. Hypotheses	35
1.9.3. Objectives	35
1.9.4. Methodology	36
Chapter 2	38
Publication 1	38
Microbicidal effectiveness of irradiation from Gamma and X-ray sources at different dose rates against the foodborne illness pathogens <i>Escherichia coli</i> , <i>Salmonella Typhimurium</i> and <i>Listeria monocytogenes</i> in rice	39
Contribution of authors	40
Résumé	41
Abstract	42
2.1. Introduction	43
2.2. Materials and methods	44
2.2.1. Bacterial species preparation	44
2.2.2. Preparation of essential oil mixture	45
2.2.3. Rice inoculation and application of EOs mixture	45
2.2.4. Irradiation of test samples	45
2.2.5. Microbiological analysis	46
2.2.6. D ₁₀ (kGy) and radio-sensitisation determination	47
2.2.7. Statistical Analysis	47
2.3. Results and Discussion	47
2.4. Conclusion	55

2.5. Acknowledgments	55
2.6. References	56
Chapter 3	59
Publication 2.....	59
Mixture design methodology and predictive modelling for developing active formulations using essential oils and citrus extract against foodborne pathogens and spoilage microorganisms in rice	60
Contribution of the authors	61
Résumé.....	62
Abstract.....	63
3.1. Introduction.....	64
3.2. Materials and methods	65
3.2.1. Preparation of essential oils (EOs).....	65
3.2.2. Preparation of bacterial/fungal cultures	66
3.2.3. Minimum inhibitory concentration (MIC)	66
3.2.4. Synergistic interaction between antibacterial and antifungal.....	67
3.2.5. Mixture design and optimize the developing active formulations	68
3.2.6. Statistical analyses for developing active formulations	68
3.2.7. <i>In situ</i> antibacterial and antifungal properties on packaged rice.....	69
3.2.8. Microbiological analysis.....	69
3.3. Results and discussion	70
3.3.1. Minimum inhibitory concentration (MIC)	70
3.3.2. Synergistic interactions between antibacterial and antifungal compounds.....	72
3.3.3. Mixture design and optimization for active formulations.....	74
3.3.4. <i>In situ</i> antibacterial and antifungal properties on packaged rice.....	85
3.4. Conclusion.....	89
3.5. Acknowledgements.....	89
3.6. References	90
Chapter 4	100
Publication 3.....	100
Silver nanoparticles-essential oils combined treatments to enhance the antibacterial and antifungal properties against foodborne pathogens and spoilage microorganisms	101
Contribution of the authors	102
Résumé.....	103
Abstract	104
4.1. Introduction.....	105
4.2. Materials and methods	106
4.2.1. Materials	106
4.2.2. Preparation of antimicrobial and antifungal compounds	107
4.2.3. Preparation of bacteria/fungi cultures and assay media	107
4.2.4. Minimal inhibitory concentration (MIC)	108
4.2.5. Synergistic interactions of essential oils and silver nanoparticles	108
4.2.6. Vapor contact assays.....	109
4.2.7. Bacterial and fungal growth model and statistical analysis	110
4.2.8. <i>In situ</i> antibacterial and antifungal efficiency of active combinations in rice	110
4.2.9. Microbiological analysis.....	111
4.3. Results and discussion	111
4.3.1. Minimal inhibitory concentration (MIC)	111
4.3.2. Synergistic interactions of essential oils and silver nanoparticles	113
4.3.3. Vapor contact assay.....	118
4.3.4. <i>In situ</i> antibacterial and antifungal efficiency of active combinations in rice	123

4.4. Conclusion.....	127
4.5. Acknowledgments	127
4.6. References	128
Chapter 5	133
Release kinetics and biological properties of active films based on cellulose nanocrystal-chitosan in combination with γ -irradiation to mitigate microbial load in rice	134
Contribution of the authors	135
Résumé.....	136
Abstract.....	137
5.1. Introduction.....	138
5.2. Materials and methods	140
5.2.1. Essential oils (EOs) and citrus extract.....	140
5.2.2. Bacterial and fungal culture preparation	140
5.2.3. Nanoemulsion development, optimization, and characterization of the active formulations	140
5.2.3.1. Measurement of particle size, zeta potential, and PDI.....	141
5.2.3.2. Encapsulation efficiency (EE).....	141
5.2.3.3. Statistical analysis for optimization	141
5.2.4. Storage stability of coarse and optimized nanoemulsions	142
5.2.5. Inhibitory capacity and turbidity measurements of the coarse and optimized nanoemulsions.....	143
5.2.6. Development of chitosan-based nanocomposite films.....	143
5.2.6.1. Water vapor permeability (WVP)	144
5.2.6.2. Mechanical properties of the films	144
5.2.7. Bioactive film development and applied in rice with irradiation treatment	144
5.2.8. Determining the % release of active components and their release kinetics from films in rice.....	145
5.2.9. Sensory analysis	146
5.3. Results and discussion	147
5.3.1. Nanoemulsion development, optimization and characterization of the active formulations	147
5.3.2. Storage stability of the coarse and optimized nanoemulsion	153
5.3.3. Inhibitory capacity and turbidity measurement of the coarse and optimized nanoemulsion	156
5.3.4. Development of chitosan-based nanocomposite films.....	159
5.3.4.1. Water Vapor Permeability (WVP)	159
5.3.4.2. Mechanical properties of the films	160
5.3.5. Bioactive film development and application in packaged rice with irradiation treatment	162
5.3.6. <i>In situ</i> release/diffusion of active components from bioactive nanocomposite films in rice	168
5.3.7. Sensory properties of treated rice	174
5.4. Conclusion.....	176
5.5. Acknowledgments	176
5.6. References	177
Chapter 6	190
Development of novel bioactive nanocomposite films using a central composite design by encapsulating active formulations: applied in stored rice to control pathogenic bacteria and spoilage fungi	191
Contribution of the authors	192
Résumé.....	193

Abstract	194
6.1. Introduction	195
6.2. Materials and methods	197
6.2.1. Materials	197
6.2.2. Preparation of active formulations using EOs and CEs	197
6.2.3. Pathogenic bacterial and spoilage fungal culture preparation.....	198
6.2.4. Experimental design for bioactive nanocomposite film	198
6.2.4.1. Antibacterial and antifungal properties of the bioactive nanocomposite films	198
6.2.4.2. Optimization and statistical analyses of the bioactive nanocomposite films	199
6.2.5. Characterization of the bioactive nanocomposite films	200
6.2.5.1. Mechanical properties.....	200
6.2.5.2. Water vapor permeability (WVP).....	200
6.2.5.3. Oxygen permeability rate (OTR)	201
6.2.5.4. <i>In vitro</i> release profiles/kinetics of the active formulations from the bioactive films	201
6.2.6. Hurdle treatment (bioactive films with γ -irradiation) in rice.....	202
6.3. Results and discussion	203
6.3.1. Experimental design for bioactive nanocomposite film	203
6.3.2. Characterization of the bioactive nanocomposite films	220
6.3.2.1. Mechanical properties.....	220
6.3.2.2. Water vapor permeability (WVP).....	221
6.3.2.3. Oxygen transmission rate (OTR)	222
6.3.2.4. <i>In vitro</i> release profiles of the active components from the bioactive films	224
6.3.3. Hurdle treatment (bioactive films with γ -irradiation) in rice.....	229
6.4. Conclusion.....	235
6.5. Acknowledgments	235
6.6. References	236
Chapter 7	251
Development of bioactive nanocomposite packaging films for control of the stored product pest <i>Sitophilus oryzae</i> in rice with and without irradiation.....	252
Contribution of authors	253
Résumé.....	254
Abstract.....	255
7.1. Introduction.....	256
7.2. Materials and methods	258
7.2.1. Rearing of rice weevil.....	258
7.2.2. Preparation of essential oils (EOs)	258
7.2.3. Dose-response fumigation toxicity tests of natural insecticides	258
7.2.4. Determination <i>in vivo</i> acetylcholine esterase (AChE) activity	259
7.2.5. Development of nanoemulsion of active formulations.....	259
7.2.6. Preparation of insecticidal film.....	260
7.2.7. <i>In situ</i> insecticidal evaluation of film combined with and without irradiation	260
7.2.8. Release profile of active components from the insecticidal films	261
7.2.9. Sensory analyses of the rice under different films treatment	261
7.2.10. Statistical analyses.....	262
7.3. Results and discussion	262
7.3.1. Dose-response fumigation toxicity tests of natural insecticides	262
7.3.2. <i>In vivo</i> determination of acetylcholine esterase (AChE) activity	266
7.3.3. Development of nanoemulsion of active formulations.....	268
7.3.4. <i>In situ</i> insecticidal evaluation of the film combined with and without irradiation.....	270
7.3.5. Release profile of active components from the insecticidal films	276

7.3.6. Sensory analyses of the rice under different films treatment	281
7.4. Conclusion.....	283
7.5. Acknowledgments	284
7.6. References	285
Chapter 8	292
Active polymers containing silver nanoparticles combined with active formulations based on essential oils: Quality effect on cereals and dairy products	293
Contribution of authors	294
Résumé.....	295
Abstract.....	296
8.1. Introduction	297
8.2. Materials and methods	299
8.2.1. Essential oils (EOs) and silver nanoparticles (AgNPs)	299
8.2.2. Bacterial and fungal culture preparation	299
8.2.3. Insect (<i>S. oryzae</i>) culture	299
8.2.4. Development and characterization of nanoemulsion of active combinations	300
8.2.5. Preparation of bioactive films	300
8.2.6. Characterization of bioactive nanocomposite films	301
8.2.6.1. Mechanical properties.....	301
8.2.6.2. Water solubility (WS)	302
8.2.6.3. Water vapor permeability (WVP).....	302
8.2.6.4. <i>In vitro</i> antibacterial and antifungal properties.....	302
8.2.6.5. <i>In vitro</i> insecticidal properties.....	303
8.2.6.6. <i>In vitro</i> release profiles of the active combinations from the bioactive films.....	303
8.2.7. Evaluate the antibacterial and antifungal properties of the films (for cereal grains)....	304
8.2.8. Evaluate the anti-insect properties of the films (for cereal grains).....	305
8.2.9. Evaluate the antibacterial and antifungal properties of the film (for dairy products) ..	305
8.3. Results and discussion	306
8.3.1. Development and characterization of nanoemulsion of active combinations	306
8.3.2. Characterization of the bioactive nanocomposite films	307
8.3.2.1. Mechanical properties.....	308
8.3.2.2. Water solubility (WS)	310
8.3.2.3. Water vapor permeability (WVP).....	311
8.3.2.4. <i>In vitro</i> antibacterial and antifungal properties.....	312
8.3.2.5. Insecticidal properties	314
8.3.2.6. <i>In vitro</i> release profile of the active combinations from the bioactive films.....	316
8.3.3. Evaluation of the antibacterial and antifungal properties of the films (for cereal grains)	321
8.3.4. Evaluation of the anti-insect properties of the films (for cereal grains).....	330
8.3.5. Evaluation of the antibacterial and antifungal properties of the film (for dairy products)	336
8.4. Conclusion.....	343
8.5. Acknowledgments	344
8.6. References	345
Chapter 9	354
Evaluation of bioactive low-density polyethylene (LDPE) nanocomposite films in combined treatment with irradiation on strawberry shelf-life extension.....	355
Contribution of authors	356
Résumé.....	357
Abstract.....	359
9.1. Introduction	360

9.2. Materials and methods	361
9.2.1. Materials	361
9.2.2. Preparation of active LDPE films	362
9.2.3. Optimization of the active ingredients in LDPE films.....	363
9.2.4. <i>In vitro</i> antibacterial and antifungal properties of the films	363
9.2.5. Optimization of the active ingredients in LDPE films.....	363
9.2.6. <i>In vitro</i> release profiles of active formulation from the active film	364
9.2.7. <i>In situ</i> application of the active LDPE films for strawberry presrvation	364
9.2.8. Physicochemical characterization of the packaged strawberries.....	368
9.2.8.1. Weight loss and decay (%) of the packaged strawberries	368
9.2.8.2. Surface color of the packaged strawberries	368
9.2.8.3. Firmness and total soluble solid of the packaged strawberries.....	368
9.2.8.4. Total phenol (TP) and total anthocyanins content measurement.....	369
9.2.9. Characterization of irradiated and non-irradiated LDPE films.....	369
9.2.9.1. Thickness and mechanical properties of the LDPE films	370
9.2.9.2. Oxygen permeability rate (OTR) of the LDPE films	370
9.2.9.3. Water vapor permeability of the LDPE films	370
9.2.9.4. Water solubility (WS) of the LDPE films.....	371
9.2.9.5. Color properties of the LDPE films	371
9.2.10. Statistical analyses	371
9.3. Results and discussion	372
9.3.1. Optimization of the active LDPE/CNCs nanocomposite films	372
9.3.2. <i>In vitro</i> release profiles of active formulation from the active film	375
9.3.3. Physicochemical characterization of the packaged strawberries.....	376
9.3.3.1. Weight loss of the packaged strawberries.....	376
9.3.3.2. Percent decay (%) of the packaged strawberries	378
9.3.3.3. Surface color of the packaged strawberries	379
9.3.3.4. Firmness and total soluble solid of the packaged strawberries.....	382
9.3.3.5. Total phenol (TP) and total anthocyanins content measurement.....	384
9.3.4. Characterization of irradiated and non-irradiated LDPE films.....	387
9.4. Conclusion.....	391
9.5. Acknowledgments	391
9.6. References	392
Chapter 10	402
General discussion and conclusions.....	402
Conclusion	412
Bibliograpgy	414
Annexe A.....	449
List of publications.....	450
List of conference presentations.....	451

List of Tables

Table 1.1. Some essential oils (EOs) and their major chemical components	9
Table 1.2. Examples of the antibacterial, antifungal, and insecticidal properties of the EOs and CEs.....	13
Table 1.3. Application chitosan (CH) as active packaging to control the growth of pathogenic bacteria, spoilage fungi and insect pests or food preservations	21
Table 1.4. Application of PLA as active packaging to control the growth of pathogenic bacteria, spoilage fungi and insect pests for food preservation	25
Table 1.5. Application of PBAT as active packaging in food preservations to control the growth of pathogenic bacteria, spoilage fungi and insect pests for food preservations	27
Table 2.1. Equipment and dosimetry systems used to apply the Gamma-ray and X-ray irradiation treatments	46
Table 2.2. D ₁₀ values for bacterial pathogens irradiated with or without oregano/thyme essential oil (EO).....	49
Table 3.1. Chemical compositions of the essential oils and citrus extracts	66
Table 3.2. Minimal inhibitory concentration (MIC, ppm) of essential oils (EOs) and citrus extracts (CEs) against two foodborne pathogens and three spoilage fungi	70
Table 3.3. Fractional inhibitory concentration (FIC) and interaction effect of double combinations between essential oils (EOs) and citrus extracts (CEs) antibacterial/antifungals.....	73
Table 3.4. Independent variables (antibacterial/antifungal compounds) of active formulation 1, their constraints (proportions from 0 to 1 and concentration of antibacterial/antifungal compounds from 0 to 10000 ppm) for the centroid-mixture design method.....	75
Table 3.5. Independent variables (antibacterial/antifungal compounds) of active formulation 2 and their constraints (proportions from 0 to 1 and concentration of antibacterial/antifungal compounds from 0 to 10000 ppm) for the centroid-mixture design method.....	75
Table 4.1. Name and compositions/chemical components of the essential oils (EOs).....	107
Table 4.2. Minimal inhibitory concentration (MIC, ppm) of AgNPs and EOs against <i>E. coli</i> O157:H7, <i>S. Typhimurium</i> , <i>A. niger</i> , <i>P. chrysogenum</i> , <i>M. circinelloides</i>	112
Table 4.3. Fractional inhibitory concentration (FIC) indices of Ag-NPs in combination with the selected EOs	115
Table 4.4. Fractional inhibitory concentration (FIC) indices of three or more combinations of EO and AgNPs	117
Table 4.5. Parameters of the modified Gompertz model for pathogenic bacterial and fungal species subjected to three active combinations containing essential oils and silver nanoparticles using vapor assay	120
Table 4.6. Antibacterial and antifungal efficiency of active combinations 1, 2, and 3 on tested bacteria and fungi in rice on day 28	124
Table 5.1. ANOVA results for optimizing nanoemulsion of AF-1 by the central composite design	148
Table 5.2. ANOVA results for optimizing nanoemulsion of AF-2 by the central composite design	150
Table 5.3. Inhibitory capacity (IC, %) against pathogenic bacteria and spoilage fungi, turbidity and digital images of coarse and nano emulsion of active formulations.....	157
Table 5.4. Effect on CNC content in the mechanical properties (TS, TM, Eb) and water vapor permeability (WVP) of the CH-based films.....	161
Table 6.1. ANOVA results for the PBAT film formulated with active formulation 1 (AF-1)	205
Table 6.2. ANOVA results for the PBAT film formulated with active formulation 2 (AF-2).....	208
Table 6.3. ANOVA results for the PLA film formulated with active formulation 1 (AF-1).....	213
Table 6.4. ANOVA results for the PLA film formulated with active formulation 2 (AF-2).....	217
Table 6.5. Effect on CNC content in the mechanical properties (TS, TM, Eb), oxygen transmission rate (OTR) and water vapor permeability (WVP) of the bioactive composite films	223

Table 6.6. Parameters of the Korsmeyer-Peppas model as kinetic release parameters (rate constant (k) and diffusional exponent (n)) of the active formulations from polymeric matrices in ethanol	226
Table 7.1. Insecticidal properties of the different volume of the essential oils against rice weevil until 72 hours of exposure	264
Table 7.2. Effect of microfluidisation pressure and number of cycles on the zeta potential (mV), PDI (poly dispersity index), size (nm) and encapsulation efficiency (EE, %) of AF-1 and AF-2	269
Table 7.3. Mortality (%) of rice weevil treated with γ -irradiation alone and in combination with bioactive CH-, PBAT- and PLA-based nanocomposite films	273
Table 8.1. Effect of microfluidisation pressure and number of cycles on the zeta potential (mV), PDI (poly dispersity index), size (nm) and encapsulation efficiency (EE, %) of AC-, AC-2 and AC-3	307
Table 8.2. Effect on CNC content in the mechanical properties (TS, TM, Eb), water vapor permeability (WVP) and water solubility (WS) of the bioactive composite films.....	309
Table 8.3. Inhibitory capacity (IC, %) against pathogenic bacteria and spoilage fungi of bioactive nanocomposite films.....	314
Table 8.4. <i>In vitro</i> insecticidal properties of the bioactive nanocomposite films against rice weevil (<i>S. oryzae</i>).....	315
Table 8.5. Parameters of the Korsmeyer-Peppas model as kinetic release parameters (rate constant (k) and diffusional exponent (n)) of the active formulations from polymeric matrices in ethanol	320
Table 8.6. Parameters of the Korsmeyer-Peppas model as kinetic release parameters (rate constant (k) and diffusional exponent (n)) of the active formulations from polymeric matrices in 3 % acetic acid	321
Table 8.7. Mortality (%) of rice weevil treated with γ -irradiation alone and in combination with bioactive CH-, PBAT- and PLA-based nanocomposite films	333
Table 9.1. Experimental design using central composite design (CCD) for developing active LDPE films.....	362
Table 9.2. Film ingredients and their constraints for the central composite design.....	363
Table 9.3. Experimental results of the inhibitory capacity (IC, %) of the active LDPE films against two pathogenic bacteria and two spoilage fungi.....	373
Table 9.4. ANOVA results for antibacterial and antifungal properties.....	374
Table 9.5. Hunter L^* values of strawberries under different packaging treatments during storage	380
Table 9.6. Hunter a^* values of strawberries under different packaging treatments during storage	381
Table 9.7. Hunter b^* values of strawberries under different packaging treatments during storage	382
Table 9.8. The firmness of strawberries under different packaging treatments	383
Table 9.9. Color measurement, mechanical properties, and water vapor permeabilities (WVP) of the active LDPE films	389

List of Supplementary Data Tables

Supplementary data table 3.1. Centroid mixture designs for four independent variables presented in the active formulation 1 and the experimental responses (MIC values) against <i>E. coli</i> O157 H7, <i>S. Typhimurium</i> , <i>A. niger</i> , <i>P. chrysogenum</i> , and <i>M. circinelloides</i>	94
Supplementary data table 3.2. Centroid mixture designs for five independent variables presented in the active formulation 2 and the experimental responses (MIC values) against <i>E. coli</i> O157 H7, <i>S. Typhimurium</i> , <i>A. niger</i> , <i>P. chrysogenum</i> , and <i>M. circinelloides</i>	95
Supplementary data table 3.3. ANOVA results for antimicrobial and antifungal properties of the active formulation 1	97
Supplementary data table 3.4. ANOVA results for antimicrobial and antifungal properties of the active formulation 2	98
Supplementary data table 3.5. Vapor effect of active formulation 1 and 2 with statistical analyses in rice for 28 days to control the growth of (a) <i>E. coli</i> O157:H7, (b) <i>S. Typhimurium</i> , (c) <i>A. niger</i> , (d) <i>P. chrysogenum</i> , (e) <i>M. circinelloides</i> . Control samples were not containing antibacterials/antifungals. Values are means±standard error. Within each row means with the same lowercase letter are not significantly different ($P > 0.05$). Within each column means with the same uppercase letter are not significantly different ($P > 0.05$).....	99
Supplementary data table 5.1. Experimental design by central composite design (CCD) for optimization of nanoemulsion active formulation 1(AF-1).....	184
Supplementary data table 5.2. Experimental design by central composite design (CCD) for optimization of nanoemulsion active formulation 2 (AF-2).....	185
Supplementary data table 5.3. ANOVA analyses for the storage stability of coarse and nanoemulsion of AF-1 and AF-1 at 4 °C, 25 °C, and 40 °C for 2 months. Values means±standard error. Within each column means with different lowercase letter are significantly different ($P \leq 0.05$). Withing each row means with different uppercase letter are significantly different ($P \leq 0.05$)	186
Supplementary data table 5.4. Inhibitory capacity (%) of bioactive chitosan film against <i>E. coli</i> , <i>S. Typhimurium</i> , <i>A. niger</i> , <i>P. chrysogenum</i> , and <i>M. circinelloides</i> . Values means ± standard error. Within each column means with different lowercase letter are significantly different ($P \leq 0.05$)	187
Supplementary data table 5.5. <i>In situ</i> antibacterial and antifungal effectiveness of different bioactive films to control <i>E. coli</i> O157:H7, <i>S. Typhimurium</i> , <i>A. niger</i> , <i>P. chrysogenum</i> , and <i>M. circinelloides</i> growth in stored rice for 8 weeks. Values means ± standard error. Within each column means with different lowercase letter are significantly different ($P \leq 0.05$). Withing each row means with different uppercase letter are significantly different ($P \leq 0.05$)	188
Supplementary data table 6.1. CCD experimental response surface design of the PBAT films formulated with active formulation 1 (AF-1), CNC and glycerol.....	243
Supplementary data table 6.2. CCD experimental response surface designs' results the PBAT films formulated with active formulation 1 (AF-1) against bacteria (<i>E. coli</i> O157:H7 and <i>S. Typhimurium</i>) and fungi (<i>A. niger</i> , <i>P. chrysogenum</i> and <i>M. circinelloides</i>).....	244
Supplementary data table 6.3. CCD experimental response surface design of the PBAT films formulated with active formulation 2 (AF-2), CNC and glycerol.....	245
Supplementary data table 6.4. CCD experimental response surface designs' results the PBAT films formulated with active formulation 2 (AF-2) against bacteria (<i>E. coli</i> O157:H7 and <i>S. Typhimurium</i>) and fungi (<i>A. niger</i> , <i>P. chrysogenum</i> and <i>M. circinelloides</i>).....	246
Supplementary data table 6.5. CCD experimental response surface design of the PLA films formulated with active formulation 1 (AF-1), CNC and glycerol.....	247

Supplementary data table 6.6. CCD experimental response surface designs' results the PLA films formulated with active formulation 1 (AF-1) against bacteria (*E. coli* O157:H7 and *S. Typhimurium*) and fungi (*A. niger*, *P. chrysogenum* and *M. circinelloides*)..... 248

Supplementary data table 6.7. CCD experimental response surface design of the PLA films formulated with active formulation 2 (AF-2), CNC and glycerol 249

Supplementary data table 6.8. CCD experimental response surface designs' results the PLA films formulated with active formulation 2 (AF-2) against bacteria (*E. coli* O157:H7 and *S. Typhimurium*) and fungi (*A. niger*, *P. chrysogenum* and *M. circinelloides*)..... 250

Supplementary data table 9.1. Weight loss (%) of strawberries under different active film packaging treatments during storage..... 399

Supplementary data table 9.2. Weight loss (%) of strawberries by placing the optimized LDPE nanocomposite films at different position inside the PET clamshell 399

Supplementary data table 9.3. Decay (%) of strawberries under different active film packaging treatments during storage..... 400

Supplementary data table 9.4. Decay (%) of strawberries after placing the optimized LDPE nanocomposite films at different positions inside the PET clamshell..... 400

Supplementary data table 9.5. Color measurement (Hunter L*, a*, b* values) of the strawberries when placing the optimized LDPE nanocomposite films at different positions inside the PET clamshell 401

List of Figures

Figure 2.1. Relative radio sensitivity (RS) of <i>E. coli</i> O157:H7, <i>S. Typhimurium</i> and <i>L. monocytogenes</i> to irradiation and irradiation plus oregano/thyme EO using different radiation sources and dose rates.	52
Figure 3.1. Optimization of the independent variables presented in the active formulation 1 using contour plot and 3D image against (a) <i>E. coli</i> O157 H7, (b) <i>S. Typhimurium</i> , (c) <i>A. niger</i> , (d) <i>P. chrysogenum</i> , and (e) <i>M. circinelloides</i> . The region of dark blue color indicates higher microbicidal effectiveness, while the green to yellow to red colors indicate increasingly weaker antimicrobial effectiveness.....	79
Figure 3.2. Optimization of the independent variables presented in the active formulation 2 using contour plot and 3D image against (a) <i>E. coli</i> O157 H7, (b) <i>S. Typhimurium</i> , (c) <i>A. niger</i> , (d) <i>P. chrysogenum</i> , and (e) <i>M. circinelloides</i> . The region of dark blue color indicates higher microbicidal effectiveness, while the green to yellow to red colors indicate increasingly weaker antimicrobial effectiveness	84
Figure 3.3. Vapor effect of active formulation 1 and 2 for controlling the growth of (a) <i>E. coli</i> O157:H7, (b) <i>S. Typhimurium</i> , (c) <i>A. niger</i> , (d) <i>P. chrysogenum</i> , (e) <i>M. circinelloides</i> in rice. Controls did not contain any antibacterial/antifungal EOs or CEs. Values are means \pm standard error	87
Figure 4.1. Effect of active combinations 1, 2, 3 on the maximum colony diameter, $\ln(D_t/D_0)$, of (a) <i>E. coli</i> O157:H7, (b) <i>S. Typhimurium</i> , (c) <i>A. niger</i> , (d) <i>P. chrysogenum</i> , and (e) <i>M. circinelloides</i> over time. The control sample did not contain active combinations. Values are means \pm standard error	122
Figure 4.2. Effect of active combinations (1, 2, and 3) in rice to control (a) <i>E. coli</i> O157:H7, (b) <i>S. Typhimurium</i> , (c) <i>A. niger</i> , (d) <i>P. chrysogenum</i> , and (e) <i>M. circinelloides</i> . The control sample did not contain antimicrobials/antifungals. Values are means \pm standard error.....	126
Figure 5.1. Optimization of the independent variables presented in the active formulation 1 using 3D image of (a) Zeta potential (mV), (b) size (nm), (c) PDI, and (d) encapsulation efficiency (EE, %).	149
Figure 5.2. Optimization of the independent variables presented in the active formulation 2 using 3D image of (a) Zeta potential (mV), (b) size (nm), (c) PDI, and (d) encapsulation efficiency (EE, %).	151
Figure 5.3. Storage stability of coarse and nanoemulsion of AF-1 and AF-1 at different temperature(a) 4 °C (b) 25 °C and (c) 40 °C for 2 months. Nanoemulsion of AF-1 and AF-2 was optimized at 8000 psi (2 nd cycle) and 15000 psi (3 rd cycle), respectively.....	154
Figure 5.4. Bacterial (<i>E. coli</i> O157:H7 and <i>S. Typhimurium</i>) and fungal (<i>A. niger</i> , <i>P. chrysogenum</i> , and <i>M. circinelloides</i>) growth profiles in storage rice under different bioactive films treatment for 8 weeks.....	165
Figure 5.5. Standard curve for active formulation 1 (AF-1) (a) and active formulation 2 (AF-2) (b), and average yield extracted active components (c) from the film at 330 nm	169
Figure 5.6. Release (%) of active components from (a) bioactive CH+AF-1 film and (b) bioactive CH+AF-film with and without CNC. Values are means \pm standard error. The same lowercase letter either in the bioactive CH-based films with or without CNC are not significantly different ($P > 0.05$). The same uppercase letter between the bioactive CH-based films with and without CNC are not significantly different ($P > 0.05$)	171
Figure 5.7. Release kinetics study of the active components from (a) CH+AF-1 film, CH+AF-1+CNC film and (b) CH+AF-2 film, CH+AF-2+CNC film	173
Figure 5.8. Sensory analyses of the cooked rice under different bioactive CH-based nanocomposite films (a) CH+AF-1+CNC film and (b) CH+AF-2+CNC film during two months of storage rice. Control samples did not contain any bioactive CH-based nanocomposite films.	

Values are means \pm standard error followed by the same lower-case letter are not significantly different ($P > 0.05$)..... 175

Figure 6.1. A numerical optimization was plotted for all dependent and independent values which showed the optimum points for PBAT film formulated with active formulation 1 (AF-1)..... 207

Figure 6.2. A numerical optimization was plotted for all dependent and independent values which showed the optimum points for PBAT film formulated with active formulation 2 (AF-2)..... 210

Figure 6.3. A numerical optimization was plotted for all dependent and independent values which showed the optimum points for PLA film formulated with active formulation 1 (AF-1) 215

Figure 6.4. A numerical optimization was plotted for all dependent and independent values which showed the optimum points for PLA film formulated with active formulation 2 (AF-2) 219

Figure 6.5. Cumulative release (%) of two active formulations in ethanol (food simulant) from PBAT and PLA polymeric matrices during extraction time 225

Figure 6.6. Ratio of the two active formulations released from polymeric films during contact time with ethanol and fitted Fick's model (Korsmeyer-Peppas model)..... 228

Figure 6.7. Bacterial (*E. coli* O157:H7 and *S. Typhimurium*) and fungal (*A. niger*, *P. chrysogenum*, and *M. circinelloides*) growth profiles in storage rice under different bioactive PBAT films treatment for 8 weeks 234

Figure 7.1. Acetylcholinesterase (AChE) enzyme activities of various EOs, CEs and active formulations against rice weevil. Values are means \pm standard error. Same values for each treatment that don't have same lowercase letters are significantly different ($P \leq 0.05$) 266

Figure 7.2. *In situ* fumigation toxicity of different insecticidal films in rice grains for 14 days against *S. oryzae* 270

Figure 7.3. Release (%) of active compounds (%) from (a-b) CH-based bioactive film with and without CNC, (c-d) bioactive PBAT-based film with and without CNC, (e-f) PLA-based bioactive film with and without CNC. Values are means \pm standard error. The same lowercase letter either in each bioactive film with or without CNC are not significantly different ($P > 0.05$). The same uppercase letter between the each bioactive films with and without CNC are not significantly different ($P > 0.05$)..... 279

Figure 7.4. Sensory evaluation scores (mean \pm SD) of cooked rice packaged with developed bioactive CH-based, PBAT-based and PLA-based nanocomposite films. Mean values for the treatment with the same area that share the common lower-case letters are not significantly different ($P > 0.05$)..... 282

Figure 8.1. Cumulative release (%) of two active formulations in ethanol (food simulant) from PBAT and PLA polymeric matrices during extraction time 317

Figure 8.2. Cumulative release (%) of two active formulations in 3 % acetic acid (food simulant) from PBAT and PLA polymeric matrices during extraction time 318

Figure 8.3. Bacterial (*E. coli* O157:H7 and *S. Typhimurium*) and fungal (*A. niger* and *P. chrysogenum*) growth profiles in storage rice under different bioactive films treatment for 8 weeks 323

Figure 8.4. Bacterial (*E. coli* O157:H7 and *S. Typhimurium*) and fungal (*A. niger* and *P. chrysogenum*) growth profiles in storage rice under different bioactive films treatment for 8 weeks 325

Figure 8.5. Effect of irradiation along with bioactive films against *E. coli* O157:H7, *S. Typhimurium*, *A. niger* and *P. chrysogenum* in stored rice after 8 weeks 329

Figure 8.6. *In situ* fumigation toxicity of different insecticidal films in rice grains for 14 days against *S. oryzae* 331

Figure 8.7. Bacterial (*E. coli* O157:H7 and *S. Typhimurium*) and fungal (*A. niger*, *P. chrysogenum*, and *M. circinelloides*) growth profiles in storage yogurt under different bioactive films treatment for 8 weeks 339

Figure 8.8. Bacterial (*E. coli* O157:H7 and *S. Typhimurium*) and fungal (*A. niger*, *P. chrysogenum*, and *M. circinelloides*) growth profiles in storage yogurt under different bioactive films treatment for 8 weeks 342

Figure 9.1. Cumulative release (%) of active formulation in ethanol (food simulant) from active LDPE-based nanocomposite film during extraction time 376

Figure 9.2. Digital images of the nanocomposite LDPE film from different Groups. Group-1: LDPE+CNCs+Glycerol (Control); Group-2: LDPE+CNCs+Glycerol+AGPPH; Group-3: LDPE+CNCs+Glycerol+cinnamom EO; Group-4: LDPE+CNCs+Glycerol+active formulation (AGPPH+cinnamom EO); and Group-5: LDPE+CNCs+Glycerol+active formulation+ γ -irradiation. LDPE nanocomposite film composed of LDPE polymer (2 g), CNCs (0.375 %), glycerol (0.625 %) 366

Figure 9.3. A schematic diagram of the film position-1, position-2, and position-3 inside the PET clamshell during strawberry preservation..... 367

Figure 9.4. Weight loss (%) (a) and % decay (b) of strawberries under different active film packaging treatments during storage..... 377

Figure 9.5. Total soluble solid (TSS) of strawberries under different packaging treatments during storage. Group-1: LDPE+CNCs+Glycerol (Control); Group-2: LDPE+CNCs+Glycerol+AGPPH; Group-3: LDPE+CNCs+Glycerol+cinnamom EO; Group-4: LDPE+CNCs+Glycerol+active formulation (AGPPH+cinnamom EO); and Group-5: LDPE+CNCs+Glycerol+active formulation+ γ -irradiation 384

Figure 9.6. Total phenol (a) and anthocyanins content (b) of strawberries under different active film packaging treatments during storage. Group-1: LDPE+CNCs+Glycerol (Control); Group-2: LDPE+CNCs+Glycerol+AGPPH; Group-3: LDPE+CNCs+Glycerol+cinnamom EO; Group-4: LDPE+CNCs+Glycerol+active formulation (AGPPH+cinnamom EO); and Group-5: LDPE+CNCs+Glycerol+active formulation+ γ -irradiation 386

List of Abbreviations

Analysis of variance (ANOVA)	Low density polyethylene (LDPE)
Active formulations (AFs)	Lactic acid bacteria (LAB)
Active combinations (ACs)	Minimal inhibitory concentration (MIC)
Acetylcholinesterase (AChE)	Natural Sciences and Engineering Research Council of Canada (NSERC)
Acetylcholinesterase inhibitor (AChEI)	Nanoparticles (NPs)
Antimicrobial diffusin film (ADF)	Poly lactic acid (PLA)
Brain heart infusion (BHI)	Poly (hydroxy butyrate adipate terephthalate) (PBAT)
Cellulose Nanocrystal (CNC)	Poly ethylene glycol (PEG)
Colony Forming Unit (CFU)	Potato dextrose agar (PDA)
Chitosan (CH)	Potato dextrose broth (PDI)
Central composite design (CCD)	Poly dispersity index (PDI)
Droplet size (DS)	Polyethylene terephthalate (PET)
Essential oils (EOs)	Relative humidity (RH)
Elongation at break (Eb)	Radio sensitization (RS)
Food and Drug Administration (FDA)	Response surface methodology (RSM)
Food and Agricultural Organization (FAO)	Silver nanoparticles (AgNPs)
Fractional inhibitory concentration (FIC)	Tensile strength (TS)
Film forming dispersion (FFD)	Tensile modulus (TM)
Generally recognized as safe (GRAS)	Total phenol (TP)
Gray (Gy)	Universal testing machine (UTM)
Gallic acid equivalent (GAE)	Water solubility (WS)
International Atomic Energy Agency (IAEA)	Water vapor permeability (WWVP)
Inhibitory capacity (IC)	World Health Organization (WHO)
Kilogray (kGy)	

Résumé

La contamination microbienne et l'infestation par les insectes des produits alimentaires stockés (par exemple, les céréales, les produits laitiers, etc.) sont une grande préoccupation pour les consommateurs, les scientifiques de l'alimentation et les industries alimentaires. La fabrication de films d'emballage bioactifs encapsulés avec des huiles essentielles d'origine végétale (HE), des extraits d'agrumes (EA) et des nanoparticules d'argent (AgNP) est une approche inventive pour lutter contre la croissance et la prolifération de bactéries pathogènes d'origine alimentaire, de champignons de détérioration et d'insectes nuisibles dans les aliments stockés. La combinaison de deux ou plusieurs traitements (technique d'obstacle) attire de plus en plus l'attention car ils agissent de manière synergique et réduisent ainsi les doses requises pour un traitement unique. Dans le contexte actuel, l'objectif de cette étude était de fabriquer des films biopolymères chargés d'HEs-EA (formulation active) ou d'HEs-AgNPs (combinaison active) ayant de fortes propriétés antibactériennes, antifongiques et insecticides. Les activités antibactériennes, antifongiques et insecticides de huit HE (HE de cannelle, HE de thym sarriette, HE d'agrumes, HE de Méditerranée, HE d'Asie, HE du Sud, HE de Lavang), de deux EA (extrait d'agrumes bio [OCE] et d'extrait naturel d'agrumes [NCE]) et de quatre AgNPs (AGPP, AGPPH, AGC0.5 et AGC1) et leurs combinaisons ont été évaluées sur la base de la capacité d'inhibition de toutes les bactéries et champignons testés. De plus, les toxicités fumigènes de ces HE, EA, AgNPs et leur mélange (deux formulations actives et trois combinaisons actives) ont été testées contre *S. oryzae*. Après analyse des résultats, deux formulations actives (AF-1 et AF-2) et trois combinaisons actives (AC-1, AC-2 et AC-3) ont montré de fortes bioactivités contre toutes les bactéries testées, les champignons de détérioration et les insectes par rapport aux agents actifs utilisés seuls. Deux formulations actives (AF-1 et AF-2) (mélange d'HE et d'EA) et trois combinaisons actives (AC-1, AC-2 et AC-3) (mélange d'HE et d'AgNP) ont été développées et encapsulées dans des matrices biopolymériques telles que le poly (butylène adipate-co-téréphtalate) (PBAT), l'acide polylactique (PLA) et le chitosane (CH) pour développer des films bioactifs ainsi que de faciliter et de contrôler la libération d'ingrédients actifs lors du stockage avec des produits alimentaires. Les films bioactifs à base de PBAT et de PLA ont été appliqués dans du yaourt stocké pour contrôler la croissance de bactéries pathogènes (*Escherichia coli* O157:H7, *Salmonella* Typhimurium) et de champignons d'altération (*Aspergillus niger*, *Penicillium chrysogenum* et *Mucor circinelloides*). De plus, les films bioactifs à base de PBAT, PLA et CH ont été appliqués sur des aliments (riz et yaourt) avec et sans la présence d'un traitement à l'irradiation γ . Le riz a été étudié pour le contrôle de la croissance de *E. coli* O157:H7, *S. Typhimurium*, *A. niger*, *P. chrysogenum*, *M. circinelloides* et un

insecte majeur *Sitophilus oryzae* (charançon du riz) pour assurer la sécurité et la qualité du riz stocké.

Ces travaux ont montré que les films biopolymères composés de PBAT et de CH contenant des formulations actives (AFs) (mélange d'HE et de EA) et de combinaisons d'agents microbiens (ACs) (mélange d'HE et de nanoparticules d'argent) ont montré plus d'efficacité que les films bioactifs à base de PLA. L'application d'un film bioactif et d'un traitement d'irradiation γ a augmenté la radiosensibilité des bactéries, des champignons et des insectes. L'ajout de cellulose nanocrystal (CNC) en tant qu'agent de renforcement dans les matrices polymériques a considérablement amélioré les propriétés barrières (perméabilité à la vapeur d'eau et aux gaz) et les propriétés mécaniques des films bioactifs. De plus, les films nanocomposites bioactifs renforcés avec du CNC (à base de CH, PBAT et PLA) ont plus tendance à retenir les agents actifs et à les libérer lentement pendant la durée de stockage que les films bioactifs sans CNC. L'application *in situ* de films nanocomposites bioactifs à base de PBAT et de PLA dans le yaourt stocké a réduit la croissance bactérienne et fongique de 25.6 à 93 % par rapport aux échantillons témoins (yaourt sans films nanocomposites bioactifs) après 8 semaines de stockage à 4 °C. D'autre part, l'application de films nanocomposites bioactifs à base de PBAT et CH seuls dans le riz stocké a réduit la croissance bactérienne et fongique de 20 à 72 % par rapport aux échantillons témoins après 8 semaines à 28 °C, tandis que le traitement combiné des films bioactifs et l'irradiation γ à une dose de 750 Gy ont significativement réduit la croissance bactérienne et fongique de 58 à 93 % à la fin du stockage. Les films nanocomposites bioactifs à base de CH, PBAT et PLA ont montré de fortes propriétés insecticides contre *S. oryzae* dans le riz stocké pendant 14 jours à 28 °C. Le niveau de mortalité des insectes dans le riz était compris entre 44.4 et 83 % après 14 jours d'incubation avec le film nanocomposite bioactif seul, tandis que l'échantillon témoin (sans film nanocomposite bioactif) ne montrait que 6 % de mortalité des insectes. De plus, le traitement combiné entre les films bioactifs et le traitement par irradiation a augmenté de manière significative la mortalité des insectes. Par exemple, un traitement d'irradiation de 300 Gy en présence des films nanocomposites bioactifs a augmenté l'efficacité insecticide entre 96 et 100 % entre les jours 7 et 14. L'évaluation sensorielle du riz stocké et le yaourt stocké pendant 2 mois conservé avec des films nanocomposites bioactifs chargés d'AF n'a montré aucun changement significatif ($P > 0.05$) de la couleur, de l'odeur, du goût et de l'appréciation globale par rapport au riz et au yaourt non traité. La thèse actuelle a été rédigée selon un format basé sur la publication suivi des directives de l'INRS (INRSGuideST-2022-eng).

Abstract

Microbial contamination and insect infestation of stored food products (e.g., cereals, dairy products, etc.) are of great concern to consumers, food scientists and food industries. Fabricating bioactive packaging films encapsulated with plant derived essential oils (EOs), citrus extracts (CEs) and silver nanoparticles (AgNPs) is an innovative approach to combat the growth and the proliferation of food-borne pathogenic bacteria, spoilage fungi and insect pests in stored food products. Combining two or more treatments (hurdle technique) are gaining more attention because they act synergistically, thus, reducing the doses required for single treatment. In the current context, the goal of this study was to fabricate EOs-CEs (active formulation) or EOs-AgNPs (active combination) loaded biopolymeric films having strong antibacterial, antifungal, and insecticidal properties. The antibacterial, antifungal, and insecticidal activities of eight EOs (cinnamon EO, savory thyme EO, citrus EO, Mediterranean EO, Asian EO, Southern EO, Lavang EO), two CEs (organic citrus extract [OCE] and natural citrus extract [NCE]) and four AgNPs (AGPP, AGPPH, AGC0.5 and AGC1) and their combinations were evaluated based on the inhibiting capacity of all tested bacteria and fungi. In addition, the fumigant toxicities of these EOs, CEs, AgNPs and their mixture (two active formulations and three active combinations) were tested against *S. oryzae*. After analysing the results, two active formulations (AF-1 and AF-2) and three active combinations (AC-1, AC-2 and AC-3) showed strong bioactivities against all tested bacteria, spoilage fungi and insect as compared to the single active agent. Two active formulations (AF-1 and AF-2) (mixture of EOs and CEs) and three active combinations (AC-1, AC-2 and AC-3) (mixture of EOs and AgNPs) were developed and encapsulated into biopolymeric matrices such as poly (butylene adipate-co-terephthalate) (PBAT), polylactic acid (PLA) and chitosan (CH) to develop bioactive films as well as facilitate and control the release of active ingredients during storage with food products. The bioactive PBAT- and PLA-based films were applied in stored yogurt to control the growth of pathogenic bacteria (*Escherichia coli* O157:H7, *Salmonella* Typhimurium) and spoilage fungi (*Aspergillus niger*, *Penicillium chrysogenum* and *Mucor circinelloides*). Furthermore, the bioactive PBAT-, PLA- and CH-based films were applied with and without the presence of γ -irradiation in stored rice to control the growth of *E. coli* O157:H7, *S. Typhimurium*, *A. niger*, *P. chrysogenum*, *M. circinelloides* and a major stored product insect *Sitophilus oryzae* (rice weevil) to ensure the safety and quality of stored rice.

However, biopolymeric films composed of PBAT and CH loaded with AFs (mixture of EOs and CEs) and ACs (mixture of EOs and silver nanoparticles) showed more efficiency than bioactive PLA-based films. Application of bioactive film and γ -irradiation increased the radiosensitivity of the tested bacteria, fungi, and insect. Addition of cellulose nanocrystals (CNCs) as reinforcing agents

into the polymeric matrices significantly improved the barrier (water vapor permeability and gas permeability) and mechanical properties of the bioactive films. Moreover, CNC-reinforced bioactive nanocomposite films (CH-, PBAT- and PLA-based) have more tendency to retain the active agents and release slowly over the storage time than the bioactive films without CNC. *In situ* application of bioactive PBAT- and PLA-based nanocomposite films in stored yogurt reduced the bacterial and fungal growth by 25.6-93 % as compared to the control samples (yogurt without bioactive nanocomposite films) after 8 weeks of storage at 4 °C. On the other hand, application of bioactive PBAT- and CH-based nanocomposite films alone in stored rice reduced the bacterial and fungal growth by 20-72 % as compared to the control samples after 8 weeks at 28 °C, while the combined treatment of bioactive films and 750 Gy γ -irradiation significantly reduced the bacterial and fungal growth by 58-93 % at the end of the storage. The bioactive CH-, PBAT- and PLA-based nanocomposite films showed strong insecticidal properties against *S. oryzae* in stored rice for 14 days at 28 °C. The mortality of insects in rice were between 44.4 to 83 % after 14 days of incubation with bioactive nanocomposite film alone, while the control sample (without bioactive nanocomposite films) showed only 6 % insect. In addition, combined treatment between bioactive films and irradiation treatment significantly increased the mortality of insects, for example, 300 Gy irradiation along with bioactive nanocomposite films increased insecticidal efficiency between 96 to 100 % at day 7 to 14. The sensorial evaluation of stored rice and stored yogurt for 2 months preserved with bioactive nanocomposite films loaded with AFs did not show any significant ($P > 0.05$) change in color, odor, taste and global appreciation as compared to untreated rice and yogurt. The current thesis has been written as publication-based format followed by the guidelines at INRS (INRSGuideST-2022-eng).

Chapter 1
Literature review

1.1. Introduction

Food packaging is a critical technology for the food industry to protect food from detrimental environmental factors including oxygen, biological and chemical hazards, water vapor, ultraviolet light, heat, pressure, mechanical damages, etc. Customers have high expectations to consume safe and healthy foods and an increasing interest for food scientists and food industries to produce advanced packaging systems that can maintain food quality and nutritional content, extend the shelf life of foods, and maintain freshness without masking the sensory properties of the foods (Mahmud *et al.*, 2022; Sharma *et al.*, 2022). Active packaging (AP) is a novel concept of adding certain active ingredients to the package itself to achieve functionality, such as antimicrobials that prevent foodborne illness to reduce the risk of food recalls, extend shelf life, and maintain food quality (Bahrami *et al.*, 2020; Sharma *et al.*, 2022). AP can be used to control the growth of many harmful biological entities such as bacteria, fungi, virus, and insect pests, via the release of bioactive compounds to protect the surface of foods during storage (Hossain *et al.*, 2018; Hossain *et al.*, 2019a; Bahrami *et al.*, 2020).

Utilization of natural antimicrobial substances during the fabrication of AP is one of the popular strategies. The major natural antimicrobial substances are plant-derived essential oils (EOs), plant extracts (PEs) (e.g., citrus extract), antimicrobial peptides, organic acids, enzymes, certain biopolymers (e.g., chitosan) (Bahrami *et al.*, 2020; Begum *et al.*, 2022b). EOs and CEs are well known for their strong bioactivities including antibacterial, antifungal, insecticidal, antiviral, and antioxidant properties (Turgis *et al.*, 2012; Hossain *et al.*, 2016a; Begum *et al.*, 2022b). EOs are typically a mixture of volatile bioactive compounds such as monoterpenes, sesquiterpenes, and their oxygenated derivatives (alcohols, aldehydes, esters, ethers, ketones, phenols, and oxides) (Turgis *et al.*, 2012; Vishwakarma *et al.*, 2016). Currently, more than 3000 different EOs have been studied and 300 of them have commercial applications in the food, pharmaceutical, sanitary, or cosmetic industries. The various terpene and polyphenol components of EOs have been accepted by the European Commission as flavorings for food products and approved by the US Food and Drug Administration (FDA) as GRAS (Generally Recognized as Safe). EOs have a strategy to apply multiple mechanisms of action for controlling microbial contaminants, thus pathogens have less chance to become resistant. However, perceivable taste and aroma changes caused by EOs at high concentrations limit their application in many food products. The combination of two or more antimicrobial/antifungal EO agents may provide synergistic and increased activity at low concentrations to avoid this limitation (Turgis *et al.*, 2012; Tongnuanchan and Benjakul, 2014; Mohammadzadeh, 2017; Tardugno *et al.*, 2019). Silver nanoparticles (AgNPs) are increasingly used in the medical, food, healthcare, and industrial fields due to their

unique physical and chemical properties, including their well-known antimicrobial activity at low concentrations (Ghosh *et al.*, 2013a; Weisany *et al.*, 2019). The microbicidal effect of AgNPs has three modes of action: (1) small size AgNPs can bind to the cell membrane surface and drastically disturb its functions, permeability, and respiration, (2) AgNPs act as a weak acid (Lewis acid) and can interact with compounds containing sulfur and phosphorus (DNA, proteins) after penetration into microbial cells, (3) the release of Ag⁺ in presence of oxygen and interaction with negatively charged microbial cell membranes can disrupt normal cell function (Morones *et al.*, 2005; Eghbalifam *et al.*, 2015; Tang and Zheng, 2018; Simbine *et al.*, 2019).

Moreover, the nano metric size of emulsions or nanoemulsions are oil-in-water or water-in-oil type emulsions that are isotopically clear dispersions stabilized by interfacial layer of surfactant molecules. The smaller particle size and narrow particle size distribution of nanoemulsions leads to distinct physicochemical properties like optical transparency, bulk viscosity and physical stability, and that contributes to superior performance of nanoemulsions over conventional emulsions (Hossain *et al.*, 2019b; Llinares *et al.*, 2018). High-pressure microfluidisation is one of the efficient techniques to produce nanoemulsions of essential oils which is suitable for wide-scale and industrial production. Though nanoemulsion of active agents or EOs have strong antimicrobial, antifungal and insecticidal properties, the direct application of nanoemulsion of active agents or EOs may affect the organoleptic and sensory properties of the foods. These problems could be minimized by immobilizing the nanoemulsions of EOs in bio-degradable polymer matrices (e.g., carbohydrates, proteins, or lipids). The biopolymers having active agents can act as bioactive packaging films that can control and prolong the release of the active compounds because encapsulation enhances and stabilizes the activity of the volatile EOs (Boumail *et al.*, 2013; Khan *et al.*, 2014; Hossain *et al.*, 2018).

Encapsulation of active agents into biopolymeric matrices could reduce the limitation of application of active agents in food products, and additionally, they can contribute to sustainable development goals by eliminating the use of petroleum-based non-degradable materials. For commercial application, it is very important to employ materials that are produced by natural sources and it must be contained good physical and chemical properties ecofriendly, readily biodegradable, non-toxic degradation by-products and low-cost. The use of biopolymers as packaging materials is an alternative to petroleum-based non-degradable packaging material. Biodegradable polymers can be divided into two main classes called natural and synthetic polymers according to their origin (Otgonzul, 2010). Natural biodegradable polymers are produced from renewable sources. Natural biodegradable polymers are polysaccharides, proteins, lipids, polyesters produced from microorganism or plant, polyesters produced from bio monomers and miscellaneous polymers.

Synthetic biodegradable polymers can be classified in 4 categories such as aliphatic polyester, aromatic polyester, polyvinyl alcohol, modified polyolefin (Siracusa *et al.*, 2008; Otgonzul, 2010). Synthetic biodegradable polymers are widely used in many fields, because of their better properties compared to natural polymers. Natural biopolymers such as polysaccharides and proteins are produced from renewable or biological sources (e.g., plant, animal, microbial, and marine sources), whereas synthetic polymers are chemically synthesized. The biodegradable polymers are used as active packing materials for food preservation. The most common active packaging materials are chitosan, corn zein, polyethylene, methyl cellulose, poly lactic acid, polyvinyl alcohol, low density polyethylene (Siracusa *et al.*, 2008; Otgonzul, 2010; Vieira *et al.*, 2011).

The use of biopolymers as a film forming materials depends on several features including cost, availability, functional attributes, mechanical properties (strength and flexibility), optical quality (gloss and opacity), barrier requisites (water vapor, O₂ and CO₂ permeability), structure resistance to water and sensorial acceptance. These characteristics are greatly influenced by parameters such as the type of material used as structural matrix (conformation, molecular mass, charge distribution), film manufacturing conditions (solvent, pH, concentration, temperature, etc.) and the type and concentration of additives (plasticizers, cross-linking agents, antimicrobials, antioxidants, etc.) (Otgonzul, 2010; Vieira *et al.*, 2011; Khan *et al.*, 2012; Khan *et al.*, 2014). Biopolymers such as chitosan (CH), Poly (butylene adipate-co-terephthalate) (PBAT), and polylactic acid (PLA) are commercially available biodegradable polymeric materials (Khan *et al.*, 2012; Su *et al.*, 2020). Chemically, PBAT is an aliphatic-aromatic copolyester, flexible and compostable certified by the European Bioplastics (EN13432 standard criteria) and the Biodegradable Polymers Institute (ASTM D6400 standard specification) (Morelli *et al.*, 2016; Shankar and Rhim, 2018). PLA is a biodegradable polymer having good mechanical properties, transparency and easy processibility prepared from renewable sources (Salmieri *et al.*, 2014a, b). CH is a biodegradable polymer used with food ingredients approved by the FDA because it is biocompatible, non-toxic, and bio-functional (Khan *et al.*, 2012; Hossain *et al.*, 2019a). Cellulose nanocrystals (CNCs) are used as reinforcing agents within polymeric matrices for improving mechanical and barrier properties of the biopolymer and also improving the controlled release of active ingredients for extended storage (Khan *et al.*, 2013; Salmieri *et al.*, 2014b; Haafiz *et al.*, 2016). Combining ionizing radiation (γ -ray) with bioactive packaging films could act synergistically with lower radiation doses for controlling foodborne pathogenic bacteria, spoilage fungi, and insect pests in stored cereal grains (Follett *et al.*, 2013; Hossain *et al.*, 2014b). Bioactive films/film patches could be applied to protect the stored

cereal grains (rice) and dairy products (yogurt) by inhibiting the growth of foodborne pathogenic bacteria, spoilage fungi and insect pests.

1.2. Level of food contamination

Today, food losses are a major concern throughout the world because one-third of the produced foods are either wasted or lost (FAO, 2011). Annually, 1.3 billion tons of foods are reported as lost by the Food and Agricultural Organization (FAO) which corresponds to about 40-50 % fruits, vegetables, root crops, about 35 % fish and sea food, 30 % cereal grains, and 20 % meat, oil, dairy products are lost or wasted (FOOD, 2016). About 30-40 % foods are lost during the post-harvest and processing stage in developing countries, while in industrialized countries, the food waste is about 30 % at the retail and consumer level (Leyva Salas *et al.*, 2017). Microbial spoilage of food is one of the major causes of these massive food losses as they alter the food and nutritional quality, and change the organoleptic properties (taste, smell, texture) of the foods. Food spoilage is a metabolic change in food making it unacceptable for consumption, or if consumed, at an increased risk for foodborne illness due to microbial contamination (Rawat, 2015; Maherani *et al.*, 2018).

Annually, hundreds of thousands of people have died worldwide due to foodborne and waterborne diseases, and alarmingly these numbers are increasing these days due to microbial antibiotic resistance as well as new emergence of pathogens. The major foodborne pathogenic bacteria are *Escherichia coli* O157:H7, *Salmonella* Typhimurium, *Listeria monocytogenes* and *Staphylococcus aureus* (Maherani *et al.*, 2018). Spoilage fungi or molds are another concern in food products and food industries that can be found in any stage of the food chain because of their ability to grow in a wide range of environmental conditions from favorable to harsh environments (Pitt and Hocking, 2009). The most common fungal species responsible for food spoilage are *Aspergillus* sp., *Penicillium* sp., and *Fusarium* sp. These fungi can produce mycotoxins as their secondary metabolites which are toxic to humans and animals (Hossain *et al.*, 2014a; Leyva Salas *et al.*, 2017). The presence of pathogenic bacteria in foods are more frequently linked to human illness outbreaks worldwide. From 1980 to 2016, a total of 571 outbreaks were recorded, accounting for 72,855 infections and 173 deaths. Among them, a total of 51.7 % outbreaks were associated with leafy green vegetables and 27.8 % outbreaks were associated with fruits (Machado-Moreira *et al.*, 2019). The major pathogenic strains associated with the outbreaks were *E. coli* O157:H7, *Salmonella*, norovirus, and hepatitis A (Machado-Moreira *et al.*, 2019). In 2011, an *E. coli* O157:H7 outbreak occurred in strawberries in the United States and 15 people were hospitalized including

two deaths (Laidler *et al.*, 2013). Delbeke *et al.* (2014) which showed that *E. coli* O157:H7 and *Salmonella* sp. can survive on the surface of strawberries for one week of storage at room temperature or refrigerated conditions.

Dairy products (milk, yogurt, cheese) are high in nutritional value and consumed worldwide (Yangilar and Yildiz, 2018). Dairy products are also highly contaminated with pathogenic bacterial species (*Salmonella* sp., Shiga toxin producing *E. coli*, *L. monocytogenes*, *Campylobacter* sp.) and spoilage fungal species (*Aspergillus* sp., *Penicillium* sp., *Eurotium* sp., *Paecilomyces* sp., *Mucor* sp.) (Snyder *et al.*, 2016b; Costard *et al.*, 2017; Sassi *et al.*, 2022). Rice, *Oryza sativa* L., is the most important cereal grain worldwide, with about 50 % of the world's population consuming it as a staple food (Das *et al.*, 2021b; Begum *et al.*, 2022a). Rice is sensitive to biodeterioration by pathogenic bacteria, spoilage fungi, and insect pests causing rice to become discolored, off-flavor, and unpleasant smelling with reduced nutritional content (Das *et al.*, 2021a; Hossain *et al.*, 2021; Begum *et al.*, 2022b). Spoilage fungi may create mycotoxins. The rice weevil, *Sitophilus oryzae* L. (Coleoptera: Curculionidae), is considered one of the most destructive and troublesome insect pests of rice worldwide (Hossain *et al.*, 2019b). Over 70 % of stored products are treated by the fumigation of methyl bromide (MeBr) and phosphine (PH₃) as SIROFLO® and ECO2FUME®. Both fumigants have become restricted under the Clean Air Act and the Montreal Protocol because of the potential ozone-depleting properties of MeBr and the increasing resistance of insects to PH₃ as well as their genotoxic properties (Lee *et al.*, 2004a). Different types of chemical food preservatives are used to prevent the growth of pathogenic microbes in stored foods. Chemical preservatives have several disadvantages such as resistance and carcinogenicity. In light of consumers' demands, food scientists and the food industry are trying to replace synthetic chemical preservatives with natural antimicrobial agents or natural active agents that have strong antimicrobial, antifungal, antiviral and insecticidal properties (Aziz and Karboune, 2018; Begum *et al.*, 2022b).

1.3. Bacteria, fungi and insect as potent biohazards

Stored food products (cereal grains, dairy products, fruits, vegetables, etc.) are at high risk of heavy losses due to the incidence of biotic agents such as pathogenic bacteria, spoilage fungi and insect pests. The pathogenic bacteria, spoilage fungi and insect pests are not only responsible for food losses during storage, but they are also life-threatening to consumers. Foodborne illness as a disease occurs due to the consumption of contaminated foods and the contamination mostly occurred by the major pathogenic bacteria such as *E. coli* O157:H7, *S. Typhimurium*, *L.*

monocytogenes, *S. aureus*, etc. (Maherani *et al.*, 2018). *E. coli* O157:H7 is one of the most important foodborne pathogenic bacteria which can lead to hemorrhagic colitis, hemolytic anemia, thrombocytopenia, renal injury, etc. In the United States, about 73,480 illnesses occurred due to *E. coli* O157:H7 each year, among them about 2,168 hospitalizations and 61 deaths were recorded each year (Rangel *et al.*, 2005). Nontyphoidal salmonellosis (NTS) disease is associated with foodborne transmission and is one of the public health risks worldwide caused by *S. Typhimurium*. NTS may lead acute gastroenteritis, bacteremia, septicemia to consumers and resulting in hospitalization and death (Won and Lee, 2017). In the United States, it has been estimated about 1 million people infected due to NTS incidence with 400 deaths annually (Scallan *et al.*, 2011). *L. monocytogenes* causes listeriosis disease which might be severe to immunocompromised patients, children, and pregnant women (Maherani *et al.*, 2018).

Fungal growth in stored foods causes a deteriorative effect including health hazards to consumers. The most common spoilage fungi in cereal grains, dairy products, fruits and vegetables are *A. niger*, *A. flavus*, *P. chrysogenum*, *M. circinelloides*, and *Saccharomyces cerevisiae* (Fleet, 1990; Moreira *et al.*, 2001; Snyder *et al.*, 2016b; Gougouli and Koutsoumanis, 2017). These fungi and their associated mycotoxins could lead enormous contamination of food commodities during postharvest and storage time and caused significant reduction in nutritional qualities (Das *et al.*, 2021a). Mycotoxins (e.g., aflatoxin B1, methylglyoxal) are teratogenic, mutagenic, cytotoxic, carcinogenic, hepatotoxic and immune suppressive agents which are mostly secreted by *Aspergillus* sp. in stored food commodities (Chen *et al.*, 2019). Their thermostability and hyperoxidant nature can increase the oxidative impairment in stored foods and reduce the shelf life of food commodities. It has been reported that about 25-40 % stored food commodities could be lost because of the fungal growth and their mycotoxins (Chen *et al.*, 2019; Das *et al.*, 2021a). Moreover, fungal growth in stored food commodities can disqualify the foods for consumption and reduce the market values by developing visible fungal growth in foods, discoloration, unpleasant odor and changing nutritional quality (Hossain *et al.*, 2014a). Apart from direct spoilage of stored food commodities due to fungal growth, the presence of fungi in foods could cheer up the development of insect pests (Abedin *et al.*, 2012). Insect pests are one of the notorious biotic agents that are responsible for damaging cereal grains at any stage from harvesting to procurement by consumers (Lee *et al.*, 2001; Ogendo *et al.*, 2008). Insect pests along with other biotic agents are responsible for 10-40 % of post harvest grain losses worldwide (Ogendo *et al.*, 2008). Coleoptera (beetles) account for three-quarters of insect pests found in stored cereal grains, and *Sitophilus* sp. and *Tribolium* sp. are the most damaging insect pests for stored grains

(wheat, rice, barley, etc.) (Hossain *et al.*, 2014b). These notorious biotic agents could be controlled by applying natural active agents.

1.4. Active agents

Active agents can come from either natural sources or via chemical synthesis. Active agents from natural sources are called natural active agents which include plant-derived essential oils (EOs) and their pure active compounds, plant extracts (PEs) such as citrus extract (CE), fermented ingredients, enzymes, peptides, biopolymers (chitosan), bacteriophage, bacteriocins, and others (Aziz and Karboune, 2018). Among the natural active agents, plant derived EOs and CEs were selected for further study in this project because of their potential application as green additives. Metallic nanoparticles (NPs) (e.g., silver, zinc, gold, etc.) are another important active agent produced by physical, chemical, or biological methods. Among metallic NPs, silver nanoparticles (AgNPs) are getting significant attention and widely used in food and food packaging, pharmaceutical, cosmetics, and clothing industries because of their strong bioactivity (antibacterial, antifungal, antiviral, insecticidal properties) (Simbine *et al.*, 2019). Hence, the present research involves examination of the bioactivity of several different types of EOs, CEs, and metallic AgNPs.

1.4.1. Essential oils (EOs) and plant extracts (PEs)

EOs contain secondary metabolites derived from plants composed of a mixture of volatile bioactive compounds including monoterpenes, monoterpenoids, sesquiterpenes and their oxygenated derivatives (alcohols, aldehydes, esters, ethers, ketones, phenols, oxides, etc.) (Turgis *et al.*, 2012; Begum *et al.*, 2022b). The EOs possess strong bactericidal, fungicidal, insecticidal, antiviral, antioxidant properties that make them potential alternatives to synthetic antimicrobial agents for increasing the shelf life of food products as well as maintaining the food safety and quality (Aziz and Karboune, 2018). Various EOs and their chemical compounds are generally recognized as safe by the US Food and Drug Administration (FDA) and the European Union (EU) (Burt, 2004). The EOs that showed strong bioactivities include oregano, cinnamon, lemongrass, citrus, orange, clove, eucalyptus, thyme, tea tree, savory thyme, rosemary, garlic, coriander etc. (Oussalah *et al.*, 2006; Tajkarimi *et al.*, 2010; Turgis *et al.*, 2012; Begum *et al.*, 2020a; Shankar *et al.*, 2021; Begum *et al.*, 2022a). A list of EOs, their major chemical compositions, Latin name and their bioactivities is presented in Table 1.1.

Table 1.1. Some essential oils (EOs) and their major bioactive chemical components.

Name of EO	Scientific name	Major active components	Reference
Oregano	<i>Origanum compactum</i>	Carvacrol, thymol	Turgis <i>et al.</i> (2012); Mith <i>et al.</i> (2014)
Oregano	<i>Origanum heracleoticum</i>	Carvacrol	Mith <i>et al.</i> (2014)
Lemongrass	<i>Cymbopogon flexuosus</i>	Geranial, neral, geraniol	Bassolé <i>et al.</i> (2011)
Cinnamon	<i>Cinnamomum verum</i>	Cinnamaldehyde, cinnamyl acetate, β -caryophyllene	Begum <i>et al.</i> (2022a); Begum <i>et al.</i> (2022b)
Orange	<i>Citrus sinensis</i>	Limonene, myrcene	Njoroge <i>et al.</i> (2009)
Clove	<i>Eugenia caryophyllata</i>	Eugenol, eugenyl acetate, β -caryophyllene, α -humulene	Mith <i>et al.</i> (2014); Begum <i>et al.</i> (2022a)
Savory thyme	<i>Thymus satureioides</i>	Borneol, α -terpineol, camphene, α -pinene+ α -thuyene, β -caryophyllene, carvacrol, p-cymene, linalool, thymol	Oussalah <i>et al.</i> (2006)
Thyme	<i>Thymus vulgaris</i>	Thymol, carvacrol, γ -terpinene	Hossain <i>et al.</i> (2016a)
Basil	<i>Ocimum basilicum</i>	Estracgol, eugenol, linalool	Hossain <i>et al.</i> (2014a); Hossain <i>et al.</i> (2016a)

The bactericidal and fungicidal properties of EOs can vary and rely on their chemical composition, active ingredients, and concentrations (Turgis *et al.*, 2012; Aziz and Karboune, 2018). The hydrophobic nature of EOs enables them to partition the lipid enriched microbial cell membrane and mitochondria, disrupting their membrane structure and increasing permeability, thereby leading to cell death (Burt, 2004). When thymol (major chemical compounds of oregano and thyme EOs) comes in contact with Gram negative bacteria, it interacts with lipopolysaccharides (LPS) and disrupts the outer membrane of the bacteria. When thymol passes through the microbial cell membrane, it interacts with intracellular substances and makes the energy generating processes dysfunctional (Hyldgaard *et al.*, 2012b). Carvacrol is an isomer of thymol and mostly found in *T. satureioides*, *O. compactum*, *O. heracleoticum* EO (Table 1.1) as one of the major active ingredients that could increase the cell permeability of the cytoplasm by releasing LPS from their outer membrane (Hyldgaard *et al.*, 2012b; Tongnuanchan and Benjakul, 2014). Oussalah *et al.* (2006) studied the effects of Chinese cinnamon, Spanish oregano and savory thyme against *E.*

coli O157:H7 and *L. monocytogenes*, and found that they caused loss of bacterial cell membrane integrity and reduced intracellular ATP concentration, which lead to cell death. Eugenol is a major active ingredient in clove EO that interrupted the production of protease and amylase by *Bacillus cereus*, causing cell wall degradation and a high level of cell lysis (Burt, 2004). Cinnamaldehyde (belongs to aldehyde group) is mostly found in cinnamon EO, and is known to covalently cross-link with bacterial proteins and DNA through amine groups thus interfering with their function (Feron *et al.*, 1991). Cinnamaldehyde enriched EO exhibits antibacterial activity in different ways at different concentrations: at low concentrations it reduces the cytokinesis process by altering associated enzymes, at higher but sub-lethal concentrations it acts as an ATPase inhibitor, and at lethal concentrations it disrupts microbial cell membrane functioning (Hyldgaard *et al.*, 2012b).

Different types of plant extracts such as citrus, tea, grape seed, cranberry, blueberry extracts are quite commonly used in the food industry because of their mild to strong antimicrobial and antioxidant properties (Aziz and Karboune, 2018; Maherani *et al.*, 2018). Plant extracts contain flavonoids, phenolic acids, phenolic diterpenes, and volatile oils which are mainly responsible for their bioactivity and antioxidant properties (Aziz and Karboune, 2018). Among them, citrus EOs or citrus extracts (CEs) have been popular because of strong antibacterial and antifungal activities, their availability, and their aroma and abundance of bioflavonoids (flavanones, flavones and their derivatives) (Maherani *et al.*, 2018). Biosecur F440D and FOODGARD F410B-K are two non-toxic commercial citrus extracts extracted from the flavedo and albedo layers of different citrus fruits; both are generally recognized as safe (GRAS) by FDA and approved by Health Canada as food ingredients (Maherani *et al.*, 2018; Begum *et al.*, 2022b). CEs havshowed strong antibacterial and antifungal properties against major food-borne pathogenic bacteria (*E. coli* O157:H7 and *S. Typhimurium*) and food spoilage fungi (*A. niger*, *P. chrysogenum* and *M. circinelloides*) (Begum *et al.*, 2022b). Antibacterial and antifungal properties of CEs depend on their concentration : at low concentration they interact with microbial enzymes and reduce energy production, whereas at high concentration they cause denaturization of microbial proteins (Maherani *et al.*, 2018).

Plant derived EOs can exhibit insecticidal properties depending on the nature of their chemical components and can act as fumigants, contact poisons, stomach poisons, or systemics (Upadhyay, 2016). The volatile chemical components present in EOs may attack the insect's nervous system via the respiratory system, resulting in abnormal hormonal signals, body temperature, behavior coordination, and response to external cues such as smell, hearing, and light (Salgado, 2013; Chand *et al.*, 2017). Two common modes of action of EOs are (i) acetylcholinesterase inhibition and (ii) blockage of octopaminergic site. Briefly, acetylcholine (ACh) is a major neurotransmitter in insects that transmits nerve impulses after denaturation by

acetylcholinesterase enzyme (AChE). Monoterpenoids (e.g., linalool, camphor, 1,8-cineole, etc.) present in EOs are AChE inhibitors which results in neuromuscular system failure and eventually death (Dambolena *et al.*, 2016; Chand *et al.*, 2017). Octopamine is another major neurotransmitter, neurohormone, and neuromodulator in the insect nervous system (Kostyukovsky *et al.*, 2002), which regulates the insect's heartbeat and hyperextension of the legs and abdomen (Chand *et al.*, 2017). Two receptors octopamine-1 and octopamine-2 united with G-protein coupled receptors for exhibiting the effect of octopamine. However, the active components from EOs could either deform the G-protein coupled receptor (e.g., carvacrol) or could block the octopamine receptor binding sites (e.g., eugenol, cinnamic alcohol, etc.) (Enan, 2001; Dambolena *et al.*, 2016; Chand *et al.*, 2017). Thus, active components present in EOs damage the nervous system of insects which may subsequently lead to death.

1.4.2. Metal nanoparticles

Metallic nanoparticles (NPs) or metallic oxides are getting more attention as antimicrobial agents over organic, inorganic acid and enzymes because of their persistence under severe environmental conditions (e.g., high temperatures). Among metallic nanoparticles, silver nanoparticles (AgNPs) have many desirable attributes for an antimicrobial agent such as high surface-to-volume ratio, stability, nano size, and are therefore finding wide application in the biomaterials industry (e.g., food and packaging, pharmaceuticals, cosmetics) (Emamifar *et al.*, 2012; Carbone *et al.*, 2016; Simbine *et al.*, 2019). As with EOs, AgNPs are generally recognized as safe by the FDA (Emamifar *et al.*, 2012). AgNPs show strong antibacterial, antifungal and insecticidal properties against a wide range of foodborne illness pathogenic bacteria, fungi, and insect pests at low concentrations, and the treated biological entities have a low probability of becoming resistant due to the multifaceted mode of action of AgNPs (Ghosh *et al.*, 2013a; Begum *et al.*, 2022a). AgNPs can easily penetrate the biofilm of bacteria and fungi and followed by ionization into the chemically active forms. The size, shape and surface chemistry of AgNPs play an important role in their antimicrobial and antifungal properties. The small-sized particles and plate- or spherical-like morphologies, and high surface to volume of AgNPs facilitate strong interaction with microbial cells and thus release high concentration of Ag⁺ ions. In the presence of oxygen, AgNPs convert to Ag⁺ ions (initiate dissolution steps) which are electrostatically attracted by negatively charged microbial cells. The AgNPs followed three mechanisms of action against microbial entities such as (1) smaller AgNPs attach to the surface of microbial cell membrane and vastly disturb cellular functions, permeability, and respiration, (2) after entering into microbial cell,

AgNPs act as a weak acid (Lewis acid) and can react with sulphur and phosphorus in DNA and proteins, and (3) in presence of O₂, the AgNPs interact with negatively charged microbial cell membranes (Morones *et al.*, 2005; Eghbalifam *et al.*, 2015; Tang and Zheng, 2018; Simbine *et al.*, 2019). In anaerobic conditions, AgNPs do not exhibit microbicidal effects even at high concentrations due to the loss of Ag⁺ release ability (Simbine *et al.*, 2019). AgNPs can deposit at outer and inner membranes of microorganisms which cause destabilization and damage the proton motive force decreasing ATP levels, thereby disrupting ribosome function and inhibiting the production of proteins and enzymes (Ghosh *et al.*, 2013a).

The insecticidal properties of the NPs rely on several factors such as surface area, particle size, morphological structure, concentration, exposure time, target species, relative humidity, etc. (Stadler *et al.*, 2012; Buteler *et al.*, 2015). The mechanism of action of AgNPs is still undetermined because it is hard to know if the toxicity shown by metal NPs by itself or by the ions generated (Benelli, 2018). After contact with or ingestion of AgNPs, insects show reduced acetylcholinesterase enzyme (AChE), and may interact with sulphur (protein) and phosphorus (DNA) compounds causing denaturation of enzymes. AgNPs also can adversely affect antioxidant and detoxifying enzymes, and create oxidative stress and thus lead to cell death. AgNPs may also reduce the activity of Cu-dependent enzymes (Bianchini and Wood, 2003; Benelli, 2018). When AgNPs generate Ag⁺, they may act via a Trojan Horse mechanism where Ag⁺ passes through the cellular barrier and produces toxic ions that destroy the cellular machinery (Foldbjerg *et al.*, 2015; Durán *et al.*, 2017).

1.4.3. Application of active compounds in foods and their limitations

Active compounds (EOs, CEs and AgNPs) are used in stored foods for extending their shelf-life due to their strong bioactivity (antibacterial, antifungal, antiviral, insecticidal properties). Minimally processed or processed foods, raw meats and meat products, dairy products (milk, yogurt, cheese), cereal grains (rice, wheat, flour), fruits and vegetables are the most vulnerable foods to microbial contamination and insect infestation (especially cereal grains) during storage. A list of the applications of EOs, CEs, AgNPs in stored foods for controlling the growth of spoilage fungi, food borne illness pathogenic bacteria, and insect pests is shown in Table 1.2.

Table 1.2. Examples of the antibacterial, antifungal, and insecticidal properties of EOs and CEs.

Food category	Food	EOs or CEs	Biological entities (bacteria, fungi or insect)	Concentration	Microbial load reduction or % mortality of insects	References
Cereal grains	Rice	Basil EO (<i>Ocimum basilicum</i>)	(1) <i>A. niger</i> (2) <i>P. chrysogenum</i>	1-2 %	<i>A. niger</i> : 1.18 log reduction (at day 14) <i>P. chrysogenum</i> : 1.12 log reduction at day 14	Hossain et al. (2014a)
	Rice	Active formulation 1: Organic CE + Mediterranean EO + citrus EO + cinnamon EO Active formulation 2: Natural CE + Asian EO + Southern EO + cinnamon EO + savory thyme EO	(1) <i>E. coli</i> O157:H7 (2) <i>S. Typhimurium</i> (3) <i>A. niger</i> (4) <i>P. chrysogenum</i> (5) <i>M. circinelloides</i>	30 µL	Bacteria: 40-60 % reduced at day 28 Fungi: 43-60 % reduced at day 28	Begum et al. (2022b)
	Rice	Basil EO (<i>Ocimum basilicum</i>)	Rice weevil (<i>S. oryzae</i>)	0.6 µL/mL	100 % insect mortality after 5 days	Hossain et al. (2014b)
	Rice	Basil EO	Rice weevil (<i>S. oryzae</i>)	10 % (3 mL)	98.3 % insect mortality after 6 days	Follett et al. (2013)
	Rice seed	<i>Cymbopogon citratus</i> , <i>Ocimum gratissimum</i> and <i>Thymus vulgaris</i>	(1) <i>Alternaria padwickii</i> (2) <i>Bipolaris oryzae</i> (3) <i>Fusarium moniliforme</i>	100 µL/g	Controlled 48 to 100 % infectious pathogens	Nguefack et al. (2008)
	Rice	Active combination 1: cinnamon EO + AgNPs	(1) <i>E. coli</i> O157:H7 (2) <i>S. Typhimurium</i> (3) <i>A. niger</i> (4) <i>P. chrysogenum</i>	50 µL	Bacteria: 40-88 % reduced at day 28 in rice Fungi: 55.2-88 % reduced at day 28 in rice	Begum et al. (2022a)

		Active combination 2: Mediterranean EO + citrus EO + AgNPs Active combination 3: cinnamon EO + Asian EO + lavang EO + AgNPs	(5) <i>M. circinelloides</i>			
	Rice seed	AgNPs	<i>Gibberella fujikuroi</i>	150µg/mL	96.2 % reduction occurred after 6 h of exposure	Jo et al. (2015)
Dairy products	Yogurt	Anise EO	Total viable bacterial, yeasts and molds count	0.1-1 g/L	Reduced bacteria and yeasts and molds count from 6.8 to 2.8 and from 6.7 to 2.7 log CFU/g at day 20	Singh et al. (2011)
	Yogurt	Lemongrass EO Cinnamon EO	(1) <i>Debaryomyces hansenii</i> (2) <i>Candida pararugosa</i> (3) <i>Yarrowia deformans</i>	1.25 µL/mL EO	Reduced a complete reduction of spoilage fungal growth (<1 CFU/g)	Milanović et al. (2021)
	Yogurt+ cucumber salad	Mint EO	<i>S. enteritidis</i>	0.5-2 %	Complete inhibition of the bacterial growth after 1 week	Tassou et al. (1995)
Fruits and vegetables	Strawberry filling (SF)	Citrus extract (FOODGARD F410B)	(1) <i>E. coli</i> O157:H7 (2) <i>S. Typhimurium</i> (3) <i>Staphylococcus aureus</i> (4) <i>Bacillus cereus</i> (5) <i>L. monocytogenes</i> (6) Total aerobic microflora (TAM) (7) Total yeasts/molds	0.2 %	A total inhibition of TAM and 90 % inhibition of total yeasts and molds, <i>E. coli</i> O157:H7 and <i>S. Typhimurium</i> were observed in SF	Maherani et al. (2018)

	Strawberry	Lemongrass EO, litsea EO, lavender EO, peppermint EO, mint EO, petitgrain EO, sage EO, and thyme EO	<i>Botrytis cinerea</i>	250 µL	Complete inhibition of the fungi by 7 days	Tančinová <i>et al.</i> (2022)
	Strawberry anthracnose	(1) Thymus daenensis+AgNPs (2) Anethum graveolens	<i>Colletotrichum nymphaeae</i>	0-625 ppm	80 % mycelium growth inhibition	Weisany <i>et al.</i> (2019)

Despite strong bioactivity, the direct application of EOs and CEs in foods as preservatives is still limited owing to their generally highly volatile nature, strong smell, instability to light and temperature, poor water solubility, and oxygen sensitivity (Mahmud *et al.*, 2022). Traditionally, antimicrobial agents are directly incorporated into the food formulations by dipping, spraying, or brushing, which may change the taste of the food (Uz and Altinkaya, 2011). Also, the antimicrobial activity may be rapidly lost due to inactivation by food components or dilution below active concentration. These limitations can be minimized by introducing nanotechnology and the possible strategies for incorporation in bioactive packaging are discussed in the following section.

1.5. Possible strategies to alleviate the limitations

The difficulties with direct application of EOs or CEs in food preservation can be overcome by encapsulating them in a suitable delivery system that improves the stability, increases the bioactivities, and minimizes off flavors in the food (Donsi and Ferrari, 2016). Developing emulsion-based film packaging or dispenser systems using food grade ingredients could be an efficient and environmentally friendly alternative to the direct application of EOs/CEs (Donsi *et al.*, 2011; Prakash *et al.*, 2018). The droplet size of emulsions can be reduced (i.e., 10-100 nm) by applying nanotechnology (e.g., high pressure microfluidization) which would have more stability to light and heat, stronger antimicrobial activity, masking of the strong smell of EOs because of their nanometric size, and uniform distribution (Ghosh *et al.*, 2013b; Prakash *et al.*, 2018). Oil-in-water (O/W) nanoemulsions consist of oil droplets (ranging from 20 to 200 nm), surfactants or emulsifiers (polysorbates, sugar esters, lecithin) or biopolymers (natural gums, proteins, modified starches). Surfactants are used not only as emulsifying agents, but also to impart several desirable features, such as specific interfacial behavior (electrostatic forces, steric repulsion, and rheology), loading capability, and resistance to environmental stresses (Chen *et al.*, 2006; Donsi and Ferrari, 2016).

According to Donsi and Ferrari (2016) the nanoemulsions of EOs have unique properties:

- (1) The nanoemulsions do not scatter light strongly because their droplet diameters are much smaller than the wavelength of light, and thus they form transparent or only slightly turbid systems.
- (2) Due to the droplet size decreased, the biological activities of the encapsulated nanoemulsion increase because small active molecules can move easily through microbial cell membranes. Also the smaller droplet size increase the surface-to-volume ratio and thus facilitates biological activity and bioavailability.

(3) Nanoemulsions are thermodynamically more stable than other emulsions because of their physical meta-stability induced by Brownian motion effects which overtake gravitational forces. Nanoemulsions also show reduced aggregation because the strength of the net attractive forces acting between droplets usually decreases droplet diameter.

Nanoemulsions are usually fabricated either using high-energy or low-energy emulsification methods. Microfluidizer or high-pressure valve homogenizers, ultra sonication, and colloid milling are commonly used high-energy methods to fabricate nanoemulsions (Llinares *et al.*, 2018; Prakash *et al.*, 2018). High-energy emulsification methods have several advantages over low-energy emulsification methods including the production of ultrafine nanoemulsions with uniform droplet size distribution. The microfluidization method for fabricating nanoemulsions is the most convenient method for scale-up from small lab scale to large industrial scale up production. With a microfluidizer, nanoemulsions are generated through shear, turbulence, and cavitation when the coarse emulsion of EOs is passed through the interaction chamber (Jafari *et al.*, 2008). The microfluidization pressure and number of cycles will greatly influence the droplet size distribution (Hossain *et al.*, 2018). During fabrication of oil-in-water (o/w) nanoemulsions, the challenge is to prevent destabilization of the nanoemulsion due to Ostwald ripening (or Lifshitz-Slyozov-Wagner theory). The Ostwald ripening destabilization mechanism is the result of diffusion of the dispersed-phase molecules leading to increased droplet size (Nazarzadeh *et al.*, 2013). By selecting an appropriate surfactant or emulsifier, the droplet stability can be increased (Llinares *et al.*, 2018). Tween 80 is a nonionic emulsifier having strong interaction with EOs by adsorbing quickly at the oil/water interface, thus forming small particles with better stability in the dispersion system (Hossain *et al.*, 2018). Characterization of the nanoemulsion using dynamic light scattering measurements (zeta (ζ)-potential, poly dispersity index (PDI), and particle size) is an important step to understanding the stability of the fabricated nanoemulsions. For example, a higher ζ -potential value of the nanoemulsion makes it more electrostatically stable (Asmawati *et al.*, 2014; Cheng *et al.*, 2016; Hossain *et al.*, 2018). Electrostatically stable nanoemulsions have either higher ζ -potential value (+30 mV) or lower ζ -potential value (-30 mV) (Asmawati *et al.*, 2014). The droplets in dispersed systems with small size, lower PDI values, and higher ζ -potential are showing less aggregation, creaming, and coalescence (Asmawati *et al.*, 2014; Hossain *et al.*, 2018; Llinares *et al.*, 2018; Ben-Fadhel *et al.*, 2022). Despite the advantages of nanoemulsions over coarse emulsions, long-term stability remains a major constraint (Prakash *et al.*, 2018). Several physicochemical mechanisms such as Ostwald ripening, coalescence, gravitational separation, and flocculation are associated with nanoemulsion destabilization process and are driven by several forces such as attractive or repulsive forces between droplets, flow forces, and molecular

forces (Karthik *et al.*, 2017; Prakash *et al.*, 2018). Immobilization or incorporation of nanoemulsions or antimicrobial agents (volatiles/non-volatiles) into different polymeric matrices to develop active packaging could be a holistic approach to overcome limitations of the application of EOs in nanoemulsions for food preservation.

1.6. Active packaging

Active packaging (AP) is a term that can be used to describe many different functions such as antimicrobial systems protection, passive or active gas exchange control, ethylene emission, and moisture control. We focused on antimicrobial AP for food safety and quality (Han *et al.*, 2018; Mahmud *et al.*, 2022). APs can be designed with different active ingredients (antimicrobials, antioxidants, vitamins, nanoparticles, plant extracts, etc.) and upon applying on food products they increase the shelf-life and maintain food safety and quality by releasing or diffusing the active compounds to the surface of the food matrix (Kuorwel *et al.*, 2015; Mahmud *et al.*, 2022). APs can be fabricated using petroleum-based polymers and/or natural biodegradable polymers. Petroleum-based polyethylene (PE), polyethylene terephthalate (PET), polypropylene (PP), polyvinylchloride (PVC) and polyamide (PA) are commonly used in the packaging industry. Globally, plastic production exceeds 320 million tons annually (Mujtaba *et al.*, 2022). These plastics are non-biodegradable, non-renewable, and may emit greenhouse gases such as methane and carbon dioxide (CO₂) that are associated with both health and environmental risks. Plastics are ubiquitous and threaten the marine environment as well. It was estimated in 2014 that there was 5.25 trillion plastics floating in the sea and plastics account for 60-95 % of marine litter (Xanthos and Walker, 2017). In Canada, the manufacture and importation of plastic bags will be banned in 2023, their sale must end by 2024, and their export must end by 2026 (PBS News Hour, 2022). Switching from petroleum-based non-degradable plastics to biopolymers from natural sources is an environmentally friendly solution (Mujtaba *et al.*, 2022).

Biopolymer-based packaging is non-toxic, biodegradable, and biocompatible (Reichert *et al.*, 2020). Biopolymer packaging based on natural materials must have good physical and chemical properties and be ecofriendly, readily biodegradable, have non-toxic degradation by-products and be low-cost. Biodegradable biopolymers can be categorized into two main classes called (Class 1) renewable resources and (Class 2) non-renewable resources. Renewable resources biopolymers (Class 1) could be sub-categorized into (i) agro-biopolymers, (ii) biomonomer chemical synthesis and (iii) microbial biopolymers. Agro-biopolymers are composed of lipids (e.g., resins, wax, fatty acids, acylglycerol, vegetable oil), polysaccharides (e.g., alginate, carrageenan,

cellulose, chitosan, pectin, starch) and protein-based (e.g., plant and animal based) polymers. Polylactic acid (PLA) belongs to the sub-categorized biomonomer chemical synthesis. Gellan, pullulan, polyhydroxyalkanoates, polyhydroxybutyrate, xanthan, poly (hydroxybutyrate co-hydroxyvalerate) belongs to the microbial biopolymers sub-category (Mujtaba *et al.*, 2022). Polycaprolactones, polyesteramides, polyglycolide, polybutylene succinate adipate, polybutylene adipate terephthalate all belong to the Class 2 (non-renewable resources). Non-renewable resource biopolymers are widely used in many fields, because of their better properties compared to renewable resource biopolymers. The most common renewable biodegradable active packaging materials are chitosan, starch, PLA, poly (butylene adipate terephthalate) (PBAT), corn zein, methyl cellulose, and polyvinyl alcohol. The use of biopolymers as film forming materials depends on several features including cost, availability, functional attributes, mechanical properties (strength and flexibility), optical quality (gloss and opacity), barrier requisites (water vapor, O₂ and CO₂ permeability), structural resistance to water, and sensorial acceptance. These characteristics are greatly influenced by parameters such as the type of material used as structural matrix (conformation, molecular mass, charge distribution), film manufacturing conditions (solvent, pH, concentration, temperature, etc.), and the type and concentration of additives (plasticizers, cross-linking agents, antimicrobials, antioxidants, etc.) (Vieira *et al.*, 2011). Below, chitosan, PLA, and PBAT-based biodegradable polymers will be discussed further.

1.6.1. Chitosan (CH)

Chitosan (CH) is an excellent biopolymer due to its film-forming ability, biodegradability, non-toxicity, antimicrobial and antioxidant properties, and biocompatibility (Khan *et al.*, 2012; Hossain *et al.*, 2019a; Oladzadabbasabadi *et al.*, 2022). Deacetylation of chitin at varying degrees is a simple way to produce chitosan. CH is an economic polymer because of the available sources of chitin in the nature such as from arthropods, crustaceans, various microorganisms, and mollusks (Garavand *et al.*, 2022; Mujtaba *et al.*, 2022). In 1811, chitin was isolated by a French Professor Henri Braconnot from an alkaline treated insoluble part of mushroom and named it “fungine”. In 1823, Antoine Odier extracted insect cuticles from the alkaline treated insects and named it “chitine”. Chitine is originated from Greek word “Khiton” meaning envelope. In 1894, Hoppe-Seyler used the term “chitosan” for the first time when he used crab, spider and scorpion shells and dissolved them in potassium hydroxide solution at 180 °C, then treated the extract with dilute acid solution (Crini, 2019; Mujtaba *et al.*, 2022). CH is chemically composed of two subunits of D-glucosamine and N-acetyl-D-glucosamine which are linearly connected with each other by 1,4-

glycosidic bonds (Khan *et al.*, 2012). The solubility, viscosity, and biodegradability of CH depend on the degree of deacetylation. The CH polymer itself offers antimicrobial properties against foodborne pathogenic bacteria and spoilage fungi because of its cationic nature (Ahmed *et al.*, 2014). CH is widely used in food industries as a packaging material alone or after incorporating essential oils (EOs), metal nanoparticles, or plant extracts to enhance its antibacterial, antifungal, insecticidal properties. A list of the application of CH as active packaging material in food preservation is shown in Table 1.3.

Table 1.3. Applications of chitosan (CH) as active packaging to control the growth of pathogenic bacteria, spoilage fungi and insect pests or food preservations.

Active CH-based film	Food	Biological targets	References
CH+oregano+thyme EO+cellulose nanocrystals (CNCs)	Rice	Spoilage fungi: <i>A. niger</i> , <i>A. flavus</i> , <i>A. parasiticus</i> , <i>P. chrusogenum</i>	Hossain <i>et al.</i> (2019a)
CH+ <i>Anethum graveolens</i> EO	Rice	<i>Aspergillus flavus</i> (aflatoxin producing fungi), <i>A. niger</i> , <i>A. candidus</i> , <i>A. sydowii</i> , <i>A. fumigatus</i> , <i>A. repens</i> , <i>A. luchuensis</i> , <i>F. poae</i> , <i>F. oxysporum</i> , <i>Cladosporium herbarum</i> , <i>Curvularia lunata</i> , <i>Alternaria alternata</i> , <i>A. humicola</i> , and <i>Mycelia sterilia</i>	Das <i>et al.</i> (2021b)
CH+ <i>Pimpinella anisum</i> EO	Rice	<i>Aspergillus flavus</i> , <i>A. sydowii</i> , <i>A. repens</i> , <i>A. fumigatus</i> , <i>A. niger</i> , <i>A. candidus</i> , <i>A. luchuensis</i> , <i>F. oxysporum</i> , <i>Cladosporium herbarum</i> , <i>F. poae</i> , <i>Mycelia sterilia</i> , <i>Curvularia lunata</i> and <i>Alternaria alternata</i> and <i>A. humicola</i>	Das <i>et al.</i> (2021a)
Modified CH+lemon EO	Leaf vegetable (Rucola)	Total microbial flora, yeast and molds of rucola leaf	Sessa <i>et al.</i> (2015)
CH+ <i>Zataria Multiflora</i> EO	Turkey meat	<i>Salmonella enteritidis</i> , <i>Listeria monocytogenes</i> , total viable bacteria, total psychrophilic, <i>Pseudomonas</i> spp., Enterobacteriaceae, lactic acid bacteria and total yeast and mold count	Keykhosravy <i>et al.</i> (2020)
CH+mandarin EO nanoemulsion+ γ -irradiation	Green beans	<i>Listeria innocua</i>	Severino <i>et al.</i> (2014)
CH+ <i>Zingiber zerumbet</i> EO nanoemulsion	<i>Salvia hispanica</i> seeds	<i>Aspergillus flavus</i>	Deepika <i>et al.</i> (2021)
CH+ <i>Cananga odorata</i> EO	Ground nuts	Aflatoxin producing fungi <i>Aspergillus flavus</i>	Upadhyay <i>et al.</i> (2021)

CH+oregano+thyme EO+CNCs	Rice	Rice weevil: <i>Sitophilus oryzae</i>	Hossain <i>et al.</i> (2019b)
CH+gelatin+AgNPs	Red grapes	Shelf-life extension study	Kumar <i>et al.</i> (2018)
CH+EO+AgNPs	Strawberries	<i>Escherichia coli</i> , <i>Listeria monocytogenes</i> , <i>Salmonella Typhimurium</i> , and <i>Aspergillus niger</i>	Shankar <i>et al.</i> (2021)
CH+gelatin+clove EO	Fish	<i>Pseudomonas fluorescens</i> , <i>Shewanella putrefaciens</i> , <i>Photobacterium phosphoreum</i> , <i>Listeria innocua</i> , <i>Escherichia coli</i> and <i>Lactobacillus acidophilus</i>	Gómez-Estaca <i>et al.</i> (2010)
Sodium alginate+chitosan+carrageenan + <i>Cinnamomum cassia</i> EO	Strawberry	<i>Colletotrichum acutatum</i>	Dong <i>et al.</i> (2020)

Several studies have shown that the incorporation of nanoemulsions of EOs into polymeric matrices increases bioactivity as compared to the incorporation of oil-in-water coarse emulsions (Donsi *et al.*, 2011; Nazzaro *et al.*, 2013; Hossain *et al.*, 2019a). Because of the smaller droplet size of the nanoemulsions, they can pass easily via porin protein channels of the outer membrane of the Gram-negative bacteria to transfer the active ingredients to the cytoplasmic membrane, thereby disrupting membrane function and causing microbial cell death (Donsi *et al.*, 2011; Nazzaro *et al.*, 2013). Hossain *et al.* (2019a) studied the bioactivity of nanoemulsions and coarse emulsions of the three active formulations of oregano+thyme EO, thyme+tea tree EO, and thyme+peppermint EO against *A. niger*, the fungicidal activity of the nanoemulsion was 83.7, 75.6, and 87.9 %, respectively, which was significantly higher than for the coarse emulsion at 39.7, 36.7, and 43 %. Similarly, Zhang *et al.* (2014) found that the nanoemulsion of D-limonene with Tween 80 emulsifier (mean droplet size: 16 nm) showed stronger antibacterial and antifungal activity against *Staphylococcus aureus*, *Bacillus subtilis*, *E. coli*, and *Saccharomyces cerevisiae* than the free oil. The cationic nature of the chitosan polymer (i.e., contains a large number of NH₂, NH, -OH, C=O, -O- groups) makes it biocompatible with other polymers or active ingredients to improve their packaging qualities and bioactivity (Mujtaba *et al.*, 2019). Chitosan has some inherent disadvantages such as poor mechanical and thermal strength, and low hydrophobicity (Wang *et al.*, 2018). These drawbacks are an impediment to the use of chitosan as a packaging material on an industrial scale. Reinforcing agents such as cellulose nanocrystals (CNCs), nanoparticles or combining crosslinking with other polymers (genipin, gelatin) could mitigate these drawbacks which will be discussed in the following sections.

1.6.2. Polylactic acid (PLA)

Poly(lactic acid) (PLA) is a commercially available biopolymer that comprises 10.3 % of the global bioplastics market (Su *et al.*, 2020). PLA is one of the most researched polyesters worldwide, with applications in diverse domains such as medicine and food packaging because of its biodegradability, biocompatibility, recyclability, renewability, and compostability (Salmieri *et al.*, 2014a; Farah *et al.*, 2016). The processibility of PLA is more convenient due to its thermoplastic nature and PLA can be easily processed into films, fibers, molded shapes. PLA was synthesized in 1932 by Carothers heating lactic acid under vacuum and removing the condensed water (Avinc and Khoddami, 2009). PLA can be produced from vegetables, corn, and rice through fermentation. The industrial scale production of PLA mostly occurs through ring-opening polymerization (Fournier *et al.*, 2022). PLA requires less energy (25 to 55 % less) for making films or fibres as

compared to poly hydroxyalkanoates (PHA), polyethylene glycol (PEG), and poly (caprolactone) (PCL), which reduce costs ([Rajeshkumar et al., 2021](#)).

PLA is increasingly used as a food packaging polymer for short shelf-life products, with common applications such as containers, drinking and salad cups, overwrap and lamination films, and blister packages. For food packaging PLA is ideal because of its ease of production, transparency, and good chemical resistance against fats and oils ([Lim et al., 2022](#)). In addition, PLA is “Generally Recognized As Safe” (GRAS) for use in foods. Indeed, PLA is widely used in the packaging of orange juice, yogurt, and dressings. Several authors developed active PLA-based packaging films to enhance preservation by incorporating plant-derived EOs, plant extracts, and metal nanoparticles ([Fortunati et al., 2012b](#); [Arrieta et al., 2014](#); [Salmieri et al., 2014b, a](#); [Rezaeigolestani et al., 2017](#)). A list of the application of PLA as active packaging material in food preservation is shown in Table 1.4.

PLA has some limitations as a packaging material such as low gas and water permeability, and distortion at high temperature ([Bordes et al., 2009](#)). Nano-scale reinforcement into the polymeric matrix can enhance the mechanical and physiological properties of the polymers and improve their functionality, processability and end-use performance ([Krishnamachari et al., 2009](#); [Fortunati et al., 2012a](#); [Hughes et al., 2012](#); [Rhim, 2013](#)). Application of organic, inorganic, nanohybrids into the polymeric matrix can overcome the limitations of PLA-based packaging materials ([Fortunati et al., 2014](#); [Salmieri et al., 2014a](#)). Several studies showed that the incorporation of CNC into the polymeric matrix as a reinforcing agent could significantly slow the controlled release of active ingredients during the storage and thus, could control microbial growth in food for an extended period of time ([Boumail et al., 2013](#); [Salmieri et al., 2014b](#); [Deng et al., 2017](#); [Hossain et al., 2018](#); [Hossain et al., 2019a](#)).

Table 1.4. Applications of PLA as active packaging to control the growth of pathogenic bacteria, spoilage fungi and insect pests for food preservation.

Active PLA-based film	Food	Biological targets	References
PLA+CNC+nisin	Sliced cook ham	<i>Listeria monocytogenes</i>	Salmieri <i>et al.</i> (2014a)
PLA+CNC+oregano EO	Mixed vegetables	<i>Listeria monocytogenes</i>	Salmieri <i>et al.</i> (2014b)
PLA+cellulose nanofiber (CNF)+ <i>Zataria multiflora</i> EO+propolis ethanolic extract (PEE)	Vacuum packaged cooked sausages	<i>Listeria monocytogenes</i> , <i>Staphylococcus aureus</i> , <i>Escherichia coli</i> O157:H7, <i>Vibrio parahaemolyticus</i>	Rezaeigolestani <i>et al.</i> (2017)
PLA+PBAT+cinnamom EO	Strawberries	Shelf-life extension	de Souza <i>et al.</i> (2022)
PLA+PBAT+trans-cinnamaldehyde	Bread	<i>Penicillium</i> sp., <i>Aspergillus niger</i> , and <i>Rhizopus</i> sp	Srisa and Harnkarnsujarit (2020)
PLA+ZnO+ <i>Zataria multiflora</i> EO	<i>Otolithes ruber</i> fillets	Aerobic count, <i>Enterobacteriaceae</i> count, <i>Pseudomonas</i> spp., Lactic acid bacteria (LAB) count	Heydari-Majd <i>et al.</i> (2019)
PLA+ <i>Origanum vulgare</i> EO	Ready-to-eat salads	<i>Staphylococcus aureus</i> , <i>Yersinia enterocolitica</i> , <i>Listeria monocytogenes</i> , <i>Enterococcus faecalis</i> , and <i>Staphylococcus carnosus</i>	Llana-Ruiz-Cabello <i>et al.</i> (2016)
PLA+propolis ethanolic extract (PE)+cellulose nanoparticle (CN)+ <i>Ziziphora clinopodioides</i> EO	Minced beef	Total mesophilic and psychrotrophic bacteria, <i>Pseudomonas</i> spp. and <i>Enterobacteriaceae</i>	Shavisi <i>et al.</i> (2017)

1.6.3. Poly (hydroxy butyrate adipate terephthalate) (PBAT)

Poly (butylene adipate-co-terephthalate) (PBAT) is a commercially available biopolymers comprising 7.2 % of global bioplastics production (Su *et al.*, 2020). PBAT is a flexible biodegradable and compostable aliphatic-aromatic copolyester certified by the Biodegradable Polymers Institute (ASTM D6400 standard specification) and European Bioplastics (EN13432 standard criteria) (Morelli *et al.*, 2016; Shankar and Rhim, 2018). Some of the biopolymers present complex issues in waste management. For biodegradable or compostable polymers-based films, sheets, bottles or injection molded products, aliphatic polyesters are an ideal structural material. However, high molecular weight aliphatic polyesters are not commercially feasible because of their high production costs and poor mechanical and physical properties (Li *et al.*, 2007). Rather than aliphatic polyesters, aromatic polyesters show excellent physical stability and are resistance to hydrolysis. Combining aromatic and aliphatic units in one polyester chain could provide biodegradable products with strong mechanical and physical stability (Li *et al.*, 2007; Fukushima *et al.*, 2012). PBAT is made of both aliphatic and aromatic units in the same polyesters chain, as PBAT thermoplastic polyester usually composed of 1,4-butanediol, adipic acid, and terephthalic acid by a polycondensation reaction (Ferreira *et al.*, 2019). Currently, linear copolyester PBAT is favored because of its biodegradability, flexibility, biocompatibility, and suitable mechanical properties [young's modulus: ~52 MPa, tensile strength: 32-36 MPa and elongation at break (Eb): 700 %] (Jiang *et al.*, 2006; Raquez *et al.*, 2008; Bordes *et al.*, 2009; Shahlari and Lee, 2012; Nagarajan *et al.*, 2013; Pinheiro *et al.*, 2017; Santana-Melo *et al.*, 2017).

Incorporation of active ingredients (EOs, CEs, AgNPs, or mixture of active EOs or CEs etc.) into PBAT polymeric matrix can form the basis of a bioactive packaging systems. A PBAT-based packaging system could release active ingredients during storage and inhibit the growth of microbial pathogens and spoilage fungi and control the growth of stored products' insect pests (Shankar and Rhim, 2016; Shankar and Rhim, 2018; Ferreira *et al.*, 2019; Felix da Silva Barbosa *et al.*, 2021; Moraes Filho *et al.*, 2022). A list of the application of PBAT as active packaging material in food preservation is shown in Table 1.5.

Table 1.5. Applications of PBAT as active packaging to control the growth of pathogenic bacteria, spoilage fungi and insect pests for food preservations.

Active PBAT-based film	Food	Biological targets	References
PBAT+ <i>Origanum vulgare</i> EO	Fish fillet	Total coliforms, <i>Staphylococcus aureus</i> and psychrotrophic microorganisms	Cardoso et al. (2017)
PBAT+PLA+cinnamon EO	Strawberry	Shelf-life extension	de Souza et al. (2022)
PBAT+poly butylene succinate (PBS)+ β -cyclodextrin (β CD)+sweet basil EO	Tomato	Total mold counts	Threepopnatkul et al. (2022)
PBAT+PLA+cinnamon EO	Strawberries	Shelf-life extension	de Souza et al. (2022)
PBAT+PLA+trans-cinnamaldehyde	Bread	<i>Penicillium</i> sp., <i>Aspergillus niger</i> , and <i>Rhizopus</i> sp	Srisa and Harnkarnsujarit (2020)
PBAT+wheat flour+oregano EO	Brazilian fresh pastry	Total molds and yeasts ocunt	Balan et al. (2021)
PBAT+PLA+starch+cinnamaldehyde	Soy protein-based meat analogue	<i>E. coli</i> and <i>Staphylococcus aureus</i>	Wang et al. (2022)
PBAT+cellulose nanofiber (CNF)+cinnamon EO	Strawberry	<i>Escherichia coli</i> , <i>Salmonella Choleraesuis</i> , <i>Staphylococcus aureus</i> , <i>Listeria monocytogenes</i>	Montero et al. (2021a)

Despite advantages, the use of biopolymers as food packaging on an industrial scale is limited because of their high molecular weight, hydrophilicity, low mechanical and barrier properties, and brittleness. All these drawbacks need to be improved to make biopolymers utilizable in the food industry (Mujtaba *et al.*, 2019). Reinforcing agents such as cellulose nanocrystals (CNCs) are useful polymers that could overcome the limitations of biopolymers. Several authors have shown that nanofiller CNCs can significantly enhance the mechanical and barrier properties and help in the controlled release of bioactive ingredients (Khan *et al.*, 2012; Salmieri *et al.*, 2014b, a; Hossain *et al.*, 2019a; Hossain *et al.*, 2019b; Mahmud *et al.*, 2022).

1.7. Cellulose nanocrystals (CNCs) as a reinforcing agent

Cellulose nanocrystals (CNCs) act as reinforcing agents in biopolymeric matrices and enhance the mechanical, thermal, and barrier properties of biopolymer matrices and improve the release of active ingredients from the active packaging polymer. CNCs are high-performing reinforcing agents in advanced materials because they are sustainable, abundant, have a large surface area to volume ratio, are light, and have high mechanical strength (Khan *et al.*, 2012; Kusmono *et al.*, 2021; Mahmud *et al.*, 2022). Cellulose is one of the most abundant biopolymers in the world and can be extracted from various plant materials including wood, hemp, and cotton (Khan *et al.*, 2012). CNC is a stable aqueous colloidal suspension with rod-like nanosized particles having 110 nm length and 5-10 nm diameter (Revol *et al.*, 1992). The hydrolysis of a cellulosic source occurs with sulfuric acid which produces a stable dispersion compared to the hydrolysis with hydrochloric acid because sulfate groups in the suspension create electrostatic repulsion and thus, forms strong stable suspension of CNC (Beck-Candanedo *et al.*, 2005). Incorporation of CNC as a reinforcing agent into biopolymeric matrices provides superior performance (mechanical properties, barrier properties, thermal properties) by forming a percolation network where CNCs H-bond to the polymeric matrices (Azeredo *et al.*, 2010; Khan *et al.*, 2012).

Reinforcing CNCs or other nano-sized materials could significantly affect the mechanical properties-tensile strength [TS], tensile modulus [TM] and elongation at break [Eb]-of the biopolymeric films by filling the free space between polymeric chains which increases molecular forces thus producing a denser biopolymeric film with reduced permeability (Jamróz *et al.*, 2019). Compared to microfibrillated cellulose (MFC), microcrystalline cellulose (MCC) or nanofibrillated cellulose (NFC), CNCs have a larger aspect ratio (length-to-width ratio) (Criado *et al.*, 2018). Due to the considerable amount of -OH groups present and its crystallinity, CNC facilitates any desired

modification such as chemical derivatization, and swelling and water-binding properties (Khan *et al.*, 2012; Jasmani *et al.*, 2016). Incorporation of CNC into polymeric matrices improves the mechanical properties of the nanocomposite films by interfacial interactions between polymeric chains and CNCs. Several studies show that a low concentration of CNCs is sufficient to improve the mechanical properties of the nanocomposite films, which is cost efficient (Khan *et al.*, 2012; Criado *et al.*, 2018; Hossain *et al.*, 2018). Hossain *et al.* (2018) reported a 15 % increase in TM values of methylcellulose nanocomposite films when 7.5 % (w/w) CNC was incorporated. Loading of 10 % (w/w) CNC into the calcium alginate polymer increased TM values by 123 % in several nanocomposite films (Ureña-Benavides *et al.*, 2010). After incorporating CNCs into biopolymeric matrices, a common phenomenon observed is that the TS and TM values are increased while the Eb values are decreasing which might be due to the intra- and inter-molecular H-bonds, and interfacial interactions between CNCs and polymeric chains. The reduction of Eb occurs due to the rigid nature of CNCs and a reduction in the polymeric chain motions after interacting with CNCs by H-bonds and interfacial interactions (Mahmud *et al.*, 2022).

Adequate barrier properties of the packaging materials are important to resist sorption and diffusion of the gases and moisture through the packaging material because moisture and gases are responsible for product's shelf-life. Water vapor permeability (WVP) and oxygen permeability (OP) are two important governing parameters (Vilarinho *et al.*, 2018a; Mahmud *et al.*, 2022). Low WVP and OP means the packaging material has low moisture transfer between the inner and outer environment thus helping prevent microbial growth (Khan *et al.*, 2012; Jamróz *et al.*, 2019). Several studies found that presence of nanofillers such as CNCs in the biopolymeric matrices can reduce the WVP and increase the barrier properties of the biopolymeric packaging films because reinforcing CNCs can create tortuous path inside the nanocomposite polymeric matrices (Khan *et al.*, 2012; Khan *et al.*, 2013; Criado *et al.*, 2018; Hossain *et al.*, 2018; Hossain *et al.*, 2019a). Also, a percolated network might be created when CNCs are incorporating into polymeric matrices by H-bonding which can reduce the molecular mobility and free volume of polymeric matrices and create more obstacles for water vapor diffusion, and thus reduced WVP (Pereda *et al.*, 2012). For instance, Khan *et al.* (2012) studied chitosan-based films with reinforcing CNCs for improving the mechanical and barrier properties and found that the WVP of the CH-based nanocomposite films after incorporating 5 % CNC into the CH-polymeric matrix was decreased by 27 % compared with the control CH-based film (Khan *et al.*, 2012).

Retaining active ingredients or antimicrobial agents into the packaging system for food preservation and extended storage is an important parameter to optimize in active packaging (AP).

It has been shown that adding reinforcing CNCs into active biopolymeric matrices can greatly improve the controlled release of active ingredients or antimicrobial agents and conserve the active ingredients for an extended time during storage (Boumail *et al.*, 2013; Salmieri *et al.*, 2014b; Hossain *et al.*, 2018; Hossain *et al.*, 2019a; Patel *et al.*, 2021). CNC as a reinforcing agent slows the release of active ingredients by helping the homogenous distribution of the active ingredients within the polymeric matrices (Boumail *et al.*, 2013). The release of active ingredients or antimicrobial agents from the active nanocomposite films could be explained by several mechanisms such as (i) the interfacial interactions between the polymeric chains and reinforcing agents could reduce the mobility of the active ingredients and polymeric chains and thus, eventually lower the release of active ingredients, (ii) the core materials or active ingredients immobilized or incorporated into nanocomposite materials are able to reduce the diffusion of active ingredients when they come in contact with foods, (iii) presence of reinforcing agents or nanomaterials in the polymeric matrix can act as a cross-linker and reduce the available hydrophilic groups in the biopolymer and reducing the swelling and biodegradation of polymers and thus eventually control the release of active ingredients, (iv) reinforcing agents or nanofillers can create tortuous path across the nanocomposite films that consequently reduces the movement of active ingredients or antimicrobial agents (Almasi *et al.*, 2021). Hossain *et al.* (2019a) developed bioactive chitosan-based nanocomposite films using an oregano-thyme EO mixture and studied the effect of CNC in the controlled release of volatile components from the films during the storage of rice; the incorporation of CNC into CH+oregano/thyme EO film slowed the release of volatile components by 26 % compared to the film without CNC (CH+oregano/thyme EO film) after 12 weeks (Hossain *et al.*, 2019a). Hossain *et al.* (2018) also developed methylcellulose/CNC-based nanocomposite films containing a blend of oregano/thyme EO and observed that incorporation of CNC slowed the release by 35 % compared to methylcellulose film without CNC during 12 weeks of storage in rice (Hossain *et al.*, 2018). Addition of CNC as a reinforcing agent into the biopolymeric matrix minimizes any drawbacks associated with biopolymer as a packaging material.

1.8. Food irradiation technology

Food irradiation has about 100 years of history as an effective, safe and environmentally clean procedure to ensure the safety of food (Lacroix and Follett, 2015; Yousefi and Razdari, 2015). Three types of ionizing radiation are commonly used in food irradiation : X-ray (machine

generated), electron beams (machine generated) and γ -rays (either by Cesium 137 or Cobalt 60). Though Cobalt-60 γ -irradiation is the most used technique for food irradiation, x-ray and electron beam are getting increasing attention in the field of food irradiation (Yousefi and Razdari, 2015). Foods could be irradiated with up to 10 kGy which is accepted by the Codex Alimentarius Commission in 1983 (Commission, 2000). Irradiation does not produce radioactive products in foods and food packaging materials, and in terms of product throughput and costs, it is a commercially feasible technology (Farkas *et al.*, 2004). Irradiation is applied not only in food and food items but also in non-food related products such as medical devices, packaging materials, cosmetics, etc. for the purpose of non-thermal sterilization (Yousefi and Razdari, 2015).

The absorbed radiation energy by the product is measured in Grays (Gy), where, 1 Gy equals 1 Joule absorbed energy per kg of food product. Food irradiation is versatile, safe, secure, highly effective and efficient technique that can control foodborne pathogenic bacteria, spoilage fungi, and insect pests without affecting the nutritional value of the food product or their packaging materials (Tauxe, 2001; Farkas *et al.*, 2004; Yousefi and Razdari, 2015). Also, irradiation does not leave any chemical residues after treatment and can be used for packaged food and irradiation treatment can significantly prolong the shelf-life of fruits, vegetables, meat, sea foods, and cereal grains (Irradiation, 1991; Follett *et al.*, 2013; Hossain *et al.*, 2014b; Hossain *et al.*, 2019a; Shankar *et al.*, 2021). Irradiation causes damage to DNA in the microbial cell by breaking the chemical bonds, thereby altering membrane permeability and affecting the other cellular functions, and possibly increasing contact between the microbial cell and active formulations (Caillet *et al.*, 2005; Caillet and Lacroix, 2006; Ayari *et al.*, 2012). Moreover, low dose irradiation could slow the ripening of fruits such as mangoes, bananas, papaya, etc., inhibit the sprouting in potatoes, onions, yams, etc. (Thomas, 2001a, b). In 1997, the World Health Organization (WHO), the International Atomic Energy Agency (IAEA) and the Food and Agricultural Organization (FAO) jointly concluded that the food irradiation with appropriate dose for the intended objective was safe to consume and nutritionally unchanged (WHO, 1999). For phytosanitary irradiation, the allowable dose of fruits and vegetables irradiation is ≤ 1 kGy which may be lower than the doses for reducing certain pathogenic bacteria and spoilage fungi (López *et al.*, 2005). Sanitary irradiation for microbial control can require significantly higher doses. Although several macronutrients, carbohydrates, protein, and lipids are resistant to radiation, some vitamins are sensitive to high-dose radiation treatments (Fadhel *et al.*, 2016; Lima *et al.*, 2018).

To get rid of this problem when using irradiation alone in food products, combining two or more preservation techniques—such as irradiation and active packaging—called hurdle technology,

may lead to synergistic or additive effects and better control of pathogens and pests than either technique alone (Lacroix and Follett, 2015; Khan *et al.*, 2017a). Active packaging or EOs in accordance with irradiation affect the bacterial membrane integrity and murein composition and induce a release of the bacterial cell constituents and a decrease of the internal pH and ATP (Caillet *et al.*, 2005; Caillet and Lacroix, 2006; Oussalah *et al.*, 2006). Combined treatment of active packaging and irradiation can act synergistically and increase the radiosensitivity of the microbial cells (Ayari *et al.*, 2012; Hossain *et al.*, 2014a). Shankar *et al.* (2021) developed chitosan-based active packaging using EO/Ag nanoparticles along with 1 kGy γ -irradiation for the extension of the shelf-life of strawberries; the combination treatment of bioactive CH-based nanocomposite films and γ -irradiation extended the shelf-life of stored strawberries by 4 days. Begum *et al.* (2020a) reported that the combined application of irradiation (γ -Ray and X-ray) along with the vapor of oregano/thyme EO against the foodborne illness pathogenic bacteria *E. coli* O157:H7, *S. Typhimurium*, and *Listeria monocytogenes* in rice sample significantly increased the microbicidal effectiveness. The D_{10} values were 326, 266, and 236 Gy for the bacteria *E. coli* O157:H7, *S. Typhimurium*, and *L. monocytogenes*, respectively, when treated with high dose rate γ -irradiation alone (9.1 kGy/h), while the corresponded D_{10} values were significantly reduced ($P \leq 0.05$) to 274, 218, and 219 Gy in combined treatment between the vapor of EO and γ -irradiation (Begum *et al.*, 2020a). Other studies have also shown the advantages of combining active films with irradiation (Caillet *et al.*, 2005; Hossain *et al.*, 2014a; Lacroix and Follett, 2015; Hossain *et al.*, 2018; Hossain *et al.*, 2019a; Shankar *et al.*, 2021). Combined treatment of the active packaging along with irradiation treatment could be an efficient way to control microbial contamination in food products under certain conditions.

In this research, active packaging films incorporated with EOs or CEs or metal nanoparticles or their mixture were developed and were tested in two different types of food model to determine their efficacy as antimicrobial, antifungal and insecticidal bioactive films or patches. The two different types of food were selected on their differences in water content : yogurt (high moisture content) and rice (low moisture content).

Food model 1: Yogurt

Milk and other dairy products are consumed all over the world. Of these, yogurt is the most popular and unique, which is a fermented dairy product and generally manufactured from pasteurized milk. Yogurt (100 gm) contains protein (3.5 gm), sugar (4.7 gm), fat (3.3 gm), and water (88%). Microbial

spoilage can occur due to the microbial growth in a wide range of processed, preserved and refrigerated food products. Fungi are recognized as one of the main contaminants of dairy products that include yogurt and sour milk (Delavenne *et al.*, 2013). Although the high acidity of yogurt (pH 4.4) allows for an extended shelf life, it is still susceptible to spoilage because fungi and yeast are able to survive and grow in an acidic environment (Viljoen *et al.*, 2003). The most common spoilage species in yogurt are *Aspergillus niger* and *Penicillium* sp., *Candida parapsilosis*, *C. maltosa*, *Debaryomyces castelli*, *D. hansenii*, *Saccharomyces cerevisiae*, and *Kluyvermyces* (Fleet, 1990; Moreira *et al.*, 2001; Gougouli and Koutsoumanis, 2017). The fungal species *Mucor circinelloides* is responsible for swelling and bloating in yogurt during storage (Snyder *et al.*, 2016b). Filtenborg *et al.* (1996) indicated that the most important spoilage species of yogurt and cheese are *Penicillium commune* and *Penicillium nalgiovense*.

Yogurt is an acidic product, so most bacterial pathogens normally cannot grow but recontamination can occur. Recontamination of yogurt can occur due to poor sanitary practices, following cooling and distribution in retail containers from: environment, personnel, added materials, containers, contamination from added cultures, micro-puncture of the container, etc. Under refrigeration temperatures, a shelf life of 4 weeks can be attained, assuming all other open manufacturing conditions are in place (Fleet, 1990). This shelf life is diminished when yeasts are introduced with raw ingredients such as fruits, nuts and honey (Fleet, 1990). Yogurt is also susceptible to bacterial contamination such as *Escherichia coli* O157:H7, *Salmonella* Typhimurium, *Listeria monocytogenes*, *Staphylococcus aureus*, etc. (Siddiqui and Nadeem, 2007; Lee *et al.*, 2014). Potassium sorbate is widely used to preserve yogurt, but consumers demand natural preservatives over chemical preservatives. Bioactive films were used in the current study to prevent spoilage during storage of yogurt.

Food model 2: Rice

Rice (*Oryza sativa* L.) is one of the most important cereal grains worldwide as around 50 % of the world's population consumes rice as a primary source of calories and nutrition (carbohydrates, fats, proteins, minerals, vitamins) (Nguefack *et al.*, 2005; Das *et al.*, 2021b). Due to its high nutritional value, rice is susceptible to biodeterioration by several categories of microbes including pathogenic bacteria (*Escherichia coli*, *Salmonella* sp., *Listeria* sp.) (Begum *et al.*, 2020a), storage fungi (*Aspergillus* sp., *Penicillium* sp., *Mucor* sp., *Fusarium* sp.) and insect pests (e.g. rice weevil) (Hossain *et al.*, 2014b; Hossain *et al.*, 2019a; Begum *et al.*, 2022b). Microbial contamination of

rice grains can cause unpleasant odors, discoloration, off-flavor, and reduction of the nutritional value of stored rice due to lipid peroxidation and production of mycotoxins and methylglyoxal (Das *et al.*, 2021a). Mycotoxins secreted by *Aspergillus* sp. in stored cereal grains (e.g., Aflatoxin B1) are carcinogenic and mutagenic (Hossain *et al.*, 2019a; Das *et al.*, 2021a). Insect pests are the most serious biotic stressors of stored products. Loss of stored commodities to insects all over the world are estimated at 10-40%, often for lack of modern storage facilities and suboptimal pest management practices (Shaaya *et al.*, 1997). Rice weevil, *Sitophilus oryzae* (L.) (Coleoptera: Curculionidae) is a major pest of stored rice, wheat, oats, rye, barley and corn worldwide (Sabbour, 2012; Hossain *et al.*, 2014b).

Management of stored product pests and molds using chemical pesticides is common worldwide. According to FAO (2002), about 2.5 million tons of chemical insecticides are used around the world to eradicate pests. Fumigation is one of the most effective methods used to protect stored food, feed stuffs and other agricultural commodities from the harmful effect of insects. Over 70 % of stored products are treated by the fumigation of methyl bromide (MeBr) and phosphine (PH₃). Both fumigants are being phased out under the Clean Air Act and Montreal Protocol because of their ozone-depleting properties and the evolution of resistance (Lee *et al.*, 2004a). However, the demand of natural food additives such as essential oils is increasing because they are environmentally friendly, safe for humans, and not prone to resistance development.

1.9. The Problem, Hypotheses and Objectives

The problematic, hypotheses, and objectives were developed based on the literature review. The following issues were investigated and developed in this study.

1.9.1. Problematic

- 1) Plant derived essential oils (EOs) are volatile in nature that can make them unable to stabilize in food products and because of their strong smell may affect the organoleptic properties of the foods.
- 2) Combining two or more EOs with other antimicrobial agents such as citrus extracts or metallic nanoparticles, can act synergistically by reducing the concentration of EOs.
- 3) Developing the nanoemulsion of EOs or mixtures of antimicrobial agents can also improve their stability, reducing their size as well as increase the bioactivities.

4) EOs or mixtures of antimicrobial agents could be degraded easily by environmental factors (UV light, temperature, etc.); have encapsulation could be an effective way to protect them from degradation while increasing their antimicrobial efficiency.

5) Direct application of EOs or mixtures of antimicrobial agents may not be acceptable by consumers, but incorporation of active agents into biopolymeric matrices could be successfully used as a active packaging or films.

6) Biopolymers have some limitations as a packaging material such as lower mechanical and barrier properties, but incorporating reinforcing agents such as cellulose nanocrystals (CNCs) could improve the limitations of biopolymers.

Development of biopolymer systems with an appropriate encapsulation process would overcome these problems.

1.9.2. Hypotheses

1. Natural antimicrobials (plant derived essential oils, plant extracts) and metallic nanoparticles can work synergistically to control bacteria, fungi, and insects.

2. Reducing the size of the emulsion will improve the bioavailability of natural antimicrobials, increase their antimicrobial properties and reduce their effective concentrations.

3. Incorporation into a polymeric matrix will protect the biological activity of bioactive compounds (during processes and storage) and control their release.

4. The techniques developed (nanoemulsion-polymer) make it possible to extend the shelf life of food.

5. The combination of bioactive films and irradiation can increase the effectiveness of bioactive films against microorganisms and insects.

1.9.3. Objectives

1. Evaluate some of the most effective antibacterial and antifungal compounds.

2. Evaluate some of the most effective active compounds having insecticidal activity.

3. Formulate and optimize a formulation and the conditions of preparation of a nanoemulsion using natural active compounds and high pressure microfluidization.

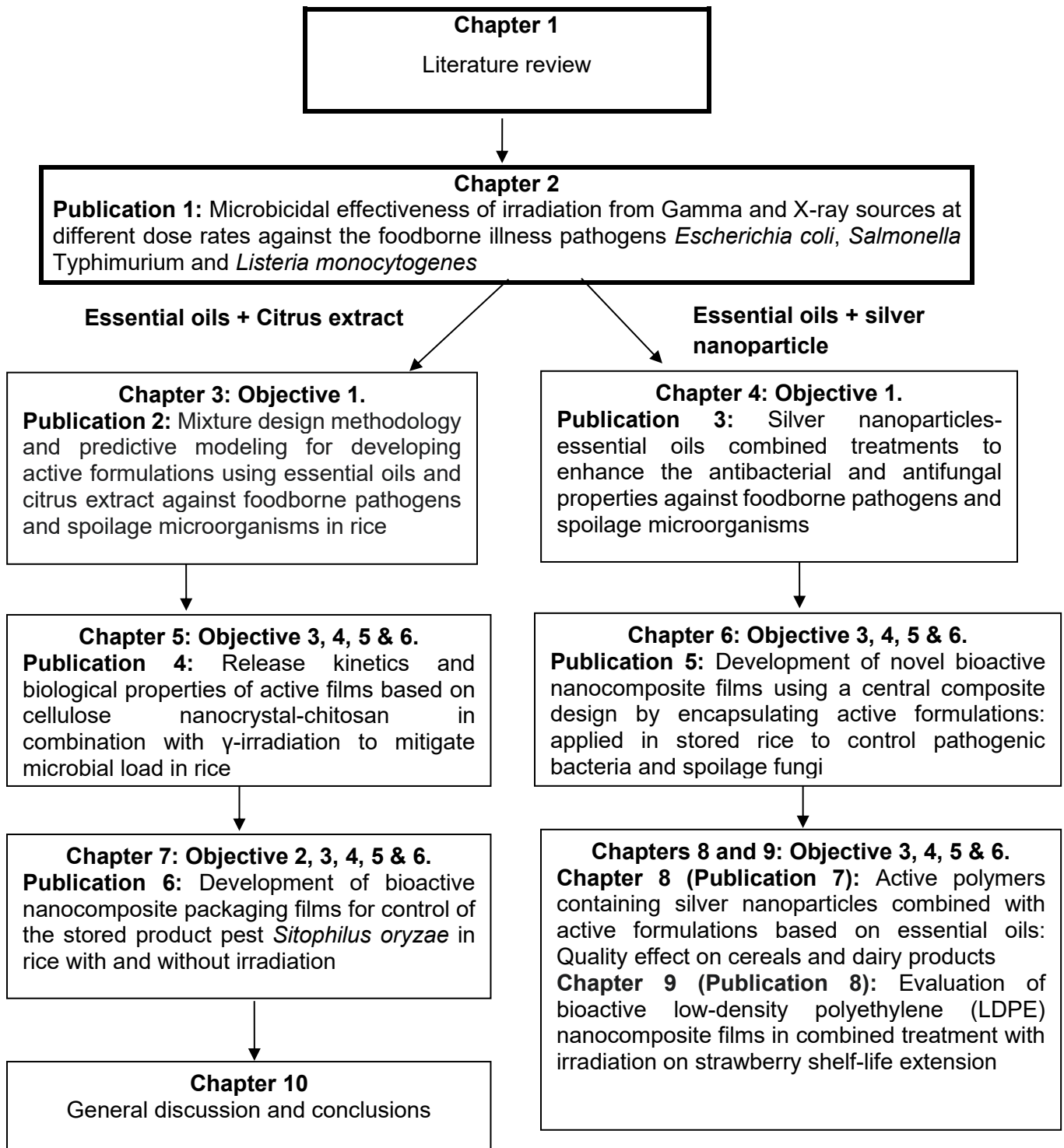
4. Develop active film packaging or patches and characterize them (water resistant, physico-chemical properties, gas permeability, antimicrobial diffusion/ volatile repellents).

5. Evaluate *in situ* antibacterial, antifungal, and insecticidal capacity of the films to assure safety, to improve food shelf life, and evaluate the controlled release of active compounds.
6. Evaluate the synergistic effects of active films and irradiation treatments to extend the shelf life and to control pathogenic microbes and insects.

1.9.4. Methodology

1. For objective 1, the most effective antibacterial and antifungal compounds will be selected using a broth microdilution assay by measuring a minimal inhibitory concentration (MIC) and the synergistic effect between two or more active compounds will be performed using a checkerboard method by measuring fractional inhibitory concentration (FIC) (Turgis *et al.*, 2008).
2. For objective 2, the most effective insecticidal compounds will be assessed using the fumigant toxicity test described by Hossain *et al.* (2019b).
3. For objective 3, Nanoemulsion will be synthesized using a high pressure microfluidizer and a central composite design will be used to optimize the nanoemulsion (Hossain *et al.*, 2018).
4. For objective 4, the development of an active film will be performed by the solvent casting and compression molding method, and the characterization of the films will be carried out by evaluating water vapor permeability, mechanical properties (tensile strength, modulus and elongation at break), permeability such as water resistance, physico-chemical properties, gas permeability and antimicrobial diffusion/ volatile repellents (Khan *et al.*, 2012; Salmieri *et al.*, 2014a; Hossain *et al.*, 2018).
5. For objective 5, the antibacterial, antifungal and insecticidal effectiveness of the developed active films will be carried out by applying the films with cereal grains (rice) and dairy products (yogurt) by measuring the microbial load or percent mortality of insects at certain time intervals as well as the *in vitro* and *in situ* release of active compounds will also be performed (Patil *et al.*, 2016; Hossain *et al.*, 2018; Ben-Fadhel *et al.*, 2020).
6. For objective 6, cold pasteurization using γ -irradiation will be employed with active film during storage on rice to control the growth of pathogenic bacteria, spoilage fungi and insect pests (Hossain *et al.*, 2019a).

Simplified organogram for the Ph.D. thesis



Chapter 2

Publication 1

Microbicidal effectiveness of irradiation from Gamma and X-ray sources at different dose rates against the foodborne illness pathogens *Escherichia coli*, *Salmonella* Typhimurium and *Listeria monocytogenes* in rice

This article has been published in ***LWT- Food Science and Technology***, 2020, 132, 109841 (IF: 4.952), h-index: 147, Overall Ranking: 3734, SCImago Journal Rank: 0.6531.059

<https://doi.org/10.1016/j.lwt.2020.109841>

Tofa Begum¹, Peter A. Follett^{2*}, Farah Hossain¹, Larry Christopher³, Stephane Salmieri¹, Monique Lacroix^{1*}

¹Research Laboratories in Sciences Applied to Food, Canadian Irradiation Center, INRS-Armand Frappier Health Biotechnology Centre, 531, Boulevard des Prairies, Laval, Quebec, Canada, H7V 1B7

²United States Department of Agriculture, Agricultural Research Service, U.S. Pacific Basin Agricultural Research Center, 64 Nowelo Street, Hilo, HI 96720, USA

³Oniris, National Veterinary and Food Science School of Nantes-Atlantic, Rue de la Geraudiere, Nantes, France

*Corresponding author:

Dr. Monique Lacroix, Tel: 450-687-5010 # 4489, Fax: 450-686-5501, E-mail: Monique.Lacroix@iaf.inrs.ca

Peter A. Follett, Tel: 808-959-4303, Fax: 808-959-5470, E-mail: peter.follett@usda.gov

Contribution of authors

Tofa Begum conducted the data curation, methodology, writing - original drafts, writing - review, and editing. This manuscript was written by the framework planned with guidance from Prof. Monique Lacroix and Dr. Peter A. Follett. Both professors corrected the main draft several times and contributed intellectual contents. I have discussed many times with Stephane Salmieri and Dr. Farah Hossain regarding some sections of the manuscript to improve the writing. Larry Christopher carried out the experiments with Tofa Begum.

Résumé:

La réponse aux rayonnements de trois agents pathogènes d'origine alimentaire a été examinée pour l'irradiation avec cobalt-60 Gamma et les rayons X à faible énergie (125 keV) à différentes doses. Du riz a été inoculé avec *Escherichia coli*, *Salmonella Typhimurium* et *Listeria monocytogenes* et irradiés à des doses cibles de 0 (témoin), 250, 500, 750, 1000 et 1500 Gy avec soit un rayonnement gamma (dose de 9.1, 3.9 ou 0.22 kGy/h) ou rayonnement X (dose de 0.76 kGy/h). Les doses ont été mesurées avec traçabilité aux étalons nationaux. Les résultats ont montré que le débit de dose n'a pas significativement affecté les valeurs de D₁₀ (efficacité microbicide) pour aucun des agents pathogènes irradiés aux rayons gamma. Les agents pathogènes irradiés aux rayons X à faible énergie ont montré des valeurs de D₁₀ significativement plus élevées (efficacité microbicide inférieure) pour tous les agents pathogènes par rapport aux agents pathogènes irradiés aux rayons gamma. La combinaison de l'irradiation aux rayons gamma ou X avec la fumigation à l'huile essentielle d'origan/thym (HE) a généralement augmenté l'efficacité microbicide par rapport à l'irradiation seule. L'irradiation aux rayons gamma ou aux rayons X de basse énergie et les huiles essentielles végétales telles que l'origan/thym, appliquées seules ou en combinaison, sont des traitements antimicrobiens efficaces.

Mots clés: contrôle microbien; irradiation; débit de dose; huile essentielle; radiosensibilisation

Abstract

The radiation response of three foodborne illness pathogens was examined for irradiation with cobalt-60 Gamma and low-energy (125 keV) X-ray at different dose rates. *Escherichia coli*, *Salmonella* Typhimurium and *Listeria monocytogenes* were inoculated into rice and irradiated at target doses of 0 (control), 250, 500, 750, 1000, and 1500 Gy with either Gamma radiation (dose rates of 9.1, 3.9 or 0.22 kGy/h) or X-ray radiation (dose rate of 0.76 kGy/h). Doses were measured with traceability to national standards. The dose rate did not significantly affect D_{10} values (microbicidal effectiveness) for any of the Gamma-irradiated pathogens. Low energy X-ray irradiated pathogens had significantly higher D_{10} values (lower microbicidal effectiveness) for all pathogens compared to Gamma-irradiated pathogens. The combination of Gamma or X-ray irradiation with oregano/thyme essential oil (EO) fumigation generally increased the microbicidal effectiveness compared to irradiation alone. Gamma or low energy X-ray irradiation and plant essential oils such as oregano/thyme, applied alone or in combination, are effective antimicrobial treatments.

Keywords: microbial control; irradiation; dose rate; essential oil; radiosensitization

2.1. Introduction

Food irradiation has the potential to reduce the incidence of foodborne illnesses (Tauxe, 2001; Eustice, 2015). The list of foods for which ionizing radiation is accepted as a pathogen reduction treatment is expanding, and treatment doses between 0.5 and 30 kGy have been approved for microbial control in different foods (USDHS, 2019). The source of irradiation can be Gamma, electron beam or X-rays and international food safety standards consider the three sources equally safe and effective for food irradiation treatments. The most common source used commercially for food treatment is the radioisotope cobalt-60 (Gamma radiation). There is currently increased interest in technologies to replace risk-significant radioactive sources used for industrial, medical and research applications, including cobalt-60 (USDHS, 2019). The most advanced and commercially available alternative technologies are devices that use electricity to produce X-rays or electron beam radiation.

Cobalt-60 Gamma rays are produced at discreet energies (1.17 MeV and 1.33 MeV). For electronic sources, electron beam radiation up to 10 MeV and X-ray radiation up to 5.0 MeV have been approved (Codex, 2003). The bremsstrahlung radiation from X-rays is comprised of a spectrum of energies, ranging as high as the electron accelerator that produces them, but with average energy about one third the maximum. The dose rate during irradiation may vary depending mainly on source energy level, source-to-product distance, and product density. None of the standards contain technical requirements referring to minimum energy level or treatment dose rate (ISO, 2012); the assumption is that the energy deposited in the target is the only important factor in effectiveness. High energy X-ray irradiation (5 or 7 MeV) is currently used for food decontamination, e.g. spices. The development of new X-ray machines with low energy (80–300 keV) has raised the question of whether energy level and by extension dose rate may influence treatment efficacy.

Tallentire *et al.* (2010) showed that radiation dose provided by cobalt-60 Gamma rays, high energy electrons (10 MeV) or low energy electrons (80–100 keV) (e-beam) had equal microbicidal effectiveness against *Bacillus pumilis*. In a follow-on study, Tallentire and Miller (2015) showed the microbial effectiveness of 5–7 MeV X-rays against *Bacillus pumilis*. Van Calenberg *et al.* (1998) found no difference between 5 MeV X-ray and 10 MeV electron beam irradiation in the microbial decontamination of spices. Jung *et al.* (2015) showed that Gamma, electron beam and X-ray applied at a dose rate of 10 kGy/h were equally effective in decontaminating dried red pepper powder. However, in a study comparing cobalt-60 Gamma rays and electron beam for

decontamination of red pepper powder. [Kyung et al. \(2019\)](#) reported that a lower dose rate (1 kGy/s) was more effective than a higher dose rate (5 kGy/s) for electron beam irradiation, and a higher dose rate (9 kGy/h) was more effective than a lower dose rate (1.8 kGy/h) for cobalt-60 Gamma irradiation. Low energy X-ray radiation, which has medical, food and research applications ([Barkai-Golan and Follett, 2017](#)), has not been tested. Similar studies with a wider range of microbial pathogens, including foodborne illness pathogens and spoilage microorganisms, would be useful to confirm the microbicidal effectiveness of irradiation across source types and dose rates.

Stored rice and rice products are contaminated by pathogenic fungi *Aspergillus niger* and bacteria *Bacillus cereus* and *Paenibacillus amylolyticus* ([Shankar et al., 2020](#)). However, rice could be also contaminated with *E. coli*, *S. Typhimurium* and *L. monocytogenes* ([Lee et al., 2006](#); [Li et al., 2018](#)). Water could be a possible source of contamination of rice in agricultural field. Listeriosis caused by foodborne illness pathogen *L. monocytogenes* which has high case-fatality rate of 20–50% with gastroenteritis, septicemia, central nervous system infections, maternal-fatal infections ([Li et al., 2018](#)). [Nyenje et al. \(2012\)](#) investigated the prevalence of *L. monocytogenes* in ready-to-eat rice and the authors found 6.7 log CFU/g of *L. monocytogenes* in rice. *L. monocytogenes* was isolated from rice, potatoes and vegetables in Italy ([Caggiano et al., 2015](#)). In this study, we tested the radiation response of three important foodborne illness pathogens, *Escherichia coli*, *Salmonella Typhimurium* and *Listeria monocytogenes*, for irradiation with cobalt-60 Gamma rays and low-energy (125 keV) X-rays at different dose rates. Irradiation was applied to rice samples with and without a plant essential oil (EO) mixture (oregano/thyme), which was previously shown to have efficacy against bacterial pathogens to examine possible radiosensitization ([Lacroix and Follett, 2015](#); [Hossain et al., 2016a](#)). Doses were measured with traceability to national standards.

2.2. Materials and Methods

2.2.1. Bacterial species preparation

The bacterial strains (*E. coli* O157: H7 NT, 14470, *S. Typhimurium* SL 1344 and *L. monocytogenes* HPB 2812) were stored at -80 °C in tryptic soy broth (TSB, BD, Franklin Lakes, NJ, USA). All the bacteria were cultured in TSB containing 10% (v/v) glycerol ([Ghabraie et al., 2016](#)). Before each experiment, the stock cultures for each bacterium were propagated through two consecutive growth cycles for 24 h at 37 °C ± 2 °C. The cultures were recovered by centrifugation and diluted

with 0.85% (w/v) saline water to obtain the desired pathogen concentration of approximately 10^6 CFU/mL.

2.2.2. Preparation of essential oil mixture

Oregano (*Origanum compactum*; Moroccan oregano) and thyme (*Thymus vulgaris*) EOs were obtained from Robert and Fils (Ghislenghien, Belgium) and stored at 4 °C before use. A mixture ratio of 1:1 oregano and thyme were prepared following [Hossain et al. \(2016a\)](#) then stored at 4 °C. The chromatogram of EOs obtained from the manufacturer showed that the major components of the oregano oil were 46.37% carvacrol, 13.7% thymol, 13.33% *p*-cymene and 12.32% γ -terpinene, and the major components of the thyme oil were 26.04% thymol, 26.36% *p*-Cymene, and 16.69% γ -terpinene.

2.2.3. Rice inoculation and application of EOs mixture

A quantity of 10 g of white long-grain rice was inoculated with 1 mL of 10^6 CFU/mL *E. coli* O157: H7 [NT, 14470](#), *S. Typhimurium* SL 1344 and *L. monocytogenes* HPB 2812 in a sterile Petri dish and mixed well. In EO treatments, a quantity of 10 μ L of oregano/thyme was added to a sterile sponge attached to the upper lid of the Petri dish. This ensured that the rice grains were exposed to the vapor of oregano/thyme EO, without direct contact.

2.2.4. Irradiation of test samples

Inoculated rice samples were treated with either irradiation (Gamma ray or X-ray) alone or irradiation in presence of a mixture of oregano: thyme EO. Samples were treated at radiation doses of 250, 500, 750, 1000, and 1500 Gy at Gamma ray dose rates of 9.1, 3.9, or 0.22 kGy/h, or an X-ray dose rate of 0.76 kGy/h. Table 2.1 lists the sources types, equipment, and dosimetry systems. All samples were irradiated at room temperature.

Table 2.1. Equipment and dosimetry systems used to apply the Gamma-ray and X-ray irradiation treatments.

Gamma high dose rate (Gamma 1)	
Radiation source:	Cobalt-60 UC-15A underwater calibrator irradiator
Dose rate:	9.1 kGy/h
Dosimetry:	Alanine dosimeter (Alanine Pellet Dosimeter, mass 66.0 ± 0.5 mg, Far West Technology) and Harwell Gammachrome YR® Perspex Dosimeter (range 0.1-3.0 kGy)
Location:	Nordion Inc., Laval, QC, Canada
Gamma medium dose rate (Gamma 2)	
Radiation source:	Cobalt-60 UC-15A underwater calibrator irradiator
Dose rate:	3.9 kGy/h
Dosimetry:	Alanine dosimeter (Alanine Pellet Dosimeter, mass 66.0 ± 0.5 mg, Far West Technology) and Harwell Gammachrome YR® Perspex Dosimeter (range 0.1-3.0 kGy)
Location:	Nordion Inc., Laval, QC, Canada
Gamma low dose rate (Gamma 3)	
Radiation source:	Cobalt-60 Gammacell GC220 cabinet irradiator
Dose rate:	0.22 kGy/h
Dosimetry:	Harwell Gammachrome YR® Perspex Dosimeter (range 0.1-3.0 kGy)
Location:	INRS-Armand Frappier Health Biotechnology Centre, Laval, QC, CANADA
X-ray	
Radiation source:	X-ray machine (Philips appliance-model MG160, 125 keV)
Dose rate:	0.76 kGy/h
Dosimetry:	Piranha 657 radiation detector (RTI) (CB2-13060931, semi-conductor) and Harwell Gammachrome YR® Perspex Dosimeter (range 0.1-3.0 kGy)
Location:	INRS-Armand Frappier Health Biotechnology Centre, Laval, QC, CANADA

2.2.5. Microbiological analysis

A standard method adopted from the International Commission of Microbiological Specification on Foods (ICMSF) was used to perform microbiological analyses of all the samples (Braide *et al.*, 2011). For each sample, 20 mL of sterile peptone water (0.1%, w/v) was added to the 10 g of rice and homogenized for 60 s at 260 rpm with a Lab-blender 400 stomacher (Laboratory Equipment, London, UK), then made serial dilution of the sample from 10⁻¹ to 10⁻⁶. An aliquot portion (0.1 mL) of each dilution (from 10⁻¹ to 10⁻⁶) was inoculated in triplicate onto the surface of solidified freshly

prepared TSA (BD, Franklin Lakes, NJ, USA). Inoculated plates were spread evenly with a sterile spreader and incubated for 24 h at 37 °C. The microbial colonies were counted following the plate count method (Hossain *et al.*, 2018).

2.2.6. D₁₀ (kGy) and radio-sensitisation determination

D₁₀ is defined as the radiation dose required to reduce the microbial population by 1 log or 90%. D₁₀-values were determined for *E. coli* O157:H7, *S. Typhimurium* and *L. monocytogenes* using the reciprocal of the slope of the regression line produced by plotting bacterial counts (log CFU/g) against the irradiation doses for the irradiation alone and irradiation plus oregano/thyme EO treatments. The D₁₀ values for each bacterium were calculated in kGy (Maity *et al.*, 2011). The relative sensitivity (RS) was calculated using the following equation (Caillet *et al.*, 2006; Hossain *et al.*, 2014a).

Relative radiation sensitivity (RS) = (D₁₀ of the sample treated irradiation alone / D₁₀ of the sample treated irradiation plus oregano/ thyme EO).

2.2.7. Statistical Analysis

Each bacterium was irradiated by the different sources at different dose rates and subjected to analysis of variance (ANOVA) and for significant effects means separation were performed using a Tukeys HSD test at alpha = 0.05 (SAS, 2013). For each bacterium and dose rate, the D₁₀ values of the irradiation alone and irradiation with oregano/thyme EO treatments were compared using a *t*-test (SAS, 2013). For each experiment, three replicates were done and for each replicate, three samples were analyzed.

2.3. Results and discussion

Results of D₁₀ values are presented on Table 2.2. Results showed that D₁₀ values were generally higher for *E. coli* than *S. Typhimurium* and *L. monocytogenes* (F = 7.9, df = 2, P ≤ 0.0006), and therefore each bacterium was analyzed separately for the effects of radiation dose rate, treatment with or without oregano/thyme, and the radiation source. For *E. coli*, D₁₀ values were significantly different for the effects of radiation dose rate (F = 8.3, df = 1, P ≤ 0.005) and treatment with or without oregano/thyme EO (F = 4.5, df = 1, P ≤ 0.03) but not for the interaction between dose rate

and oregano/thyme EO treatment ($F = 0.2$, $df = 1$, $P > 0.6$). The two slowest dose rates (Gamma ray 0.22 kGy/h and X-ray 0.76 kGy/h) had the highest D_{10} values for both the irradiation alone and irradiation and oregano/thyme combination treatments (Table 2.2). Across all treatments, D_{10} values were higher for *E. coli* treated with X-ray (0.403) than Gamma ray (mean: 0.307) ($t = -2.48$, $df = 1$, $P \leq 0.02$). Irradiation combined with oregano/thyme resulted in lower D_{10} values for all dose rate treatments compared with irradiation alone. The highest RS was observed for samples treated with Gamma ray at a dose rate of 9.1 kGy/h (RS:1.20), 3.9 kGy/h (RS:1.22) and X-ray (0.76 kGy/h) (RS:1.14) (Table 2.2).

For *S. Typhimurium*, D_{10} values were significantly different for the effects of radiation dose rate ($F = 98.3$, $df = 1$, $P \leq 0.0001$) and treatment with or without oregano/thyme EO ($F = 23.1$, $df = 1$, $P \leq 0.0002$) but not for the interaction between dose rate and oregano/thyme EO treatment ($F = 0.9$, $df = 1$, $P > 0.47$). Dose rate effects were inconsistent but the highest D_{10} values for both the irradiation alone and irradiation and oregano/thyme combination treatments were in the X-ray treatment (0.76 kGy/h) (Table 2.2). Across all treatments, D_{10} values were higher for *S. Typhimurium* treated with X-ray (0.377 kGy) than Gamma ray (mean: 0.252 kGy) ($t = -8.73$, $df = 1$, $P \leq 0.001$). Irradiation combined with oregano/thyme resulted in lower D_{10} values for all dose rate treatments compared with irradiation alone. The highest RS was observed on samples treated with Gamma ray at 9.1 kGy (RS:1.22) and 0.22 kGy/h (RS:1.28) (Table 2.2).

For *L. monocytogenes*, D_{10} values were significantly different for the effects of radiation dose rate ($F = 30.7$, $df = 1$, $P \leq 0.001$) and treatment with or without oregano/thyme EO ($F = 15.9$, $df = 1$, $P \leq 0.001$) but not for the interaction between dose rate and oregano/thyme EO treatment. ($F = 1.9$, $df = 1$, $P > 0.18$). Dose rate effects were inconsistent but the highest D_{10} values for both the irradiation alone and irradiation with oregano/thyme combination treatments were in the X-ray treatment (0.76 kGy/h), as was the case for *E. coli* and *S. Typhimurium* (Table 2.2). Across all treatments, D_{10} values were higher for *L. monocytogenes* treated with X-ray (0.302 kGy) than Gamma (D_{10} values from 0.232 to 0.236 kGy) ($t = -5.95$, $df = 1$, $P \leq 0.001$). Irradiation combined with oregano/thyme resulted in lower D_{10} values for all dose rate treatments compared with irradiation alone. The highest RS was observed for samples treated with Gamma irradiation at the dose rate of 3.9 kGy/h (RS:1.17) and X-ray at 0.76 kGy/h (RS:1.14) (Table 2.2).

Table 2.2. D₁₀ values for bacterial pathogens irradiated with or without oregano/thyme essential oil (EO).

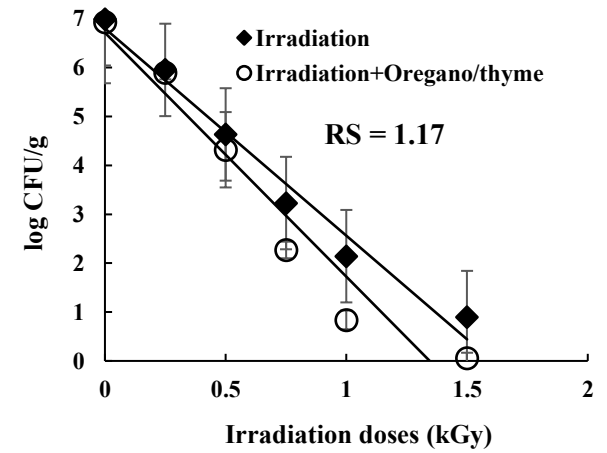
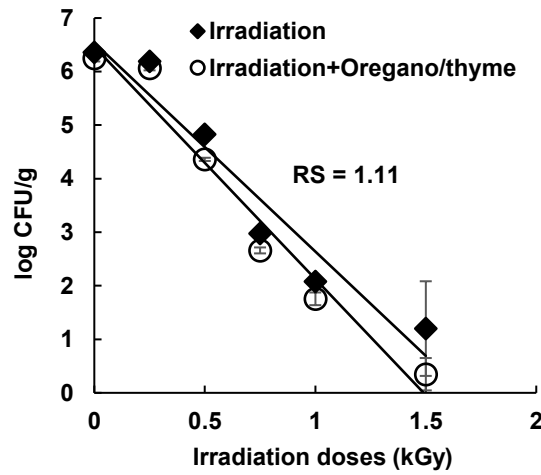
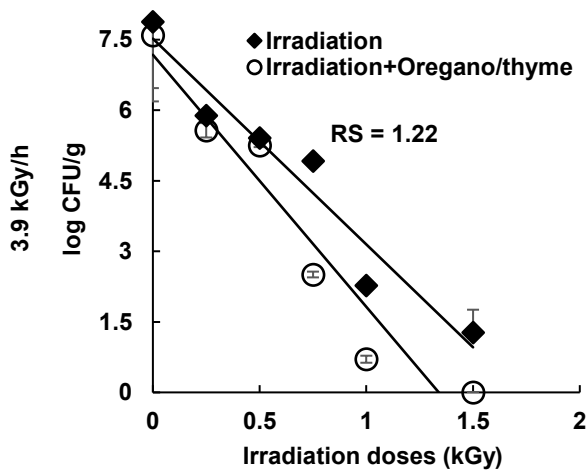
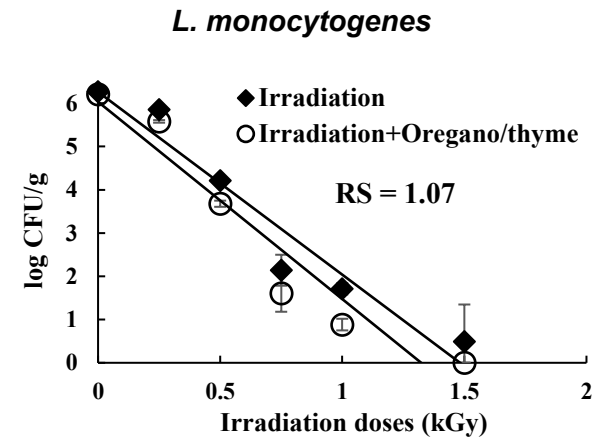
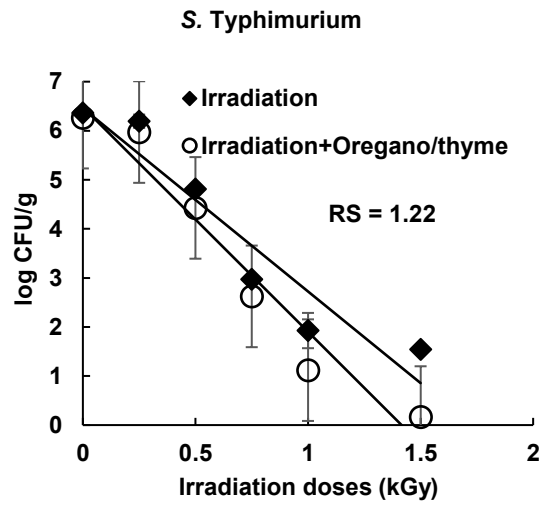
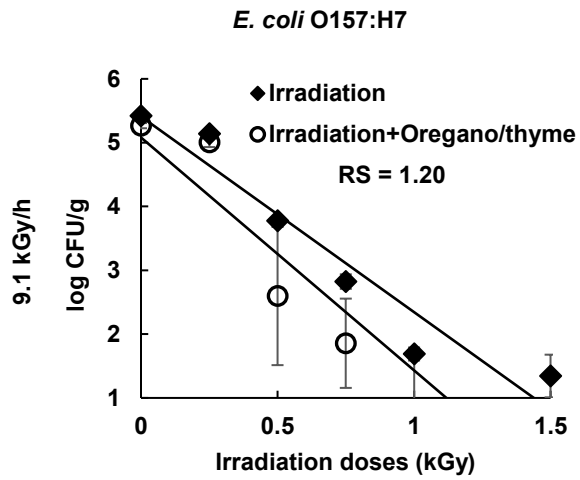
Pathogens	Source	Dose rate (kGy/h)	Irradiation (kGy)	Irradiation + EO (kGy)	F-value ¹	df	P	RS
<i>E. coli</i> O157:H7	Gamma	9.1	0.326b	0.274b	1.87	4	0.24	1.20
	Gamma	3.93	0.228c	0.187c	2.48	4	0.19	1.22
	Gamma	0.22	0.367a	0.360a	1.87	4	0.24	1.02
	X-ray	0.76	0.403a	0.351a	54.8	4	0.002	1.14*
<i>S. Typhimurium</i>	Gamma	9.1	0.266b	0.218b	28.0	4	0.006*	1.22*
	Gamma	3.93	0.257c	0.231b	2.21	4	0.21	1.12
	Gamma	0.22	0.234c	0.184c	113.0	4	0.0004*	1.28*
	X-ray	0.76	0.377a	0.351a	1.26	4	0.32	1.07
<i>L. monocytogenes</i>	Gamma	9.1	0.236b	0.219bc	3.25	4	0.14	1.07
	Gamma	3.93	0.235b	0.200c	4.2	4	0.11	1.17
	Gamma	0.22	0.232c	0.227b	6.4	4	0.06	1.02
	X-ray	0.76	0.302a	0.265a	16.0	4	0.016*	1.14*

¹For each bacterium, D₁₀ values in columns followed by a different letter are significantly different by Tukey's test at alpha = 0.5. P-values and RS values followed by an asterisk (*) indicate a significant decrease in D₁₀ values between the irradiation plus oregano/thyme EO and the irradiation alone treatments, and therefore an increase on efficacy.

Overall, the dose rate did not significantly affect D₁₀ values (microbicidal effectiveness) for any of the Gamma-irradiated pathogens. Low energy X-ray irradiated pathogens had significantly higher D₁₀ values (lower microbicidal effectiveness) for all pathogens compared to Gamma-irradiated pathogens. The combination of Gamma ray or X-ray irradiation with oregano/thyme essential oil (EO) fumigation generally increased the bacterial radiosensitization compared to irradiation alone.

Microbial control of all three bacteria in rice increased with increasing radiation dose in both the irradiation and irradiation with oregano/thyme EO treatments (Figure 2.1). Over the doses tested, the log reduction was higher for *L. monocytogenes* than for *E. coli* and *S. Typhimurium* regardless of dose rate and source. For *E. coli*, the bacteria count was 1.1, 1.6 and 0.3 log CFU/g when treated at 1500 Gy with three different Gamma dose rates of 9.1, 3.9 and 0.22 kGy/h, respectively, resulting in log reductions of 4.3, 4.7 and 3.6 log CFU/g as compared to *E. coli* counts at 0 Gy (control). The combined treatment of irradiation and oregano/thyme EO further increased the microbial control for all bacteria. For the combined irradiation with oregano/ thyme EO treatment at Gamma dose rates of 9.1, 3.9 and 0.22 kGy/h, *E. coli* counts was 0, 0, 0.16 log CFU/g, respectively at 1500 Gy which corresponded to 5.3, 6 and 3.6 log CFU/g reductions compared to *E. coli* counts at 0 Gy. Reductions in microbial counts with X-ray irradiation (0.76 kGy/h) were less pronounced. *E. coli* counts were 0.64 and 0.16 log CFU/g with X-ray irradiation alone and X-ray irradiation with oregano/thyme EO treatments, respectively, at 1500 Gy which corresponded to a 3.3 and 3.8 log CFU/g reduction as compared to the *E. coli* count at 0 kGy (Figure 2.1).

S. Typhimurium counts were 1.5, 1.7 and 1.1 log CFU/g at 1.5 kGy at the three Gamma-radiation dose rates of 9.1, 3.9 and 0.22 kGy/h, respectively, which corresponded to 4.8, 4.6 and 5.5 log CFU/g reductions of *S. Typhimurium* in rice compared to the bacterial count at 0 kGy. The combined treatments of Gamma-radiation with oregano/ thyme EO increased the microbial control of *S. Typhimurium* at each irradiation dose (Figure 2.1). *S. Typhimurium* counts were 0.2, 0.5 and 0 log CFU/g at 1500 Gy at dose rates of 9.1, 3.9 and 0.22 kGy/h, respectively, which represented 6.1, 5.7 and 7.3 log CFU/g reductions of *S. Typhimurium* compared to the bacterial counts at 0 Gy. *S. Typhimurium* appeared to be more resistant to X-ray irradiation compared to Gamma-irradiation (Figure 2.1). The bacterial counts were 0 and 0.42 log CFU/g at 1500 Gy with and without oregano/thyme EO at 0.76 kGy/h (X-ray) which corresponded to 3.8 and 3.6 log CFU/g reductions of *S. Typhimurium*, respectively.



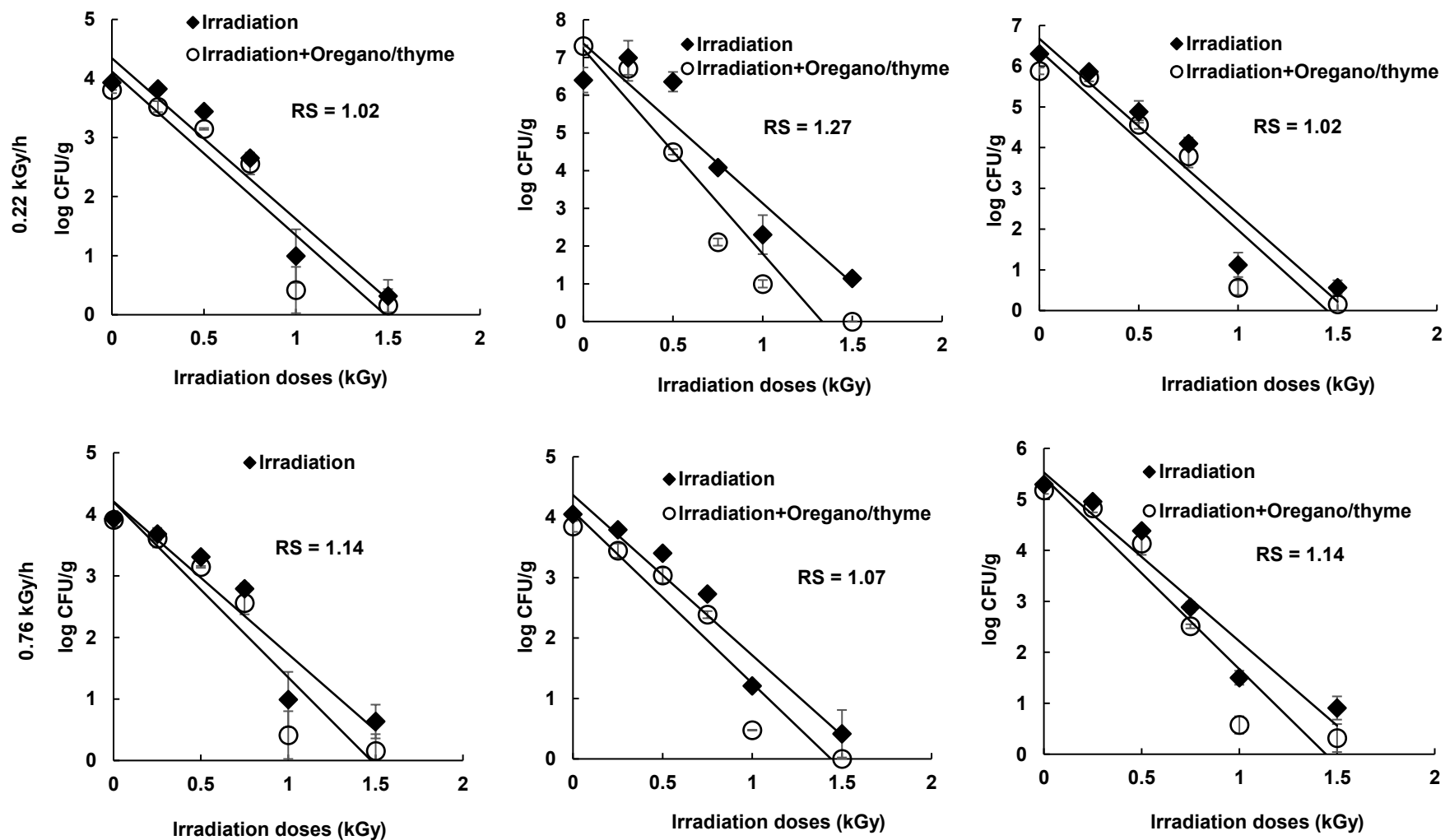


Figure 2.1. Relative radio sensitivity (RS) of *E. coli* O157:H7, *S. Typhimurium* and *L. monocytogenes* to irradiation and irradiation plus oregano/thyme EO using different radiation sources and dose rates.

L. monocytogenes was the least radio-tolerant bacterium tested. The bacterial count of *L. monocytogenes* was 0.55, 0.89 and 0.56 at 1500 Gy at radiation dose rates of 9.1, 3.9 and 0.22 kGy/h, respectively, with corresponding reductions of 5.7, 5.4 and 5.7 log CFU/g compared to the bacterial count at 0 kGy. The combination of Gamma-radiation with oregano/thyme EO increased the reduction of *L. monocytogenes* to 6.2, 6.0 and 5.7 log CFU/g at dose rates of 9.1, 3.9 and 0.22 kGy/h, respectively. The bacterial counts were 0.9 and 0.3 log CFU/g when *L. monocytogenes* was treated with X-ray irradiation at 0.76 kGy/h alone and in combination with oregano/thyme EO, respectively, which corresponded to 4.4 and 4.7 log CFU/g reductions in rice compared to 0 kGy.

Other studies have found similar reductions in food-borne pathogens after irradiation and irradiation combined with EOs. For example, [Turgis et al. \(2008\)](#) evaluated the effect of essential oils with Gamma-irradiation under modified atmosphere packaging on the radiosensitivity of *Escherichia coli* O157: H7 and *Salmonella typhi* in Gamma-irradiated ground beef; *Escherichia coli* and *S. typhi* inoculated at 10^6 CFU/g in ground beef and irradiated in combination with 0.5% (w/w) Chinese cinnamon or Spanish oregano essential oils showed increased of the relative radiation sensitivities (RS) of 3.57 at 1 kGy for *E. coli* O157: H7 and 3.26 at 1.75 kGy for *S. typhi* compared to untreated controls. [Ayari et al. \(2012\)](#) reported that cinnamaldehyde (1.47% w/w) increased the radiosensitivity of *Bacillus cereus* in minced meat; the D₁₀ value in the control sample was 3.71 kGy, whereas the D₁₀ value in the combined treatment of Gamma-irradiation and cinnamaldehyde was 2.48 kGy showing a RS of more than 1.5. [Caillet and Lacroix \(2006\)](#) investigated the radiosensitization of *L. monocytogenes* in the presence of *trans*-cinnamaldehyde, Spanish oregano, winter savory, and Chinese cinnamon on peeled mini carrots packed under air or under a modified atmosphere (60% O₂, 30% CO₂, and 10% N₂). The carrots were inoculated with *L. monocytogenes* HPB 2812 (10^6 CFU/g) and then, were coated separately with each active compound (0.5%, wt/wt) before being packaged under air or the modified atmosphere and irradiated at doses from 0.07 to 2.4 kGy. The dose required to reduce *L. monocytogenes* population by 1 log CFU (D₁₀) was 0.36 kGy for carrots packed under air and 0.17 kGy for carrots packed under the modified atmosphere. The most efficient compound was *trans*-cinnamaldehyde which increased the RS 3.8-fold under both atmospheres compared with untreated controls. [Hossain et al. \(2019a\)](#) studied the antifungal activity of combined treatments of irradiation and oregano and thyme EOs incorporated into chitosan nanocomposite films; nanocrystal cellulose (NCC) reinforced bioactive chitosan films combined with irradiation at 750 Gy showed significantly higher antifungal activities without altering the sensorial properties of rice against *Aspergillus niger*, *A. flavus*, *A. parasiticus*, and *Penicillium chrysogenum* than irradiation alone. [Yemiş and](#)

Candoğan (2017) studied the antimicrobial effects of oregano and thyme EOs incorporated in a soy edible coating to control *E. coli* O157: H7, *L. monocytogenes* and *Staphylococcus aureus* in beef during storage; the incorporation of 3% oregano and thyme EO in the soy edible coating showed 1.83 to 2.86 log CFU/g reductions of pathogenic microorganisms compared to untreated controls.

Ionizing radiation can break the chemical bonds within the DNA in microbial cells or alter membrane permeability or other cellular functions (Caillet *et al.*, 2005; Caillet and Lacroix, 2006). EOs and irradiation affect the bacterial membrane integrity and murein composition and induce a release of the bacterial cell constituents, and a decrease of the internal pH and ATP (Caillet *et al.*, 2005; Caillet and Lacroix, 2006; Oussalah *et al.*, 2006). The combined treatment of irradiation and EOs act in synergy and may also facilitate contact between antimicrobial compounds and cell membranes and thereby increase cell damage (Ayari *et al.*, 2012). For example, Park and Ha (2019) investigated the efficacy of X-ray irradiation for the inactivation of the food-borne pathogens *E. coli* O157: H7, *S. Typhimurium* and *L. monocytogenes* on sliced cheese. The cheese samples inoculated with bacteria were treated with X-ray doses of 0, 0.2, 0.4, 0.6, and 0.8 kGy, with the 0.6 kGy dose causing approximately a 5 log reduction in pathogens without changing the color and texture of the cheese. The underlying antimicrobial mechanisms of the X-ray and curcumin combination included the increased generation of intracellular reactive oxygen species (ROS) in bacterial cells and bacterial cell membrane damage.

In the present study, we showed the radiation response of three foodborne illness pathogens *Escherichia coli*, *Salmonella Typhimurium* and *Listeria monocytogenes* in rice to irradiation with cobalt-60 Gamma ray and low-energy (125 keV) X-ray at different dose rates. Stored rice is also prone to contamination by pathogenic fungi and bacteria that cause spoilage. In a companion study to the present one, Shankar *et al.* (2020) inoculated rice with *Aspergillus niger*, *Bacillus cereus* or *Paenibacillus amylolyticus* then irradiated the rice with or without fumigation with oregano/thyme EO using Gamma or X-ray irradiation at the same dose rates as in the present study. The fungus *A. niger* exhibited higher relative sensitivity to X-ray irradiation than the bacteria *B. cereus* and *P. amylolyticus*, whereas the bacteria showed higher relative sensitivity to Gamma irradiation than the fungus, but there was no consistent positive or negative correlation between relative sensitivity and dose rate for these pathogens (Shankar *et al.*, 2020). Overall, it seems clear that both irradiation and plant essential oils such as oregano/thyme, applied alone or in combination, are effective antimicrobial treatments.

2.4. Conclusion

A comparative study was conducted between Gamma and X-ray at four different dose rates for microbial decontamination of rice of the food-borne illness pathogens *E. coli* 0157:H7, *S. Typhimurium* and *L. monocytogenes*. The dose rate did not significantly affect D₁₀ values (microbicidal effectiveness) for any of the Gamma-irradiated pathogens. Low energy X-ray irradiated pathogens had significantly higher D₁₀ values (lower microbicidal effectiveness) for all pathogens compared to Gamma-irradiated pathogens. The combination of Gamma or X-ray irradiation with oregano/thyme essential oil (EO) fumigation increased the radiosensitivity of all bacteria and generally increased the microbicidal effectiveness compared to irradiation alone. Combination treatment with plant essential oils can reduce the irradiation dose required for a prescribed level of bacterial reduction. For packaged foods such as rice, plant essential oils can be deployed as sachets or as bioactive films to improve food safety.

2.5. Acknowledgments

The authors are sincerely thankful to the Natural Sciences and Engineering Research Council of Canada (NSERC) discovery program project #RGPIN-2017-05947 and the U.S. Department of Agriculture, Agricultural Research Service (USDA ARS), U.S. Pacific Basin Agricultural Research Centre for their financial support. This research was part of an IAEA-sponsored coordinated research project (CRP no: F23033) on radiation inactivation of biohazards. The authors are indebted to Nordion, Inc., Laval, QC, Canada for providing Gamma-irradiation treatment.

Conflicts of interest

All authors state that there is no conflict of interest.

2.6. References

- Ayari, S., Dussault, D., Jerbi, T., Hamdi, M., Lacroix, M., 2012. Radiosensitization of *Bacillus cereus* spores in minced meat treated with cinnamaldehyde. *Radiation Physics and Chemistry* 81, 1173-1176.
- Barkai-Golan, R., Follett, P.A., 2017. Irradiation for quality improvement, microbial safety and phytosanitation of fresh produce. Academic Press.
- Braide, W., Nwaoguikpe, R., Oranus, S., Udegbonam, L., Akobundu, C., Okorundu, S., 2011. The effect of biodeterioration on the nutritional composition and microbiology of an edible long-winged reproductive termite, *Macrotermes bellicosus*. Smeathman. *International Journal of Food Safety* 13, 107-114.
- Caggiano, G., De Giglio, O., Lovero, G., Rutigliano, S., Diella, G., Balbino, S., Napoli, C., Montagna, M.T., 2015. Detection of *Listeria monocytogenes* in ready-to-eat foods sampled from a catering service in Apulia, Italy. *Annali Di Igiene Medicina Preventiva E Di Comunita* 27, 590-594.
- Caillet, S., Lacroix, M., 2006. Effect of gamma radiation and oregano essential oil on murein and ATP concentration of *Listeria monocytogenes*. *Journal of Food Protection* 69, 2961-2969.
- Caillet, S., Millette, M., Turgis, M., Salmieri, S., Lacroix, M., 2006. Influence of antimicrobial compounds and modified atmosphere packaging on radiation sensitivity of *Listeria monocytogenes* present in ready-to-use carrots (*Daucus carota*). *Journal of Food Protection* 69, 221-227.
- Caillet, S., Shareck, F., Lacroix, M., 2005. Effect of gamma radiation and oregano essential oil on murein and ATP concentration of *Escherichia coli* O157: H7. *Journal of Food Protection* 68, 2571-2579.
- Codex, C.A., 2003. General standard for irradiated foods: CODEX STAN 106–1983, REV. 1–2003. Food and Agriculture Organization of the United Nations, Rome.
- Eustice, R.F., 2015. Using irradiation to make safe food safer. *Stewart Postharvest Review* 11, 1-5.
- Ghabraie, M., Vu, K.D., Tata, L., Salmieri, S., Lacroix, M., 2016. Antimicrobial effect of essential oils in combinations against five bacteria and their effect on sensorial quality of ground meat. *LWT-Food Science and Technology* 66, 332-339.
- Hossain, F., Follett, P., Dang Vu, K., Harich, M., Salmieri, S., Lacroix, M., 2016. Evidence for synergistic activity of plant-derived essential oils against fungal pathogens of food. *Food Microbiology* 53, 24-30.

- Hossain, F., Follett, P., Salmieri, S., Vu, K.D., Frascini, C., Lacroix, M., 2019. Antifungal activities of combined treatments of irradiation and essential oils (EOs) encapsulated chitosan nanocomposite films in *in vitro* and *in situ* conditions. *International Journal of Food Microbiology* 295, 33-40.
- Hossain, F., Follett, P., Vu, K.D., Salmieri, S., Frascini, C., Jamshidian, M., Lacroix, M., 2018. Antifungal activity of combined treatments of active methylcellulose-based films containing encapsulated nanoemulsion of essential oils and γ -irradiation: *in vitro* and *in situ* evaluations. *Cellulose* 26, 1335-1354.
- Hossain, F., Follett, P., Vu, K.D., Salmieri, S., Senoussi, C., Lacroix, M., 2014. Radiosensitization of *Aspergillus niger* and *Penicillium chrysogenum* using basil essential oil and ionizing radiation for food decontamination. *Food Control* 45, 156-162.
- Jung, K., Song, B.-S., Kim, M.J., Moon, B.-G., Go, S.-M., Kim, J.-K., Lee, Y.-J., Park, J.-H., 2015. Effect of X-ray, gamma ray, and electron beam irradiation on the hygienic and physicochemical qualities of red pepper powder. *LWT-Food Science and Technology* 63, 846-851.
- Kyung, H.K., Ramakrishnan, S.R., Kwon, J.H., 2019. Dose rates of electron beam and gamma ray irradiation affect microbial decontamination and quality changes in dried red pepper (*Capsicum annuum* L.) powder. *Journal of the Science of Food and Agriculture* 99, 632-638.
- Lacroix, M., Follett, P., 2015. Combination irradiation treatments for food safety and phytosanitary uses. *Stewart Postharvest Review* 11, 1-10.
- Lee, S.-Y., Chung, H.-J., Shin, J.-H., Dougherty, R.H., Kang, D.-H., 2006. Survival and growth of foodborne pathogens during cooking and storage of oriental-style rice cakes. *Journal of Food Protection* 69, 3037-3042.
- Li, W., Bai, L., Fu, P., Han, H., Liu, J., Guo, Y., 2018. The epidemiology of *Listeria monocytogenes* in China. *Foodborne Pathogens and Disease* 15, 459-466.
- Maity, J.P., Kar, S., Banerjee, S., Sudershan, M., Chakraborty, A., Santra, S.C., 2011. Effects of gamma radiation on fungi infected rice (*in vitro*). *International Journal of Radiation Biology* 87, 1097-1102.
- Nyenje, M.E., Odjadjare, C.E., Tanih, N.F., Green, E., Ndip, R.N., 2012. Foodborne pathogens recovered from ready-to-eat foods from roadside cafeterias and retail outlets in Alice, Eastern Cape Province, South Africa: public health implications. *International Journal of Environmental Research and Public Health* 9, 2608-2619.

- Oussalah, M., Caillet, S., Lacroix, M., 2006. Mechanism of action of Spanish oregano, Chinese cinnamon, and savory essential oils against cell membranes and walls of *Escherichia coli* O157: H7 and *Listeria monocytogenes*. *Journal of Food Protection* 69, 1046-1055.
- Park, J.S., Ha, J.W., 2019. X-ray irradiation inactivation of *Escherichia coli* O157:H7, *Salmonella enterica* Serovar Typhimurium, and *Listeria monocytogenes* on sliced cheese and its bactericidal mechanisms. *International Journal of Food Microbiology* 289, 127-133.
- SAS, I., 2013. JMP 11 basic analysis. SAS Institute.
- Shankar, S., Follett, P., Ayari, S., Hossain, F., Salmieri, S., Lacroix, M., 2020. Microbial radiosensitization using combined treatments of essential oils and irradiation-part B: Comparison between gamma-ray and X-ray at different dose rates. *Microbial Pathogenesis* 143, 104118.
- Tallentire, A., Miller, A., 2015. Microbicidal effectiveness of X-rays used for sterilization purposes. *Radiation Physics and Chemistry* 107, 128-130.
- Tallentire, A., Miller, A., Helt-Hansen, J., 2010. A comparison of the microbicidal effectiveness of gamma rays and high and low energy electron radiations. *Radiation Physics and Chemistry* 79, 701-704.
- Tauxe, R.V., 2001. Food safety and irradiation: protecting the public from foodborne infections. *Emerging Infectious Diseases* 7, 516.
- Turgis, M., Borsa, J., Millette, M., Salmieri, S., Lacroix, M., 2008. Effect of selected plant essential oils or their constituents and modified atmosphere packaging on the radiosensitivity of *Escherichia coli* O157: H7 and *Salmonella* Typhi in ground beef. *Journal of Food Protection* 71, 516-521.
- USDHS, U.S.D.o.H.S., 2019. CISA (cybersecurity and infrastructure security agency) (p. 155). Non-radioisotopic alternative technologies white paper.
- Van Calenberg, S., Vanhaelewyn, G., Van Cleemput, O., Callens, F., Mondelaers, W., Huyghebaert, A., 1998. Comparison of the effect of X-ray and electron beam irradiation on some selected spices. *LWT-Food Science and Technology* 31, 252-258.
- Yemiş, G.P., Candoğan, K., 2017. Antibacterial activity of soy edible coatings incorporated with thyme and oregano essential oils on beef against pathogenic bacteria. *Food Science and Biotechnology* 26, 1113-1121.

Chapter 3
Publication 2

Mixture design methodology and predictive modelling for developing active formulations using essential oils and citrus extract against foodborne pathogens and spoilage microorganisms in rice

This article has been published in *Journal of Food Science*, 2022, 87(1), 353-369, Impact factor: 3.167, h-index: 160, Overall Ranking: 7454, SCImago Journal Rank: 0.653

<https://doi.org/10.1111/1750-3841.15988>

Tofa Begum¹, Peter A. Follett², Shiv Shankar¹, Jumana Mahmud¹, Stephane Salmieri¹, Monique Lacroix^{1,*}

¹Research Laboratories in Sciences, Applied to Food, Canadian Irradiation Center, INRS, Armand Frappier Health and Biotechnology Centre, Institute of Nutrition and Functional Food (INAF), Chair of the MAPAQ on stabilized natural antimicrobial and food quality, 531, Boulevard des Prairies, Laval, Quebec, Canada, H7V 1B7

²United States Department of Agriculture, Agricultural Research Service, U.S. Pacific Basin Agricultural Research Center, 64 Nowelo Street, Hilo, HI 96720, USA

*Corresponding author: Monique Lacroix, Ph.D, Email: Monique.Lacroix@inrs.ca

Tel: 450-687-5010 # 4489, Fax: 450-686-5501

Contribution of the authors

Tofa Begum curated the data, developed the methodology and wrote the manuscript. Monique Lacroix and Peter Follett conceived the project, designed the general methodology, supervised the research, and edited the manuscript. Stephane Salmieri and Shiv Shankar assisted with methodology, software, and statistical analysis, and reviewed the manuscript. Jumana Mahmud helped with the data curation and statistical analysis.

Résumé

Les effets antibactériens et antifongiques de six huiles essentielles (HE) végétales et de deux types d'extraits d'agrumes (EA) ont été étudiés contre deux bactéries pathogènes (*Salmonella Typhimurium* et *Escherichia coli* O157:H7) et trois champignons (*Aspergillus niger*, *Penicillium chrysogenum*, et *Mucor circinelloides*). Un test de microdilution en bouillon et une méthode en damier ont été utilisés pour mesurer la concentration minimale inhibitrice (CMI) de chaque extrait et les interactions possibles entre eux. Le test MIC a montré que l'HE de cannelle, l'HE méditerranéenne, la formulation du Sud, l'HE d'agrumes, l'extrait d'agrumes organique (OCE) et l'extrait naturel d'agrumes (NCE) avaient l'activité antimicrobienne et antifongique la plus élevée. La méthode du damier a montré que la combinaison méditerranéenne HE+OCE agissait en synergie contre tous les agents pathogènes testés. Une conception de mélange centroïde a été utilisée pour développer des formulations actives en prédisant les concentrations optimales d'OE/EA pour une activité antibactérienne/antifongique accrue. Un mélange de quatre formulations (625 ppm d'OCE, 313 ppm d'HE de Méditerranée, 625 ppm d'HE d'agrumes et 313 ppm d'HE de cannelle) désignée comme formulation active 1, et le mélange de cinq formulations (625 ppm NCE, 625 ppm de formulation asiatique, 313 ppm La formulation Southern, 625 ppm d'HE de cannelle et 313 ppm d'HE de thym sarriette) désignée comme formulation active 2, ont été formulées et testées en raison de leur efficacité microbicide élevée. Des tests *in situ* avec du riz ont montré une réduction significative ($P \leq 0.05$) de toutes les bactéries et champignons pathogènes testés à partir de la vapeur des formulations actives 1 et 2 après 28 jours de stockage.

Application pratique

Les formulations actives (huiles essentielles et extraits d'agrumes) développées dans l'étude sont très efficaces contre les agents pathogènes d'origine alimentaire. Les formulations actives dans l'étude actuelle pourraient être utilisées comme conservateurs naturels dans l'industrie alimentaire pour contrôler les maladies d'origine alimentaire et les organismes de détérioration dans les aliments stockés.

Mots clés: huile essentielle; extrait d'agrumes; pathogènes alimentaires; activité antimicrobienne; riz stocké

Abstract

The antibacterial and antifungal effects of six plant-derived essential oils (EOs) and two types of citrus extracts (CEs) were studied against two pathogenic bacteria (*Salmonella* Typhimurium and *Escherichia coli* O157:H7) and three fungi (*Aspergillus niger*, *Penicillium chrysogenum*, and *Mucor circinelloides*). A broth microdilution assay and checkerboard method were used to measure the minimal inhibitory concentration (MIC) of each extract and the possible interactions between them. The MIC assay showed that cinnamon EO, Mediterranean EO, Southern formulation, citrus EO, organic citrus extract (OCE), and natural citrus extract (NCE) had the highest antimicrobial and antifungal activity. The checkerboard method showed that the Mediterranean EO+OCE combination acted in synergy against all tested pathogens. A centroid mixture design was used to develop active formulations by predicting optimal concentrations of EO/CEs for increased antibacterial/antifungal activity. A mixture of four formulations (625 ppm OCE, 313 ppm Mediterranean EO, 625 ppm citrus EO, and 313 ppm cinnamon EO) named as active formulation 1, and the mixture from five formulations (625 ppm NCE, 625 ppm Asian formulation, 313 ppm Southern formulation, 625 ppm cinnamon EO, and 313 ppm savory thyme EO) named as active formulation 2, were formulated and tested because of their high microbicidal effectiveness. *In situ* tests with rice showed a significant reduction ($P \leq 0.05$) of all tested pathogenic bacteria and fungi from the vapor of active formulations 1 and 2 after 28 days of storage.

Practical application

Active formulations (essential oils and citrus extracts) developed in the study are highly effective against foodborne pathogens. Active formulations in the current study could be used as natural preservatives in the food industry for controlling foodborne diseases and spoilage organisms in stored foods.

Keywords: essential oil; citrus extract; food pathogens; antimicrobial activity; stored rice

3.1. Introduction

Rice (*Oryza sativa* L.) is the third most important cereal crop in the world after wheat and maize, with an annual production of over 600 million (Nguefack *et al.*, 2005). It is a staple food for about 50 % of the world's population and provides more calories per hectare for human consumption than wheat. However, specific conditions of temperature, relative humidity, and moisture content which arise during storage may contribute to the rapid deterioration of rice by promoting bacterial and fungal growth (Nguefack *et al.*, 2005). Fungal contamination of rice negatively affects grain color and nutritional value. Fungi may also contaminate the rice with mycotoxins, eg. aflatoxin, which can cause serious food poisoning (Paster *et al.*, 1993). Fungi such as *Penicillium* spp., *Aspergillus* spp., *Fusarium* spp., and *Mucor* spp. are the most important fungi responsible for food loss (Betts *et al.*, 1999; Viuda-Martos *et al.*, 2007; Hossain *et al.*, 2014a). Several pathogenic bacteria can also cause food poisoning in cereals, especially *Escherichia coli*, *Salmonella* spp., *Staphylococcus aureus*, and *Listeria monocytogenes* (Oussalah *et al.*, 2007; Ghabraie *et al.*, 2016; Mohammadzadeh, 2017; Ju *et al.*, 2019). Different chemical preservatives, plant-based extracts, and biological agents have been used to control postharvest microbial (bacterial and fungal) contamination during grain storage, such as synthetic chemicals, acids (acetic, formic, propionic, butyric, and isobutyric acids), potassium sorbate, potassium benzoate, iodine, cinnamic acid, and ferulic acid (Bullerman, 1983; Kumar *et al.*, 1993; Nesci and Etcheverry, 2006; Mannaa and Kim, 2018). However, chemical residues and microbial resistance are problematic, and consumers increasingly want to replace chemical preservatives with plant-based antimicrobial agents (Mannaa and Kim, 2018).

The use of plant extracts could be a viable alternative to protect rice quality and extend shelf life. Many plant-derived essential oils (EOs) possess antibacterial, antifungal, antiviral, insecticidal, and antioxidant properties (Burt, 2004; Turgis *et al.*, 2012; Hossain *et al.*, 2014a; Hossain *et al.*, 2014b; Hossain *et al.*, 2016a). EOs are typically a mixture of volatile bioactive compounds such as monoterpenes, and sesquiterpenes, and their oxygenated derivatives (alcohols, aldehydes, esters, ethers, ketones, phenols, and oxides) (Turgis *et al.*, 2012; Hossain *et al.*, 2016a). The various terpene and polyphenol components of EOs have been accepted by the European Commission as flavorings for food products and approved by the US Food and Drug Administration (FDA) as GRAS (Generally Recognized as Safe). The commercial use of EOs has been limited because of negative impacts on taste and aroma, especially at high concentrations. Therefore, it is important to determine the minimal inhibitory concentration (MIC) for specific EOs and to develop EO mixtures showing synergistic effects at low concentrations, thereby limiting the

impact on food flavor and aroma (Turgis *et al.*, 2012; Tongnuanchan and Benjakul, 2014; Mohammadzadeh, 2017; Tardugno *et al.*, 2019).

In the present study, the antibacterial and antifungal activities of EOs and CEs against two foodborne pathogenic bacteria and three spoilage fungi were assessed by (i) determining MIC values using a broth microdilution assay, (ii) identifying possible synergistic interactions of combinations using the checkerboard method, (iii) developing active formulations by centroid mixture design, and (iv) evaluating the *in situ* antibacterial and antifungal effects of active formulations in rice during storage.

3.2. Materials and methods

3.2.1. Preparation of essential oils (EOs)

The essential oils (EOs) of Asian formulation, Mediterranean EO, Southern formulation were obtained from BSA (Montreal, Quebec, Canada). The cinnamon EO, savory thyme EO, and citrus EO were purchased from Zayat Aroma (Bromont, QC, Canada). The organic citrus extract (OCE) and natural citrus extract (NCE) were kindly provided by Kerry (Beloit, Wisconsin, USA). The chemical compositions of EOs and CEs are presented in Table 3.1. The chemical compositions of EOs and CEs were provided by BSA (Montreal, Quebec, Canada) and Zayat Aroma (Bromont, QC, Canada). EOs were prepared as oil-in-water (O/W) emulsions for use in the bioassays. Each emulsion contained 2 % (v/v) EO, 1 % (w/v) Tween-80 (Sigma-Aldrich Ltd, St. Louis, Missouri, USA, and 97 % distilled water (w/w) and was homogenized for 1 min at 15000 rpm using Ultra Turrax (TP18/1059 homogenizer) before use.

Table 3.1. Chemical compositions of the essential oils and citrus extracts.

Antibacterial/antifungal compounds	Major chemical compounds
Cinnamon EO	cinnamaldehyde (55.09%), cinnamyle acetate (9.57%), β -caryophyllene (4%), p-cymene (2.5%).
Savory thyme	borneol (27%), α -terpineol (11.9%), camphene (10.5%), α -pinene + α -thuyene (6.5%), β -caryophyllene (5.5%), Carvacrol (5.3%), p-cymene (3.9%), Linalol (3.7%), Terpinene-4-ol + methyl carvacrol ether (2.9%), 1,8-cineole + β -phellandrene (2.9%), Thymol (2.8%).
Asian formulation	geranial (39.1%), neral (31.6%), geraniol (6.7%), geranyl acetate (3.7%).
Mediterranean EO	carvacrol (46.1%), thymol (17.6%), γ -terpinene+ trans- β -ocimene (14.8%), p-cymene (8.5%).
Southern formulation	carvacrol (82%).
Citrus EO	limonene (69.5%), β -pinene (18.18%).
Organic citrus extract	polyphenols (3.36%) and flavonoids (0.62%).
Natural citrus extract	organic citrus extract, lauric arginate, fructo-oligosaccharide.

3.2.2. Preparation of bacterial/fungal cultures

The bacterial strains (*Salmonella* Typhimurium and *Escherichia coli* O157:H7) were stored at -80 °C in tryptic soy broth (TSB, BD, Franklin Lakes, NJ, USA), and the fungal strains (*Aspergillus niger*, *Penicillium chrysogenum*, *Mucor circinelloides*) were stored at -80 °C in potato dextrose broth (PDB, Alpha Biosciences, Inc., Baltimore, MD, USA). The bacteria were cultured in TSB and the fungi in PDB broth containing 10 % (v/v) glycerol (Ghabraie *et al.*, 2016). Before each experiment, the stock cultures were propagated through two consecutive growth cycles in TSB at 37 °C for 24 h (bacteria) or in PDB at 28 °C for 48 h (fungi). The cultures were recovered by centrifugation and washed with 0.85 % (w/v) saline water to obtain the desired pathogen concentrations for inoculation. Final bacterial and conidia culture concentrations were approximately 10⁵ CFU/mL or 10⁵ conidia/mL, respectively, for *in vitro* and *in situ* experiments.

3.2.3. Minimum inhibitory concentration (MIC)

A modified broth microdilution method was used to determine the minimum inhibitory concentration (MIC) of the EOs and CEs (Turgis *et al.*, 2012). A 100 μ L aliquot of 2-fold serial dilution (from 156.25-10,000 ppm) of EOs/CEs suspension was prepared and deposited in each well of a 96-well microplate (SARSTEDT, St. Leonard, QC, Canada) using TSB broth for bacteria

or PDB for fungi. Each well was then inoculated with 100 μL of 10^5 CFU/mL bacteria or 10^5 conidia/mL fungi and incubated for 24 or 48 h at 37 or 28 $^\circ\text{C}$, respectively. The positive control contained pathogen+TSB medium, while the negative control contained nutrient media+EOs/CEs (no pathogen). An Ultra Microplate Reader (Biotek Instruments, Winooski, USA) was used to evaluate microbial growth at 595 nm. The MIC was defined as the lowest concentration of the EOs/CEs suspension that completely inhibited bacterial and fungal growth. All experiments were performed in triplicate. The EOs and CEs were classified into three distinct groups based on MIC interval values, (i) highly effective (312.5-1,250 ppm), (ii) moderately effective (2,500-5,000 ppm), and (iii) less effective (10,000 ppm).

3.2.4. Synergistic interaction between antibacterial and antifungal

Interactions of antibacterial and antifungal compounds were evaluated using a checkerboard microdilution test. The checkerboard tests were performed using 96-well microplates to measure the fractional inhibitory concentration (FIC) index of EOs and CEs against each bacterium and fungus (Requena *et al.*, 2019). Fourteen combinations (dual combinations) were evaluated, including Mediterranean EO/OCE, Southern formulation/OCE, cinnamon EO/OCE, Asian formulation/OCE, citrus EO/OCE, cinnamon EO/NCE, Asian formulation/NCE, citrus EO/NCE, Southern formulation/citrus EO, cinnamon EO/Asian formulation, cinnamon EO/citrus EO, cinnamon EO/Mediterranean EO, cinnamon EO/savory thyme EO, savory thyme EO/Mediterranean EO. A volume of 100 μL of bacterial/fungal suspension (10^5 CFU/mL) was added to the wells of the microplate. The microplates were then incubated in a shaking incubator at 37 $^\circ\text{C}$ (bacteria)/28 $^\circ\text{C}$ (fungi) for 24 h (bacteria) or 48 h (fungi), respectively. The corresponding readings were taken with a microplate reader (BioTek, Elx800™) at 595 nm. All assays were performed in triplicate. The FIC values were calculated by the following Eq. 3.1:

$$\text{FIC} = \text{FIC}_1 + \text{FIC}_2 \quad \text{Eq. 3.1}$$

Where, $\text{FIC}_1 = (\text{MIC}_{1 \text{ combined}} / \text{MIC}_{1 \text{ alone}})$

$\text{FIC}_2 = (\text{MIC}_{2 \text{ combined}} / \text{MIC}_{2 \text{ alone}})$

An $\text{FIC} < 1$ was interpreted as a synergistic effect, $\text{FIC} = 1$ represented as an additive effect, $\text{FIC} > 1$ represented an antagonistic effect.

3.2.5. Mixture design to optimize the active formulations

Based on the results of MIC and FIC tests, two groups (Group-1 and Group-2) of antibacterials and antifungals containing a mixture of EOs and CEs were selected for the development of active formulations using a centroid mixtures plan (Design Expert® version 11). The two groups, Group-1 and Group-2 were named as active formulation 1 and active formulation 2, respectively, and mixture concentrations were determined based on optimization points. Group-1 contained OCE, Mediterranean EO, citrus EO, and cinnamon EO, and Group-2 contained NCE, Asian formulation, Southern formulation, cinnamon EO, and savory thyme EO. The independent variables for Group-1 (Total number of mixture formulations =24) and Group-2 (Total number of mixture formulations = 36) are presented in supplementary data Tables 3.1 and 3.2, respectively; the independent variables were varied from 0 to 1 without constraints on the experimental design plan and represented the different concentrations (from 0 to 10000 ppm) of each antibacterial and antifungal in the mixture. The composition data and their constraints for the mixture design for Group-1 and Group-2 are presented in Table 3.4 and Table 3.5, respectively.

3.2.6. Statistical analyses for developing active formulations

Each of the dependent variables was plotted in the design expert software for predicting the optimal values of each component present in Group-1 and Group-2 and fitted to special cubic and quadratic models Eq. 3.2 and Eq. 3.3:

$$Y = C_0 + \sum_{i=1}^n C_i X_i + \sum_{1 \leq i < j}^n C_{ij} X_i X_j \quad \text{Eq. 3.2}$$

$$Y = C_0 + \sum_{i=1}^n C_i X_i + \sum_{1 \leq i < j}^n C_{ij} X_i X_j + \sum_{1 \leq i < j < k}^n C_{ijk} X_i X_j X_k \quad \text{Eq. 3.3}$$

Where, Y is the dependent variable (MIC against each microorganism); C_0 , C_i , C_{ij} are the constant coefficient, linear coefficient, and the interactive coefficient, respectively; $X_i..X_j...X_k$ are independent variables; and n is the number of variables. The experiments were repeated three times. Model results were subjected to analysis of the variance (ANOVA), with significance at $P \leq 0.05$ (Falleh *et al.*, 2019; Radfar *et al.*, 2020).

The role of the different mixture parameters (independent variables) on the antimicrobial and antifungal responses was evaluated using contour plots and 3D images (Figure 3.1 and Figure

3.2). Contour plots and 3D images allow visualization of responses under different parameters by connecting all points within two-dimensional and three-dimensional planes, respectively (Falleh *et al.*, 2019; Radfar *et al.*, 2020). The plots also help visualize results when varying the constraints from 0 to 1 to obtain precise optimum points which were then tested experimentally.

3.2.7. *In situ* antibacterial and antifungal properties on packaged rice

The active formulation 1 and the active formulation 2 obtained from mixture design analysis were selected for testing in packaged rice against pathogenic bacteria (*E. coli* O157:H7, *S. Typhimurium*) and fungi (*A. niger*, *P. chrysogenum*, and *M. circinelloides*) following the method of (Hossain *et al.*, 2014a). Long-grain white rice was purchased from a local supermarket (Super quality basmati rice, Pitfield Ville St, Laurent, Quebec, Canada). A quantity of 50 g of rice (water activity: 0.90) was inoculated with 200 μ L of pathogenic bacteria (10^5 CFU/mL) or fungi (10^5 conidia/mL) in sterile plastic bags. Based on preliminary results, a quantity of 30 μ L of active formulation 1 or 2 was added to a sterile filter and placed inside a sterile plastic cup. The filter in plastic cups was covered with a muslin screen to prevent direct contact. The cups with a filter containing active formulation 1 or 2 were placed inside the packaged rice, which was inoculated with pathogenic bacteria and fungi. The samples were divided into two groups: (1) rice containing only inoculum (also called control sample), and (2) rice containing inoculum and active formulation 1 or 2. The triplicate of the experimental samples was incubated at 37 °C for bacteria and 27 °C for fungi for 28 days, and microbiological analyses were conducted after 1, 7, 14, 21, and 28 days of storage.

3.2.8. Microbiological analysis

The International Commission of Microbiological Specification on Foods (ICMSF) was followed as a standard method to perform microbiological analyses of packaged rice (Braide *et al.*, 2011). A quantity of 10 g of rice (water activity: 0.90) from each sample was placed into 20 mL of sterile peptone water (0.1 %, w/v) and homogenized for 60 sec at 260 rpm using a Lab-blender 400 stomacher (Laboratory Equipment, London, UK). A serial dilution of the homogenized sample was prepared (from 10^{-1} to 10^{-6}). A quantity of 0.1 mL of the diluted sample was inoculated onto the freshly prepared TSA (bacteria) and PDA (fungi) media. Then the plates were incubated at 37 °C for 24 h (bacteria) or 27 °C for 48h (fungi). The microbial colonies were counted using the plate count method (Begum *et al.*, 2020a).

3.3. Results and discussion

3.3.1. Minimum inhibitory concentration (MIC)

The antibacterial and antifungal effects of EOs and CEs in terms of MICs against selected pathogens are presented in Table 3.2. Results showed that among all the tested EOs and CEs, cinnamon EO, Mediterranean EO, Southern formulation, citrus EO, OCE, and NCE showed the highest antibacterial activity against *E. coli* O157:H7 and *S. Typhimurium* with MIC values of 312.5 to 1250 ppm. The Asian formulation showed moderate antibacterial activity (MIC = 5000 ppm) against the tested bacteria.

The EOs and CEs of cinnamon EO, Mediterranean EO, Southern formulation, citrus EO, OCE exhibited high activity against *A. niger*, *P. chrysogenum*, and *M. circinelloides*, with MIC values of 312.5-1250 ppm. The Asian formulation of EOs showed high activity against both *A. niger* and *P. chrysogenum*, with MIC values of 1250 and 625 ppm, respectively, but moderate antifungal activity against *M. circinelloides* (MIC = 5000 ppm). The NCE showed high antifungal activity against *P. chrysogenum* (MIC = 1250 ppm), but moderate antifungal activity against *A. niger* and *M. circinelloides* (MIC = 2500 ppm) (Table 3.2).

Table 3.2. Minimal inhibitory concentration (MIC, ppm) of essential oils (EOs) and citrus extracts (CEs) against two foodborne pathogens and three spoilage fungi.

Antibacterial/antifungal compounds	Minimal Inhibitory Concentration (ppm)				
	<i>E. coli</i> 0157:H7	<i>S. Typhimurium</i>	<i>A. niger</i>	<i>P. chrysogenum</i>	<i>M. circinelloides</i>
Cinnamon EO	1250	1250	625	312.5	1250
Savory thyme EO	2500	5000	5000	2500	2500
Asian formulation	5000	5000	1250	612	5000
Mediterranean EO	1250	1250	1250	1250	1250
Southern formulation	625	625	625	625	625
Citrus EO	1250	1250	625	625	625
Organic citrus extract	1250	312.5	625	625	1250
Natural citrus extract	1250	312.5	2500	1250	2500

The antibacterial, antifungal, and antioxidant activities of EOs and CEs depend on the mixture of chemical compounds, their active ingredients, and concentrations (Turgis *et al.*, 2012; Aziz and Karboune, 2018). The EOs are complex mixtures of up to 45 different compounds (Hyldgaard *et al.*, 2012b). Based on the literature, the major components of cinnamon EO, Mediterranean EO, Southern formulation, citrus EO, and citrus extracts are mostly cinnamaldehyde, carvacrol, thymol, eugenol, limonene, terpineol, geraniol, neral, myrcene, trans-caryophyllene, and borneol, which all possess strong antibacterial and antifungal properties (Zachariah and Leela, 2006; Dzamic *et al.*, 2008). Mith *et al.* (2014) reported the strong antibacterial activity of *Cinnamomum verum*, *Origanum compactum*, and *Origanum heracleoticum* EOs against *S. Typhimurium*, *E. coli* O157:H7, *Listeria monocytogenes*. The main phenolic compounds carvacrol and thymol in oregano and trans cinnamaldehyde in cinnamon are responsible for antibacterial activity in oregano EO (Dussault *et al.*, 2014; Mith *et al.*, 2014).

Thymol and carvacrol are the dominant chemical compounds found in Mediterranean EO and Southern formulation. The major mode of antimicrobial action of thymol is to interact with the outer and inner membrane proteins as well as intracellular targets. Thymol interacts with gram-negative bacteria causing the release of lipopolysaccharides (LPS) and disrupts the outer membrane of the bacteria. When thymol interacts with intracellular targets, it affects energy-generating processes, and the exposed bacterial cell cannot recover (Hyldgaard *et al.*, 2012b). Carvacrol is a phenolic monoterpenoid and closely related isomer of thymol. The savory thyme EO, Mediterranean EO, Southern formulation contain carvacrol, which causes the release of LPS from the outer membrane of gram-negative bacteria and thus enhances the cell permeability of the cytoplasmic membrane (Hyldgaard *et al.*, 2012b; Tongnuanchan and Benjakul, 2014). The activity of Spanish oregano, Chinese cinnamon, and savory thyme (*Satureja montana*) EOs against *E. coli* O157:H7 and *L. monocytogenes* was studied by Oussalah *et al.* (2006); these EOs affected the membrane integrity of the bacteria and caused a reduction of the intracellular ATP concentration resulting in cell death. Dussault *et al.* (2014) evaluated sixty-seven EOs, oleoresins (OR), and pure compounds against *Staphylococcus aureus*, *L. monocytogenes*, *Bacillus cereus*, *E. coli*, *S. Typhimurium*, and *Pseudomonas aeruginosa*; allyl isothiocyanate, cinnamon Chinese cassia, cinnamon OR, oregano, and red thyme all showed high antibacterial activity; oregano and cinnamon cassia EOs reduced the growth rate of *L. monocytogenes* on ham by 19 and 10 % at a concentration of 500 ppm, respectively.

The citrus extracts (OCE and NCE) showed stronger antibacterial and antifungal activity in the broth microdilution assay against all tested microorganisms. OCE and NCE are commercial citrus extracts and contain phenolic acids and bioflavonoids as active ingredients with antibacterial and

antifungal properties (Maherani *et al.*, 2018); these active components cause conformational and compositional damage to the cell membrane (Bilbao *et al.*, 2007; Maherani *et al.*, 2018). The mode of action of citrus extracts depends on the quantity of active components. At low concentrations, active compounds interfere with microbial enzymes related to energy production, whereas, at high concentrations, the microbial proteins are denatured (Maherani *et al.*, 2018). The main constituents of *Zataria multiflora* EOs (carvacrol, thymol, and eugenol) inhibited the synthesis of microbial DNA and transcription of genes involved in aflatoxin synthesis (Yahyaraeyat *et al.*, 2013).

3.3.2. Synergistic interactions between antibacterial and antifungal compounds

The antibacterial and antifungal effects of the combined EOs and CEs by the checkerboard method are presented in Table 3.3. Results showed that the combinations of Mediterranean EO+OCE, Southern formulation+OCE, Asian formulation+NCE, cinnamon EO+citrus EO, and savory thyme EO+Mediterranean EO caused a synergistic effect against the bacteria (*E. coli* O157:H7 and *S. Typhimurium*) because their FIC values were below 1. The mixture of cinnamon EO and Asian formulation showed a synergistic and additive effect against *E. coli* O157:H7 (FIC < 1) and *S. Typhimurium* (FIC = 1), respectively. The dual combinations of cinnamon EO+OCE, and Asian formulation+OCE, and cinnamon EO+Mediterranean EO exhibited synergistic activity against *E. coli* O157:H7 (FIC < 1), while those combinations showed antagonistic activity against *S. Typhimurium*. The combination of citrus EO+OCE and Southern formulation+citrus EO showed synergistic activity against *S. Typhimurium*, while those combinations showed antagonistic activity against *E. coli* O157:H7 (FIC > 1) (Table 3.3).

The mixture of Mediterranean EO+OCE, citrus EO+OCE showed synergy against *A. niger*, *P. chrysogenum*, and *M. circinelloides* (FIC < 1). The combinations of cinnamon EO+OCE and savory thyme EO+Mediterranean EO showed synergy against *A. niger* and *P. chrysogenum* (FIC < 1), however, this formulation showed antagonistic activity against *M. circinelloides* (FIC > 1). Citrus EO mixed with NCE showed synergy against *A. niger* and *P. chrysogenum* but showed additive effect against *M. circinelloides* (FIC = 1). The combinations of Asian formulation+OCE, Asian formulation+NCE, cinnamon EO+NCE, and cinnamon EO+citrus EO showed synergistic effects against *A. niger*. Southern formulation+OCE, and Southern formulation+citrus EO showed a synergistic effect against *P. chrysogenum*. The mixture of Asian formulation NCE, cinnamon EO+Asian formulation, cinnamon EO+citrus EO showed a synergistic effect against *M. circinelloides* (Table 3.3).

Table 3.3. Fractional inhibitory concentration (FIC) and interaction effect of double combinations between essential oils (EOs) and citrus extracts (CEs) antibacterial/antifungals.

Antimicrobial combination (antimicrobial compound 1/antimicrobial compound 2)	<i>E. coli</i> O157: H7		<i>S. Typhimurium</i>		<i>A. niger</i>		<i>P. chrysogenum</i>		<i>M. circinelloides</i>	
	FIC	Effect	FIC	Effect	FIC	Effect	FIC	Effect	FIC	Effect
Mediterranean EO/organic citrus extract	0.75±0.21 ^a	S	0.50±0.23 ^a	S	0.75±0.11 ^{ab}	S	0.62±0.13 ^a	S	0.50±0.20 ^a	S
Southern formulation/organic citrus extract	0.62±0.19 ^a	S	0.75±0.26 ^a	S	1.50±0.36 ^c	AG	0.62±0.11 ^a	S	1.25±0.2 ^{abc}	AG
Cinnamon EO/organic citrus extract	0.50±0.21 ^a	S	3.00±1.04 ^b	AG	0.75±0.31 ^{ab}	S	0.38±0.08 ^a	S	2.00±0.51 ^b	AG
Asian formulation/organic citrus extract	0.75±0.27 ^a	S	4.50±1.06 ^c	AG	0.50±0.10 ^a	S	2.00±0.56 ^b	AG	1.00±0.33 ^{ab}	AD
Citrus EO/organic citrus extract	1.50±0.54 ^b	AG	0.75±0.13 ^a	S	0.75±0.25 ^{ab}	S	0.75±0.43 ^a	S	0.62±0.41 ^a	S
Cinnamon EO/natural citrus extract	1.0±0.17 ^{ab}	AD	0.75±0.22 ^a	S	0.50±0.07 ^a	S	3.00±0.71 ^{bc}	AG	1.50±0.32 ^{bc}	AG
Asian formulation/natural citrus extract	0.50±0.15 ^a	S	0.31±0.23 ^a	S	0.62±0.26 ^a	S	5.00±1.51 ^{de}	AG	0.50±0.09 ^a	S
Citrus EO/natural citrus extract	3.00±0.79 ^c	AG	3.00±1.21 ^b	AG	0.62±0.18 ^a	S	0.50±0.21 ^a	S	1.00±0.08 ^{ab}	AD
Southern formulation/Citrus EO	1.50±0.44 ^b	AG	0.75±0.33 ^a	S	1.00±0.13 ^b	AD	0.50±0.19 ^a	S	1.50±0.61 ^{bc}	AG
Cinnamon EO/Southern formulation	0.50±0.17 ^a	S	1.00±0.22 ^a	AD	2.50±1.72 ^d	AG	4.00±1.02 ^{cd}	AG	0.75±0.13 ^{ab}	S
Cinnamon EO/Citrus EO	0.75±0.11 ^a	S	0.75±0.13 ^a	S	0.75±0.23 ^{ab}	S	2.50±1.51 ^b	AG	0.50±0.22 ^a	S
Cinnamon EO/Mediterranean EO	0.50±0.13 ^a	S	3.00±1.31 ^b	AG	2.50±0.23 ^d	AG	6.00±2.23 ^e	AG	4.00±1.12 ^c	AG
Cinnamon EO/Savory thyme EO	6.00±1.12 ^d	AG	1.25±0.28 ^a	AG	1.50±0.41 ^c	AG	2.50±0.63 ^b	AG	1.50±0.19 ^{bc}	AG
Savory thyme EO/Mediterranean EO	0.75±0.12 ^a	S	0.75±0.19 ^a	S	0.50±0.09 ^a	S	0.50±0.13 ^a	S	2.00±0.42 ^b	AG

Abbreviations: FIC, Fractional Inhibitory Concentration; S, Synergistic; AD, Additive; AG, Antagonistic. FIC index < 1: Synergistic; FIC index = 1: Additive; FIC index > 1: Antagonistic. Results expressed as ppm. Within each column means with the same lowercase letter are not significantly different (P > 0.05).

The combinations of antibacterial and antifungal compounds above were assessed for possible synergistic activity so that lower effective concentrations of compounds might be used to reduce any undesirable organoleptic properties in foods. When the combination of antimicrobials showed synergy, it meant that the effect of the combined compounds was greater than the sum of the individual effects (Burt, 2004). It is well known that the minor components of EOs may play a significant role in their activity and may have a synergistic or potentiating effect (Burt, 2004). The potential synergistic activity between EOs and citrus extracts provides a means of reducing the active doses needed to achieve antimicrobial effects in food (Requena *et al.*, 2019).

The FIC results showed that the combination of Mediterranean EO+OCE had synergistic antibacterial and antifungal activities against all tested microorganisms. When carvacrol from Mediterranean EO, an acid phenol, is combined with monoterpenes (e.g., α -pinene, camphene, myrcene, α -terpinene, and p-cymene) from the Mediterranean EO, they may interact with the microbial cell membrane to facilitate the carvacrol to penetrate into the cell and show synergistic effect (Ultee *et al.*, 2002; de Azeredo *et al.*, 2011; Ghabraie *et al.*, 2016). The combination of oregano EO and Citrox® (containing citric acid and acid phenols (bioflavonoids) as active ingredients) reduced by 3.7-4.0 log CFU/g the level of *E. coli* O157:H7 in spinach and lettuce samples without color change (Poimenidou *et al.*, 2016a). The present study reported similar observations for the combination of Mediterranean EO and OCE against *E. coli*, *S. Typhimurium*, *A. niger*, *P. chrysogenum* and *M. circinelloides*. Overall, MIC and FIC results demonstrated that combinations of EOs and CEs can have synergistic effects and could be proposed for food preservation as bioactive formulations at low concentrations that may avoid problems with off flavors while preserving food (Turgis *et al.*, 2012; Hossain *et al.*, 2016a).

3.3.3. Mixture design and optimization for active formulations

The mixture designs with three or four EOs with CEs and their responses with each compound are presented in Figure 3.1-3.2. The ANOVA analyses for the two active formulations 1 and 2 are presented in supplementary data Table 3.3 and 3.4, respectively. The statistical models and ANOVA analyses for active formulation 1 and 2 predicted the effect of the different mixtures against tested bacteria and fungi by measuring MIC values. In the case of active formulation 1, the quadratic and special cubic models were highly significant for *E. coli* O157:H7 (F-value = 22.22; P = 0.0001; df = 9) and *S. Typhimurium* (F-value = 6.94; P = 0.0021; df = 13), respectively (Supplementary data Table 3.3). The higher coefficient of determination values (R^2 values) of the quadratic and special cubic model for *E. coli* O157:H7 (R^2 = 93 %) and *S. Typhimurium* (R^2 = 90

%) indicated a good agreement between the experimental and the predicted values of the models. The special cubic model was significant for *A. niger* and *M. circinelloides* while showing the respected F-values were 14.1 (P = 0.0001) and 3.82 (P = 0.0201) (Supplementary data Table 3.3). The R² values (coefficient of determination values) of the special cubic model for *A. niger* and *M. circinelloides* were 95 % and 83 %, respectively, signifying the good agreement between the experimental and the predicted values.

Table 3.4. Independent variables (antibacterial/antifungal compounds) of active formulation 1, their constraints (proportions from 0 to 1 and concentration of antibacterial/antifungal compounds from 0 to 10000 ppm) for the centroid-mixture design method.

Component	Name	Symbol (unit)						
		0	0.125	0.25	0.33	0.5	0.6	1
A	Organic citrus extract (OCE) (ppm)	0	313	625	1250	2500	5000	10000
B	Mediterranean EO (ppm)	0	157	313	625	1250	2500	5000
C	Citrus EO (ppm)	0	313	625	1250	2500	5000	10000
D	Cinnamon (ppm)	0	157	313	625	1250	2500	5000

Table 3.5. Independent variables (antibacterial/antifungal compounds) of active formulation 2 and their constraints (proportions from 0 to 1 and concentration of antibacterial/antifungal compounds from 0 to 10000 ppm) for the centroid-mixture design method.

Component	Name	Symbol (unit)						
		0	0.125	0.25	0.33	0.5	0.6	1
A	Natural citrus extract (NCE) (ppm)	0	313	625	1250	2500	5000	10000
B	Asian formulation (ppm)	0	313	625	1250	2500	5000	10000
C	Southern formulation (ppm)	0	157	313	625	1250	2500	5000
D	Cinnamon EO (ppm)	0	313	625	1250	2500	5000	10000
E	Savory thyme EO (ppm)	0	157	313	625	1250	2500	5000

The mathematical models for representing response expressed as the minimal inhibitory concentration (MIC) against *E. coli* O157:H7, *S. Typhimurium*, *A. niger*, *P. chrysogenum*, and *M. circinelloides* in terms of the four independent variables (A: OCE, B: Mediterranean EO, C: citrus EO, and D: cinnamon EO) are as follows equation 3.4, 3.5, 3.6, 3.7 and 3.8, respectively:

E. coli O157:H7 (MIC, ppm) = 1244.7A + 1263.6B + 1250.6C + 1252.6D - 3362.7AB - 1075.2AC - 4065.9AD - 4124.2BC - 3364.9BD - 4031.4CD Eq. 3.4

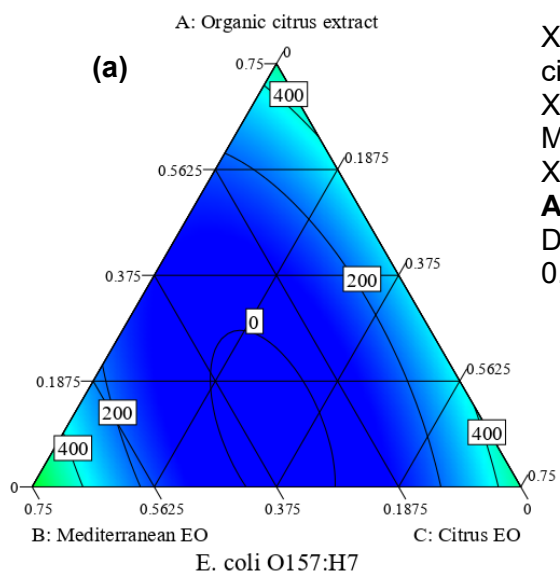
S. Typhimurium (MIC, ppm) = 329.2A + 1220.4B + 1258.8C + 1213D - 167.2AB - 686.5AC + 1696AD - 180.4BC + 4702.6BD - 2698.8CD - 1522.9ABC - 11386.7ACD - 33922.5BCD Eq. 3.5

A. niger (MIC, ppm) = 626A + 1211B + 629C + 637D - 1333AB - 1282AC - 1887AD - 1386BC + 1133BD - 1881CD - 7865ABC - 11169ABD + 2403ACD - 11836BCD Eq. 3.6

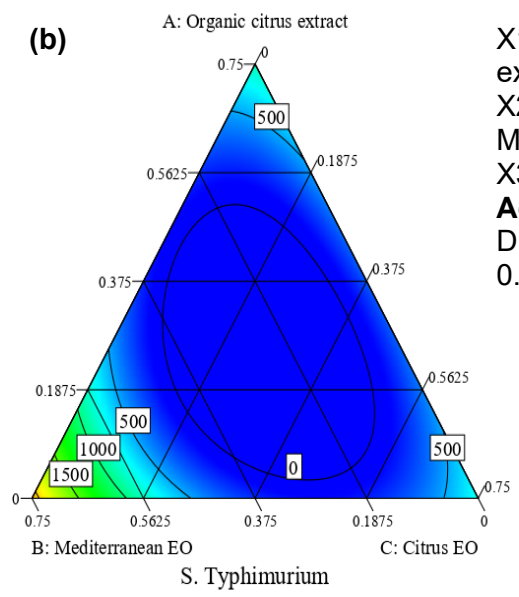
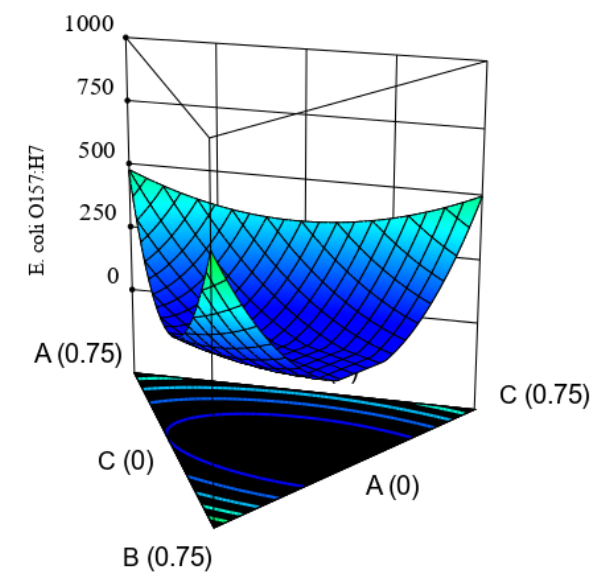
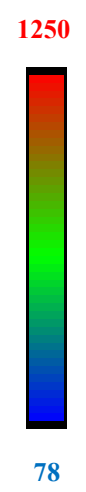
P. chrysogenum (MIC, ppm) = 643A + 1200B + 625C + 1715D + 1408AB - 1371AC - 2319AD + 5957BC - 1241BD - 2365CD - 35856ABC - 19935ABD - 2996ACD - 33918BCD Eq. 3.7

M. circinelloides (MIC, ppm) = 1249A + 1191B + 644C + 1247D - 487AB - 2643AC - 200AD + 5959BC + 4652BD - 2648CD - 29744ABC - 38012ABD - 4338ACD - 44928BCD Eq. 3.8

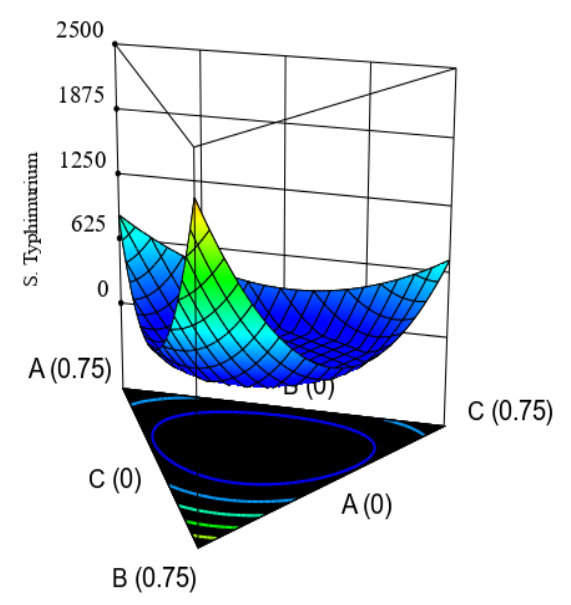
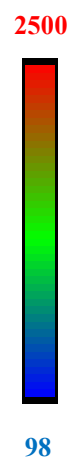
The combinations containing OCE, Mediterranean EO, citrus EO, and cinnamon EO among the twenty-four runs for Group-1 showed the strongest antibacterial and antifungal properties against *E. coli* O157:H7, *S. Typhimurium*, *A. niger*, *P. chrysogenum*, and *M. circinelloides*. Figure 3.1 a-e showed the ternary diagrams (contour plot and 3D images) of interactions among each independent variable used in active formulation 1 (Group-1) against two pathogenic bacteria (*E. coli* O157:H7 and *S. Typhimurium*) and three spoilage fungi (*A. niger*, *P. chrysogenum* and *M. circinelloides*). The region of dark blue color in the contour plot and 3D images indicated lower MIC values (higher microbicidal effectiveness), while the green to the red color indicated medium to higher MIC values (less strong antimicrobial effectiveness). When OCE (625 ppm), the Mediterranean EO (313 ppm), the citrus EO (625 ppm), and the cinnamon EO (313 ppm) were mixed following the symbolic variable unit of 0.25 for each independent variable, they significantly reduced the inhibition concentrations of 78, 98, 89, 92, and 110 ppm for *E. coli* O157:H7, *S. Typhimurium*, *A. niger*, *P. chrysogenum*, and *M. circinelloides*, respectively, while the combination of OCE and Mediterranean EO (without citrus EO and cinnamon EO) at the independent variable symbolic unit 0.5 (OCE: 2500 ppm and Mediterranean EO: 12560 ppm) were increased the corresponded MIC values 8 (625 ppm), 3 (313 ppm), 7 (625 ppm), 6.8 (625 ppm) and 2.8 (313 ppm) times higher (reduced microbicidal effectiveness) (Supplementary data Table 3.1). According to the data in supplementary data Table 3.1 and Figure 3.1 a-e (contour plot and 3D images), the centroid-mixture design optimized that the combination of OCE, Mediterranean EO, citrus EO, and cinnamon EO at the respected concentration of 625, 313, 625, and 313 ppm expressed the lowest MIC (strongest antibacterial and antifungal efficiencies) against all tested pathogenic bacteria and fungi.

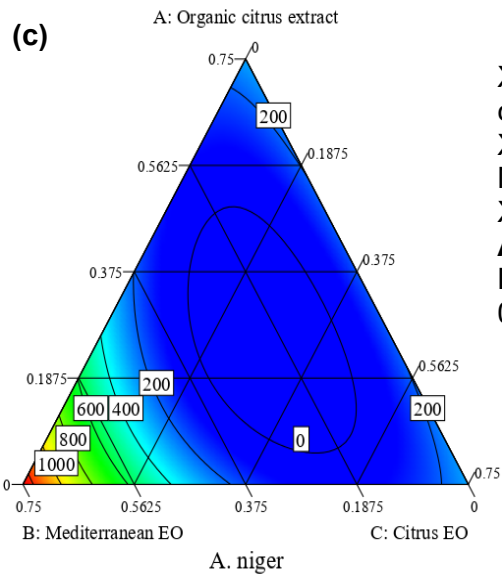


X1 = A: Organic citrus extract
X2 = B: Mediterranean EO
X3 = C: Citrus EO
Actual component
D: Cinnamon EO = 0.25



X1 = A: Organic citrus extract
X2 = B: Mediterranean EO
X3 = C: Citrus EO
Actual component
D: Cinnamon EO = 0.25



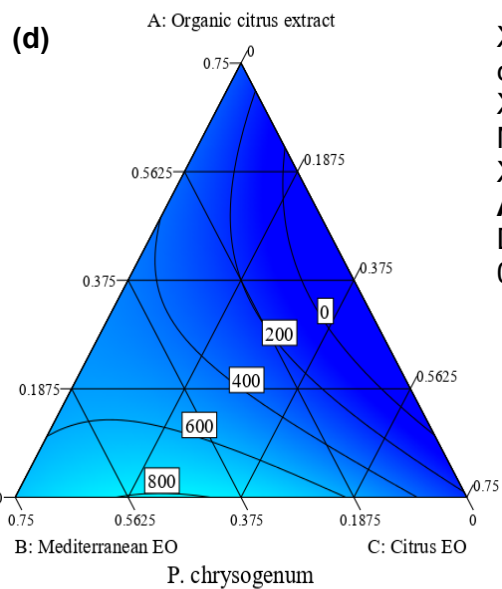
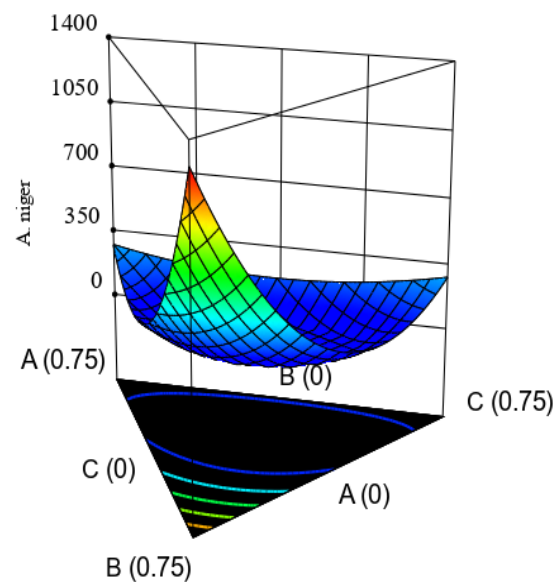


X1 = A: Organic citrus extract
 X2 = B: Mediterranean EO
 X3 = C: Citrus EO
Actual component
 D: Cinnamon EO = 0.25

1250

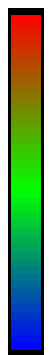


89

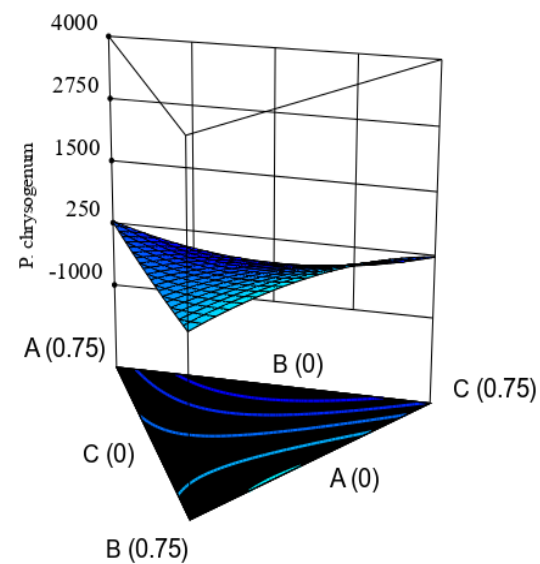


X1 = A: Organic citrus extract
 X2 = B: Mediterranean EO
 X3 = C: Citrus EO
Actual component
 D: Cinnamon EO = 0.25

3126



78



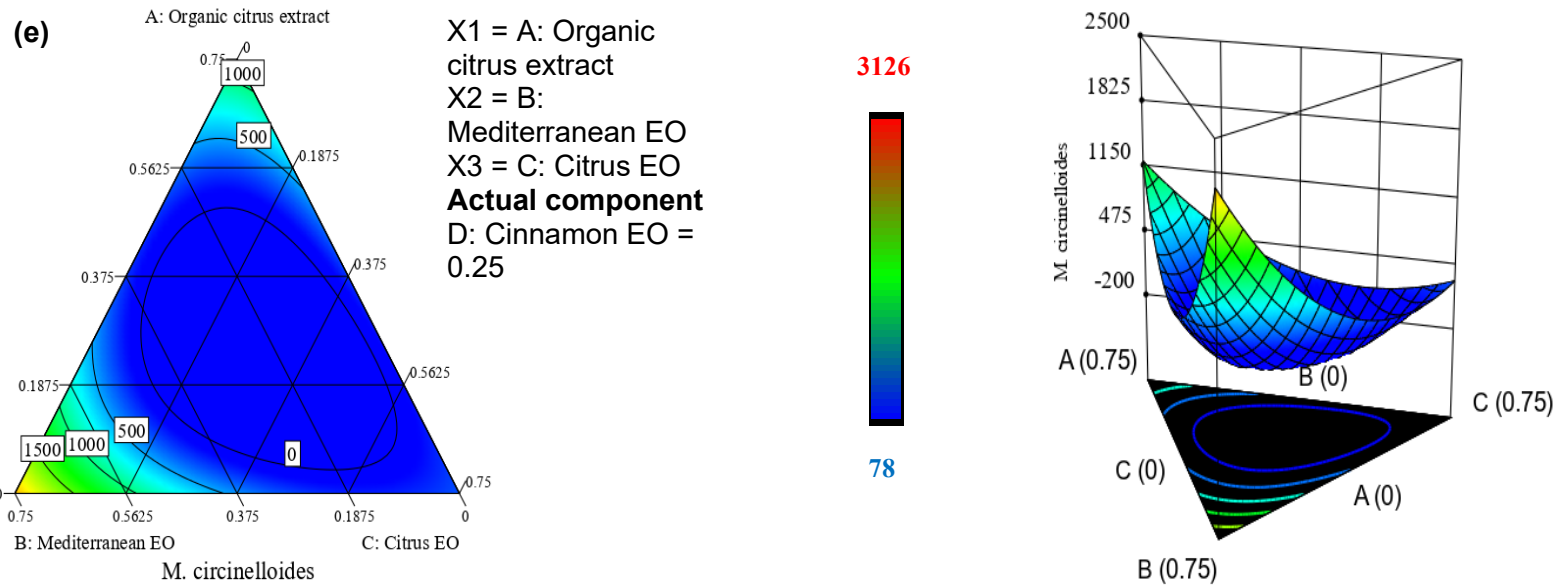


Figure 3.1. Optimization of the independent variables presented in the active formulation 1 using contour plot and 3D image against (a) *E. coli* O157 H7, (b) *S. Typhimurium*, (c) *A. niger*, (d) *P. chrysogenum*, and (e) *M. circinelloides*. The region of dark blue color indicates higher microbicidal effectiveness, while the green to yellow to red colors indicate increasingly weaker antimicrobial effectiveness.

The mixture of NCE, Asian formulation, Southern formulation, cinnamon EO, and savory thyme EO among the thirty-six runs for Group-2 showed the strong antibacterial and antifungal properties against *E. coli* O157:H7, *S. Typhimurium*, *A. niger*, *P. chrysogenum*, and *M. circinelloides*. Further, by considering the antibacterial and antifungal properties the Group-2 was named as active formulation 2. For active formulation 2, the quadratic model was significant for both *E. coli* O157:H7 (F-value: 6.83; $P \leq 0.0001$; df: 14) and *S. Typhimurium* (F-value: 6.20; $P = 0.0001$; df: 14) (Supplementary data Table 3.4). The coefficient of determination (R^2 values) of the quadratic model for both *E. coli* O157:H7 ($R^2 = 82\%$) and *S. Typhimurium* ($R^2 = 80\%$) indicated a good agreement between the experimental and the predicted values of the models. A quadratic, special cubic and quadratic model was significant for *A. niger*, *P. chrysogenum* and *M. circinelloides*, respectively, and showing their corresponded F-values were 6.72 ($P \leq 0.0001$; df: 14; $R^2 = 82\%$), 5.88 ($P = 0.002$; df: 24; $R^2 = 93\%$) and 7.26 ($P \leq 0.0001$; df: 14; $R^2 = 83\%$) (Supplementary data Table 3.4). The mathematical models for representing response expressed as the minimal inhibitory concentration (MIC) against *E. coli* O157:H7, *S. Typhimurium*, *A. niger*, *P. chrysogenum*, and *M. circinelloides* in terms of the five independent variables (A: NCE, B: Asian formulation, C: Southern formulation, D: cinnamon EO, and E: savory thyme EO) are as follows equation 3.9, 3.10, 3.11, 3.12, and 3.13, respectively:

$$E. coli \text{ O157:H7 (MIC, ppm)} = 1469A + 4976B + 866C + 1365D + 2673E - 7569AB - 4151AC - 3952AD - 1764AE - 7701BC - 11562BC \text{ Eq. 3.9}$$

$$S. Typhimurium \text{ (MIC, ppm)} = 473A + 4864B + 976C + 1268D + 5016E - 8848AB - 1764AC - 291AD - 7999AE - 7822BC - 8764BD - 11969BE - 2801CD + 1899CE - 8108DE \text{ Eq. 3.10}$$

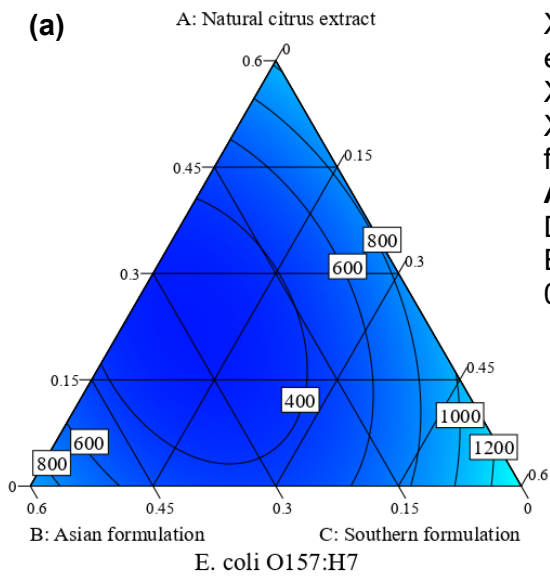
$$A. niger \text{ (MIC, ppm)} = 2530A + 1385B + 967C + 743D + 5013E - 4759AB - 6112AC - 4603AD - 11872AE - 4782BC + 728BD - 9730BE - 2480CD + 2138CE - 9864DE \text{ Eq. 3.11}$$

$$P. chrysogenum \text{ (MIC, ppm)} = 1196A + 621B + 652C + 345D + 2360E + 6065AB - 1451AC - 626AD - 2589AE - 229BC + 596BD - 1368BE - 669CD + 3616CE - 3059DE - 22978ABC - 21015ABD - 3905ABE - 3041ACD - 30462ACE - 1781ADE - 8812BCD - 27795BCE - 3332BDE - 14421CDE \text{ Eq. 3.12}$$

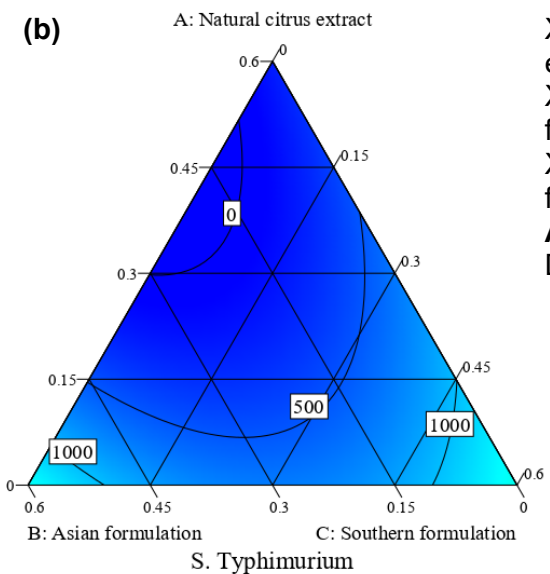
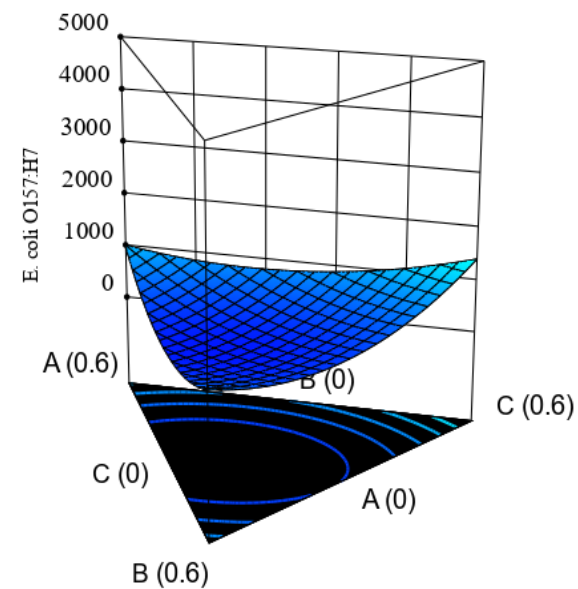
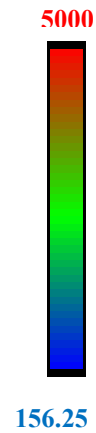
$$M. circinelloides \text{ (MIC, ppm)} = 2609A + 4827B + 885C + 1394D + 2663E - 9173AB - 6316AC - 3733AD - 4225AE - 9142BC - 9111BD - 11227BE - 687CD + 212CE - 4395DE \text{ Eq. 3.13}$$

The mixture of NCE, Asian formulation, Southern formulation, cinnamon EO, and savory thyme EO among the thirty-six runs for Group-2 showed strong antibacterial and antifungal properties against two pathogenic bacteria and three spoilage fungi. Considering the antibacterial and antifungal properties of Group-2 was named as active formulation 2. Figure 3.2 a-e showed the ternary diagrams (contour plot and 3D images) of interactions among each independent variable

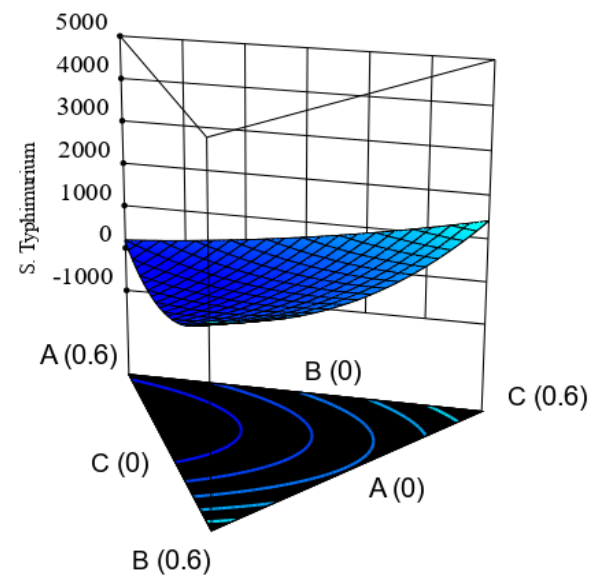
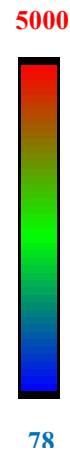
used in active formulation 2 against the tested bacteria and fungi. The dark blue color region in the contour plot and 3D images indicated the strongest microbicidal effectiveness (lower MIC values), while the green to the red color indicated medium to higher MIC values (not strong antimicrobial effectiveness). The NCE, Asian formulation, Southern formulation, cinnamon EO, and savory thyme EO was mixed in the concentration of 0.2 for each independent variable (symbolic variable unit), they significantly reduced the inhibition concentrations of 156, 156, 78, 78, and 92, and 156 ppm for *E. coli* O157:H7, *S. Typhimurium*, *A. niger*, *P. chrysogenum*, and *M. circinelloides*, respectively, while the combination of Asian formulation and Southern formulation (without NCE, cinnamon and savory thyme EO) at the independent variable symbolic unit 0.5 were increased the corresponded MIC values (reduced microbicidal effectiveness) 8 (1250 ppm), 8 (156 ppm), 4 (313 ppm), 8 (625 ppm) and 4 (625 ppm) times higher (Supplementary data Table 3.2). The centroid-mixture design optimized that the combination of NCE, Asian formulation, Southern formulation, cinnamon EO, and savory thyme EO at the respected concentration of 625, 625, 313, 625, and 313 ppm expressed the lowest MIC (strongest antibacterial and antifungal efficiencies) against all tested pathogenic bacteria and fungi (Supplementary data Table 3.2 and Figure 3.2 a-e).



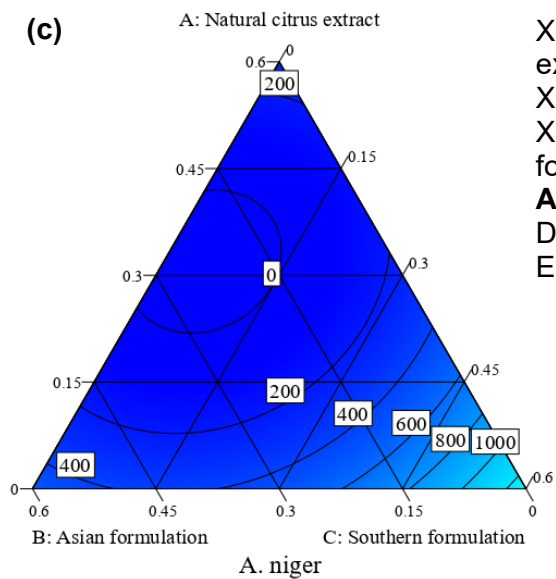
X1 = A: Natural citrus extract
 X2 = B: Asian formulation
 X3 = C: Southern formulation
Actual component
 D: Cinnamon EO = 0.2
 E: Savory thyme EO = 0.2



X1 = A: Natural citrus extract
 X2 = B: Asian formulation
 X3 = C: Southern formulation
Actual component
 D: Cinnamon EO = 0.2

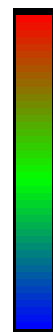


(c)

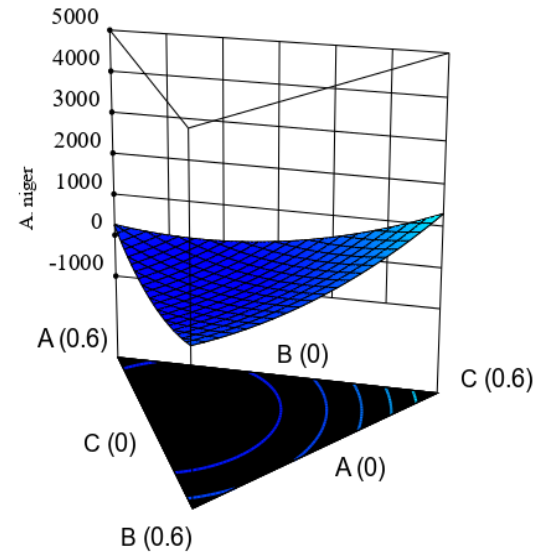


X1 = A: Natural citrus extract
 X2 = B: Asian formulation
 X3 = C: Southern formulation
Actual component
 D: Cinnamon EO = 0.2
 E: Savory thyme EO =

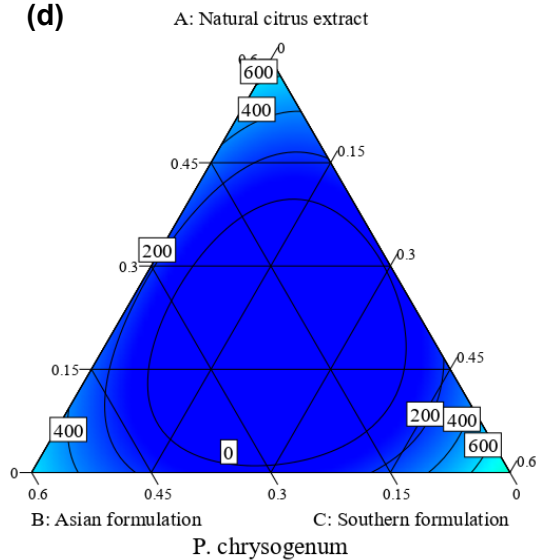
5000



78

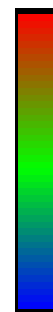


(d)

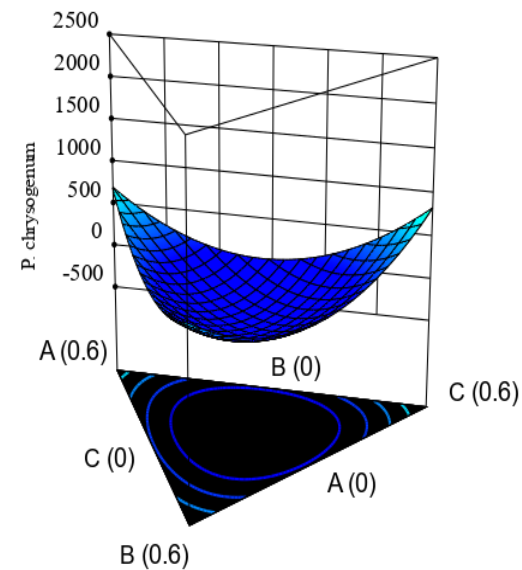


X1 = A: Natural citrus extract
 X2 = B: Asian formulation
 X3 = C: Southern formulation
Actual component
 D: Cinnamon EO = 0.2

2500



78



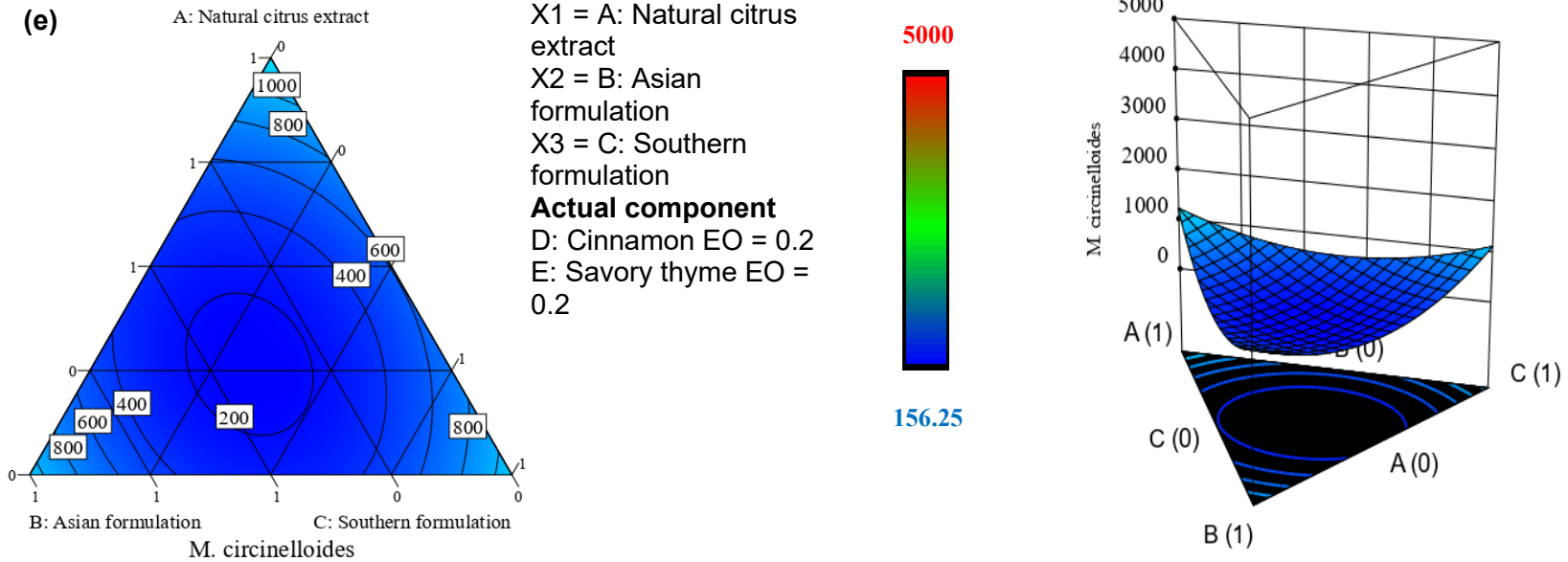


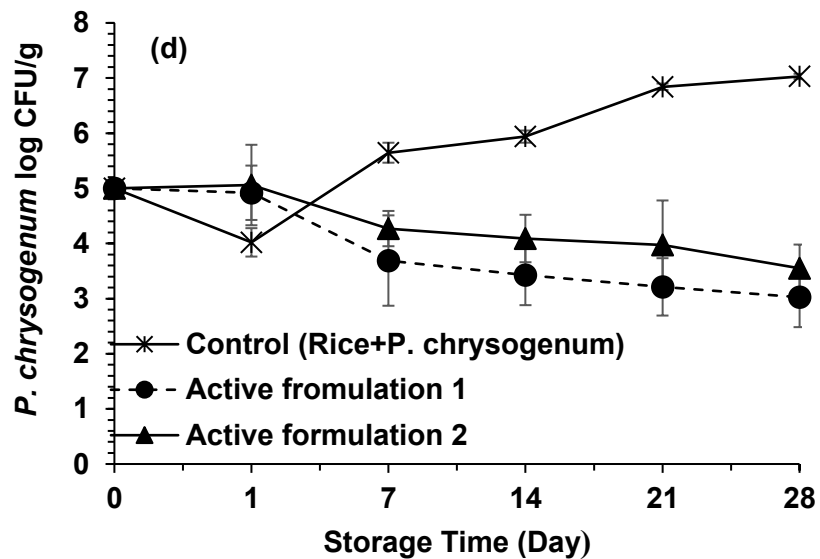
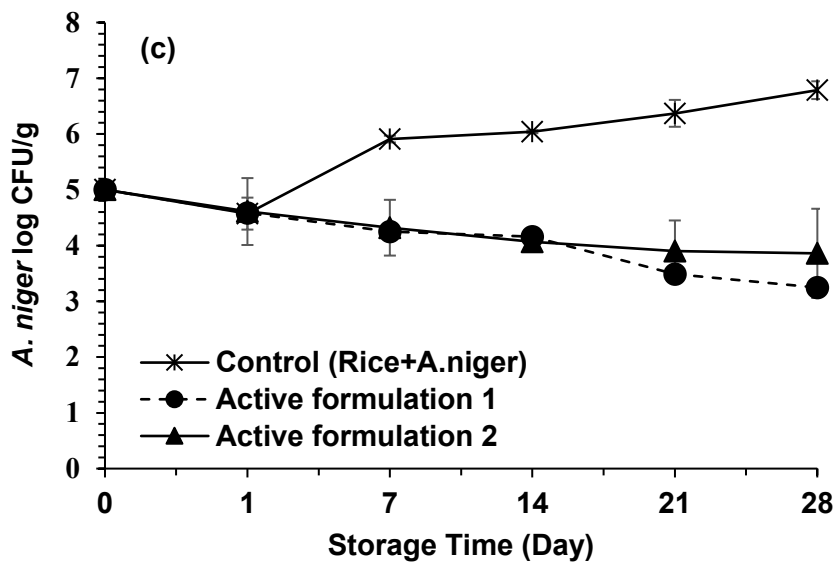
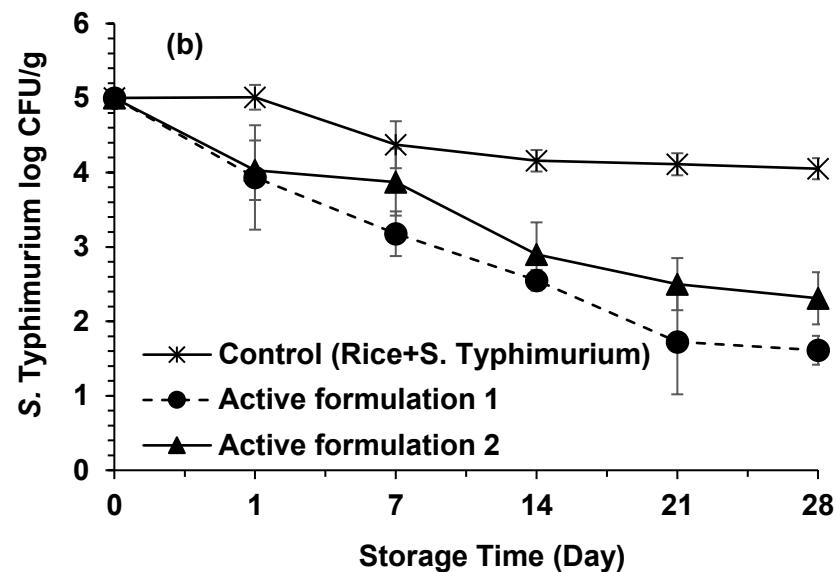
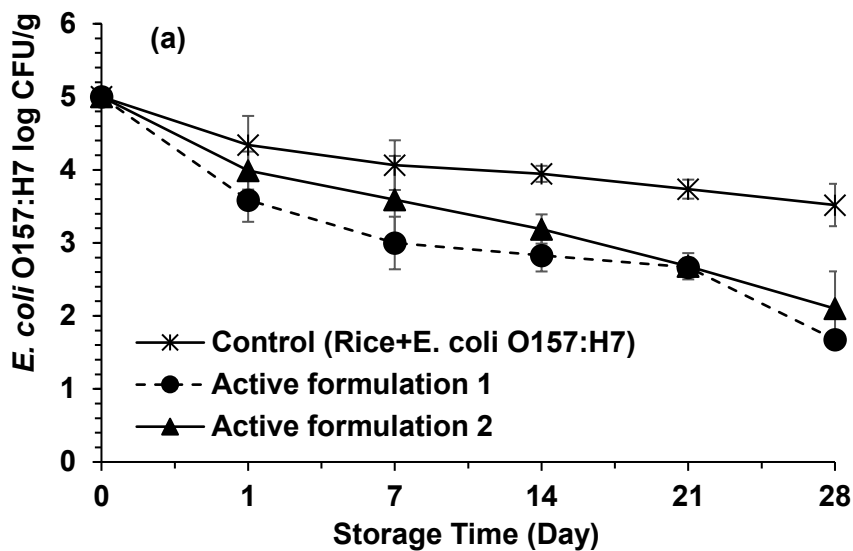
Figure 3.2. Optimization of the independent variables presented in the active formulation 2 using contour plot and 3D image against (a) *E. coli* O157 H7, (b) *S. Typhimurium*, (c) *A. niger*, (d) *P. chrysogenum*, and (e) *M. circinelloides*. The region of dark blue color indicates higher microbicidal effectiveness, while the green to yellow to red colors indicate increasingly weaker antimicrobial effectiveness.

Many chemical ingredients are presented in the optimal formulation and each of these molecules has several sites to act on microbial cells. For example, the enzyme action of *E. coli* might be disabled by the action of hydroxyl and carbonyl groups present in the eugenol and cinnamaldehyde (Falleh *et al.*, 2019). The oxygenated terpenoids (phenolic terpenes, phenylpropanoids, and alcohols) are the major antibacterial/antifungal components in EOs and CEs. The hydrocarbons (α -pinene, camphene, myrcene, α -terpinene and *p*-cymene) present in EOs and plant extracts showed low antimicrobial/antifungal activities when applied alone, but in combinations, they increased their effectiveness (Hossain *et al.*, 2016a; Nikkhah *et al.*, 2017b). For example, *p*-cymene showed relatively weak antimicrobial activity when used alone but combination with other strong components like carvacrol significantly enhanced its effectiveness (Poimenidou *et al.*, 2016a); *p*-cymene of EOs and plant extracts is considered as a substitutional impurity in the membrane which has a high affinity to bind membranes and decreased the membrane enthalpy and melting temperature, thus helping carvacrol to penetrate easily inside the cell (Poimenidou *et al.*, 2016a).

The current approach to develop an active formulation of EOs/CEs using the centroid mixture design could be an important way to replace chemical preservatives in the food industry and develop natural preservatives to control foodborne pathogens without compromising the organoleptic and sensory properties of the food. Falleh *et al.* (2019) worked on the development of antimicrobial formulations using a mixture design methodology and presented an optimized mixture of *Syzygium aromaticum*, *Cinnamomum zeylanicum*, *Myrtus communis*, and *Lavandula stoechas* EOs against *E. coli*. To increase the sensitivity of *S. Typhimurium*, Fadil *et al.* (2018) studied the EOs of *Thymus vulgaris*, *Rosmarinus officinalis*, and *Myrtus communis*; the optimized antimicrobial formulation using a mixture design methodology showed that 55 % *T. vulgaris* and 45 % *M. communis* EOs was synergistic in its effect against *S. Typhimurium*.

3.3.4. *In situ* antibacterial and antifungal properties on packaged rice

The vapor effect of active formulations 1 and 2 were selected for the *in situ* tests in packaged rice against growth of pathogenic bacteria and fungi (Figure 3.3 a-e, Supplementary data Table 3.5) during 28 days of storage. The rice samples (water activity: 0.90) were initially inoculated with 5 log CFU/g of bacteria or 5 log conidia/g of fungi. The control samples did not contain active formulations.



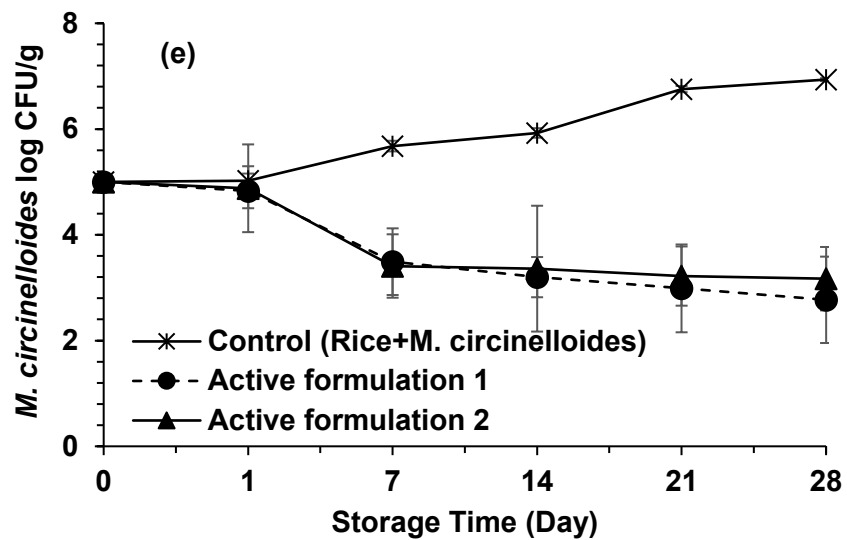


Figure 3.3. Vapor effect of active formulation 1 and 2 for controlling the growth of (a) *E. coli* O157:H7, (b) *S. Typhimurium*, (c) *A. niger*, (d) *P. chrysogenum*, (e) *M. circinelloides* in rice. Controls did not contain any antibacterial/antifungal EOs or CEs. Values are means \pm standard error.

Results showed that active formulations 1 and 2 both had significant antibacterial activity against *E. coli* O157:H7 and *S. Typhimurium* compared to control samples ($P \leq 0.05$). For *E. coli* O157:H7, the bacterial count was significantly reduced ($P \leq 0.05$) to 1.67 and 2.1 log CFU/g when treated with active formulation 1 and active formulation 2, respectively, while the control sample showed a bacterial count of 3.52 log CFU/g in rice after 28 days storage. *S. Typhimurium* counts were significantly reduced ($P \leq 0.05$) under the vapor treatment of active formulation 1 (1.61 log CFU/g) and 2 (2.31 log CFU/g) and the control sample showed *S. Typhimurium* counts of 4.05 log CFU/g in rice at day 28. It was observed that active formulation 1 had significantly stronger antibacterial effects against *E. coli* O157:H7 and *S. Typhimurium* than active formulation 2 ($P \leq 0.05$) (Figure 3.3 a-b and Supplementary data Table 3.5).

The active formulation 1 and 2, significantly reduced *A. niger*, *P. chrysogenum*, and *M. circinelloides* counts in rice samples after 28 days storage ($P \leq 0.05$) compared to the control samples (Figures 3.3c-e). For *A. niger*, the fungal count was 3.24, 3.86, and 6.78 log conidia/g in the sample treated with active formulation 1, 2, and control (with active formulation), respectively, on day 28 which showed a significant ($P \leq 0.05$) reduction of *A. niger* in rice (Figure 3.3c). *P. chrysogenum* and *M. circinelloides* counts were 3.02 and 2.77 log conidia/g in rice under the vapor treatment of active formulation 1, respectively, while the corresponding fungal growth in control samples was 7.03 and 6.93 log conidia/g ($P \leq 0.05$) (Figure 3.3d and 3.3e). Active formulation 2 significantly reduced ($P \leq 0.05$) the growth of *P. chrysogenum* and *M. circinelloides* 3.55 and 3.17 log conidia/g, respectively, compared to control. *M. circinelloides* was more sensitive to active formulations 1 and 2, followed by *P. chrysogenum* and *A. niger*.

As in our study, [Ben-Fadhel et al. \(2020\)](#) studied the mixture of citrus extracts (CEs) and essential oils EOs and developed two active formulations entrapped in a pectin-based matrix for controlling *Listeria monocytogenes* and *P. chrysogenum* in pre-cut carrots; the mixture of EOs and CE increased the shelf-life of stored carrots with improved antimicrobial properties ([Ben-Fadhel et al., 2020](#)). The vapor effect of clove buds EO, fruit peel, and leaves of makrut lime, eucalyptus leaves, and lemongrass stems against the grain storage fungi *Aspergillus flavus*, *A. niger*, *Curvularia lunata*, and *Fusarium proliferatum* was studied by [Ahebwa et al. \(2020\)](#); the mixture of lemongrass and makrut lime leaf EOs showed potent antifungal activity compared to the application of the individual EOs to suppress the growth of the four fungi ([Ahebwa et al., 2020](#)).

3.4. Conclusions

This study showed that, cinnamon EO, Mediterranean EO, Southern formulation, citrus EO, OCE, and NCE were potent antibacterial/antifungal agents. Either alone or in combination, those EOs and CEs were effective in reducing foodborne pathogenic bacteria (*E. coli* O157:H7 and *S. Typhimurium*) and spoilage fungi (*A. niger*, *P. chrysogenum*, and *M. circinelloides*). Considering the data obtained from the centroid mixture design, two active formulations (1 and 2) were developed based on their synergistic effect against the tested bacteria and fungi. A centroid mixture design was used to determine the optimal concentrations for active formulation 1 which corresponded to 625 ppm OCE, 313 ppm Mediterranean EO, 625 ppm citrus EO, and 313 ppm cinnamon EO. The optimized concentrations for active formulation 2 corresponded to 625 ppm NCE, 625 ppm Asian formulation, 313 ppm Southern formulation, 625 ppm cinnamon EO, and 313 ppm savory thyme EO. Active formulations 1 and 2 significantly increased the microbicidal/fungicidal effectiveness under both *in vitro* and *in situ* conditions compared to using the EO/CE alone. Active formulation 1 showed significantly higher microbicidal effectiveness compared to active formulation 2 during *in situ* tests in rice for controlling the growth of pathogenic bacteria and fungi. These findings highlight the need for further studies of the potential for use of natural preservatives in the food industry to control postharvest pathogens of foods.

3.5. Acknowledgments

The authors sincerely thank the Ministère de l'Économie, et de l'Innovation (MEI) du Québec (PSR SIIIRI 985), Biosecur Lab Inc., Kerry Group, the Ministère de l'Agriculture, des Pêcheries, et de l'Agriculture du Québec (MAPAQ) for a chair on antimicrobial compounds (PPIA-12) and the U.S. Department of Agriculture, Agricultural Research Service (USDA ARS), U.S. Pacific Basin Agricultural Research Centre for financial support. Finally, the authors sincerely thank Farah Hossain for her scientific and technical contributions.

Conflicts of interest

All authors state that there is no conflict of interest.

3.6. References

- Ahebwa, A., Mongkol, R., Sawangsri, P., Kanjanamaneesathian, M., 2020. Vapour-phase efficacy of selected essential oils individually and in combination against *Aspergillus flavus*, *A. niger*, *Fusarium proliferatum*, and *Curvularia lunata*. *New Zealand Plant Protection* 73, 40-48.
- Aziz, M., Karboune, S., 2018. Natural antimicrobial/antioxidant agents in meat and poultry products as well as fruits and vegetables: A review. *Critical Reviews in Food Science and Nutrition* 58, 486-511.
- Begum, T., Follett, P.A., Hossain, F., Christopher, L., Salmieri, S., Lacroix, M., 2020. Microbicidal effectiveness of irradiation from Gamma and X-ray sources at different dose rates against the foodborne illness pathogens *Escherichia coli*, *Salmonella* Typhimurium and *Listeria monocytogenes* in rice. *LWT-Food Science and Technology* 132, 109841.
- Ben-Fadhel, Y., Maherani, B., Manus, J., Salmieri, S., Lacroix, M., 2020. Physicochemical and microbiological characterization of pectin-based gelled emulsions coating applied on pre-cut carrots. *Food Hydrocolloids* 101.
- Betts, G., Linton, P., Betteridge, R., 1999. Food spoilage yeasts: effects of pH, NaCl and temperature on growth. *Food Control* 10, 27-33.
- Bilbao, M.d.L.M., Andrés-Lacueva, C., Jáuregui, O., Lamuela-Raventos, R.M., 2007. Determination of flavonoids in a Citrus fruit extract by LC–DAD and LC–MS. *Food Chemistry* 101, 1742-1747.
- Braide, W., Nwaoguikpe, R., Oranusi, S., Udegbonam, L., Akobondu, C., Okorundu, S., 2011. The effect of biodeterioration on the nutritional composition and microbiology of an edible long-winged reproductive termite, *Macrotermes bellicosus*. *Smeathman. International Journal of Food Safety* 13, 107-114.
- Bullerman, L.B., 1983. Effects of potassium sorbate on growth and aflatoxin production by *Aspergillus parasiticus* and *Aspergillus flavus*. *Journal of Food Protection* 46, 940-942.
- Burt, S., 2004. Essential oils: their antibacterial properties and potential applications in foods—a review. *International Journal of Food Microbiology* 94, 223-253.
- de Azeredo, G.A., Stamford, T.L.M., Nunes, P.C., Gomes Neto, N.J., de Oliveira, M.E.G., de Souza, E.L., 2011. Combined application of essential oils from *Origanum vulgare* L. and *Rosmarinus officinalis* L. to inhibit bacteria and autochthonous microflora associated with minimally processed vegetables. *Food Research International* 44, 1541-1548.

- Dussault, D., Vu, K.D., Lacroix, M., 2014. *In vitro* evaluation of antimicrobial activities of various commercial essential oils, oleoresin and pure compounds against food pathogens and application in ham. *Meat Science* 96, 514-520.
- Dzamic, A., Sokovic, M., Ristic, M., Grujic-Jovanovic, S., Vukojevic, J., Marin, P., 2008. Chemical composition and antifungal activity of *Origanum heracleoticum* essential oil. *Chemistry of Natural Compounds* 44, 659-660.
- Fadil, M., Fikri-Benbrahim, K., Rachiq, S., Ihssane, B., Lebrazi, S., Chraibi, M., Haloui, T., Farah, A., 2018. Combined treatment of *Thymus vulgaris* L., *Rosmarinus officinalis* L. and *Myrtus communis* L. essential oils against *Salmonella typhimurium*: Optimization of antibacterial activity by mixture design methodology. *European Journal of Pharmaceutics and Biopharmaceutics* 126, 211-220.
- Falleh, H., Ben Jemaa, M., Djebali, K., Abid, S., Saada, M., Ksouri, R., 2019. Application of the mixture design for optimum antimicrobial activity: Combined treatment of *Syzygium aromaticum*, *Cinnamomum zeylanicum*, *Myrtus communis*, and *Lavandula stoechas* essential oils against *Escherichia coli*. *Journal of Food Processing and Preservation* 43, 14257.
- Ghabraie, M., Vu, K.D., Tata, L., Salmieri, S., Lacroix, M., 2016. Antimicrobial effect of essential oils in combinations against five bacteria and their effect on sensorial quality of ground meat. *LWT-Food Science and Technology* 66, 332-339.
- Hossain, F., Follett, P., Dang Vu, K., Harich, M., Salmieri, S., Lacroix, M., 2016. Evidence for synergistic activity of plant-derived essential oils against fungal pathogens of food. *Food Microbiology* 53, 24-30.
- Hossain, F., Follett, P., Vu, K.D., Salmieri, S., Senoussi, C., Lacroix, M., 2014a. Radiosensitization of *Aspergillus niger* and *Penicillium chrysogenum* using basil essential oil and ionizing radiation for food decontamination. *Food Control* 45, 156-162.
- Hossain, F., Lacroix, M., Salmieri, S., Vu, K., Follett, P.A., 2014b. Basil oil fumigation increases radiation sensitivity in adult *Sitophilus oryzae* (Coleoptera: Curculionidae). *Journal of Stored Products Research* 59, 108-112.
- Hyldgaard, M., Mygind, T., Meyer, R.L., 2012. Essential oils in food preservation: mode of action, synergies, and interactions with food matrix components. *Frontiers in Microbiology* 3, 12.
- Ju, J., Xie, Y., Guo, Y., Cheng, Y., Qian, H., Yao, W., 2019. The inhibitory effect of plant essential oils on foodborne pathogenic bacteria in food. *Critical Reviews in Food Science and Nutrition* 59, 3281-3292.

- Kumar, S., Sinha, R., Prasad, T., 1993. Propionic acid as a preservative of maize grains in traditional storage in India. *Journal of Stored Products Research* 29, 89-93.
- Maherani, B., Harich, M., Salmieri, S., Lacroix, M., 2018. Comparative evaluation of antimicrobial efficiency of FOODGARD F410B citrus extract and sodium benzoate against foodborne pathogens in strawberry filling. *Journal of Food Processing and Preservation* 42, e13549.
- Mannaa, M., Kim, K.D., 2018. Biocontrol activity of volatile-producing *Bacillus megaterium* and *Pseudomonas protegens* against *Aspergillus* and *Penicillium* spp. predominant in stored rice grains: study II. *Mycobiology* 46, 52-63.
- Mith, H., Dure, R., Delcenserie, V., Zhiri, A., Daube, G., Clinquart, A., 2014. Antimicrobial activities of commercial essential oils and their components against food-borne pathogens and food spoilage bacteria. *Food Science and Nutrition* 2, 403-416.
- Mohammadzadeh, A., 2017. In vitro antibacterial activity of essential oil and ethanolic extract of Ajowan (*Carum copticum*) against some food-borne pathogens. *Journal of Global Pharma Technology* 9, 20-25.
- Nesci, A.V., Etcheverry, M.G., 2006. Control of *Aspergillus* growth and aflatoxin production using natural maize phytochemicals under different conditions of water activity. *Pest Management Science: formerly Pesticide Science* 62, 775-784.
- Nguefack, J., Somda, I., Mortensen, C., Amvam Zollo, P., 2005. Evaluation of five essential oils from aromatic plants of Cameroon for controlling seed-borne bacteria of rice (*Oryza sativa* L.). *Seed Science and Technology* 33, 397-407.
- Nikkhah, M., Hashemi, M., Najafi, M.B.H., Farhoosh, R., 2017. Synergistic effects of some essential oils against fungal spoilage on pear fruit. *International Journal of Food Microbiology* 257, 285-294.
- Oussalah, M., Caillet, S., Lacroix, M., 2006. Mechanism of action of Spanish oregano, Chinese cinnamon, and savory essential oils against cell membranes and walls of *Escherichia coli* O157: H7 and *Listeria monocytogenes*. *Journal of Food Protection* 69, 1046-1055.
- Oussalah, M., Caillet, S., Saucier, L., Lacroix, M., 2007. Inhibitory effects of selected plant essential oils on the growth of four pathogenic bacteria: *E. coli* O157: H7, *Salmonella typhimurium*, *Staphylococcus aureus* and *Listeria monocytogenes*. *Food Control* 18, 414-420.
- Paster, N., Droby, S., Chalutz, E., Menasherov, M., Nitzan, R., Wilson, C., 1993. Evaluation of the potential of the yeast *Pichia guilliermondii* as a biocontrol agent against *Aspergillus flavus* and fungi of stored soya beans. *Mycological Research* 97, 1201-1206.

- Poimenidou, S.V., Bikouli, V.C., Gardeli, C., Mitsi, C., Tarantilis, P.A., Nychas, G.-J., Skandamis, P.N., 2016. Effect of single or combined chemical and natural antimicrobial interventions on *Escherichia coli* O157: H7, total microbiota and color of packaged spinach and lettuce. *International Journal of Food Microbiology* 220, 6-18.
- Radfar, R., Hosseini, H., Farhodi, M., Ghasemi, I., Srednicka-Tober, D., Shamloo, E., Khaneghah, A.M., 2020. Optimization of antibacterial and mechanical properties of an active LDPE/starch/nanoclay nanocomposite film incorporated with date palm seed extract using D-optimal mixture design approach. *International Journal of Biological Macromolecules* 158, 790-799.
- Requena, R., Vargas, M., Chiralt, A., 2019. Study of the potential synergistic antibacterial activity of essential oil components using the thiazolyl blue tetrazolium bromide (MTT) assay. *LWT-Food Science and Technology* 101, 183-190.
- Tardugno, R., Serio, A., Pellati, F., D'Amato, S., Chaves López, C., Bellardi, M.G., Di Vito, M., Savini, V., Paparella, A., Benvenuti, S., 2019. *Lavandula x intermedia* and *Lavandula angustifolia* essential oils: phytochemical composition and antimicrobial activity against foodborne pathogens. *Natural Product Research* 33, 3330-3335.
- Tongnuanchan, P., Benjakul, S., 2014. Essential oils: extraction, bioactivities, and their uses for food preservation. *Journal of Food Science* 79, R1231-R1249.
- Turgis, M., Vu, K.D., Dupont, C., Lacroix, M., 2012. Combined antimicrobial effect of essential oils and bacteriocins against foodborne pathogens and food spoilage bacteria. *Food Research International* 48, 696-702.
- Ultee, A., Bennik, M.H., Moezelaar, R., 2002. The phenolic hydroxyl group of carvacrol is essential for action against the food-borne pathogen *Bacillus cereus*. *Applied and Environmental Microbiology* 68, 1561-1568.
- Viuda-Martos, M., Ruiz-Navajas, Y., Fernández-López, J., Pérez-Álvarez, J., 2007. Antifungal activities of thyme, clove and oregano essential oils. *Journal of Food Safety* 27, 91-101.
- Yahyaraeyat, R., Khosravi, A., Shahbazzadeh, D., Khalaj, V., 2013. The potential effects of *Zataria multiflora* Boiss essential oil on growth, aflatoxin production and transcription of aflatoxin biosynthesis pathway genes of toxigenic *Aspergillus parasiticus*. *Brazilian Journal of Microbiology* 44, 649-655.
- Zachariah, T.J., Leela, N.K., 2006. Volatiles from herbs and spices. *Handbook of Herbs and Spices*, pp. 177-218.

Supplementary data Table 3.1. Centroid mixture designs for four independent variables presented in the active formulation 1 and the experimental responses (MIC values) against *E. coli* O157 H7, *S. Typhimurium*, *A. niger*, *P. chrysogenum*, and *M. circinelloides*.

Run	OCE	Mediterranean EO	Citrus EO	Cinnamon EO	Minimal Inhibitory Concentration (MIC, ppm)				
					<i>E. coli</i> O157:H7	<i>S. Typhimurium</i>	<i>A. niger</i>	<i>P. chrysogenum</i>	<i>M. circinelloides</i>
1	0.125	0.625	0.125	0.125	256	253	156	165	186
2	0.25	0.25	0.25	0.25	78	98	89	92	110
3	0.625	0.125	0.125	0.125	125	102	110	98	123
4	0	0	0	1	1250	1250	625	3125.5	1250
5	0	1	0	0	1250	1250	1250	1250	1250
6	0.5	0.5	0	0	625	312.5	625	625	312.5
7	0	0	1	0	1250	1250	625	625	625
8	0.125	0.125	0.625	0.125	129	253	101	125	153
9	0	0	0.5	0.5	313	625	156	625	312.5
10	0.125	0.125	0.125	0.625	156	186	256	256	301
11	0	0.5	0	0.5	313	2500	1250	1250	2500
12	0.5	0	0.5	0	1250	625	313	312.5	312.5
13	0	0	0	1	1250	1250	625	312.5	1250
14	0	0.33	0.33	0.33	135	180	156	156	186
15	0	1	0	0	1250	1250	1250	1250	1250
16	0.33	0.33	0.33	0	125	178	108	98	176
17	1	0	0	0	1250	312.5	625	625	1250
18	0	0	1	0	1250	1250	625	625	625
19	0.33	0.33	0	0.33	214	256	189	152	231
20	0.5	0	0	0.5	313	1250	156	625	1250
21	0	0.5	0.5	0	313	1250	625	2500	2500
22	0.5	0.5	0	0	300	1200	600	2000	2000
23	0.33	0	0.33	0.33	125	256	102	78	125
24	1	0	0	0	1250	312.5	625	625	1250

Supplementary data Table 3.2. Centroid mixture designs for five independent variables presented in the active formulation 2 and the experimental responses (MIC values) against *E. coli* O157 H7, *S. Typhimurium*, *A. niger*, *P. chrysogenum*, and *M. circinelloides*.

Run	NCE	Asian formulation	Southern formulation	Cinnamon EO	Savory thyme EO	Minimal Inhibitory Concentration (MIC, ppm)				
						<i>E. coli</i> O157:H7	<i>S. Typhimurium</i>	<i>A. niger</i>	<i>P. chrysogenum</i>	<i>M. circinelloides</i>
1	0	0	0.5	0	0.5	2500	5000	5000	2500	2500
2	0.1	0.6	0.1	0.1	0.1	313	156	156	156	156
3	0	0	0.33	0.33	0.33	2500	1250	625	625	1250
4	0.33	0	0.33	0.33	0	313	625	156	313	313
5	0.1	0.1	0.1	0.6	0.1	156	78	78	78	313
6	1	0	0	0	0	1250	313	2500	1250	2500
7	0.25	0.25	0	0.25	0.25	313	156	78	156	313
8	0	0	0.5	0.5	0	1250	625	625	313	1250
9	0	0	0	0.5	0.5	2500	1250	625	625	1250
10	0.6	0.1	0.1	0.1	0.1	156	78	78	78	156
11	0	0.5	0	0.5	0	313	625	1250	625	625
12	0	0	1	0	0	625	625	625	625	625
13	0	0.33	0	0.33	0.33	625	1250	625	625	625
14	0.5	0.5	0	0	0	1250	156	625	2500	1250
15	0.33	0.33	0	0.33	0	625	625	625	625	1250
16	0.5	0	0	0	0.5	2500	1250	1250	1250	2500
17	0.25	0.25	0.25	0	0.25	313	313	78	78	156
18	0.25	0.25	0.25	0.25	0	313	313	156	78	156
19	0.33	0.33	0.33	0	0	625	625	313	313	625
20	0	0	0	1	0	1250	1250	625	313	1250
21	0.1	0.1	0.1	0.1	0.6	313	156	78	78	156
22	0	0.5	0	0	0.5	1250	2500	1250	1250	1250
23	0	0.5	0.5	0	0	1250	1250	313	625	625
24	0.33	0	0	0.33	0.33	1250	1250	625	625	625
25	0.1	0.1	0.6	0.1	0.1	156	325	156	156	156
26	0	0.33	0.33	0	0.33	625	1250	625	313	625
27	0.33	0.33	0	0	0.33	625	625	313	313	625

28	0	0	0	0	1	2500	5000	5000	2500	2500
29	0	0.25	0.25	0.25	0.25	156	156	78	78	156
30	0	1	0	0	0	5000	5000	1250	625	5000
31	0.2	0.2	0.2	0.2	0.2	156	156	78	78	156
32	0.5	0	0	0.5	0	625	313	156	625	1250
33	0.5	0	0.5	0	0	625	625	625	625	625
34	0	0.33	0.33	0.33	0	313	625	313	156	313
35	0.25	0	0.25	0.25	0.25	156	326	156	78	156
36	0.33	0	0.33	0	0.33	625	326	156	156	313

Supplementary data Table 3.3. ANOVA results for antimicrobial and antifungal properties of the active formulation 1.

Bacteria/fungi	Model	F-Value	P-value	df	R²	Predicted equation
<i>E. coli</i> O157:H7	Quadratic	22.22	0.0001	9	0.9346	+ 1244.7A + 1263.6B + 1250.6C + 1252.6D - 3362.7AB - 1075.2AC - 4065.9AD - 4124.2BC - 3364.9BD - 4031.4CD
<i>S. Typhimurium</i>	Special cubic	6.94	0.0021	13	0.9002	+ 329.2A + 1220.4B + 1258.8C + 1213D - 167.2AB - 686.5AC + 1696AD - 180.4BC + 4702.6BD - 2698.8CD - 1522.9ABC - 11386.7ACD - 33922.5BCD
<i>A. niger</i>	Special cubic	14.1	0.0001	13	0.9482	+ 626A + 1211B + 629C + 637D - 1333AB - 1282AC - 1887AD - 1386BC + 1133BD - 1881CD - 7865ABC - 11169ABD + 2403ACD - 11836BCD
<i>P. chrysogenum</i>	Special cubic	1.34	0.3	13	0.6352	+ 643A + 1200B + 625C + 1715D + 1408AB - 1371AC - 2319AD + 5957BC - 1241BD - 2365CD - 35856ABC - 19935ABD - 2996ACD - 33918BCD
<i>M. circinelloides</i>	Special cubic	3.82	0.0201	13	0.8324	+ 1249A + 1191B + 644C + 1247D - 487AB - 2643AC - 200AD + 5959BC + 4652BD - 2648CD - 29744ABC - 38012ABD - 4338ACD - 44928BCD

Supplementary data Table 3.4. ANOVA results for antimicrobial and antifungal properties of the active formulation 2.

Bacteria/fungi	Model	F-Value	P-value	df	R²	Predicted equation
<i>E. coli</i> O157:H7	Quadratic	6.83	≤ 0.0001	14	0.8199	+ 1469A + 4976B + 866C + 1365D + 2673E - 7569AB - 4151AC - 3952AD - 1764AE - 7701BC - 11562BC
<i>S. Typhimurium</i>	Quadratic	6.20	0.0001	14	0.8051	+ 473A + 4864B + 976C + 1268D + 5016E - 8848AB - 1764AC - 291AD - 7999AE - 7822BC - 8764BD - 11969BE - 2801CD + 1899CE - 8108DE
<i>A. niger</i>	Quadratic	6.72	≤ 0.0001	14	0.8176	+ 2530A + 1385B + 967C + 743D + 5013E - 4759AB - 6112AC - 4603AD - 11872AE - 4782BC + 728BD - 9730BE - 2480CD + 2138CE - 9864DE
<i>P. chrysogenum</i>	Special cubic	5.88	0.0020	24	0.9277	+ 1196A + 621B + 652C + 345D + 2360E + 6065AB - 1451AC - 626AD - 2589AE - 229BC + 596BD - 1368BE - 669CD + 3616CE - 3059DE - 22978ABC - 21015ABD - 33905ABE - 3041ACD - 30462ACE - 1781ADE - 8812BCD - 27795BCE - 3332BDE - 14421CDE
<i>M. circinelloides</i>	Quadratic	7.26	≤ 0.0001	14	0.8287	+ 2609A + 4827B + 885C + 1394D + 2663E - 9173AB - 6316AC - 3733AD - 4225AE - 9142BC - 9111BD - 11227BE - 687CD + 212CE - 4395DE

Supplementary data Table 3.5. Vapor effect of active formulation 1 and 2 with statistical analyses in rice for 28 days to control the growth of (a) *E. coli* O157:H7, (b) *S. Typhimurium*, (c) *A. niger*, (d) *P. chrysogenum*, (e) *M. circinelloides*. Control samples were not containing antibacterials/antifungals. Values are means±standard error.

Pathogens	Bacterial and fungal count (log CFU/g) in stored rice (Day)				
	1	7	14	21	28
<i>E. coli</i> O157:H7					
Control*	4.34±0.4 ^{eC}	4.06±0.3 ^{dC}	3.94±0.1 ^{cC}	3.73±0.1 ^{bC}	3.52±0.3 ^{aC}
Active formulation 1	3.59±0.3 ^{eA}	2.99±0.4 ^{dA}	2.83±0.2 ^{cA}	2.66±0.1 ^{bA}	1.67±0 ^{aA}
Active formulation 2	3.99±0.5 ^{eB}	3.59±0.6 ^{dB}	3.19±0.2 ^{cB}	2.68±0.2 ^{bB}	2.1±0.5 ^{aB}
<i>S. Typhimurium</i>					
Control*	5.01±0.2 ^{dC}	4.37±0.3 ^{cC}	4.16±0.1 ^{bC}	4.11±0.2 ^{abC}	4.05±0.1 ^{aC}
Active formulation 1	3.93±0.7 ^{eA}	3.18±0.3 ^{dA}	2.55±0.1 ^{cA}	1.73±0.7 ^{bA}	1.61±0.2 ^{aA}
Active formulation 2	4.03±0.4 ^{eB}	3.87±0.6 ^{dB}	2.9±0.4 ^{cB}	2.5±0.3 ^{bB}	2.31±0.3 ^{aB}
<i>A. niger</i>					
Control*	4.57±0.3 ^{aA}	5.91±0.1 ^{bC}	6.04±0.1 ^{cC}	6.37±0.2 ^{dC}	6.78±0.2 ^{eC}
Active formulation 1	4.58±0.7 ^{eA}	4.25±0.4 ^{dA}	4.16±0.5 ^{cB}	3.49±0.5 ^{bA}	3.24±0.4 ^{aA}
Active formulation 2	4.61±0.6 ^{eB}	4.32±0.5 ^{cB}	4.07±0.2 ^{bA}	3.9±0.6 ^{aB}	3.86±0.8 ^{aB}
<i>P. chrysogenum</i>					
Control*	4.02±0.7 ^{aA}	5.64±0.2 ^{bC}	5.94±0.1 ^{cC}	6.84±0.1 ^{dC}	7.03±0.05 ^{eC}
Active formulation 1	4.92±0.5 ^{eB}	3.69±0.8 ^{dA}	3.43±0.5 ^{cA}	3.21±0.5 ^{bA}	3.02±0.5 ^{aA}
Active formulation 2	5.06±0.7 ^{cC}	4.27±0.3 ^{dB}	4.1±0.4 ^{cB}	3.97±0.8 ^{bB}	3.55±0.4 ^{aB}
<i>M. circinelloides</i>					
Control*	5.02±0.3 ^{aC}	5.7±0.1 ^{bB}	5.93±0.1 ^{cC}	6.76±0.1 ^{dC}	6.93±0.1 ^{eC}
Active formulation 1	4.83±0.3 ^{eB}	3.49±0.6 ^{dA}	3.2±0.4 ^{cA}	2.98±0.8 ^{bA}	2.77±0.8 ^{aA}
Active formulation 2	4.88±0.8 ^{dA}	3.41±0.6 ^{cA}	3.36±1.2 ^{cB}	3.22±0.6 ^{bB}	3.17±0.6 ^{aB}

Within each row means with the same lowercase letter are not significantly different ($P > 0.05$). Within each column means with the same uppercase letter are not significantly different ($P > 0.05$).

Chapter 4

Publication 3

Silver nanoparticles-essential oils combined treatments to enhance the antibacterial and antifungal properties against foodborne pathogens and spoilage microorganisms

This article has been published in *Microbial Pathogenesis*, 2022, 164, 105411, Impact factor: 3.848, h-index: 80, Overall Ranking: 6948, SCImago Journal Rank: 0.693

<https://doi.org/10.1016/j.micpath.2022.105411>

Tofa Begum^a, Peter A. Follett^b, Jumana Mahmud^a, Lana Moskovchenko^c, Stephane Salmieri^a, Zahra Allahdad^a, Monique Lacroix^{a*}

^aResearch Laboratories in Sciences, Applied to Food, Canadian Irradiation Center, INRS, Armand Frappier Health and Biotechnology Centre, Institute of Nutrition and Functional Food (INAF), Chair of the MAPAQ on stabilized natural antimicrobial and food quality, 531, Boulevard des Prairies, Laval, Quebec, Canada, H7V 1B7

^bUnited States Department of Agriculture, Agricultural Research Service, U.S. Pacific Basin Agricultural Research Center, 64 Nowelo Street, Hilo, HI 96720, USA

^cNano Brand, 230 Rue Bernard Belleau, Laval, Quebec, Canada, H7V 4A9

*Corresponding author. Dr. Monique Lacroix, Tel: 450-687-5010 # 4489, Fax: 450-686-5501, E-mail: Monique.Lacroix@inrs.ca

Contribution of the authors

Tofa Begum conducted the data curation, methodology, writing - original drafts, writing - review and editing. Monique Lacroix and Peter Follett designed the methodology, conceptualization, supervision and software. Stephane Salmieri, Lana Moskovchenko and Zahra Allahdad assisted with reviewing the methodology. Jumana Mahmud helped for the data curation.

Résumé

Des huiles essentielles d'origine végétale (HE) et des nanoparticules commerciales d'argent (AgNP) ont été testées pour évaluer leur efficacité antibactérienne et antifongique contre deux bactéries pathogènes (*Salmonella* Typhimurium et *Escherichia coli* O157:H7) et trois champignons d'altération (*Aspergillus niger*, *Penicillium chrysogenum*, *Mucor circinelloides*). Les tests de microdilution en bouillon ont été utilisés pour déterminer la concentration minimale inhibitrice (CMI) des HE et des AgNP. Dans le test MIC, l'HE de cannelle, l'HE de Méditerranée, l'HE d'agrumes et les nanoparticules d'argent de forme sphérique (AgNPs) (AGC 1, AGC 0.5, AGPP et AGPPH), ont montré des valeurs modérées à élevées (7.8 à 62.5 ppm pour les AgNPs et 312.5 à 1250 ppm pour les HE) propriétés antibactériennes et antifongiques contre toutes les bactéries et champignons testés. Une éventuelle interaction entre les HE et les AgNPs a été déterminée à l'aide d'une méthode en damier en évaluant les valeurs de FIC (Fractional inhibiting concentration). De nombreuses combinaisons doubles ont montré des effets synergiques (FIC < 1.0) contre certaines bactéries et champignons, cependant, les triples combinaisons parmi les HE et les AgNP (AGPPH + HE de cannelle, AGC 0.5 + HE méditerranéenne + HE d'agrumes, AGPP + HE de cannelle + La formulation asiatique EO + lavang EO) a également montré des effets synergétiques (FIC < 1.0) contre toutes les bactéries et champignons testés. Un modèle mathématique modifié de Gompertz a été appliqué pour évaluer les paramètres de croissance, y compris le diamètre maximal de la colonie (A), le taux de croissance maximal (V_m) et la phase de latence (λ), sous les trois composés actifs développés par la méthode Checkerboard en utilisant le test de vapeur. La vapeur de trois composés actifs a réduit le taux de croissance et le diamètre maximal des colonies de *E. coli*, *S. Typhimurium*, *A. niger*, *P. chrysogenum* et *M. circinelloides* de manière significative ($P \leq 0.05$), et a prolongé leur phase de latence de 1- 5 jours. Les tests *in situ* ont montré une réduction significative ($P \leq 0.05$) de toutes les bactéries et champignons pathogènes testés en utilisant la vapeur de trois composés actifs au 28e jour d'entreposage du riz par rapport au témoin.

Mots clé: huile essentielle; nanoparticules; effet synergique; propriété antibactérienne; riz entreposé

Abstract

Plant-derived essential oils (EOs) and commercial silver nanoparticles (AgNPs) were tested to evaluate their antibacterial and antifungal efficiency against two pathogenic bacteria (*Escherichia coli* O157:H7 and *Salmonella* Typhimurium) and three spoilage fungi (*Aspergillus niger*, *Penicillium chrysogenum*, and *Mucor circinelloides*). A broth microdilution assay was used to determine the minimal inhibitory concentration (MIC) of EOs and AgNPs. In the MIC assay, the cinnamon EO, Mediterranean formulation, citrus EO and spherical-shaped silver nanoparticles (AgNPs) (AGC 1, AGC 0.5, AGPP and AGPPH) showed moderate to high antibacterial and antifungal properties, with MIC ranging from 7.8 to 62.5 ppm for AgNPs and 312.5 to 1250 ppm for EOs against the tested bacteria and fungi. The possible interaction between the EOs and the AgNPs was determined using a checkerboard method by evaluating fractional inhibitory concentration (FIC) values. The combination of two or more EOs and AgNPs (Active combination 1: AGPPH+cinnamon EO, Active combination 2: AGC 0.5+Mediterranean formulation+citrus EO, Active combination 3: AGPP+cinnamon EO+Asian formulation+lavang EO) showed synergistic effects (FIC < 1.0) against all tested bacteria and fungi. A modified Gompertz model was used to evaluate growth parameters including maximum colony diameter (A), maximum growth rate (V_m), and lag phase (λ), under the three active combinations suggested by the checkerboard method using a vapor assay. The three active combinations 1, 2 and 3 reduced the growth rate and maximum colony diameter of *E. coli*, *S. Typhimurium*, *A. niger*, *P. chrysogenum*, and *M. circinelloides*, and extended their lag phase from 1-5 days. In *in situ* tests with inoculated rice, the three active combinations showed a significant ($P \leq 0.05$) reduction of all tested bacteria and fungi at 27 °C for 28 days.

Keywords: essential oil; nanoparticles; synergistic effect; antibacterial property; storage rice

4.1. Introduction

Rice (*Oryza sativa* L.) is an important cereal crop with a worldwide annual production of over 600 million tons annually (Nguefack *et al.*, 2005). Stored rice is prone to deterioration under storage conditions (temperature, relative humidity, moisture contents) that promote bacterial and fungal growth. The most common spoilage fungi are *Aspergillus* sp., *Penicillium* sp., *Fusarium* sp., and may produce mycotoxins which are highly toxic to human and animals. Spoilage fungi can cause grain discoloration, chemical and nutritional changes, and reduced germination (Paster *et al.*, 1993; Hossain *et al.*, 2014a). Rice is also susceptible to contamination by bacteria such as *Escherichia coli*, *Salmonella* Typhimurium, and *Listeria monocytogenes* (Begum *et al.*, 2020a).

Natural food extracts such as plant essential oils (EOs) are a safe alternative to the use of synthetic chemical food preservatives. Plant EOs are widely known to have antibacterial, antifungal, antiviral, insecticidal, and antioxidant properties (Burt, 2004; Turgis *et al.*, 2012; Hossain *et al.*, 2014a; Hossain *et al.*, 2014b; Hossain *et al.*, 2016b). EOs are secondary metabolites of plants with a complex mixture of volatile active compounds especially monoterpenes, sesquiterpenes, and their oxygenated derivatives (alcohols, aldehydes, esters, ethers, ketones, phenols, and oxides) (Turgis *et al.*, 2012; Hossain *et al.*, 2016b; Vishwakarma *et al.*, 2016). More than 300 EOs are playing an important role in the food, pharmaceutical, sanitary, or cosmetic industries and they are generally recognized as safe (GRAS) by the US Food and Drug Administration (FDA) and the European Commission. However, perceivable taste and aroma changes caused by EOs at high concentrations limit their application in many food products. The combination of two or more antimicrobial/antifungal EO agents may provide synergistic and increased activity at low concentrations to avoid this limitation (Turgis *et al.*, 2012; Tongnuanchan and Benjakul, 2014; Mohammadzadeh, 2017; Tardugno *et al.*, 2019).

Silver nanoparticles (AgNPs) are increasingly used in the medical, food, healthcare, and industrial fields due to their unique physical and chemical properties, including their well-known antimicrobial activity at low concentrations (Ghosh *et al.*, 2013a; Weisany *et al.*, 2019). The microbicidal effect of AgNPs could be identified under three mechanisms of actions: (1) small size AgNPs can bind to the cell membrane surface and drastically disturb its functions, permeability, and respiration, (2) AgNPs as weak acid (Lewis acid) can interact with compounds containing sulfur and phosphorus (DNA, proteins) after penetration into microbial cells, (3) The release of Ag⁺ in presence of Oxygen and interaction with negatively charged microbial cell membranes provide additional contribution to microbicidal effects (Morones *et al.*, 2005; Eghbalifam *et al.*, 2015; Tang and Zheng, 2018; Simbine *et al.*, 2019).

In the present study, the antibacterial and antifungal activities of five EOs and four spherical silver nanoparticle types (AGC 1, AGC 0.5, AGPP and AGPPH) were investigated against pathogenic bacteria and spoilage fungi by determining (i) the minimal inhibitory concentration (MIC), (ii) possible synergistic antibacterial and antifungal interaction among EOs and AgNPs, (iii) the growth kinetics of bacteria and fungi in the presence of selected EO/AgNP combinations, and (iv) the *in situ* antibacterial and antifungal effectiveness of select EO/AgNP combinations in rice during storage.

4.2. Materials and methods

4.2.1. Materials

The essential oils (EOs) of Asian formulation and Mediterranean formulation were purchased from BSA (Montreal, Quebec, Canada), and cinnamon EO, citrus EO and lavang EO were obtained from Zayat Aroma (Bromont, QC, Canada). The Mediterranean formulation composed of seven oils (origanum oil : black pepper oil : capsicum oleoresin (OR) : garlic oil : pimento berry oil : lemongrass oil : citral oil (5.85: 0.25: 0.25: 0.25: 1.4: 1.15: 0.85)) and Asian formulation composed of twelve oils (lemongrass : citral oil : pimento berry oil : ginger oleoresin : Indian celery seed oil : black pepper oleoresin : cumin oil : nutmeg oil : coriander seed oil : caraway oil : capsicum oleoresin : garlic oil (1.78: 1.2: 0.57: 0.65: 0.47: 0.47: 0.22: 1.94: 0.8: 0.29: 0.6: 1)). The compositions/chemical components of EOs were mentioned in Table 4.1. Four different types of commercial silver nanoparticle (AgNPs) containing formulations namely as AGC 1, AGC 0.5, AGPP, and AGPPH were provided by NanoBrand (Bernard-Belleau, Laval, Quebec, Canada). Tween 80 (emulsifier), NaCl (for saline water) and glycerol were purchased from Sigma-Aldrich Ltd. (St. Louis, Missouri, United States), the stabilizer polyvinylpyrrolidone (PVP) (average molecular weight 40000) and chitosan (8 % deacetylated Chitosan) were purchased from Alfa Aesar (Ward Hill, Massachusetts, United States), and polyethylene glycol (average molecular weight 600) was bought from Acros Organics (Fair Lawn, New Jersey, United States). The potato dextrose broth (PDB) and tryptic soy broth (TSB) were purchased from Alpha Biosciences Inc. (Baltimore, MD, USA) and BD, Franklin Lakes, NJ, USA), respectively.

Table 4.1. Name and compositions/chemical components of the essential oils (EOs).

Name of antibacterials / antifungals	Compositions/chemical components
Mediterranean formulation	origanum oil, black pepper oil, capsicum oleoresin (OR), garlic oil, pimento berry oil, lemongrass oil, citral oil.
Asian formulation	lemongrass, citral oil, pimento berry oil, ginger oleoresin, Indian celery seed oil, black pepper oleoresin, cumin oil, nutmeg oil, coriander seed oil, caraway oil, capsicum oleoresin, garlic oil.
Cinnamon EO	cinnamaldehyde, cinnamyle acetate, β -caryophyllene, p-cymene.
Citrus EO	Sweet orange (limonene, myrcene).
Lavang EO	beta-caryophyllene, alpha-humulene, eugenol, eugenyle acetate.

4.2.2. Preparation of antimicrobial and antifungal compounds

The plant-derived essential oils (EOs) Mediterranean formulation, citrus, cinnamon, lavang, and Asian formulation were tested as natural antibacterial and antifungal agents. The oil-in-water (O/W) emulsions were prepared using 2 % (v/v) EO, 1 % (w/v) Tween 80, and 97 % distilled water (w/w), and were homogenized for 1 min at 15000 rpm using Ultra Turrax (TP18/1059 homogenizer) before use. All the samples containing silver nanoparticles (AGC 1, AGC 0.5, AGPP, and AGPPH) had a silver concentration of 1000 ppm. AGPP and AGPPH samples contained silver nanoparticles stabilized by polyvinylpyrrolidone and polyethylene glycol with different pH (AGPP: pH = 3; AGPPH: pH = 6). The nanoparticles containing formulations AGC 0.5 and AGC 1 were dispersed in 0.5 % and 1 % of chitosan, respectively.

4.2.3. Preparation of bacteria/fungi cultures and assay media

The bacteria (*S. Typhimurium* SL 1344 and *E. coli* O157:H7 NT 1931) and fungi (*A. niger* ATCC 1015, *P. chrysogenum* ATCC 10106, and *M. circinelloides* ATCC 56649) were collected from the American Type Culture Collection (ATCC), except, *E. coli* O157:H7. *E. coli* O157:H7 was collected from United States Department of Agriculture (USDA), Albany, CA, United States. All bacterial and fungal strains were stored at -80 °C in 10 % (v/v) glycerol on TSB and in PDB, respectively (Ghabraie *et al.*, 2016). Before each experiment, the stock cultures were propagated through two consecutive growth cycles in TSB at 37 °C for 24 h (bacteria) or in PDB at 28 °C for 48 h (fungi) (Ghabraie *et al.*, 2016). The bacterial cultures were recovered by centrifugation and washed with 0.85 % (w/v) saline water to obtain the desired pathogen concentrations for inoculation. However, the fungal cultures were pre-cultured in sterile PDA media for 2-4 days at 28 °C and the spores

were collected from the culture media using sterile saline water and filtered. Final bacterial and fungal spore culture concentrations were adjusted to 1×10^5 CFU/mL or 1×10^5 spores/mL respectively, for all *in vitro* and *in situ* experiments (Ghabraie *et al.*, 2016; Hossain *et al.*, 2016a; Snyder *et al.*, 2016a).

4.2.4. Minimal inhibitory concentration (MIC)

A modified broth microdilution method was used to determine the minimum inhibitory concentration (MIC) of the AgNPs and EOs as described by Turgis *et al.* (2012). The AgNPs and EOs were classified into three distinct groups based on MIC values, and the groups were i) highly effective (< 625 ppm) ii) moderately effective (625-1250 ppm), and iii) less effective (> 1250 ppm). A 100 μ L aliquot of a 2-fold serial dilution (from 0.48 to 500 ppm) of AgNPs and from 156 to 10,000 ppm for EO suspensions were prepared and deposited in each well of a 96-well microplate (Sarstedt, St-Leonard, QC, Canada) using TSB for bacteria or PDB for fungi. Each well was then inoculated with 100 μ L of a pathogen at a concentration of 10^5 CFU/mL (bacteria) or 10^5 spores/mL (fungi) and incubated for 24 h at 37 °C or 48 h at 28 °C. In the 96-well plate, one well served as a positive control containing the pathogen and TSB/PDB, and a negative control contained no pathogen. Microbial growth was evaluated using an Ultra Microplate Reader (Biotek Instruments, Winooski, VT, USA) by measuring the optical density (OD) at 595 nm. The MIC was defined as the lowest concentration of the AgNPs or EOs suspension that completely inhibited the bacterial and fungal growth.

4.2.5. Synergistic interactions of essential oils and silver nanoparticles

Interactions of EOs and AgNPs were evaluated using a checkerboard microdilution test. The checkerboard tests were performed using 96-well microplates to measure the fractional inhibitory concentration (FIC) index of EOs and AgNPs against each bacterium and fungus (Turgis *et al.*, 2012; Tongnuanchan and Benjakul, 2014; Hossain *et al.*, 2016a; Requena *et al.*, 2019). For selected double combinations, the checkerboard test was used against all tested bacteria and fungi with two-fold dilutions of twenty treatments, including AGC 0.5+Mediterranean formulation, AGC 0.5+cinnamon EO, AGC 0.5+Asian formulation, AGC 0.5+citrus EO, AGC 0.5+lavang EO, AGPP+cinnamon EO, AGPP+Asian formulation, AGPP+lavang EO, AGPP+citrus EO, AGPP+Mediterranean formulation, AGPPH+ Mediterranean formulation, AGPPH+cinnamon EO, AGPPH+Asian formulation, AGPPH+citrus EO, AGPPH+lavang EO, AGC 1+Mediterranean formulation, AGC 1+cinnamon EO, AGC 1+Asian formulation, AGC 1+citrus EO, AGC1+lavang EO. A volume of 100 μ L of bacterial/fungal suspension (containing 10^5 CFU/mL) was added to

each well of the microplate. The microplates were then incubated in a shaking incubator at 37 °C (bacteria)/ and 28 °C (fungi) for 24 (bacteria) or 48 (fungi) hours, respectively. The corresponding readings were taken with a microplate reader (BioTek, ELx800™) at 595 nm.

The dual combinations of EOs and AgNPs which showed synergy were combined with a third component for assessing 3-way synergistic interactions using a three-dimensional checkerboard method (Nikkhah *et al.*, 2017a). For the three-dimensional checkerboard method, nine combinations including (AGC 0.5 + Mediterranean formulation) and citrus EO, (AGC 0.5 + cinnamon EO) and Asian formulation, (AGPP + cinnamon EO) and lavang EO, (AGPP + cinnamon EO) and Asian formulation, (AGPP + Asian formulation) and lavang EO, (AGC 1 + cinnamon EO) and Asian formulation, (AGC 1 + cinnamon EO) and citrus EO, (AGPP + cinnamon EO + Asian formulation) and lavang EO were selected for evaluation. The well of the microplate containing the nutrient medium (TSB or PDB) with bacterial or fungal inoculum served as a positive control and the well without inocula (containing active EO and Ag components only) served as a negative control. All assays were performed in triplicate. The FIC values for 2 (Eq. 4.1), 3 or more (Eq. 4.2) EOs, and AgNPs were calculated using Eq. 4.1.

$$\text{FIC} = \text{FIC1} + \text{FIC2} \text{ Eq. (4.1)}$$

Where, FIC1 = (MIC1 combined/MIC1 alone) and FIC2 = (MIC2 combined/MIC2 alone)

$$\text{FIC} = \text{FIC} (1+2) + \text{FIC3} \text{ Eq. (4.2)}$$

Where, FIC (1+2) = (MIC1+2 combined/MIC1+2 alone) and FIC3 = (MIC3 combined/MIC3 alone)

A FIC < 1.0 was interpreted as a synergistic effect, FIC = 1 represented as additive effect, FIC > 1 represented an antagonistic effect.

The three active combinations of EOs and AgNPs such as AGPPH + cinnamon EO, AGC 0.5 + Mediterranean formulation + citrus EO, and AGPP + cinnamon EO + Asian formulation + lavang EO named active combination 1, 2 and 3, respectively, were selected for further tests because of their synergistic effect against all tested pathogens.

4.2.6. Vapor contact assays

An inverted lid technique was used to test the efficacy of active combinations in a volatile state for food packaging applications (Avila-Sosa *et al.*, 2012; Hossain *et al.*, 2016a). Briefly, a 10 µL aliquot bacterial or fungal suspension (1×10^5 CFU/mL or 1×10^5 spores/mL) was placed in the center of the TSA plate (Trypto Soy Agar) for bacteria and PDA plate (Potato Dextrose Agar) for fungi and were dried in a laminar flow hood under aseptic conditions at room temperature for 30 min. Sterile filter paper (10 mm diameter) was placed at the center of the upper lid of the plate. A quantity of 10 µL of each active combination was added at the center of individual paper filters. A growth

control was prepared in parallel to ensure that viable microorganisms were present. The Petri dishes were incubated at 37 °C for bacteria and 27 °C for fungi for 8 days. Every test was performed in triplicate. Bacterial and fungal growth modeling was fitted using a modified Gompertz model as reported by [Char et al. \(2007\)](#).

4.2.7. Bacterial and fungal growth model and statistical analysis

The growth model and parameters for each bacteria and fungi under the vapor treatment of active combinations on pure nutrient media (TSA or PDA) and compared with control plate (without active combinations) and fitted using the modified Gompertz equation ([Char et al., 2007](#); [Avila-Sosa et al., 2012](#)):

$$\ln \frac{D_t}{D_0} = A \cdot \exp \left\{ -\exp \left[\frac{V_{m.e}}{A} \right] (\lambda - t) + 1 \right\} \quad \text{Eq. 4.3}$$

Where D_t is the average colony diameter (cm) at time t (day); D_0 is the average colony diameter (cm) at the initial time (day 0); A stands for the maximum growth achieved during the stationary phase; V_m is the maximum specific growth rate (1/day); λ is the lag phase (day).

The one-way analysis of variance (ANOVA) and Duncan test at $\alpha = 0.05$ was performed for statistical analysis using SPSS software (IBM Corporation, Somers, NY, USA). Three replicates were performed for each treatment and the differences between mean values at $P \leq 0.05$ were considered significant.

4.2.8. *In situ* antibacterial and antifungal efficiency of active combinations in rice

An *in situ* test was performed in packaged rice to evaluate the antibacterial and antifungal properties against the pathogenic bacteria (*E. coli* O157:H7, *S. Typhimurium*) and fungi (*A. niger*, *P. chrysogenum*, and *M. circinelloides*) according to [Hossain et al. \(2014a\)](#). A volume of 200 μL of bacteria or fungi (1×10^5 CFU/mL for bacteria or 1×10^5 spores/mL for fungi) was inoculated in 50 g of sterile rice (Super quality basmati rice, St. Laurent, Quebec, Canada). A sterile sponge cube ($5 \times 5 \times 5$ cm) containing a volume of 50 μL of the active combination was placed inside a sterile plastic cup. A muslin screen was used to cover the cup to prevent contact between rice grains and the active combinations and placed them inside the rice. The samples were containing rice and inocula denoted as control groups (without active combinations). The samples were incubated for 28 days at 37 °C and 27 °C for bacteria and fungi, respectively, and the microbiological analyses were performed at 1, 7, 14, 21, and 28 days of storage.

4.2.9. Microbiological analysis

The microbiological analyses of stored rice were carried out using a standard method International Commission of Microbiological Specification on Foods (ICMSF) (Braide *et al.*, 2011). A volume of 20 mL of sterile peptone water (0.1 %, w/v) was added in 10 g of rice and homogenized for 60 s at 260 rpm by a Lab-blender 400 stomacher (Laboratory Equipment, London, UK). A serial dilution (from 10^{-1} to 10^{-6}) of the homogenized sample was prepared and a 0.1 mL of diluted sample was inoculated onto TSA media for bacteria and PDA media for fungi. Then the plates were incubated at 37 °C and 27 °C for 24 h (bacteria) and 48 h (fungi), and the microbial colonies were counted as per Begum *et al.* (2020a). Each experiment was performed in triplicate.

4.3. Results and discussion

4.3.1. Minimal inhibitory concentration (MIC)

The antibacterial and antifungal effects of EOs and AgNPs in terms of MICs against pathogenic bacteria (*E. coli* O157:H7 and *S. Typhimurium*) and spoilage fungi (*A. niger*, *P. chrysogenum*, and *M. circinelloides*) are presented in Table 4.2. Results showed that among all tested AgNPs (AGC 1, AGC 0.5, AGPP, and AGPPH) have significant antibacterial activity against all tested pathogenic bacteria (*E. coli* O157:H7 and *S. Typhimurium*) with MIC values ranging from 7.8 to 62.5 ppm. The AGC 1, AGC 0.5, and AGPPH formulations showed the highest antibacterial activity against *E. coli* O157:H7 and *S. Typhimurium*, with MIC values of 7.8 ppm. The AGPP formulation showed a significant inhibitory effect against *E. coli* O157:H7 and *S. Typhimurium*, with an MIC of 15.6 ppm. All tested AgNPs showed strong antifungal activity against *A. niger*, *P. chrysogenum*, and *M. circinelloides*. AGPP showed the highest antifungal activity against *A. niger* and *P. chrysogenum*, with MIC values of 7.8 ppm. AGPPH exhibited the highest antifungal activity against *A. niger* and *M. circinelloides*, with MIC values of 7.8 ppm. AGC 0.5 was most effective against *A. niger* (MIC of 7.8 ppm).

The cinnamon EO, Mediterranean formulation, and citrus EO showed moderate antibacterial activity (MIC of 1250 ppm) against *E. coli* O157:H7 and *S. Typhimurium*. Similarly, Mith *et al.* (2014) also found cinnamon EO, oregano EO, clove, and lemongrass EOs had antibacterial activity against pathogenic bacteria *E. coli* O157:H7, *S. Typhimurium* and *Listeria monocytogenes*. Cinnamon EO showed highly effective antifungal activity whose MIC value was 312.5 ppm against *P. chrysogenum*, while cinnamon EO showed moderate antifungal activities against *A. niger* and

M. circinelloides. The citrus EO showed moderately effective antifungal activity (MIC of 625 ppm) against all tested fungi.

Table 4.2. Minimal inhibitory concentration (MIC, ppm) of AgNPs and EOs against *E. coli* O157:H7, *S. Typhimurium*, *A. niger*, *P. chrysogenum*, *M. circinelloides*.

Antibacterials / Antifungals	Minimal Inhibitory Concentration (ppm)				
	<i>E. coli</i> O157:H7	<i>S. Typhimurium</i>	<i>A. niger</i>	<i>P. chrysogenum</i>	<i>M. circinelloides</i>
AGC 1	7.8	7.8	15.6	31.2	31.2
AGC 0.5	7.8	7.8	7.8	62.5	31.2
AGPP	15.6	15.6	7.8	7.8	15.6
AGPPH	7.8	7.8	7.8	62.5	7.8
Cinnamon EO	1250	1250	625	312.5	1250
Asian formulation	5000	5000	1250	612	5000
Mediterranean formulation	1250	1250	1250	1250	1250
Citrus EO	1250	1250	625	625	625
Lavang EO	5000	5000	2500	2500	1250

Silver nanoparticles (AgNPs) have strong antibacterial and antifungal properties and they are widely used in the food industry as an antimicrobial agent within FDA recommended limits (Emamifar *et al.*, 2010; Metak *et al.*, 2015; Bocate *et al.*, 2019). AgNPs have higher bactericidal efficacy toward Gram-negative bacteria due to their thinner cell wall, while EOs are more effective against Gram-positive bacteria. AgNPs can create pits on the cell surface of microorganisms which can lead to cell damage; they can also inhibit the production of microbial proteins and enzymes by disrupting the ribosomal activities of the bacterial cell. Moreover, AgNPs are also commonly used as antifungal agents to treat resistant fungi (Emamifar *et al.*, 2010; Bocate *et al.*, 2019). Generally, the bioactivities (*e.g.*, cellular uptake, cellular activation, intercellular distribution) of the nanoparticles depend on their size, shape, surface charge, functionalization, and core structure. In the current study, we worked with spherical and small-sized AgNPs (3-45 nm) which release Ag⁺ faster, and thus leading to higher bactericidal and antifungal effects due to higher concentrations of silver ions (Sotiriou and Pratsinis, 2011; Helmlinger *et al.*, 2016). Martinez-Castanon and co-authors found spherical shaped AgNPs that were 7, 29 and 89 nm in diameter all exhibited strong antibacterial activity against *E. coli* (Martínez-Castañón *et al.*, 2008). Helmlinger *et al.* (2016) demonstrated the role of AgNPs shape on antibacterial activities against

Staphylococcus aureus. They found nanoplatelets (20-60 nm) exhibited the highest toxicity, followed by nanospheres (diameter 40-70 nm and 120–180 nm), and finally nanocubes (140-180 nm), and attributed this pattern to the effects of surface area and dissolution rate of particles, i.e., spherical and nanoplatelet shaped AgNPs have the highest specific area and formed more Ag⁺ ions (Helmlinger *et al.*, 2016; Tang and Zheng, 2018).

The bioactivity of EOs mainly depends on the mixture of chemical components, their functional groups, and concentrations (Burt, 2004; Weisany *et al.*, 2019). The cinnamon EO, Mediterranean formulation, citrus EO, lavang EO, and Asian formulation contain cinnamaldehyde (63 %), carvacrol (46 %) and thymol (14 %), limonene (95 %), eugenol (> 85 %) and geraniol (45 %) and neral (32 %), respectively (Zachariah and Leela, 2006; Oussalah *et al.*, 2007; Mith *et al.*, 2014). High antifungal activity of oregano EO against *A. niger* and *P. chrysogenum* (MIC of 62.5 ppm) supports the findings of Hossain *et al.* (2016a). The phenolic compounds carvacrol and thymol (60 to 74 %) found in oregano EO are mainly responsible for its bioactivity (Dussault *et al.*, 2014; Tongnuanchan and Benjakul, 2014; Ayari *et al.*, 2020). EOs targets the fungal cell membranes, thus increasing cell permeability which leads to loss of cellular contents. Moreover, EOs disrupt the mitochondrion of fungi causing energy depletion, inhibiting respiration, and disrupting aflatoxin biosynthesis by inhibiting the synthesis of DNA and transcription genes (Abd-Alla and Haggag, 2013; Yahyaraeyat *et al.*, 2013; Hossain *et al.*, 2016b).

4.3.2. Synergistic interactions of essential oils and silver nanoparticles

The antibacterial and antifungal effects of combined AgNPs and EOs by the checkerboard method against two foodborne bacteria (*E. coli* O157:H7, *S. Typhimurium*) and three spoilage fungi (*A. niger*, *P. chrysogenum*, and *M. circinelloides*) are presented in Tables 4.3-4.4. The selection of EOs and AgNPs was based on the high efficiency (low MIC) values. The silver nanoparticles AGC 0.5, AGPP, AGC 1 and AGPPH, and EOs of Mediterranean formulation, cinnamon EO, Asian formulation, lavang EO, and citrus EO was selected for the checkerboard tests against *E. coli* O157:H7, *S. Typhimurium*, *A. niger*, *P. chrysogenum*, and *M. circinelloides*. The dual combination between AGC 0.5+cinnamon EO, AGPP+Asian formulation EO, AGPPH+cinnamon EO, AGC 1+citrus EO, AGPP+cinnamon EO, AGPPH+Asian formulation, AGPPH+citrus EO, AGC1+cinnamon EO, and AGC 1+Asian formulation exhibited the highest synergistic activity against *E. coli* O157:H7 and *S. Typhimurium* (FIC < 1). The mixture of AGC 0.5+Asian formulation as well as AGPPH+Mediterranean formulation showed synergistic activity against *E. coli* O157:H7 and *S. Typhimurium* (FIC < 1), respectively. The combination of AGC 0.5+Mediterranean

formulation, AGC 0.5+lavang EO, AGPP+lavang EO, AGPP+citrus EO, AGPPH+lavang EO, AGC 1+Mediterranean formulation, and AGC 1+lavang EO showed synergistic activity against *S. Typhimurium* (FIC < 1) only.

The mixture of AGC 0.5+Mediterranean formulation, AGC 0.5+cinnamon EO, AGC 0.5+citrus EO, AGPP+Asian formulation, AGPP+lavang EO, AGPPH+cinnamon EO, AGPPH+lavang EO, AGC 1+citrus EO, AGC 1+lavang EO showed synergy against all tested fungal species such as *A. niger*, *P. chrysogenum* and *M. circinelloides* having FIC values below 1.0. The mixtures of AGPP+Mediterranean formulation and AGPP+citrus EO showed synergy against both *P. chrysogenum* and *M. circinelloides* (FIC < 1.0), however, antagonistic activity against *A. niger* (FIC > 1.0). The mixtures of AGC 0.5+Asian formulation, AGC 0.5+lavang EO, AGPP+cinnamon EO showed synergistic activity against both *A. niger* and *M. circinelloides*. The combination of AGC 1+cinnamon EO showed a synergistic effect against *A. niger* only. The AGPPH with citrus EO, AGC 1 with cinnamon EO, AGC 1 with Asian formulation exerted synergy only against *P. chrysogenum* (Table 4.3).

Combining antimicrobial and antifungal agents showing synergistic effects and thereby reducing the required concentration of active compounds may have several advantages including slower development of resistance and minimizing any undesirable organoleptic effects in foods. Oregano EO (*Origanum vulgare*) combined with AgNPs showed synergistic activity against resistant *E. coli* with bactericidal effects (Scandorieiro *et al.*, 2016). The interactions between two or more active compounds can be influenced by the type of the antibacterial/antifungal component, their concentrations, the microbial strain, and their size and shape (Sheikholeslami *et al.*, 2016). In some cases, the plant extract may aggregate AgNPs in the mixture which may change the size and shape of the nanoparticles and could reduce the antibacterial and antifungal effects (Asghar Heydari *et al.*, 2017).

Table 4.3. Fractional inhibitory concentration (FIC) indices of Ag-NPs in combination with the selected EOs.

Combination of EOs/AgNPs	<i>E. coli</i> O157:H7		<i>S. Typhimurium</i>		<i>A. niger</i>		<i>P. chrysogenum</i>		<i>M. circinelloides</i>	
	FIC	Act ¹	FIC	Act ¹	FIC	Act ¹	FIC	Act ¹	FIC	Act ¹
AGC 0.5+Mediterranean formulation	1.24	AG	0.74	S	0.49	S	0.74	S	0.74	S
AGC 0.5+cinnamon EO	0.53	S	0.49	S	0.56	S	0.99	S	0.62	S
AGC 0.5+Asian formulation	0.56	S	1.49	AG	0.75	S	1.24	AG	0.49	S
AGC 0.5+citrus EO	1.5	AG	0.99	S	0.53	S	0.49	S	0.74	S
AGC 0.5+lavang EO	1.25	AG	0.49	S	0.62	S	1.12	AG	0.99	S
AGPP+cinnamon EO	0.75	S	0.37	S	0.31	S	1.00	AD	0.62	S
AGPP+Asian formulation	0.28	S	0.31	S	0.62	S	0.55	S	0.49	S
AGPP+lavang EO	1.00	AD	0.49	S	0.75	S	0.75	S	0.5	S
AGPP+citrus EO	4.12	AG	0.75	S	2.25	AG	0.50	S	0.37	S
AGPP+Mediterranean formulation	0.5	S	1.00	AD	1.12	AG	0.62	S	0.37	S
AGPPH+Mediterranean formulation	1.12	AG	0.74	S	1.00	AD	1.12	AG	1.00	AD
AGPPH+cinnamon EO	0.49	S	0.37	S	0.37	S	0.75	S	0.62	S
AGPPH+Asian formulation	0.62	S	0.56	S	1.12	AG	1.00	AD	2.24	AG
AGPPH+citrus EO	0.62	S	0.49	S	1.25	AG	0.5	S	1.00	AD
AGPPH+lavang EO	2.25	AG	0.49	S	0.50	S	0.74	S	0.75	S
AGC 1+Mediterranean formulation	1.00	AD	0.74	S	1.00	AD	2.06	AG	1.00	AD
AGC 1+cinnamon EO	0.53	S	0.74	S	0.56	S	0.74	S	1.00	AD
AGC 1+Asian formulation	0.37	S	0.49	S	1.00	AD	0.56	S	2.24	AG
AGC 1+citrus EO	0.74	S	0.99	S	0.31	S	0.99	S	0.25	S
AGC 1+lavang EO	2.24	AG	0.49	S	0.74	S	0.74	S	0.37	S

Act¹: activity; FIC < 1.0: synergic effect (S); FIC = 1.0: additive effect (AD); FIC > 1.0: antagonistic effect (AG). FIC = FIC_{Ag-NPs} + FIC_{EOs}; FIC_{Ag-NPs} = MIC_{Ag-NPs} combined to EO / MIC_{Ag-NPs} alone; FIC_{EOs} = MIC_{EO} combined to Ag-NPs / MIC_{EOs} alone; FIC < 1.0: synergic effect (S); FIC = 1.0: additive effect (AD); FIC > 1.0: antagonistic effect (AG).

The results of antibacterial and antifungal effects of triple combinations of EO-AgNP in combination with other EOs were evaluated by the checkerboard method and the results are presented in Table 4.4. The triple combinations of (AGC 0.5+Mediterranean formulation) with citrus EO, (AGPP+cinnamom EO) with lavang EO, (AGPP+cinnamom EO) with Asian formulation, (AGC 1+cinnamom EO) with Asian formulation, (AGC 1+cinnamom EO) with citrus EO, and (AGPP+cinnamom EO+Asian formulation) with lavang EO showed synergistic effects against both *E. coli* O157: H7 and *S. Typhimurium* (FIC < 1.0) (Table 4.4).

For fungi, the triple combinations of (AGC 0.5+Mediterranean formulation) with citrus EO, (AGPP+cinnamom EO) with lavang EO, (AGPP+cinnamom EO) with Asian formulation, and (AGPP+cinnamom EO+Asian formulation) with lavang EO were effective against *A. niger*, *P. chrysogenum*, and *M. circinelloides*. The triple combination of (AGC 0.5+cinnamom EO) with Asian formulation showed synergistic antifungal activity against *P. chrysogenum* and *M. circinelloides*, while an antagonistic activity was observed for (AGC 0.5+cinnamom EO) with Asian formulation against only *A. niger* (FIC > 1.0) (Table 4.4).

The current study showed that AgNPs (AGPPH) with cinnamon EO have synergistic activities against pathogenic bacteria (*E. coli* O157:H7 and *S. Typhimurium*) and fungi (*A. niger*, *P. chrysogenum*, and *M. circinelloides*). Cinnamaldehyde is the main active chemical component found in cinnamon EO. The AgNP and cinnamaldehyde are engaged in the surface of pathogens which lead to the disruption of membrane and energy balance, and consequently the death of microorganisms (Ghosh *et al.*, 2013a). Ghosh *et al.* (2013a) found a combination of AgNPs and cinnamaldehyde was synergistic against spore-forming *Bacillus cereus* and *Clostridium perfringens*, which supports the current study.

Table 4.4. Fractional inhibitory concentration (FIC) indices of three or more combinations of EO and AgNPs.

Combination of EOs/AgNPs	<i>E. coli</i> O157: H7		<i>S. Typhimurium</i>		<i>A. niger</i>		<i>P. chrysogenum</i>		<i>M. circinelloides</i>	
	FIC	Act ¹	FIC	Act ¹	FIC	Act ¹	FIC	Act ¹	FIC	Act ¹
(AGC 0.5+Mediterranean formulation)/citrus EO	0.24	S	0.53	S	0.34	S	0.71	S	0.32	S
(AGC 0.5+cinnamon EO)/Asian formulation	2.50	AG	1.12	AG	1.56	AG	0.58	S	0.99	S
(AGPP+cinnamon EO)/lavang EO	0.37	S	0.53	S	0.76	S	0.34	S	0.71	S
(AGPP+cinnamon EO)/Asian formulation	0.62	S	0.58	S	0.32	S	0.74	S	0.34	S
(AGPP+Asian formulation)/lavang EO	2.66	AG	5.01	AG	1.0	AD	1.21	AG	2.44	AG
(AGC 1+cinnamon EO)/Asian formulation	0.58	S	0.99	S	1.23	AG	2.01	AG	1.0	AD
(AGC 1+cinnamon EO)/citrus EO	0.99	S	0.43	S	1.72	AG	2.56	AG	2.38	AG
(AGPP+cinnamon EO+Asian formulation)/lavang EO	0.74	S	0.99	S	0.99	S	0.82	S	0.51	S

Act¹: activity; FIC < 1.0: synergic effect (S); FIC = 1.0: additive effect (AD); FIC > 1.0: antagonistic effect (AG).

Generally, the major antibacterial and antifungal components in EOs are oxygenated terpenoids (such as phenolic terpenes, phenyl-propanoids, and alcohols). However, they contain hydrocarbons (α -pinene, camphene, myrcene, α -terpinene, and *p*-cymene) showing low bioactivity when applied alone, but their effectiveness will increase in combination with the others (Hossain *et al.*, 2016a; Nikkhah *et al.*, 2017a). For example, the hydrocarbon of *p*-cymene, found in Mediterranean formulation and cinnamon EO is known as a weaker antimicrobial component, but it can enhance the efficacy when combined with strong antimicrobial components (e.g., carvacrol). Because *p*-cymene is a substitutional impurity in the membrane having strong affinity binding to membranes resulting in the decreased enthalpy and melting temperature of the membrane that facilitates carvacrol penetration easily into the cell (Poimenidou *et al.*, 2016b). The minor components in the EOs may have a significant influence on the major components to exert and cause synergistic effect. It has been hypothesized that the combined treatment of EOs and AgNPs could increase their applicability and EOs encapsulated by AgNPs may increase the physical stability and bioactivity of EOs thereby protecting the EOs from environmental influences (Weisany *et al.*, 2019).

Based on the FIC results, three active combinations (AGPPH+cinnamon EO, AGC 0.5+Mediterranean formulation+citrus EO and AGPP+cinnamon EO+Asian formulation+lavang EO) were selected for further tests as those combinations showed synergistic effect (FIC index) against all tested pathogenic bacteria (*E. coli* O157:H7, *S. Typhimurium*) and spoilage fungi (*A. niger*, *P. chrysogenum*, and *M. circinelloides*). The active combinations were denoted as active combination 1 (AGPPH : cinnamon EO (0.1 : 6)), active combination 2 (AGC 0.5 : Mediterranean formulation : citrus EO (0.1 : 12 : 6)), and active combination 3 (AGPP : cinnamon EO : Asian formulation : lavang EO (0.1 : 12 : 6 : 6)). However, no study has been conducted in which the combination of two or more EOs with AgNPs is used to develop active combinations having synergistic effects. Hence, in the present study we verified the antibacterial and antifungal activities of the developed active combinations with synergistic effects from *in vitro* to *in situ* tests without contacting foods.

4.3.3. Vapor contact assay

The bacterial (*E. coli* O157:H7 and *S. Typhimurium*) and fungal (*A. niger*, *P. chrysogenum*, and *M. circinelloides*) colony diameter variation under the treatment of active combinations 1, 2, and 3 were evaluated and presented in Figure 4.1. The modified Gompertz model was applied to compare the bacterial and fungal growth in the presence of active combinations 1, 2, and 3 through

the parameters obtained from the model including the maximum colony diameter of the bacteria and fungi in stationary phase (A), the maximum exponential growth rate (V_m), and the lag time (λ) values (Char *et al.*, 2007; Avila-Sosa *et al.*, 2012; Hossain *et al.*, 2016a).

It can be seen from Figure 4.1 and Table 4.5 that the active combination 1 shows the highest antimicrobial activity against *E. coli* O157:H7 having the maximum colony diameter or $\ln(D_t/D_0)$ of 0.51, while that of the control is 2.32 on day 8. The lowest maximum growth rate (0.3/day) was observed in *E. coli* O157:H7 when treated with active combination 1, while the control sample showed the maximum growth rate of 1.4/day which was significantly different from that of active combination 1 ($P \leq 0.05$). Active combinations 2 and 3 showed the $\ln(D_t/D_0)$ values of 0.72 and 0.74 against *E. coli* O157:H7, respectively. The three active combinations (1, 2, and 3) extended the lag phase of *E. coli* O157:H7 and *S. Typhimurium* from 1-2 days. The active combinations 1, 2, and 3 showed strong antimicrobial activity against *S. Typhimurium*, and the maximum colony diameter was 0.42, 0.66, and 0.59, respectively, while the control sample's $\ln(D_t/D_0)$ was 1.79 ($P \leq 0.05$) (Figure 4.1 b, Table 4.5).

The developed active combinations 1, 2, and 3 extended the lag phase of all tested fungal species *A. niger*, *P. chrysogenum*, and *M. circinelloides* to 2-5 days, while the control lag phase of tested fungi was 1-1.92 days ($P \leq 0.05$) (Figure 4.1, Table 4.5). Active combination 3 was the most active against all three fungal species of *A. niger*, *P. chrysogenum*, and *M. circinelloides*. The maximum colony diameters (cm) of *A. niger*, *P. chrysogenum*, and *M. circinelloides* were 0.2, 0.1, and 0.16 when treated with active combination 3, respectively, while the corresponded maximum colony diameters for controls were significantly different 3.1, 3.2, and 5.1 cm at day 8 ($P \leq 0.05$) (Table 4.5). It was concluded that the active combinations 1, 2, and 3 limited the fungal growth, colony diameter, and extended the lag times. Similarly, Nikkhah *et al.* (2017a) studied the synergistic antifungal properties of the mixture of thyme, cinnamon, and rosemary EO against *P. expansum* and *Botrytis cinerea* by applying the modified Gompertz model to analyze the fungal growth profile. The authors found the mixture of thyme/cinnamon/rosemary EO was able to significantly reduce the fungal growth (*P. expansum* and *B. cinerea*) with an extended lag phase (Nikkhah *et al.*, 2017a). The combined oregano and thyme EO showed synergistic antifungal activity against *A. niger*, *A. flavus*, *A. parasiticus*, and *P. chrysogenum* reported by Hossain *et al.* (2016a). Those authors introduced a modified Gompertz model to evaluate the antifungal efficacy of oregano/thyme EO which significantly reduced the growth of *A. niger*, *A. parasiticus*, *A. flavus*, and *P. chrysogenum* and extended lag phase (Hossain *et al.*, 2016a). These findings provide valuable insights into how the active combinations exerted their antibacterial and antifungal activities by altering the growth kinetics of the tested pathogenic bacteria and fungi.

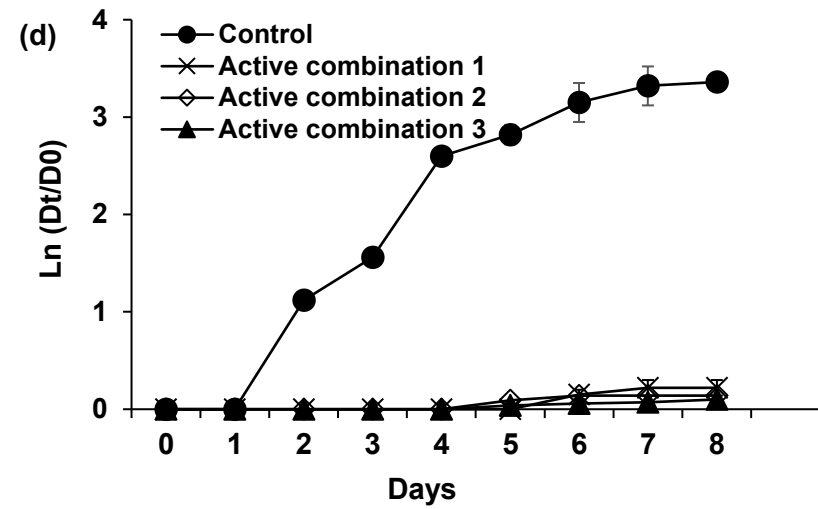
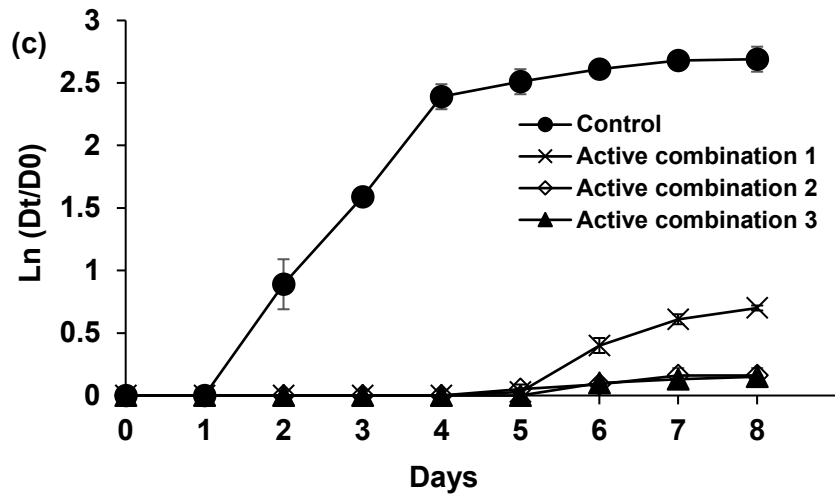
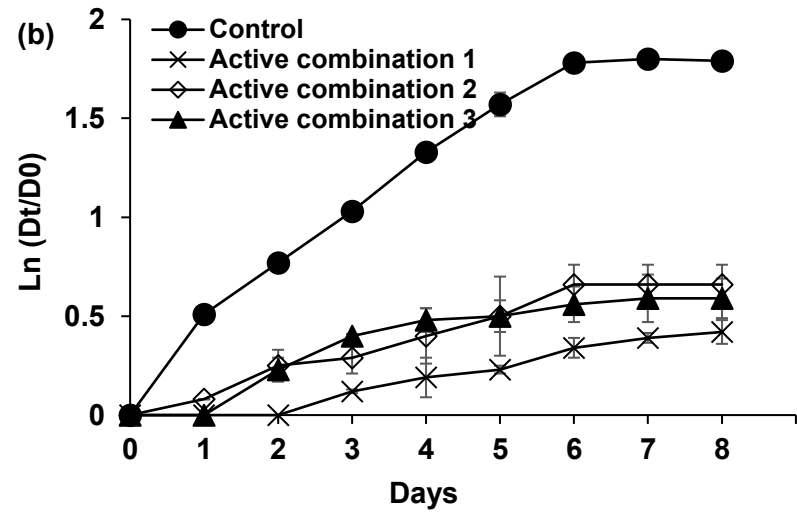
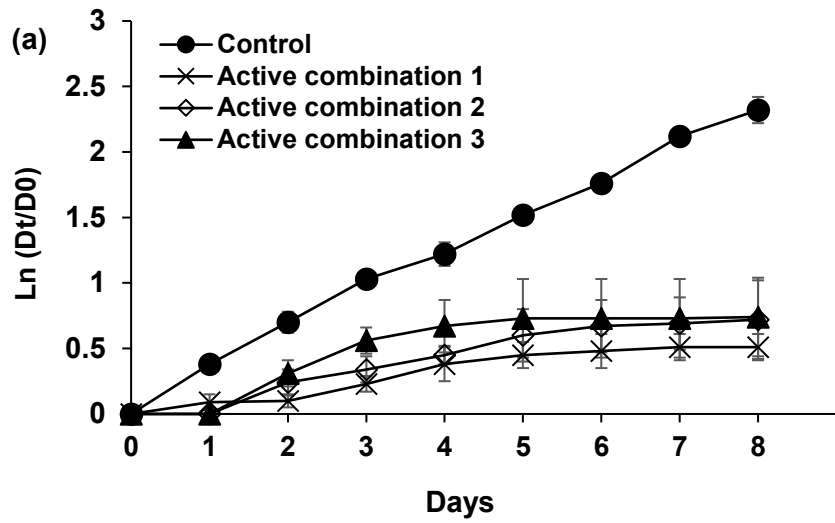
Table 4.5. Parameters of the modified Gompertz model for pathogenic bacterial and fungal species subjected to three active combinations containing essential oils and silver nanoparticles using vapor assay.

Active combinations	<i>E. coli</i> O157:H7			<i>S. Typhimurium</i>			<i>A. niger</i>			<i>P. chrysogenum</i>			<i>M. circinelloides</i>		
	A (cm)	$V_m d^{-1}$	λ (d)	A (cm)	$V_m d^{-1}$	λ (d)	A (cm)	$V_m d^{-1}$	λ (d)	A (cm)	$V_m d^{-1}$	λ (d)	A (cm)	$V_m d^{-1}$	λ (d)
Control*	2.4±0.2 _b	1.4±0.0 _{4b}	0.7±0.1 _a	2.3±0.0 _{4c}	1.3±0.0 _{4c}	1±0.2 _a	3.1±0.3 _b	1.9±0.04 _c	1±0 _a	3.2±0.1 _b	2.2±0.04 _b	1±0 _a	5.1±0.1 _c	3.3±0.02 _b	1±0 _a
Active combination 1	0.6±0.1 _a	0.3±0.0 _{6a}	1±0 _a	0.5±0.0 _{1a}	0.2±0.0 _{1a}	2±0 _b	0.7±0.1 _a	0.2±0 _b	4±0 _b	0.23±0 _a	0.08±0.03 _a	5±0 _b	0.54±0.06 _b	0.3±0.02 _a	2±0 _a _b
Active combination 2	0.7±0.0 _{3a}	0.5±0.1 _a	1±0 _a	0.5±0.0 _{7a}	0.4±0.1 _b	1±0 _{ab}	0.2±0 _a	0.1±0.01 _a	4±0 _b	0.19±0 _a	0.07±0.02 _a	4±0 _b	0.41±0.02 _b	0.2±0.08 _a	3±0 _b _c
Active combination 3	0.7±0.0 _{3a}	0.5±0.0 _{2a}	1±0 _a	0.7±0.0 _{9b}	0.4±0.1 _b	1±0 _{ab}	0.2±0 _a	0.05±0 _a	5±0 _b	0.1±0 _a	0.03±0.02 _a	4±0 _b	0.16±0.01 _a	0.1±0 _a	4±0 _c

Control*, did not contain active combinations.

Values are means±standard error. Within each column means with the same lowercase letter are not significantly different ($P \geq 0.05$).

A, Maximum colony diameter in cm during stationary phase; V_m , Maximum growth rate; λ , Lag time.



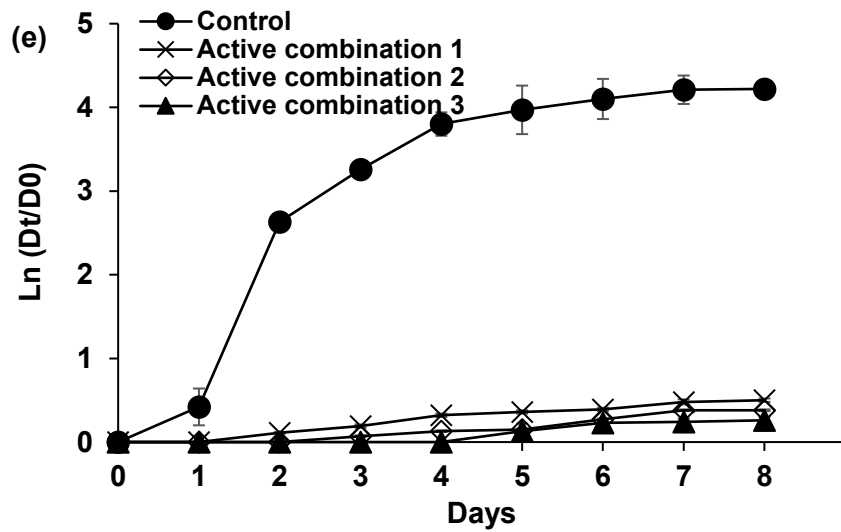


Figure 4.1. Effect of active combinations 1, 2, 3 on the maximum colony diameter, $\ln(D_t/D_0)$, of (a) *E. coli* O157:H7, (b) *S. Typhimurium*, (c) *A. niger*, (d) *P. chrysogenum*, and (e) *M. circinelloides* over time. The control sample did not contain active combinations. Values are means \pm standard error.

4.3.4. *In situ* antibacterial and antifungal efficiency of active combinations in rice

The vapor effect of active combinations 1, 2, and 3 containing essential oils and silver nanoparticles for controlling the pathogenic bacteria is presented in Figure 4.2a and 2b and the result corresponding to fungi is shown in Figure 4.2c, 4.2d, and 4.2e for a 28-day storage period in packaged rice. A 5 log CFU/g of bacteria or 5 log spores/g of fungi was inoculated in sterile rice samples with active combinations and the control samples contained only pathogens (did not contain active combinations).

The result showed that the active combination 1 had strong antimicrobial activity against *E. coli* O157:H7 and *S. Typhimurium*. A significant 3.52 and 4.52 log reduction of *E. coli* O157:H7 and *S. Typhimurium* was observed in rice when treated with active combination 1 as compared to control, respectively ($P \leq 0.05$). For *E. coli* O157:H7, the bacterial count was significantly ($P \leq 0.05$) reduced by 2.9 and 3.15 log CFU/g on 28th day of storage when treated with active combinations 2 and 3, while the bacterial count was 3.52 log CFU/g in the control. For *S. Typhimurium*, the bacterial count was 1.23 and 0.85 log CFU/g when treated with active combinations 2 and 3, respectively, while the control sample showed 4.05 log CFU/g after a 28-day storage period ($P \leq 0.05$). However, it was observed that *S. Typhimurium* was more sensitive to all three active combinations compared to *E. coli* O157:H7 (Figure 4.2 a,b; Table 4.6).

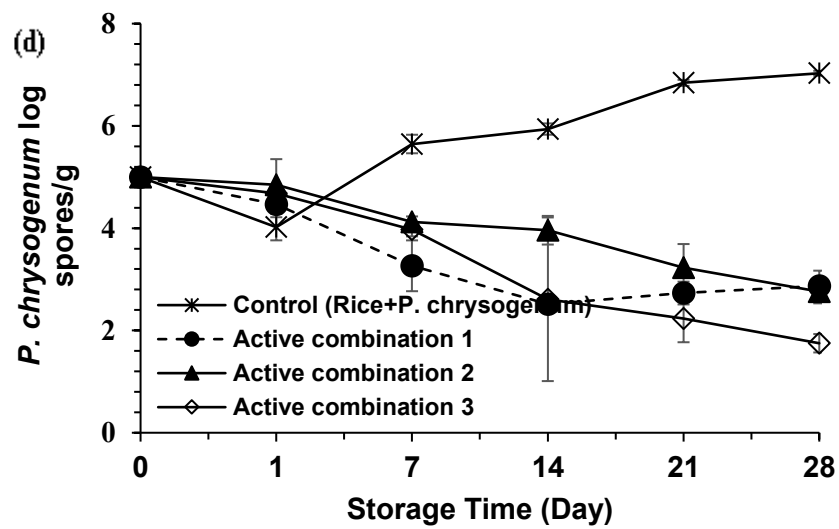
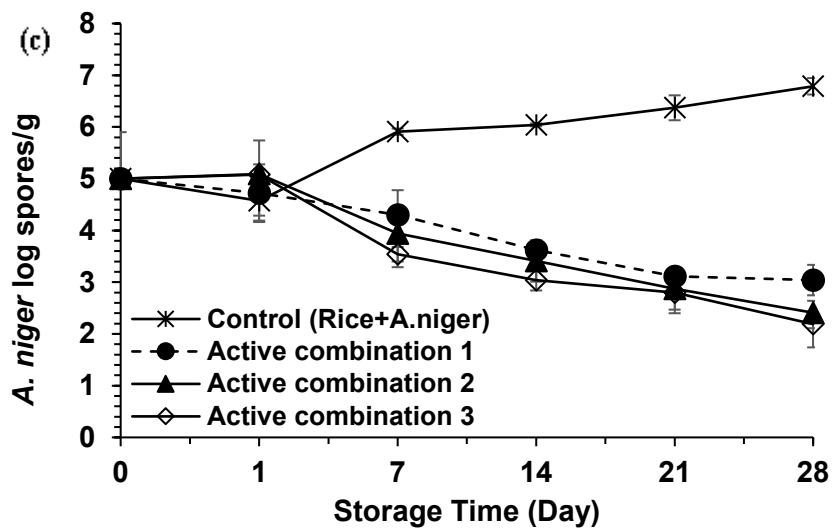
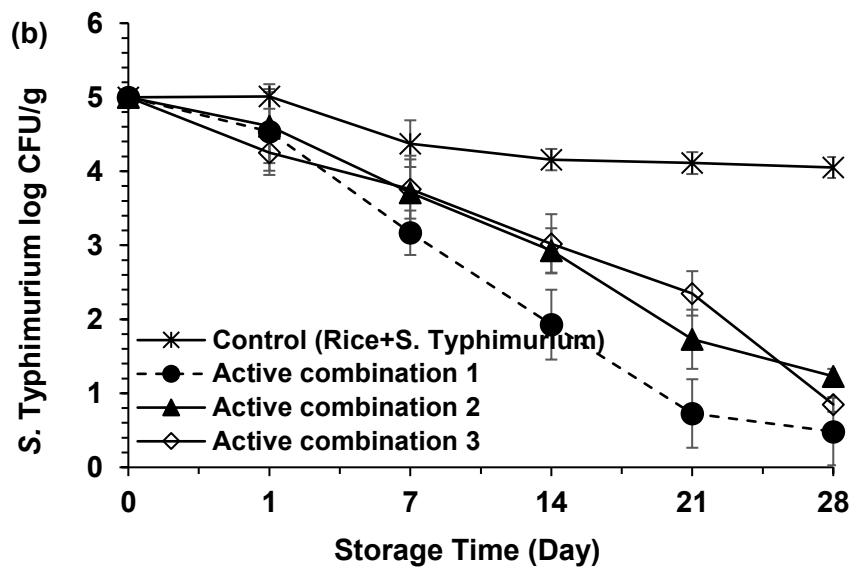
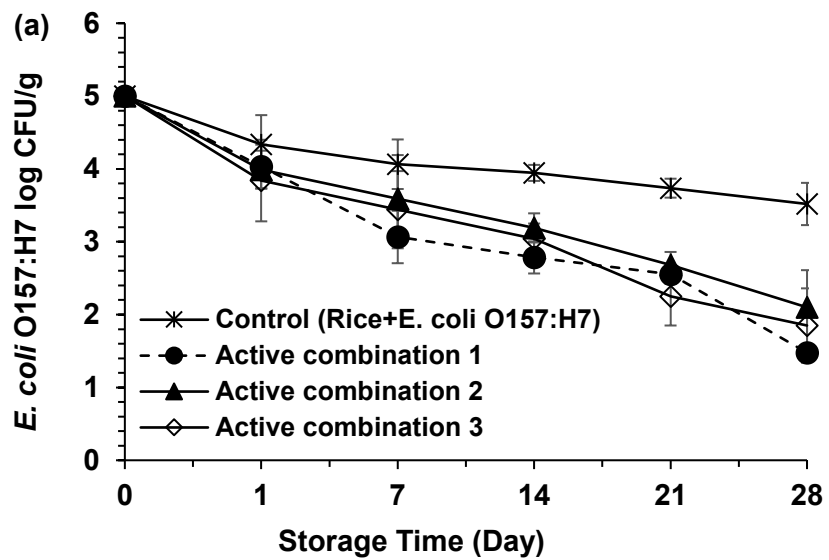
The active combinations 1, 2, and 3 were significantly ($P \leq 0.05$) reduced *A. niger*, *P. chrysogenum*, and *M. circinelloides* count in packaged rice on 28th day (Figure 4.2 c,d,e). Active combination 3 showed the highest antifungal activities against all tested fungi as compared to the control. At 28 days of the storage period, the three fungal (*A. niger*, *P. chrysogenum*, and *M. circinelloides*) counts significantly reduced by 2.19, 1.75, and 0.85 spores/g when treated with active combination 3, respectively, while the corresponded fungal counts in controls were 6.79, 7.03 and 6.93 spores/g ($P \leq 0.05$) (Table 4.6).

Table 4.6. Antibacterial and antifungal efficiency of active combinations 1, 2, and 3 on tested bacteria and fungi in rice on day 28.

Bacterial and fungal growth in rice at 28 days (log CFU/g or spores/g)					
Active combinations	<i>E. coli</i> O157:H7	<i>S.</i> Typhimurium	<i>A. niger</i>	<i>P.</i> <i>chrysogenum</i>	<i>M.</i> <i>circinelloides</i>
Control	3.52±0.29 ^{bA}	4.05±0.14 ^{cB}	6.79±0.16 ^{cC}	7.03±0.05 ^{cC}	6.93±0.03 ^{cC}
Active combination 1	1.48±0 ^{aB}	0.48±0.1 ^{aA}	3.04±0.29 ^{bD}	2.87±0.29 ^{bD}	2.31±0.22 ^{bC}
Active combination 2	2.9±0.5 ^{aBC}	1.23±0.1 ^{bA}	2.41±0.3 ^{aC}	2.76±0.23 ^{bC}	1.75±0.21 ^{bAB}
Active combination 3	3.15±0.5 ^{aB}	0.85±0.1 ^{abA}	2.19±0.45 ^{aB}	1.75±0.18 ^{aAB}	0.85±0.51 ^{aA}

Footnote: Values are means ± standard error. The same lowercase letter within each column either in the control or in the treated sample is not significantly different ($P > 0.05$). The same uppercase letters within each row are not significantly different ($P > 0.05$).

For *A. niger*, the fungal count was 3.04 and 2.41 spores/g in the sample treated with active combinations 1 and 2 ($P \leq 0.05$), respectively. The active combinations 1 and 2 reduced *P. chrysogenum* count by 2.87 and 2.76 spores/g ($P > 0.05$), respectively. These values for *M. circinelloides* were 2.31 and 1.75 spores/g in rice stored for 28 days, respectively. *M. circinelloides* was more sensitive to active combinations 1, 2, and 3, followed by *P. chrysogenum* and *A. niger*. Overall, the vapor of combined EOs and AgNPs can significantly ($P \leq 0.05$) reduce the pathogenic bacteria and spoilage fungi during the storage of rice. Likewise, low-density polyethylene (LDPE) film containing bimetallic nanoparticles (4 % Ag-Au NPs) with *cinnamon* EO showed strong antibacterial activities against *S. Typhimurium*, *L. monocytogenes*, and *Campylobacter jejuni* at during 21 days meat storage at 4 °C. It was also observed that combined Ag-Au/cinnamon EO was capable of a 100 % reduction of *S. Typhimurium* and *C. jejuni* from meat during storage (Ahmed *et al.*, 2018). Another study was conducted by Dehkordi *et al.* (2019) to evaluate the antibacterial properties of the AgNPs and eugenol, alone and in combination, against *S. aureus* and *S. Typhimurium* in meat and milk. The authors found combined (AgNPs/eugenol) treatment achieved 6 log reduction of *S. Typhimurium* and *S. aureus* from meat and milk samples within 3 h and 24 h, respectively, while it took a long time to reach a 6-log reduction of those bacteria when a single antimicrobial agent was applied (Dehkordi *et al.*, 2019).



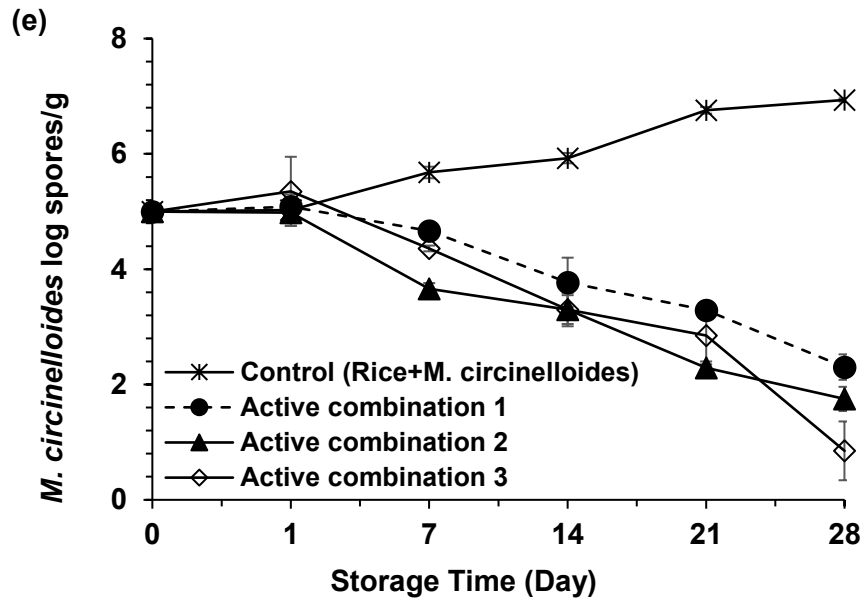


Figure 4.2. Effect of active combinations (1, 2, and 3) in rice to control (a) *E. coli* O157:H7, (b) *S. Typhimurium*, (c) *A. niger*, (d) *P. chrysogenum*, and (e) *M. circinelloides*. The control sample did not contain antimicrobials/antifungals. Values are means±standard error.

4.4. Conclusion

The study highlights the antimicrobial and antifungal efficiency of EOs and AgNPs alone and in combination to control pathogenic bacteria (*E. coli* O157:H7 and *S. Typhimurium*) and spoilage fungi (*A. niger*, *P. chrysogenum*, and *M. circinelloides*) during the storage of rice. The spherical shaped AgNPs (AGPP, AGPPH, AGC 1, and AGC 0.5) and EOs (cinnamon EO, Mediterranean formulation, citrus EO) showed strong to moderate antibacterial and antifungal efficacy in MIC assays. Three active combinations 1, 2 and 3 were developed using Checkerboard analyses which showed synergistic activity (FIC < 1.0) against all tested bacteria and fungi, and active combinations were (1) AGPPH+cinnamon EOs (active combination 1) (2) AGC 0.5+Mediterranean formulation+citrus EO (active combination 2) and (3) AGPP+cinnamon EO+Asian formulation+lavang EO (active combination 3). A modified Gompertz model was used to obtain more information on the growth profile of bacteria and fungi when treated with active combinations 1, 2, and 3 in the vapor state. *In vitro* vapor effect of active combinations 1, 2 and 3 significantly reduced the growth rate of the tested bacteria and fungi by prolonging their lag phase as compared to the control sample (without active compounds). The more challenging *in situ* tests were performed in rice to evaluate the antimicrobial and antifungal effects of active combinations under more realistic conditions. The antimicrobial and antifungal effect of active combinations 1, 2, and 3 significantly decreased the count of *E. coli* O157:H7, *S. Typhimurium*, *A. niger*, *P. chrysogenum*, and *M. circinelloides* in rice samples during a 28-day storage period. The findings of this study could be a potential, alternative and natural way to control pathogens and spoilage fungi in food products during storage with increased shelf life which can prevent postharvest losses of foods.

4.5. Acknowledgments

The authors are grateful for the financial support from Natural Sciences and Engineering Research Council of Canada (NSERC) no: RDCPJ 534563 - 18 and through a research agreement with NanoBrand Lab, the U.S. Department of Agriculture, Agricultural Research Service (USDA ARS), U.S. Pacific Basin Agricultural Research Centre and by a chair granted by Quebec Ministry of Agriculture, Fishery and Food (MAPAQ) no: PPIA12.

4.6. References

- Abd-Alla, M., Haggag, W.M., 2013. Use of some plant essential oils as post-harvest botanical fungicides in the management of anthracnose disease of Mango fruits (*Mangi feraindica* L.) caused by *Colletotrichum gloeosporioides* (Penz). International Journal of Agriculture and Forestry 3, 1-6.
- Ahmed, J., Mulla, M., Arfat, Y.A., Bher, A., Jacob, H., Auras, R., 2018. Compression molded LLDPE films loaded with bimetallic (Ag-Cu) nanoparticles and cinnamon essential oil for chicken meat packaging applications. Lwt-Food Science and Technology 93, 329-338.
- Asghar Heydari, M., Mobini, M., Salehi, M., 2017. The Synergic Activity of Eucalyptus Leaf Oil and Silver Nanoparticles Against Some Pathogenic Bacteria. Archives of Pediatric Infectious Diseases In Press.
- Avila-Sosa, R., Palou, E., Munguía, M.T.J., Nevárez-Moorillón, G.V., Cruz, A.R.N., López-Malo, A., 2012. Antifungal activity by vapor contact of essential oils added to amaranth, chitosan, or starch edible films. International Journal of Food Microbiology 153, 66-72.
- Ayari, S., Shankar, S., Follett, P., Hossain, F., Lacroix, M., 2020. Potential synergistic antimicrobial efficiency of binary combinations of essential oils against *Bacillus cereus* and *Paenibacillus amylolyticus*-Part A. Microbial Pathogenesis 141, 104008.
- Begum, T., Follett, P.A., Hossain, F., Christopher, L., Salmieri, S., Lacroix, M., 2020. Microbicidal effectiveness of irradiation from Gamma and X-ray sources at different dose rates against the foodborne illness pathogens *Escherichia coli*, *Salmonella* Typhimurium and *Listeria monocytogenes* in rice. LWT-Food Science and Technology 132, 109841.
- Bocate, K.P., Reis, G.F., de Souza, P.C., Oliveira Junior, A.G., Duran, N., Nakazato, G., Furlaneto, M.C., de Almeida, R.S., Panagio, L.A., 2019. Antifungal activity of silver nanoparticles and simvastatin against toxigenic species of *Aspergillus*. International Journal of Food Microbiol 291, 79-86.
- Braide, W., Nwaoguikpe, R., Oranus, S., Udegbonam, L., Akobondu, C., Okorundu, S., 2011. The effect of biodeterioration on the nutritional composition and microbiology of an edible long-winged reproductive termite, *Macrotermes bellicosus*. Smeathman. International Journal of Food Safety 13, 107-114.
- Burt, S., 2004. Essential oils: their antibacterial properties and potential applications in foods—a review. International Journal of Food Microbiology 94, 223-253.
- Char, C.D., Guerrero, S.N., Alzamora, S.M., 2007. Growth of *Eurotium chevalieri* in milk jam: influence of pH, potassium sorbate and water activity. Journal of Food Safety 27, 1-16.

- Dehkordi, N.H., Tajik, H., Moradi, M., Kousheh, S.A., Molaei, R., 2019. Antibacterial Interactions of Colloid Nanosilver with Eugenol and Food Ingredients. *Journal of Food Protection* 82, 1783-1792.
- Dussault, D., Vu, K.D., Lacroix, M., 2014. *In vitro* evaluation of antimicrobial activities of various commercial essential oils, oleoresin and pure compounds against food pathogens and application in ham. *Meat Science* 96, 514-520.
- Eghbalifam, N., Frounchi, M., Dadbin, S., 2015. Antibacterial silver nanoparticles in polyvinyl alcohol/sodium alginate blend produced by gamma irradiation. *International Journal of Biological Macromolecules* 80, 170-176.
- Emamifar, A., Kadivar, M., Shahedi, M., Soleimanian-Zad, S., 2010. Evaluation of nanocomposite packaging containing Ag and ZnO on shelf life of fresh orange juice. *Innovative Food Science and Emerging Technologies* 11, 742-748.
- Ghabraie, M., Vu, K.D., Tata, L., Salmieri, S., Lacroix, M., 2016. Antimicrobial effect of essential oils in combinations against five bacteria and their effect on sensorial quality of ground meat. *LWT-Food Science and Technology* 66, 332-339.
- Ghosh, I.N., Patil, S.D., Sharma, T.K., Srivastava, S.K., Pathania, R., Navani, N.K., 2013. Synergistic action of cinnamaldehyde with silver nanoparticles against spore-forming bacteria: a case for judicious use of silver nanoparticles for antibacterial applications. *International Journal of Nanomedicine* 8, 4721-4731.
- Helmlinger, J., Sengstock, C., Groß-Heitfeld, C., Mayer, C., Schildhauer, T.A., Köller, M., Epple, M., 2016. Silver nanoparticles with different size and shape: equal cytotoxicity, but different antibacterial effects. *RSC Advances* 6, 18490-18501.
- Hossain, F., Follett, P., Dang Vu, K., Harich, M., Salmieri, S., Lacroix, M., 2016a. Evidence for synergistic activity of plant-derived essential oils against fungal pathogens of food. *Food Microbiology* 53, 24-30.
- Hossain, F., Follett, P., Salmieri, S., Vu, K.D., Jamshidian, M., Lacroix, M., 2016b. Perspectives on essential oil-loaded nano-delivery packaging technology for controlling stored cereal and grain pests.
- Hossain, F., Follett, P., Vu, K.D., Salmieri, S., Senoussi, C., Lacroix, M., 2014a. Radiosensitization of *Aspergillus niger* and *Penicillium chrysogenum* using basil essential oil and ionizing radiation for food decontamination. *Food Control* 45, 156-162.
- Hossain, F., Lacroix, M., Salmieri, S., Vu, K., Follett, P.A., 2014b. Basil oil fumigation increases radiation sensitivity in adult *Sitophilus oryzae* (Coleoptera: Curculionidae). *Journal of Stored Products Research* 59, 108-112.

- Martínez-Castañón, G.A., Niño-Martínez, N., Martínez-Gutierrez, F., Martínez-Mendoza, J.R., Ruiz, F., 2008. Synthesis and antibacterial activity of silver nanoparticles with different sizes. *Journal of Nanoparticle Research* 10, 1343-1348.
- Metak, A.M., Nabhani, F., Connolly, S.N., 2015. Migration of engineered nanoparticles from packaging into food products. *LWT - Food Science and Technology* 64, 781-787.
- Mith, H., Dure, R., Delcenserie, V., Zhiri, A., Daube, G., Clinquart, A., 2014. Antimicrobial activities of commercial essential oils and their components against food-borne pathogens and food spoilage bacteria. *Food Science and Nutrition* 2, 403-416.
- Mohammadzadeh, A., 2017. In vitro antibacterial activity of essential oil and ethanolic extract of Ajowan (*Carum copticum*) against some food-borne pathogens. *Journal of Global Pharma Technology* 9, 20-25.
- Morones, J.R., Elechiguerra, J.L., Camacho, A., Holt, K., Kouri, J.B., Ramirez, J.T., Yacaman, M.J., 2005. The bactericidal effect of silver nanoparticles. *Nanotechnology* 16, 2346-2353.
- Nguefack, J., Somda, I., Mortensen, C., Amvam Zollo, P., 2005. Evaluation of five essential oils from aromatic plants of Cameroon for controlling seed-borne bacteria of rice (*Oryza sativa* L.). *Seed Science and Technology* 33, 397-407.
- Nikkhah, M., Hashemi, M., Habibi Najafi, M.B., Farhoosh, R., 2017. Synergistic effects of some essential oils against fungal spoilage on pear fruit. *International Journal Food Microbiol* 257, 285-294.
- Oussalah, M., Caillet, S., Saucier, L., Lacroix, M., 2007. Inhibitory effects of selected plant essential oils on the growth of four pathogenic bacteria: *E. coli* O157: H7, *Salmonella typhimurium*, *Staphylococcus aureus* and *Listeria monocytogenes*. *Food Control* 18, 414-420.
- Paster, N., Droby, S., Chalutz, E., Menasherov, M., Nitzan, R., Wilson, C., 1993. Evaluation of the potential of the yeast *Pichia guilliermondii* as a biocontrol agent against *Aspergillus flavus* and fungi of stored soya beans. *Mycological Research* 97, 1201-1206.
- Poimenidou, S.V., Bikouli, V.C., Gardeli, C., Mitsi, C., Tarantilis, P.A., Nychas, G.J., Skandamis, P.N., 2016. Effect of single or combined chemical and natural antimicrobial interventions on *Escherichia coli* O157:H7, total microbiota and color of packaged spinach and lettuce. *International Journal of Food Microbiology* 220, 6-18.
- Requena, R., Vargas, M., Chiralt, A., 2019. Study of the potential synergistic antibacterial activity of essential oil components using the thiazolyl blue tetrazolium bromide (MTT) assay. *LWT-Food Science and Technology* 101, 183-190.

- Scandorieiro, S., de Camargo, L.C., Lancheros, C.A., Yamada-Ogatta, S.F., Nakamura, C.V., de Oliveira, A.G., Andrade, C.G., Duran, N., Nakazato, G., Kobayashi, R.K., 2016. Synergistic and Additive Effect of Oregano Essential Oil and Biological Silver Nanoparticles against Multidrug-Resistant Bacterial Strains. *Frontiers in Microbiology* 7, 760.
- Sheikholeslami, S., Mousavi, S.E., Ahmadi Ashtiani, H.R., Hosseini Doust, S.R., Mahdi Rezayat, S., 2016. Antibacterial Activity of Silver Nanoparticles and Their Combination with *Zataria multiflora* Essential Oil and Methanol Extract. *Jundishapur Journal of Microbiology* 9, e36070.
- Simbine, E.O., Rodrigues, L.d.C., Lapa-GuimarÃEs, J., Kamimura, E.S., Corassin, C.H., Oliveira, C.A.F.d., 2019. Application of silver nanoparticles in food packages: a review. *Food Science and Technology* 39, 793-802.
- Snyder, A.B., Churey, J.J., Worobo, R.W., 2016. Characterization and control of *Mucor circinelloides* spoilage in yogurt. *International Journal of Food Microbiology* 228, 14-21.
- Sotiriou, G.A., Pratsinis, S.E., 2011. Engineering nanosilver as an antibacterial, biosensor and bioimaging material. *Current Opinion in Chemical Engineering* 1, 3-10.
- Tang, S., Zheng, J., 2018. Antibacterial Activity of Silver Nanoparticles: Structural Effects. *Advanced Healthcare Materials* 7, e1701503.
- Tardugno, R., Serio, A., Pellati, F., D'Amato, S., Chaves López, C., Bellardi, M.G., Di Vito, M., Savini, V., Paparella, A., Benvenuti, S., 2019. *Lavandula x intermedia* and *Lavandula angustifolia* essential oils: phytochemical composition and antimicrobial activity against foodborne pathogens. *Natural Product Research* 33, 3330-3335.
- Tongnuanchan, P., Benjakul, S., 2014. Essential oils: extraction, bioactivities, and their uses for food preservation. *Journal of Food Science* 79, R1231-R1249.
- Turgis, M., Vu, K.D., Dupont, C., Lacroix, M., 2012. Combined antimicrobial effect of essential oils and bacteriocins against foodborne pathogens and food spoilage bacteria. *Food Research International* 48, 696-702.
- Vishwakarma, G.S., Gautam, N., Babu, J.N., Mittal, S., Jaitak, V., 2016. Polymeric encapsulates of essential oils and their constituents: A review of preparation techniques, characterization, and sustainable release mechanisms. *Polymer Reviews* 56, 668-701.
- Weisany, W., Amini, J., Samadi, S., Hossaini, S., Yousefi, S., Struik, P.C., 2019. Nano silver-encapsulation of *Thymus daenensis* and *Anethum graveolens* essential oils enhances antifungal potential against strawberry anthracnose. *Industrial Crops and Products* 141.
- Yahyaraeyat, R., Khosravi, A., Shahbazzadeh, D., Khalaj, V., 2013. The potential effects of *Zataria multiflora* Boiss essential oil on growth, aflatoxin production and transcription of aflatoxin

biosynthesis pathway genes of toxigenic *Aspergillus parasiticus*. Brazilian Journal of Microbiology 44, 649-655.

Zachariah, T.J., Leela, N.K., 2006. Volatiles from herbs and spices. Handbook of Herbs and Spices, pp. 177-218.

Chapter 5

Release kinetics and biological properties of active films based on cellulose nanocrystal-chitosan in combination with γ -irradiation to mitigate microbial load in rice

This manuscript submitted to the *Journal of Food Hydrocolloids*, Impact factor: 11.504, h-index: 174, Overall Ranking: 1120, SCImago Journal Rank: 2.132

Tofa Begum¹, Peter A. Follett², Lily Jaiswal¹, Domitille de Guibert³, Stephane Salmieri¹, Monique Lacroix^{1*}

¹INRS-Armand Frappier Health Biotechnology Research Centre, Research Laboratories in Sciences, Applied to Food (RESALA), MAPAQ Research Chair in food safety and quality, Canadian Irradiation Center (CIC), Institute of Nutrition and Functional Foods (INAF), 531 des Prairies Blvd, Laval, QC, H7V 1B7, Canada

²United States Department of Agriculture, Agricultural Research Service, U.S. Pacific Basin Agricultural Research Center, 64 Nowelo Street, Hilo, HI 96720, USA

³Institute Agro - Agrocampus West Rennes, 65 Rue de Saint-Brieuc, 35042 Rennes, France

*Corresponding author. Dr. Monique Lacroix, Tel: 450-687-5010 # 4489, Fax: 450-686-5501, E-mail: Monique.Lacroix@inrs.ca

Contribution of the authors

Tofa Begum curated the data, developed the methodology and wrote the whole manuscript. Monique Lacroix and Peter A. Follett conceived the project, designed the general methodology, supervised the research, and edited the manuscript. Stephane Salmieri assisted with methodology, software, and statistical analysis, and reviewed the manuscript. Lily Jaiswal reviewed the manuscript. Domitille de Guibert helped with the data curation.

Résumé

Des nanoémulsions de deux formulations antimicrobiennes (AF-1 et AF-2) composées d'extraits d'agrumes et d'un mélange d'huiles essentielles (HE) ont été préparées par microfluidisation. Une conception composite centrale a été réalisée pour l'optimisation de la nanoémulsion AF-1 et AF-2 en étudiant l'influence de variables indépendantes telles que la haute pression (8 KPSI (2ème cycle) pour AF-1 et 15 KPSI (3ème cycle) pour AF-2), nombre de cycles et concentration d'émulsifiant 2 % Tween 80 sur les réponses, à savoir la taille moyenne des gouttelettes (nm), l'indice de polydispersité (PDI), le potentiel zêta (mV) et l'efficacité d'encapsulation (EE, %). Les formulations AF-1 et AF-2 optimisées avaient des potentiels zêta de 49 et 32.3 mV, taille : 116 et 40 nm, PDI : 0.17 et 0.2 et EE : 77 et 79 %, respectivement. Pour déterminer la stabilité physique, différents paramètres de fabrication, y compris les effets de la température de stockage (4, 25 et 40 ° C), la bioactivité et la turbidité de deux émulsions à savoir (i) émulsion grossière (préparée par ultraturax) et (ii) nanoémulsion (à l'aide d'un microfluidiseur) ont été comparés. Un essai de diffusion sur disque d'agar a montré que les propriétés microbicides des nanoémulsions AF-1 et AF-2 contre *Escherichia coli* O157:H7, *Salmonella* Typhimurium, *Aspergillus niger*, *Penicillium chrysogenum* et *Mucor circinelloides* étaient significativement supérieures à celles de l'émulsion grossière ($P \leq 0.05$). De plus, des tests *in situ* ont été effectués avec du riz stocké pendant deux mois en utilisant AF1 et AF2 incorporés dans des films nanocomposites à base de chitosan (CH) renforcés de nanocristaux de cellulose (CNC) et testés contre *E. coli* O157:H7, *S. Typhimurium*, *A. niger*, *P. chrysogenum* et *M. circinelloides* en combinaison avec ou sans un traitement d'irradiation γ (750 Gy). L'action combinée de l'irradiation γ et des films nanocomposites bioactifs à base de CH a entraîné une réduction de 3,89 à 7,3 log des bactéries et champignons testés après 8 semaines de stockage par rapport au témoin (sans films ni irradiation). L'incorporation de CNC dans des films bioactifs à base de CH a démontré un schéma prévisible de libération plus lente des composants actifs (32 à 39 %) sur 8 semaines par rapport aux films bioactifs sans CNC. Le riz traité avec différents films nanocomposites bioactifs n'a présenté aucun changement significatif ($P > 0.05$) dans les attributs sensoriels, y compris la couleur, l'odeur, le goût et l'appréciation générale par rapport au riz non traité.

Abstract

Nanoemulsions of two antimicrobial formulations (AF-1 and AF-2) composed of citrus extracts and a mixture of essential oils (EOs) were prepared by microfluidisation. A central composite design was performed for optimization of AF-1 and AF-2 nanoemulsions by studying the influence of independent variables such as high pressure (8 KPSI (2nd cycle) for AF-1 and 15 KPSI (3rd cycle) for AF-2), number of cycles, and concentration of emulsifier (2 % Tween 80) on responses namely mean droplet size (nm), polydispersity index (PDI), zeta potential (mV), and encapsulation efficiency (EE, %). The optimized AF-1 and AF-2 had zeta potentials of 49 and 32.3 mV, size: 116 and 40 nm, PDI: 0.17, and 0.2, and EE: 77 and 79 %, respectively. To determine the physical stability, different fabrication parameters including the effects of storage temperature (4, 25, and 40 °C), bioactivity, and turbidity of two emulsions namely (i) coarse emulsion (prepared by ultraturax) and (ii) nanoemulsion (using microfluidizer) were compared. An agar disc diffusion assay exhibited that the microbicidal properties of the AF-1 and AF-2 nanoemulsions against *Escherichia coli* O157:H7, *Salmonella* Typhimurium, *Aspergillus niger*, *Penicillium chrysogenum*, and *Mucor circinelloides*, were significantly greater than the coarse emulsion ($P \leq 0.05$). In addition, *in situ* tests were performed in stored rice for two months using AF1 and AF2 incorporated into Chitosan-based (CH) nanocomposite films reinforced with cellulose nanocrystals (CNCs) and tested against *E. coli* O157:H7, *S. Typhimurium*, *A. niger*, *P. chrysogenum*, and *M. circinelloides* in combination with (750 Gy) and without γ -irradiation. The combined action of γ -irradiation and bioactive CH-based nanocomposite films caused a 3.89 to 7.3 log reduction of the bacteria and fungi tested after 8 weeks of storage compared to control (without the films or irradiation). Incorporation of CNC into bioactive CH-based films demonstrated predictable pattern of slower release of active components (32 to 39 %) over 8 weeks compared to the bioactive films without CNC. Rice treated with different bioactive nanocomposite films exhibited no significant change ($P > 0.05$) in sensory attributes including color, odor, taste, and general appreciation compared to untreated rice.

5.1. Introduction

Across the world, one-third of the food production is lost or wasted each year, which causes significant economic losses for farmers, the food industry, and consumers. In this context, foodborne pathogenic bacteria and spoilage fungi are major culprits that can play a substantial role in food losses, waste, and foodborne illness (Zhang *et al.*, 2021). As a primary source of calories and nutrition (carbohydrates, fats, proteins, minerals, vitamins), rice (*Oryza sativa* L.) has been one of the most important cereal grains worldwide, account for 50 % of the world population's consumption (Nguefack *et al.*, 2005; Das *et al.*, 2021b). In addition, to its nutritive value, rice grains are highly susceptible to biodeterioration by several categories of microbes including pathogenic bacteria (*Escherichia coli*, *Salmonella* sp., *Listeria* sp.) (Begum *et al.*, 2020a) and storage fungi (*Aspergillus* sp., *Penicillium* sp., *Mucor* sp., *Fusarium* sp.) (Hossain *et al.*, 2019a; Begum *et al.*, 2022b). The above mentioned microbial infestation can cause lipid peroxidation that can lead to unpleasant odors, discoloration, off-flavor, hydro-peroxides formation, and eventually the reduction of nutritional quality of stored rice. In addition, upon infestation *Aspergillus* sp. secretes mycotoxins such as Aflatoxin B1 and metabolite by product such as methylglyoxal which is designated as mycotoxin's biosynthesis inducer (Das *et al.*, 2021a). It has been reported that Aflatoxin B1 is potent carcinogen and mutagen (Hossain *et al.*, 2019a; Das *et al.*, 2021a). Currently, several synthetic chemical preservatives have been used to curb microbial infestation which has adverse consequences on microbial resistance, health and the environment.

Plant-derived essential oils (EOs), plant extracts (PEs), and citrus extracts (CEs) have antibacterial, antifungal, insecticidal, antiviral, and antioxidant properties and have great potential to substitute synthetic preservatives to prevent bio-deteriorating agents in stored rice (Turgis *et al.*, 2012; Hossain *et al.*, 2016a; Begum *et al.*, 2022b). EOs have various mechanisms of action for controlling a wide range of microbes and are less prone to microbial resistance. However, the application of EOs in the food industry is still in early stage due to their highly volatile nature, low water solubility, chemical instability under environmental factors including temperature, moisture, pH, oxidation, light, and isomerisation (Das *et al.*, 2021b). In addition, direct application of EO nanoemulsions may affect the organoleptic and sensory properties of the foods which may further reduce their utility. The above mentioned drawbacks of EOs can be addressed by incorporating them in an oil-in-water emulsion thereby improving properties such as transparency, physical stability, increased bioactivity, and enhanced encapsulation efficiency (Hossain *et al.*, 2018; Llinares *et al.*, 2018). High-pressure microfluidisation is an efficient technique to produce nanoemulsions (droplet size from 2 to 200 nm) of essential oils which can be exploited for scale up and industrial production. It has been observed that the high homogenization shear pressure

and cycle number of cycles of microfluidization significantly influence the droplet size and eventually enhances the nanoemulsion attributes (Hossain *et al.*, 2018; Llinares *et al.*, 2018).

Nanoemulsion of EOs can be incorporated into biodegradable polymers to form bioactive nanocomposite polymeric films which can prevent direct contact of EO with foods, without compromising antimicrobial efficacy (Hossain *et al.*, 2019a). Chitin is a polysaccharide mostly found in exoskeletons of crustaceans whose partial deacetylation produces chitosan. Chitosan is non-toxic, bio-functional, biocompatible biopolymers composed of *N*-acetyl D-glucosamine and D-glucosamine units and positively charged amine groups. Chitosan is also found in the cell wall of fungi and insect cuticles and approved by the FDA as a food ingredient (Khan *et al.*, 2012; Hossain *et al.*, 2019a). Another abundant biopolymer found in wood, cotton, and other plant sources is cellulose (Khan *et al.*, 2012). Cellulose Nanocrystals (CNC) are prepared from cellulose via acid hydrolysis. The nanosized (5-10 nm) CNC has been used as a reinforcing agent in biopolymers for improving mechanical, thermal, barrier properties, and controlled release of active compounds during storage (Azeredo *et al.*, 2010; Hossain *et al.*, 2018; Hossain *et al.*, 2019a).

Food irradiation (cold pasteurization) is an efficient and promising technology to mitigate foodborne illness and spoilage organisms (Eustice, 2015; Maherani *et al.*, 2016). However, depending on the food dose, optimization is prerequisite for microbial inactivation ranging from 0.5 to 30 kGy (USDHS-U.S. Department of Homeland Security, 2019). In particular, irradiation breaks down the chemical bonds in DNA, altering membrane permeability and disrupting normal cellular activity (Caillet *et al.*, 2005; Caillet and Lacroix, 2006). It has been observed that EOs and irradiation in combination can work synergistically through affecting the bacterial membrane integrity, and murein composition thereby releasing the bacterial cell constituents, decreasing internal pH and ATP consumption (Caillet *et al.*, 2005; Caillet and Lacroix, 2006; Oussalah *et al.*, 2006). Combined treatment of active packaging and irradiation can act synergistically and be quite effective to increase the radiosensitivity of the microbial cells (Ayari *et al.*, 2012; Hossain *et al.*, 2014a).

Therefore, the current research is undertaken (i) to develop and optimize active nanoemulsion formulations using plant-derived essential oils and citrus extracts, (ii) to develop essential oils and citrus extracts impregnated bioactive nanocomposite chitosan-based packaging film, (iii) to evaluate the effect of reinforcing agent (CNC) on mechanical, permeability and control release of the active components, (iv) to determine *in vitro* and *in situ* antibacterial and antifungal properties of bioactive chitosan films against foodborne pathogens in stored rice, (v) to evaluate possible synergistic effects between γ -irradiation and active packaging films, and (vi) to evaluate the sensorial properties of the stored rice with and without storage in chitosan-based bioactive films.

5.2. Materials and Methods

5.2.1. Essential oils (EOs) and citrus extract

Cinnamon essential oil (EO), savory thyme EO, and citrus EO were purchased from Zayat Aroma (Bromont, QC, Canada). The Southern formulation, Asian formulation, and Mediterranean formulation was obtained from BSA (Montreal, QC, Canada). The citrus extracts (CEs)—organic citrus extract (OCE) and natural citrus extract (NCE)—were kindly provided by Kerry (Mont St-Hilaire, QC, Canada). Two active formulations (AF-1 and AF-2) were prepared using citrus extracts (CEs) and mixtures of essential oils (EOs) based on our previous research (Begum *et al.*, 2022b). AF-1 was composed of organic citrus extract (OCE), Mediterranean formulation, citrus EO, cinnamon EO in the ratio of 2 : 1 : 2 : 1, and the AF-2 composed of natural citrus extract (NCE), Asian formulation, Southern formulation, cinnamon EO, savory thyme EO with the corresponded ratio of 2 : 2 : 1 : 2 : 1.

5.2.2. Bacterial and fungal culture preparation

Two foodborne pathogenic bacteria (*Escherichia coli* O157:H7 NT 1931 and *Salmonella* Typhimurium SL 1344) and three food spoilage fungi (*Aspergillus niger* ATCC 1015, *Penicillium chrysogenum* ATCC 10106, and *Mucor circinelloides* ATCC 56649) were selected for *in vitro* and *in situ* experiments. All pathogenic bacteria and spoilage fungi were preserved in tryptic soy broth (TSB for bacteria) or in potato dextrose broth (PDB for fungi) containing 10 % (v/v) glycerol kept at -80 °C (Ghabraie *et al.*, 2016). At the onset of each experiment, the cryopreserved cultures were passed through two consecutive growth cycles in the corresponding nutrient media at 37 °C for 24 h (bacteria) or at 28 °C for 48 h (fungi). Upon obtaining the desired concentration of bacterial cultures (1×10^5 CFU/mL), the cultures were centrifuged and washed with sterile saline water. From PDA media, pre-cultured fungi (for 2 - 4 days) were collected using sterile saline water and filtered and adjusted to approximately 1×10^5 spores/mL final fungal concentrations for all tests.

5.2.3. Nanoemulsion development, optimization, and characterization of the active formulations

A central composite design was performed for the development and optimization of active formulations (AF-1 and AF-2) using Design Expert (Version 11). The independent variables were concentration of AF-1 and AF-2 (2 %), pressure (8 KPSI to 20 KPSI), number of cycles (0 to 4), and concentration of emulsifier (Tween 80) (1-3 %, v/v). The dependent variables were zeta

potential (mV), size (nm), poly dispersity index (PDI), and encapsulation efficiency (EE, %). The independent variables for AF-1 (total number of mixtures runs = 20 with 6 replicates as central points) and AF-2 (total number of mixtures runs = 20 with 6 replicates) are presented in Supplementary data Table 5.1 and Supplementary data Table 5.2, respectively. The oil-in-water (O/W) emulsion for each sample run was homogenized for 1 min at 15000 rpm using Ultra Turrax (TP18/1059 homogenizer) which was considered as coarse emulsion with zero number of cycles and zero microfluidisation pressure, then the emulsion was passed through a high-pressure microfluidizer (Microfluidics Inc., Newton, MA, USA) at different pressures and cycles to obtain stable nanoemulsions.

5.2.3.1. Measurement of particle size, zeta potential, and PDI

The ζ -potential (zeta) (mV), average particle size (nm), and size distribution (PDI-Poly dispersity index) were determined by dynamic light scattering using photon correlation spectroscopy (Malvern Zetasizer Nano-ZS, Model ZEN3600, Westborough, MA, USA) at 25 °C. The samples were diluted in deionized water in the ratio of 1:50 to prevent multiple scattering effects following [Ben-Fadhel *et al.* \(2022\)](#). Each experiment was performed in triplicate (n = 3). The results are presented in Figures 5.1 (a-c) and 5.2 (a-c) for AF-1 and AF-2, respectively.

5.2.3.2. Encapsulation efficiency (EE)

The encapsulation efficiency of AF-1 and AF-2 nanoemulsions for each mixture run was determined according to [Hossain *et al.* \(2019b\)](#). Briefly, 3 mL of nanoemulsion was transferred to a centrifuge tube and centrifuged at 6000 rpm (revolution per minute of rotor) for 10 mins at 4 °C. A volume of 3 mL methanol was added after removing the supernatant and followed by a second centrifugation for another 30 min. Then, the supernatant was quantified using a UV-VIS spectrophotometer at a UV-length of 360 nm. The encapsulation efficiency (EE) was measured by the following equation:

$$EE = (\text{Total oil} - \text{Free oil}) / \text{Total oil} \times 100 \text{ Eq. 5.1}$$

The results are presented in Figure 5.1d and 5.2d for the AF-1 and AF-2 nanoemulsions, respectively.

5.2.3.3. Statistical analysis for optimization

To optimize the final conditions of microfluidization (pressure, number of cycles, emulsifier concentration) to prepare AF-1 and AF-2 nanoemulsions with the best stability, EE, highest antibacterial and antifungal properties, the dependent variables (ζ -potential, size, PDI, and EE)

were fitted into the design expert software. The measured independent variables were fitted to linear and quadratic models as Eq. 5.2 and Eq. 5.3, respectively.

$$Y = C_0 + \sum_{i=1}^n C_i X_i + \sum_{i=1}^n C_j X_j \quad \text{Eq. 5.2}$$

$$Y = C_0 + \sum_{i=1}^n C_i X_i + \sum_{1 \leq i < j}^n C_{ij} X_i X_j + \sum_{1 \leq i < j < k}^n C_{ijk} X_i X_j X_k \quad \text{Eq. 5.3}$$

Where, Y = dependent variables (ζ -potential, size, PDI, and EE); C_0 = constant-coefficient; C_i = linear coefficient; C_{ij} = interactive coefficient; $X_i \dots X_j \dots X_k$ = independent variables; n = number of variables. Each experiment was performed in triplicate. Data for each variable were subjected to analysis of the variance (ANOVA), and the P-value ($P \leq 0.05$: significant and $P > 0.05$: insignificant) was used to accept or reject the null hypothesis (H_0 : no effect of varying the level of a variable) (Radfar *et al.*, 2020; Begum *et al.*, 2022b).

For evaluating the effect of different microfluidisation pressures, the number of cycles, and concentration of emulsifier on AF-1 and AF-2 nanoemulsions (Figure 5.1a-d and Figure 5.2a-d), the dependent variables (ζ -potential, size, PDI, and EE) were plotted creating 3D images. Deciphering the effect of independent variables on dependent variables using 3D images is crucial because through this, the optimum conditions for developing stable nanoemulsions could be achieved which can connect all points within the three-dimensional plane (Falleh *et al.*, 2019; Radfar *et al.*, 2020; Begum *et al.*, 2022b).

5.2.4. Storage stability of coarse and optimized nanoemulsion

The effect of storage time and temperature on the stability of nanoemulsions was measured following the methods of Nirmal *et al.* (2018). A volume of 15 mL of the coarse and nanoemulsions were stored in airtight glass bottles and kept at 4 °C, 25 °C, or 40 °C for 60 days. Each week, the stability of the nanoemulsions was examined by measuring mean particle size (nm) (Figure 5.3a-c). Stability may be compromised due to coagulation, phase separation, or creaming during storage.

5.2.5. Inhibitory capacity and turbidity measurement of the coarse and optimized nanoemulsions

To evaluate the bactericidal and fungicidal activity against *E. coli* O157:H7, *S. Typhimurium*, *A. niger*, *P. chrysogenum* and *M. circinelloides*, the inhibitory capacity (IC, %) of the coarse and nanoemulsion of AF-1 and AF-2 was performed against above mentioned microbes by agar disc diffusion assay (Dussault *et al.*, 2014; Ghabraie *et al.*, 2016). In detail, 30 μ L emulsion was added to a small filter disc (8 mm diameter), and the disc was placed at the center of a tryptic soy agar/potato dextrose agar plate (92 \times 16 mm, St. Leonard, QC, Canada) which was previously inoculated with a 100 μ L suspension of either bacteria (10^5 CFU/mL) or fungi (10^5 spores/mL). The plates were sealed with parafilm to prevent evaporation of the volatile compounds found in AF-1 and AF-2 and then kept at 37 $^{\circ}$ C for 24 h or 28 $^{\circ}$ C for 48 h for bacteria and fungi, respectively. The zone of inhibition (no colony growth) around the filter disc was measured using a traceable carbon fiber digital caliper (resolution: 0.1 mm accuracy: 0.2 mm; Fisher Scientific). The inhibitory capacity (IC, %) was calculated as follows:

$$\text{Inhibitory Capacity (IC, \%)} = (D_{\text{IN}} / D_{\text{PD}}) \times 100 \text{ Eq. 5.4}$$

Where D_{IN} is the diameter of the zone of inhibition and D_{PD} is the diameter of the Petri dish.

The turbidity of the coarse and optimized nanoemulsions of AF-1 and AF-2 was determined by UV-VIS spectrophotometer at 360 nm (Model Cary 8454, Agilent Technologies, Santa Clara, CA, USA) (Nirmal *et al.*, 2018).

5.2.6. Development of chitosan-based nanocomposite films

Chitosan (CH) based composite film reinforced with cellulose nanocrystals (CNCs) was developed following the methods of Khan *et al.* (2012) and Hossain *et al.* (2019a) with some modification. In brief, 2 % (w/v) chitosan was dissolved in a 2 % aqueous solution of acetic acid (CH_3COOH). A quantity of 2 % CNC (w/w) was prepared in distilled water, mixed well under magnetic stirring for 3 h at room temperature, and then sonicated for 30 min in the cold-water bath. The CNC suspension (0, 1, 2, 4, 6, 8, and 10 %) (v/w) was then added into the CH-based film-forming solution, followed by 0.5 % (w/v) polyethylene glycol (PEG) addition as a plasticizer. The CH-based solutions were then homogenized with a high shear mixer (23000 rpm) for 6 h using IKA RW-20 mechanical homogenizer. Then, 15 mL of CH-based film-forming solution was casted into

Petri plates (95×16 mm; Sarstedt, Newton, USA) and dried at room temperature for 24 h. The chitosan films without CNC were taken as controls (Khan *et al.*, 2012; Hossain *et al.*, 2019a).

5.2.6.1 Water vapor permeability (WVP)

WVP tests of the CH-based films containing different concentrations of CNC were examined following the methods described by Salmieri *et al.* (2014b). Each CH-based nanocomposite film was mechanically sealed onto Vapometer cells (model 68-1; Twining-Albert Instrument Co., West Berlin, NJ, USA) containing anhydrous CaCl₂ (30 g). The initial weight of the cells was recorded and then were placed in a humidity chamber (model Shellab 9010L, Sheldon Manufacturing Inc., Cornelius, OR, USA) for 24 h at 25 °C and 60 % relative humidity (RH). The final weight of the Vapometer cells was taken after 24 h. The weight gained by CaCl₂ indicated the amount of H₂O vapor absorbed through the CH-based nanocomposite films, which were fitted to Fick and Henry's laws of gas diffusion and follows Eq. 5.5 for evaluating WVP of the film.

$$\text{WVP (g mm m}^{-2}\text{day}^{-1}\text{kPa}^{-1}) = \Delta w \cdot x / A \cdot \Delta P \text{ Eq. 5.5}$$

Where Δw : Vapometer cell weight (g) gain after 24 h; x : Film thickness (mm); A : Area of exposed film ($31.67 \times 10^{-4} \text{ m}^2$); ΔP : differential vapor pressure of water through the film ($\Delta P = 3.282 \text{ kPa}$ at 25 °C).

5.2.6.2. Mechanical properties of the films

The mechanical properties (tensile strength [TS], tensile modulus [TM], and elongation at break [Eb]) of the chitosan-based films with and without CNC were measured (Salmieri *et al.*, 2014b). Briefly, the thickness of the films was measured at five random positions using a Mitutoyo Digimatic Indicator with 1 μm resolution; (Model ID-110E, Mitutoyo MFG Co. Ltd, Tokyo, Japan). The width of the film was measured by a Traceable Carbon Fiber Digital Caliper (Fisher Scientific, Quebec, Canada). A Universal Testing Machine Model H5KT (Tinius Olsen Testing Machine Co., Inc., Horsham, PA, USA) equipped with a 100 N-load cell and 1.5 kN-specimen grips was used for measuring mechanical properties of the films (ASTM, 1995). The position of the machine was controlled by the initial grip separation: 30 mm, crosshead speed: 50 mm/min, and a load cell: 100 N. A total of 5 measurements were taken for each film, and average values were presented with standard error.

5.2.7. Bioactive film development and irradiation treatment with rice

The concentration of CNC was optimized to prepare CNC reinforced CH-based nanocomposite films. Later the nanoemulsions of AF-1 and AF-2 were incorporated into films to form solutions at

different concentrations (0 - 1 % AF-1, AF-2), then mixed well and cast following the method described by [Hossain et al. \(2019a\)](#). The films without bioactive nanoemulsions (0 % AF-1 and AF-2) were taken as controls. The *in vitro* antibacterial and antifungal activities of the developed nanocomposite CH-based films were determined by the agar volatilization test described by [Cardiet et al. \(2012\)](#); [Begum et al. \(2022a\)](#). Briefly, the bacterial and fungal species (approximately 10^5 CFU/mL or 10^5 spores/mL) were inoculated on the surface of nutrient media (TSA for bacteria and PDA for fungi). The plates were inverted and a 1 cm² piece of the film was placed in the middle of the lid of the Petri plate. All plates were sealed with Parafilm® to prevent vapor transfer and incubated at 37 °C for 24 h for bacteria or 27 °C for 48 h for fungi. The antibacterial and antifungal properties of the films were measured as inhibitory capacity (IC, %).

The antibacterial and antifungal properties of bioactive films with and without γ -irradiation in rice for controlling pathogenic bacteria (*E. coli* O157:H7 and *S. Typhimurium*) and spoilage fungi (*A. niger*, *P. chrysogenum*, and *M. circinelloides*) were evaluated following the methods by [Hossain et al. \(2018\)](#); [Hossain et al. \(2019a\)](#); [Begum et al. \(2022b\)](#). Briefly, 500 g of sterile rice was submerged in an inoculation bath of peptone water containing 10^5 CFU/mL of bacteria or 10^5 spores/mL of fungi. The rice was mixed well for 30 sec and dried for 2 h under sterile conditions. Fifty grams of the inoculated rice was transferred to a sterile plastic bag and two strips of the most efficient bioactive CH-based nanocomposite films (8.5 cm in diameter) containing a nanoemulsion of either AF-1 or AF-2 were added. The concentrations of AF-1 and AF-2 in the films were selected based on the *in vitro* test results. Some samples with or without bioactive films were also irradiated at 750 Gy using a UC-15A γ -irradiator equipped with Cobalt-60 (Nordion, Laval, QC, Canada) and having a dose rate of 7.1 kGy/h. The samples treatments were: control (Rice+pathogenic bacteria/fungi), γ -irradiation alone (Rice+pathogenic bacteria/fungi+750 Gy irradiation), Treatment-1 (CH+AF-1+CNC film), Treatment-2 (CH+AF-1+CNC film+750 Gy), Treatment-3 (CH+AF-2+CNC film), and Treatment-4 (CH+AF-2+CNC film+750 Gy). Then the samples were incubated at 37 °C (for bacteria) and 27 °C (for fungi) for 8 weeks and subjected weekly to microbiological analysis using the agar plate count method.

5.2.8. Determining the % release of active components and their release kinetics from films in rice

The controlled release of active components from bioactive CH-based nanocomposite films loaded with the AF-1 and AF-2 nanoemulsion and the effect of CNC on controlled release was studied following the methods of [Hossain et al. \(2018\)](#) (Figure 5.4a-b). Four types of films were tested: 1) CH+AF-1 film (CH-based film containing 1 % nanoemulsion of AF-1), 2) CH+AF-1+CNC

film (CH-based film reinforced with 6 % CNC and 1 % nanoemulsion of AF-1), 3) CH+AF-2 film (CH-based film loaded with 1 % nanoemulsion of AF-2), and 4) CH+AF-2+CNC film (CH-based film reinforced with 6 % CNC and 1 % nanoemulsion of AF-2). A sample of 250 g of rice grains was placed in a closed plastic bag with an 8.5 cm diameter circle bioactive CH-based film at 28 °C for 8 weeks (65 % RH). Each week until 8 weeks, a piece of film (1 cm diameter) was cut and removed and placed into 10 mL of ethanol with constant stirring for 5 h (CH+AF-1 bioactive film and CH+AF-1+CNC bioactive nanocomposite film) and 6 h (CH+AF-2 bioactive film and CH+AF-2+CNC bioactive nanocomposite film) for EO extraction. The extract solution was analyzed using a UV-VIS spectrophotometer at 330 nm. The initial concentration of the active components of the films was calculated before keeping them in the incubation chamber. The difference in the concentration of active compounds in each week was considered as release of the active compounds from films to stored rice, therefore, % release of the active compounds was subtracted from the total active compounds to measure available active compounds in the film (Hossain *et al.*, 2019a).

The release kinetics of the active components from bioactive CH-based films with and without CNC was measured by plotting the UV-VIS absorption profiles at 330 nm and analyzing the release rate by first-order kinetics (Patil *et al.*, 2016). The first order velocity constant (K) was calculated by the following equation 5.5

$$K = \frac{2.303}{t} \log (A_{\infty}-A_0) / (A_{\infty}-A_t) \text{ Eq 5.5.}$$

Where, K = velocity constant; A_{∞} = absorption values of infinity; A_0 = absorption values at initial time; and A_t = absorption value at time (t) at 330 nm.

5.2.9. Sensory analysis

After optimizing the bactericidal and fungicidal properties of the bioactive CH-based antimicrobial nanocomposite films containing AF-1 and AF-2 nanoemulsion, the sensory attributes (color, odor, taste, and global appreciation) of rice stored for two months with the films were evaluated following the methods described by Das *et al.* (2021b) and Hossain *et al.* (2019a). The sensory attributes of cooked rice in the control and treatment group were assessed (i) CH+AF-1+CNC bioactive nanocomposite film and (ii) CH+AF-2+CNC bioactive nanocomposite film by 13 panelists of a sensory panel. The rice without bioactive CH-based nanocomposite films was considered as a control. Rice and water were taken in the ratio of 1 : 2 and cooked for 20 - 25 min in a cooking pot and the samples were placed into coded cups with closed lids. The coded cups were randomized and served individually to the panel members and evaluated on nine-point hedonic scale: Like

extremely (9), Like very much (8), Like moderately (7), Like slightly (6), Neither like nor dislike (5), Dislike slightly (4), Dislike moderately (3), Dislike very much (2), Dislike extremely (1).

5.3. Results and discussion

5.3.1. Nanoemulsion development, optimization and characterization of the active formulations

The central composite design (CCD) with three independent variables and their responses (ζ -potential, particle size, PDI, and encapsulation efficiency) are presented in Figures 5.1a-d and 5.2a-d for AF-1 and AF-2, respectively. The one-way analysis of variance (ANOVA) for AF-1 and AF-2 is shown in Tables 5.1 and 5.2, respectively. The ANOVA analyses and statistical models were used to optimize the stability, in terms of ζ -potential (mV), particle size (nm), PDI, and encapsulation efficiency (EE, %), and antimicrobial and antifungal properties of the AF-1 and AF-2 nanoemulsions. In the case of AF-1, the quadratic models were highly significant for ζ -potential (F-value = 8.12; df = 9; P = 0.0015), size (F-value = 6.97; df = 9; P = 0.0027) and EE (F-value = 4.55; df = 9; P = 0.0134), while the linear model was significant for PDI (F-value = 6.91; df = 3; P = 0.0034) (Table 5.1). The high coefficient of determination values (R^2 values) for ζ -potential (mV), size (nm), EE, and PDI were 88, 86, 80, and 56 %, respectively. indicated a good agreement between the experimental and the predicted values of the models.

The interactions among microfluidisation pressure, number of cycles, and concentration of emulsifier, and their effect on the stability of the AF-1 nanoemulsion, are shown by ternary diagrams (3D images) (Figure 5.1a-d). The dark red region in the 3D image of ζ -potential (Figure 5.1a) indicated a higher particle surface charge of the emulsion (highly stable), while the green to dark blue color indicated medium to lower particle surface charge of the emulsion (less stable). Figure 5.1b showed the small particle size to larger particle size which was indicated in the 3D image from dark blue color to red color (from 36 to 232 nm). Figures 5.1c and 5.1d indicated the PDI and EE (%), respectively, the dark blue indicated the lower PDI and encapsulation efficiency (%), and the green to red color denoted the medium to higher PDI and EE (%) of the nanoemulsion. When the microfluidisation pressure was 8 kPSI at the 2nd cycle with 2 % emulsifier (Tween 80) (Run 4) (Supplementary data Table 5.1), the AF-1 nanoemulsion showed the highest EE (77 %), ζ -potential (49 mV), lowest size (116 nm), and PDI (0.17), suggesting a significant improvement of nanoemulsion properties over the coarse emulsion (with zero microfluidisation cycles) with corresponding values of 30 %, 22 mV, 232 nm, and 0.556 ($P \leq 0.05$).

Table 5.1. ANOVA results for optimizing nanoemulsion of AF-1 by the central composite design.

Dependent variables	Model	F-Value	P-value	df	R²	Predicted equation
Zeta potential (mV)	Quadratic	8.12	0.0015	9	0.8796	+38-2.05A-1.18B+1.32C-2.34AB+0.345AC+3.83BC+9.23A ² -10.12B ² -1.92C ²
Size (nm)	Quadratic	6.97	0.0027	9	0.8625	+61.73+3.59A-69.24B-8.41C-13.92AB+1.25AC-8.50BC+61.13A ² +49.98B ² -11.57C ²
PDI	Linear	6.91	0.0034	3	0.5643	+0.3517+0.0857A-0.0425B-0.0194C
Encapsulation efficiency (EE, %)	Quadratic	4.55	0.0134	9	0.8038	+55.99-9.29A+6.39B+4.22C-5.99AB-0.8125AC-1.14BC+1.69A ² -16.27B ² -0.3359C ²

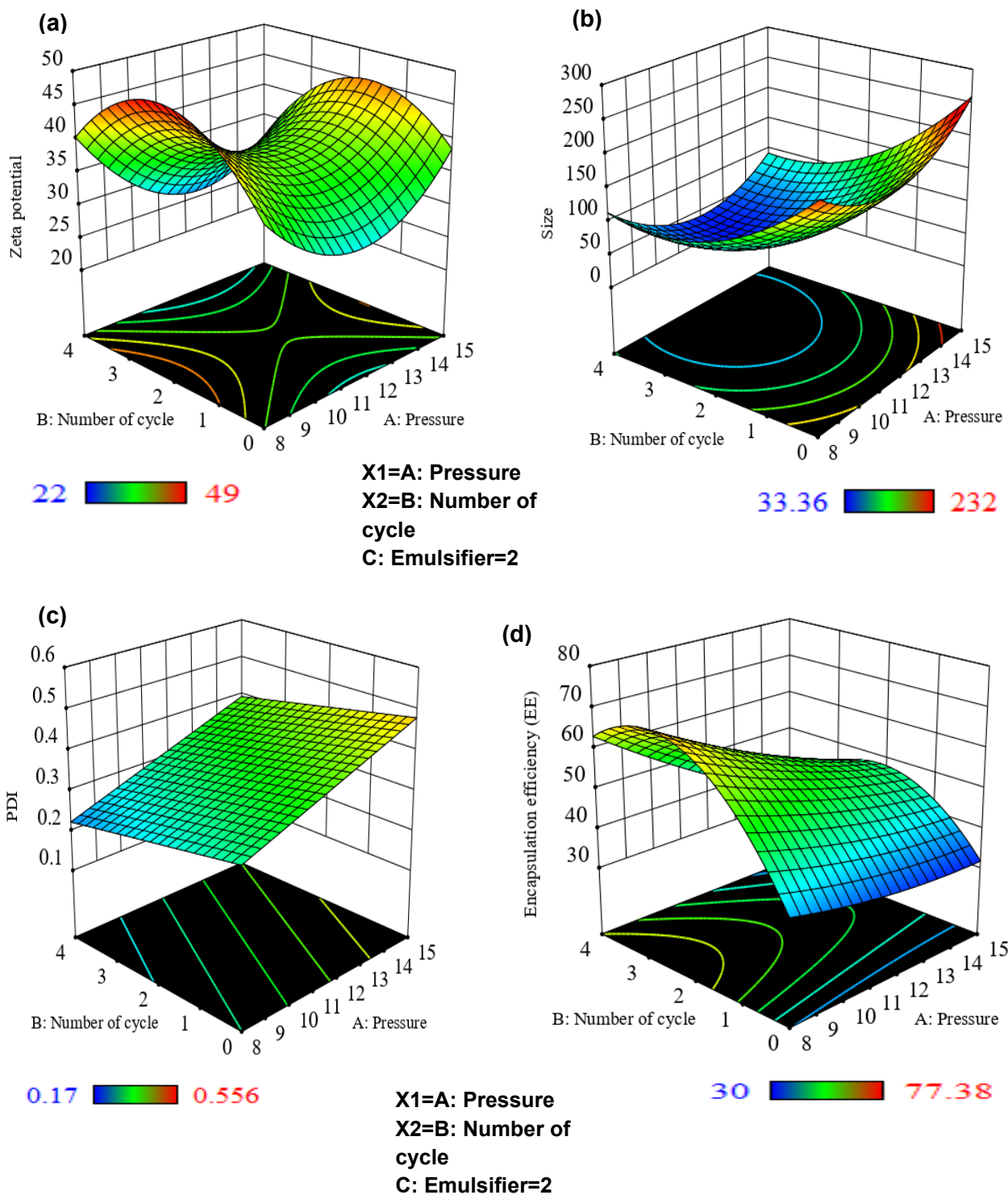


Figure 5.1. Optimization of the independent variables presented in the active formulation 1 using 3D image of (a) Zeta potential (mV), (b) size (nm), (c) PDI, and (d) encapsulation efficiency (EE, %).

A CCD design was performed for AF-2 to optimize the independent variables including the microfluidizer pressure (10-15 kPSI), number of cycles (0-3), and concentration of emulsifier (1-3 %, v/v) and their effect on the dependent variables such as ζ -potential, particle size, PDI, and encapsulation efficiency (Figure 5.2, Supplementary data Table 5.2). The one-way analysis of variance (ANOVA) for AF-2 is presented in Table 5.2. The ANOVA analyses and statistical models for optimization of AF-2 nanoemulsion were used to predict the effect of the different independent variable combinations on ζ -potential (mV), particle size (nm), PDI, and encapsulation efficiency (EE, %) to obtain a more stable nanoemulsion with higher antimicrobial and antifungal properties. In the case of AF-2, the quadratic models were highly significant for ζ -potential (F-value = 4.07; df = 9; P = 0.019), size (F-value = 20.92; df = 9; P < 0.0001), PDI (F-value = 5.68; df = 9; P = 0.006) and EE (F-value = 11.39; df = 9; P = 0.0004) (Table 5.2). The R² values for ζ -potential (mV), size (nm), EE and PDI were 78, 95, 91, and 84 %, respectively, indicating a good agreement between the experimental and the predicted values of the models.

Table 5.2. ANOVA results for optimizing nanoemulsion of AF-2 by the central composite design.

Dependent variables	Model	F-Value	P-value	df	R ²	Predicted equation
Zeta potential (mV)	Quadratic	4.07	≤ 0.019	9	0.7854	+26.47+0.82A+1.58B-0.89C+0.125AB-0.075AC+1.80BC-9.54A ² -1.24B ² -0.591C ²
Size (nm)	Quadratic	20.92	≤ 0.0001	9	0.9496	+72.07-5.0A-57.67B-24.66C-7.23AB-3.59AC-18.92BC+17.06A ² +46.41B ² +18.06C ²
PDI	Quadratic	5.68	≤ 0.0060	9	0.8365	+0.2708+0.0303A-0.0226B-0.01C-0.0005AB-0.007AC+0.0305BC+0.1836A ² +0.0881B ² +0.0311C ²
Encapsulation efficiency (EE, %)	Quadratic	11.39	≤ 0.0004	9	0.9111	+67.85-2.68A+15.19B-1.29C-0.19AB+1.96AC-0.2113BC-23.15A ² -20.4B ² -1.60C ²

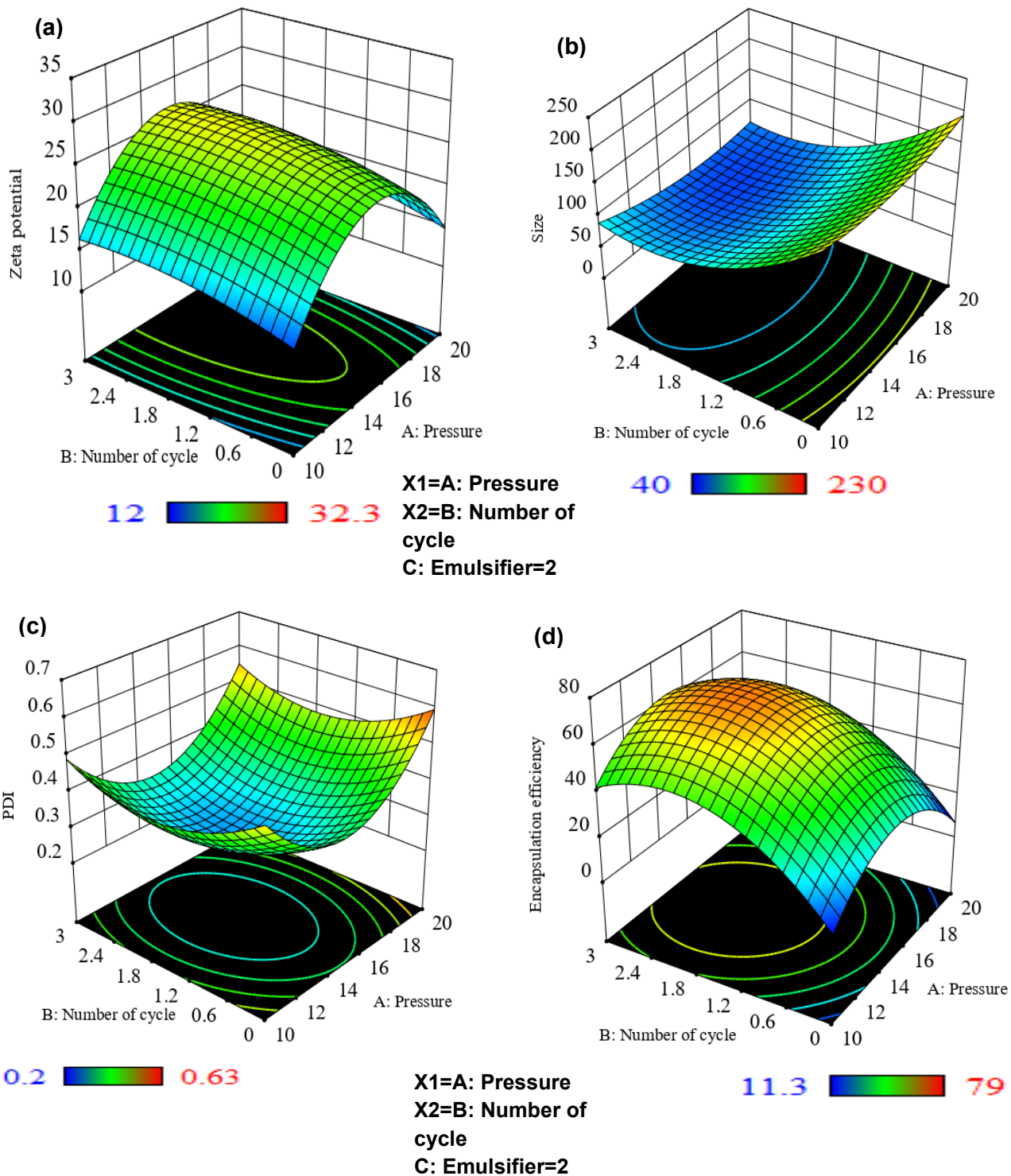


Figure 5.2. Optimization of the independent variables presented in the active formulation 2 using 3D image of (a) Zeta potential (mV), (b) size (nm), (c) PDI, and (d) encapsulation efficiency (EE, %).

The interactions among microfluidisation pressure, number of cycles, and concentration of emulsifier, and their effect on the stability of the AF-2 nanoemulsion are shown by ternary diagrams (3D images) (Figure 5.2a-d). The dark red color in the 3D image of ζ -potential (Figure 5.2a) indicated higher particle surface charge of the emulsion (highly stable), while the green to dark blue color signified medium to lower particle surface charge (less stable). Figure 5.2b showed the small particle size to larger particle size which was designated in the 3D image from dark blue color to red color (from 40 to 230 nm). For figures 5.2c and 5.2d showing the PDI and EE (%), respectively, the dark blue signified the lower PDI and encapsulation efficiency (%), and the green to red color indicated the medium to higher PDI and EE (%) of the nanoemulsion. When the microfluidisation pressure was 15 kPSI at 3rd cycle with 2 % emulsifier (Run 12), the AF-2 nanoemulsion showed the highest EE (79 %), ζ -potential (32.3 mV), lowest size and lowest PDI values, signifying a substantial improvement of nanoemulsion over the coarse emulsion (with zero microfluidisation cycles) with corresponding values of 11.3 %, 12 mV, 230 nm, and 0.63 ($P \leq 0.05$). The ζ -potential, PDI, and particle size are the most important parameters to optimize the stability of nanoemulsions, from the above-mentioned results. It is stated that all these parameters are greatly influenced by microfluidisation pressure, the number of cycles, and the emulsifier concentration. Several studies have demonstrated that the higher the ζ -potential value, the greater the chances of obtaining an electrostatically stable nanoemulsion ([Asmawati et al., 2014](#); [Cheng et al., 2016](#); [Hossain et al., 2018](#)). Nanoemulsions with very high (+30 mV) or very low (-30 mV) ζ -potential values are generally considered electrostatically stable emulsions ([Asmawati et al., 2014](#)). In the current study, we obtained 49 mV and 32.3 mV ζ -potentials for the optimized nanoemulsion of AF-1 (at 8KPSI, 2nd cycle) and AF-2 (15KPSI, 3rd cycle), respectively signifying them to be electrostatically stable. In addition, the emulsifier concentration had a strong influence on the stabilization of active nanoemulsion formulations. In the present study, 2 % Tween 80 was optimized for both AF-1 and AF-2, and both nanoemulsions showed an increased tendency to be destabilized at > 2 % Tween which might be due to the Ostwald ripening destabilization mechanism (ORDM) (or Lifshitz-Slyozov-Wagner theory) ([Llinares et al., 2018](#)). ORDM occurs as a result of dispersed phase molecule's diffusion leading to increased droplet size ([Nazarzadeh et al., 2013](#)). Tween 80 is a nonionic emulsifier which works efficiently upon optimization and can have a strong interaction with active formulations (mixture of essential oils) by adsorbing them quickly at the oil/water interface, thus forming small particles with better stability in the dispersion system ([Hossain et al., 2018](#)). It is well conceived that the nanosized droplets in dispersed systems with lower PDI values, and higher ζ -potential tend to have better stability, higher encapsulation efficiency, minimal aggregation, creaming, and coalescence during long term storage under

different conditions. Also, nanosized droplets of the active formulation could result in stronger bioactivity compared to coarse emulsions. Based on the results of the mixture design methodology, AF-1 and AF-2 were optimized at 8 KPSI, 2nd cycle, and 15 KPSI, 3rd cycle, respectively. The stability of the optimized AF-1 and AF-2 nanoemulsions should be tested at different storage conditions to evaluate their stability and bioactivity on a broader scale.

5.3.2. Storage stability of the coarse and optimized nanoemulsion

The stability of the coarse emulsion and AF-1 and AF-2 nanoemulsions during storage at 4, 25, and 40 °C for 56 days is shown in Figure 5.3a-c. The stability determination of active nanoemulsion formulations during storage is a prerequisite in order to monitor change in droplet size at different temperatures with time during storage because any change can severely affect the antimicrobial and antifungal properties of a nanoemulsion. Moreover, the storage temperature and time had a significant effect on the particle size (nm) ($P \leq 0.05$) of the emulsions (Supplementary data Table 5.3). At 4 °C, the optimized nanoemulsions of AF-1 (8 KPSI microfluidisation pressure at 2nd cycle) and AF-2 (15 KPSI microfluidisation pressure at 3rd cycle) attained more stability without significant fluctuations ($P > 0.05$) during the storage. For example, the droplet size of the AF-1 nanoemulsion was 116.2, 112.4, 116.1, 116.3, 115.2, and 115.6 nm at day 1, 5, 14, 28, 42, and 56, respectively, while the same for coarse emulsion of AF-1 increased significantly ($P \leq 0.05$) with respective values of 208.3, 212.2, 225.6, 221.1, 232.9, and 234.4 nm at the corresponding storage time (days) at 4 °C (Figure 5.3a, Supplementary data Table 5.3).

At 25 °C, the droplet size of the coarse emulsion of AF-1 was 207, 213, 223, 218, 236, and 242 nm at day 1, 5, 14, 28, 42, and 56 ($P \leq 0.05$), whereas the same for nanoemulsion of AF-1 was increased from 115 nm to 119 nm over this stipulated time which was not significant ($P > 0.05$) (Figure 5.1b, Supplementary data Table 5.3). At 40 °C, the coarse and AF-1 nanoemulsions were significantly destabilized, although AF-1 nanoemulsion showed less instability in droplet size than coarse emulsion. Droplet size in the AF-1 nanoemulsion decreased in size from 113, 103, 106, 108 nm at day 1, 5, 14, and 28, respectively, then increased to 123 and 137 nm at day 42 and 56 days of storage at 40 °C, respectively. The high storage temperature (40 °C) and storage time profoundly affected the droplet size of AF-1 emulsion, which augmented from 189 nm to 259 nm from day 1 to 56 of storage ($P \leq 0.05$) (Figure 5.1c, Supplementary data Table 5.3). These findings reflect that droplet size of the AF-1 nanoemulsion was more stable at 4 °C and 25 °C during 56 days of storage compared to the coarse emulsion of AF-1.

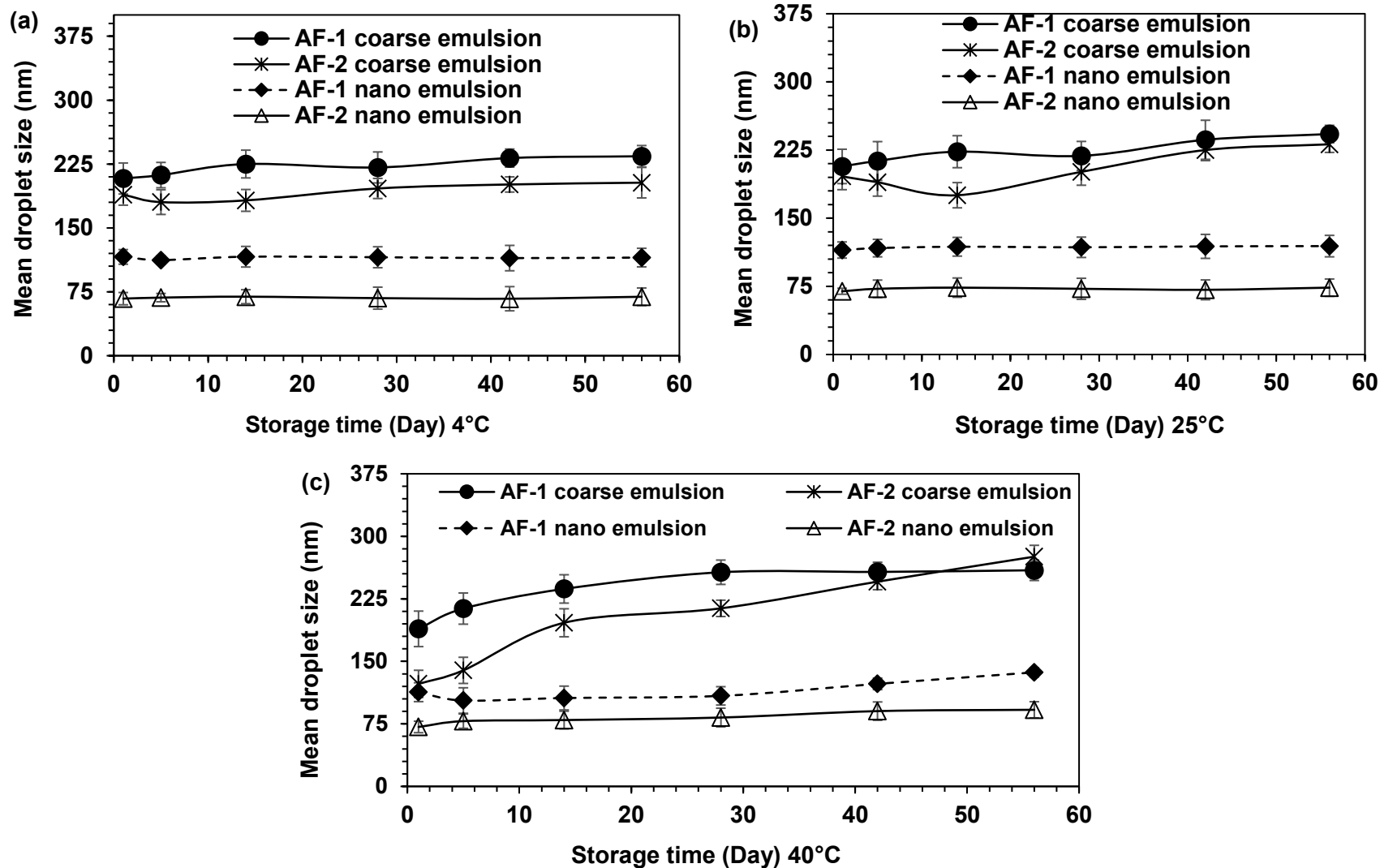


Figure 5.3. Storage stability of coarse and nanoemulsion of AF-1 and AF-1 at different temperature (a) 4 °C (b) 25 °C and (c) 40 °C for 2 months. Nanoemulsion of AF-1 and AF-2 was optimized at 8000 psi (2nd cycle) and 15000 psi (3rd cycle), respectively.

Likewise, the droplet size of AF-2 emulsion was also dependent on the storage time and temperature (Figure 5.3 and Supplementary data Table 5.3). At 4 °C, the AF-2 nanoemulsion was more stable with an insignificant increase in droplet size from 67.6 to 69.5 nm during 1 to 56 days of storage ($P > 0.05$), while droplet size of AF-2 coarse emulsion significantly increased from 189.6 to 203.1 nm (from day 1 to 56) ($P \leq 0.05$) (Figure 5.3a and Supplementary data Table 5.3). At 25 °C, the nanoemulsion of AF-2 was more stable during storage, with specified droplet size of 69.6 and 73.6 nm at day 1 and day 56, respectively, but the droplet size of the coarse emulsion significantly increased with storage time (from 196.2 to 231.3 nm = from day 1 to day 56) (Figure 5.3b and Supplementary data Table 5.3). At 40 °C, both the coarse and AF-2 nanoemulsions, droplet size increased significantly ($P \leq 0.05$) with storage time which was measured as 71.3, 78.3, 79.6, 82.6, 90.3, and 91.9 nm at days 1, 5, 14, 28, 42, and 56, respectively, while the corresponded droplet size of the coarse emulsion of AF-2 was 123.8, 139.2, 196.3, 213.6, 245.6, and 275.6 nm (Figure 5.3c and Supplementary data Table 5.3).


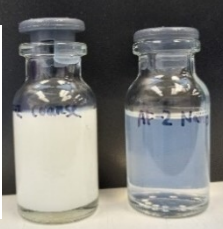
In the present study, the emulsions of AF-1 and AF-2 (especially nanoemulsion) showed a smaller droplet size during initial storage that eventually increased toward the end of the storage that might be due to continuous reconstruction of the droplet to acquire kinetic stability. At high temperature (40 °C), Ostwald ripening occurred during long storage time causing a drastic change in the mean droplet size of an oil-in-water coarse emulsion of both AF-1 and AF-2. Therefore, the droplet size of the coarse emulsion of AF-1 and AF-2 attained almost double the size at the end of the storage. Furthermore, the rapid movement of the droplets in the continuous phase enhanced the chances of collisions among droplets which accelerated the Ostwald ripening or coalescence and ultimately created phase separation at 56 days of storage. It is well documented that higher temperature causes an increase in the Ostwald ripening rate (Li and Chiang, 2012; Nirmal *et al.*, 2018). The optimized nanoemulsion of AF-1 and AF-2 showed better stability in terms of droplet size than the coarse emulsions over a wide range of storage temperatures from 4 °C to 25 °C. However, at 40 °C the nanoemulsions showed the lowest increase in the droplet size at the end of the storage time compared to the coarse emulsion of AF-1 and AF-2. This study aligned with the findings of Abbas *et al.* (2015) who worked on the development of the nanocapsules of curcumin oil using the ultrasonication method and stored the nanocapsules at 4, 25, and 40 °C for 1 month, and found that the nanocapsules showed the lowest aggregation (increase in droplet size) when stored at 4 °C followed storage at 25 °C temperature (Abbas *et al.*, 2015). Therefore, it can be safely inferred from the current study that 4 and 25 °C are ideal temperatures for the long-term storage of nanoemulsion of AF-1 and AF-2 with enhanced stability.

5.3.3. Inhibitory capacity and turbidity measurement of the coarse and optimized nanoemulsion

The antibacterial and antifungal properties of the coarse and optimized nanoemulsions of AF-1 and AF-2 were measured as inhibitory capacity (IC, %) using the agar disc diffusion assay and the results are presented in Table 5.3. The antibacterial and antifungal tests were performed against pathogenic bacteria (*E. coli* O157:H7 and *S. Typhimurium*) and spoilage fungi (*A. niger*, *P. chrysogenum*, and *M. circinelloides*). The antibacterial and antifungal properties of AF-1 and AF-2 were profoundly dependent on the droplet size of the emulsions. The nanoemulsion of AF-1 showed a significantly strong bactericidal effect of 67 and 73.1 % IC against *E. coli* O157:H7 and *S. Typhimurium*, respectively, while the corresponding IC was 24.4 and 33.1 % for the coarse emulsion of AF-1 ($P \leq 0.05$). The nanoemulsion of AF-1 also exhibited strong fungicidal properties against *A. niger* (IC = 74.9 %), *P. chrysogenum* (IC = 77.4 %), and *M. circinelloides* (IC = 67.8 %), while the coarse emulsion of AF-1 showed 39, 30, and 27.5 % IC against the corresponded fungi ($P \leq 0.05$).

The optimized AF-2 nanoemulsion also had stronger bactericidal properties against *E. coli* O157:H7 (IC = 75 %) and *S. Typhimurium* (IC = 72 %) than the coarse emulsion of AF-2. The coarse emulsion of AF-2 had an IC of 34 and 27 % for *E. coli* O157:H7 and *S. Typhimurium*, respectively, which was significantly lower than the bactericidal effect shown by AF-2 nanoemulsion ($P \leq 0.05$) (Table 5.3). The AF-2 nanoemulsion showed significant antifungal properties of 82, 88, and 69 % IC against *A. niger*, *P. chrysogenum*, and *M. circinelloides*, respectively, while the corresponded antifungal properties were 22, 19, and 21 % for the coarse emulsion of AF-2 ($P \leq 0.05$). Although AF-1 and AF-2 nanoemulsions exhibited stronger antibacterial and antifungal properties than their coarse emulsions, the AF-2 nanoemulsion demonstrated better bactericidal and fungicidal properties than AF-1 nanoemulsion likely because of the smaller droplet size (~67 nm) compared to AF-1 (droplet size ~113 nm) ($P \leq 0.05$).

Table 5.3. Inhibitory capacity (IC, %) against pathogenic bacteria and spoilage fungi, turbidity and digital images of coarse and nano emulsion of active formulations.

Active formulation	Type of emulsion	Inhibitory capacity (IC, %)					Turbidity (600 nm)	Digital image of the emulsion
		Pathogenic bacteria			Spoilage fungi			
		<i>E. coli</i> O157:H7	<i>S. Typhimurium</i>	<i>A. niger</i>	<i>P. chrysogenum</i>	<i>M. circinelloides</i>		
AF-1	Coarse	24.4±3.9 ^a A	33.1±7.1 ^{bB}	39±4.1 ^{bC}	30±2.2 ^{bB}	27.5±3.2 ^{bA}	1.17±0.1 ^d	
	Nano	67±2.1 ^{cA}	73.1±7.2 ^{cB}	74.9±3.8 ^{cB}	77.4±1.9 ^{cB}	67.8 ±1.1 ^{cA}	0.51±0.06 ^b	
AF-2	Coarse	34±2.8 ^{bC}	27±3.1 ^{aB}	22±1.1 ^{aA}	19±0.7 ^{aA}	21±0.4 ^{aA}	1.01±0.10 ^c	
	Nano	75±4.7 ^{dB}	72±5.1 ^{cA}	82±1.8 ^{dC}	88±3.2 ^{dD}	69±3.7 ^{dA}	0.17±0.02 ^a	

Values means ± standard error. Within each column means with different lowercase letter are significantly different ($P \leq 0.05$), while the means with the different uppercase letter are significantly different ($P \leq 0.05$).

The current study showed that the antibacterial and antifungal properties of AF-1 and AF-2 nanoemulsions were strongly dependent on their droplet size that determined bactericidal and fungicidal effects against pathogenic Gram-negative bacteria (*E. coli* O157:H7 and *S. Typhimurium*) and spoilage fungi (*A. niger*, *P. chrysogenum*, and *M. circinelloides*) than coarse emulsions which was probably due to the smaller droplet size of the nanoemulsions. Several other studies have also shown that nanoemulsions of active formulations exhibit greater microbicidal activity than free active formulations (Donsi *et al.*, 2011; Li *et al.*, 2015b; Moghimi *et al.*, 2016; Hossain *et al.*, 2019a). The smaller droplet size of the nanoemulsions has a greater surface-to-volume ratio, which increases their dissolution rate and bioavailability (Hossain *et al.*, 2019a). Because of nano size, the nanoemulsion can easily pass through porin protein channels of the outer membrane of the Gram-negative bacteria and effectively deliver the active ingredients to the cytoplasmic membrane, disrupt membrane function, thereby causing microbial cell death (Donsi *et al.*, 2011; Nazzaro *et al.*, 2013). Hossain *et al.* (2019a) studied the bioactivity of nanoemulsions and coarse emulsions of the three active formulations of oregano+thyme EO, thyme+tea tree EO, and thyme+peppermint EO against *A. niger*, and found higher fungicidal activity of the nanoemulsion was 83.7, 75.6, and 87.9 %, respectively, with respect to coarse emulsion at 39.7, 36.7, and 43 %. Similarly, Zhang *et al.* (2014) found that the nanoemulsion of D-limonene with Tween 80 emulsifier (mean droplet size: 16 nm) showed stronger antibacterial and antifungal activity against *Staphylococcus aureus*, *Bacillus subtilis*, *E. coli*, and *Saccharomyces cerevisiae* than free oil.

The turbidity measurements of the coarse and nanoemulsion of AF-1 and AF-2 are shown in Table 5.3, along with a visual image. For the application of emulsions in food packaging, turbidity is an crucial property because cloudy emulsions may alter the color of the food compared to optically transparent emulsions (Qian and McClements, 2011). The optimized nanoemulsion of AF-2 had the lowest turbidity, followed by AF-1 nanoemulsion, the coarse emulsion of AF-2, and the coarse emulsion of AF-1. The turbidity of AF-1 nanoemulsion (turbidity: 0.51) was significantly ($P \leq 0.05$) lower than the coarse emulsion of AF-1 (turbidity: 1.17). The turbidity of the coarse emulsion of AF-2 was significantly higher (1.01) than the turbidity of AF-2 nanoemulsion (0.17) ($P \leq 0.05$) (Table 5.3). It is well reported that the smaller droplet size aids in lowering the turbidity value, through absorbing and scattering less light, thereby producing higher clarity. Transparency is also an indicator of a more stable emulsion with less creaming and precipitation (McClements, 2002; Ha *et al.*, 2015). All these properties (determination of stability of the nanoemulsions of active formulations, the antibacterial and antifungal properties, turbidity) indicated that the optimized AF-1 and AF-2 nanoemulsion were better in terms of stability, displaying strong bactericidal and

fungicidal properties, and transparency than their corresponding coarse emulsions. The above mentioned attributes make the stabilized nanoemulsions of AF-1 and AF-2 ideal candidates for their incorporation into biopolymeric matrices (chitosan) for developing bioactive packaging films for controlling pathogenic bacteria and fungi in stored rice.

5.3.4. Development of chitosan-based nanocomposite films

Chitosan-based (CH) nanocomposite films were developed using reinforced CNCs at different concentrations (0 to 10 % CNC solutions) to optimize the best concentration of CNC in the polymeric matrix by measuring several mechanical properties (tensile strength [TS], tensile modulus [TM], and Elongation at break [Eb]) and the water vapor permeability (WVP) of the films. The results are presented in Table 5.4. Several studies found that upon reinforcing CNC, the mechanical properties and WVP of bioactive films can be improved ([Khan et al., 2012](#); [Salmieri et al., 2014b](#); [Hossain et al., 2018](#); [Hossain et al., 2019a](#)). The effect of CNC on the mechanical properties and WVP of the CH-based nanocomposite films is discussed below:

5.3.4.1. Water vapor permeability (WVP)

The effect of CNC at different concentrations ranging from 0 to 10 % on the WVP of the chitosan films is presented in Table 5.4. The chitosan-based film without reinforcing CNC (Control) showed the highest WVP of $10.2 \text{ g m mm}^{-2} \text{ day}^{-1} \text{ kPa}^{-1}$ which was significantly higher ($P \leq 0.05$) than all the CH-based films containing 1-10 % CNC. The WVP values of the CH-based films dropped significantly ($P \leq 0.05$) with rising concentration of CNC until 6 %, and adding 6 % CNC into CH-based polymeric matrices exhibited the lowest WVP ($6.03 \text{ g m mm}^{-2} \text{ day}^{-1} \text{ kPa}^{-1}$). The incorporation of 6 % CNC into the CH-based polymeric matrices decreased the WVP of the film by 41 % compared to the control film. The WVP values of the CH-based films were 9.8, 9.07, and 8.01 upon adding 1, 2, and 4 % of CNC, respectively. It is noteworthy that the WVP values started to increase with higher concentrations, and the values were 7.28 and $7.78 \text{ g m mm}^{-2} \text{ day}^{-1} \text{ kPa}^{-1}$ when the CH-based films contained 8 and 10 % of CNC, respectively (Table 5.4).

WVP is a crucial parameter of packaging films as the moisture content in the air tends to degrade the films by accelerating the chemical and enzymatic reactions in the polymer, thereby increasing the microbial growth in foods and deterioration of the food quality during storage ([Hossain et al., 2019a](#)). In the present study, the reinforcing agent CNC significantly reduced the WVP of the CH-based films. This reduction is attributed to the increased tortuosity in the film matrices as a result of reduced water vapor diffusion and permeability ([Khan et al., 2012](#)). It has been reported that

upon incorporating CNC, a percolated network might be created into polymeric matrices by H-bonding which can reduce the molecular mobility and free volume of polymeric matrices and serves as obstacles for water vapor diffusion, and thus reduced WVP (Pereda *et al.*, 2012). Khan *et al.* (2012) studied chitosan-based films by reinforcing CNCs (5 %) for improving the mechanical and barrier properties, and found that the WVP of the CH-based nanocomposite films was decreased by 27 % compared with the control CH-based film (Khan *et al.*, 2012).

5.3.4.2. Mechanical properties of the films

The effect of CNC at different concentrations ranging from 1 to 10 (w/w) on the tensile strength (TS) of CH-based films was studied and the results are presented in Table 5.6. The incorporation of CNC as a reinforcing agent significantly increased ($P \leq 0.05$) the TS values of the CH-based films than the control film (CH-based film without CNC). The TS values were 78.2, 83.4, 90.1, 93.7, 87.5, and 81.9 MPa in the CH-based nanocomposite films containing 1, 2, 4, 6, 8, and 10 % CNC (w/w), respectively, while the TS value was 75.3 Mpa in the control film. The highest TS value (24%) was observed when 6 % CNC was incorporated into the CH-based polymeric film compared to the control film. Tensile strength increased by 20, 16, 11, 10, and 4 % when CNC was added into CH-based films at 4, 8, 2, 10 and 1 % respectively, compared to the control film (Table 5.4).

These results showed that TS of the CH-based nanocomposite films increased by 24.4 % (from 75.3 to 93.7 MPa) as compared to the control film (CH-film) upon adding CNC up to 6 % (w/w). The increase in TS might be due to ionic interactions between the cationic amine groups present in the CH polymer and the anionic sulfate groups in the CNC, which effectively augmented the interface between the filler and the matrix that eventually led to higher TS values (de Mesquita *et al.*, 2010). The high TS values might be due to the mean-field mechanical force caused by the uniform distribution of CNC throughout the CH-polymeric matrices without interactions (Khan *et al.*, 2012). Greater than 6 % of CNC incorporation into CH-based polymeric matrices caused a reduction in TS values of the CH-nanocomposite films, possibly due to the higher aggregation of CNC and feeble interaction with polymer matrix (Khan *et al.*, 2012; Hossain *et al.*, 2019a). This result can be aligned with the findings of other studies, where incorporation of CNC as a reinforcing agent can increase the TS of the polymeric matrices at certain concentrations (Li *et al.*, 2009; Khan *et al.*, 2012; Salmieri *et al.*, 2014b; Hossain *et al.*, 2019a).

Table 5.4 shows the tensile modulus (TM) and elongation at break (Eb) of CH-based polymeric films with and without different concentrations of CNC. The TM value of the CH-based film (control) was 1279 MPa. Integration of 1 % CNC into the CH-based polymer matrix caused a significant (P

≤ 0.05) increase of TM value to 1830 MPa, or 43% above than the control. At 6 % CNC content, TM value of the CH-film was 2248 MPa (76 % increased as compared to the control film). TM values of the films were decreased to 66 % (2129 MPa) and 63 % (2084 MPa) when 8 and 10 % (w/w) of CNC was incorporated into CH-based polymeric matrices, respectively, reflecting a similar trend as the TS values mentioned above. It is generally perceived that polymeric films with the higher TM values tend to be more brittle and stiffer. The increase in brittleness with the incorporation of CNC into CH-based polymers is a common phenomenon in filler-reinforced films (Lee *et al.*, 2004b; Rhim, 2011; Khan *et al.*, 2012). Hossain *et al.* (2018) reported a 15 % hike in TM values of the methylcellulose nanocomposite films when 7.5 % (w/w) CNC was incorporated. Addition of 10 % (w/w) CNC into the calcium alginate polymer increased TM values by 123 % in several nanocomposite films (Ureña-Benavides *et al.*, 2010).

Table 5.4. Effect on CNC content in the mechanical properties (TS, TM, Eb) and water vapor permeability (WVP) of the CH-based films.

Films	Mechanical properties			WVP (g m mm ⁻² day ⁻¹ kPa ⁻¹)
	TS (MPa)	TM(MPa)	Eb (%)	
CH-film (Control)	75.3±5.8 ^a	1279±120 ^a	61±7.1 ^e	10.2±1.1g
CH+CNC (1 %)	78.2±3.9 ^a	1830±80.5 ^b	58±5.6 ^{de}	9.80±0.8f
CH+CNC (2 %)	83.4±3.7 ^b	2010±105 ^c	51±3.6 ^{cd}	9.07±0.3 ^e
CH+CNC (4 %)	90.1±5.5 ^c	2126±127 ^d	45±3.0 ^{bc}	8.01±1.1d
CH+CNC (6 %)	93.7±5.2 ^d	2248±146 ^e	42±2.7 ^b	6.03±0.3a
CH+CNC (8 %)	87.5±6.3 ^c	2129±208 ^d	39.6±4.8 ^{ab}	7.28±1.0b
CH+CNC (10 %)	81.9±6.8 ^b	2084±44.6 ^c	34±2.1 ^a	7.78±0.3c

Values means ± standard error. Within each column means with different lowercase letter are significantly different ($P \leq 0.05$).

The Eb of the control film (pure CH-based) was 61 %. Eb values decreased significantly ($P \leq 0.05$) with increasing concentrations of CNC into the CH-based nanocomposite films compared to the control film. The Eb values were 58, 51, 45, 42, 39.6, and 34 % of the CH-based nanocomposite films when reinforced with 1, 2, 4, 6, 8, and 10 % CNC (w/w), respectively, which corresponded to a 5, 16, 26, 31, 35, and 44 % reduction of Eb values compared to the control film. Several studies have shown similar results (Li *et al.*, 2009; Khan *et al.*, 2012; Dhar *et al.*, 2015). The reduction of Eb of the nanocomposite films after adding CNC might be due to strong interactions between polymeric matrices and CNCs that limit the movement of the polymeric matrices and thus lower

the Eb values (Samir *et al.*, 2004; Hossain *et al.*, 2019a). Based on the results obtained from the mechanical and WVP properties of the CH-based nanocomposite films, it can be inferred that the incorporation of 6 % (w/w) CNC into CH-based matrices improved film performance, and thus, for further experiments 6 % CNC was considered.

5.3.5. Bioactive film development and application in packaged rice with irradiation treatment

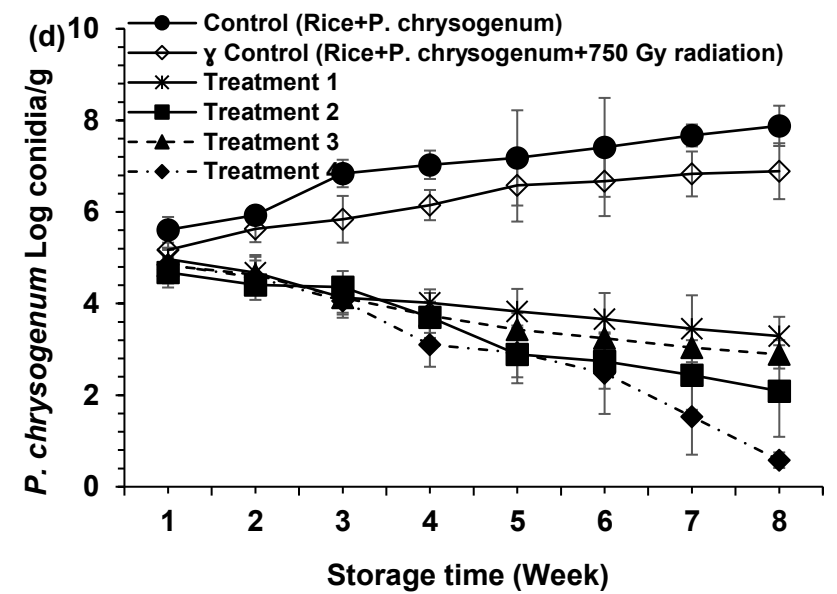
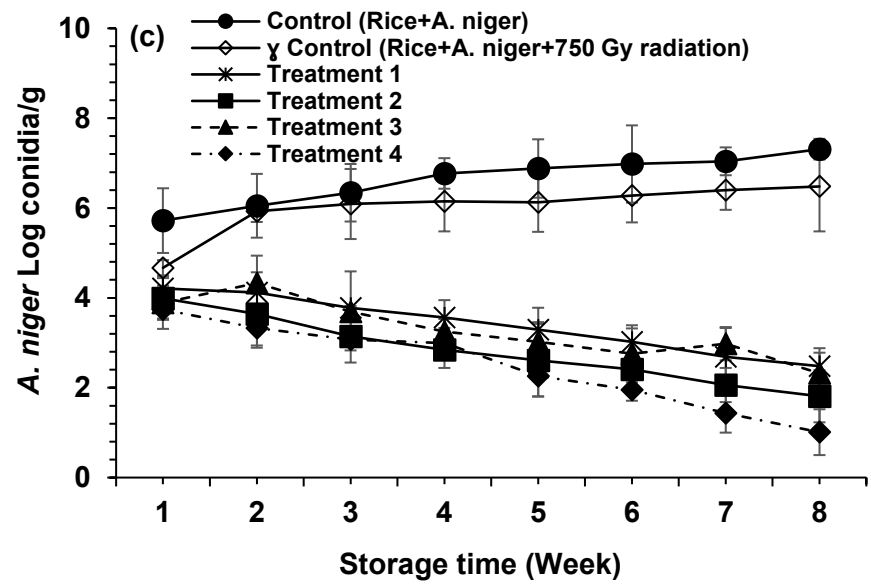
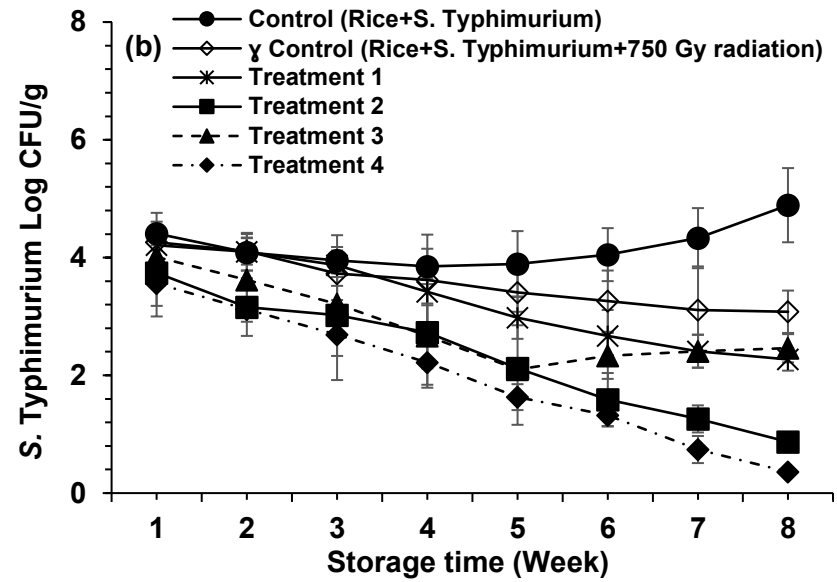
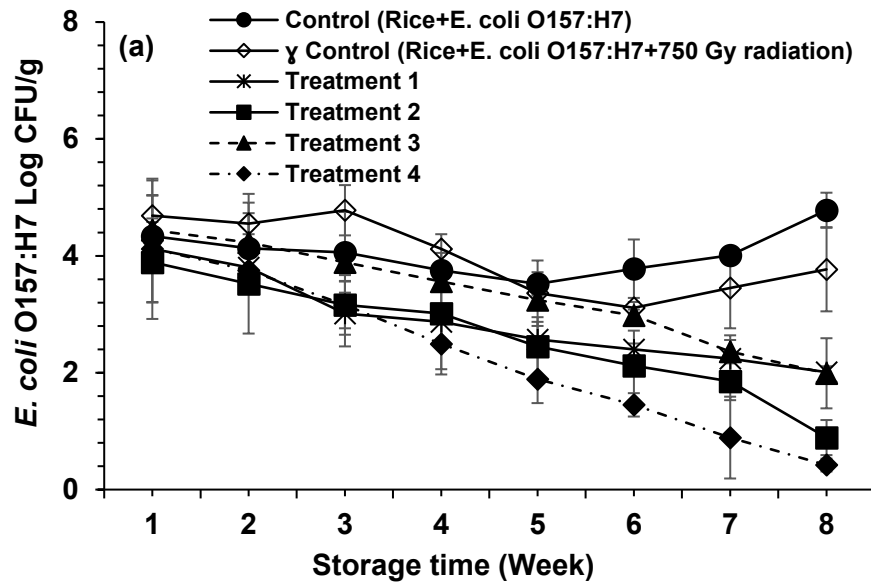
After CNC optimization, the CH-based nanocomposite films AF-1 and AF-2 nanoemulsions were incorporated into CH-based nanocomposite film-forming solutions at different concentrations (0, 0.125, 0.25, 0.5, and 1 %). The CH-based nanocomposite films without active formulations (0 %) were considered as control films. The antibacterial and antifungal properties of the bioactive CH-based nanocomposite films were measured using an *in vitro* agar volatilization test to identify the best concentration of AF-1 and AF-2 nanoemulsions. The results are presented in Supplementary data Table 5.4. The bioactive CH-based film containing 1 % AF-1 and AF-2 nanoemulsions showed significant ($P \leq 0.05$) bactericidal and fungicidal effectiveness against *E. coli* O157:H7, *S. Typhimurium*, *A. niger*, *P. chrysogenum*, and *M. circinelloides* compared to the control film (Supplementary data Table 5.4), therefore 1 % AF-1 and AF-2 nanoemulsions containing CH-based nanocomposite films were selected for further antimicrobial tests.

The antibacterial and antifungal properties of the bioactive CH-based nanocomposite films containing 1 % AF-1 (CH+AF-1+CNC film) or AF-2 (CH+AF-2+CNC film) with and without γ -irradiation (750 Gy) in rice to control pathogenic bacteria (*E. coli* O157:H7 and *S. Typhimurium*) and spoilage fungi (*A. niger*, *P. chrysogenum*, and *M. circinelloides*) were tested and the results are presented in Figure 5.4 and Supplementary data Table 5.5. The treated samples were categorized as Treatment 1 (CH+AF-1+CNC film), Treatment 2 (CH+AF-1+CNC film+750 Gy γ -irradiation), Treatment 3 (CH+AF-2+CNC), and Treatment 4 (CH+AF-2+CNC film+750 Gy γ -irradiation).

The results showed that the bacterial growth in rice was significantly reduced after 8 weeks of storage with bioactive CH-based nanocomposite films containing 1 % AF-1 and AF-2 nanoemulsions compared to the control sample ($P \leq 0.05$). The rice was inoculated with 5 log CFU/g of pathogenic bacteria (either *E. coli* O157:H7 or *S. Typhimurium*). The growth of *E. coli* O157:H7 was 4.78 log CFU/g in the control sample after 8 weeks of storage time (Figure 5.4a, Supplementary data table 5.5). The growth of *E. coli* O157:H7 was significantly lower ($P \leq 0.05$) when the samples treated with γ -irradiation alone (750 Gy), treatment 1, treatment 2, treatment 3

and treatment 4 as compared to control sample and their corresponded count was 3.77, 2.01, 0.89, 1.99, and 0.42 log CFU/g, respectively, after 8 weeks of rice storage. Moreover, the combined treatment of bioactive films and γ -irradiation in treatment 2 and treatment 4 drastically reduced the *E. coli* O157:H7 counts by 3.89 and 4.36 log CFU/g, respectively, compared to the control sample. A similar phenomenon was observed in the growth profile of *S. Typhimurium*, where the growth reached to 4.89 log CFU/g in the control sample after 8 weeks of storage (Figure 5.4b). The highest bacterial growth (*S. Typhimurium*) reduction was observed in treatment 4, followed by treatment 2, treatment 1, treatment 3, and γ irradiation alone, and the bacterial count was 0.36, 0.87, 2.27, 2.46, and 3.08 log CFU/g, respectively, after 8 weeks of rice storage. The combined treatment between irradiation and bioactive nanocomposite films (either CH+AF-1+CNC film or CH+AF-2+CNC film) showed a significant bacterial counts reduction ($P \leq 0.05$) in stored rice than the treatment alone (either treated samples by bioactive film alone or by irradiation alone) (Supplementary data Table 5.5).

The antifungal activities of the developed bioactive CH-based films were tested with and without irradiation treatment against three spoilage fungi *A. niger*, *P. chrysogenum*, and *M. circinelloides* in stored rice for 8 weeks (Figure 5.4c-e and Supplementary data Table 5.5). The bioactive CH-based films with and without irradiation showed a stronger fungicidal effect than the control samples (no irradiation or no bioactive film) ($P \leq 0.05$) after 8 weeks of storage. The initial inoculation was 5 log spores/g for each fungus. In the first control sample (no bioactive film), the fungal count of *A. niger* reached 7.31 log spores/g in stored rice after 8 weeks which was significantly higher ($P \leq 0.05$) than the samples treated with 750 Gy irradiation alone, CH+AF-1+CNC film (treatment 1), CH+AF-1+CNC film+750 Gy irradiation (treatment 2), CH+AF-2+CNC film (treatment 3), and CH+AF-2+CNC film+750 Gy irradiation (treatment 4). The samples treated with bioactive films alone either by treatment 1 or by treatment 3 reached the fungal growth (*A. niger*) of 2.48 and 2.32 log spores/g after 8 weeks of storage, respectively. With the rice samples treated with treatment 2 and treatment 4, the growth of *A. niger* growth was 1.81 and 1.01 log conidia/g, respectively, which efficiently reduced the fungal (*A. niger*) counts by 5.5 and 6.3 log spores/g at the end of storage (Figure 5.4c and Supplementary data table 5.5). The nanocomposite film treatment 4 exhibited significantly higher ($P \leq 0.05$) fungicidal effect against *A. niger* than control, γ irradiation alone, treatment 1, treatment 2, and treatment 3.



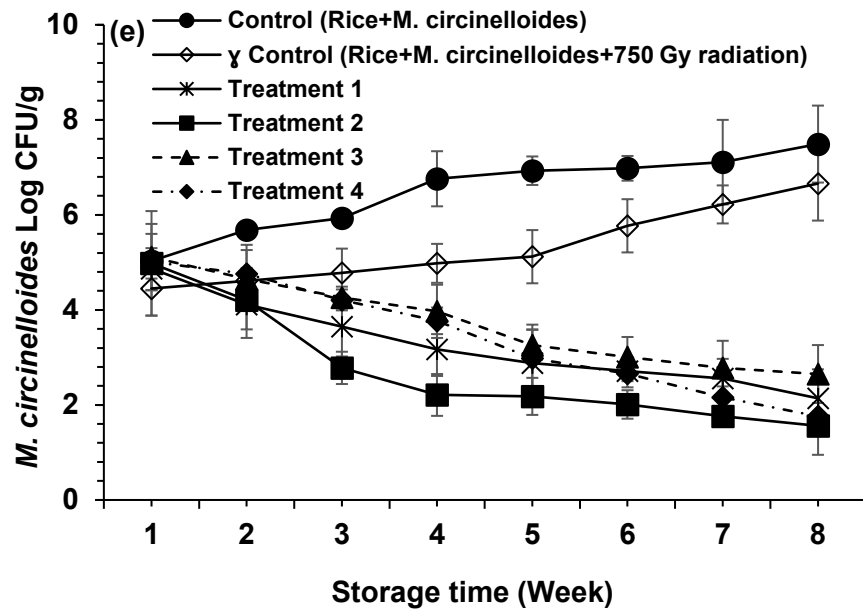


Figure 5.4. Bacterial (*E. coli* O157:H7 and *S. Typhimurium*) and fungal (*A. niger*, *P. chrysogenum*, and *M. circinelloides*) growth profiles in storage rice under different bioactive films treatment for 8 weeks.

Figure 5.4d shows the antifungal efficiency of bioactive CH-based nanocomposite films alone or in combination with γ -irradiation against *P. chrysogenum* in stored rice. The growth of *P. chrysogenum* in control samples (no bioactive film) reached 7.88 log spores/g after 8 weeks of storage. The fungal (*P. chrysogenum*) growth was 3.29 and 2.89 log spores/g while the samples treated with films alone by treatment 1 and by treatment 3, respectively, after 8 weeks of rice storage compared to the control sample (no bioactive film) (Supplementary data Table 5.5). To decontaminate *P. chrysogenum* in stored rice, the application of 750 Gy irradiation alone resulted in fungal growth of 6.89 log spores/g at the end of the incubation period. But the combined treatment of γ -irradiation with the bioactive films containing 1 % nanoemulsion of AF-1 (treatment 2) and AF-2 (treatment 4) caused a reduction by 5.79 and 7.3 log spores/g, respectively, compared to control sample (no bioactive film) ($P \leq 0.05$).

Figure 5.4e depicts the fungicidal effectiveness shown by the bioactive CH-based nanocomposite films with and without γ -irradiation treatment to control infestation of *M. circinelloides* in stored rice for 8 weeks. The growth of *M. circinelloides* in control samples was 7.49 log conidia/g after 8 weeks of incubation while the samples treated with films alone CH+AF-1+CNC (treatment 1) and CH+AF-2+CNC (treatment 3) showed 2.14 and 2.56 log conidia/g, respectively, suggesting a substantial reduction by 5.35 and 4.48 log spores/g (Supplementary data Table 5.5). To decontaminate *M. circinelloides* in stored rice, the 750 Gy irradiation treatment alone caused the fungal (*M. circinelloides*) reduction by 0.88 log spores/g at the end of the incubation period, while the combined treatment of γ -irradiation with the bioactive films used in treatment 2 and treatment 4 caused fungal inhibition by 5.93 and 5.73 log spores/g, respectively, compared to control sample (no bioactive film) ($P \leq 0.05$).

The active formulations (AF-1 and AF-2) used in the current study were composed of a mixture of EOs and citrus extracts [AF-1: organic citrus extract (OCE), Mediterranean EO, citrus EO, and cinnamon EO; AF-2: natural citrus extract (NCE), Asian formulation, Southern formulation, cinnamon EO, and savory thyme EO]. Recently, [Begum et al. \(2022b\)](#) reported the effective antibacterial and antifungal properties of the organic citrus extract, natural citrus extract, Mediterranean EO, citrus EO, cinnamon EO, Asian formulation, Southern formulation, and savory thyme EO against pathogenic bacteria (*E. coli* O157:H7 and *S. Typhimurium*) and spoilage fungi (*A. niger*, *P. chrysogenum*, and *M. circinelloides*). The authors found that the vapor effect of AF-1 and AF-2 can remarkably reduce the pathogenic bacteria and spoilage fungi in stored rice as compared to the control sample (no active formulations). In the current study, the CH-based nanocomposite films containing 1 % AF-2 showed a higher microbial and fungal growth inhibition than 1 % AF-1 in stored rice, possibly due to the smaller droplet size of the AF-2 nanoemulsion

(~67 nm) than AF-1 nanoemulsion (~115 nm). In particular, owing to the enhanced surface-to-volume ratio of nano droplet sized-EOs and their active components' release from bioactive CH-based nanocomposite films enabled them to interact efficiently with microbial cellular membrane, leading to apoptosis, facilitating their translocation across the membrane, destroying their cellular functions and eventually cell death (Donsi *et al.*, 2012).

It is noted from above mentioned results that the bioactive CH-based nanocomposite films released the active components present in the (AF-1 and AF-2) from the films to stored rice and inhibited the growth of pathogenic bacteria and fungi during the storage time. The most dominant active components found in Mediterranean EO, Southern formulation, citrus EO, cinnamon EO, and citrus extracts are enriched with cinnamaldehyde, carvacrol, thymol, eugenol, limonene, terpineol, geraniol, neral, myrcene, trans-caryophyllene, and borneol (Zachariah and Leela, 2006; Dzamic *et al.*, 2008; Begum *et al.*, 2022b). In addition, the reinforcing agent CNC reportedly improving the gradual release of active components of the nanoemulsions of EOs in polymeric matrices during extended storage (Boumail *et al.*, 2013; Deng *et al.*, 2017). Similar trends were observed by da Rosa *et al.* (2020b) when incorporated zein nanoparticles into polyethylene oxide matrices that increased the stability and facilitated the controlled release of carvacrol and thymol EOs from active packaging for stored products. Luzi *et al.* (2017) developed antimicrobial polyvinyl alcohol/chitosan-based nanocomposite films reinforced with CNC films and carvacrol as antimicrobial agents where CNC greatly improved the mechanical properties of the film and the active ingredient carvacrol acted as both an antioxidant and an antimicrobial compound.

Hurdle technology is an eminent approach for microbial inactivation where two or more preservation techniques are combined in order to achieve synergistic or additive effects by showing superior inhibitory potential against tested pathogenic bacteria and fungi compared to a single preservation technique (Lacroix and Follett, 2015; Khan *et al.*, 2017a). In the current study, the application of irradiation treatment along with bioactive CH-based nanocomposite films synergistically reduced the microbial load by 58 to 93 % after 8 weeks of storage as compared to the initial microbial inoculation in rice (5 log CFU/g) (Figure 5.4 and Supplementary data Table 5.5). It is well documented that irradiation treatment can damage microbial cell DNA by breaking the chemical bonds, thereby altering membrane permeability and affecting the other cellular functions, and possibly increasing contact between the microbial cell and active formulations (Caillet *et al.*, 2005; Caillet and Lacroix, 2006; Ayari *et al.*, 2012). The vapor of active formulations present in CH-based nanocomposite films and γ -irradiation in combination can affect the integrity of the microbial cell, influence the release of bacterial and fungal cell ingredients, and reduce the internal pH and ATP synthesis (Caillet *et al.*, 2005; Oussalah *et al.*, 2006). Shankar *et al.* (2021)

developed 1 kGy γ -irradiated chitosan-based active packaging using EO/Ag nanoparticles for the shelf-life extension of strawberries; the combined treatment of bioactive CH-based nanocomposite films and γ -irradiation remarkably extended the shelf-life of stored strawberries by 4 days. [Begum et al. \(2020a\)](#) reported that the combined irradiation treatment (γ -rays and X-rays) along with oregano/thyme EO against the foodborne pathogenic bacteria *E. coli* O157:H7, *S. Typhimurium*, and *Listeria monocytogenes* in rice samples significantly increased the microbicidal effectiveness. The D_{10} values were 326, 266, and 236 Gy for *E. coli* O157:H7, *S. Typhimurium*, and *L. monocytogenes*, respectively, when treated with a high dose rate of γ -irradiation alone (9.1 kGy/h), while the corresponded D_{10} values were significantly reduced ($P \leq 0.05$) to 274, 218, and 219 Gy upon combined treatment of EO and γ -irradiation ([Begum et al., 2020a](#)). Other studies have also demonstrated the higher efficacy of combining active films with irradiation against microbes ([Caillet et al., 2005](#); [Hossain et al., 2014a](#); [Lacroix and Follett, 2015](#); [Hossain et al., 2018](#); [Hossain et al., 2019a](#); [Shankar et al., 2021](#)). In a nutshell, the current study suggested that the combined treatment of the bioactive CH-based nanocomposite films with irradiation treatment could be a viable approach to control microbial contamination in stored cereal grains without compromising the sensory qualities of the stored foods.

5.3.6. *In situ* release/diffusion of active components from bioactive nanocomposite films in rice

In order to ascertain the active components' release profile of AF-1 and AF-2 from bioactive CH-based films, a standard curve was made with concentrations ranging from 0.5 to 2.5 mg/mL. A volume of 1 mL of pure AF-1 and AF-2 was subjected to a UV-VIS spectrophotometer and the spectra were recorded between wavelengths of 900-190 nm following the methods of [Hossain et al. \(2018\)](#) with slight modification. A major peak was observed 330 nm for both AF-1 and AF-2 nanoemulsions (Figure 5.5a, 5.5b). In Figure 5.5c, an extraction profile of active components from the bioactive CH-based was depicted, carried out for 24 h until constant release values were achieved and expressed as yield extracted active components (%) at 330 nm. The highest yield of extracted active components was 17.8 % for the AF-1 nanoemulsion (CH+AF-1) and 14.7% for AF-2 (CH+AF-2 film) at 24 h.

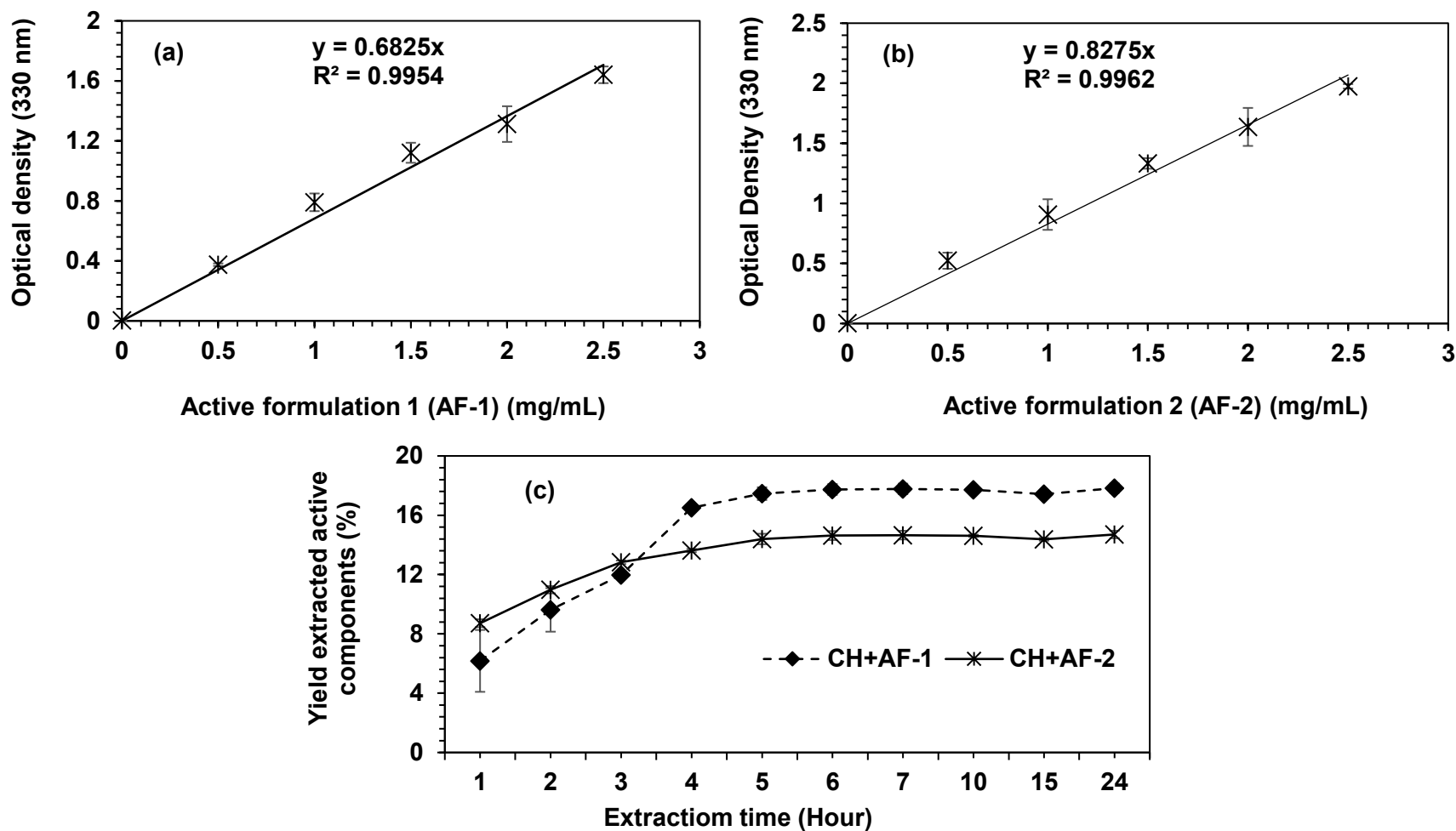


Figure 5.5. Standard curve for active formulation 1 (AF-1) (a) and active formulation 2 (AF-2) (b), and average yield extracted active components (c) from the film at 330 nm.

Figure 5.6 describes the gradual release of active components from the bioactive CH-based films with and without CNC during the storage of films with rice for 2 months. Four types of CH-based films were tested: Group-1: CH+AF-1 film, Group-2: CH+AF-1+CNC film, Group-3: CH+AF-2 film, and Group-4: CH+AF-2+CNC film. Figure 5.6a shows the release profile of active components from CH+AF-1 (Group-1) and CH+AF-1+CNC (Group-2) films. The active components in the CH+AF-1 film were significantly ($P \leq 0.05$) reduced from 43.9 at day 0 to 9.62 % at day 60 (week 8) during storage of rice. The storage time 1, 2, 3, 4, 5, 6, 7, and 8 weeks had significantly ($P \leq 0.05$) increased the quantity of % release of active components from CH+AF-1 film (Group-1), and the values were 12.1, 22.5, 33.6, 45, 61, 66, 73, and 78.1 %, respectively (Figure 5.6a). In addition, the incorporation of CNC into the CH-based film matrix (Group2: CH+AF-1+CNC film) significantly ($P \leq 0.05$) slowed down (38.74 %) the release of active components during the end of the storage compared to Group-1 (CH+AF-1 film). Moreover, it has been observed from Figure 5.6a that there is a significant difference ($P \leq 0.05$) in the release of active components (%) between two films of CH+AF-1 and CH+AF-1+CNC (Group-1 and Group-2). The % release of the active components from the CH+AF-1+CNC film was 8.9, 18.4, 21.1, 25.6, 31.6, 35, 41.1, and 48 % at 1, 2, 3, 4, 5, 6, 7, and 8 weeks, respectively. After 8 weeks of storage, the available active components were 19 % in CH+AF-1+CNC films which were significantly higher ($P \leq 0.05$) than the film CH+AF-1.

Figure 5.6b shows the % release of active formulation 2 (AF-2) from CH+AF-2 (Group-3) and CH+AF-2+CNC (Group-4) film for 8 weeks in stored rice. The release of active components (%) in CH+AF-2 film (Group-3) was significantly increased with storage time and values were 21.8, 37.5, 51.6, 62.7, 67.6, 69.7, 78.1, and 85.3 % at 1, 2, 3, 4, 5, 6, 7, and 8 weeks, respectively ($P \leq 0.05$). The release (%) from the CH+AF-2 film was significantly faster compared to the film CH+AF-2+CNC as shown in Figure 5.6b. The reinforcement of CNC into CH-based bioactive polymeric matrices (Group-4: CH+AF-2+CNC film) significantly improved the controlled release of active components compared to the CH+AF-2 film (Group-3). The active components released from CH+AF-2+CNC film (Group-4) was 32 % lower compared to the film CH+AF-2 (Group-3) at the 8th week. The active component release was 8.1, 12.8, 17.8, 33.6, 39.5, 40.4, 48.4, and 58.1 % from the CH+AF-2+CNC films during the storage at 1, 2, 3, 4, 5, 6, 7, and 8 weeks, respectively, (Figure 5.6b).

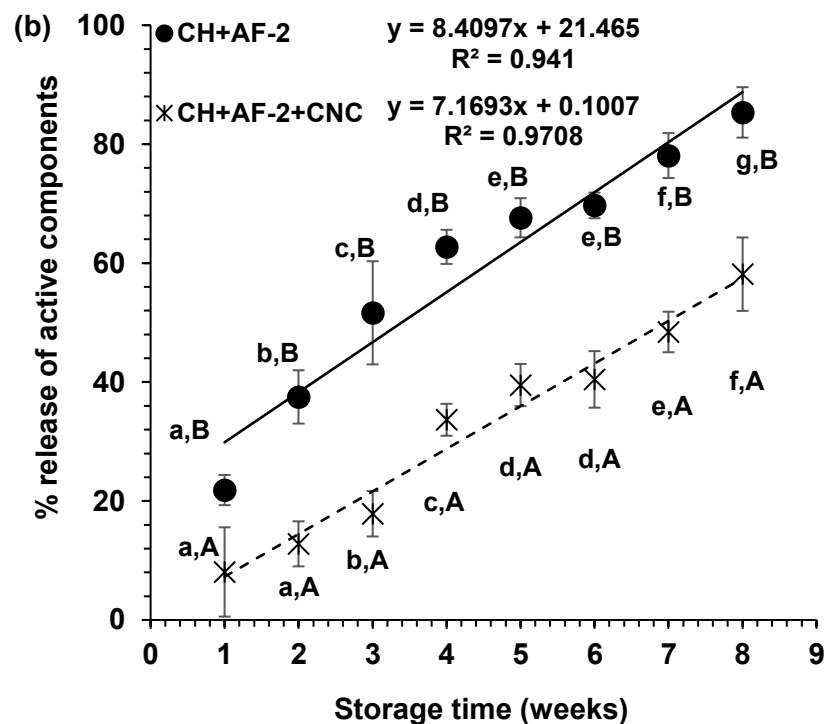
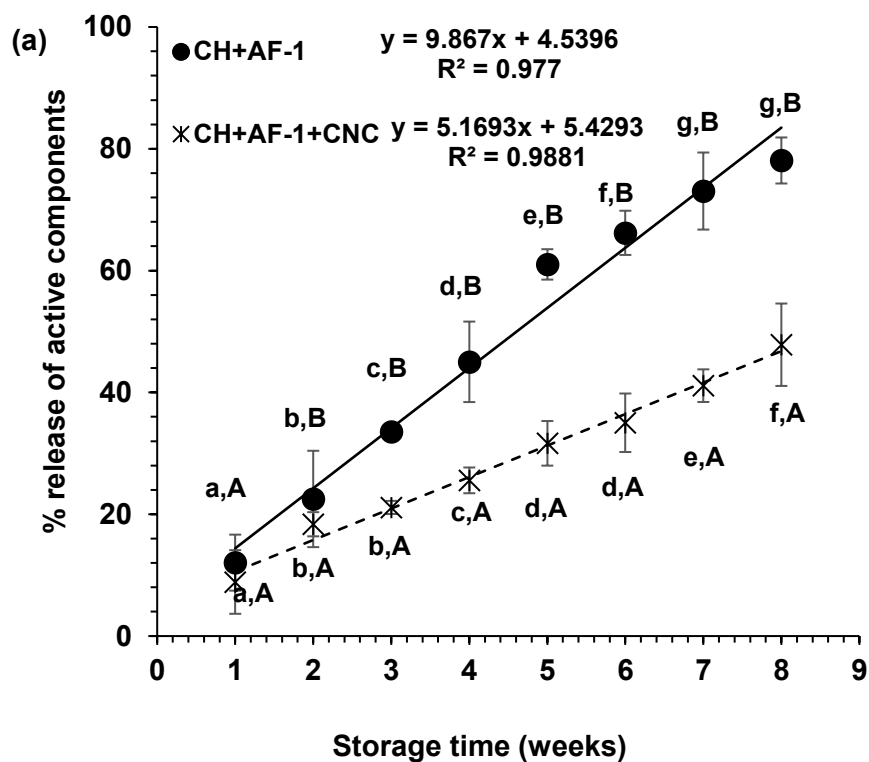


Figure 5.6. Release (%) of active components from (a) bioactive CH+AF-1 film and (b) bioactive CH+AF-film with and without CNC. Values are means \pm standard error. The same lowercase letter either in the bioactive CH-based films with or without CNC are not significantly different ($P > 0.05$). The same uppercase letter between the bioactive CH-based films with and without CNC are not significantly different ($P > 0.05$).

In the present study, the incorporation of CNC into bioactive CH-based matrices (either CH+AF-1 film or CH+AF-2 film) remarkably improved the controlled release of active formulations and preserved their bioactivities through holding them firmly (either AF-1 or AF-2) during storage time thereby preventing fast release. Several authors studied the application of CNC into polymeric matrices as reinforcing agents and also showed that their incorporation considerably improved the controlled release of active components from bioactive films and preserved the bioactivities of active formulations or antimicrobials for an extended period of time during storage (Boumail *et al.*, 2013; Salmieri *et al.*, 2014b; Hossain *et al.*, 2018; Hossain *et al.*, 2019a; Patel *et al.*, 2021). In particular, CNCs also help improving and governing the release of active formulations from nanocomposite matrices through this homogenous distribution of nanoemulsion within the polymeric matrices (Boumail *et al.*, 2013). Hossain *et al.* (2019a) developed bioactive chitosan-based nanocomposite films using an oregano-thyme essential oil mixture and studied the effect of CNC on the controlled release of volatile components from the films during the storage of rice; the incorporation of CNC into CH+oregano/thyme EO film slowed down the % release of volatile components by 26 % compared to the film without CNC (CH+oregano/thyme EO film) (Hossain *et al.*, 2019a). The authors also noticed a similar trend when they used methylcellulose/CNC-based nanocomposite films containing a blend of oregano/thyme EO and CNC slowed the release rate by 35 % compared to methylcellulose film without CNC during 12 weeks of storage in rice (Hossain *et al.*, 2018).

The kinetic release profiles of active components from CH+AF-1 film and AH+AF-1+CNC film (Figure 5.7a) and CH+AF-2 and CH+AF-2+CNC films (Figure 5.7b) were measured and plotted as absorption values at different times (hours). The release kinetic models for CH+AF-1, CH+AF-1+CNC, CH+AF-2, and CH+AF-2+CNC films can be described as first order release models based on their respective R^2 values 0.8887, 0.9192, 0.8963, and 0.9169, respectively, for model fit. The first-order release model is dependent on the released concentration which was first applied by Gibaldi and Feldman (1967) based on Fick's law of diffusion. Moreover, the concentration of active components presented inside the polymeric matrices decayed during the release of active components through the packaging film (Malekjani and Jafari, 2021). In the current study, absorbance prominently decreased with storage time which indicated the slow release of active components from the matrices. Incorporation of CNC into CH-based bioactive films (either CH+AF-1+CNC film or CH+AF-2+CNC film) caused drastic reduction in the release of active components compared to the bioactive films without CNC. A similar observation was reported by Patil *et al.* (2016); Hossain *et al.* (2018). Hossain *et al.* (2018) studied the release kinetics of oregano/thyme essential oils through methylcellulose and methylcellulose/CNC polymeric

matrices and found that release kinetics models were best described by first-order models with high R^2 values of 0.82 (methylcellulose) and 0.88 (methylcellulose/CNC polymeric films). Bruschi (2015) stated that the concentration of released active components from polymeric matrices was proportional to the concentration of remaining active components which decayed with time. The present study suggested the incorporation of CNC into bioactive packaging films could preserve the active formulations for extended storage time due to the slow release of active components.

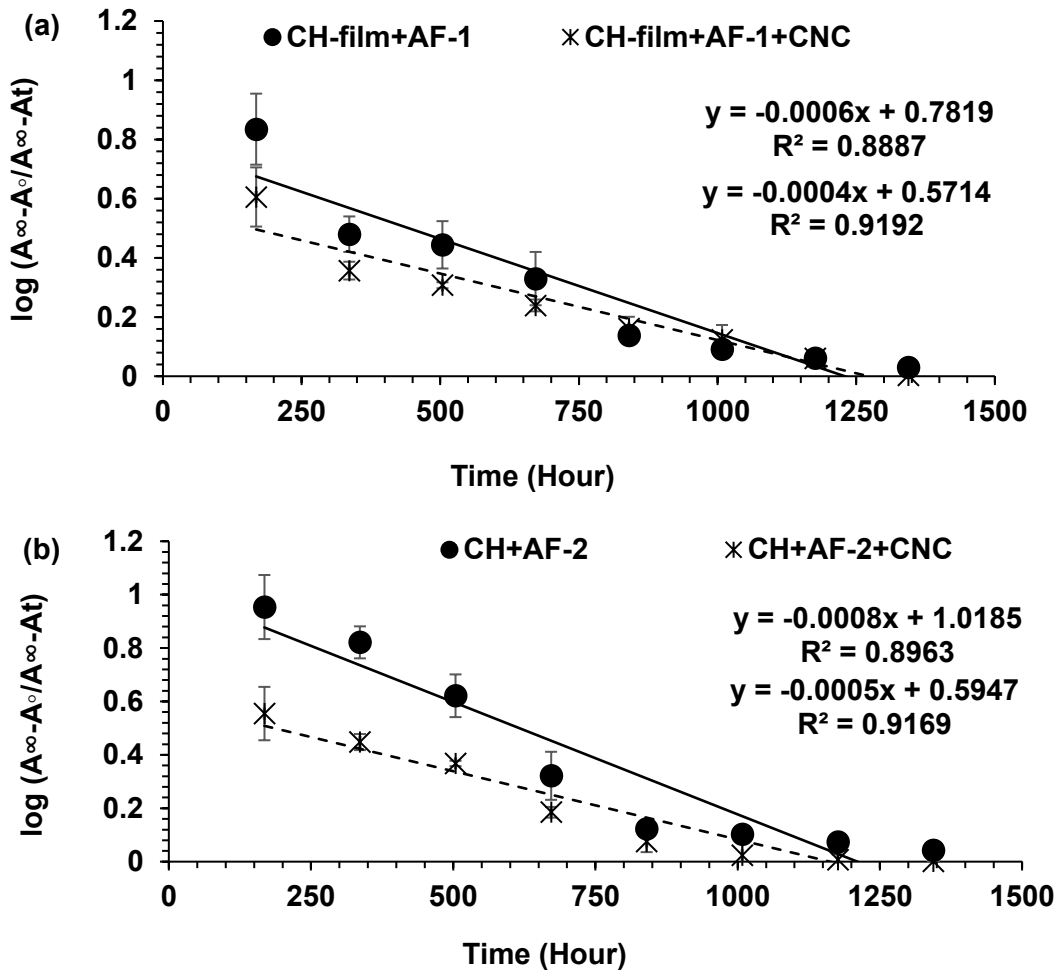


Figure 5.7. Release kinetics study of the active components from (a) CH+AF-1 film, CH+AF-1+CNC film and (b) CH+AF-2 film, CH+AF-2+CNC film.

5.3.7. Sensory properties of treated rice

Sensory profiling (odor, color, taste, and global appreciation) of the stored rice after cooking under the treatment of CH+AF-1+CNC (Figure 5.8a), CH+AF-2+CNC (Figure 5.8b), and without bioactive film (control) were studied for 2 months of storage period (Figure 5.8). The sensory evaluation of bioactive nanocomposite films in the food industry is a critical parameter for their application in food preservation and allied industries to replace synthetic preservatives (Das *et al.*, 2021b). Figure 5.8a-b shows that all the control samples and treated samples with bioactive films (either by CH+AF-1+CNC film or by CH+AF-2+CNC film) did not significantly ($P > 0.05$) change the color, odor, and taste of the rice throughout the storage period, hence received high scores assigned by the sensory panel members. Scores for odor, color, taste, and general appreciation ranged between 7.4 to 8.0 when rice was preserved with CH+AF-1+CNC film and that score corresponded to 'like moderately' to 'like very much', compared to the control sample with similar score range 7.6 to 8.1 ($P > 0.05$) (Figure 5.8a). On the other hand, the rice sample preserved with CH+AF-2+CNC film, scored between 8 to 8.4 ('like very much'), compared to control samples (8.2 to 8.6 'like very much') ($P > 0.05$) during the 2 months of storage (Figure 5.8b). It is worth noted that for both treatment groups, there were no negative evaluations by the panel members. These results reflect that incorporation of nanosized CNC and nanoemulsion formed a stable system of matrix with chitosan that possibly tuned a slow release of essential oil without influencing the sensory profile.

It has been reported that direct application of active formulations on rice can affect the organoleptic properties, particularly during long-term storage (Hossain *et al.*, 2019a). Therefore, from the consumers' perspective, it is imperative that the sensory quality of the product should not be compromised upon packaging treatment. In the current study, all sensory attributes of rice stored with bioactive CH-based nanocomposite films were positive. This might be due to the incorporation of stable antimicrobial nanoemulsion of active formulations into polymeric matrices that in turn tuned the slow release rate of active components at low concentration during storage. Similar reports were found where nanocomposite films augmented the physical stability of the active formulations during storage time, protected them from evaporation and light effects, and helped their gradual release over the storage period (Hossain *et al.*, 2019a). In addition, Hossain *et al.* (2019a) described that the CH-based nanocomposite films containing oregano/thyme EO nanoemulsion did not exhibit any significant effect on odor, taste, color, and appreciation of stored rice after 2 months of storage compared to the control sample. The authors obtained sensory attributes scores between 7.4 to 8.0 for color, odor, taste, and global appreciation for both control and treated samples (Hossain *et al.*, 2019a), analogous to the present study. Chitosan

nanoparticles containing carvacrol maintained acceptable sensory attributes when applied in freshly cut carrots for 13 days of storage (Martínez-Hernández *et al.*, 2017). The above mentioned characteristics of bioactive CH-based nanocomposite films loaded with the nanoemulsion of active antimicrobial formulations for rice preservation could be a viable substitute that has immense potential to pave the way to develop green shelf-life enhancers by replacing synthetic preservatives.

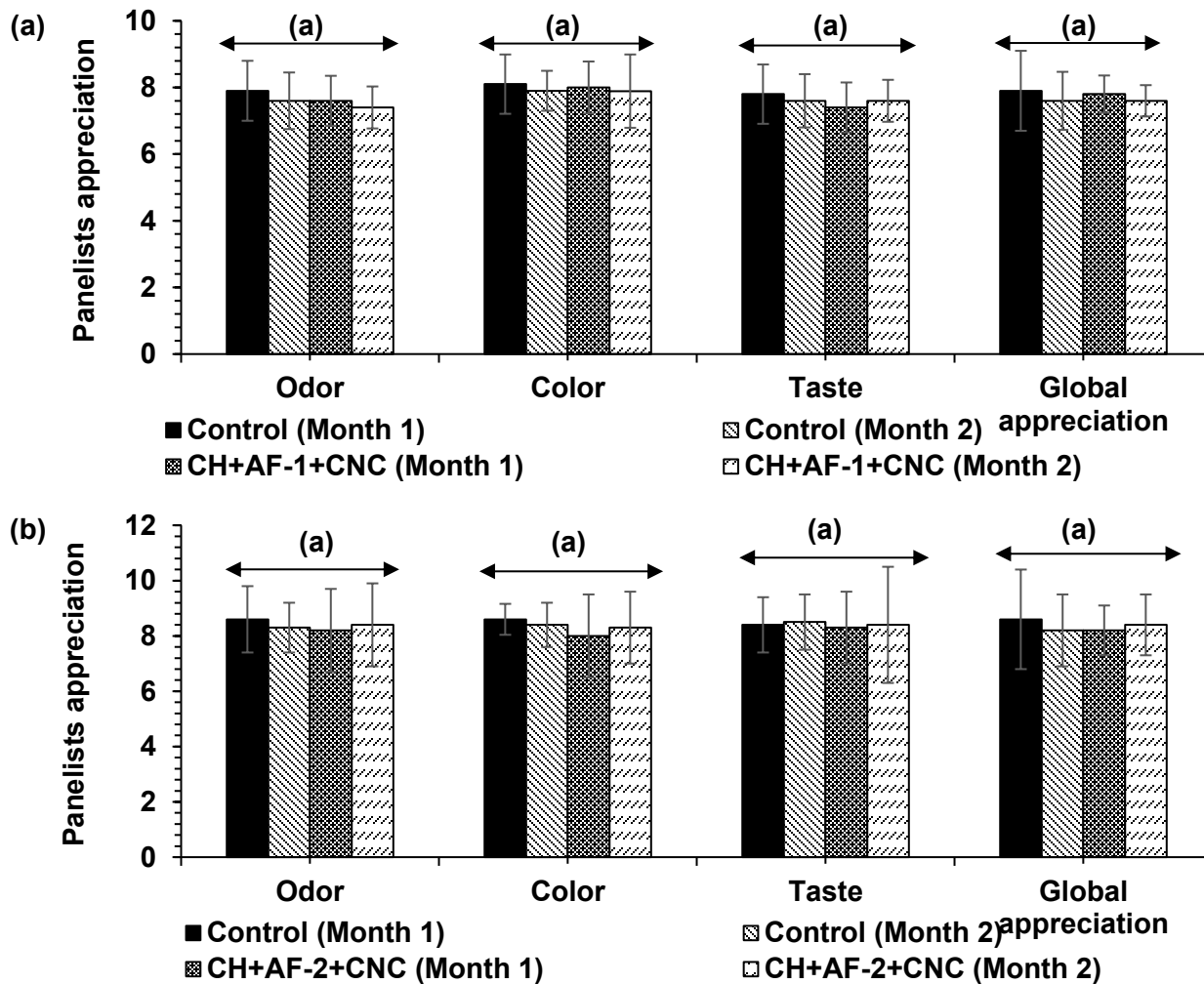


Figure 5.8. Sensory analyses of the cooked rice under different bioactive CH-based nanocomposite films (a) CH+AF-1+CNC film and (b) CH+AF-2+CNC film during two months of storage rice. Control samples did not contain any bioactive CH-based nanocomposite films. Values are means \pm standard error followed by the same lower-case letter are not significantly different ($P > 0.05$).

5.4. Conclusions

The nanoemulsions of active formulations (AF-1 and AF-2) were characterized and optimized by central composite design to obtain stable nanoemulsions with higher microbicidal effectiveness and better stability under different storage conditions. The optimized nanoemulsion of AF-1 and AF-2 significantly increased the encapsulation efficiency by 77 and 79 %, respectively. CH-based nanocomposite films were developed by incorporating different concentrations of CNC. Based on mechanical properties, water vapor permeability, *in vitro* and *in situ* antimicrobial tests against *E. coli* O157:H7, *S. Typhimurium*, *A. niger*, *P. chrysogenum*, and *M. circinelloides*, 6 % CNC with 1 % nanoemulsion of AF-1 and AF-2 incorporated into CH polymeric matrices were optimized as the best bioactive nanocomposite films. Upon combining bioactive nanocomposite films with γ -irradiation, the bacterial and fungal contamination significantly decreased in stored rice for 8 weeks. In addition, reinforcement of CNC in the bioactive CH matrices significantly governed the controlled release of active components for extended period during storage. Sensorial attributes of rice samples under different bioactive packaging treatments showed no significant ($P > 0.05$) difference in color, odor, taste, and overall appreciation with untreated rice. Considering above mentioned results, it can be inferred that the application of CNC-loaded CH-based bioactive films combined with γ -irradiation treatment could be an effective alternative to combat foodborne pathogenic bacteria and fungi in stored cereal grains for extended time in storage without compromising their sensory profiling.

5.5. Acknowledgments

The authors are grateful to the Ministère de l'Économie, et de l'Innovation (MEI) du Québec (PSR SIIIRI 985), Kerry Group, Biosecur Lab Inc., the Ministère de l'Agriculture, des Pêcheries, et de l'Agriculture du Québec (MAPAQ) for a chair on antimicrobial compounds (PPIA-12) and the U.S. Department of Agriculture, Agricultural Research Service (USDA ARS), U.S. Pacific Basin Agricultural Research Centre for supporting this research. The authors would like to acknowledge Dr. Farah Hossain for her scientific and technical contributions.

5.6. References

- Abbas, S., Karangwa, E., Bashari, M., Hayat, K., Hong, X., Sharif, H.R., Zhang, X., 2015. Fabrication of polymeric nanocapsules from curcumin-loaded nanoemulsion templates by self-assembly. *Ultrasonics Sonochemistry* 23, 81-92.
- Asmawati, Mustapha, W.A.W., Yusop, S.M., Maskat, M.Y., Shamsuddin, A.F., 2014. Characteristics of cinnamaldehyde nanoemulsion prepared using APV-high pressure homogenizer and ultra turrax. *AIP Conference Proceedings*. American Institute of Physics, pp. 244-250.
- ASTM, D., 1995. Standard test method for tensile properties of thin plastic sheeting. *Annual book of ASTM standards* 8, 182-190.
- Ayari, S., Dussault, D., Jerbi, T., Hamdi, M., Lacroix, M., 2012. Radiosensitization of *Bacillus cereus* spores in minced meat treated with cinnamaldehyde. *Radiation Physics and Chemistry* 81, 1173-1176.
- Azeredo, H.M.C., Mattoso, L.H.C., Avena-Bustillos, R.J., Filho, G.C., Munford, M.L., Wood, D., McHugh, T.H., 2010. Nanocellulose Reinforced Chitosan Composite Films as Affected by Nanofiller Loading and Plasticizer Content. *Journal of Food Science* 75, N1-N7.
- Begum, T., Follett, P.A., Hossain, F., Christopher, L., Salmieri, S., Lacroix, M., 2020. Microbicidal effectiveness of irradiation from Gamma and X-ray sources at different dose rates against the foodborne illness pathogens *Escherichia coli*, *Salmonella* Typhimurium and *Listeria monocytogenes* in rice. *LWT-Food Science and Technology* 132, 109841.
- Begum, T., Follett, P.A., Mahmud, J., Moskovchenko, L., Salmieri, S., Allahdad, Z., Lacroix, M., 2022a. Silver nanoparticles-essential oils combined treatments to enhance the antibacterial and antifungal properties against foodborne pathogens and spoilage microorganisms. *Microbial Pathogenesis* 164, 105411.
- Begum, T., Follett, P.A., Shankar, S., Mahmud, J., Salmieri, S., Lacroix, M., 2022b. Mixture design methodology and predictive modeling for developing active formulations using essential oils and citrus extract against foodborne pathogens and spoilage microorganisms in rice. *Journal of Food Science* 87, 353-369.
- Ben-Fadhel, Y., Maherani, B., Salmieri, S., Lacroix, M., 2022. Preparation and characterization of natural extracts-loaded food grade nanoliposomes. *LWT-Food Science and Technology* 154, 112781.
- Boumail, A., Salmieri, S., Klimas, E., Tawema, P.O., Bouchard, J., Lacroix, M., 2013. Characterization of trilayer antimicrobial diffusion films (ADFs) based on methylcellulose-polycaprolactone composites. *Journal of Agricultural Food Chemistry* 61, 811-821.

- Bruschi, M.L., 2015. Strategies to modify the drug release from pharmaceutical systems. Woodhead Publishing, 1-92.
- Caillet, S., Lacroix, M., 2006. Effect of gamma radiation and oregano essential oil on murein and ATP concentration of *Listeria monocytogenes*. Journal of Food Protection 69, 2961-2969.
- Caillet, S., Shareck, F., Lacroix, M., 2005. Effect of gamma radiation and oregano essential oil on murein and ATP concentration of *Escherichia coli* O157: H7. Journal of Food Protection 68, 2571-2579.
- Cardiet, G., Fuzeau, B., Barreau, C., Fleurat-Lessard, F., 2012. Contact and fumigant toxicity of some essential oil constituents against a grain insect pest *Sitophilus oryzae* and two fungi, *Aspergillus westerdijkiae* and *Fusarium graminearum*. Journal of Pest Science 85, 351-358.
- Cheng, D., Wen, Y., An, X., Zhu, X., Cheng, X., Zheng, L., Nasrallah, J.E., 2016. Improving the colloidal stability of Cellulose nano-crystals by surface chemical grafting with polyacrylic acid. Journal of Bioresources and Bioproducts 1, 114-119.
- da Rosa, C.G., Sganzerla, W.G., Maciel, M.V.d.O.B., de Melo, A.P.Z., da Rosa Almeida, A., Nunes, M.R., Bertoldi, F.C., Barreto, P.L.M., 2020. Development of poly (ethylene oxide) bioactive nanocomposite films functionalized with zein nanoparticles. Colloids and Surfaces A: Physicochemical and Engineering Aspects 586, 124268.
- Das, S., Kumar Singh, V., Kumar Dwivedy, A., Kumar Chaudhari, A., Deepika, Kishore Dubey, N., 2021a. Nanostructured *Pimpinella anisum* essential oil as novel green food preservative against fungal infestation, aflatoxin B1 contamination and deterioration of nutritional qualities. Food Chemistry 344, 128574.
- Das, S., Singh, V.K., Dwivedy, A.K., Chaudhari, A.K., Dubey, N.K., 2021b. *Anethum graveolens* Essential Oil Encapsulation in Chitosan Nanomatrix: Investigations on In Vitro Release Behavior, Organoleptic Attributes, and Efficacy as Potential Delivery Vehicles Against Biodeterioration of Rice (*Oryza sativa* L.). Food and Bioprocess Technology 14, 831-853.
- de Mesquita, J.P., Donnici, C.L., Pereira, F.V., 2010. Biobased nanocomposites from layer-by-layer assembly of cellulose nanowhiskers with chitosan. Biomacromolecules 11, 473-480.
- Deng, Z., Jung, J., Simonsen, J., Wang, Y., Zhao, Y., 2017. Cellulose Nanocrystal Reinforced Chitosan Coatings for Improving the Storability of Postharvest Pears Under Both Ambient and Cold Storages. Journal of Food Science 82, 453-462.
- Dhar, P., Tarafder, D., Kumar, A., Katiyar, V., 2015. Effect of cellulose nanocrystal polymorphs on mechanical, barrier and thermal properties of poly (lactic acid) based bionanocomposites. Rsc Advances 5, 60426-60440.

- Donsì, F., Annunziata, M., Sessa, M., Ferrari, G., 2011. Nanoencapsulation of essential oils to enhance their antimicrobial activity in foods. *LWT-Food Science and Technology* 44, 1908-1914.
- Donsì, F., Annunziata, M., Vincensi, M., Ferrari, G., 2012. Design of nanoemulsion-based delivery systems of natural antimicrobials: effect of the emulsifier. *Journal of Biotechnology* 159, 342-350.
- Dussault, D., Vu, K.D., Lacroix, M., 2014. *In vitro* evaluation of antimicrobial activities of various commercial essential oils, oleoresin and pure compounds against food pathogens and application in ham. *Meat Science* 96, 514-520.
- Dzamic, A., Sokovic, M., Ristic, M., Grujic-Jovanovic, S., Vukojevic, J., Marin, P., 2008. Chemical composition and antifungal activity of *Origanum heracleoticum* essential oil. *Chemistry of Natural Compounds* 44, 659-660.
- Eustice, R.F., 2015. Using irradiation to make safe food safer. *Stewart Postharvest Review* 11, 1-5.
- Falleh, H., Ben Jemaa, M., Djebali, K., Abid, S., Saada, M., Ksouri, R., 2019. Application of the mixture design for optimum antimicrobial activity: Combined treatment of *Syzygium aromaticum*, *Cinnamomum zeylanicum*, *Myrtus communis*, and *Lavandula stoechas* essential oils against *Escherichia coli*. *Journal of Food Processing and Preservation* 43, 14257.
- Ghabraie, M., Vu, K.D., Tata, L., Salmieri, S., Lacroix, M., 2016. Antimicrobial effect of essential oils in combinations against five bacteria and their effect on sensorial quality of ground meat. *LWT-Food Science and Technology* 66, 332-339.
- Gibaldi, M., Feldman, S., 1967. Establishment of sink conditions in dissolution rate determinations. Theoretical considerations and application to nondisintegrating dosage forms. *Journal of Pharmaceutical Sciences* 56, 1238-1242.
- Ha, T.V.A., Kim, S., Choi, Y., Kwak, H.-S., Lee, S.J., Wen, J., Oey, I., Ko, S., 2015. Antioxidant activity and bioaccessibility of size-different nanoemulsions for lycopene-enriched tomato extract. *Food Chemistry* 178, 115-121.
- Hossain, F., Follett, P., Dang Vu, K., Harich, M., Salmieri, S., Lacroix, M., 2016. Evidence for synergistic activity of plant-derived essential oils against fungal pathogens of food. *Food Microbiology* 53, 24-30.
- Hossain, F., Follett, P., Salmieri, S., Vu, K.D., Fraschini, C., Lacroix, M., 2019a. Antifungal activities of combined treatments of irradiation and essential oils (EOs) encapsulated

- chitosan nanocomposite films in *in vitro* and *in situ* conditions. International Journal of Food Microbiology 295, 33-40.
- Hossain, F., Follett, P., Salmieri, S., Vu, K.D., Harich, M., Lacroix, M., 2019b. Synergistic Effects of Nanocomposite Films Containing Essential Oil Nanoemulsions in Combination with Ionizing Radiation for Control of Rice Weevil *Sitophilus oryzae* in Stored Grains. Journal Food Science 84, 1439-1446.
- Hossain, F., Follett, P., Vu, K.D., Salmieri, S., Frascini, C., Jamshidian, M., Lacroix, M., 2018. Antifungal activity of combined treatments of active methylcellulose-based films containing encapsulated nanoemulsion of essential oils and γ -irradiation: *in vitro* and *in situ* evaluations. Cellulose 26, 1335-1354.
- Hossain, F., Follett, P., Vu, K.D., Salmieri, S., Senoussi, C., Lacroix, M., 2014. Radiosensitization of *Aspergillus niger* and *Penicillium chrysogenum* using basil essential oil and ionizing radiation for food decontamination. Food Control 45, 156-162.
- Khan, A., Khan, R.A., Salmieri, S., Le Tien, C., Riedl, B., Bouchard, J., Chauve, G., Tan, V., Kamal, M.R., Lacroix, M., 2012. Mechanical and barrier properties of nanocrystalline cellulose reinforced chitosan based nanocomposite films. Carbohydrate Polymers 90, 1601-1608.
- Khan, I., Tango, C.N., Miskeen, S., Lee, B.H., Oh, D.-H., 2017. Hurdle technology: A novel approach for enhanced food quality and safety—A review. Food Control 73, 1426-1444.
- Lacroix, M., Follett, P., 2015. Combination irradiation treatments for food safety and phytosanitary uses. Stewart Postharvest Review 11, 1-10.
- Lee, S.-Y., Yang, H.-S., Kim, H.-J., Jeong, C.-S., Lim, B.-S., Lee, J.-N., 2004. Creep behavior and manufacturing parameters of wood flour filled polypropylene composites. Composite Structures 65, 459-469.
- Li, P.-H., Chiang, B.-H., 2012. Process optimization and stability of D-limonene-in-water nanoemulsions prepared by ultrasonic emulsification using response surface methodology. Ultrasonics Sonochemistry 19, 192-197.
- Li, Q., Zhou, J., Zhang, L., 2009. Structure and properties of the nanocomposite films of chitosan reinforced with cellulose whiskers. Journal of Polymer Science Part B: Polymer Physics 47, 1069-1077.
- Li, W., Chen, H., He, Z., Han, C., Liu, S., Li, Y., 2015. Influence of surfactant and oil composition on the stability and antibacterial activity of eugenol nanoemulsions. LWT-Food Science and Technology 62, 39-47.

- Llinares, R., Santos, J., Trujillo-Cayado, L.A., Ramírez, P., Muñoz, J., 2018. Enhancing rosemary oil-in-water microfluidized nanoemulsion properties through formulation optimization by response surface methodology. *LWT-Food Science and Technology* 97, 370-375.
- Luzi, F., Fortunati, E., Giovanale, G., Mazzaglia, A., Torre, L., Balestra, G.M., 2017. Cellulose nanocrystals from *Actinidia deliciosa* pruning residues combined with carvacrol in PVA-CH films with antioxidant/antimicrobial properties for packaging applications. *International Journal of Biological Macromolecules* 104, 43-55.
- Maherani, B., Hossain, F., Criado, P., Ben-Fadhel, Y., Salmieri, S., Lacroix, M., 2016. World market development and consumer acceptance of irradiation technology. *Foods* 5, 79.
- Malekjani, N., Jafari, S.M., 2021. Modeling the release of food bioactive ingredients from carriers/nanocarriers by the empirical, semiempirical, and mechanistic models. *Comprehensive Reviews in Food Science and Food Safety* 20, 3-47.
- Martínez-Hernández, G.B., Amodio, M.L., Colelli, G., 2017. Carvacrol-loaded chitosan nanoparticles maintain quality of fresh-cut carrots. *Innovative Food Science and Emerging Technologies* 41, 56-63.
- McClements, D.J., 2002. Theoretical prediction of emulsion color. *Advances in Colloid and Interface Science* 97, 63-89.
- Moghimi, R., Ghaderi, L., Rafati, H., Aliahmadi, A., McClements, D.J., 2016. Superior antibacterial activity of nanoemulsion of *Thymus daenensis* essential oil against *E. coli*. *Food Chemistry* 194, 410-415.
- Nazarzadeh, E., Anthonypillai, T., Sajjadi, S., 2013. On the growth mechanisms of nanoemulsions. *Journal of Colloid and Interface Science* 397, 154-162.
- Nazzaro, F., Fratianni, F., De Martino, L., Coppola, R., De Feo, V., 2013. Effect of essential oils on pathogenic bacteria. *Pharmaceuticals* 6, 1451-1474.
- Nguefack, J., Somda, I., Mortensen, C., Amvam Zollo, P., 2005. Evaluation of five essential oils from aromatic plants of Cameroon for controlling seed-borne bacteria of rice (*Oryza sativa* L.). *Seed Science and Technology* 33, 397-407.
- Nirmal, N.P., Mereddy, R., Li, L., Sultanbawa, Y., 2018. Formulation, characterisation and antibacterial activity of lemon myrtle and anise myrtle essential oil in water nanoemulsion. *Food Chemistry* 254, 1-7.
- Oussalah, M., Caillet, S., Lacroix, M., 2006. Mechanism of action of Spanish oregano, Chinese cinnamon, and savory essential oils against cell membranes and walls of *Escherichia coli* O157: H7 and *Listeria monocytogenes*. *Journal of Food Protection* 69, 1046-1055.

- Patel, D.K., Dutta, S.D., Ganguly, K., Lim, K.T., 2021. Multifunctional bioactive chitosan/cellulose nanocrystal scaffolds eradicate bacterial growth and sustain drug delivery. *International Journal of Biological Macromolecules* 170, 178-188.
- Patil, D.K., Agrawal, D.S., Mahire, R.R., More, D.H., 2016. Synthesis, characterization and controlled release studies of ethyl cellulose microcapsules incorporating essential oil using an emulsion solvent evaporation method. *American Journal of Essential Oils and Natural Products* 4, 23-31.
- Pereda, M., Amica, G., Marcovich, N.E., 2012. Development and characterization of edible chitosan/olive oil emulsion films. *Carbohydrate Polymers* 87, 1318-1325.
- Qian, C., McClements, D.J., 2011. Formation of nanoemulsions stabilized by model food-grade emulsifiers using high-pressure homogenization: Factors affecting particle size. *Food Hydrocolloids* 25, 1000-1008.
- Radfar, R., Hosseini, H., Farhodi, M., Ghasemi, I., Srednicka-Tober, D., Shamloo, E., Khaneghah, A.M., 2020. Optimization of antibacterial and mechanical properties of an active LDPE/starch/nanoclay nanocomposite film incorporated with date palm seed extract using D-optimal mixture design approach. *International Journal of Biological Macromolecules* 158, 790-799.
- Rhim, J.-W., 2011. Effect of clay contents on mechanical and water vapor barrier properties of agar-based nanocomposite films. *Carbohydrate Polymers* 86, 691-699.
- Salmieri, S., Islam, F., Khan, R.A., Hossain, F.M., Ibrahim, H.M.M., Miao, C., Hamad, W.Y., Lacroix, M., 2014. Antimicrobial nanocomposite films made of poly(lactic acid)-cellulose nanocrystals (PLA-CNC) in food applications—part B: effect of oregano essential oil release on the inactivation of *Listeria monocytogenes* in mixed vegetables. *Cellulose* 21, 4271-4285.
- Samir, M.A.S.A., Alloin, F., Sanchez, J.-Y., Dufresne, A., 2004. Cellulose nanocrystals reinforced poly (oxyethylene). *Polymer* 45, 4149-4157.
- Shankar, S., Khodaei, D., Lacroix, M., 2021. Effect of chitosan/essential oils/silver nanoparticles composite films packaging and gamma irradiation on shelf life of strawberries. *Food Hydrocolloids* 117, 106750.
- Turgis, M., Vu, K.D., Dupont, C., Lacroix, M., 2012. Combined antimicrobial effect of essential oils and bacteriocins against foodborne pathogens and food spoilage bacteria. *Food Research International* 48, 696-702.
- Ureña-Benavides, E.E., Brown, P.J., Kitchens, C.L., 2010. Effect of jet stretch and particle load on cellulose nanocrystal- alginate nanocomposite fibers. *Langmuir* 26, 14263-14270.

- Zachariah, T.J., Leela, N.K., 2006. Volatiles from herbs and spices. Handbook of Herbs and Spices, pp. 177-218.
- Zhang, X., Liu, D., Jin, T.Z., Chen, W., He, Q., Zou, Z., Zhao, H., Ye, X., Guo, M., 2021. Preparation and characterization of gellan gum-chitosan polyelectrolyte complex films with the incorporation of thyme essential oil nanoemulsion. Food Hydrocolloids 114, 106570.
- Zhang, Z., Vriesekoop, F., Yuan, Q., Liang, H., 2014. Effects of nisin on the antimicrobial activity of D-limonene and its nanoemulsion. Food Chemistry 150, 307-312.

Supplementary data Table 5.1. Experimental design by central composite design (CCD) for optimization of nanoemulsion active formulation 1(AF-1).

Runs	Independent variables			
	Active formulation 1 (AF-1) (%, v/v)	A: Pressure (kPSI)	B: Number of cycles	C: Emulsifier (%, v/v)
1	2	11.5	2	2
2	2	11.5	2	2
3	2	11.5	2	2
4	2	8	2	2
5	2	11.5	2	2
6	2	11.5	2	2
7	2	11.5	2	1
8	2	15	4	3
9	2	15	0	1
10	2	8	4	3
11	2	11.5	0	2
12	2	8	4	1
13	2	11.5	4	2
14	2	15	4	1
15	2	8	0	1
16	2	15	2	2
17	2	11.5	2	2
18	2	15	0	3
19	2	8	0	3
20	2	11.5	2	3

Supplementary data Table 5.2. Experimental design by central composite design (CCD) for optimization of nanoemulsion active formulation 2 (AF-2).

Runs	Independent variables			
	Active formulation 2 (AF-2) (% v/v)	A: Pressure (kPSI)	B: Number of cycles	C: Emulsifier (% v/v)
1	2	10	3	3
2	2	15	2	2
3	2	15	2	3
4	2	10	0	3
5	2	15	2	2
6	2	15	2	2
7	2	20	0	1
8	2	10	3	1
9	2	20	3	1
10	2	15	2	2
11	2	15	2	2
12	2	15	3	2
13	2	10	0	1
14	2	15	0	2
15	2	20	0	3
16	2	20	3	3
17	2	20	2	2
18	2	15	2	2
19	2	15	2	1
20	2	10	2	2

Supplementary data Table 5.3. ANOVA analyses for the storage stability of coarse and nanoemulsion of AF-1 and AF-1 at 4 °C, 25 °C, and 40 °C for 2 months.

Storage time (Day)	Coarse emulsion AF-1			Nanoemulsion AF-1		
	4 °C	25 °C	40 °C	4 °C	25 °C	40 °C
1	208.3±18.2 ^a _B	207±18.9 ^a _B	189±21.3 ^{aA}	116.2±8.60 ^{aA}	115±8.90 ^{aA}	113±11.3 ^c _A
5	212.2±14.9 ^a _A	213±21.3 ^b _A	213±18.7 ^{bA}	112.4±4.90 ^{aB}	117±9.60 ^{aC}	103±15.3 ^a _A
14	225.6±16.3 ^b _A	223±17.6 ^d _A	237±17.0 ^{cB}	116.1±12.1 ^{aB}	118±10.3 ^{aB}	106±14.3 ^a _A
28	221.1±18.2 ^b _A	218±15.9 ^c _A	257±14.6 ^{dB}	116.3±12.3 ^{aB}	118±11.2 ^{aB}	108±11.0 ^b _A
42	232.9±10.6 ^c _A	236±21.5 ^e _A	257±11.6 ^{dB}	115.2±14.9 ^{aA}	119±13.2 ^{aA}	123±6.90 ^d _B
56	234.4±12.6 ^c _A	242±9.60 ^{fB}	259±12.3 ^{cC}	115.6±10.9 ^{aA}	119±11.8 ^{aA}	137±5.60 ^e _B
Storage time (Day)	Coarse emulsion AF-2			Nanoemulsion AF-2		
	4 °C	25 °C	40 °C	4 °C	25 °C	40 °C
1	189.6±12.3 ^b _B	196.2±14.6 ^{bC}	123.8±16.3 ^{aA}	67.6±7.2 ^{aA}	69.6±3.3 ^{aA}	71.3±6.9 ^{aA}
5	180.3±14.5 ^a _B	189.6±15.3 ^{aC}	139.2±15.7 ^{bA}	68.1±4.9 ^{aA}	72.3±9.6 ^{aA}	78.3±8.6 ^{bB}
14	182.3±12.8 ^a _B	175.3±13.9 ^{aA}	196.3±16.8 ^{cC}	69.6±8.2 ^{aA}	73.6±10.6 ^a _A	79.6±10.6 ^{bB}
28	196.3±11.8 ^c _A	201.3±14.7 ^{cB}	213.6±9.8 ^{dC}	68.2±12.9 ^{aA}	72.3±11.6 ^a _A	82.6±11.2 ^{bB}
42	201.2±8.9 ^{eA}	225.6±11.6 ^{dB}	245.6±9.6 ^{eC}	67.3±14.2 ^{aA}	71.2±10.9 ^a _A	90.3±11 ^{cB}
56	203.1±17.9 ^e _A	231.3±8.9 ^e _B	275.6±13.6 ^f _C	69.5±10.3 ^{aA}	73.6±9.5 ^{aA}	91.9±9.7 ^{cB}

Values means ± standard error. Within each column means with different lowercase letter are significantly different ($P \leq 0.05$). Withing each row means with different uppercase letter are significantly different ($P \leq 0.05$).

Supplementary data Table 5.4. Inhibitory capacity (%) of bioactive chitosan film against *E. coli*, *S. Typhimurium*, *A. niger*, *P. chrysogenum*, and *M. circinelloides*.

Films	Conc. Of formulation (%)	Inhibitory Capacity (%)				
		<i>E. coli</i> 0157:H7	<i>S. Typhimurium</i>	<i>A. niger</i>	<i>P. chrysogenum</i>	<i>M. circinelloides</i>
Chitosan AF-1	Control	0 ^a	0 ^a	0 ^a	0 ^a	0 ^a
	0.125	17.0±6.3 ^b	27.3±2.9 ^b	28.1±2.2 ^b	11.8±0.6 ^b	11.3±1.6 ^b
	0.25	27.6±4.6 ^c	28.4±8.4 ^b	31.4±3.4 ^b	25.3±4.2 ^c	23.0±6.4 ^c
	0.5	37.9±1.4 ^d	35.3±1.6 ^c	40.1±1.9 ^c	31.9±6.8 ^d	32.3±1.8 ^d
	1	52.0±7.3 ^e	40.0±3.1 ^d	66.0±3.2 ^d	53.0±3.3 ^e	57.0±2.8 ^e
	Chitosan AF-2	Control	0 ^a	0 ^a	0 ^a	0 ^a
0.125		10.2±1.2 ^b	10.1±3.6 ^b	23.5±2.9 ^b	37.3±5.5 ^b	30.1±4.1 ^b
0.25		18.0±3.1 ^c	15.8±2.5 ^c	41.0±1.8 ^c	39.7±2.9 ^b	36.5±1.9 ^c
0.5		34.2±2.5 ^d	29.1±2.7 ^d	49.9±4.5 ^d	54.3±3.0 ^c	46.2±3.9 ^d
1		55.0±2.2 ^e	44.0±1.5 ^e	68.1±5.3 ^e	63.0±4.1 ^d	62.0±7.1 ^e

Values means ± standard error. Within each column means with different lowercase letter are significantly different ($P \leq 0.05$).

Supplementary data Table 5.5. *In situ* antibacterial and antifungal effectiveness of different bioactive films to control *E. coli* O157:H7, *S. Typhimurium*, *A. niger*, *P. chrysogenum*, and *M. circinelloides* growth in stored rice for 8 weeks.

Pathogens	Bacterial and fungal count (log CFU/g) in stored rice (Week)							
	1	2	3	4	5	6	7	8
<i>E. coli</i> O157:H7								
Control	4.34±0.30 ^{cB}	4.13±0.80 ^{cA}	4.06±0.69 ^{bD}	3.75±0.30 ^{cC}	3.52±0.20 ^{dB}	3.78±0.50 ^{fC}	4.01±0.12 ^{eD}	4.78±0.30 ^{eE}
y Control	4.69±0.60 ^{eE}	4.55±0.51 ^{dE}	4.78±0.43 ^{cF}	4.12±0.25 ^{dD}	3.36±0.56 ^{cB}	3.11±0.10 ^{eA}	3.45±0.69 ^{dB}	3.77±0.72 ^{dC}
Treatment 1	4.12±1.20 ^{bF}	3.80±0.30 ^{bE}	3.01±0.56 ^{aD}	2.87±0.90 ^{bD}	2.57±0.30 ^{bC}	2.40±0.10 ^{cB}	2.24±0.40 ^{cB}	2.01±0.10 ^{cA}
Treatment 2	3.89±0.69 ^{aG}	3.52±0.85 ^{aF}	3.16±0.40 ^{aE}	3.01±0.47 ^{bE}	2.45±0.50 ^{bD}	2.12±0.60 ^{bC}	1.85±0.32 ^{bB}	0.89±0.30 ^{bA}
Treatment 3	4.44±0.60 ^{dH}	4.23±0.50 ^{cG}	3.89±0.20 ^{bF}	3.55±0.10 ^{cE}	3.24±0.10 ^{cD}	2.98±0.10 ^{dC}	2.36±0.20 ^{cB}	1.99±0.60 ^{cA}
Treatment 4	4.12±0.91 ^{bH}	3.75±0.40 ^{bG}	3.16±0.51 ^{aF}	2.49±0.43 ^{aE}	1.89±0.41 ^{aD}	1.45±0.20 ^{aC}	0.89±0.70 ^{aB}	0.42±0.11 ^{aA}
<i>S. Typhimurium</i>								
Control	4.41±0.20 ^{cC}	4.09±0.31 ^{cB}	3.95±0.43 ^{dA}	3.85±0.30 ^{dA}	3.89±0.56 ^{eA}	4.05±0.45 ^{fA}	4.33±0.51 ^{eC}	4.89±0.63 ^{eD}
y Control	4.26±0.50 ^{cD}	4.11±0.23 ^{cD}	3.73±0.45 ^{cC}	3.62±0.77 ^{cC}	3.41±0.56 ^{dB}	3.26±0.52 ^{eA}	3.11±0.74 ^{dA}	3.08±0.36 ^{dA}
Treatment 1	4.21±0.21 ^{bF}	4.10±0.32 ^{cF}	3.87±0.20 ^{cE}	3.42±0.23 ^{cD}	2.98±0.36 ^{cC}	2.67±0.44 ^{dB}	2.41±0.28 ^{cA}	2.27±0.19 ^{cA}
Treatment 2	3.74±0.56 ^{aG}	3.16±0.49 ^{aF}	3.02±1.10 ^{bF}	2.73±0.89 ^{bE}	2.12±0.96 ^{bD}	1.59±0.45 ^{bC}	1.26±0.23 ^{bB}	0.87±0.10 ^{bA}
Treatment 3	4.01±0.36 ^{bF}	3.62±0.71 ^{bE}	3.21±0.52 ^{bD}	2.67±0.55 ^{bC}	2.10±0.13 ^{bA}	2.33±0.39 ^{cB}	2.41±0.28 ^{cB}	2.46±0.24 ^{cB}
Treatment 4	3.56±0.56 ^{aH}	3.12±0.12 ^{aG}	2.69±0.36 ^{aF}	2.22±0.43 ^{aE}	1.63±0.22 ^{aD}	1.32±0.19 ^{aC}	0.74±0.23 ^{aB}	0.36±0.06 ^{aA}
<i>A. niger</i>								
Control	5.72±0.72 ^{eA}	6.05±0.71 ^{fB}	6.34±0.64 ^{dC}	6.77±0.34 ^{fD}	6.88±0.65 ^{fD}	6.98±0.86 ^{fE}	7.04±0.31 ^{fF}	7.31±0.23 ^{fF}
y Control	4.67±0.17 ^{dA}	5.93±0.24 ^{eB}	6.09±0.78 ^{cB}	6.15±0.67 ^{eC}	6.13±0.66 ^{eC}	6.28±0.60 ^{eC}	6.40±0.44 ^{eD}	6.48±1.00 ^{eD}
Treatment 1	4.21±0.27 ^{cG}	4.12±0.82 ^{cG}	3.78±0.81 ^{bF}	3.56±0.39 ^{dE}	3.29±0.49 ^{dD}	3.02±0.37 ^{dC}	2.69±0.64 ^{cB}	2.48±0.30 ^{cA}
Treatment 2	3.99±0.45 ^{bG}	3.64±0.70 ^{bF}	3.14±0.58 ^{aE}	2.84±0.40 ^{bD}	2.61±0.81 ^{bC}	2.41±0.29 ^{bC}	2.06±0.38 ^{bB}	1.81±0.58 ^{bA}
Treatment 3	3.89±0.38 ^{aE}	4.33±0.24 ^{dF}	3.69±0.13 ^{bE}	3.25±0.28 ^{cD}	3.02±0.44 ^{cC}	2.76±0.56 ^{cB}	2.98±0.37 ^{dB}	2.32±0.56 ^{cA}
Treatment 4	3.74±0.43 ^{aG}	3.33±0.44 ^{aF}	3.07±0.24 ^{aE}	2.99±0.34 ^{aE}	2.26±0.45 ^{aD}	1.95±0.24 ^{aC}	1.43±0.43 ^{aB}	1.01±0.51 ^{aA}
<i>P. chrysogenum</i>								

Control	5.61±0.28 ^{ca}	5.93±0.20 ^{db}	6.84±0.30 ^{dc}	7.03±0.31 ^{ed}	7.18±1.04 ^{ed}	7.41±1.08 ^{fe}	7.67±0.24 ^{ff}	7.88±0.44 ^{ff}
γ Control	5.17±0.36 ^{ba}	5.63±0.29 ^{cb}	5.84±0.51 ^{cb}	6.15±0.33 ^{dc}	6.58±0.79 ^{dc}	6.67±0.76 ^{ed}	6.83±0.49 ^{ee}	6.89±0.61 ^{ee}
Treatment 1	4.97±0.24 ^{be}	4.67±0.35 ^{bd}	4.13±0.37 ^{ac}	4.02±0.29 ^{cc}	3.83±0.49 ^c B	3.66±0.57 ^{db}	3.45±0.73 ^{da}	3.29±0.42 ^{da}
Treatment 2	4.68±0.33 ^{ae}	4.41±0.14 ^{ad}	4.36±0.35 ^{bd}	3.70±0.34 ^{bc}	2.89±0.63 ^{ac}	2.74±0.60 ^{bc}	2.44±0.76 ^{bb}	2.09±1.00 ^{ba}
Treatment 3	4.83±0.39 ^{ae}	4.63±0.31 ^{be}	4.13±0.33 ^{ad}	3.74±0.49 ^{bc}	3.43±0.36 ^{bb}	3.24±0.42 ^{cb}	3.04±0.39 ^{ca}	2.89±0.31 ^{ca}
Treatment 4	4.85±0.32 ^{ag}	4.57±0.49 ^{af}	4.06±0.37 ^{ae}	3.10±0.48 ^{ad}	2.93±0.54 ^{ad}	2.48±0.89 ^{ac}	1.53±0.83 ^{ab}	0.58±0.17 ^{aa}

M. circinelloides

Control	5.03±0.27 ^{ba}	5.68±0.10 ^{cb}	5.93±0.10 ^{ec}	6.76±0.58 ^{ed}	6.93±0.30 ^{ed}	6.98±0.26 ^{ee}	7.11±0.89 ^{fe}	7.49±0.81 ^{ef}
γ Control	4.45±0.57 ^{aa}	4.61±0.27 ^{ba}	4.78±0.51 ^{db}	4.98±0.41 ^{db}	5.12±0.56 ^{dc}	5.77±0.56 ^{dd}	6.22±0.40 ^{ee}	6.66±0.78 ^{df}
Treatment 1	4.87±0.21 ^{bg}	4.11±0.70 ^{af}	3.65±0.63 ^{be}	3.17±0.56 ^{bd}	2.88±0.71 ^{bc}	2.71±0.21 ^{bb}	2.56±0.41 ^{cb}	2.14±0.61 ^{ba}
Treatment 2	4.98±1.10 ^{be}	4.21±0.62 ^{ad}	2.78±0.34 ^{ac}	2.21±0.44 ^{ab}	2.18±0.39 ^{ab}	2.01±0.30 ^{ab}	1.76±0.11 ^{aa}	1.56±0.21 ^{aa}
Treatment 3	5.11±0.70 ^{cg}	4.65±0.61 ^{bf}	4.26±0.23 ^{ce}	3.97±0.56 ^{cd}	3.26±0.32 ^{cc}	3.01±0.42 ^{cb}	2.78±0.57 ^{da}	2.65±0.61 ^{ca}
Treatment 4	5.01±0.59 ^{bh}	4.76±0.61 ^{bg}	4.21±0.22 ^{cf}	3.77±0.28 ^{ce}	2.98±0.71 ^{bd}	2.66±0.29 ^{bc}	2.16±0.23 ^{bb}	1.76±0.81 ^{aa}

Values means ± standard error. Within each column means with different lowercase letter are significantly different ($P \leq 0.05$). Within each row means with different uppercase letter are significantly different ($P \leq 0.05$).

Chapter 6

Development of novel bioactive nanocomposite films using a central composite design by encapsulating active formulations: applied in stored rice to control pathogenic bacteria and spoilage fungi

This manuscript will be submitted to *Journal of Food Microbiology*, Impact factor: 6.374, h-index: 128, Overall Ranking: 3353, SCImago Journal Rank: 1.131

Tofa Begum^a, Peter A. Follett^b, Shiv Shankar^a, Domitille de Guibert^c, Aymen Ben Abdeljalil^a, Stephane Salmieri^a, Monique Lacroix^{a,*}

^aResearch Laboratories in Sciences, Applied to Food, Canadian Irradiation Center, INRS, Armand Frappier Health and Biotechnology Centre, 531, Boulevard des Prairies, Laval, Quebec, Canada, H7V 1B7

^bUnited States Department of Agriculture, Agricultural Research Service, U.S. Pacific Basin Agricultural Research Center, 64 Nowelo Street, Hilo, HI 96720, USA

^cInstitute Agro-Agrocampus Ouest, 65 Rue de Saint-Brieuc, 35042 Rennes, France

*Corresponding author: Monique Lacroix, Ph.D, Email: Monique.Lacroix@inrs.ca

Tel: 450-687-5010 # 4489, Fax: 450-686-5501

Contribution of the authors

Tofa Begum curated the data, developed the methodology and wrote the whole manuscript. Monique Lacroix and Peter Follett conceived the project, designed the general methodology, supervised the research, and edited the manuscript. Stephane Salmieri and Shiv Shankar assisted with methodology and statistical analysis and reviewed the manuscript. Domitille de Guibert and Aymen Ben Abdeljalil helped with the data curation.

Résumé

Des films nanocomposites à base de poly (butylène adipate-co-téréphtalate) (PBAT) et d'acide polylactique (PLA) conçus à l'aide de deux formulations actives (AF-1 et AF-2), des nanocristaux de cellulose (CNC) et de glycérol comme variables indépendantes par analyse de conception centrale (CCD) ont été évalués. La capacité inhibitrice (CI, %) des films conçus en tant que variables dépendantes contre deux bactéries pathogènes (*Escherichia coli* O157:H7 et *Salmonella* Typhimurium) et trois champignons de détérioration (*Aspergillus niger*, *Penicillium chrysogenum* et *Mucor circinelloides*) ont été mesurés en utilisant un test de volatilisation sur gélose d'agar. Les formulations antimicrobiennes AF-1 et AF-2 sont à base d'un mélange d'extraits d'agrumes (EA) et d'huiles essentielles (HE). Les films nanocomposites bioactifs optimisés ont été caractérisés par des tests de propriétés mécaniques, de perméabilité à la vapeur d'eau (WVP), de taux de transmission d'oxygène (OTR) et de cinétique de libération des agents bioactifs. La cinétique de libération et les mécanismes de libération de l'AF-1 et de l'AF-2 à partir de matrices polymères ont été calculés à l'aide des données intégrées au modèle de Korsmeyer-Peppas. De plus, l'incorporation de CNC/Glycérol dans des films bioactifs de PBAT et de PLA bioactifs pourrait ralentir considérablement la libération des formulations actives de 44-50 % et 20-32 %, respectivement. De plus, la libération d'AF-1 et d'AF-2 dans l'éthanol à partir de films à base de PBAT ou de PLA s'est produite par un mécanisme de diffusion Fickien ou quasi-Fickien pendant la durée d'extraction (70 h). Par la suite, le riz a été stocké pendant 2 mois avec les films nanocomposites bioactifs et traité par irradiation gamma à une dose de 750 Gy pour obtenir un effet synergique afin de contrôler les bactéries pathogènes et les champignons de détérioration testés. Les films optimisés PBAT+AF-1+CNC+Gly et PBAT+AF-2+CNC+Gly ont montré la plus forte efficacité microbicide comparativement aux films nanocomposites bioactifs à base de PLA. Les films bioactifs à base de PBAT avec irradiation pourraient réduire de manière synergique la charge bactérienne et fongique de 73 à 93 % dans le riz stocké après 2 mois par rapport aux échantillons témoins.

Abstract

Poly (butylene adipate-co-terephthalate) (PBAT) and polylactic acid (PLA)-based nanocomposite films were designed using two active formulations (AF-1 and AF-2), cellulose nanocrystals (CNCs) and glycerol as independent variables were analyzed by central composite design (CCD). The inhibitory capacity (IC, %) of the designed films as dependent variables against two pathogenic bacteria (*Escherichia coli* O157:H7 and *Salmonella* Typhimurium) and three spoilage fungi (*Aspergillus niger*, *Penicillium chrysogenum*, and *Mucor circinelloides*) were measured using the agar volatilization assay. The antimicrobial formulations AF-1 and AF-2 are a mixture of citrus extracts (CEs) and essential oils (EOs). The optimized bioactive nanocomposite films were characterized by mechanical properties, water vapor permeability (WVP), oxygen transmission rate (OTR), and release kinetics mechanism tests of the bioactive agents. The release kinetics and release mechanisms of AF-1 and AF-2 from polymeric matrices were calculated using the data fitted into the Korsmeyer-Peppas model. Moreover, incorporation of CNC/Glycerol into bioactive PBAT and bioactive PLA films could significantly slow the active formulations release by 44-50 % and 20-32 %, respectively. Moreover, the release of AF-1 and AF-2 in ethanol from either PBAT or PLA-based films occurred through Fickian or quasi-Fickian diffusion mechanism over the extraction time (70 h). Thereafter, the rice was stored for 2 months with the bioactive nanocomposite films and 750 Gy γ -irradiation to obtain a synergistic effect for controlling all tested pathogenic bacteria and spoilage fungi. The optimized PBAT+AF-1+CNC+Gly and PBAT+AF-2+CNC+Gly films showed the strongest microbicidal effectiveness as compared to the bioactive PLA-based nanocomposite films. The bioactive PBAT-based films with irradiation could synergistically reduce the bacterial and fungal load by 73 to 93 % in stored rice after 2 months compared to the control samples.

6.1. Introduction

Biodegradable environmentally friendly polymers have been gaining interest to achieve sustainable development goals. Poly (butylene adipate-co-terephthalate) (PBAT) and polylactic acid (PLA), commercially available biopolymers, are getting more attention as they comprise 7.2 and 10.3 % of global bioplastics production, respectively (Su *et al.*, 2020). PBAT is a flexible biodegradable and compostable aliphatic-aromatic copolyester certified by the Biodegradable Polymers Institute (ASTM D6400 standard specification) and the European Bioplastics (EN13432 standard criteria) (Morelli *et al.*, 2016; Shankar and Rhim, 2018). However, to increase its application widely, it is important to improve its barrier and mechanical resistance properties. Another biodegradable polymer, PLA, is getting more popular as a packaging material owing to its transparency, high mechanical properties, commercial availability, low cost, and easy processability (Arrieta *et al.*, 2014; Salmieri *et al.*, 2014b, a). PLA could be produced from both renewable sources (such as sugar, and starch) and chemical synthesis (Su *et al.*, 2020). The application of PLA in the food industry as a packaging material is still limited because of its brittleness, lower thermal stability, poor oxygen and water vapor barrier properties, and lower melt strength (Arrieta *et al.*, 2014; Shankar and Rhim, 2018). These drawbacks of the PLA and PBAT polymers could be improved by incorporating a reinforcing filler, plasticizers, and developing nanocomposite films (Morelli *et al.*, 2016; Sung *et al.*, 2017). Cellulose nanocrystals (CNCs) are attractive nanofillers used by several authors to improve the drawbacks of the natural biopolymers (Khan *et al.*, 2012; Khan *et al.*, 2013; Salmieri *et al.*, 2014b; Haafiz *et al.*, 2016; Sung *et al.*, 2017; Hossain *et al.*, 2019a). As a reinforcing filler CNC possesses unique properties such as high specific strength (10 GPa), elasticity (150 GPa), commercial availability with low cost, biocompatibility, ease of chemical modification, which makes it an attractive nanofiller (Sung *et al.*, 2017).

CNC-reinforced nanocomposite PLA and PBAT films can be used as a biodegradable packaging material for food packaging and replace the nonbiodegradable petroleum-based packaging materials. However, the incorporation of bioactive agents into polymeric matrices can help to develop bioactive packaging films which could extend the food's shelf life by preventing the growth of foodborne pathogenic bacteria and spoilage fungi (Salmieri *et al.*, 2014a; Ghabraie *et al.*, 2016; Hossain *et al.*, 2016b). Bioactive agents such as plant-derived essential oils (EOs), and plant-based extracts (citrus extracts-CEs) possess strong antibacterial, antifungal, insecticidal, and antiviral properties (Turgis *et al.*, 2012; Begum *et al.*, 2020a; Begum *et al.*, 2022b). EOs and CEs contain a mixture of complex volatile and non-volatile compounds such as monoterpenes, sesquiterpenes, aldehydes, alcohols, phenols, ketones, oxides, flavonoids, and they control

microbial growth or biological contaminants by multiple mechanisms of action (Turgis *et al.*, 2012; Hossain *et al.*, 2016b; Maherani *et al.*, 2018; Begum *et al.*, 2022b). However, the direct application of natural bioactive agents in foods might affect the market values of the products because of the strong smell. Hence, the mixture of EOs and CEs can work together synergistically and the incorporation of the mixture of active agents into nanocomposite polymeric matrices improves the controlled release of the active agents as well as prolong the shelf-life of stored foods while maintaining food safety and quality (Hossain *et al.*, 2014a; Hossain *et al.*, 2019b; Begum *et al.*, 2020a; Begum *et al.*, 2022b).

Oryza sativa L. (rice) is rich with carbohydrates, fats, proteins, minerals, and vitamins, and is one of the most dominant cereal grains throughout the world consumed by of the 50 % population (Das *et al.*, 2021b; Begum *et al.*, 2022a). Because of its high nutritional value, rice is sensitive to biodeterioration by several pathogenic bacteria, spoilage fungi, and insect pests (Begum *et al.*, 2020a; Hossain *et al.*, 2021; Begum *et al.*, 2022b). Microbial growth in stored rice grains could lead to discoloration, off-flavor, unpleasant smell, decreased nutritional value and may contain mycotoxins and methylglyoxal (Das *et al.*, 2021a). Various synthetic preservatives such as methyl-bromide, phosphine, and organophosphates are commonly used for preventing biodeterioration of rice during storage which has serious health and environmental issues, and may cause pathogens to become resistant after a long time of exposure (Follett *et al.*, 2013; Hossain *et al.*, 2021).

Ionizing irradiation is a technique for controlling foodborne pathogenic bacteria, spoilage fungi, and insect pests in stored cereal grains (Follett *et al.*, 2013; Hossain *et al.*, 2014b). Irradiation controls the biological contaminants in foods by breaking down the chemical bonds in microbial DNA, altering the membrane permeability, disrupting cellular activity, and thus leading to microbial death (Oussalah *et al.*, 2006; Begum *et al.*, 2020a). Bioactive packaging in combination with irradiation act synergistically and increase the radiosensitivity to the biological contaminants (Ayari *et al.*, 2012; Hossain *et al.*, 2014a; Hossain *et al.*, 2019a; Ayari *et al.*, 2020). The goals of the current studies were (i) developing bioactive PBAT and PLA-based nanocomposite films for food packaging; (ii) determining the effect of CNC, glycerol and active formulations on the antibacterial and antifungal properties of the bioactive nanocomposite films; (iii) evaluate the effect of reinforcing agents on mechanical, water vapor permeability, oxygen transmission rate, and *in vitro* controlled release of active formulations; (iv) determine *in situ* antibacterial and antifungal properties of bioactive nanocomposite films to control foodborne pathogens in stored rice; and (v) evaluate the synergistic effect between γ -irradiation and bioactive nanocomposite packaging films.

6.2. Materials and methods

6.2.1. Materials

A film grade bioplastic PBAT pellet (EnPol PBG7070) was purchased from S-EnPol Co. Ltd. (Wonju, South Korea) (Specific gravity: 1.10-1.25; Melting point: 125 °C). PLA was bought from Nature Works LLC (Blair, NE, USA) (Ingeo™ 3,251 grade; Mw: 90,000–120,000). Reinforcing agent cellulose nanocrystal (CNC) was provided by FPIInnovations (Pointe-Claire, Quebec, Canada). The emulsifier Glycerol (Gly) was procured from Sigma-Aldrich Ltd. (St. Louis, Missouri, United States). The bacterial nutrient media tryptic soy broth/agar (TSB/TSA) and fungal nutrient media potato dextrose broth/agar (PDB/PDA) were purchased from BD, Franklin Lakes, NJ, USA, and Alpha Biosciences Inc. (Baltimore, MD, USA), respectively. The Mediterranean EO, Southern EO, and Asian EO were procured from BSA (Montreal, QC, Canada), while the citrus EO, cinnamon EO, and savory thyme EO were bought from Zayat Aroma (Bromont, QC, Canada). The natural citrus extract (NCE) and organic citrus extract (OCE) were provided by Kerry (Beloit, WI, USA).

6.2.2. Preparation of active formulations using EOs and CEs

Active formulations were composed of citrus extracts (CEs) and a mixture of essential oils (EOs) was developed based on our previous study ([Begum et al., 2022b](#)). Two active formulations were developed and coded as AF-1 (active formulation 1) and AF-2 (active formulation 2). The AF-1 was prepared by organic citrus extract (OCE), Mediterranean EO, citrus EO, cinnamon EO (2 : 1 : 2 : 1), and the AF-2 was prepared by natural citrus extract (NCE), Asian EO, Southern EO, cinnamon EO, savory thyme EO (2 : 2 : 1 : 2 : 1).

6.2.3. Pathogenic bacterial and spoilage fungal culture preparation

Pathogenic bacteria: *Escherichia coli* O157:H7 NT 1931 and *Salmonella* Typhimurium SL 1344 and spoilage fungi: *Aspergillus niger* ATCC 1015, *Penicillium chrysogenum* ATCC 10106, and *Mucor circinelloides* ATCC 56649 were selected for the current study. The bacterial and fungal stock cultures were preserved at -80 °C in TSB and PDB with a volume of 10 % (v/v) glycerol ([Ghabraie et al., 2016](#)). Before each experiment, the stock cultures were recuperated by passing through two consecutive growth cycles in the TSB for 24 h at 37 °C for bacteria and in the PDB

for at least 48 h at 28 °C for fungi. Bacterial and fungal concentrations of 1×10^5 CFU/mL were used for *in vitro* and *in situ* experiments. The desired bacterial concentration was obtained by centrifugation and then by washing with sterile saline water, while the fungal concentrations were adjusted by inoculating fungus into PDA media, culturing them for 2-4 days, collecting the spores using sterile saline water and filtered, and finally, the concentrations were adjusted at approximately 1×10^5 CFU/mL for the experiments.

6.2.4. Experimental design for bioactive nanocomposite film

The bioplastic-based films (PLA, PBAT) were selected for the development of bioactive packaging films for controlling the growth of pathogenic bacteria and fungi in stored cereal grains. All ingredients, including 2 g of polymer granules (PBAT or PLA granules), active formulation (either AF-1 or AF-2) (100-300 μ L), CNC (0-1.5 %), and Gly (0.25-1.5 %), were mixed at different concentrations (polymeric blend formulations). Finally, the polymeric blend formulations were hot-pressed using a compression molding machine (Carver Inc., Indiana, USA, Model 3912) under the pressure of 5500-7500 pounds at 280-300 °F for 1-2 min to get the desired bioactive PBAT and PLA nanocomposite films (Radfar *et al.*, 2020).

A central composite design (CCD) (Design-Expert software, version 11, Stat-Ease, Inc.) was performed for optimizing the levels and proportions of the independent variables (active formulations, CNC, Gly) for developing the efficient antibacterial and antifungal bioactive packaging films (Radfar *et al.*, 2020; Begum *et al.*, 2022b). A total of 17-20 experimental runs (polymeric blend formulations) were designed for each bioactive packaging film with three replicates. The antibacterial and antifungal properties of each film were considered dependent variables against pathogenic bacteria (*E. coli* O157:H7 and *S. Typhimurium*) and spoilage fungi (*A. niger*, *P. chrysogenum*, and *M. circinelloides*).

6.2.4.1. Antibacterial and antifungal properties of the bioactive nanocomposite films

An inverted lid agar volatilization assay method was used to measure the antibacterial and antifungal properties of the films by calculating inhibitory capacity (IC, %) (Hossain *et al.*, 2019a; Begum *et al.*, 2022a). Briefly, the bacterial and fungal strains (approximately 10^5 CFU/mL) were inoculated on the surface of TSA or PDA media. Then, the plate was inverted, and a piece of film (1 cm²) was placed in the middle of the lid of the Petri plate, followed by sealing the plates with

Parafilm®, incubating all plates at 37 °C for 24 h (bacteria) and at 27 °C for 48 h (fungi). The inhibitory capacity of the films was calculated as follows Eq. 6.1

$$\text{Inhibitory capacity (\%, IC)} = D_i/D_p \times 100 \text{ Eq. 6.1}$$

Where, D_i = Diameter of the inhibition zone (mm); D_p = diameter of the petri plate (mm).

6.2.4.2. Optimization and statistical analyses of the bioactive nanocomposite films

The independent variables (active formulations, CNC, Gly) were fitted into the experimental design to obtain the bioactive nanocomposite film having the strongest bactericidal and fungicidal properties. The measured independent variables were fitted into linear and quadratic models as follows-

$$Y = C_0 + \sum_{i=1}^n C_i X_i + \sum_{i=1}^n C_j X_j \text{ Eq. 6.2}$$

$$Y = C_0 + \sum_{i=1}^n C_i X_i + \sum_{1 \leq i < j}^n C_{ij} X_i X_j + \sum_{1 \leq i < j < k}^n C_{ij} X_i X_j X_k \text{ Eq. 6.3}$$

Where, Y: Dependent variables (Inhibitory Capacity against tested pathogenic bacteria and spoilage fungi); C_0 : Constant-coefficient; C_i : Linear coefficient; C_{ij} : Interactive coefficient; $X_i..X_j...X_k$: Independent variables; n: Number of variables. Each experiment was performed in triplicate. One-way ANOVA analyses were performed for the level of significance of the models where the significant P-values were ≤ 0.05 and insignificant P-values were > 0.05 for rejecting the null hypotheses (Radfar *et al.*, 2020; Begum *et al.*, 2022b). However, the effect of different independent variables at the different concentrations on the dependent variables was depicted as 3D images for visualizing IC (%) of the bioactive nanocomposite films against *E. coli* O157:H7, *S. Typhimurium*, *A. niger*, *P. chrysogenum*, and *M. circinelloides*. However, the relationship between independent and dependent variables depicted through 3D images can describe different conditions by connecting all points within the three-dimensional plane (Falleh *et al.*, 2019; Radfar *et al.*, 2020). When the polymeric blend formulation for PBAT and PLA-based nanocomposite films were optimized in terms of strong antibacterial and antifungal properties, further characterization of the bioactive nanocomposite films could be performed before applying them for food preservation.

6.2.5. Characterization of the bioactive nanocomposite films

The mechanical properties, water vapor permeability (WVP), oxygen transmission rate (OTR), and *in vitro* release kinetics tests of the optimized bioactive nanocomposite films (PBAT and PLA) were examined. The effect of CNC on mechanical properties, WVP, OTR, and *in vitro* release tests was also examined. The tested films were categorized as Control-1: neat PBAT film, Group-1: PBAT+AF-1+CNC+Gly, Group-2: PBAT+AF-2+CNC+Gly, Control-2: neat PLA film, Group-3: PLA+AF-1+CNC+Gly, and Group-4: PLA+AF-2+CNC+Gly.

6.2.5.1. Mechanical properties

The mechanical properties such as tensile strength (TS), modulus (TM), and Elongation at break (Eb) of the films were tested ([Salmieri *et al.*, 2014b](#); [Morelli *et al.*, 2016](#)). Mechanical properties are indicating the film processing capability, handling, and storage of the packaged materials properties which are the important characterization of the films that will be used in food packaging ([Salmieri *et al.*, 2014b](#); [Shankar and Rhim, 2016](#)). Briefly, the film thickness was measured at five different random points using a Mitutoyo Digimatic Indicator (Tokyo, Japan) and the film width was measured using a Traceable Carbon® Fiber Digital Caliper (Fisher Scientific). All films were cut into 60 × 12 mm pieces before testing and the mechanical properties were measured using a Universal Testing Machine (100 N-load cell; specimen grips: 1.5 kN) (Tinius Olsen Testing Machine Co., Inc., Horsham, PA, USA). Moreover, the position of machine control was fixed at 50 mm/min, Y- and X-axes were imposed to a 100 N-range load and a 500 mm-range position coordinates, respectively. Using a Test Navigator® program, TS (maximum stress, MPa) and TM (modulus, MPa), and elongation at break (Eb, %) values were automatically recorded when the films were broken owing to elongation.

6.2.5.2. Water vapor permeability (WVP)

The WVP of the films was performed followed by [Salmieri *et al.* \(2014a\)](#). Briefly, a vapometer cell (model 68-1; Twining-Albert Instrument Co., West Berlin, NJ, USA) was filled up with 30 g of anhydrous CaCl₂ (RH: 0 %). Then, the films were placed onto the vapometers and the cells were mechanically sealed. After recording the initial weight the cells were kept in a controlled humidity chamber (Shellab 9010L, Sheldon Manufacturing Inc., Cornelius, OR, USA) at 25 °C (RH: 60 %) for 24 h. After incubation of 24 h, the final weight of the cells was recorded as the amount of water

vapor transferred through the film and absorbed by the anhydrous CaCl_2 . WVP was calculated using Fick and Henry's laws of gas diffusion through films and coatings as follows-

$$\text{WVP (g mm m}^{-2} \text{ day}^{-1} \text{ kPa}^{-1}) = \Delta w \cdot x / A \cdot \Delta P \text{ Eq. 6.4}$$

Where Δw : Gained weight (g) of the cell after 24 h; x : Film thickness (mm); A : Area of exposed film ($31.679 \cdot 10^{-4} \text{ m}^2$); and ΔP : Differential vapor pressure of water through the film ($\Delta P = 3.282 \text{ kPa}$ at $25 \text{ }^\circ\text{C}$).

6.2.5.3. Oxygen permeability rate (OTR)

The oxygen transmission rate (OTR) of the films was measured using an OX-TRAN Model 1/50 (Minneapolis, MN, USA) machine following the method adopted by [Criado *et al.* \(2020\)](#) and [Kang *et al.* \(2021\)](#). Briefly, a 5 cm^2 film area was adjusted to an aluminum foil mask, and a test was performed at 0 % relative humidity at $23 \text{ }^\circ\text{C}$. Prior to the experiment, the thickness of each film was measured at five random points using a Mitutoyo micrometer (BDI Canada Inc., Laval, QC, Canada). The measured thickness was each film between $78\text{-}90 \text{ }\mu\text{m}$. The results were expressed as $\text{cm}^3 \cdot \text{m}^{-2} \cdot \text{day}^{-1}$. The test cells were divided into two chambers separated by the film samples and the gas (N_2 and O_2) pressure ranges were stabilized at 33 PSIG. An oxy-dot sensor measured the O_2 absorption over time at 20-min intervals to get OTR for 24 h. The tests were performed in triplicate for each film.

6.2.5.4. *In vitro* release profiles/kinetics of the active formulations from the bioactive films

The *in vitro* release kinetics of the active formulations from the bioactive films were performed in an ethanolic medium with different contact times ([Requena *et al.*, 2017](#); [Hossain *et al.*, 2018](#); [Ben-Fadhel *et al.*, 2020](#); [Felix da Silva Barbosa *et al.*, 2021](#)). Briefly, a 500 mg bioactive film sample was placed in a flask containing 200 mL of ethanol for 70 h of extraction time. A total of eight types of films were tested named Control-1: PBAT+AF-1 film; Control-2: PBAT+AF-2 film; Control-3: PLA+AF-1 film; Control-4: PLA+AF-2 film; PBAT+AF-1+CNC+Gly film; PBAT+AF-2+CNC+Gly film; PLA+AF-1+CNC+Gly film; and PLA+AF-2+CNC+Gly film. Thereafter, each film in ethanol was kept under mild magnetic stirring throughout the extraction time at room temperature. The extracted samples (1 mL) were collected at certain time intervals until reached an equilibrium and the flask was filled with 1 mL of fresh ethanol to keep the same volume. The absorbance of the extracted sample was measured using a UV-Vis spectrophotometer and calculated the cumulative release (%) of AF-1 and AF-2 from the bioactive films as follows-

$$\text{Cumulative release (\%)} = \frac{\text{Volume of sample withdraw}}{\text{Bath volume}} \times P(t-1) + P_t \quad \text{Eq 6.5}$$

Where, P_t is released (% w/v) at time t ; $P_{(t-1)}$ is released (% w/v) at a time previous to “ t ”. All experiments were performed in triplicate. The film without active formulations or active formulation+CNC+Gly in the liquid phase was considered blank for the absorbance measurement. Likewise, the obtained data were fitted into the Korsmeyer-Peppas model (Eq. 6.6) for investigating the release kinetics and the mechanisms associated with the release of active formulations through the polymeric matrices.

$$M_t/M_\infty = kt^n \quad \text{Eq 6.6}$$

Where M_t/M_∞ : Fraction of the released active formulation at the time “ t ”; k : Rate constant of apparent release (related to the diffusion process); n : Release exponent (“ n ” values are given information associated with the release mechanism). Herein, an “ n ” value ≤ 0.45 : release through Fickian diffusion or quasi-Fickian diffusion, “ n ” value between 0.45 and 0.89: release through anomalous transportation (means the polymer relaxation and the diffusion rates are coupled), “ n ” value equal to 0.89: release follows a zero-order release mechanism (means through swelling processing), and “ n ” value > 0.89 : release through non-Fickian transportation mechanism (means deterioration of the polymeric chain and release occurs both diffusion and relaxation process) (Requena *et al.*, 2017; Ben-Fadhel *et al.*, 2020).

6.2.6. Hurdle treatment (bioactive films with γ -irradiation) in rice

The optimized bioactive nanocomposite films with higher bactericidal and fungicidal properties along with satisfactory mechanical, WVP, and release kinetics properties were selected for a challenging test in stored rice (*in situ* tests) for controlling pathogenic bacteria (*E. coli* O157:H7 and *S. Typhimurium*) and spoilage fungi (*A. niger*, *P. chrysogenum* and *M. circinelloides*) (Hossain *et al.*, 2018; Hossain *et al.*, 2019a; Begum *et al.*, 2022a). Moreover, the bioactive nanocomposite films were also tested with 750 Gy γ -irradiation in rice for controlling the growth of bacteria and fungi. Briefly, an inoculation bath having 10^5 CFU/mL of bacteria/fungi was prepared and sterile rice (500 g) was added to the inoculation bath. After mixing the rice with pathogens very well (30 sec), the rice was dried under sterile conditions for 2 h. Then, a 50 g of inoculated rice was placed into a sterile plastic bag containing the bioactive nanocomposite films (1 g/cm^2). The samples with and without bioactive nanocomposite films went under irradiation treatment (750 Gy) using a Cobalt-60 UC-15A γ -irradiator at a 7.1 kGy/h dose rate (Sterigenics, Laval, QC, Canada) for increasing the microbicidal effectiveness in combined (Hurdle) treatment. The samples were categorized as Control: (Rice+pathogenic bacteria/fungi), γ -Control: Rice+pathogenic

bacteria/fungi+750 Gy irradiation, Treatment 1: PBAT+AF-1+CNC+Gly film, Treatment-2: PBAT+AF-1+CNC+Gly film+750 Gy), Treatment 3: PBAT+AF-2+CNC+Gly film), and Treatment 4: PBAT+AF-2+CNC+Gly film+750 Gy. Then the samples were stored for 8 weeks and a microbiological analysis was performed each week (Begum *et al.*, 2020b).

6.3. Results and Discussion

6.3.1. Experimental design for bioactive nanocomposite film

The effect of each independent variable on dependent variables (antibacterial and antifungal properties) of the produced films was fitted in different models using CCD and optimized the best conditions of the films based on the highest bioactivities. The dependent variables' results as inhibitory capacity (IC, %) against the tested bacteria (*E. coli* O157:H7 and *S. Typhimurium*) and fungi (*A. niger*, *P. chrysogenum*, and *M. circinelloides*) of PBAT and PLA films are depicted in Figures 6.1-6.4. The statistical analyses (ANOVA) of the effect of each independent variable on the dependent variables were shown in Tables 6.1-6.4, and Supplementary data Tables 6.1-6.8 shows the film-forming formulation at different levels.

In the case of PBAT films, a quadratic model was significant for all tested pathogenic bacteria and fungi (Table 6.1 and Table 6.2). The independent variables such as active formulation 1 (AF-1) (100 to 300 μ L), CNC (0 to 0.75 %), and Gly (0.25 to 1 %) were incorporated into PBAT polymeric matrices at the different concentrations for producing the bioactive PBAT-based nanocomposite films (Table 6.1, Figure 6.1a-e, Supplementary data Tables 6.6.1-6.2). A strong significant interaction among the independent variables was observed in the study. The quadratic model was significant for the pathogenic bacteria *E. coli* O157:H7 and *S. Typhimurium* ($P \leq 0.05$). The quadratic model was statistically significant ($P \leq 0.05$) for the tested bacteria as the model showed the F-values for *E. coli* O157:H7 and *S. Typhimurium* were 48.85 ($P < 0.0001$; df: 9; Lack of fit: 0.77; Lack of fit P-value: 0.61) and 56.94 ($P < 0.0001$; df: 9; Lack of fit: 0.76; Lack of fit P-value: 0.62), respectively. The insignificant Lack of fit (LOF) ($LOF > 0.05$) values for *E. coli* O157:H7 and *S. Typhimurium* implied that the LOF values were not occurring due to error as well as there was a 61-62 % chance to get large LOF F-values due to noise. The quadratic model for *E. coli* O157:H7 and *S. Typhimurium* showed a higher coefficient of determination values (R^2 values) at 97 and 98 %, respectively, which stated that the corresponding quadratic model had a good agreement between the experimental and the predicted values (Table 6.1). A quadratic model was significant

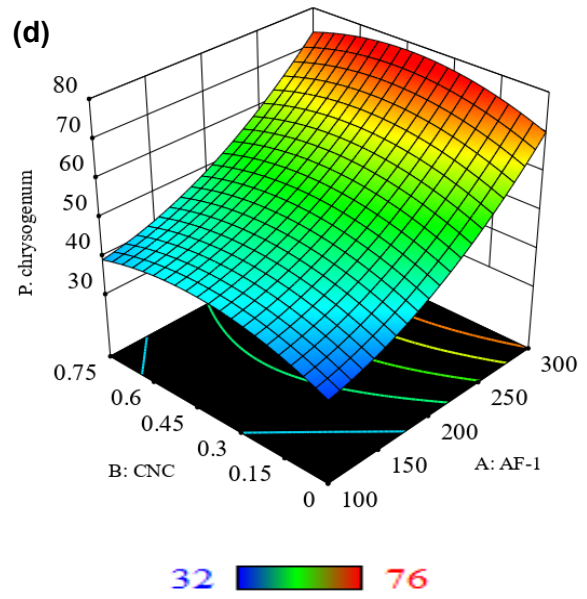
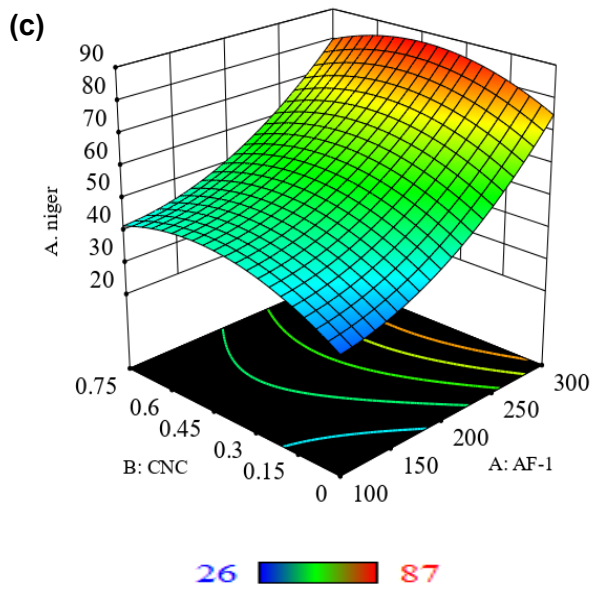
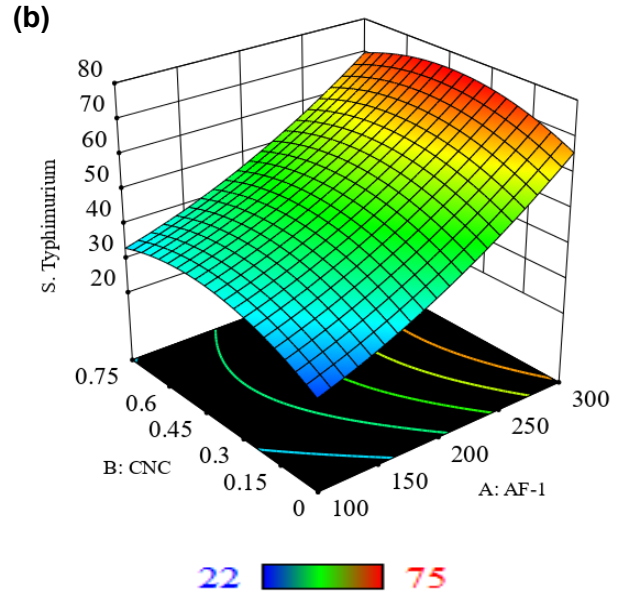
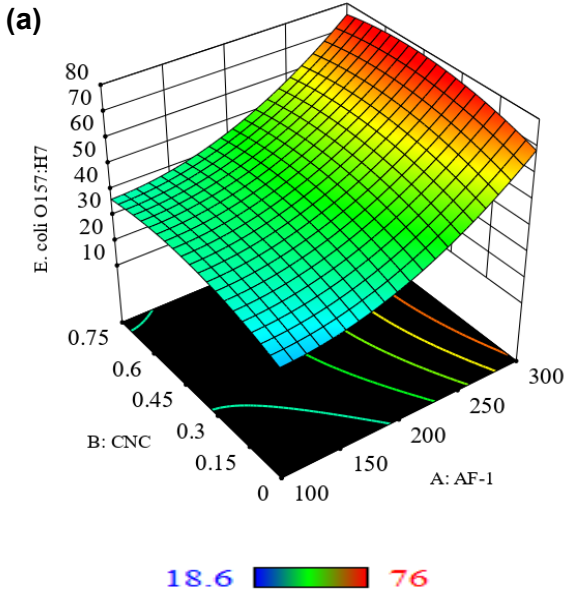
for spoilage fungi *A. niger*, *P. chrysogenum*, and *M. circinelloides* having F-values of 21.36 ($P < 0.0001$; df: 9; Lack of fit: 1.40; Lack of fit P-value: 0.36), 49.89 ($P < 0.0001$; df: 9; Lack of fit: 2.47; Lack of fit P-value: 0.17), and 29.98 ($P < 0.0001$; df: 9; Lack of fit: 0.11; Lack of fit P-value: 0.98) (Table 6.1). There was a good agreement between the experimental and predictive values with higher R^2 values (coefficient of determination) of the quadratic model for *A. niger*, *P. chrysogenum*, and *M. circinelloides* at 95, 98, and 96 %, respectively. The mixture of PBAT (2 g), CNC (0.375 %), AF-1 (300 μ L), and Gly (0.625 %) (film formulation blend number 4) showed the highest antibacterial and antifungal properties among twenty film formulation blend numbers (Figures 6.1a-e, Supplementary data Tables 6.1-6.2).

The interactions among independent variables and their effect on dependent variables were shown by using the ternary diagrams (3D images) against two foodborne pathogenic bacteria (*E. coli* O157:H7 and *S. Typhimurium*) and three spoilage fungi (*A. niger*, *P. chrysogenum*, and *M. circinelloides*). The region of red color in the 3D images indicated the higher microbicidal effectiveness (IC, %), while the blue and green to the yellow color zone indicated lower and medium microbicidal effectiveness. The PBAT-based film designed with 300 μ L of AF-1, 0.375 % of CNC, and 0.625 % of Gly showed a significantly higher ($P \leq 0.05$) inhibitory capacity against *E. coli* O157:H7, *S. Typhimurium*, *A. niger*, *P. chrysogenum*, and *M. circinelloides*, and their IC values were 76, 75, 87, 76, and 74 %, respectively. It has been found that the higher the concentration of AF-1, the higher the inhibitory capacity (Supplementary data Table 6.2). However, the addition of CNC and Gly had a significant effect on microbicidal effectiveness. The PBAT films having 300 μ L AF-1, 0 % CNC, and 0.25 % Gly (film formulation blend 8) reduced significantly the antibacterial and antifungal effects of PBAT films compared to film formulation blend number 4 while the IC values were 62, 63, 69, 66, and 63 % for *E. coli* O157:H7, *S. Typhimurium*, *A. niger*, *P. chrysogenum*, and *M. circinelloides* ($P \leq 0.05$). According to the data in Table 6.1, Supplementary data Table 6.2, and Figure 6.1 a-e (3D images), the central composite design optimized (based on the highest microbicidal effectiveness) that the mixture of PBAT, AF-1, CNC, and Gly at the corresponded amount of 2 g, 300 μ L, 0.375 %, and 0.625 % expressed the highest IC (%) against all tested bacteria and fungi.

Table 6.1. ANOVA results for the PBAT film formulated with active formulation 1 (AF-1).

Bacteria/fungi	Model	F-Value	Model P-value	Lack of fit	Lack of fit P-value	df	R²	Predicted equation
<i>E. coli</i> O157:H7	Quadratic	48.85	≤ 0.0001	0.7735	0.6075	9	0.9735	+ 48.66 + 19.56A + 3.54B + 1.29C - 0.1250AB - 1.72AC - 1.20BC + 9.39A ² - 5.31B ² - 6.96C ²
<i>S. Typhimurium</i>	Quadratic	56.94	≤ 0.0001	0.7574	0.6160	9	0.9809	+ 51.64 + 19.3A + 2.97B + 1.6C - 1.0AB - 0.75AC + 1.75BC + 4.13A ² - 7.22B ² - 3.37C ²
<i>A. niger</i>	Quadratic	21.36	≤ 0.0001	1.40	0.3598	9	0.9505	+ 57.39 + 20.54A + 3.83B + 1.9C - 1.38AB - 0.375AC - 0.375BC + 8.56A ² - 8.89B ² - 5.24C ²
<i>P. chrysogenum</i>	Quadratic	49.89	≤ 0.0001	2.47	0.1722	9	0.9782	+ 54.09 + 17.54A + 2.09B + 1.03C - 0.375AB + 0.625AC + 0.375BC + 6.06A ² - 5.79B ² - 3.09C ²
<i>M. circinelloides</i>	Quadratic	29.98	≤ 0.0001	0.1134	0.9839	9	0.9643	+ 48.28 + 18.6A + 2.40B + 1.67C - 0.25AB + 0.5AC + 0.0BC + 7.51A ² - 3.39B ² - 3.84C ²

P ≤ 0.05: significant; P > 0.05: not significant.



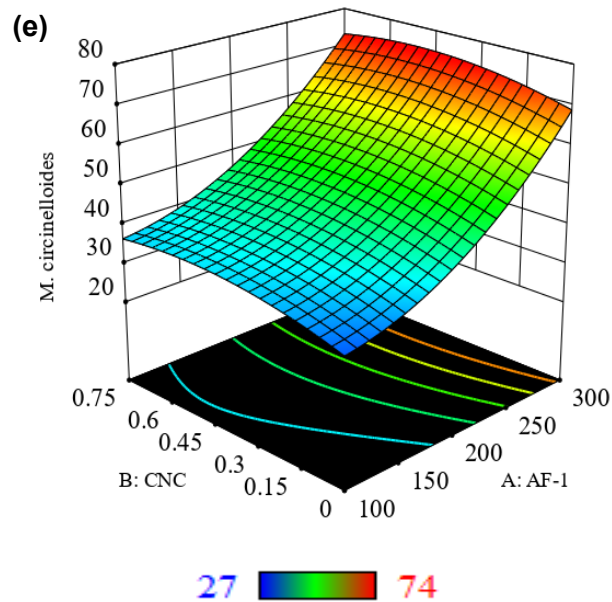


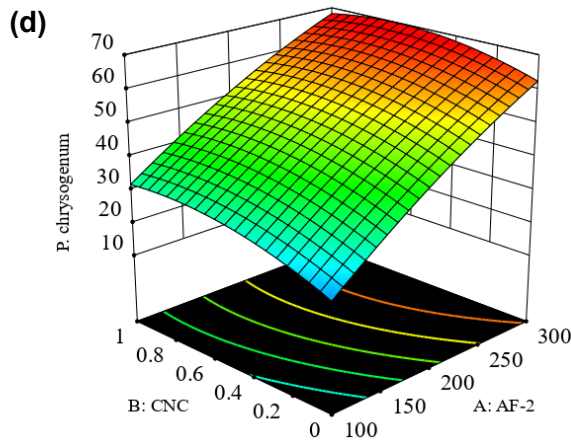
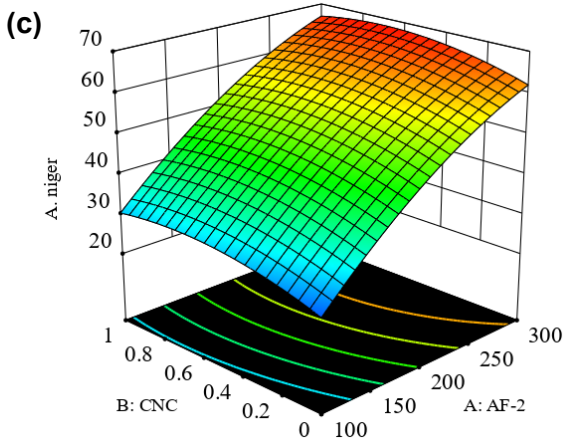
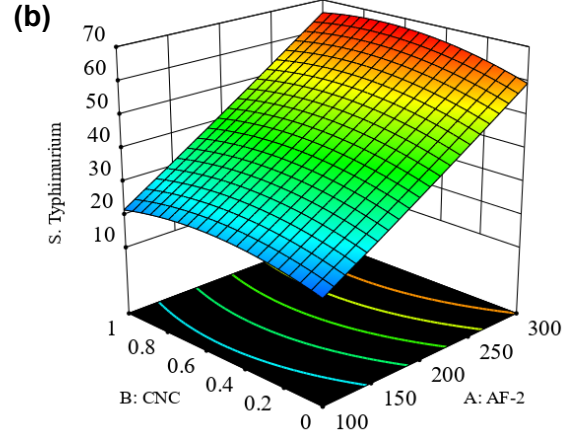
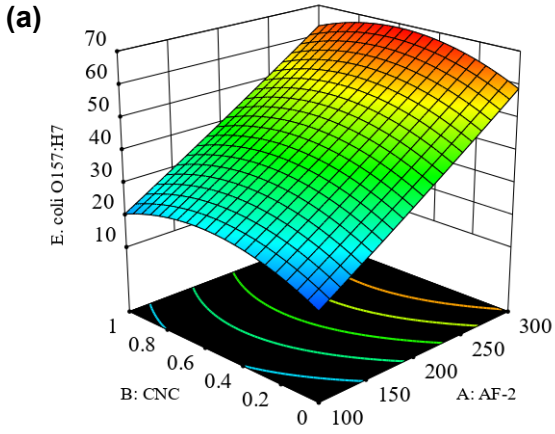
Figure 6.1. A numerical optimization was plotted for all dependent and independent values which showed the optimum points for PBAT film formulated with active formulation 1 (AF-1).

Table 6.2 showed the ANOVA results of the PBAT films formulated with active formulation 2 (AF-2) (100 to 300 μL), CNC (0 to 1 %), and Gly (0.25 to 1 %) to evaluate the effect on dependent variables in terms of the antibacterial and the antifungal properties (Table 6.2, Figure 6.2a-e, Supplementary data Tables 6.3-6.4). Like the previous result, the quadratic models were significant for both pathogenic bacteria (*E. coli* O157:H7 and *S. Typhimurium*) and spoilage fungi (*A. niger*, *P. chrysogenum*, and *M. circinelloides*). The quadratic model was statistically significant ($P \leq 0.05$) for the tested bacteria as the model showed a F-value for *E. coli* O157:H7 of 177.09 ($P < 0.0001$; df: 9; Lack of fit: 0.46) and for *S. Typhimurium* was 226.76 ($P < 0.0001$; df: 9; Lack of fit: 3.07). The LOF > 0.05 values for *E. coli* O157:H7 and *S. Typhimurium* meant that the LOF values did not occur because of error as well as there was a 79 to 12 % chance to get large LOF F-values due to noise. Moreover, the higher coefficient of determination values (R^2 values) of 99 % implied that the quadratic model for *E. coli* O157:H7 and *S. Typhimurium* had a good agreement between the experimental and the predicted values (Table 6.2).

Table 6.2. ANOVA results for the PBAT film formulated with active formulation 2 (AF-2).

Bacteria/fungi	Model	F-Value	Model P-value	Lack of fit	Lack of fit P-value	df	R ²	Predicted equation
<i>E. coli</i> O157:H7	Quadratic	177.09	≤ 0.0001	0.4599	0.7930	9	0.9938	+ 46.51 + 21.5A + 2.3B + 0.7C - 0.125AB + 1.88AC + 0.125BC + 0.5364A ² - 7.46B ² - 3.46C ²
<i>S. Typhimurium</i>	Quadratic	226.76	≤ 0.0001	3.07	0.1217	9	0.9951	+ 45.36 + 21A + 2.1B - 0.2C + 1.13AB - 0.625AC + 1.385BC + 0.4A ² - 4.1B ² - 4.6C ²
<i>A. niger</i>	Quadratic	33.05	≤ 0.0001	2.17	0.2076	9	0.9675	+ 53.77 + 18.3A + 2.5B + 1C - 0.125AB + 0.375AC + 1.135BC - 4.34A ² - 3.34B ² - 5.84C ²
<i>P. chrysogenum</i>	Quadratic	67.22	≤ 0.0001	6.49	0.0305	9	0.9837	+ 52.6 + 19.4A + 4.1B - 0.4C - 1.25AB + 0.0AC - 1.0BC - 2.61A ² - 4.11B ² - 6.61C ²
<i>M. circinelloides</i>	Quadratic	54.97	≤ 0.0001	1.21	0.4206	9	0.9802	+ 44.16 + 17.1A + 3.1B + 0.6C - 0.875AB - 1.38AC - 0.375BC + 1.59A ² - 3.41B ² - 3.91C ²

P ≤ 0.05: significant; P > 0.05: not significant.



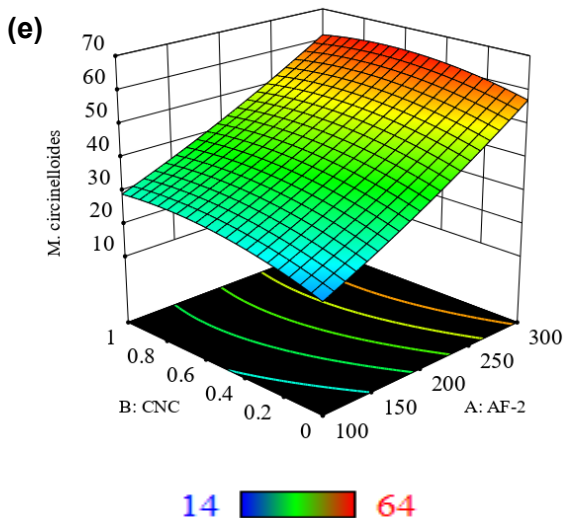


Figure 6.2. A numerical optimization was plotted for all dependent and independent values which showed the optimum points for PBAT film formulated with active formulation 2 (AF-2).

The AF-2, CNC, and Gly loaded PBAT polymeric matrix for preparing the strongest fungicidal films are shown in Table 6.2, Figure 6.2c-e, Supplementary data Tables 6.3-6.4. ANOVA analyses showed the quadratic model was significant for all tested fungi (*A. niger*, *P. chrysogenum*, and *M. circinelloides*) and their corresponding F-values were 33.05 ($P < 0.0001$; df: 9; Lack of fit: 2.17; Lack of fit P-value: 0.21), 67.22 ($P < 0.0001$; df: 9; Lack of fit: 6.49; Lack of fit P-value: 0.03), and 54.97 ($P < 0.0001$; df: 9; Lack of fit: 1.21; Lack of fit P-value: 0.42) (Table 6.2). Furthermore, there was a good agreement between the experimental and predictive values which were supported by higher R^2 values (coefficient of determination) of the quadratic model for *A. niger*, *P. chrysogenum*, and *M. circinelloides* 97, 98, and 98 %, respectively.

The mixture of PBAT (2 g), CNC (0.5 %), AF-2 (300 μL), and Gly (0.625 %) (film formulation blend number 8) exhibited the highest antibacterial and antifungal properties among twenty film formulation blend numbers (Figure 6.2a-e, Supplementary data Tables 6.3-6.4). Moreover, the interactions among independent variables and their effect on dependent variables were depicted through 3D images against all tested pathogenic bacteria and spoilage fungi whereas the red-green-yellow-blue color zone indicated the higher-higher medium-medium-lower microbicidal effectiveness. The PBAT-based film designed with 300 μL of AF-2, 0.5 % of CNC, and 0.625 % of Gly showed a significantly higher ($P \leq 0.05$) inhibitory capacity against *E. coli* O157:H7, *S. Typhimurium*, *A. niger*, *P. chrysogenum*, and *M. circinelloides*, and their IC values were 69, 67, 69, 68, and 64 %, respectively. It has been found that the higher the concentration of AF-2, the higher the inhibitory capacity (Supplementary data Table 6.4). However, the addition of CNC and

Gly had a significant effect on microbicidal effectiveness. The PBAT films having 300 μ L AF-2, 0 % CNC, and 1 % Gly (film formulation blend 3) significantly reduced the antibacterial and antifungal effects of PBAT films as compared to film formulation blend number 8 while the IC values were 58, 52, 58, 56, and 52 % for *E. coli* O157:H7, *S. Typhimurium*, *A. niger*, *P. chrysogenum*, and *M. circinelloides* ($P \leq 0.05$). According to the data in Table 6.2, Supplementary data Table 6.4, and Figure 6.2a-e (3D images), the central composite design optimized (based on the highest microbicidal effectiveness) that the mixture of PBAT, AF-2, CNC, and Glycerol at the corresponded amount of 2 g, 300 μ L, 0.5 %, and 0.625 % expressed the highest IC (%) against all tested bacteria and fungi.

The bioactive PBAT-based nanocomposite film optimized with 300 μ L AF-1, 0.375 % CNC, and 0.625 % Glycerol showed the highest bactericidal and fungicidal properties (IC \geq 74 %) over the bioactive PBAT-based nanocomposite film optimized with 300 μ L AF-2, 0.5 % CNC and 0.625 % Glycerol (IC \leq 69 %) against all tested bacteria and fungi. The antibacterial and antifungal effects of the bioactive PBAT-based nanocomposite films are shown by mainly active formulations. Active formulation 1 (AF-1) was designed with a mixture of organic citrus extract (OCE), Mediterranean EO, citrus EO, and cinnamon EO, while the AF-2 was designed with natural citrus extract (NCE), Asian formulation, Southern formulation, cinnamon EO, and savory thyme EO by [Begum et al. \(2022b\)](#). The authors found that the direct application of the vapor of AF-1 had strong microbicidal and fungicidal effectiveness over the vapor of AF-2 for inhibiting the growth of *E. coli* O157:H7, *S. Typhimurium*, *A. niger*, *P. chrysogenum*, and *M. circinelloides* in the rice samples. A similar phenomenon has been observed in the current study when PBAT polymeric matrix loaded with AF-1 showed higher bioactivities than PBAT film with AF-2 against all tested bacteria and fungi. The major chemical components are cinnamaldehyde, carvacrol and thymol, limonene, and polyphenols in cinnamon EO, Mediterranean EO, citrus EO, and OCE, respectively, which had strong bactericidal and fungicidal properties ([Dzamic et al., 2008](#); [Begum et al., 2022b](#)). When the vapor of AF-1 was released from the PBAT+AF-1+CNC+Gly film and exposed to the bacterial and fungal growth, it might interact with the inner and outer membrane proteins, intracellular targets, affect the energy-generating process, disrupt the lipopolysaccharides and outer membrane, thus leading to the cell death ([Hyldgaard et al., 2012b](#); [Mith et al., 2014](#)). However, PBAT-based capsule loaded with linalool showed strong effectiveness against *E. coli* in agar disc diffusion assay ([Felix da Silva Barbosa et al., 2021](#)). [Srisa and Harnkarnsujarit \(2020\)](#) developed antifungal films based on PBAT/PLA blends containing trans-cinnamaldehyde as antifungal agents using cast-extrusion. The authors tested their bioactive PBAT/PLA-trans cinnamaldehyde films against *Penicillium* sp., *A. niger*, and *Rizophus* sp. using the disc diffusion method and vapor phase

method, and the study found that the release of trans-cinnamaldehyde has fungicidal effect against tested fungi (Srisa and Harnkarnsujarit, 2020).

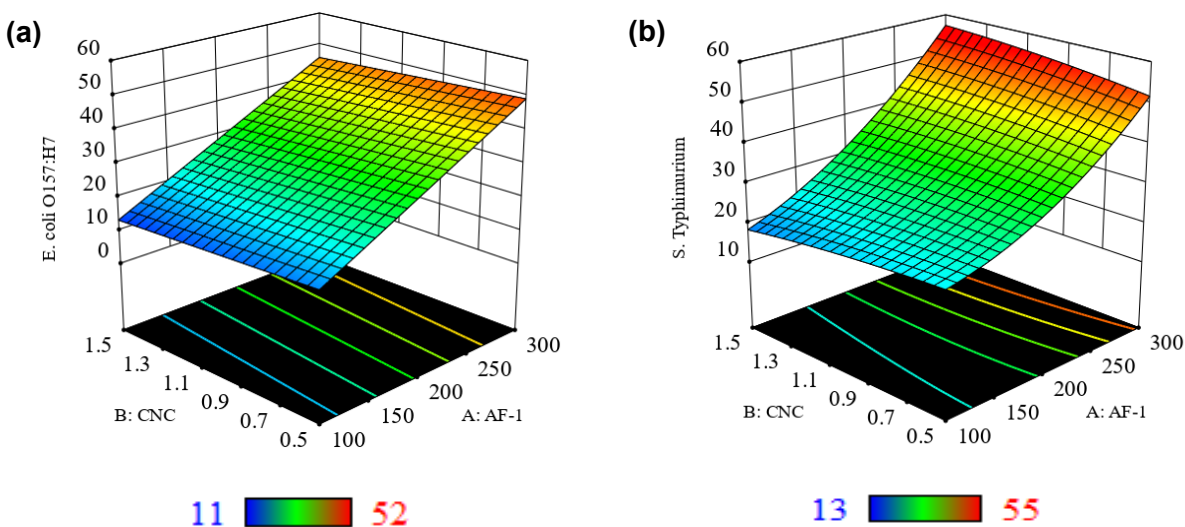
For the PLA-based film, the results are presented in Tables 6.3-6.4, Figure 6.3a-e, Figure 6.4a-e, and Supplementary data Tables 6.5-6.8. In the case of PLA films, a linear and quadratic model was significant for tested pathogenic bacteria and fungi (Table 6.3 and Table 6.4). The AF-1 (100-300 μ L), CNC (1-1.5 %), and Gly (0.5-1.5 %) were incorporated into PLA polymeric matrix to develop bioactive PLA-based nanocomposite films for controlling bacteria and spoilage fungi (Table 6.3, Figure 6.3a-e, Supplementary data Tables 6.5-6.6). All film-forming ingredients (independent variables) showed strong interaction with the responses. Linear and quadratic models were significant for the pathogenic bacteria *E. coli* O157:H7 and *S. Typhimurium*, respectively. The linear model was statistically significant ($P \leq 0.05$) for the tested bacteria as the model showed the F-values for *E. coli* O157:H7 and *S. Typhimurium* were 97.66 ($P < 0.0001$; df: 3; Lack of fit: 5.10; R^2 : 95 %) and 30.82 ($P < 0.0001$; df: 9; Lack of fit: 7.02; R^2 : 96 %), respectively. The higher coefficient of determination values (R^2) for *E. coli* O157:H7 and *S. Typhimurium* stated that the corresponding linear and quadratic models had a good agreement between the experimental and the predicted values (Table 6.3). Moreover, a linear model was significant for spoilage fungi *A. niger*, *P. chrysogenum*, and *M. circinelloides* having F-values of 53.30 ($P < 0.0001$; df: 3; Lack of fit: 0.62; R^2 : 91 %), 42.38 ($P < 0.0001$; df: 3; Lack of fit: 0.60; R^2 : 89 %), and 64.42 ($P < 0.0001$; df: 3; Lack of fit: 0.67; R^2 : 92 %) (Table 6.3).

Table 6.3. ANOVA results for the PLA film formulated with active formulation 1 (AF-1).

Bacteria/fungi	Model	F-Value	Model P-value	Lack of fit	Lack of fit P-value	df	R²	Predicted equation
<i>E. coli</i> O157:H7	Linear	97.66	≤ 0.0001	5.10	0.0424	3	0.9482	+ 31.15 + 16.3A - 1.62B - 0.55C
<i>S. Typhimurium</i>	Quadratic	30.82	≤ 0.0001	7.02	0.0259	9	0.9652	+ 33.59 + 16.8A + 0.1B - 0.7C + 2.62AB - 0.125AC - 0.125BC + 4.77A ² - 0.7273B ² - 5.73C ²
<i>A. niger</i>	Linear	53.30	≤ 0.0001	0.6214	0.7630	3	0.9090	+ 38.14 + 18.71A + 1.28B - 1.39C
<i>P. chrysogenum</i>	Linear	42.38	≤ 0.0001	0.6039	0.7745	3	0.8882	+ 36.45 + 17.08A - 1.47B - 0.09C
<i>M. circinelloides</i>	Linear	64.42	≤ 0.0001	0.6694	0.7315	3	0.9235	+ 34.11 + 17.14A - 0.85B - 0.45C

P ≤ 0.05: significant; P > 0.05: not significant.

The mixture of PLA (2 g), CNC (1 %), AF-1 (300 μ L), and Gly (1 %) (film formulation blend number 7) showed the highest antibacterial and antifungal properties among twenty film formulation blend numbers (Figure 6.3a-e, Supplementary data Tables 6.5-6.6). The interactions among independent variables and their effect on dependent variables were shown by using the ternary diagrams (3D images) against two foodborne pathogenic bacteria (*E. coli* O157:H7 and *S. Typhimurium*) and three spoilage fungi (*A. niger*, *P. chrysogenum*, and *M. circinelloides*). The region of red color in the 3D images indicated the higher microbicidal effectiveness (IC, %), while the blue and green to the yellow color zone indicated lower and medium microbicidal effectiveness. The PLA-based film designed with 300 μ L AF-1, 1 % CNC, and 1 % Gly showed a significantly higher ($P \leq 0.05$) inhibitory capacity against *E. coli* O157:H7, *S. Typhimurium*, *A. niger*, *P. chrysogenum*, and *M. circinelloides*, and their IC values were 49.6, 52, 59, 54.6, and 54 %, respectively. It has been found that the higher the concentration of AF-1, the higher the inhibitory capacity (Supplementary data Table 6.6). However, the PLA films having 300 μ L AF-1, 1.5 % CNC, and 1.5 % Gly (film formulation blend 16) were reducing the antibacterial and antifungal effects of PLA films compared to film formulation blend number 7 while the IC values were 42, 50, 53, 48, and 52 % for *E. coli* O157:H7, *S. Typhimurium*, *A. niger*, *P. chrysogenum*, and *M. circinelloides*, respectively. According to the data in Table 6.3, Supplementary data Table 6.6, and Figure 6.3a-e (3D images), the central composite design optimized (based on the highest microbicidal effectiveness) that the mixture of PLA, AF-1, CNC, and Gly at the corresponding amount of 2 g, 300 μ L, 1 %, and 1 % expressed the highest IC (%) against all tested bacteria and fungi.



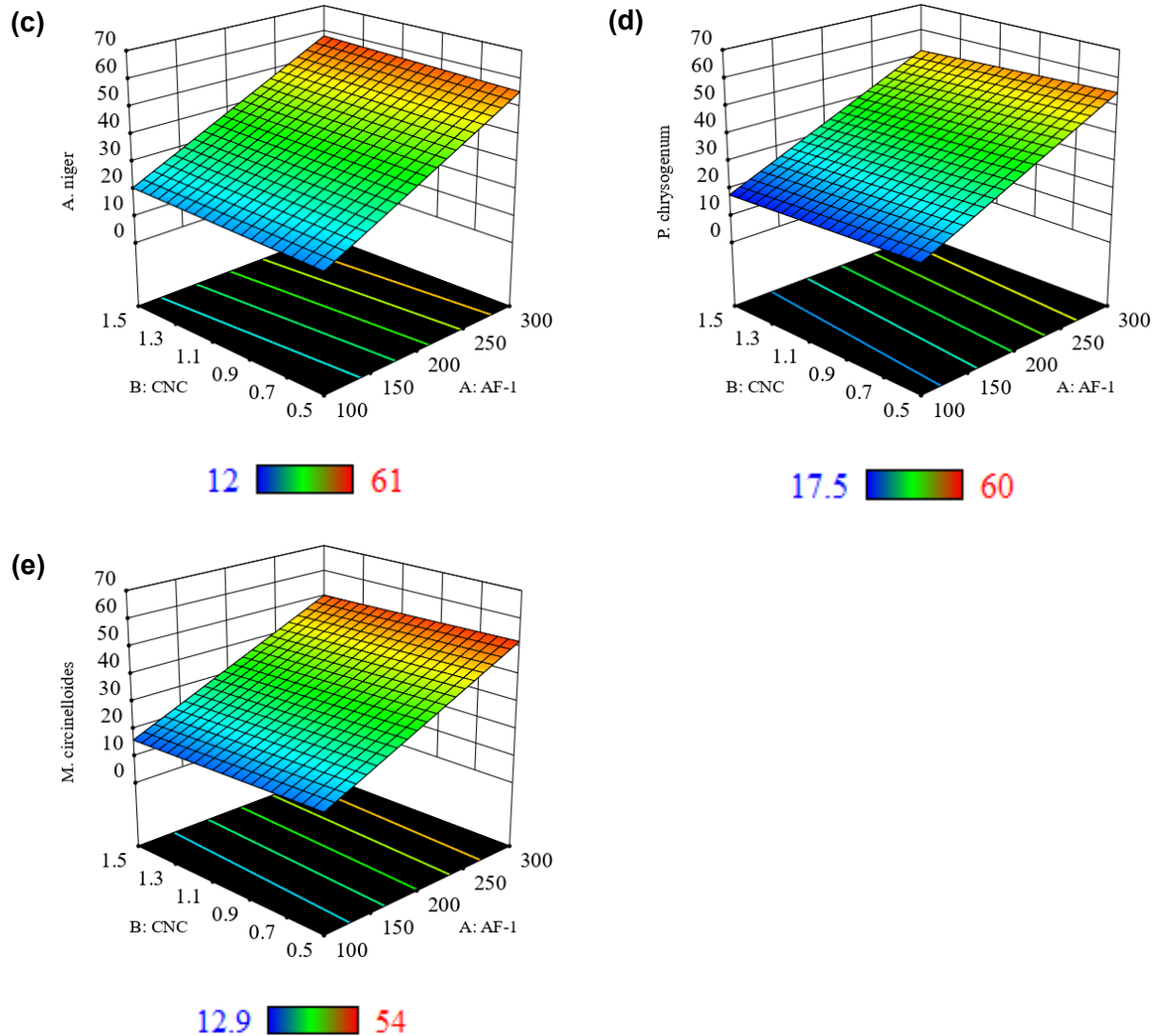


Figure 6.3. A numerical optimization was plotted for all dependent and independent values which showed the optimum points for PLA film formulated with active formulation 1 (AF-1).

For the PLA-based film containing active formulation 2 (AF-2) (100-300 μL), CNC (0.5-1 %), and Gly (0.25-1 %), the results are presented in Table 6.4, Figure 6.4a-e, Supplementary data Tables 6.7-6.8. The quadratic and linear models were significant for tested pathogenic bacteria *E. coli* O157:H7 and *S. Typhimurium*, respectively. The statistically significant models ($P \leq 0.05$) for the tested bacteria showed the F-values for *E. coli* O157:H7 and *S. Typhimurium* were 128.79 ($P < 0.0001$; df: 9; Lack of fit: 1.09; R^2 : 99 %) and 43.23 ($P < 0.0001$; df: 3; Lack of fit: 0.79; R^2 : 91 %), respectively. A linear model was significant for spoilage fungi *A. niger*, *P. chrysogenum*, and *M. circinelloides* having the respected F-values were 143.35 ($P < 0.0001$; df: 3; Lack of fit: 0.79; R^2 : 97 %), 62.17 ($P < 0.0001$; df: 3; Lack of fit: 1.80; R^2 : 93 %), and 100.7 ($P < 0.0001$; df: 3; Lack of

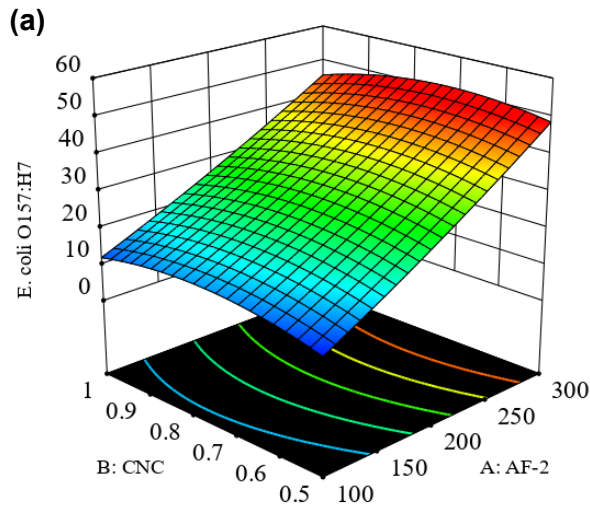
fit: 4.91; R^2 : 96 %) (Table 6.4). The higher R^2 values (≥ 91 %) for all tested bacteria and fungi proved a good agreement between the experimental and predictive values of the designed models (Table 6.4).

The mixture of 2 g PLA, 0.5 % CNC, 300 μ L AF-2, and 1 % Gly (film formulation blend number 4) showed the highest antibacterial and antifungal properties among seventeen film formulation blend numbers (Figure 6.4a-e, Supplementary data Table 6.7-6.8). The ternary diagrams were used to visualize the interactions among independent and dependent variables (*E. coli* O157:H7, *S. Typhimurium*, *A. niger*, *P. chrysogenum*, and *M. circinelloides*) through different color sheds. In the ternary diagram, the red color indicated the higher microbicidal effectiveness (IC, %), followed by green to yellow, and the blue color indicated medium and lower microbicidal effectiveness. The PLA-based film designed with 300 μ L AF-2, 0.5 % CNC, and 1 % Gly showed a significantly higher ($P \leq 0.05$) inhibitory capacity against *E. coli* O157:H7, *S. Typhimurium*, *A. niger*, *P. chrysogenum*, and *M. circinelloides*, and their IC values were 48, 45, 59, 58, and 57 %, respectively. It has been found that the higher the concentration of AF-2, the higher the inhibitory capacity (Supplementary data Table 6.8). However, the PLA films having 300 μ L AF-2, 1 % CNC, and 0.25 % Gly (film formulation blend 10) reduced the antibacterial and antifungal effects of PLA films compared to film formulation blend number 4 while the IC values were 41, 42, 51, 47, and 49 % for *E. coli* O157:H7, *S. Typhimurium*, *A. niger*, *P. chrysogenum*, and *M. circinelloides*. According to the data in Table 6.4, Supplementary data Table 6.8, and Figure 6.4a-e (3D images), the central composite design predicted (based on the highest microbicidal effectiveness) that the mixture of PLA, AF-2, CNC, and Gly at the corresponded amount of 2 g, 300 μ L, 0.5 %, and 1 % expressed the highest IC (%) against all tested bacteria and fungi.

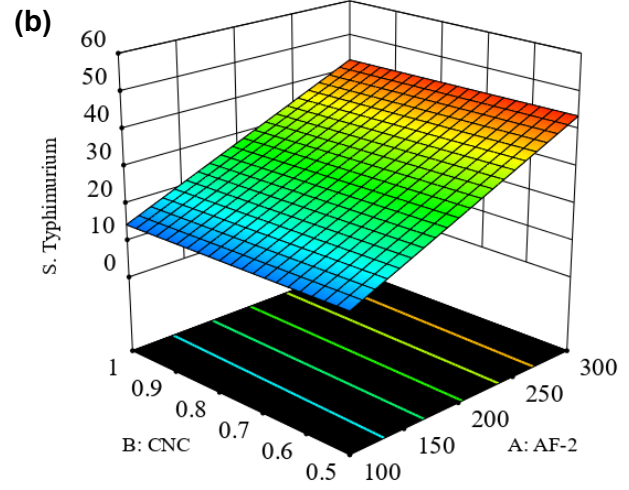
Table 6.4. ANOVA results for the PLA film formulated with active formulation 2 (AF-2).

Bacteria/fungi	Model	F-Value	Model P-value	Lack of fit	Lack of fit P-value	df	R ²	Predicted equation
<i>E. coli</i> O157:H7	Quadratic	128.79	≤0.0001	1.09	0.5430	9	0.9940	+ 31.3 + 16.64A - 0.4B + 1.1C - 1.25AB + 1.5AC + 0.25BC + 1.18A ² - 4.02B ² - 0.5225C ²
<i>S. Typhimurium</i>	Linear	43.23	≤ 0.0001	0.7877	0.6809	3	0.9089	+ 28.53 + 14.2A - 0.4B + 0.6C
<i>A. niger</i>	Linear	143.35	≤ 0.0001	0.7873	0.6811	3	0.9707	+ 36.84 + 19.03A + 0.0B + 1.5C
<i>P. chrysogenum</i>	Linear	62.17	≤ 0.0001	1.80	0.4118	3	0.9348	+ 36.11 + 17.50A - 0.1B + 1.4C
<i>M. circinelloides</i>	Linear	100.7	≤ 0.0001	4.91	0.1813	3	0.9587	+ 33.93 + 18.49A + 0.68B + 2.51C

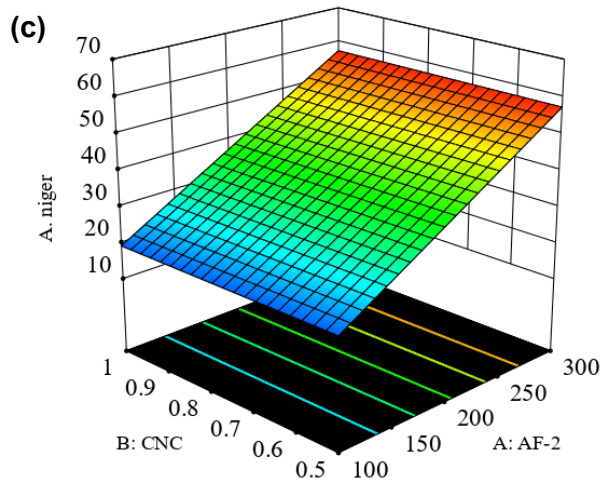
P ≤ 0.05: significant; P > 0.05: not significant.



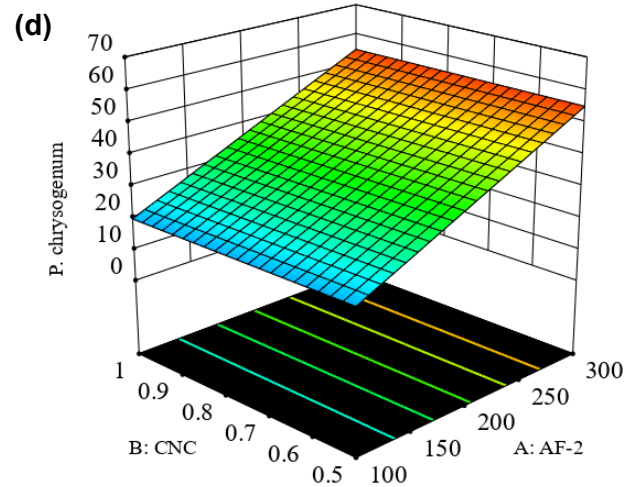
9 48.4



11 45



15 59



12 58

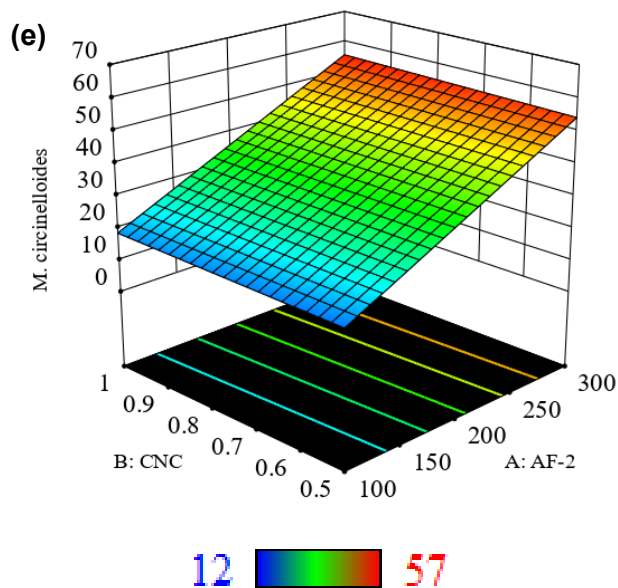


Figure 6.4. A numerical optimization was plotted for all dependent and independent values which showed the optimum points for PLA film formulated with active formulation 2 (AF-2).

The bioactive PLA-based films optimized with either AF-1 (300 μ L), 1 % CNC, and 1 % Gly or AF-2 (300 μ l), 0.5 % CNC, and 1 % Gly showed the similar antibacterial and antifungal properties (IC: 48-59 %) against all tested bacteria and fungi. [Subbuvel and Kavan \(2021\)](#) prepared bioactive PLA-based film using neem oil and curcumin oil. The authors found the strong bactericidal properties of the developed PLA/neem/curcumin oil-based film against *E. coli*, *Bacillus subtilis*, *Pseudomonas aeruginosa*, and *Staphylococcus aureus* ([Subbuvel and Kavan, 2021](#)). Moreover, PLA-CNC-based nanocomposite films containing oregano EO and nisin were shown strong bactericidal properties against *Listeria monocytogenes* ([Salmieri et al., 2014a, b](#)). In comparison between PBAT and PLA-based bioactive nanocomposite films in terms of bioactivities, the bioactive PBAT+AF-1+CNC+Gly nanocomposite film showed the strongest antibacterial and antifungal properties against all tested bacteria and fungi, followed by PBAT+AF-2+CNC+Gly film, and finally by either PLA+AF-1+CNC+Gly or by PLA+AF-2+CNC+Gly film in the *in vitro* agar volatilization assay tests. However, the polymeric nature and their structural features where the active formulations are dispersed, and film-forming methods could play an important role in the antimicrobial effectiveness of the bioactive nanocomposite films ([Hosseini et al., 2009](#)). Moreover, antibacterial and antifungal properties of the bioactive films depend also on the degree of migration of the active components from the bioactive films which are influenced by several factors such as the volatility and polarity of the active formulations, the chemical interactions between the polymeric chains and active formulations, as well as their hydrophobicity and hydrophilicity

(Suppakul *et al.*, 2003; Tawakkal *et al.*, 2016). The current approach to developing bioactive PBAT and PLA-based nanocomposite films using CNC, Gly, and active formulations (AF-1 and AF-2) by central composite design method could be an efficient and innovative way to develop active packaging for extending the shelf life of stored products.

6.3.2. Characterization of the bioactive nanocomposite films

After obtaining the best conditions for the bioactive PBAT and PLA nanocomposite films, all films required to characterize such as mechanical tests (tensile, modulus, and elongation at break), water vapor permeability (WVP) test, oxygen transmission rate (OTR), *in vitro* release kinetics of the active components for further application of the films in real foods. The films were divided into several groups Control-1: neat PBAT film, Group-1: PBAT+AF-1+CNC+Gly, Group-2: PBAT+AF-2+CNC+Gly, Control-2: neat PLA film, Group-3: PLA+AF-1+CNC+Gly, and Group-4: PLA+AF-2+CNC+Gly.

6.3.2.1. Mechanical properties

The mechanical properties (such as TM, TS and Eb) of the PBAT and PLA-based films were presented in Table 6.5. The TM values of the neat PBAT and PLA films were found as 77 MPa and 1253 MPa, respectively. The TM indicates the rigidity of the material. The higher the TM value, the higher the rigidity of the film. Incorporation of CNC+AF-1+Gly (Group-1) and CNC+AF-2+Gly (Group-2) into PBAT polymeric matrices significantly ($P \leq 0.05$) reduced the TM of the films when compared to Control-1. The TM values were 63 and 67 MPa for the PBAT+AF-1+CNC+Gly and PBAT+AF-2+CNC+Gly nanocomposite films, respectively, which implied that the TM values were reduced by 13-18 % compared to the Control-1 film. A similar phenomenon was observed in the case of TS values of the PBAT film. The TS value of the Control-1 was 24.43 MPa, while the TS values were 15.67 and 19 MPa for the PBAT+AF-1+CNC+Gly and PBAT+AF-2+CNC+Gly nanocomposite films, respectively. On the other hand, an opposite tendency was observed in the case of the films' Eb values after incorporation of CNC+AF-1+Gly and CNC+AF-2+Gly into PBAT polymeric matrices, the Eb (significantly increased the flexibility of the nanocomposite films) of the films were increased compared to Control-1 film. The Eb values were 627, 652.3, and 641.3 % for the Control-1, Group-1, and Group-2 films, respectively (Table 6.5). The TS, TM, and Eb values of pure PBAT film were 22 MPa, 90.4 MPa, and 817.8 % found by Li *et al.* (2015a) which supported the results obtained in the current study. Moreover, the incorporation of active formulations+CNC+Gly into the PBAT polymeric matrices acted as a plasticizer and reduced the

intermolecular forces between polymeric chains, thus improving the flexibility and extensibility, and lessening the rigidity compared to the neat PBAT film.

The TS of the neat PLA film (Control-2) was found to be 66.7 MPa, which was reduced significantly ($P \leq 0.05$) by 33 to 43 % after incorporation of AF-1+CNC+Gly and AF-2+CNC+Gly into the neat PLA matrices. This TS value is similar to that of the neat PLA film (TS: 62 MPa) found by [Wang et al. \(2016\)](#). The TS values were 44.7 and 37.7 MPa of the films in Group-3 (PLA/CNC/Gly/AF-1) and Group-4 (PLA+AF-2+CNC+Gly), respectively. Similarly, the TM values of the nanocomposite PLA films were also significantly ($P \leq 0.05$) reduced by 24 to 41 % after incorporation of AF-1+CNC+Gly and AF-2+CNC+Gly compared to Control-2. The TM values were 956.7 and 735 MPa for the films in Group-3 and Group-4, respectively, while the TM value in neat PLA film was 1253 MPa. After incorporation of AF-1+CNC+Gly and AF-2+CNC+Gly into PLA polymeric matrices, the Eb values increased significantly ($P \leq 0.05$) compared to the Control-2 film. The Eb values were 36.3, 58, and 82 % for the Control-2, Group-3, and Group-4 nanocomposite films, respectively (Table 6.5). The Eb values indicate the flexibility of the films which was significantly raised in both bioactive PLA and PBAT nanocomposite films than in the control films. The plasticizer effect of CNC+active formulations could weaken the intermolecular interactions of the polymeric chains, thus, raising the mobility of the polymeric motion with less rigidity as well as higher flexibility and extensibility of the nanocomposite PLA and PBAT films ([Rhim et al., 2006](#); [Cardoso et al., 2017](#)). A similar trend has been observed by [Sharma et al. \(2020\)](#) where the authors prepared the bioactive PLA/PBAT composite polymeric film by incorporating clove oils (1-10 %). They found that the TS and Eb values of the PLA/PBAT composite films were 1.35 MPa and 5.63 %, respectively. However, after the incorporation of clove oil into the PLA/PBAT polymeric matrices, the clove acted as a plasticizer, and thus, the flexibility of the composite films was raised significantly (Eb: from 26 to 40 %) and reduced the TS values (TS: from 0.79 to 0.94 MPa) ([Sharma et al., 2020](#)).

6.3.2.2. Water vapor permeability (WVP)

The effect of CNC+Gly+active formulation (either AF-1 or AF-2) on WVP of the PLA and PBAT films was measured, and the results are presented in Table 6.5. WVP of the film is an important test used in food packaging because water is one of the important parameters responsible for food deterioration and allows microbial growth in stored foods. However, several factors such as vapor diffusion, adsorption, desorption, and polymeric affinity to water affect the WVP of the films ([Srisa and Harnkarnsujarit, 2020](#)). Table 6.5 shows the WVP of the neat PBAT (Control-1) and PLA film

(Control-2) and bioactive PLA and PBAT-based nanocomposite films. The WVP of the Control-1 and Control-2 was found at 2.35 and 3.45 g.m.mm².day⁻¹.kPa⁻¹, respectively, and the values well agreed with the previous studies by [Morelli *et al.* \(2016\)](#) and [Wang *et al.* \(2016\)](#). After incorporation of AF-1+CNC+Gly and AF-2+CNC+Gly into PBAT matrices, the WVP was significantly reduced by 21 % (WVP: 1.86 g.m.mm².day⁻¹.kPa⁻¹) and 19 % (WVP: 1.91 g.m.mm².day⁻¹.kPa⁻¹), respectively, as compared to the Control-1 film ($P \leq 0.05$). The presence of CNC throughout the bioactive PBAT nanocomposite film could create a tortuous path which decreased the diffusion process and hence, slowed the WVP of the bioactive PBAT nanocomposite films ([Khan *et al.*, 2012](#); [Khan *et al.*, 2013](#)). Moreover, the presence of hydrophobic essential oils in active formulations might also effectively prevent the diffusion of vapor from the bioactive PBAT nanocomposite and result in improved WVP of the films ([Srisa and Harnkarnsujarit, 2020](#)).

On the other hand, an opposite phenomenon was observed in the case of PLA films when incorporated with AF-1+CNC+Gly and AF-2+CNC+Gly. The WVP values of the PLA films were increased when AF-1+CNC+Gly (WVP: 3.95 g.m.mm².day⁻¹.kPa⁻¹) and AF-2+CNC+Gly (WVP: 3.58 g.m.mm².day⁻¹.kPa⁻¹) were compared to Control-2 (WVP: 3.45 g.m.mm².day⁻¹.kPa⁻¹). Similar observations have been obtained by several authors ([Salmieri *et al.*, 2014a](#); [Hossain *et al.*, 2018](#); [Shankar and Rhim, 2018](#); [Hossain *et al.*, 2019a](#)). [Salmieri *et al.* \(2014a\)](#) developed bioactive PLA-CNC-nisin nanocomposite films for meat preservation and the authors found that the WVP values of bioactive PLA-CNC-nisin films (WVP: 3.8 g.m.mm².day⁻¹.kPa⁻¹) were comparatively higher than the PLA-CNC film (control film) (WVP: 3.2 g.m.mm².day⁻¹.kPa⁻¹) at day 0 (17 % increment). The increment of WVP values of the PLA films after incorporation of either AF-1+CNC+Gly or AF-2+CNC+Gly might be owed to the presence of micro voids in the polymeric matrices, diffusion of the active formulations which affected tortuosity and nanocomposite's internal structure ([Salmieri *et al.*, 2014b](#); [Morelli *et al.*, 2016](#)). Moreover, the presence of Gly in bioactive PLA-nanocomposite films could increase the molecular mobility of the solids as a plasticizer which could lead to higher diffusion rate of the water vapor and thus, increased the WVP values of the bioactive PLA nanocomposite films ([Srisa and Harnkarnsujarit, 2020](#)).

6.3.2.3. Oxygen transmission rate (OTR)

The oxygen transmission rate (OTR) test of the bioactive film is very important because food's quality and shelf life are greatly affected by the OTR value which indicates the oxygen gas transmission through the films at different time intervals under oxygen partial pressure, relative humidity and temperature ([Sharmin *et al.*, 2012](#)). The OTR of each film was characterized and

summarized in Table 6.5. The OTR values of the Control-1 and Control-2 were of 192 and 182 $\text{cm}^3.\text{m}^{-2}.\text{day}^{-1}$ ($P > 0.05$), respectively. After incorporation of AF-1+CNC+Gly and AF-2+CNC+Gly into the PBAT polymeric matrix, the OTR values were significantly reduced at 153 and 169 $\text{cm}^3.\text{m}^{-2}.\text{day}^{-1}$, respectively ($P \leq 0.05$). A tortuous path might be created in the presence of CNC into the PBAT polymeric matrix which created a longer diffusion path for oxygen gas and increased the film's impermeability, reducing the OTR values of the nanocomposite films (Vilarinho *et al.*, 2018b; Vatansever *et al.*, 2020). Vatansever *et al.* (2020) developed the PBAT-based nanocomposite films loaded with CNC nanoparticles at different contents (1-5 %) and the authors found that the incorporation of 5 % CNC into the PBAT matrix significantly reduced the OTR of PBAT nanocomposite film by 41 % which is the similar phenomenon of the current study. Criado *et al.* (2020) found that after incorporation of CNC into an alginate matrix reduced the OTR values from 125 to 92 of the neat alginate and alginate-CNC films, respectively.

Table 6.5. Effect on CNC content in the mechanical properties (TS, TM, Eb), oxygen transmission rate (OTR) and water vapor permeability (WVP) of the bioactive composite films.

Films	Mechanical properties			WVP ($\text{g}.\text{m}.\text{mm}^{-2}.\text{day}^{-1}.\text{kPa}^{-1}$)	OTR ($\text{cm}^3.\text{m}^{-2}.\text{day}^{-1}$)
	TS (MPa)	TM(MPa)	Eb (%)		
Control-1: PBAT-film	24.4±2.9 ^b	76.8±5.8 ^b	627±11.3 ^d	2.35±0.59 ^a	192±9.6 ^c
Group-1: PBAT/AF-1/CNC/Gly	15.7±1.5 ^a	63.3±6.6 ^a	652.3±4.9 ^f	1.86±0.56 ^b	153±3.9 ^a
Group-2: PBAT/AF-2/CNC/Gly	19.0±3.6 ^a	67.3±2.5 ^a	641.3±3.0 ^e	1.91±0.52 ^a	169±4.1 ^b
Control-2: PLA-film	66.7±7.6 ^e	1253±45 ^e	36.3±5.1 ^a	3.45±0.50	182±12.3 ^c
Group-3: PLA/AF-1/CNC/Gly	44.7±10 ^d	956±8.5 ^d	58.0±5.6 ^b	3.95±0.74	187±6.7 ^c
Group-4: PLA/AF-2/CNC/Gly	37.7±6.7 ^c	735±21 ^c	82.0±6.6 ^c	3.58±0.27	199±4.8 ^d

Values means ± standard error. Within each column means with different lowercase letter are significantly different ($P \leq 0.05$).

The OTR values of Group-3 and Group-4 films increased from 182 $\text{cm}^3.\text{m}^{-2}.\text{day}^{-1}$ (control 2) to 187 $\text{cm}^3.\text{m}^{-2}.\text{day}^{-1}$ ($P > 0.05$) (Group-3) and 199 $\text{cm}^3.\text{m}^{-2}.\text{day}^{-1}$ ($P \leq 0.05$) (Group-4), respectively. The addition of AF-1+CNC+Gly into the PLA matrix acted as a plasticizer which increased the free volume of the polymeric matrix, and increased oxygen diffusivity, thus resulting in an increased OTR value when compared to Control-2 (Arrieta *et al.*, 2014; Subbuvel and Kavan, 2021). A similar

trend has been found by [Subbuvel and Kavan \(2021\)](#) and the authors reported that the OTR values were augmented from 179.45 to 203.4 $\text{cm}^3 \cdot \text{m}^{-2} \cdot \text{day}^{-1}$ after loading 10 % neem oil (NO) into PLA composite film due to the plasticization effect of NO. An augmentation in oxygen permeation (OTR values) of the bioactive PLA and PBAT/PLA-based composite films were observed after the incorporation of D-limonene and trans-cinnamaldehyde, respectively ([Arrieta et al., 2014](#); [Srisa and Harnkarnsujarit, 2020](#)). Moreover, the incorporation of active formulations+CNC+Gly into the PLA composite film that increased the OTR values of the bioactive PLA-based nanocomposite films might be due to the plasticizing effect, a reduction in the orientation and non-homogeneity of the polymeric network, and a creation of a micropore in the films which allowed oxygen to dissolve into the matrices and augmented oxygen transportation ([Srisa and Harnkarnsujarit, 2020](#)).

6.3.2.4. *In vitro* release profiles of the active components from the bioactive films

Controlled release behavior and release kinetics mechanism of the active formulations (AF-1 and AF-2) from bioactive PBAT and PLA films in ethanol was studied with optical absorbance measurement as a function of time (Figure 6.5a-b, Figure 6.6a-b, Table 6.6). Figure 6.5a shows the % cumulative release of AF-1 and AF-2 from the control films (Control-1: PBAT+AF-1 film; Control-2: PBAT+AF-2 film) and bioactive PBAT nanocomposite films (PBAT+AF-1+CNC+Gly and PBAT+AF-2+CNC+Gly) for 70 h of extraction time in ethanol. Control-1 and Control-2 showed significantly higher release of active formulations (%) than the PBAT nanocomposite films (Figure 6.5a). At the beginning of the extraction, the % release of AF-1 and AF-2 was 4.38, 5.74, 3.23, and 5.26 % at 0.5 h from the Control-1 (PBAT+AF-1), Control-2 (PBAT+AF-2), PBAT+AF-1+CNC+Gly and PBAT+AF-2+CNC+Gly, respectively. Afterward, the % release increased with extraction time and became stabilized after ~36 h and ~12 h of extraction for Controls and bioactive PBAT nanocomposite films. A 51 and 55 % release of the total retained active formulations (AF-1 or AF-2) occurred with the PBAT+AF-1 and PBAT+AF-2 films, respectively, at 70 h contact with ethanol. But the incorporation of the CNC+Gly into either PBAT+AF-1 or PBAT+AF-2 matrices was significant ($P \leq 0.05$) reducing the release by 50 % (% release: 25.45 %) and 44 % (% release: 30.83 %), respectively.

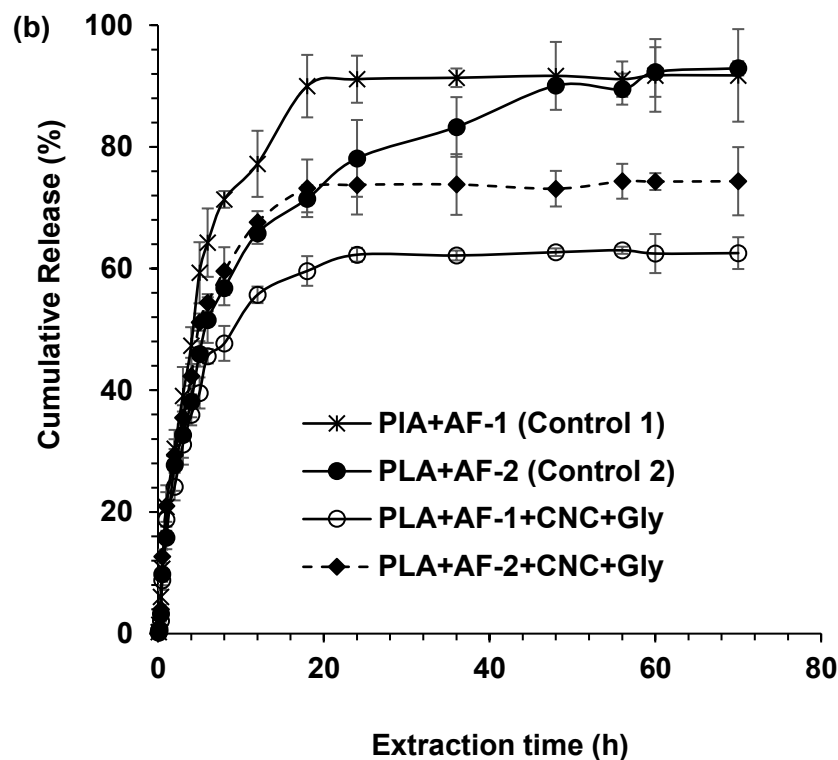
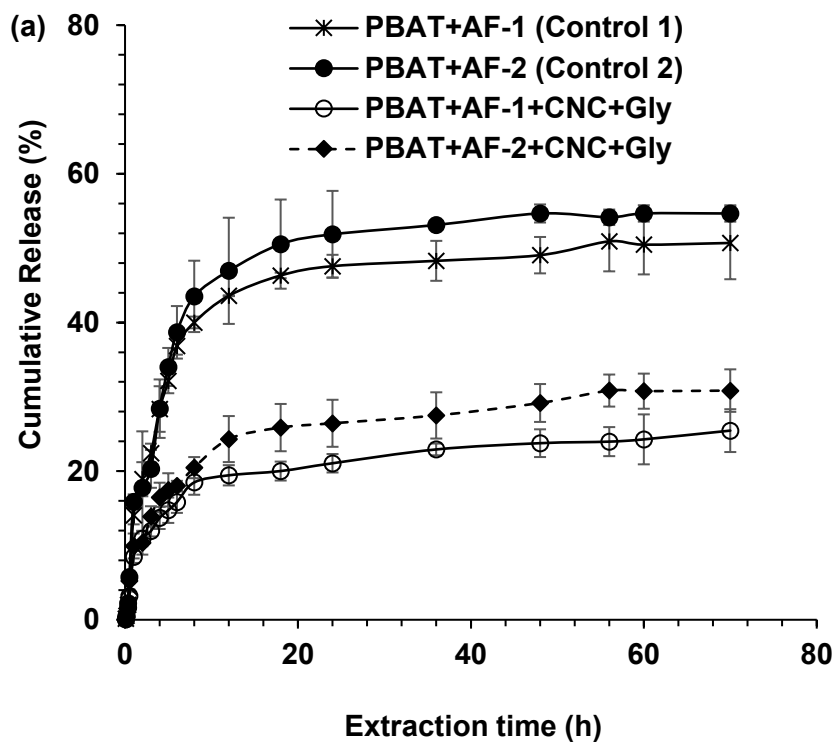


Figure 6.5. Cumulative release (%) of two active formulations in ethanol (food simulant) from (a) PBAT and (b) PLA polymeric matrices during extraction time.

The cumulative release measurement (%) of AF-1 and AF-2 as a function of time from the control films (Control 3: PLA+AF-1 film; Control 4: PLA+AF-2 film) and bioactive PLA nanocomposite films (PLA+AF-1+CNC+Gly film and PLA+AF-2+CNC+Gly film) was tested and depicted in Figure 6.5b. At the beginning of the extraction in ethanol (at 0.33 h), the % release of the active formulations (both AF-1 and AF-2) was much less and the range was between 2.11 to 6.04 % for four different types of PLA films. The % release of active formulations increased with time and the release from the Control-3, Control-4, PLA+AF-1+CNC+Gly film, and PLA+AF-2+CNC+Gly film was stabilized at 18, 48, 18, 18 h, respectively. The % release was 91.74 and 93 % from the Control-3 and Control-4 films at 70 h, respectively. However, the incorporation of CNC+Gly into the PLA+active formulations matrices noticeably reduced the release of AF-1 and AF-2 by 32 % (% release: 62.54 %) and 20 % (% release: 74.35 %) at 70 h of extraction from PLA+AF-1+CNC+Gly and PLA+AF-2+CNC+Gly, respectively, as compared to the Control films. These results suggested that the incorporation of CNC/Gly significantly improved the controlled release of active formulations from PBAT films and prevented the fast release which is very important for extending the shelf life of preserved foods with bioactive packaging films.

Table 6.6. Parameters of the Korsmeyer-Peppas model as kinetic release parameters (rate constant (k) and diffusional exponent (n)) of the active formulations from polymeric matrices in ethanol.

Types of bioactive films	Korsmeyer-Peppas parameters		
	N	k	R ²
Control-1: PBAT+AF-1	0.29	0.48	0.8637
PBAT+AF-1+CNC+Gly	0.24	0.36	0.9543
Cnontrol-2: PBAT+AF-2	0.30	0.48	0.8562
PBAT+AF-2+CNC+Gly	0.28	0.38	0.9434
Control-3: PLA+AF-1	0.32	0.59	0.8443
PLA+AF-1+CNC+Gly	0.27	0.53	0.8725
Control-4: PLA+AF-2	0.37	0.52	0.9284
PLA+AF-2+CNC+Gly	0.27	0.58	0.8395

The Korsmeyer-Peppas parameters such as n, k, and R² were calculated for analyzing release kinetics and their mechanism of release of the AF-1 and AF-2 from PLA and PBAT films (Table 6.6). The higher R² values (> 80 %) for all tested films indicated that the Korsmeyer-Peppas model is fitted for the release of active formulations from the bioactive PLA and PBAT films. The

coefficient n values ranged between 0.24 to 0.37 for eight different types of tested films (Control-1: PBAT+AF-1, Control-2: PBAT+AF-2, Control-3: PLA+AF-1, Control-4: PLA+AF-2, PBAT+AF-1+CNC+Gly, PBAT+AF-2+CNC+Gly, PLA+AF-1+CNC+Gly, PLA+AF-2+CNC+Gly). The coefficient n values lower than 0.5 indicated that the release of active formulations occurred through Fickian or quasi-Fickian diffusion mechanisms for both polymeric matrices. The current results were in line with the results obtained by several authors as they observed the release of active ingredients or essential oils from polymeric matrices by a diffusional mechanism (Petchwattana and Naknaen, 2015; Bustos *et al.*, 2016; Tawakkal *et al.*, 2016; Requena *et al.*, 2017; Ben-Fadhel *et al.*, 2020). Requena *et al.* (2017) studied the release kinetics mechanism of the eugenol and carvacrol from the poly (hydroxybutyrate-co-hydroxyvalerate) (PHBV) films in different food simulants (10 % ethanol, 50 % ethanol, 3 % acetic acid, and isooctane) and the authors found that the release of eugenol and carvacrol occurred through Fickian and quasi-Fickian diffusion in the PHBV matrix. As the diffusional release of AF-1 and AF-2 from the PBAT and PLA matrices were not coupled with polymeric chain relaxation, it could be assumed that the release occurred by (i) ethanol diffusion through polymeric matrices, (ii) the polymeric network relaxation after incorporating CNC/Gly/active formulations, and (iii) active formulations diffused through the relaxed polymeric matrices until the thermodynamic equilibrium condition was reached between polymer and ethanol (Requena *et al.*, 2017).

The release mass (M_t/M_∞) of AF-1 and AF-2 from PBAT and PLA polymeric matrices at different contact times with ethanol were measured and depicted in Figure 6.6a-b. Figure 6.6a-b shows the ratio of active formulations released from PBAT and PLA films at different extraction times respecting the final amount released at equilibrium values and the fitted Fick's model in ethanol. In Figure 6.6a the diffusion of AF-1 and AF-2 was significantly faster in ethanol from the PBAT+AF-1 (M_t/M_∞ : 0.5 at 70 h) and PBAT+AF-2 (M_t/M_∞ : 0.54 at 70 h), however, it remarkably reduced the diffusion of AF-1 and AF-2 when bioactive PBAT films loaded with CNC+Gly. The M_t/M_∞ values obtained for the films PBAT+AF-1+CNC+Gly and PBAT+AF-2+CNC+Gly were respectively 0.25 and 0.31 at 70 h of extraction with the ethanol. On the other hand, bioactive PLA film showed the fastest release of active formulations as compared to the PBAT films. Figure 6.6b shows M_t/M_∞ ratio of the released AF-1 and AF-2 from PLA+AF-1, PLA+AF-2, PLA+AF-1+CNC+Gly, and PLA+AF-2+CNC+Gly films were 0.91, 0.92, 0.62, and 0.74, respectively. A similar phenomenon as PBAT has been observed in the case of bioactive PLA nanocomposite films, after incorporating CNC+Gly into the bioactive PLA matrix has greatly reduced the diffusion of AF-1 and AF-2. This phenomenon suggested that the incorporation of CNC/Gly into polymeric matrices improved the interactions with active formulations which reduced their migration through the polymeric network

by the restriction of compound mobility (Requena *et al.*, 2017). After analyzing the release kinetics results, it could be concluded that the PBAT films containing AF-1+CNC+Gly and AF-2+CNC+Gly have a greater ability to retain the active formulations for longer times than bioactive PLA nanocomposite films.

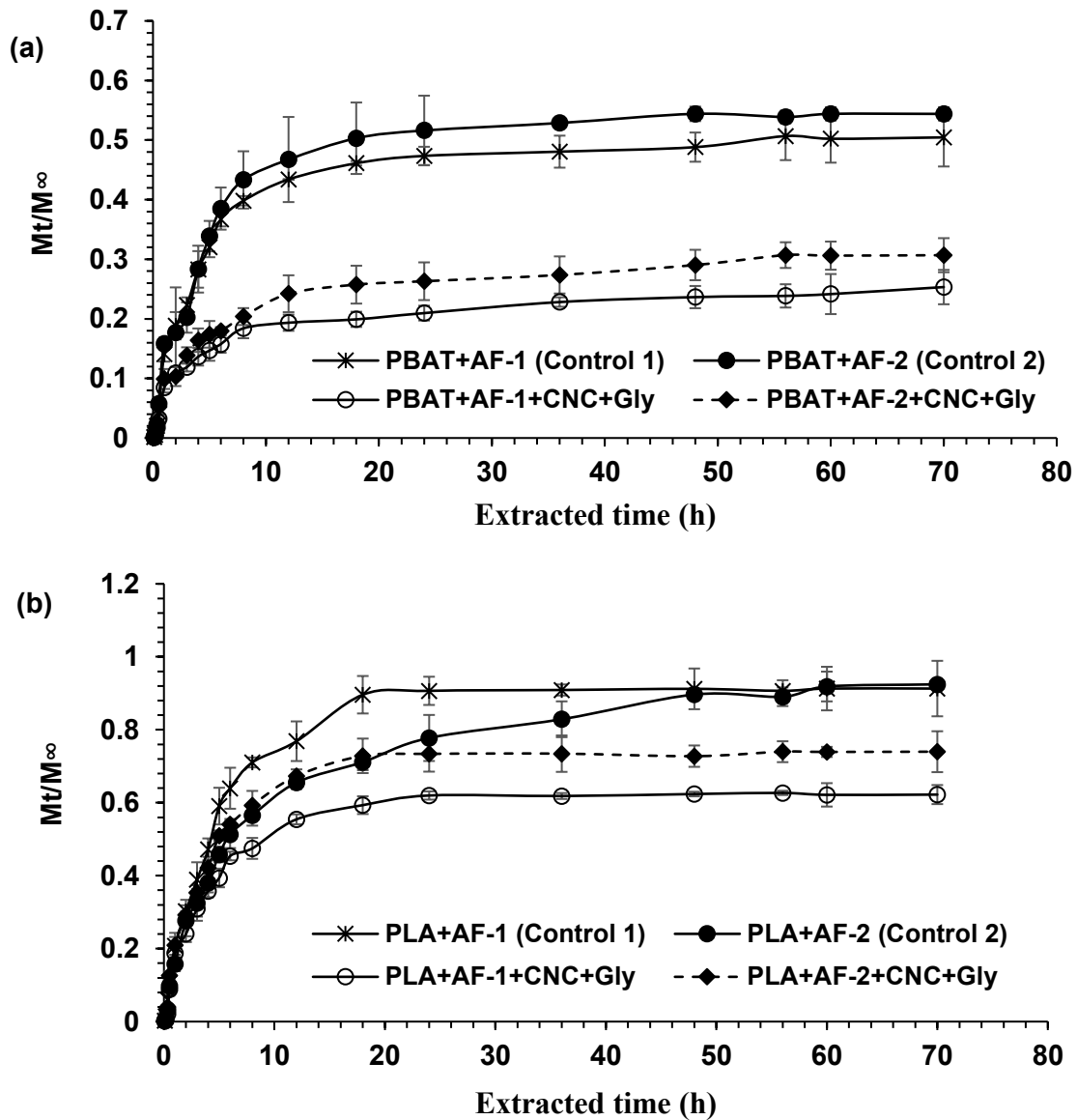


Figure 6.6. Ratio of the two active formulations released from polymeric films during contact time with ethanol and fitted Fick's model (Korsmeyer-Peppas model).

6.3.3. Hurdle treatment (bioactive films with γ -irradiation) in rice

Two bioactive nanocomposite films were selected for the *in situ* tests in stored rice against *E. coli* O157:H7, *S. Typhimurium*, *A. niger*, *P. chrysogenum*, and *M. circinelloides* with and without the treatment with 750 Gy γ -irradiation (Figure 6.7a-e). The nanocomposite films were selected based on the results of mechanical properties, WVP, OTR, and *in vitro* release kinetics tests. However, treated rice was categorized as Control (Rice+bacteria/fungi), γ -Control (Rice+bacteria/fungi+750 Gy radiation), Treatment-1 (Rice+bacteria/fungi+bioactive PBAT+AF-1+CNC+Gly nanocomposite film), Treatment-2 (Rice+bacteria/fungi+bioactive PBAT+AF-1+CNC+Gly nanocomposite film+irradiation), Treatment-3 (Rice+bacteria/fungi+bioactive PBAT+AF-2+CNC+Gly nanocomposite film), and Treatment-4 (Rice+bacteria/fungi+bioactive PBAT+AF-2+CNC+Gly nanocomposite film+irradiation).

Figure 6.7a-b shows the growth profile of *E. coli* O157:H7 and *S. Typhimurium* in stored rice for 8 weeks under different treatments. The tested bacterial growth profile was significantly affected in rice after 8 weeks stored with bioactive PBAT+AF-1+CNC+Gly (Treatment-1) and PBAT+AF-2+CNC+Gly (Treatment-3) films compared to the Control (no film) and γ -Control. Briefly, rice was inoculated with 5 log CFU/g of *E. coli* O157:H7 and *S. Typhimurium*. The growth of *E. coli* O157:H7 reached 4.96 log CFU/g in Control sample after 8 weeks (Figure 6.7a). After 8 weeks of storage, *E. coli* O157:H7 was significantly reduced by 24 % (3.65 log CFU/g), 59 % (2.04 log CFU/g), 81 % (0.93 log CFU/g), 52 % (2.36 log CFU/g), and 71 % (1.42 log CFU/g) in γ -Control, Treatment-1, Treatment-2, Treatment-3, and Treatment-4, respectively, as compared to the Control (4.96 log CFU/g) ($P \leq 0.05$). However, the combined treatment of bioactive films and γ -irradiation in Treatment-2 and Treatment-4 reduced the load of *E. coli* O157:H7 in stored rice. A similar observation was found in the case of the growth profile of *S. Typhimurium* in stored rice and the result was depicted in Figure 6.7b. *S. Typhimurium* growth in the Control sample declined with storage time until 4 weeks (from 4.41 to 3.85 log CFU/g), then the bacterial growth started to increase upto 4.89 log CFU/g after 8 weeks. The highest bacterial growth (*S. Typhimurium*) reduction was observed in Treatment-2 (82.4 %), followed by Treatment-4 (77 %), Treatment-1 (66 %), Treatment-3 (43 %), and γ -Control (36.6 %) with respect to the Control sample, and the corresponding bacterial count were 0.86, 1.14, 1.67, 2.78, and 3.1 log CFU/g of *S. Typhimurium* after 8 weeks in stored rice. The combined treatment of γ -irradiation and bioactive nanocomposite films (either PBAT+AF-1+CNC+Gly film or PBAT+AF-2+CNC+Gly film) showed a synergistic efficiency to control the growth of *E. coli* O157:H7 and *S. Typhimurium* in stored rice (Figure 6.7a-b).

The antifungal activities of the developed bioactive PBAT nanocomposite films were tested with and without irradiation treatment against three spoilage fungi *A. niger*, *P. chrysogenum*, and *M. circinelloides* in stored rice for 8 weeks (Figure 6.7c-e). The bioactive PBAT nanocomposite films with irradiation showed the strongest fungicidal effect over the treatment alone (either by bioactive films alone or by γ -irradiation alone). The initial inoculation was 5 log CFU/g for each fungus. In the case of *A. niger*, the fungal count reached 7.31 log CFU/g in stored rice after 8 weeks (Figure 6.7c). The samples treated with PBAT+AF-1+CNC+Gly film (Treatment-1) and PBAT+AF-2+CNC+Gly film (Treatment-3) reduced the fungal (*A. niger*) growth by 53 % (3.42 log CFU/g) and 63.5 % (2.67 log CFU/g) with respect to the control sample after 8 weeks, respectively. However, the corresponding films in addition to 750 Gy γ -irradiation eliminated *A. niger* growth by 92 % (0.56 log CFU/g) and 85 % (1.11 log CFU/g) in Treatment-2 and Treatment-4, respectively, after 8 weeks compared to the control sample. Moreover, the application of γ -irradiation alone could reduce 11 % *A. niger* growth in rice after 8 weeks compared to the control sample (Figure 6.7c).

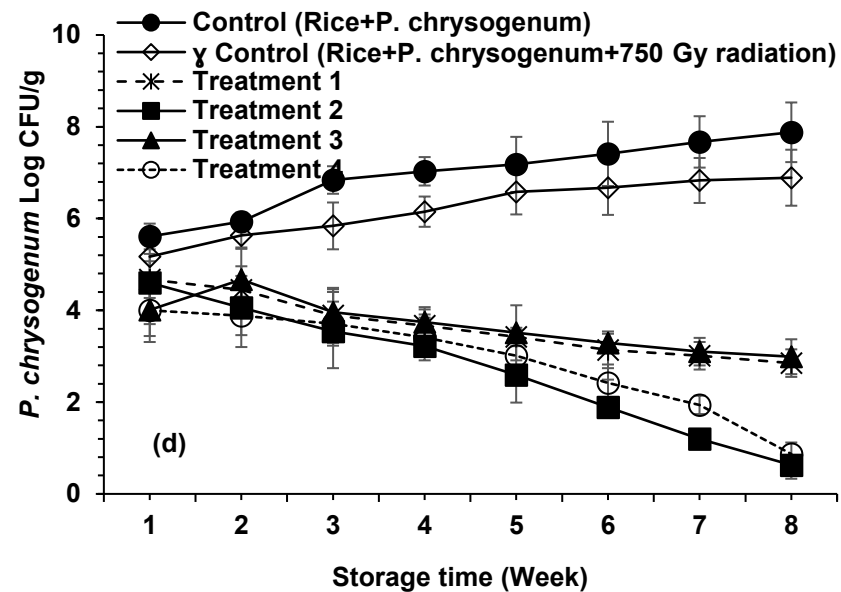
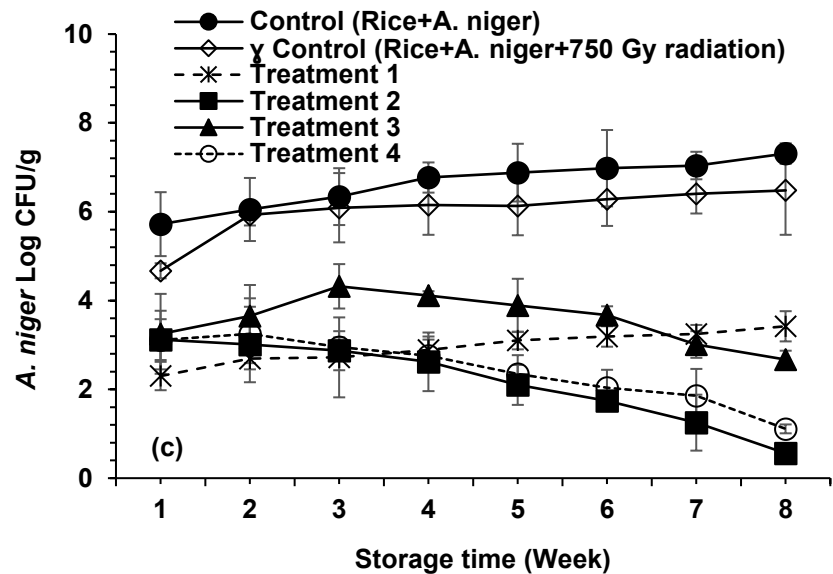
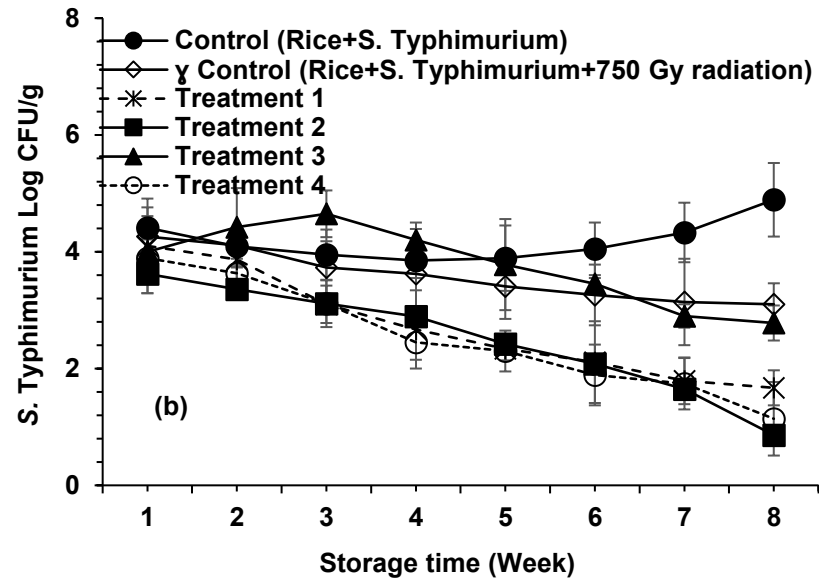
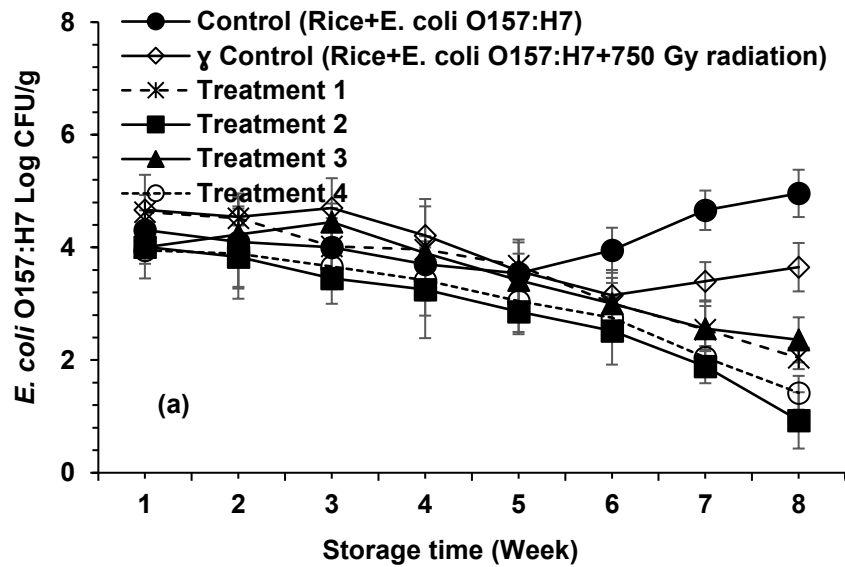
Figure 6.7d shows the antifungal efficiency of bioactive PBAT-based nanocomposite films alone or in combination with γ -irradiation against *P. chrysogenum* in stored rice. The growth of *P. chrysogenum* in control samples reached 7.88 log CFU/g after 8 weeks of storage. The fungal (*P. chrysogenum*) growth was 2.85 and 2.99 log CFU/g for the samples treated with films alone by PBAT+AF-1+CNC+Gly (Treatment-1) and by PBAT+AF-2+CNC+Gly (Treatment-3), respectively, had reductions by 64 and 62 % of *P. chrysogenum* after 8 weeks of stored rice as compared to the control. The growth of *P. chrysogenum* reduced 12.5 % as compared to the control sample in stored rice after 8 weeks by applying 750 Gy irradiation alone, while the combined treatment of γ -irradiation with the bioactive films PBAT+AF-1+CNC+Gly (Treatment-2) and PBAT+AF-2+CNC+Gly (Treatment-4) caused a reduction by 92 % (0.63 log CFU/g) and 89 % (0.87 log CFU/g), respectively, as compared to the control sample ($P \leq 0.05$) (Figure 6.7d). Figure 6.7e shows the fungicidal effectiveness given by the bioactive PBAT-based nanocomposite films with and without γ -irradiation treatment to control *M. circinelloides* in stored rice for 8 weeks. The growth of *M. circinelloides* in control samples was 7.49 log CFU/g after 8 weeks of storage. The fungal (*M. circinelloides*) growth was 2.18 and 2.53 log CFU/g with the samples treated with films alone by PBAT+AF-1+CNC+Gly (Treatment-1) and by PBAT+AF-2+CNC+Gly (Treatment-3), respectively, which represents a corresponding reduction by 71 and 66 % of *M. circinelloides* after 8 weeks of stored rice as compared to the control sample. The application of 750 Gy irradiation alone, the fungal (*M. circinelloides*) growth reduced by 11.1 % at the end of the incubation period, while the combined treatment of γ -irradiation with the bioactive films used in Treatment-2 and

Treatment-4 caused a reduction by 88 and 83 %, respectively, with respect to the control ($P \leq 0.05$).

In the current study, two types of bioactive PBAT-based nanocomposite films were used containing 300 μL of AF-1 and AF-2 with CNC and plasticizer to control pathogenic bacteria (*E. coli* O157:H7 and *S. Typhimurium*) and spoilage fungi (*A. niger*, *P. chrysogenum*, and *M. circinelloides*) in stored rice. The active components presented in AF-1 and AF-2 were released from the bioactive PBAT-based nanocomposite films which prevent the growth of pathogenic bacteria and spoilage fungi in rice. The EOs and citrus extracts used in the active formulations mainly contain cinnamaldehyde, carvacrol, thymol, eugenol, limonene, terpineol, geraniol, neral, myrcene, trans-caryophyllene, and borneol which have strong bactericidal and fungicidal effects proven by several studies (Burt, 2004; Zachariah and Leela, 2006; Dzamic *et al.*, 2008; Turgis *et al.*, 2012; Begum *et al.*, 2022a; Begum *et al.*, 2022b).

Incorporation of CNC into the polymeric matrix as a reinforcing agent could slow the controlled release of active components over the storage period and control the microbial growth in foods for a long time (Boumail *et al.*, 2013; Salmieri *et al.*, 2014b; Deng *et al.*, 2017; Hossain *et al.*, 2018; Hossain *et al.*, 2019a). In line with our current study, Hossain *et al.* (2018) developed bioactive methylcellulose-based films reinforced with CNC and oregano/thyme EO (MC/CNC/Oregano/thyme) to control fungal growth (*A. niger*, *A. flavus*, *A. parasiticus*, and *P. chrysogenum*) in rice samples. The authors observed that the MC/CNC/Oregano/thyme-based nanocomposite films could reduce 2 log CFU/g of fungal growth in contaminated rice at 28 °C after 8 weeks. Moreover, the authors also proved that the incorporation of CNC could slow the release of volatile components by 35 % from bioactive MC-based nanocomposite film after 12 weeks in stored rice (Hossain *et al.*, 2018). de Souza *et al.* (2022) prepared PBAT-based film incorporated with bioactive PLA capsules containing cinnamon EO by the solvent casting method for developing biodegradable bioactive food packaging. The authors used PBAT/PLA/cinnamon EO films for strawberry preservation and observed the bioactive film potentially extended the shelf life of strawberries maintaining fruit quality without dehydration (de Souza *et al.*, 2022). Cardoso *et al.* (2017) developed bioactive PBAT-based film loaded with oregano EO for fish fillet preservation and they found bioactive PBAT-based film significantly reduced the growth of total coliforms, *Staphylococcus aureus*, and psychrotrophic microorganisms in fish fillet during storage. Polyvinyl alcohol/chitosan-based nanocomposite films reinforced with CNC and carvacrol could modulate the mechanical properties and increase the antioxidant properties of the bioactive films, thus, controlling the microbial growth and preventing the oxidation of stored products (Luzi *et al.*, 2017).

Hurdle techniques, combining two or more preservation techniques, are a new idea to achieve a superior way to control pathogenic bacteria and spoilage fungi in stored food commodities rather than a single preservation technique (Khan *et al.*, 2017b). In the current study, the application of irradiation treatment along with bioactive PBAT-based nanocomposite films synergistically reduced the microbial load by 77 to 92 % after 8 weeks of storage as compared to the control sample, while the single treatment either by irradiation alone or bioactive PBAT-based nanocomposite film alone could reduce only by 11 to 37 % and by 53 to 71 %, respectively, as compared to control sample. Ionizing irradiation can attack microbial cell DNA, then break their chemical bonds, alter membrane permeability, as well as affect other cellular functions. When irradiation is applied along with active packaging, irradiation could increase contact between the microbial cell and active components released from bioactive packaging and facilitate cell destruction (Caillet *et al.*, 2005; Caillet and Lacroix, 2006; Ayari *et al.*, 2012; Begum *et al.*, 2020a). The release of active components present in the active formulations (AF-1 and AF-2) from the bioactive PBAT-based films and γ -irradiation might be affect cell integrity, accelerate the release of the bacterial and fungal cell ingredients and imbalance internal pH and ATP synthesis (Caillet *et al.*, 2005; Oussalah *et al.*, 2006). In agreement with our current study, Shankar *et al.* (2021) worked with strawberry preservation using active chitosan-based nanocomposite film loaded with EO/Ag nanoparticles along with 1 kGy γ -irradiation. The authors observed that the combined treatment between active Chitosan nanocomposite film and irradiation extended the shelf-life of stored strawberries by 4 days (Shankar *et al.*, 2021). Similar observations were found by several authors (Caillet *et al.*, 2005; Hossain *et al.*, 2014a; Lacroix and Follett, 2015; Hossain *et al.*, 2018; Hossain *et al.*, 2019a). The combined application of irradiation (either γ -ray or X-ray) and oregano/thyme EO successfully reduced the growth of *E. coli* O157:H7, *S. Typhimurium*, and *Listeria monocytogenes* in rice (Begum *et al.*, 2020b). The authors stated that the combined treatment of irradiation and EO could significantly increase the microbicidal effectiveness. Moreover, the authors found that the D_{10} values were 326, 266, and 236 Gy for the bacteria *E. coli* O157:H7, *S. Typhimurium*, and *L. monocytogenes*, respectively, when treated with a high dose rate of γ -irradiation alone (9.1 kGy/h), while the corresponding D_{10} values were significantly reduced ($P \leq 0.05$) to 274, 218, and 219 Gy in combined treatment between the vapor of EO and γ -irradiation (Begum *et al.*, 2020b). Therefore, it could be stated that the combined treatment between irradiation and bioactive PBAT-based nanocomposite films could be an effective strategy for controlling biological contaminants in stored rice as well as could replace chemical preservatives and plastic packaging.



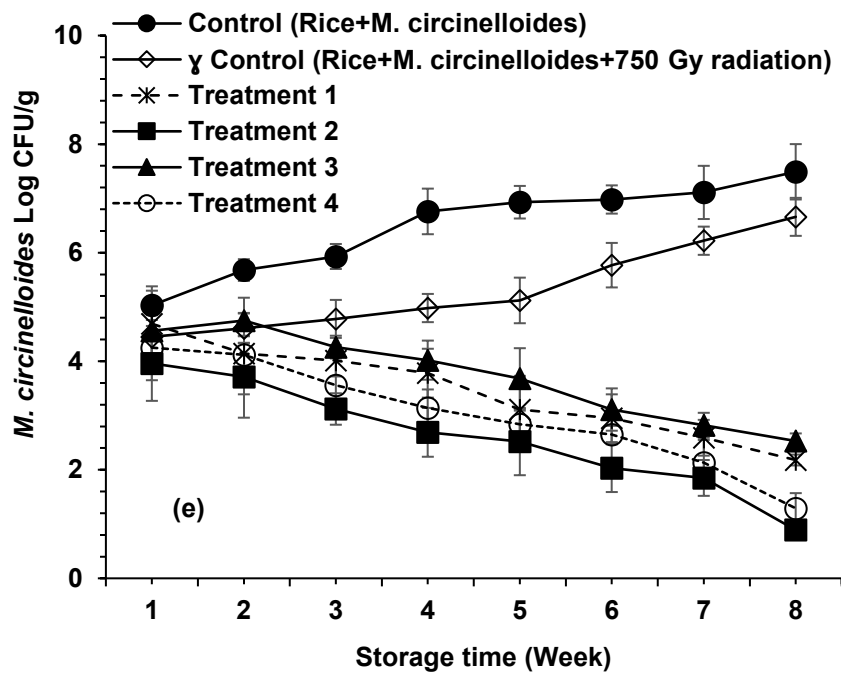


Figure 6.7. Bacterial (*E. coli* O157:H7 and *S. Typhimurium*) and fungal (*A. niger*, *P. chrysogenum*, and *M. circinelloides*) growth profiles in storage rice under different bioactive PBAT films treatment for 8 weeks.

6.4. Conclusions

Central composite design (CCD) was applied to optimize the bioactive PBAT and PLA nanocomposite films having the highest bactericidal and fungicidal effectiveness by combining the following parameters- polymeric matrix, active formulations (AF-1 and AF-2), CNC, Gly. The IC (%) values of the films were measured using an agar volatilization assay against *E. coli* O157:H7, *S. Typhimurium*, *A. niger*, *P. chrysogenum*, and *M. circinelloides* to obtain bioactive nanocomposite films having strong antibacterial and antifungal properties. Incorporation of active formulations+CNC+Gly into either PBAT or PLA matrices improved the mechanical strength and WVP of the bioactive nanocomposite films, while the OTR values were improved only for bioactive PBAT-based nanocomposite films. The entrapment of AF-1 and AF-2 into the PBAT+CNC+Gly nanocomposite matrix significantly slowed down the release of active components compared to the bioactive films without CNC+Gly. Bioactive PBAT-based nanocomposite films were able to retain more active formulations during the extraction time over bioactive PLA-based nanocomposite films. Furthermore, the bioactive PBAT-based nanocomposite films were applied with the presence of 750 Gy γ -irradiation to control pathogenic bacteria and fungi for 2 months in stored rice. The current study proved that the combination between bioactive PBAT-based nanocomposite films and irradiation could work synergistically and increase the microbicidal effectiveness significantly compared to the treatment alone (either by bioactive film or by irradiation alone). Finally, it could be concluded that the application of bioactive PBAT-based films and irradiation together could be an effective and safe way to protect cereal grains during long-term storage as well as contribute to “Green Consumerism” and “Sustainable Packaging” in the agriculture sector and food industry.

6.5. Acknowledgments

The authors grateful to the Ministère de l'Économie, et de l'Innovation (MEI) du Québec (PSR SIIRI 985), Kerry Group, Biosecur Lab Inc., the Ministère de l'Agriculture, des Pêcheries, et de l'Agriculture du Québec (MAPAQ) for a chair on antimicrobial compounds (PPIA-12) and the U.S. Department of Agriculture, Agricultural Research Service (USDA ARS), U.S. Pacific Basin Agricultural Research Centre for supporting this research.

6.6. References

- Arrieta, M.P., López, J., Hernández, A., Rayón, E., 2014. Ternary PLA–PHB–Limonene blends intended for biodegradable food packaging applications. *European Polymer Journal* 50, 255-270.
- Ayari, S., Dussault, D., Jerbi, T., Hamdi, M., Lacroix, M., 2012. Radiosensitization of *Bacillus cereus* spores in minced meat treated with cinnamaldehyde. *Radiation Physics and Chemistry* 81, 1173-1176.
- Ayari, S., Shankar, S., Follett, P., Hossain, F., Lacroix, M., 2020. Potential synergistic antimicrobial efficiency of binary combinations of essential oils against *Bacillus cereus* and *Paenibacillus amylolyticus*-Part A. *Microbial pathogenesis* 141, 104008.
- Begum, T., Follett, P.A., Hossain, F., Christopher, L., Salmieri, S., Lacroix, M., 2020a. Microbicidal effectiveness of irradiation from Gamma and X-ray sources at different dose rates against the foodborne illness pathogens *Escherichia coli*, *Salmonella* Typhimurium and *Listeria monocytogenes* in rice. *LWT-Food Science and Technology* 132, 109841.
- Begum, T., Follett, P.A., Mahmud, J., Moskovchenko, L., Salmieri, S., Allahdad, Z., Lacroix, M., 2022a. Silver nanoparticles-essential oils combined treatments to enhance the antibacterial and antifungal properties against foodborne pathogens and spoilage microorganisms. *Microbial Pathogenesis* 164, 105411.
- Begum, T., Follett, P.A., Shankar, S., Mahmud, J., Salmieri, S., Lacroix, M., 2022b. Mixture design methodology and predictive modeling for developing active formulations using essential oils and citrus extract against foodborne pathogens and spoilage microorganisms in rice. *Journal of Food Science* 87, 353-369.
- Ben-Fadhel, Y., Maherani, B., Manus, J., Salmieri, S., Lacroix, M., 2020. Physicochemical and microbiological characterization of pectin-based gelled emulsions coating applied on pre-cut carrots. *Food Hydrocolloids* 101, 105573.
- Boumail, A., Salmieri, S., Klimas, E., Tawema, P.O., Bouchard, J., Lacroix, M., 2013. Characterization of trilayer antimicrobial diffusion films (ADFs) based on methylcellulose-polycaprolactone composites. *Journal of Agricultural and Food Chemistry* 61, 811-821.
- Burt, S., 2004. Essential oils: their antibacterial properties and potential applications in foods—a review. *International Journal of Food Microbiology* 94, 223-253.
- Bustos, C.R., Alberti, R.F., Matiacevich, S.B., 2016. Edible antimicrobial films based on microencapsulated lemongrass oil. *Journal of Food Science and Technology* 53, 832-839.
- Caillet, S., Lacroix, M., 2006. Effect of gamma radiation and oregano essential oil on murein and ATP concentration of *Listeria monocytogenes*. *Journal of Food Protection* 69, 2961-2969.

- Caillet, S., Shareck, F., Lacroix, M., 2005. Effect of gamma radiation and oregano essential oil on murein and ATP concentration of *Escherichia coli* O157: H7. *Journal of Food Protection* 68, 2571-2579.
- Cardoso, L.G., Pereira Santos, J.C., Camilloto, G.P., Miranda, A.L., Druzian, J.I., Guimarães, A.G., 2017. Development of active films poly (butylene adipate co-terephthalate) – PBAT incorporated with oregano essential oil and application in fish fillet preservation. *Industrial Crops and Products* 108, 388-397.
- Criado, P., Frascini, C., Salmieri, S., Lacroix, M., 2020. Cellulose nanocrystals (CNCs) loaded alginate films against lipid oxidation of chicken breast. *Food Research International* 132, 109110.
- Das, S., Kumar Singh, V., Kumar Dwivedy, A., Kumar Chaudhari, A., Deepika, Kishore Dubey, N., 2021a. Nanostructured *Pimpinella anisum* essential oil as novel green food preservative against fungal infestation, aflatoxin B1 contamination and deterioration of nutritional qualities. *Food Chemistry* 344, 128574.
- Das, S., Singh, V.K., Dwivedy, A.K., Chaudhari, A.K., Dubey, N.K., 2021b. *Anethum graveolens* Essential Oil Encapsulation in Chitosan Nanomatrix: Investigations on *In Vitro* Release Behavior, Organoleptic Attributes, and Efficacy as Potential Delivery Vehicles Against Biodeterioration of Rice (*Oryza sativa* L.). *Food and Bioprocess Technology* 14, 831-853.
- de Souza, A.G., Barbosa, R.F.d.S., Quispe, Y.M., Rosa, D.d.S., 2022. Essential oil microencapsulation with biodegradable polymer for food packaging application. *Journal of Polymers and the Environment* 30, 3307-3315.
- Deng, Z., Jung, J., Simonsen, J., Wang, Y., Zhao, Y., 2017. Cellulose Nanocrystal Reinforced Chitosan Coatings for Improving the Storability of Postharvest Pears Under Both Ambient and Cold Storages. *Journal of Food Science* 82, 453-462.
- Dzamic, A., Sokovic, M., Ristic, M., Grujic-Jovanovic, S., Vukojevic, J., Marin, P., 2008. Chemical composition and antifungal activity of *Origanum heracleoticum* essential oil. *Chemistry of Natural Compounds* 44, 659-660.
- Falleh, H., Ben Jemaa, M., Djebali, K., Abid, S., Saada, M., Ksouri, R., 2019. Application of the mixture design for optimum antimicrobial activity: Combined treatment of *Syzygium aromaticum*, *Cinnamomum zeylanicum*, *Myrtus communis*, and *Lavandula stoechas* essential oils against *Escherichia coli*. *Journal of Food Processing and Preservation* 43, 14257.

- Felix da Silva Barbosa, R., Gabrieli de Souza, A., Rangari, V., Rosa, D.D.S., 2021. The influence of PBAT content in the nanocapsules preparation and its effect in essential oils release. *Food Chemistry* 344, 128611.
- Follett, P.A., Snook, K., Janson, A., Antonio, B., Haruki, A., Okamura, M., Bisel, J., 2013. Irradiation quarantine treatment for control of *Sitophilus oryzae* (Coleoptera: Curculionidae) in rice. *Journal of Stored Products Research* 52, 63-67.
- Ghabraie, M., Vu, K.D., Tata, L., Salmieri, S., Lacroix, M., 2016. Antimicrobial effect of essential oils in combinations against five bacteria and their effect on sensorial quality of ground meat. *LWT-Food Science and Technology* 66, 332-339.
- Haafiz, M.K., Hassan, A., Khalil, H.P., Fazita, M.R., Islam, M.S., Inuwa, I.M., Marliana, M.M., Hussin, M.H., 2016. Exploring the effect of cellulose nanowhiskers isolated from oil palm biomass on polylactic acid properties. *International Journal of Biological Macromolecules* 85, 370-378.
- Hossain, F., Follett, P., Salmieri, S., Vu, K.D., Frascini, C., Lacroix, M., 2019a. Antifungal activities of combined treatments of irradiation and essential oils (EOs) encapsulated chitosan nanocomposite films in *in vitro* and *in situ* conditions. *International Journal of Food Microbiology* 295, 33-40.
- Hossain, F., Follett, P., Salmieri, S., Vu, K.D., Harich, M., Lacroix, M., 2019b. Synergistic Effects of Nanocomposite Films Containing Essential Oil Nanoemulsions in Combination with Ionizing Radiation for Control of Rice Weevil *Sitophilus oryzae* in Stored Grains. *Journal of Food Science* 84, 1439-1446.
- Hossain, F., Follett, P., Salmieri, S., Vu, K.D., Jamshidian, M., Lacroix, M., 2016. Perspectives on essential oil-loaded nano-delivery packaging technology for controlling stored cereal and grain pests. CRC Press, 487-508.
- Hossain, F., Follett, P., Shankar, S., Begum, T., Salmieri, S., Lacroix, M., 2021. Radiosensitization of rice weevil *Sitophilus oryzae* using combined treatments of essential oils and ionizing radiation with gamma-ray and X-Ray at different dose rates. *Radiation Physics and Chemistry* 180, 109286.
- Hossain, F., Follett, P., Vu, K.D., Salmieri, S., Frascini, C., Jamshidian, M., Lacroix, M., 2018. Antifungal activity of combined treatments of active methylcellulose-based films containing encapsulated nanoemulsion of essential oils and γ -irradiation: *in vitro* and *in situ* evaluations. *Cellulose* 26, 1335-1354.

- Hossain, F., Follett, P., Vu, K.D., Salmieri, S., Senoussi, C., Lacroix, M., 2014a. Radiosensitization of *Aspergillus niger* and *Penicillium chrysogenum* using basil essential oil and ionizing radiation for food decontamination. *Food Control* 45, 156-162.
- Hossain, F., Lacroix, M., Salmieri, S., Vu, K., Follett, P.A., 2014b. Basil oil fumigation increases radiation sensitivity in adult *Sitophilus oryzae* (Coleoptera: Curculionidae). *Journal of Stored Products Research* 59, 108-112.
- Hosseini, M., Razavi, S., Mousavi, M., 2009. Antimicrobial, physical and mechanical properties of chitosan-based films incorporated with thyme, clove and cinnamon essential oils. *Journal of Food Processing and Preservation* 33, 727-743.
- Hyltdgaard, M., Mygind, T., Meyer, R.L., 2012. Essential oils in food preservation: mode of action, synergies, and interactions with food matrix components. *Frontiers in Microbiology* 3, 12.
- Kang, J.H., Jeon, Y.J., Min, S.C., 2021. Effects of packaging parameters on the microbial decontamination of Korean steamed rice cakes using in-package atmospheric cold plasma treatment. *Food Science and Biotechnology* 30, 1535-1542.
- Khan, A., Khan, R.A., Salmieri, S., Le Tien, C., Riedl, B., Bouchard, J., Chauve, G., Tan, V., Kamal, M.R., Lacroix, M., 2012. Mechanical and barrier properties of nanocrystalline cellulose reinforced chitosan based nanocomposite films. *Carbohydrate Polymers* 90, 1601-1608.
- Khan, I., Tango, C.N., Miskeen, S., Lee, B.H., Oh, D.-H., 2017. Hurdle technology: A novel approach for enhanced food quality and safety – A review. *Food Control* 73, 1426-1444.
- Khan, R.A., Beck, S., Dussault, D., Salmieri, S., Bouchard, J., Lacroix, M., 2013. Mechanical and barrier properties of nanocrystalline cellulose reinforced poly(caprolactone) composites: Effect of gamma radiation. *Journal of Applied Polymer Science* 129, 3038-3046.
- Lacroix, M., Follett, P., 2015. Combination irradiation treatments for food safety and phytosanitary uses. *Stewart Postharvest Review* 11, 1-10.
- Li, G., Shankar, S., Rhim, J.-W., Oh, B.-Y., 2015. Effects of preparation method on properties of poly(butylene adipate-co-terephthalate) films. *Food Science and Biotechnology* 24, 1679-1685.
- Luzi, F., Fortunati, E., Giovanale, G., Mazzaglia, A., Torre, L., Balestra, G.M., 2017. Cellulose nanocrystals from *Actinidia deliciosa* pruning residues combined with carvacrol in PVA_CH films with antioxidant/antimicrobial properties for packaging applications. *International Journal of Biological Macromolecules* 104, 43-55.
- Maherani, B., Harich, M., Salmieri, S., Lacroix, M., 2018. Comparative evaluation of antimicrobial efficiency of FOODGARD F410B citrus extract and sodium benzoate against foodborne pathogens in strawberry filling. *Journal of Food Processing and Preservation* 42, 13549.

- Mith, H., Dure, R., Delcenserie, V., Zhiri, A., Daube, G., Clinquart, A., 2014. Antimicrobial activities of commercial essential oils and their components against food-borne pathogens and food spoilage bacteria. *Food Science and Nutrition* 2, 403-416.
- Morelli, C.L., Belgacem, N., Bretas, R.E.S., Bras, J., 2016. Melt extruded nanocomposites of polybutylene adipate-co-terephthalate (PBAT) with phenylbutyl isocyanate modified cellulose nanocrystals. *Journal of Applied Polymer Science* 133, 43678.
- Oussalah, M., Caillet, S., Lacroix, M., 2006. Mechanism of action of Spanish oregano, Chinese cinnamon, and savory essential oils against cell membranes and walls of *Escherichia coli* O157: H7 and *Listeria monocytogenes*. *Journal of Food Protection* 69, 1046-1055.
- Petchwattana, N., Naknaen, P., 2015. Utilization of thymol as an antimicrobial agent for biodegradable poly(butylene succinate). *Materials Chemistry and Physics* 163, 369-375.
- Radfar, R., Hosseini, H., Farhodi, M., Ghasemi, I., Srednicka-Tober, D., Shamloo, E., Khaneghah, A.M., 2020. Optimization of antibacterial and mechanical properties of an active LDPE/starch/nanoclay nanocomposite film incorporated with date palm seed extract using D-optimal mixture design approach. *International Journal of Biological Macromolecules* 158, 790-799.
- Requena, R., Vargas, M., Chiralt, A., 2017. Release kinetics of carvacrol and eugenol from poly(hydroxybutyrate-co-hydroxyvalerate) (PHBV) films for food packaging applications. *European Polymer Journal* 92, 185-193.
- Rhim, J.-W., Mohanty, A.K., Singh, S.P., Ng, P.K.W., 2006. Effect of the processing methods on the performance of polylactide films: Thermocompression versus solvent casting. *Journal of Applied Polymer Science* 101, 3736-3742.
- Salmieri, S., Islam, F., Khan, R.A., Hossain, F.M., Ibrahim, H.M.M., Miao, C., Hamad, W.Y., Lacroix, M., 2014a. Antimicrobial nanocomposite films made of poly(lactic acid)-cellulose nanocrystals (PLA-CNC) in food applications: part A—effect of nisin release on the inactivation of *Listeria monocytogenes* in ham. *Cellulose* 21, 1837-1850.
- Salmieri, S., Islam, F., Khan, R.A., Hossain, F.M., Ibrahim, H.M.M., Miao, C., Hamad, W.Y., Lacroix, M., 2014b. Antimicrobial nanocomposite films made of poly(lactic acid)-cellulose nanocrystals (PLA-CNC) in food applications—part B: effect of oregano essential oil release on the inactivation of *Listeria monocytogenes* in mixed vegetables. *Cellulose* 21, 4271-4285.
- Shankar, S., Khodaei, D., Lacroix, M., 2021. Effect of chitosan/essential oils/silver nanoparticles composite films packaging and gamma irradiation on shelf life of strawberries. *Food Hydrocolloids* 117, 106750.

- Shankar, S., Rhim, J.-W., 2016. Tocopherol-mediated synthesis of silver nanoparticles and preparation of antimicrobial PBAT/silver nanoparticles composite films. *LWT - Food Science and Technology* 72, 149-156.
- Shankar, S., Rhim, J.W., 2018. Preparation of antibacterial poly(lactide)/poly(butylene adipate-co-terephthalate) composite films incorporated with grapefruit seed extract. *International Journal of Biological Macromolecules* 120, 846-852.
- Sharma, S., Barkauskaite, S., Duffy, B., Jaiswal, A.K., Jaiswal, S., 2020. Characterization and Antimicrobial Activity of Biodegradable Active Packaging Enriched with Clove and Thyme Essential Oil for Food Packaging Application. *Foods* 9, 1117.
- Sharmin, N., Khan, R.A., Salmieri, S., Dussault, D., Lacroix, M., 2012. Fabrication and Characterization of Biodegradable Composite Films Made of Using Poly(caprolactone) Reinforced with Chitosan. *Journal of Polymers and the Environment* 20, 698-705.
- Srisa, A., Harnkarnsujarit, N., 2020. Antifungal films from trans-cinnamaldehyde incorporated poly(lactic acid) and poly(butylene adipate-co-terephthalate) for bread packaging. *Food Chemistry* 333, 127537.
- Su, S., Duhme, M., Kopitzky, R., 2020. Uncompatibilized PBAT/PLA Blends: Manufacturability, Miscibility and Properties. *Materials (Basel)* 13, 4897.
- Subbuvel, M., Kavan, P., 2021. Development and investigation of antibacterial and antioxidant characteristics of poly lactic acid films blended with neem oil and curcumin. *Journal of Applied Polymer Science* 139, 51891.
- Sung, S.H., Chang, Y., Han, J., 2017. Development of polylactic acid nanocomposite films reinforced with cellulose nanocrystals derived from coffee silverskin. *Carbohydrate Polymers* 169, 495-503.
- Suppakul, P., Miltz, J., Sonneveld, K., Bigger, S.W., 2003. Active packaging technologies with an emphasis on antimicrobial packaging and its applications. *Journal of Food Science* 68, 408-420.
- Tawakkal, I.S.M.A., Cran, M.J., Bigger, S.W., 2016. Release of thymol from poly(lactic acid)-based antimicrobial films containing kenaf fibres as natural filler. *LWT - Food Science and Technology* 66, 629-637.
- Turgis, M., Vu, K.D., Dupont, C., Lacroix, M., 2012. Combined antimicrobial effect of essential oils and bacteriocins against foodborne pathogens and food spoilage bacteria. *Food Research International* 48, 696-702.
- Vatansever, E., Arslan, D., Sarul, D.S., Kahraman, Y., Gunes, G., Durmus, A., Nofar, M., 2020. Development of CNC-reinforced PBAT nanocomposites with reduced percolation threshold:

a comparative study on the preparation method. *Journal of Materials Science* 55, 15523-15537.

Vilarinho, F., Sanches Silva, A., Vaz, M.F., Farinha, J.P., 2018. Nanocellulose in Green Food Packaging. *Critical Reviews in Food Science and Nutrition* 58, 1526-1537.

Wang, L.-F., Rhim, J.-W., Hong, S.-I., 2016. Preparation of poly(lactide)/poly(butylene adipate-co-terephthalate) blend films using a solvent casting method and their food packaging application. *LWT - Food Science and Technology* 68, 454-461.

Zachariah, T.J., Leela, N.K., 2006. Volatiles from herbs and spices. *Handbook of Herbs and Spices*, pp. 177-218.

Supplementary data Table 6.1. CCD experimental response surface design of the PBAT films formulated with active formulation 1 (AF-1), CNC and glycerol.

Film formulation blend number	PBAT (g)	A : Active compound 1 (μL)	B : CNC (%)	C : Glycerol (%)
1	2	300	0.75	0.25
2	2	200	0.375	0.625
3	2	100	0.375	0.625
4	2	300	0.375	0.625
5	2	200	0.375	0.625
6	2	200	0.75	0.625
7	2	100	0	1
8	2	300	0	0.25
9	2	200	0.375	0.625
10	2	100	0	0.25
11	2	300	0.75	1
12	2	200	0.375	0.625
13	2	300	0	1
14	2	200	0.375	0.25
15	2	200	0.375	0.625
16	2	200	0.375	0.625
17	2	200	0	0.625
18	2	100	0.75	0.25
19	2	200	0.375	1
20	2	100	0.75	1

Supplementary data Table 6.2. CCD experimental response surface designs' results the PBAT films formulated with active formulation 1 (AF-1) against bacteria (*E. coli* O157:H7 and *S. Typhimurium*) and fungi (*A. niger*, *P. chrysogenum* and *M. circinelloides*).

Run	Inhibitory capacity, IC %				
	<i>E. coli</i> O157:H7	<i>S.</i> Typhimurium	<i>A. niger</i>	<i>P.</i> <i>chrysogenum</i>	<i>M. circinelloides</i>
1	70	65	73	69	68
2	52	58	67	58	50.3
3	35.6	34	38.6	39.6	36
4	76	75	87	76	74
5	47	51	62	55	46.2
6	45.3	44	52	47.9	46.1
7	28.3	22	31	32	28
8	62	63	69	66	63
9	46	53	55	58	46.3
10	18.6	22	26	32	27
11	68	69	75	73	71
12	53	52	60	53	42
13	63	61	72	69	67
14	38.9	44	46	48	40.3
15	48	52	58	56	52
16	55	48.9	55	54	56
17	36.9	42.3	38.7	44	42.1
18	28.9	27	36	36	32
19	40	50	52	49.3	47
20	32	35	39	38	34

Supplementary data Table 6.3: CCD experimental response surface design of the PBAT films formulated with active formulation 2 (AF-2), CNC and glycerol.

Film formulation blend number	PBAT (g)	A : Active compound 2 (µL)	B : CNC (%)	C : Glycerol (%)
1	2	200	0.5	0.25
2	2	100	0	0.25
3	2	300	0	1
4	2	200	0.5	1
5	2	200	0.5	0.625
6	2	200	0.5	0.625
7	2	100	0	1
8	2	300	0.5	0.625
9	2	200	0.5	0.625
10	2	100	1	1
11	2	300	0	0.25
12	2	100	1	0.25
13	2	300	1	1
14	2	200	0.5	0.625
15	2	200	0	0.625
16	2	200	0.5	0.625
17	2	200	0.5	0.625
18	2	100	0.5	0.625
19	2	200	1	0.625
20	2	300	1	0.25

Supplementary data Table 6.4. CCD experimental response surface designs' results the PBAT films formulated with active formulation 2 (AF-2) against bacteria (*E. coli* O157:H7 and *S. Typhimurium*) and fungi (*A. niger*, *P. chrysogenum* and *M. circinelloides*).

Run	Inhibitory capacity, IC %				
	<i>E. coli</i> O157:H7	<i>S.</i> Typhimurium	<i>A.</i> <i>niger</i>	<i>P.</i> <i>chrysogenum</i>	<i>M. circinelloides</i>
1	44	42	47	46	41
2	13	15	22	13	14
3	58	52	58	56	52
4	42	39	46	42	38
5	48	45	55	53	48
6	47.6	46.2	52.6	54	42
7	12	16	21	18	22
8	69	67	69	68	64
9	44	47	50	53.5	44
10	16	18	27	23	27
11	53	58	56	57	54
12	18	16	22	28	25
13	63	63	62	62	58
14	46.6	44	56	52	46
15	36	38	42	41	37
16	44	46	56.8	55	46
17	49	45	58	56	42
18	25	24	27	28	26
19	42	44	56	52	43
20	56	59	57	61	57

Supplementary data Table 6.5: CCD experimental response surface design of the PLA films formulated with active formulation 1 (AF-1), CNC and glycerol.

Film formulation blend number	PLA (g)	A : Active compound 1 (μL)	B : CNC (%)	C : Glycerol (%)
1	2	300	1.5	0.5
2	2	200	1	1
3	2	200	1.5	1
4	2	200	1	1.5
5	2	100	1	1
6	2	100	1.5	1.5
7	2	300	1	1
8	2	200	1	1
9	2	100	0.5	1.5
10	2	200	0.5	1
11	2	100	1.5	0.5
12	2	200	1	1
13	2	200	1	0.5
14	2	300	0.5	0.5
15	2	200	1	1
16	2	300	1.5	1.5
17	2	100	0.5	0.5
18	2	200	1	1
19	2	200	1	1
20	2	300	0.5	1.5

Supplementary Data Table 6.6. CCD experimental response surface designs' results the PLA films formulated with active formulation 1 (AF-1) against bacteria (*E. coli* O157:H7 and *S. Typhimurium*) and fungi (*A. niger*, *P. chrysogenum* and *M. circinelloides*).

Run	Inhibitory capacity, IC %				
	<i>E. coli</i> O157:H7	<i>S.</i> Typhimurium	<i>A.</i> <i>niger</i>	<i>P.</i> <i>chrysogenum</i>	<i>M. circinelloides</i>
1	44	55	61	53	51
2	32	36	46	38	36.9
3	30	29	40.9	34	33
4	29.1	25	35	35	31
5	16	19	22	17.5	12.9
6	16	14	21	22	16.5
7	49.6	52	59	54.6	54
8	33	37	45	35	34
9	11	16	12	18	17.6
10	29.6	31	38	33	36
11	12	13	16.9	21.3	17.6
12	36	34	43	47	42
13	26	25	31	27.6	26
14	52	46	56	58	53
15	32	33	41	30	29.7
16	42	50	53	48	52
17	18.6	20	22	24	23
18	33	36	32	35	36
19	32	37	36	38	31
20	49	47	52	60	49

Supplementary data Table 6.7: CCD experimental response surface design of the PLA films formulated with active formulation 2 (AF-2), CNC and glycerol.

Film formulation blend number	PLA (g)	A : Active compound 2 (μL)	B : CNC (%)	C : Glycerol (%)
1	2	100	0.75	0.625
2	2	200	0.75	0.625
3	2	200	0.75	1
4	2	300	0.5	1
5	2	100	0.5	1
6	2	300	0.5	0.25
7	2	100	0.5	0.25
8	2	100	1	0.25
9	2	300	1	1
10	2	300	1	0.25
11	2	300	0.75	0.625
12	2	200	0.75	0.625
13	2	100	1	1
14	2	200	0.5	0.625
15	2	200	0.75	0.625
16	2	200	0.75	0.25
17	2	200	1	0.625

Supplementary data Table 6.8. CCD experimental response surface designs' results the PLA films formulated with active formulation 2 (AF-2) against bacteria (*E. coli* O157:H7 and *S. Typhimurium*) and fungi (*A. niger*, *P. chrysogenum* and *M. circinelloides*).

Run	Inhibitory capacity, IC %				
	<i>E. coli</i> O157:H7	<i>S.</i> Typhimurium	<i>A.</i> <i>niger</i>	<i>P.</i> <i>chrysogenum</i>	<i>M. circinelloides</i>
1	16	12	15	17	12
2	32	36	42	42.8	39.2
3	33	32	38	37	35
4	48	45	59	58	57
5	9	11	16	12	13
6	44	43	56	52	48.9
7	11	14	16	17	13
8	13	15	19	17	16
9	46	38	56	52	53
10	41	42	51	47	49
11	48.4	42	56.3	53	54
12	33	35	41	42	37
13	12	16	22	24	23
14	29	28	35	36	32
15	30	28	36	37	36
16	28	22	34	36	29
17	25	26	34	34	29.7

Chapter 7

Development of bioactive nanocomposite packaging films for control of the stored product pest *Sitophilus oryzae* in rice with and without irradiation

This manuscript will be submitted to ***Journal of Stored Products Research***, Impact factor: 2.831, h-index: 82, Overall Ranking: 7350, SCImago Journal Rank: 0.66

Tofa Begum^a, Peter A. Follett^b, Lily Jaiswal^a, Anais Nehr^c, Stephane Salmieri^a, Monique Lacroix^{a,*}

^aResearch Laboratories in Sciences, Applied to Food, Canadian Irradiation Center, INRS, Armand Frappier Health and Biotechnology Centre, 531, Boulevard des Prairies, Laval, Quebec, Canada, H7V 1B7

^bUnited States Department of Agriculture, Agricultural Research Service, U.S. Pacific Basin Agricultural Research Center, 64 Nowelo Street, Hilo, HI 96720, USA

^cPolytechnic Lille, Lille, Hauts-de-France

*Corresponding author: Monique Lacroix, Ph.D., Email: Monique.Lacroix@inrs.ca

Tel: 450-687-5010 # 4489, Fax: 450-686-5501

and Peter A. Follett, Ph.D., Email: peter.follett@usda.gov

Tel: (808) 959-4303, Fax: (808) 959-5470

Contribution of authors

Tofa Begum conducted the data curation, methodology, writing, review, and manuscript editing. This manuscript was written by the framework planned with guidance from Prof. Monique Lacroix and Dr. Peter A. Follett and they corrected the manuscript several times while contributing intellectual contents. Lily Jaiswal and Stephane Salmieri corrected the manuscript. Anais Nehr participated in the experiments with Tofa Begum.

Résumé

La toxicité fumigène de six huiles essentielles (HE) (HE méditerranéenne, formulation méridionale, HE agrumes, HE cannelle, formulation asiatique, HE thym sarriette), deux extraits d'agrumes (extrait d'agrumes bio-OCE et extrait naturel d'agrumes-NCE), et deux des formulations actives (AF-1 et AF-2) a été étudiée pour lutter contre *Sitophilus oryzae* (charançon du riz). AF-1 était composé d'OCE, d'HE méditerranéenne, d'HE d'agrumes, d'HE de cannelle (2 : 1 : 2 : 1) et AF-2 était composé d'HE, d'HE d'Asie, d'HE du Sud, d'HE de cannelle, d'HE de thym salé (2 : 2 : 1 : 2 : 1). Dans les essais biologiques, deux formulations actives ont montré des propriétés insecticides ($P \leq 0.05$) supérieures à celles des HE et CE individuels, et AF-1 et AF-2 causant 92 et 100 % de mortalité des insectes à 0.6 $\mu\text{L/mL}$ après 72 h d'exposition. De plus, une nanoémulsion huile-dans-eau d'AF-1 et d'AF-2 a été développée en utilisant une technique d'homogénéisation à haute pression de 8000 psi (2e cycle) et 15000 psi (3e cycle) (microfluidisation). Les résultats ont montré que la taille des gouttelettes des émulsions d'AF-1 et d'AF-2 diminuait de 232 à 116 nm et de 230 à 40 nm, respectivement, après microfluidisation tandis que l'efficacité d'encapsulation (EE) correspondante augmentait de 30 à 77 % et de 11.3 à 79 %. Les formulations AF-1 et AF-2 ont montré la plus forte inhibition de l'enzyme acétylcholinestérase (AChE) de 42.6 et 44.5 % ($P > 0.05$) chez les insectes. Par conséquent, un total de six types différents de films nanocomposites bioactifs ont été développés à l'aide de chitosane/nanocrystal de cellulose/polyéthylène glycol (CH/CNC/PEG), poly (adipate de butylène-co-téréphtalate)/nanocrystal de cellulose/glycérol (PBAT/CNC/Gly) et des matrices de diffusion composites à base d'acide polylactique/nanocrystal de cellulose/glycérol (PLA/CNC/Gly) en présence des formulations AF-1 et AF-2 (CH/CNC/PEG/AF-1, CH/CNC/PEG/AF- 2, films PBAT/CNC/Gly/AF-1, PBAT/CNC/Gly/AF-2, PLA/CNC/Gly/AF-1 et PLA/CNC/Gly/AF-2). Les films CH/CNC/PEG/AF-1 et CH/CNC/PEG/AF-2 ont causé 78 et 83 % de mortalité des insectes dans le riz stocké pendant 14 jours, respectivement, tandis que les échantillons témoins (sans films bioactifs) ont montré de manière significative ($P \leq 0.05$) une mortalité inférieure de 6 % après 14 jours de stockage. L'irradiation à 200 Gy seule a causé 62 % de mortalité et a augmenté à 82-100 % lorsqu'elle est combinée avec les films nanocomposites bioactifs à base de CH, PBAT et PLA après 14 jours d'incubation. L'incorporation de CNC dans les matrices polymères a considérablement réduit le pourcentage de libération de composés actifs de 15 à 39 % à partir des films nanocomposites bioactifs à base de CH, PBAT et PLA pendant le stockage par rapport aux films sans CNC. De plus, les analyses sensorielles (odeur, couleur, goût et appréciation globale) des échantillons de riz cuit traités avec des films nanocomposites bioactifs ont été très bien acceptées par les consommateurs.

Abstract

The fumigant toxicity of six essential oils (EOs) (Mediterranean EO, Southern formulation, citrus EO, cinnamon EO, Asian formulation, savory thyme EO), two citrus extracts (organic citrus extract-OCE and natural citrus extract-NCE), and two active formulations (AF-1 and AF-2) were investigated for control of *Sitophilus oryzae* (rice weevil). AF-1 was composed of OCE, Mediterranean EO, citrus EO, cinnamon EO (2 : 1 : 2 : 1), and AF-2 was composed of NCE, Asian EO, Southern EO, cinnamon EO, savory thyme EO (2 : 2 : 1 : 2 : 1). In bioassays, two active formulations showed significantly ($P \leq 0.05$) higher insecticidal properties as compared to the individual EOs and CEs, and AF-1 and AF-2 causing 92 and 100 % mortality of insects at 0.6 $\mu\text{L/mL}$ after 72 h of exposure. Furthermore, an oil-in-water nanoemulsion of AF-1 and AF-2 was developed using 8000 psi (2nd cycle) and 15000 psi (3rd cycle) high-pressure homogenization technique (microfluidization). The droplet size of the emulsions of AF-1 and AF-2 was found to decrease from 232 to 116 nm and from 230 to 40 nm, respectively, while the corresponding encapsulation efficiency (EE) increased from 30 to 77 % and from 11.3 to 79 %. AF-1 and AF-2 showed the highest acetylcholinesterase (AChE) enzyme inhibition of 42.6 and 44.5 % ($P > 0.05$) of insects. Therefore, a total of six different types of bioactive nanocomposite films were developed using chitosan/cellulose nanocrystal/polyethylene glycol (CH/CNC/PEG), Poly (butylene adipate-co-terephthalate)/cellulose nanocrystal/Glycerol (PBAT/CNC/Gly) and Poly lactic acid/cellulose nanocrystal/Glycerol (PLA/CNC/Gly)-based composite diffusion matrices loaded with AF-1 and AF-2 (CH/CNC/PEG/AF-1, CH/CNC/PEG/AF-2, PBAT/CNC/Gly/AF-1, PBAT/CNC/Gly/AF-2, PLA/CNC/Gly/AF-1 and PLA/CNC/Gly/AF-2 film). CH/CNC/PEG/AF-1 and CH/CNC/PEG/AF-2 films caused 78 and 83 % mortality of insects in stored rice for 14 days, respectively, while the control samples (without bioactive films) showed ($P \leq 0.05$) a low mortality of 6 % after 14 days of storage. Irradiation treatment at 200 Gy alone caused 62 % mortality and increased to 82-100 % when combined with the bioactive CH-, PBAT- and PLA-based nanocomposite films after 14 days of incubation. Incorporation of CNC into the polymeric matrices significantly reduced the % release of active compounds by 15-39 % from the bioactive CH-, PBAT- and PLA-based nanocomposite films during the storage as compared to the films without CNC. Furthermore, the sensory analyses (odor, color, taste, and global appreciation) of cooked rice samples treated with bioactive nanocomposite films were highly acceptable by consumers.

7.1. Introduction

Stored products' insect pests can seriously damage the quality and quantity of post-harvest agricultural products such as cereals, grains, dried fruits, and vegetables up to 10-40 % in temperate and tropical zones (Ogendo *et al.*, 2008; Khani *et al.*, 2017). Moreover, insect pests contaminate the cereal grains by excreting as well as influencing the growth of storage molds. The rice weevil, *Sitophilus oryzae* L. (Coleoptera: Curculionidae), is considered one of the most destructive and troublesome insects worldwide (Hossain *et al.*, 2019b). Over 70 % of stored products are treated by the fumigation of methyl bromide (MeBr) and phosphine (PH₃) as SIROFLO® and ECO2FUME® for more than 70 years. Both fumigants have become restricted under the Clean Air Act and Montreal Protocol because of the potential ozone-depleting properties of MeBr and the increasing resistance of insects to PH₃ as well as their genotoxic properties (Lee *et al.*, 2004a).

In recent years, essential oils (EOs) and their chemical constituents derived from plants are getting more focus as a possible replacement for MeBr and PH₃ because of their insecticidal, repellent, antibacterial, antifungal, antiviral properties (Hossain *et al.*, 2016b; Hossain *et al.*, 2018; Begum *et al.*, 2020b; Hossain *et al.*, 2021; Begum *et al.*, 2022a). The EOs could be used safely as natural fumigants against harmful insect pest infestation of cereal grains during storage owing to their lower mammalian toxicity and low persistence in the environment (Ogendo *et al.*, 2008). Moreover, there is a very low chance to develop insect resistance to EOs because the major and minor components that exist in the EO that show multiple modes of action against a wide range of stored product insects (Hategekimana and Erler, 2020). The EOs (*Origanum compactum*, *Origanum heracleoticum*, *Citrus sinensis*, *Cinnamomum verum*, *Cymbopogon flexuosus*, *Thymus satureioides*, etc.) from the plant families of Rutaceae, Poaceae, Lauraceae, Citraceae, Asteraceae, Lamiaceae, Meliaceae, and Myrtaceae have been broadly studied because of their insecticidal activities against stored product insects (Demirel and Erdogan, 2017; Hategekimana and Erler, 2020; Castillo-Morales *et al.*, 2021).

The use of EOs for stored products preservation has some limitations because of their high volatile nature, lower water solubility, and lower stability, moreover, EOs are sensitive to several environmental factors such as high temperature, pH, moisture, light, oxidation, and so on (Das *et al.*, 2021b). Researchers have long wondered that the development of oil-in-water (o/w) emulsion of EOs, then passed through a high-pressure homogenization technique (e.g., microfluidizer) could reduce the drawbacks of EOs and thus, help to achieve submicrometer droplet size with improved solubility, bioavailability, physical stability and enhanced encapsulation efficiency

(Llinares *et al.*, 2018; Hossain *et al.*, 2019a). Moreover, the incorporation of EOs and o/w nanoemulsion into the polymeric matrix as a bio-based delivery system and their use as insecticidal packaging films could be an alternative way to control stored product insect pests (Hossain *et al.*, 2014b; Hossain *et al.*, 2019b). Incorporation of EOs into polymeric matrices can improve the controlled release of active ingredients during a long storage time as well as reduce the utilization of chemical insecticides (Kim *et al.*, 2016).

Currently, biodegradable biopolymers (polysaccharides, proteins, lipids) are getting more attention to reach sustainable development goals by the replacement of synthetic non-degradable materials. Biopolymers such as chitosan (CH), Poly (butylene adipate-co-terephthalate) (PBAT), and polylactic acid (PLA) are commercially available polymeric materials (Khan *et al.*, 2012; Su *et al.*, 2020). Chemically, PBAT is an aliphatic-aromatic copolyester that is flexible, biodegradable, and compostable certified by the European Bioplastics (EN13432 standard criteria) and the Biodegradable Polymers Institute (ASTM D6400 standard specification) (Morelli *et al.*, 2016; Shankar and Rhim, 2018). PLA is another type of biodegradable polymer produced from renewable sources and it is getting more attention because of its availability, good mechanical properties, transparency, and easy processibility (Salmieri *et al.*, 2014a, b). Chitosan (CH) is derived from chitin and is mostly found in insect cuticles and in the cell wall of fungi. Moreover, CH is approved by the FDA as a food ingredient because it is biocompatible, non-toxic, and bio-functionality (Khan *et al.*, 2012; Hossain *et al.*, 2019a). Cellulose nanocrystals (CNCs) are used as reinforcing agents into polymeric matrices which can improve the mechanical and barrier properties of the biopolymer as well as can improve the controlled release of active ingredients over storage time (Khan *et al.*, 2012; Hossain *et al.*, 2018).

Another efficient and emerging technique for insect disinfestation is ionizing irradiation (Follett *et al.*, 2013; Hossain *et al.*, 2014b). 400 Gy to 1000 Gy irradiation doses are recommended for insect disinfestation (Hallman, 2013). A 120 Gy irradiation dose can sterilize the rice weevil *S. oryzae* for two weeks of storage (Follett *et al.*, 2013). However, bioactive packaging in combination with irradiation could work synergistically to reduce the concentration of EOs as well as the radiation dose and improve the radiosensitivity of the insect pests (Hossain *et al.*, 2014a; Lacroix and Follett, 2015; Hossain *et al.*, 2019a). The objectives of the current study were to (i) evaluate the fumigation effect of EOs and two active formulations against rice weevil, (ii) evaluate the acetylcholinesterase enzyme inhibition capacity of EOs, (iii) develop anti-insect films by incorporating EOs and a reinforcing agent, (iv) determine the insecticidal efficiency of the developed films in combination with γ -irradiation, (v) evaluate the effect of reinforcing agents in terms of controlled release of

active ingredients, and (v) evaluate the sensorial properties of the rice stored on the bioactive films.

7.2. Materials and Methods

7.2.1. Rearing of rice weevil

The rice weevil (*S. oryzae* L.) was collected from the Cereal Research Center, Agriculture and Agri-food Canada, Winnipeg, Manitoba. The weevils (~200 adults) were reared in a well-ventilated 2 L plastic container that was contained rice (Super quality basmati rice, Quebec, Canada). Then, the container was incubated at 28 °C (65 % RH) for 12 : 12 h light : dark conditions inside the controlled incubator. Rice used throughout the experiments was sterilized by applying γ -irradiation at 3 kGy (Hossain *et al.*, 2021).

7.2.2. Preparation of essential oils (EOs)

The essential oils (EOs) of citrus, cinnamon, and savory thyme were procured from Zayat Aroma (Bromont, QC, Canada). Southern formulation, Asian formulation, and Mediterranean formulation were bought from BSA (Montreal, Quebec, Canada). The organic citrus extract (OCE) and natural citrus extract (NCE) were supplied by Kerry (Beloit, Wisconsin, USA). Two active formulations, mixture of EOs and citrus extracts, were used throughout the experiment which was developed based on our previous study (Begum *et al.*, 2022b). The active formulations were named AF-1 and AF-2. AF-1 was prepared by a mixture of OCE, Mediterranean EO, citrus EO, and cinnamon EO at the ratio of 2 : 1 : 2 : 1, while the AF-2 was prepared by a mixture of NCE, Asian EO, Southern EO, cinnamon EO, savory thyme EO at 2 : 2 : 1 : 2 : 1.

7.2.3. Dose-response fumigation toxicity tests of natural insecticides

The fumigation toxicity tests of eight EOs/CEs (OCE, NCE, Southern formulation, Asian formulation, Mediterranean formulation, citrus, cinnamon, and savory thyme) and two active formulations (AF-1 and AF-2) were tested against *S. oryzae* following Hossain *et al.* (2019b). Briefly, an aliquot of 0.2, 0.4, 0.6, 0.8, and 1.6 μ L/mL of EOs/CEs and active formulations were applied to a small sponge (5 × 5 × 4 mm) and transferred into a 10 mL cup covered with muslin screen. The EOs/CEs and active formulation containing cups were fixed onto the lid of the Petri

dish (95 × 15 mm) with sterile rice (10 g) and combined with 25 adult rice weevils. Each Petri dish was covered and sealed with laboratory Parafilm® and incubated at 28 °C (65 % RH) for 72 h. Each experiment was performed in triplicate (n = 3). The mortality (%) of insects was calculated at 24, 48, and 72 h with Eq. 7.1.

Mortality (%) = (Number of dead insect / Total number of insect) × 100 Eq. 7.1

7.2.4. Determination *in vivo* acetylcholine esterase (AChE) activity

To understand the mechanism of insect mortality after fumigation of EOs/CEs and active formulations, a colorimetric method was used to determine the AChE enzyme (Abdelgaleil *et al.*, 2009; Ali-Shtayeh *et al.*, 2014). Briefly, 0.5 g of a whole-body preparation of rice weevil (*S. oryzae*) was homogenized in 5 mL ice-cold phosphate buffer (0.1 M, pH 7.0), followed by the resulting homogenates passed through a centrifugation treatment at 5,000 rpm for 20 min at 0 °C. Then, the supernatants were collected for AChE activity assessment. The EOs/CEs, AF-1, and AF-2 were diluted in methanol to obtain 20 µL/mL of concentration. A 96-well plate was loaded with 25 µL of 15 mM Acetylthiocholine iodide (ATChI) in water, 125 µL of 3 mM 5, 5'-dithio-bis (2-nitrobenzoic) acid (DTNB) in buffer, and 25 µL of insecticide diluted in methanol, then the absorbance of the reaction mixture was measured at 405 nm. Thereafter, an aliquot of 25 µL of AChE enzyme solution was added to each well and followed by incubation at 37 °C for 10 min and read the absorbance at 405 nm 10 times at 1 min intervals. The control samples were prepared by using 25 µL of methanol instead of the insecticide. The AChE enzyme inhibition (%) was calculated with Eq. 7.2.

Inhibition (%) = 1 - (Absorbance of sample / Absorbance of control) × 100 Eq. 7.2

7.2.5. Development of nanoemulsion of active formulations

An oil-in-water (o/w) emulsion of AF-1 and AF-2 was prepared using a 2 % (v/v) active formulation and a 2 % (w/v) Tween-80 as emulsifier. Thereafter, the o/w emulsions were homogenized using an Ultra Turax (TP18/1059 homogenizer) at 15000 rpm for 1 min which was considered as coarse emulsion. Then, the coarse emulsions of AF-1 and AF-2 were passed through a high-pressure microfluidizer (Microfluidics Inc., Newton, MA, USA) at 8000 PSI (2nd cycle) and 15000 PSI (3rd cycle), respectively, to obtain the nanoemulsion of AF-1 and AF-2.

7.2.6. Preparation of insecticidal film

CH/CNC/PEG, PBAT/CNC/Glycerol, and PLA/CNC/Glycerol-based composite diffusion matrices loaded with AF-1 and AF-2 formulations were developed. Briefly, a quantity of 0.12 g CNC (from 2 % w/w suspension) was added to 2 g of chitosan (CH) dissolved in 2 % aqueous acetic acid and followed by a 1 % nanoemulsion of AF-1 or AF-2 was added and then 0.5 % polyethylene glycol (PEG) was mixed with the film forming solution. The film-forming solution was homogenized overnight using with IKA RW-20 mechanical homogenizer at 1,500 rpm. After mixing properly, the film-forming solutions (15 mL) were poured onto a petri dish (95×16 mm; Sarstedt, Newton, USA) and dried for 24 h at room temperature. The CH-based nanocomposite films were prepared based on our previous experiment (Chapter 5). PBAT-based nanocomposite films prepared using a 2 g of PBAT were mixed with 0.375 % CNC, 300 µL of AF-1, and 0.625 % glycerol (0.375 %) and then hot pressed by a compression molding machine. Similarly, a mixture of PBAT (2 g), CNC (0.5 %), AF-2 (300 µL), and Gly (0.625 %) was hot pressed to develop PBAT-based nanocomposite film containing AF-2. For PLA-based films, a quantity of 1 % CNC, 300 µL AF-1, and 1 % glycerol were incorporated into PLA (2 g) matrices using hot-pressed compression molding. A quantity of 0.5 % CNC, 300 µL AF-2, and 1 % glycerol were loaded into 2 g of PLA matrix to develop insecticidal films.

7.2.7. *In-situ* insecticidal evaluation of the film combined with and without irradiation

The insecticidal properties of the six nanocomposite films (CH/CNC/PEG/AF-1 film, CH/CNC/PEG/AF-2 film, PBAT/CNC/Gly/AF-1 film, PBAT/CNC/Gly/AF-2 film, PLA/CNC/Gly/AF-1 film, PLA/CNC/Gly/AF-2 film) were tested against the rice weevil (*S. oryzae*) (Hossain *et al.*, 2014b; Hossain *et al.*, 2019b). Briefly, a total of 15 rice weevils were inoculated into a plastic bag containing 30 g of rice, then two pieces of each insecticidal film were inserted into the plastic bag and stored for 14 days. The samples were divided into two sets: one set of samples were containing only insecticidal film and 2nd set of the film was combined with 100-300 Gy of γ -irradiation using UC-15A γ -irradiator equipped with Cobalt-60 (Nordion, Laval, QC, Canada). The rice samples without insecticidal nanocomposite films were considered as control. Moreover, the rice samples were also treated alone with irradiation at 100, 200, and 300 Gy to determine the insecticidal effect of irradiation during 14 days of storage. The insect mortality was recorded on days 1, 3, 7, 10, and 14. The rice weevils were considered as dead when their appendages were not moving even after probing with a fine camel hair brush. The experiments were performed in three replicates for each set of samples.

7.2.8. Release profile of active components from the insecticidal films

The controlled release of active formulations from the insecticidal films with and without the presence of CNCs was studied as described by [Hossain *et al.* \(2019a\)](#). Twelve types of insecticidal films (CH/CNC/PEG/AF-1 film, CH/PEG/AF-1 film, CH/CNC/PEG/AF-2 film, CH/PEG/AF-2 film, PBAT/CNC/Gly/AF-1 film, PBAT/Gly/AF-1 film, PBAT/CNC/Gly/AF-2 film, PBAT/Gly/AF-2 film, PLA/CNC/Gly/AF-1 film, PLA/Gly/AF-1 film, PLA/CNC/Gly/AF-2 film, and PLA/Gly/AF-2 film) for evaluating the effect of reinforcing agents CNCs on controlled release in two months stored rice. Briefly, the sterile rice grains were stored with the insecticidal films (1 g/cm²) at 28 °C (65 % RH) for 8 weeks. Each week a small piece of film sample (500 mg) was excerpted from the rice grains and mixed with a volume of 10 mL ethanol for 5-6 hours with mild agitation. After 5-6 hours, the extraction of active formulations was collected, and the absorbance was measured using UB-Vis spectrophotometer at 320 nm. The initial concentration of active compounds in each type of film was determined before they were put into the chamber. The decreased concentration of active compounds in the film samples was considered as the release of active compounds.

7.2.9. Sensory analyses of the rice under different films treatment

The sensory attributes (odor, color, taste, and global appreciation) of rice were evaluated under the treatment of six insecticidal nanocomposite films (CH/CNC/PEG/AF-1 film, CH/CNC/PEG/AF-2 film, PBAT/CNC/Gly/AF-1 film, PBAT/CNC/Gly/AF-2 film, PLA/CNC/Gly/AF-1 film, PLA/CNC/Gly/AF-2 film) for 1 month of storage ([Hossain *et al.*, 2019a](#); [Das *et al.*, 2021b](#)). The rice samples without insecticidal nanocomposite films were considered as control. A total of 13 panelists participated in the sensory attributes of the control and treated rice under six different insecticidal films. One stored rice (with and without insecticidal films) was cooked with water at a ratio of 1 : 2 (rice-to-water) for about 25 min, thereafter the cooked rice samples were taken into small coded cups and served to the consumers. All consumers were asked to evaluate the cooked rice using a nine-point hedonic scale and the scales were “Like extremely = 9, Like very much = 8, Like moderately = 7, Like slightly = 6, Neither like nor dislike = 5, Dislike slightly = 4, Dislike moderately = 3, Dislike very much = 2, Dislike extremely = 1”.

7.2.10. Statistical analyses

The fumigation toxicity effect of EOs/CEs, AF-1 and AF-2 against the rice weevil was measured as % mortality after 24, 48, and 72 h of exposure. The experiments were carried out in triplicates. The % mortality of insects was subjected to ANOVA analyses for variance and means separations by Duncan's test at $\alpha = 0.05$ using SAS Institute, 2014. Moreover, the effect of CNCs in the insecticidal films on the controlled release of active formulations was performed in triplicates and the comparison was performed using t-tests. Each experiment was performed three times and each time contained three samples.

7.3. Results and discussions

7.3.1. Dose-response fumigation toxicity tests of natural insecticides

The insecticidal properties of the six EOs, two citrus extracts, and two active formulations at different concentrations against rice weevil (*S. oryzae*) were measured for 24, 48, and 72 h (Table 7.1). At the lowest contact time (24 h), the AF-1 showed the highest % mortality of 12 and 31 % against *S. oryzae* when exposed to 0.2 and 0.4 $\mu\text{L}/\text{mL}$ of AF-1 ($P \leq 0.05$), respectively. A quantity of 0.6, 0.8, and 1.6 $\mu\text{L}/\text{mL}$ AF-2 showed 32, 38, and 52 % of insect mortality ($P \leq 0.05$), respectively, at the shortest exposure time of 24 h. A 32, 39, and 43 % ($P \leq 0.05$) insect mortality was found when the rice weevil was exposed to 0.6, 0.8, and 1.6 $\mu\text{L}/\text{mL}$ AF-1, respectively, at 24 h. The EOs of cinnamon and Mediterranean showed 41 and 30 % mortality ($P \leq 0.05$) of insects, respectively, at 1.6 $\mu\text{L}/\text{mL}$ after 24 h. It is noticeable that the % mortality of insects was higher when treated with a higher concentration of insecticidal agents.

After 48 h of incubation time, the vapor of AF-2 showed significantly ($P \leq 0.05$) higher mortality (53 %) of rice weevil at the lowest concentration (0.2 $\mu\text{L}/\text{mL}$), followed by cinnamon EO (40 %), Mediterranean EO (38 %), AF-1 (36 %) at 0.2 $\mu\text{L}/\text{mL}$. 91 and 84 % mortalities were shown by AF-2 and AF-1 (0.8 $\mu\text{L}/\text{mL}$) which was significantly ($P \leq 0.05$) higher than the insecticidal agent performed alone. After 72 h of incubation, the number of dead insects was significantly increased ($P \leq 0.05$) as compared to 24 and 48 h. The vapor of AF-2 showed significantly higher toxicity against rice weevil (mortality: 82 %), followed by Asian formulation (73 % mortality), AF-1 (69 % mortality), Mediterranean EO (66 % mortality), Southern formulation (58 % mortality), cinnamon EO (56 %), citrus EO (54 %), savory thyme (53 %), OCE (4 %) and NCE (2.7 %) at the lowest concentration (0.2 $\mu\text{L}/\text{mL}$) after 72 h of fumigation effect. The AF-1 and AF-2 caused 92 and 100

% insect mortality, respectively, at 0.6 $\mu\text{L/mL}$ after 72 h which was significantly higher than the insecticidal efficiency of EO and CE alone. At 0.8 $\mu\text{L/mL}$ concentration of AF-1 and AF-2 caused 100 % insect mortality after 72 h, while the single insecticidal agents OCE, NCE, Mediterranean EO, Southern formulation, Citrus EO, Cinnamon EO, Asian formulation, savory thyme caused 11, 4, 84, 92, 80, 64, 93 and 71 % of insects, respectively, at 0.8 $\mu\text{L/mL}$ after 72 h of incubation time.

A review of the literature revealed that the plant-derived EOs and their components including the current EOs used in the study showed fumigation toxicity effects against several stored product insects. For instance, [Hossain et al. \(2019b\)](#) tested eight EOs such as cinnamon, basil, mandarin, eucalyptus, tea tree, oregano, thyme, and peppermint, and one mixture of EOs (oregano : thyme EO) against *S. oryzae* using fumigation toxicity test. The authors reported that the eucalyptus EO caused 100 % insect mortality after 24 h of exposure at 0.8 $\mu\text{L/mL}$. Moreover, the authors also observed that the individual EO of oregano and thyme caused 33.33 and 80 % mortality of *S. oryzae*, while the combination of oregano:thyme EO caused 100 % insect mortality at 2.4 $\mu\text{L/mL}$ after 72 h of exposure ([Hossain et al., 2019b](#)). [Hategekimana and Erler \(2020\)](#) conducted a comparative repellent study of a single, binary, and ternary combination of EOs (anise EO, eucalyptus EO, and peppermint EO) and their major chemical components correspondingly (trans-anethole, 1,8-cineole, and L-menthol) on *S. oryzae*. The authors found that the binary and ternary combinations required a lower concentration of EO to show RC_{50} (Repellency concentration: the concentration required to show 50 % repellency) as compared to the single EO and their major chemical components ([Hategekimana and Erler, 2020](#)). The results obtained in the current study suggest that the mixtures of EOs and CEs (AF-1 and AF-2) have strong fumigation activities against *S. oryzae* as compared to the individual EO or CE.

Table 7.1. Insecticidal properties of the different volume of the essential oils against rice weevil until 72 hours of exposure.

Time (hours)	µL/mL	OCE	NCE	Mediterranean EO	Southern formulation	Citrus EO	Cinnamon EO	Asian formulation	Savory thyme EO	Active formulation 1	Active formulation 2
24	0.2	1.3±0.5 ^{aB}	1.3±0.5 ^{bB}	10±0.5 ^{aC}	2.0±0.5 ^{bB}	0±0 ^{aA}	10±2.0 ^{aC}	0±0 ^{aA}	1.3±0.5 ^{aB}	12±1.0 ^{aD}	8±1.0 ^{bC}
	0.4	2.7±0.5 ^{aB}	1.3±0.5 ^{bB}	20±2.6 ^{bD}	0±0 ^{aA}	1.0±0.5 ^{bB}	17±2.0 ^{bD}	8.0±1.7 ^{cC}	2.1±0.3 ^{aB}	31±3.1 ^{bE}	4±2.0 ^{aB}
	0.6	4.0±1.0 ^{aA}	2.7±1.1 ^{bA}	17±2.5 ^{bB}	1.0±0.5 ^{bA}	1.0±0.5 ^{bA}	19±1.5 ^{bB}	4.0±1.0 ^{bA}	3.1±0.5 ^{aA}	32±4.2 ^{bC}	32±1.0 ^{cC}
	0.8	2.7±1.1 ^{aB}	0±0 ^{aA}	13±2.0 ^{aC}	12±1.7 ^{cC}	0±0 ^{aA}	28±1.7 ^{dD}	2.0±1.1 ^{bB}	4.0±1.1 ^{aB}	39±1.5 ^{cE}	38±2.3 ^{dE}
	1.6	2.7±1.0 ^{aB}	0±0 ^{aA}	30±1.5 ^{cE}	2.0±1.1 ^{bB}	9.0±1.1 ^{cD}	41±6.5 ^{eF}	0±0 ^{aA}	5.4±1.6 ^{bC}	43±1.5 ^{dF}	52±2.6 ^{eG}
48	0.2	2.7±1.1 ^{aA}	2.7±1.1 ^{bA}	38±2.8 ^{dE}	29±1.1 ^{dD}	1.3±0.5 ^{bA}	40±2.6 ^{fF}	18±0.5 ^{dC}	5.3±0.5 ^{bB}	36±3.6 ^{cE}	53±2.5 ^{eG}
	0.4	4.0±1.0 ^{aA}	1.3±0.5 ^{bA}	45±4.6 ^{eF}	37±3.2 ^{eE}	13±0.5 ^{dC}	24±2.6 ^{cD}	25±3.0 ^{eD}	7.1±0.3 ^{bB}	51±3.0 ^{eG}	56±2.9 ^{fH}
	0.6	6.7±0.5 ^{bA}	4.0±1.7 ^{bA}	65±4.0 ^{gG}	34±2.5 ^{eE}	20±3.0 ^{eC}	23±2.5 ^{cC}	26±2.5 ^{eD}	14±1.9 ^{cB}	57±3.1 ^{fF}	67±0.6 ^{gG}
	0.8	6.7±1.1 ^{bB}	0±0 ^{aA}	54±5.1 ^{fG}	50±3.2 ^{fF}	28±1.7 ^{fD}	51±1.5 ^{hF}	32±1.0 ^{fE}	21±3.1 ^{dC}	84±1.0 ^{iG}	91±2.1 ^{hH}
	1.6	6.7±1.0 ^{bB}	0±0 ^{aA}	54±0.6 ^{fF}	51±1.5 ^{fE}	48±3.0 ^{gE}	56±4.5 ⁱ	30±5.0 ^{fC}	38±4.2 ^{eD}	72±4.6 ^{gG}	76±2.0 ^{hH}
72	0.2	4.0±1.7 ^{aA}	2.7±1.1 ^{bA}	66±3.2 ^{gD}	58±4.5 ^{gC}	54±2.0 ^{hB}	56±2.6 ^{iB}	73±3.1 ^{gE}	53±1.5 ^{fB}	69±2.5 ^{gD}	82±1.5 ^{fF}
	0.4	5.3±0.5 ^{bB}	1.3±0.5 ^{bA}	70±4.1 ^{hE}	75±2.5 ^{hF}	69±1.5 ^{iE}	38±1.5 ^{eC}	78±2.3 ^{hF}	61±4.1 ^{gD}	80±4.2 ^{hG}	94±2.3 ^{iH}
	0.6	8.0±1.0 ^{bA}	7.0±1.1 ^{cA}	76±6.2 ^{iD}	83±1.5 ^{iE}	69±3.0 ^{iC}	47±3.7 ^{gB}	85±3.5 ^{eE}	69±3.9 ^{hC}	92±1.0 ^{jF}	100±0 ^{kG}
	0.8	11±1.5 ^{cB}	4.0±1.0 ^{bA}	84±2.0 ^{jF}	92±2.1 ^{jG}	80±2.6 ^{jE}	64±4.5 ^{jC}	93±1.5 ^{jG}	71±1.1 ^{iD}	100±0 ^{kH}	100±0 ^{kH}
	1.6	13±2.3 ^{cB}	7.0±0.5 ^{cA}	86±1.1 ^{jD}	92±2.1 ^{jE}	92±2.1 ^{KE}	77±3.7 ^{kC}	95±4.1 ^{KE}	75±3.7 ^{jC}	100±0 ^{kF}	100±0 ^{kF}

Values means ± standard error. Within each column means with different lowercase letter are significantly different ($P \leq 0.05$), while the means with the different uppercase letter are significantly different ($P \leq 0.05$).

It has been observed from the current study that the toxicity of EOs/CEs, AF-1 and AF-2 was both concentration-dependent and time-dependent. The active formulations used in the current study were composed of Mediterranean EO, Southern formulation, citrus EO, cinnamon EO, Asian formulation, savory thyme, OCE, and NCE (Begum *et al.*, 2022b). These components have been reported by several authors because of their high insecticidal efficiency against several stored product insect pests (Karabörklü *et al.*, 2010; Tandorost and Karimpour, 2012; Trivedi *et al.*, 2017; Hossain *et al.*, 2021). Monoterpenoids are present in the many plant EOs which are responsible for insecticidal efficiency. Monoterpenoids are lipophilic volatile compounds that can penetrate insects and disrupt their physiological functions (Khani *et al.*, 2017). Besides, OCE and NCE showed the least insecticidal efficiency when they were applied alone even though with high concentration and longest incubation time which might be because of their non-volatile nature and different levels of major and minor chemical constituents. Moreover, the presence of more hydroxyl groups (-OH) in the major and minor chemical constituents of EOs/CEs could lower the insecticidal efficacy and the presence of more carbonyl groups (C=O) in the EOs/CEs could raise the insecticidal efficiency (Abdelgaleil *et al.*, 2009; Hossain *et al.*, 2019b). Insecticidal efficiency caused by EOs may occur in direct action as well as indirect action. In direct action, the oil vapor can exert the insecticidal effect by inhibiting acetylcholinesterase (AChE) enzyme and blocking the octopamine and γ -aminobutyric acid receptor sites, which could lead to neurotoxicity and death. In the indirect action, EOs can interact with the insect hormone and pheromone systems, cytochrome P450 monooxygenase, and insect growth regulators, and thus, affect their biochemical and physiological levels and lead to death (Fierascu *et al.*, 2020). Moreover, the EOs can be ingested, absorbed by the skin as well as inhaled by insect pests.

In the current study, AF-1 and AF-2 showed stronger insecticidal properties as compared to the single EO and CE because of their phytochemical diversity from different EOs/CEs in the formulation. The active formulation showed broad-spectrum insecticidal activity as they contain several major and minor chemical ingredients as well as there is less chance for insect to resistant. Different chemical ingredients presented in the active formulations show multiple ways to control insect growth. Some minor chemical ingredients may not have strong insecticidal efficiency when applied alone, but they may act synergistically with other chemical ingredients (Bakkali *et al.*, 2008; Hossain *et al.*, 2019b).

7.3.2. *In vivo* determination of acetylcholine esterase (AChE) activity

In the present study, the inhibitory effects of individual EOs, CEs, and two active formulations (AF-1 and AF-2) were studied on the inhibitory activity of AChE that was extracted from the insects and the results are depicted in Figure 7.1. All tested EOs, CEs, AF-1 and AF-2 showed AChE inhibitory activities. Among them, AF-2 was found to exert the highest AChE inhibitory activity (44.5 %), followed by AF-1 which showed an insignificantly lower AChE inhibitory activity of 42.6 % ($P > 0.05$) as compared to AF-2. The EOs from Asian formulation, citrus, Southern formulation, savory thyme, cinnamon, OCE, Mediterranean, and NCE exerted significantly ($P \leq 0.05$) lower AChE inhibitory activity as compared to AF-1 and AF-2, and the catalytic activity of AChE was 34.8, 31.8, 29.5, 25.7, 24.7, 22.9, 21.9, and 19.7 %, respectively (Figure 7.1). Upon assessing the results, it has been stated that the higher mortality (%) of insects by EOs was not always related to the higher inhibitory efficiency of the AChE enzyme. For example, the OCE and Mediterranean EO showed 2.7 and 30 % insect mortality at 1.6 $\mu\text{L}/\text{mL}$ after 24 h of exposure ($P \leq 0.05$), respectively, however, OCE showed higher AChE inhibitory capacity than Mediterranean EO.

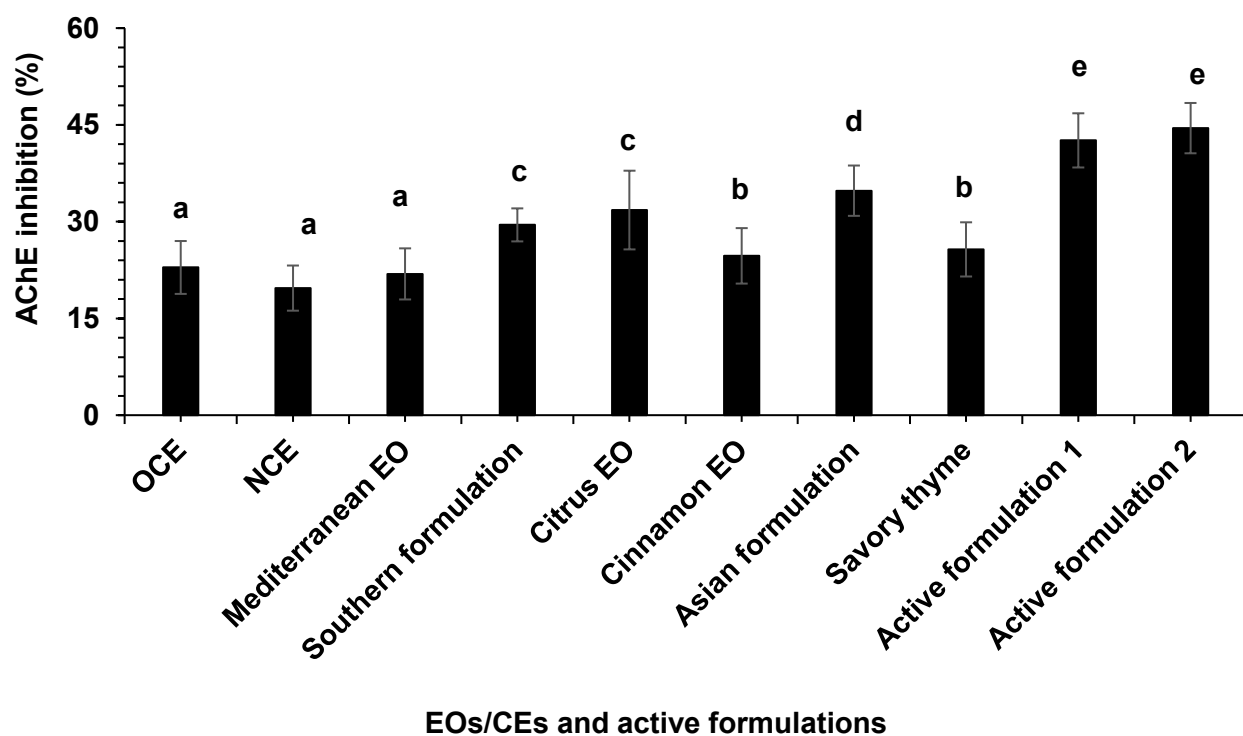


Figure 7.1. Acetylcholinesterase (AChE) enzyme activities of various EOs, CEs and active formulations against rice weevil. Values are means \pm standard error. Same values for each treatment that don't have same lowercase letters are significantly different ($P \leq 0.05$).

EOs and their compounds are absorbed through insect cuticles in direct contact application and fumigation/indirect application, and the EOs and their compounds are ingested through the respiratory and digestive systems (Lee *et al.*, 2004a; Garrido-Miranda *et al.*, 2022). There, they target the AChE enzyme of insects because AChE is the major key enzyme in the central nervous system of insects, and inhibiting AChE activity in insects is one of the major targets of developing insecticidal agents (Zarrad *et al.*, 2015). EOs and their chemical compounds in the active formulations act as competitive and uncompetitive inhibitors and block the activity of the AChE enzyme. AF-1 and AF-2 showed higher AChE inhibitory activity because two or more monoterpenoids or other compounds from the mixture of EOs can interact with one AChE enzyme molecule at a time and the 1st bound EO favors the binding of the 2nd EO, and thus, active formulations used in the study showed higher mortality as well as high AChE enzyme inhibition activity (Lopez *et al.*, 2015; Jankowska *et al.*, 2017). According to manufacturer, the major chemical compounds of cinnamon EO are cinnamaldehyde (55.09 %), cinnamaldehyde acetate (9.75 %), β -caryophyllene (4 %) and p-cymene (2.5 %), savory thyme are borneol (27 %), α -terpineol (11.9 %), camphene (10.5 %), α -pinene+ α -thuyene (6.5 %), β -caryophyllene (5.5 %), carvacrol (5.3 %), p-cymene (3.9 %), linalool (3.7 %), terpinene-4-ol+methyl carvacrol ether (2.9 %), 1,8-cineole+ β -phellandrene (2.9 %) and thymol (2.8 %), Asian formulation contains geraniol (39.1 %), neral (31.6 %), geraniol (6.7 %) and geranyl acetate (3.7 %), Mediterranean EO consists of carvacrol (46.1 %), thymol (17.6 %), γ -terpinene+trans- β -ocimene (14.8 %) and p-cymene (8.5 %) and Southern formulation are composed of carvacrol (82 %), organic citrus extract (OCE) are polyphenols (3.36 %) and flavonoids (0.62 %), and natural citrus extract (NCE) are polyphenols (3.36 %), flavonoids (0.62 %), lauric arginate and fructo-oligosaccharide (Begum *et al.*, 2022b). The active formulations (AF-1 and AF-2) are composed of all those major compounds associated with the EOs and CEs, and thus showed the highest AChE inhibition activity as well as insecticidal activity as compared to single EOs/CEs. Thus, the anti-AChE activity exerted by the active formulations, EOs, and CEs through the neurotoxic mode of action disrupted neurotransmission in insects and caused paralysis and death (Priestley *et al.*, 2006).

In agreement with our study, several authors found that the limonene containing EOs such as citrus EO, orange EO, and citrus extract (CE) was a non-competitive inhibitor of insect AChE enzyme which means they were able to interact with the AChE enzyme alone as well as the enzyme-substrate complex simultaneously (Kim *et al.*, 2013; Zarrad *et al.*, 2015). Limonene showed 51.23 % AChE inhibition of *S. oryzae* at a very low concentration of 1 mg/mL (Kim *et al.*, 2013). Carvacrol and thymol (major chemical compounds of Mediterranean and Southern formulation) showed a potent AChE inhibitory of *S. oryzae* and *Drosophila suzukii* (Lee *et al.*,

2001; Park *et al.*, 2016). López *et al.* (2008); López and Pascual-Villalobos (2010) studied eight monoterpenoids such as linalool, camphor, terpinene, geranyl, S-carvone, E-anethole, fenchone and estragole to inhibit AChE enzyme in three stored products insects (*S. oryzae*, *Rhyzopertha dominica* and *Cryptolestes pusillus*). The authors found that the tested monoterpenoids exerted strong anti-AChE activity except E-anethole (López *et al.*, 2008; López and Pascual-Villalobos, 2010). Moreover, the high anti-AChE activity by EO or CE is not necessarily an indication of high insecticidal activity. For example, Mediterranean EO showed relatively higher fumigant toxicity as compared to organic citrus extract (OCE) against rice weevil, while AChE enzyme inhibition was higher with OCE than above mentioned EOs in the current study which was supported by the observation of Picollo *et al.* (2008), although several studies reported that there is a direct correlation between AChE enzyme inhibition and insecticidal activities by plant-derived EOs. To the best of our knowledge, it is the first time that the mixture of EOs was used as an anti-AChE inhibitor as well as an insecticidal agent against major stored product insects. Upon assessing the previous results, the AF-1 and AF-2 showed higher insecticidal properties as well as higher anti-AChE activities against *S. oryzae*.

7.3.3. Development of nanoemulsion of active formulations

The zeta potential, polydispersity index (PDI), size, and encapsulation efficiency (EE) of AF-1 and AF-2 were evaluated (Table 7.2). Results showed that the o/w emulsion of AF-1 passed through the microfluidisation treatment at a pressure of 8000 PSI and 2 cycles formed a nanoemulsion of AF-1 with a droplet size of 116 nm, a zeta potential of 49 mV and an EE of 77 % which were significantly different ($P \leq 0.05$) as compared to the coarse emulsion of AF-1. The coarse emulsion of AF-1 exhibited a higher droplet size of 232 nm, a lower zeta potential of 22 mV, and a lower EE value of 30 %. Likewise, the nanoemulsion of AF-2 was formed when a microfluidisation pressure of 15000 PSI and 3 cycles were applied, and the nanoemulsion of AF-2 showed a higher EE value of 79 %, a droplet size of 40 nm and a zeta potential of 32.3 mV. The coarse emulsion of AF-2 showed a higher droplet size of 230 nm, an EE of 11.3 %, and a zeta potential of 12 mV (Table 7.2). The polydispersity index (PDI) value is an important parameter that indicates the particle size distribution throughout the o/w emulsion. For example, a larger PDI signifies a broader size distribution and a smaller PDI value signifies a narrower size distribution in an o/w emulsion. In the current study, the coarse emulsions of AF-1 and AF-2 exhibited a significantly ($P \leq 0.05$) broader range of the droplet size distribution as compared to the nanoemulsions of AF-1 and AF-2, with PDI values were 0.56 and 0.63, respectively. However, the droplet size distributions were

significantly ($P \leq 0.05$) narrow for the nanoemulsion of AF-1 and AF-2 with the PDI values were 0.17 and 0.2, respectively, in comparison with the coarse emulsions of AF-1 and AF-2.

Table 7.2. Effect of microfluidisation pressure and number of cycles on the zeta potential (mV), PDI (poly dispersity index), size (nm) and encapsulation efficiency (EE, %) of AF-1 and AF-2.

Active formulations (AF)	Zeta potential (mV)	PDI	Size (nm)	Encapsulation efficiency, EE (%)
Coarse emulsion AF-1	22±3.9 ^a	0.56±0.1 ^b	232±6.1 ^b	30±3.9 ^a
Nanoemulsion AF-1	49±2.16 ^b	0.17±0.02 ^a	116±2.1 ^a	77±3.4 ^b
Coarse emulsion AF-2	12±2.8 ^a	0.63±0.15 ^b	230±9.14 ^b	11.3±5.1 ^a
Nanoemulsion AF-2	32.3±2.8 ^b	0.20±0.02 ^a	40±1.5 ^a	79±1.07 ^b

Values means \pm standard error. Within each column means with different lowercase letter are significantly different ($P \leq 0.05$).

It is well known that the droplets in dispersed systems with lower PDI, higher zeta potential, and smaller size have better encapsulation efficiency and stronger stability which was also proven in the current study when compared to the coarse and nanoemulsions of active formulations. Moreover, a droplet with higher zeta potential, lower size, and narrow PDI could become more stable during the storage period at different conditions by preventing aggregation, creaming, and coalescence which was proven in several studies ([Hossain et al., 2019a](#); [Hossain et al., 2019b](#); [Ben-Fadhel et al., 2020](#)). High-pressure microfluidisation treatment had a significant effect on the stability of the emulsions. Studies found that the nanoemulsions are electrostatically stable and have higher zeta potential values (ranges between very high +30mV and very low -30mV) ([Asmawati et al., 2014](#); [Cheng et al., 2016](#); [Hossain et al., 2019a](#)). In the current study, we obtained the zeta potential for the nanoemulsion of AF-1 (at 8KPSI, 2 cycles) and AF-2 (15KPSI, 3 cycles) was 49 mV and 32.3 mV, respectively, which indicated we obtained electrostatically stable nanoemulsions of AF-1 and AF-2. The stable nanoemulsions of AF-1 and AF-2 as well as active formulations were therefore encapsulated into polymeric matrices to develop biopolymeric films for controlling the rice weevil during storage.

7.3.4. *In-situ* insecticidal evaluation of the film combined with and without irradiation

The six nanocomposite films, named CH/CNC/PEG/AF-1 film, CH/CNC/PEG/AF-2 film, PBAT/CNC/Gly/AF-1 film, PBAT/CNC/Gly/AF-2 film, PLA/CNC/Gly/AF-1 film, PLA/CNC/Gly/AF-2 film, were developed as diffusion matrices to control *S. oryzae* in stored rice as a model of cereal grains and results are depicted in Figure 7.2. The results showed that CH/CNC/PEG-, PBAT/CNC/Gly- and PLA/CNC/Gly-based polymeric matrices having either AF-1 or AF-2 showed a wide range (from lower to higher) of insecticidal properties against rice weevil (*S. oryzae*) (Figure 7.2). The highest insecticidal properties were shown by the bioactive CH/CNC/PEG/AF-2 nanocomposite film against *S. oryzae* at 14 days of storage, followed by CH/CNC/PEG/AF-1 film, PBAT/CNC/Gly/AF-1 film, PBAT/CNC/Gly/AF-2 film, PLA/CNC/Gly/AF-1 film and PLA/CNC/Gly/AF-2 film. Bioactive CH/CNC/PEG/AF-2 nanocomposite film caused 3, 29, 43, 67, and 83 % mortality of insects on day 1, 3, 7, 10, and 14, respectively, whereas the bioactive PLA/CNC/Gly/AF-2 film caused 3, 12, 26, 34 and 49 % mortality over the same period which was significantly lower ($P \leq 0.05$) as compared to the bioactive CH/CNC/PEG/AF-2 film. Samples treated under the treatment of bioactive CH/CNC/PEG/AF-1 film, PBAT/CNC/Gly/AF-1 film, PBAT/CNC/Gly/AF-2 film, PLA/CNC/Gly/AF-1 film and PLA/CNC/Gly/AF-2 film showed 78, 74, 68, 52 and 49 % mortality of insects at day 14, respectively, whereas the control sample (no bioactive nanocomposite films) caused only 6 % mortality at day 14 (Figure 7.2).

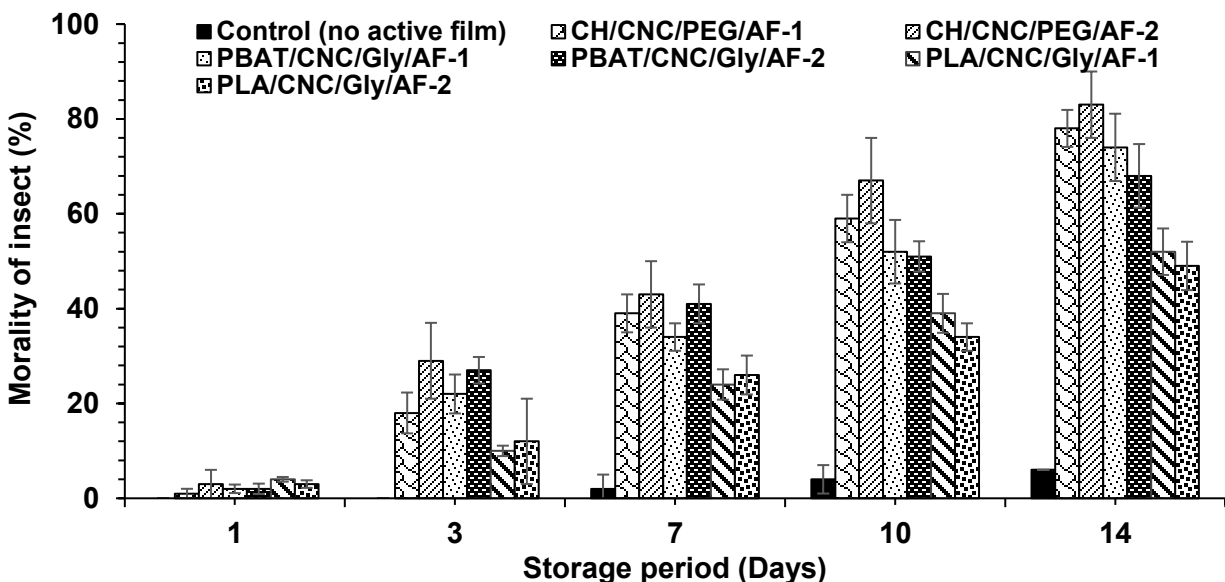


Figure 7. 2. *In situ* fumigation toxicity of different insecticidal films in rice grains for 14 days against *S. oryzae*.

In the above mentioned statement, the *in situ* insecticidal properties shown by six different types of insecticidal nanocomposite films against rice weevil were different even though they contained either AF-1 or AF-2 as insecticidal agents. The significant difference in insect mortality depended on the diffusion rate of the insecticidal compounds which mostly relied on several factors such as the nature and chemical structure of the molecules, type of polymer, the binding affinity between the polymeric matrices and the active compounds, solubility, temperatures, storage time, as well as the degree of crystallinity (Hossain *et al.*, 2019b; Sharma *et al.*, 2021). The significant mortality of insects was shown by CH-based nanocomposite films containing nanoemulsion of AF-2 and followed by CH/CNC/PEG/AF-1 film as compared to PLA-based and PBAT-based nanocomposite films and such results might have occurred because of the smaller droplet size of the nanoemulsion of the AF-2 (40 nm) than AF-1 (116 nm). The nanoemulsions with smaller droplet sizes have better insecticidal properties than coarse emulsions of EOs which was proven by several authors and current studies corroborated those findings (Anjali *et al.*, 2012; Suresh Kumar *et al.*, 2013; Choupanian *et al.*, 2017; Adak *et al.*, 2020). For example, Adak *et al.* (2020) worked with the eucalyptus EO and nanoemulsion of eucalyptus EO against *S. oryzae* and *Tribolium castaneum*. The authors found that the nanoemulsion of eucalyptus EO showed stronger insecticidal properties with the LC₅₀ values from 0.51-0.58 $\mu\text{L}/\text{cm}^2$ and 0.86-1.86 $\mu\text{L}/\text{cm}^2$ against *S. oryzae* and *T. castaneum*, respectively, while the eucalyptus EO required higher concentration of LC₅₀ values of 0.83 and 4.17 $\mu\text{L}/\text{cm}^2$ for *S. oryzae* and *T. castaneum*, respectively (Adak *et al.*, 2020).

Moreover, in the current study the reinforcing agent CNC was incorporated into the polymeric matrices to improve the controlled release of active formulations over the storage period (Boumail *et al.*, 2013; Salmieri *et al.*, 2014b; Deng *et al.*, 2017; Hossain *et al.*, 2018; Hossain *et al.*, 2019a). In line with our current study, Hossain *et al.* (2019b) developed insecticidal chitosan (CH), methylcellulose (MC), and PLA-based nanocomposite films using a mixture of EOs (oregano : thyme) as insecticidal agent and CNC as a reinforcing agent to control the rice weevil in stored rice for 14 days. The authors observed that the CH/CNC-based film containing a nanoemulsion of oregano:thyme EO had the highest insecticidal properties against *S. oryzae* with % mortality of 43 % at 14 days, then followed by MC/CNC-based film containing a nanoemulsion of oregano : thyme EO (% mortality: 27 % at 14 days) and PLA/CNC-based film containing oregano : thyme EO with 20 % mortality of *S. oryzae* at 14 days, and these results were strongly supported by our current findings (Hossain *et al.*, 2019b). The current findings suggest that the encapsulation of active formulations (mixture of EOs and CEs) within the polymeric matrices could control the release of

active ingredients progressively from the bioactive films and thus, protect the stored product cereals from the infestation of insects for a longer storage time.

In the current study, hurdle technology was introduced to control stored product cereal grains. The hurdle technique is to combine two or more techniques for getting a synergistic effect, thus reducing the concentration of each treatment applied alone. There are numerous experiments performed on the use of EOs or CEs to protect stored grains from insect infestation but there were very few studies performed on the combination of ionizing radiation and insecticidal nanocomposite film (hurdle technique) against insect pests. In the current study, the effect of γ -irradiation at different doses on insect mortality was applied alone as well as in combined treatment between six different types of bioactive nanocomposite films and γ -irradiation doses (Table 7.3). The results showed that the mortality of rice weevil increased significantly ($P \leq 0.05$) with increased radiation dose as well as increased incubation period. When the γ -irradiation was applied alone to control *S. oryzae* in store rice for 14 days, an increase of % mortality of insects was observed from 7 days of incubation with higher doses (200-300 Gy) and mortality increased progressively. A 71 % insect mortality was evident when the sample was treated with 300 Gy γ -irradiation alone at day 14, whereas 51 and 62 % mortality was found when the samples were treated with 100 and 200 Gy γ -irradiation, respectively. The control sample (no bioactive film, no irradiation dose) showed only 6 % insect mortality at day 15 (Table 7.3). The mortality observed in this study was slightly lower than previously reported by [Hossain et al. \(2019b\)](#), who irradiated rice weevil present in rice at 100-300 Gy and recorded the mortality 14 days after the irradiation; these authors reported 65, 79 and 100 % insect mortality at the corresponded irradiation doses. Moreover, [Tunçbilek \(1995\)](#) reported that 90 Gy γ -irradiation caused 100 % of *S. oryzae* following 2 week of incubation. So the insecticidal effectiveness shown by γ -irradiation alone may vary depending on several factors such as the dose rate of the radiation source, source-to-product distance, age of insects, and so on ([Begum et al., 2020a](#); [Hossain et al., 2021](#)).

Table 7.3. Mortality (%) of rice weevil treated with γ -irradiation alone and in combination with bioactive CH-, PBAT- and PLA-based nanocomposite films.

Name of samples	Mortality (%)				
	Day 1	Day 3	Day 7	Day 10	Day 14
Control (no film, no radiation)	0±0 ^{aA}	0±0 ^{aA}	2±1.2 ^{aB}	4±1.5 ^{aC}	6±1.8 ^{aE}
100 Gy	0±0 ^{aA}	4±0.32 ^{bB}	16±1.2 ^{bC}	29±2.9 ^{bD}	51±3.4 ^{bE}
200 Gy	0±0 ^{aA}	10±4.1 ^{cdB}	21±2.9 ^{cC}	41±5.1 ^{cdD}	62±4.5 ^{cE}
300 Gy	0±0 ^{aA}	9±1.1 ^{cB}	22±4.1 ^{cC}	55±4.2 ^{cdD}	71±4.1 ^{dE}
100 Gy+CH+CNC+PEG+AF-1	0±0 ^{aA}	45±4.2 ^{iB}	59±3.5 ^{gC}	68±5.4 ^{gD}	92±5.8 ^{hE}
200 Gy+CH+CNC+PEG+AF-1	8±1.8 ^{fA}	56±3.8 ^{klB}	69±3.5 ^{ijC}	85±5.2 ^{lD}	100±0 ^{iE}
300 Gy+CH+CNC+PEG+AF-1	12±3.2 ^{gA}	69±2.7 ^{nB}	89±3.8 ^{nC}	100±0 ^{oD}	100±0 ^{iD}
100 Gy+CH+CNC+PEG+AF-2	2±0.3 ^{bA}	55±6.2 ^{kB}	68±4.8 ^{iC}	86±4.8 ^{iD}	100±0 ^{iE}
200 Gy+CH+CNC+PEG+AF-2	4±0.8 ^{cdA}	69±4.6 ^{nB}	86±3.6 ^{mC}	100±0 ^{oD}	100±0 ^{iD}
300 Gy+CH+CNC+PEG+AF-2	26±3.6 ^{iA}	88±4.1 ^{oB}	100±0 ^{oC}	100±0 ^{oC}	100±0 ^{iC}
100 Gy+PBAT+CNC+Gly+AF-1	4±0.5 ^{cdA}	49±2.5 ^{jB}	65±3.9 ^{hC}	75±5.1 ^{iD}	91±5.5 ^{hE}
200 Gy+PBAT+CNC+Gly+AF-1	8±2.5 ^{fA}	58±2.9 ^{lmB}	75±6.3 ^{lC}	88±4.7 ^{mD}	100±0 ^{iE}
300 Gy+PBAT+CNC+Gly+AF-1	14±2.5 ^{hA}	67±3.6 ^{nB}	86±5.2 ^{mC}	100±0 ^{oD}	100±0 ^{iD}
100 Gy+PBAT+CNC+Gly+AF-2	5±2.1 ^{deA}	36±2.6 ^{gB}	56±3.6 ^{fcC}	67±6.3 ^{gD}	86±4.5 ^{gE}
200 Gy+PBAT+CNC+Gly+AF-2	6±0.5 ^{eA}	50±4.3 ^{jB}	70±4.9 ^{jC}	80±5.5 ^{kD}	100±0 ^{iE}
200 Gy+PBAT+CNC+Gly+AF-2	3±0.6 ^{bcA}	60±5.3 ^{mB}	85±6.2 ^{mC}	100±0 ^{oD}	100±0 ^{iD}
100 Gy+PLA+CNC+Gly+AF-1	2±1.2 ^{bA}	32±4.8 ^{fbB}	42±6.8 ^{ecC}	65±2.9 ^{fdD}	78±4.2 ^{eeE}
200 Gy+PLA+CNC+Gly+AF-1	15±4.1 ^{hA}	49±0.9 ^{jB}	69±5.2 ^{ijC}	85±5.8 ^{iD}	93±4.5 ^{hE}
300 Gy+PLA+CNC+Gly+AF-1	11±2.8 ^{gA}	69±4.5 ^{nB}	72±4.2 ^{kcC}	95±6.8 nD	100±0 ^{iE}
100 Gy+PLA+CNC+Gly+AF-2	0±0 ^{aA}	12±2.3 ^{dB}	30±1.4 ^{dcC}	58±2.8 ^{edD}	72±6.3 ^{deE}
200 Gy+PLA+CNC+Gly+AF-2	4±1.8 ^{cdA}	28±2.5 ^{eB}	56±5.1 ^{fcC}	70±3.6 ^{hdD}	82±5.2 ^{feE}
300 Gy+PLA+CNC+Gly+AF-2	8±2.3 ^{fA}	42±2.5 ^{hB}	65±4.2 ^{hcC}	78±3.9 ^{jdD}	92±4.1 ^{heE}

Values means ± standard error. Within each column means with different lowercase letter are significantly different ($P \leq 0.05$), while the means with the different uppercase letter are significantly different ($P \leq 0.05$).

In the combined treatment between γ -irradiation and CH-based nanocomposite films, the % mortality of insects was significantly higher ($P \leq 0.05$) as compared to the treatment alone (either by γ -irradiation alone or by bioactive CH-based nanocomposite film alone) (Figure 7.2 and Table 7.3). In the case of combined treatment between 100 Gy and CH/CNC/PEG/AF-1 film, the % mortality of rice weevil increased from 45 to 92 % between 3 to 14 days of incubation. Higher irradiation doses of 200 and 300 Gy combined with CH/CNC/PEG/AF-1 film caused 100 % insect mortality both day 14 and day 10. On day 3, the combined treatment between 300 Gy and CH/CNC/PEG/AF-1 film caused 69 % mortality, while the treated sample with 300 Gy irradiation alone caused significantly lower mortality of 9 %. The bioactive CH/CNC/PEG/AF-2 nanocomposite film along with γ -irradiation showed the highest insect mortality among all treatments. The combination between 100 Gy γ -irradiation and CH/CNC/PEG/AF-2 film caused 55 % insect mortality on day 3 while at day 14 the mortality of insects reached at 100 %, while the application of 100 Gy γ -irradiation alone showed significantly lower ($P \leq 0.05$) mortality of 4, 16, 29 and 51 % at day 3, 7, 10 and 14, respectively. Complete mortality of insects was observed in the combination treatment of 200 Gy with CH/CNC/PEG/AF-2 film and 300 Gy with CH/CNC/PEG/AF-2 film at day 10 and day, respectively, whereas the samples treated with 200 and 300 Gy caused only 41 and 22 % ($P \leq 0.05$) mortality at incubation time of 10 and 7 days, respectively (Table 7.3).

Similar observations were found in the case of the bioactive PBAT- and PLA-based nanocomposite films. The bioactive films (PBAT- and PLA-based nanocomposite films) along with 200 and 300 Gy of γ -irradiation were responsible for the complete mortality of experimental insects in between 10-14 days of the incubation period. PBAT-based nanocomposite film containing AF-1 (PBAT/CNC/Gly/AF-1) with 100 Gy γ -irradiation showed from 4-91 % of mortality between days 1 to 14; the insect mortality was increased when radiation doses were increased in combined treatment. Upon assessing the results, the mortality of insects was significantly ($P \leq 0.05$) higher from 8-100 % and 14-100 % at day 1-14 and day 1-10, respectively, in the corresponding treatments 200Gy/PBAT/CNC/Gly/AF-1 film and 300 Gy/PBAT/CNC/Gly/AF-1 film (Table 7.3). PBAT-based nanocomposite film containing AF-2 (PBAT/CNC/Gly/AF-2) along with 100, 200, and 300 Gy γ -irradiation caused 36-86 %, 50-100 % and 60-100 % mortality of insects during the incubation period between 3 to 14 days, respectively. Bioactive PLA-based nanocomposite film having AF-1 (PLA/CNC/Gly/AF-1 film) and AF-2 (PLA/CNC/Gly/AF-2 film) alone caused 4 to 52 % and 3 to 49 % mortality from day 3 to 14 of incubation time, respectively (Figure 7.2). The mortality of rice weevils was significantly increased along with 100, 200, and 300 Gy γ -irradiation doses, and the mortality increased with higher doses of radiation and a longer incubation period. The

results of combined treatment between irradiation and PLA-based nanocomposite film showed increased mortality, which is significantly higher as compared to the effect of each treatment as well as control samples. Bioactive PLA/CNC/Gly/AF-1 film in combination with 100, 200, and 300 Gy γ -irradiation caused 78, 93 and 100 % mortality at day 14 of incubation, respectively, while the bioactive PLA/CNC/Gly/AF-2 film along with 100, 200 and 300 Gy of γ -irradiation treatment caused 72, 82 and 92 % mortality, respectively, at 14 days of incubation (Table 7.3).

It has also been well-established and proven by several authors that the combined treatment between irradiation and bioactive films or plant-derived EOs could enhance the radiosensitivity of foodborne pathogenic bacteria, spoilage fungi, and stored products insect pests (Caillet *et al.*, 2005; Ayari *et al.*, 2012; Hossain *et al.*, 2014b; Hossain *et al.*, 2019b; Ayari *et al.*, 2020; Begum *et al.*, 2020a; Hossain *et al.*, 2021). Hossain *et al.* (2021) worked with tea tree and eucalyptus EO along with γ -radiation and X-rays at different dose rates against *S. oryzae* and the authors stated that the application of EOs and irradiation treatment increased the mortality of rice weevils by 3-6 times versus the treatment alone. In accordance, Ahmadi *et al.* (2013) reported a synergistic effect of the treatment between EOs (*Rosmarinus officinalis* EO and *Perovskia atriplicifolia* EO) and γ -irradiation on the major stored product insect *Tribolium castaneum*. *R. officinalis* EO at 4.2 μ L/mL showed only 1 % *T. castaneum* mortality and 130-230 Gy γ -irradiation caused 1-5 % mortality of insects when applied alone, however, the insect mortality increased to 20 and 30.3 %, respectively, while both treatments combined (Ahmadi *et al.*, 2013). A study found that *S. oryzae* became 4.8 and 6.2 times more sensitive to γ -irradiation dose when they were exposed to basil EO at 0.2 and 0.4 μ L/mL concentration, respectively, than the rice weevils used in the control samples (120 Gy irradiation treatment alone) (Hossain *et al.*, 2014b). Moreover, the application of bioactive nanocomposite films in stored rice can release active ingredients slowly during the storage period and kill the adult rice weevils, although fumigation of EOs cannot have a negative effect on their eggs and larvae because of their location inside the kernel. But the application of low doses of γ -radiation could pass through the kernel and affect the development of insects in all stages. Thus, combining two treatments showed a synergistic effect to control insect pests in stored rice. Furthermore, the application of bioactive nanocomposite films and irradiation treatment separately to complete the elimination of the stored product insect pests required higher radiation doses and higher concentrations of EO which is expensive as well as time-consuming. The current study came up with an innovative solution to reduce the time, costs as well as pest infestation in stored cereal grains by combining γ -irradiation and bioactive nanocomposite films.

7.3.5. Release profile of active components from the insecticidal films

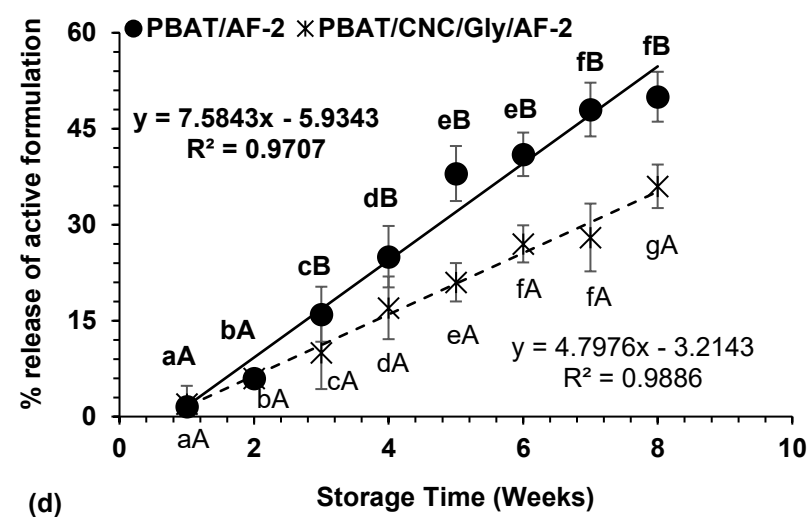
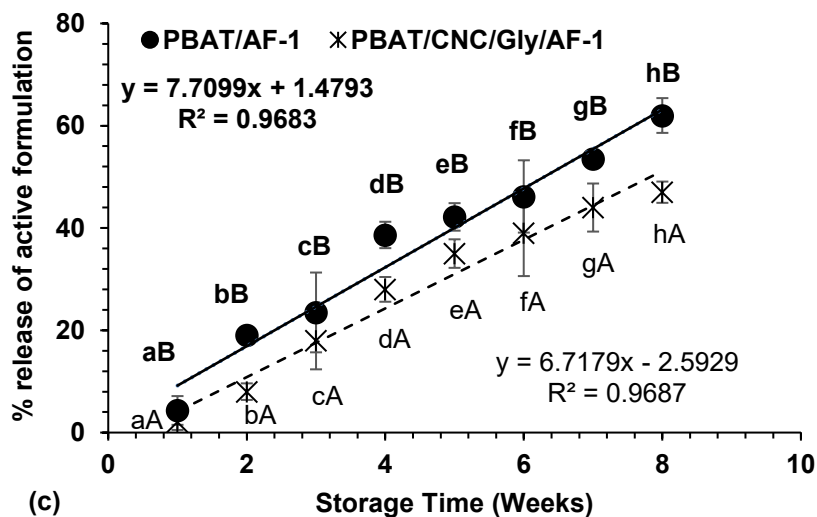
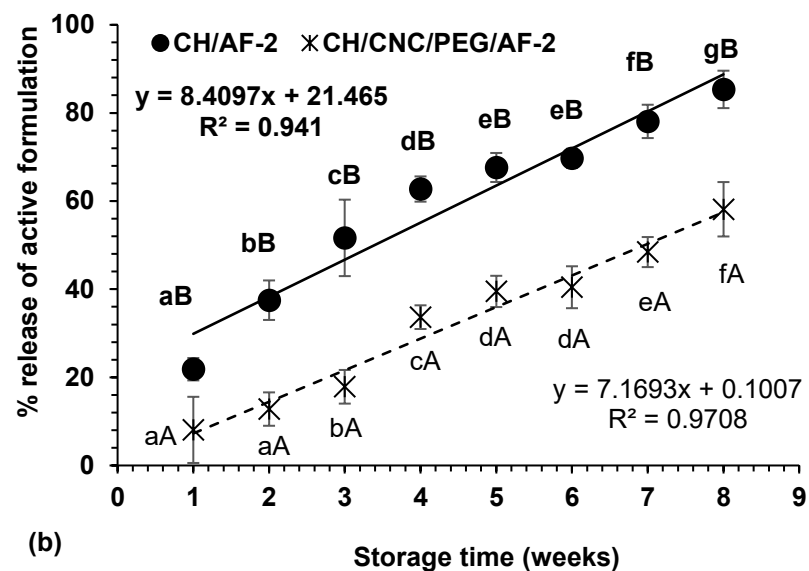
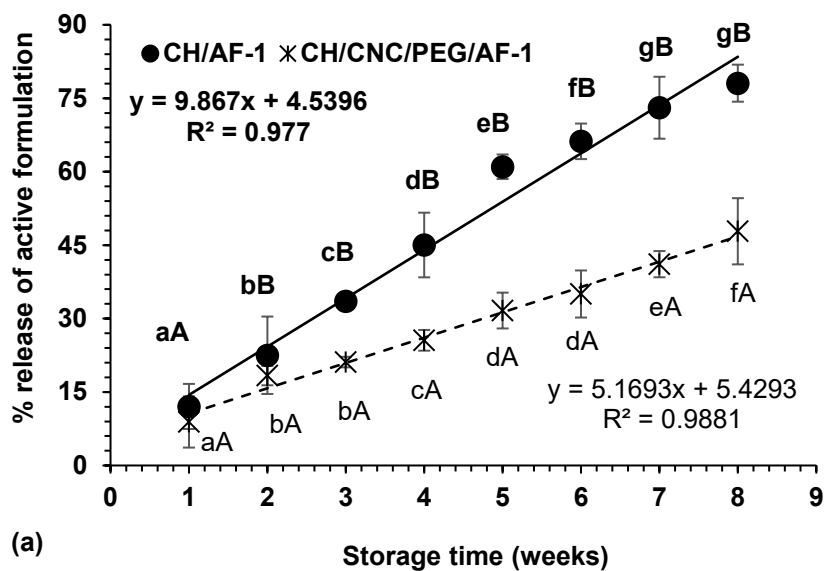
Anti-insect pest packaging films should maintain their insecticidal effect from storage time to consumption because insect pests can reduce food quality anytime. Therefore, the release profile of AF-1 and AF-2 from bioactive CH-, PBAT- and PLA-based nanocomposite films with the presence of CNC and without CNC were analyzed in terms of % release of active formulations for 2 months in stored rice. The total twelve bioactive nanocomposite films were analyzed such as (1) CH/CNC/PEG/AF-1 film, (2) CH/AF-1 film, (3) CH/CNC/PEG/AF-2 film, (4) CH/AF-2 film, (5) PBAT/CNC/Gly/AF-1 film, (6) PBAT/AF-1 film, (7) PBAT/CNC/Gly/AF-2 film, (8) PBAT/AF-2 film, (9) PLA/CNC/Gly/AF-1 film, (10) PLA/AF-1 film, (11) PLA/CNC/Gly/AF-2 film and (12) PLA/AF-2 film, and the results are depicted in Figure 7.3 a-f. To determine the release profile of active formulations from the polymeric matrices, two standard curves were obtained for the AF-1 and AF-2 at 320 nm. The absorbance of extracted eluents was measured using a UV-Vis spectrophotometer and a reduction of the concentration of active formulations in the polymeric matrix with storage time was considered as the release of active compounds.

The results showed (Figure 7.3) gradual release of the active formulations from the CH-based, PBAT-based, and PLA-based composite films. It was noticed that all polymeric matrices loaded with CNC (bioactive nanocomposite films) could significantly ($P \leq 0.05$) lower the release of active compounds as compared to the composite films (bioactive films without CNC). Figure 7.3a-b shows the gradual % release of active formulation 1 (AF-1) and active formulation 2 (AF-2) from the bioactive CH-based films with and without CNC during the storage of films in rice for 2 months. Here, four types of CH-based films (CH/AF-1 film, CH/CNC/PEG/AF-1 film, CH/AF-2 film, and CH/CNC/AF-2 film) were tested. Figure 7.3a describes the release profile of active ingredients from CH/AF-1 film and CH/CNC/PEG/AF-1 film. The available active components in the CH/AF-1 film were significantly ($P \leq 0.05$) reduced from 43.9 to 9.62 % at day 0 to day 60 (week 8) during storage in rice. The storage time 1, 2, 3, 4, 5, 6, 7, and 8 weeks had significantly ($P \leq 0.05$) increased the quantity of % release of active ingredients from CH/AF-1 film, and the values were 12.1, 22.5, 33.6, 45, 61, 66, 73, and 78.1 %, respectively (Figure 7.3a). In addition, the incorporation of CNC into the CH-based film matrix (CH/CNC/PEG/AF-1 film) was significantly ($P \leq 0.05$) slower (38.74 %) the release of active compounds during the end of the storage compared to the CH/AF-1 film. Moreover, it has been observed from Figure 7.3a that there was a significantly difference ($P \leq 0.05$) in the release of active compounds (%) between two films of CH/AF-1 and CH/CNC/PEG/AF-1 film. The release (%) of the active compounds from the CH/CNC/PEG/AF-1 film was 8.9, 18.4, 21.1, 25.6, 31.6, 35, 41.1, and 48 % at 1, 2, 3, 4, 5, 6, 7, and 8 weeks,

respectively. At 8 weeks of storage, the available active components were 19 % in CH/CNC/PEG/AF-1 films which were significantly higher ($P \leq 0.05$) than the film CH/AF-1.

Figure 7.3b shows the % release of active formulation 2 (AF-2) from CH/AF-2 and CH/CNC/PEG/AF-2 film for 8 weeks in stored rice. The release of active components (%) in CH/AF-2 film was significantly increased with storage time and values were 21.8, 37.5, 51.6, 62.7, 67.6, 69.7, 78.1, and 85.3 % at weeks 1, 2, 3, 4, 5, 6, 7, and 8, respectively. The release (%) from the CH/AF-2 film was significantly faster as compared to the film CH/CNC/PEG/AF-2 which has been noticeable in Figure 7.3b. The reinforcement of CNC into CH-based bioactive polymeric matrices (CH/CNC/PEG/AF-2 film) significantly improved the controlled release of active compounds as compared to the CH/AF-2 film ($P \leq 0.05$). The active compounds released from CH/CNC/PEG/AF-2 film were 32 % lower compared to the film CH/AF-2 at week 8. The release was 8.1, 12.8, 17.8, 33.6, 39.5, 40.4, 48.4, and 58.1 % from the CH/CNC/PEG/AF-2 films during storage at weeks 1, 2, 3, 4, 5, 6, 7, and 8, respectively, (Figure 7.3b).

The gradual release (%) of active formulations (AF-1 and AF-2) from the bioactive PBAT-based films in stored rice were examined with and without the presence of CNC (Figure 7.3c and Figure 7.3d). Therefore, four types of bioactive PBAT-based films (PBAT/AF-1 film, PBAT/CNC/Gly/AF-1 film, PBAT/AF-2 film, and PBAT/CNC/Gly/AF-2 film) were investigated. Briefly, the release (%) of active compounds from bioactive PBAT/AF-1 film was 4.32, 19.07, 23.49, 38.64, 42.17, 46.17, 53.53 and 62 % at week 1, 2, 3, 4, 5, 6, 7 and 8, respectively, while the PBAT/CNC/Gly/AF-1 nanocomposite film released 2.1, 8, 18, 28, 35, 39, 44 and 47 % at the corresponding weeks of storage (Figure 7.3c). This means that the CNC reinforcing agent significantly ($P \leq 0.05$) reduced the release of active compounds by 24.2 % from the PBAT/CNC/Gly/AF-1 nanocomposite film while compared with PBAT/AF-1 film after 8 weeks of storage. Similar findings were observed in the case of the release profile of AF-2 from the PBAT-based composite films (PBAT/AF-2 film and PBAT/CNC/Gly/AF-2 nanocomposite film) (Figure 7.3d). Incorporation of CNC into the PBAT/Gly/AF-2 matrix significantly ($P \leq 0.05$) reduced the release of active compounds by 28 % as compared to the PBAT/AF-2 composite film after 8 weeks of storage in the rice sample. The % release was 1.56, 6, 16, 25, 38, 41, 48 and 50 % from the bioactive PBAT/AF-2 film at week 1, 2, 3, 4, 5, 6, 7 and 8, respectively, while the corresponding release was 2, 6, 10, 17, 21, 27, 28 and 36 % from the bioactive PBAT/CNC/Gly/AF-2 nanocomposite film when stored in rice (Figure 7.3d).



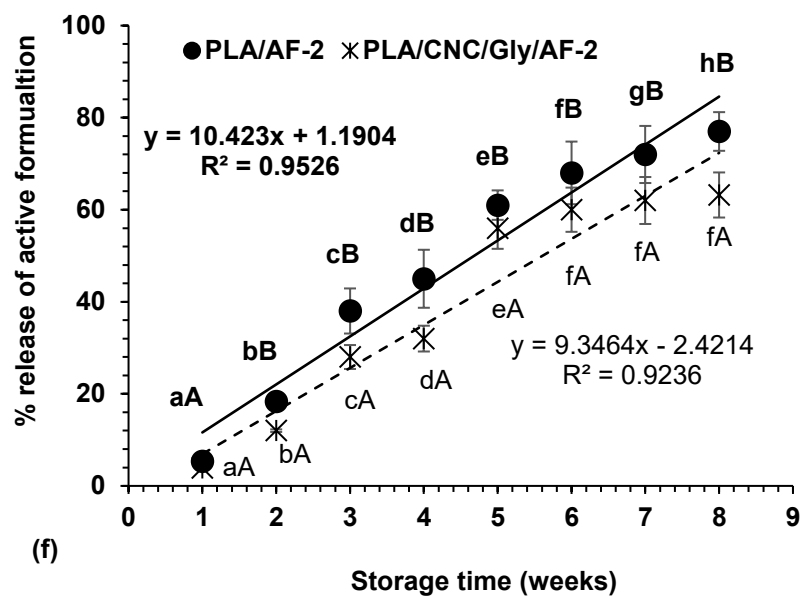
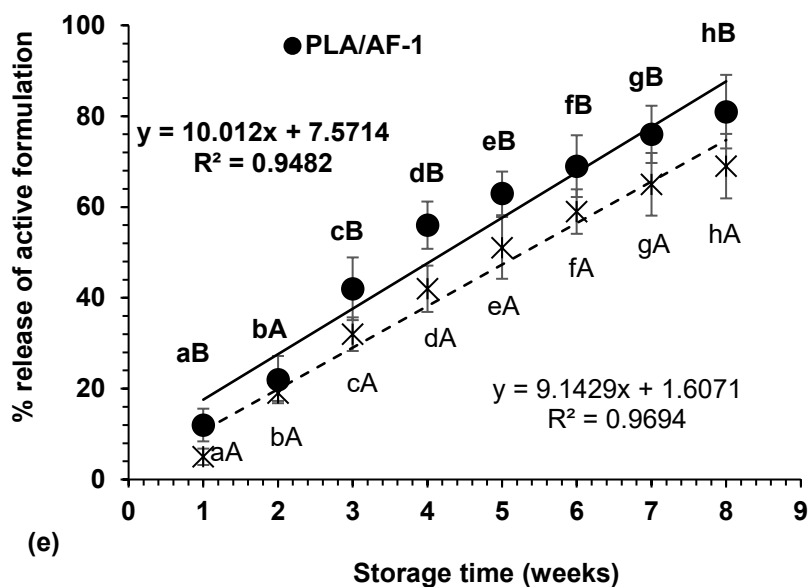


Figure 7.3. Release (%) of active compounds (%) from (a-b) CH-based bioactive film with and without CNC, (c-d) bioactive PBAT-based film with and without CNC, (e-f) PLA-based bioactive film with and without CNC. Values are means±standard error. The same lowercase letter either in each bioactive film with or without CNC are not significantly different ($P > 0.05$). The same uppercase letter between the each bioactive films with and without CNC are not significantly different ($P > 0.05$).

The release profile of active compounds from the PLA/AF-1 film and PLA/CNC/Gly/AF-1 film was measured to evaluate the effectiveness of CNC in the bioactive films (Figure 7.3e). The presence of CNC in the PLA-based polymeric matrix (PLA/CNC/Gly/AF-1 film) could significantly ($P \leq 0.05$) reduce the release of AF-1 by 14.8 % after 8 weeks of storage in stored rice as compared to the PLA/AF-1 film. Briefly, the release (%) of active compounds from bioactive PLA/AF-1 film increased by 12-81 % from week 1 to 8 in stored rice, while the PLA/CNC/Gly/AF-1 nanocomposite film caused from 5 to 69 % release of active compounds from week 1 to week 8 ($P \leq 0.05$). In the case of AF-2, similar findings were observed that the incorporation of CNC was significantly lower the release of AF-2 (by 19.9 %) from PLA/CNC/Gly/AF-2 film than the PLA/AF-2 film at the end of the storage period (8 weeks) (Figure 7.3f). The % release was 5.36, 18.4, 38, 45, 61, 68, 72 and 77 % from the bioactive PLA/AF-2 film at week 1, 2, 3, 4, 5, 6, 7 and 8, respectively, while the corresponded release was 3.9, 12, 28, 32, 56, 60, 62 and 63.2 % from the bioactive PLA/CNC/Gly/AF-2 nanocomposite film when stored in rice (Figure 7.3f).

It has been proven from the current study that the incorporation of CNC into bioactive CH-, PBAT- and PLA-based matrices greatly improved the controlled release of active formulations and preserved the active formulations (either AF-1 or AF-2) during storage time by preventing the fast release. These findings were in agreement with several authors' findings ([Boumail *et al.*, 2013](#); [Salmieri *et al.*, 2014b](#); [Hossain *et al.*, 2018](#); [Hossain *et al.*, 2019a](#); [Patel *et al.*, 2021](#)). Briefly, the authors stated that the application of CNC into polymeric matrices as reinforcing agents could profoundly improve the controlled release of active compounds from bioactive films and preserve the bioactivities of active formulations or antimicrobials for long storage times ([Boumail *et al.*, 2013](#); [Hossain *et al.*, 2019a](#); [Patel *et al.*, 2021](#)). Moreover, CNC also helps to improve and slow the release of active formulations from nanocomposite matrices by helping the homogenous distribution of the nanoemulsion of active formulations within the polymeric matrices ([Boumail *et al.*, 2013](#)). [Hossain *et al.* \(2019a\)](#) developed bioactive chitosan-based nanocomposite films using an oregano-thyme essential oil mixture and studied the effect of CNC in the controlled release of volatile components from the films during the storage of rice. The authors found that the incorporation of CNC into CH+oregano/thyme EO film slowed the release of volatile components by 26 % compared to the film without CNC (CH+oregano/thyme EO film) ([Hossain *et al.*, 2019a](#)). A study hypothesized that the PLA-CNC matrix was slower in the release of oregano EO because of the molecular hydrophobic interactions between matrix and EO that influence the release rate of volatile oregano EO ([Salmieri *et al.*, 2014b](#)). Moreover, [Hossain *et al.* \(2018\)](#) observed similar results when they worked with methylcellulose films. Briefly, the authors worked to develop methylcellulose/CNC-based nanocomposite films containing a blend of oregano/thyme EO. They

observed that incorporation of CNC slowed the release by 35 % compared to the methylcellulose film without CNC over 12 weeks of storage in rice (Hossain *et al.*, 2018). Release of active compounds from bioactive nanocomposite films plays an important role to preserve and extend the shelf-life of stored foods. Moreover, bioactive films reinforced with CNC could modify the polymeric matrices and thus help to control release in a slow manner (Fortunati *et al.*, 2013). Moreover, the release of active ingredients from the bioactive nanocomposite films could be related to several factors such as the chemical nature of the active ingredients, polymer morphology, molecular weight distribution, polymer-active formulation interactions, distribution nature in the polymeric matrix, storage environmental parameters, porosity of the polymer, polymer preparation method, temperature, types of food and so on (Salmieri *et al.*, 2014b; da Rosa *et al.*, 2020a; Malekjani and Jafari, 2021). The incorporation of CNC into polymeric matrices could improve the interactions with active formulations which reduced their migration through the polymeric network by the restriction of compound mobility (Requena *et al.*, 2017). The present study suggested the incorporation of CNC into bioactive packaging films could preserve the active formulations for a long storage time and delay the fast release of active components.

7.3.6. Sensory analyses of the rice under different films treatment

Sensory analyses (odor, color, taste, and global appreciation) of the stored rice after cooking under the treatment of six bioactive films (CH/CNC/PEG/AF-1, CH/CNC/PEG/AF-2, PBAT/CNC/Gly/AF-1, PBAT/CNC/Gly/AF-2, PLA/CNC/Gly/AF-1 and PLA/CNC/Gly/AF-2) and control sample (without bioactive films) were evaluated after 1 month of rice storage (Figure 7.4). The sensory evaluation of treated foods is considered an important parameter when developing new bioactive packaging to understand the migration level of chemical agents from the bioactive films (Chang *et al.*, 2017). The bioactive films not only affect the insect pests but also affect the food qualities too, therefore, the sensory properties of the rice were determined to check the effect of the active films on cooked rice. The results of sensory analyses for 1 month of stored rice with six bioactive packaging films, the intensity of odor and color of rice after cooking were not significantly ($P > 0.05$) different as compared to the control sample. Thereafter, Figure 7.4 shows that all the control samples and treated samples with bioactive films (CH/CNC/PEG/AF-1, CH/CNC/PEG/AF-2, PBAT/CNC/Gly/AF-1, PBAT/CNC/Gly/AF-2, PLA/CNC/Gly/AF-1 and PLA/CNC/Gly/AF-2) did not significantly ($P > 0.05$) affect the taste as well as the global appreciation of cooked treated and control rice as it has been recorded that all samples were accepted with high scores assigned by the panelists. The obtained scores for odor, color, taste, and general appreciation ranged between

7.7 to 8.5 when rice was preserved with the six bioactive films which corresponded to like moderately to like very much, while in the control sample the scores were obtained between 8.4 to 8.5 ($P > 0.05$) for the corresponded sensory attributes for 1 month of storage (Figure 7.4).

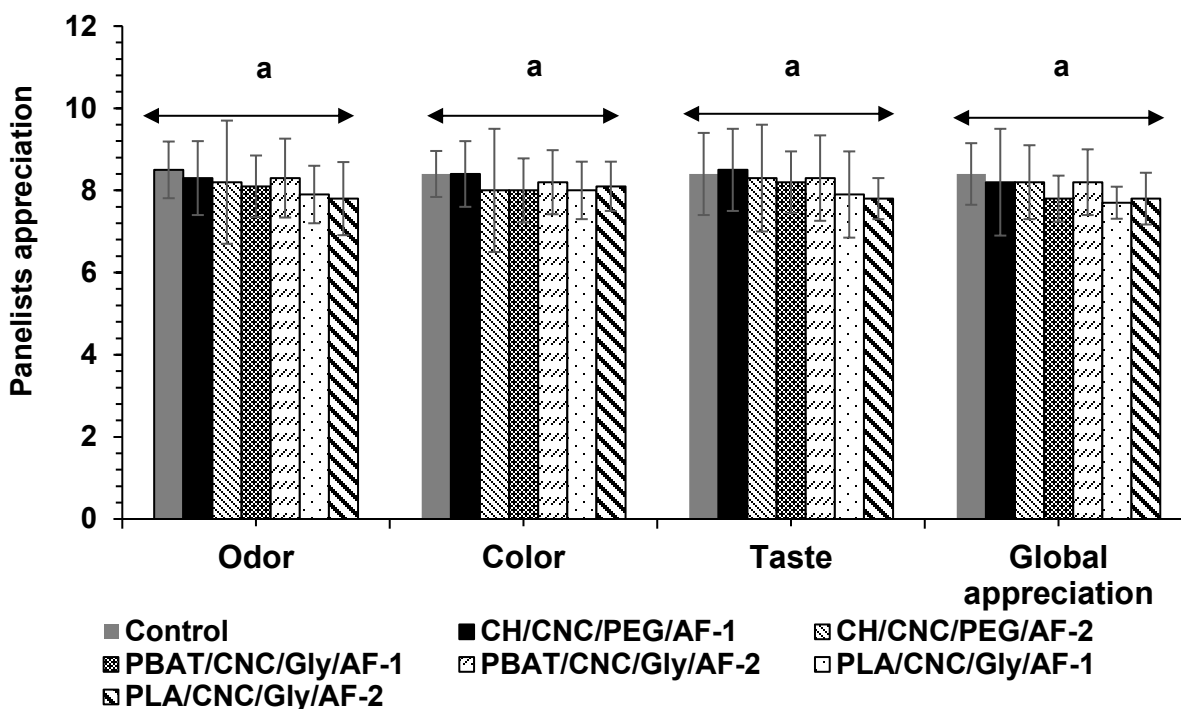


Figure 7.4. Sensory evaluation scores (mean \pm SD) of cooked rice packaged with developed bioactive CH-based, PBAT-based and PLA-based nanocomposite films. Mean values for the treatment with the same area that share the common lower-case letters are not significantly different ($P > 0.05$).

Direct application of EOs in stored rice for preventing insect infestation may affect the quality of stored rice by changing the organoleptic properties. Meanwhile, the current study showed the sensory attributes of stored rice were acceptable because the active formulations (mixture of EOs and CEs) were encapsulated into the polymeric matrices which allowed for the slow release of active formulations during storage (Badr *et al.*, 2013; Hossain *et al.*, 2019a). Moreover, nanocomposite films also increased the physical stability of the active formulations during storage time, protected them from evaporation and light, and helped to control gradual release over the storage time (Hossain *et al.*, 2019a). Moreover, the authors described that the chitosan-based nanocomposite films containing oregano/thyme EO nanoemulsion did not have any significant

effect on odor, taste, color, and appreciation of stored rice after two months as compared to the control sample. Moreover, the authors obtained sensory attributes scores between 7.4 to 8.0 for color, odor, taste, and global appreciation for both control and treated samples which agreed with our current investigation (Hossain *et al.*, 2019a). Chang *et al.* (2017) developed an anti-insect repellent sachet using allyl mercaptan (AM) to control *S. oryzae* in rice. AM is an organosulphur compound found in onion and garlic which is volatile and encapsulated in a packaging sachet. The sensory properties (odor, color, texture, and overall preference) of brown uncooked and cooked rice were investigated under active sachet and control treatment. However, the authors found there was no significant ($P > 0.05$) difference between the treated and control samples which strongly supports the current study (Chang *et al.*, 2017). Moreover, there was no negative evaluation obtained by the panelists such as “Dislike slightly” which brings us hope that our developed active packaging will be a practical application in the cereal grain industry.

7.4. Conclusion

The fumigation toxicities of six individual EOs, two citrus extracts (CEs), and two active formulations (mixture of EOs and CEs) against the rice weevil (*S. oryzae*) were evaluated. The two active formulations (AF-1 and AF-2) showed the strongest fumigant toxicity against the rice weevil at the lowest concentration and shortest exposure time than the individual EOs or CEs. Subsequently, AF-1 and AF-2 acted as the highest anti-acetylcholinesterase (AChE) inhibitors which suggested that the fumigation of insecticidal properties by AF-1 and AF-2 depended on AChE inhibition. Microfluidisation pressure of 8000 psi at the 2nd cycle and 15000 psi at the 3rd cycle produced a stable nanoemulsion of AF-1 and AF-2, respectively, with a particle size of 116 nm, and EE of 77 % for AF-1 nanoemulsion and particle size of 40 nm and EE of 79 % for AF-2 nanoemulsion. The active formulations were encapsulated into three different polymeric matrices such as CH-, PBAT- and PLA-based nanocomposite films containing CNC and plasticizer to develop bioactive nanocomposite packaging films. Six different types of bioactive films (CH/CNC/PEG/AF-1, CH/CNC/PEG/AF-2, PBAT/CNC/Gly/AF-1, PBAT/CNC/Gly/AF-2, PLA/CNC/Gly/AF-1 and PLA/CNC/Gly/AF-2) were applied to stored rice to control rice weevil's infestation for 14 days. All tested bioactive films showed significant insecticidal properties during the storage time. Among them, CH-based bioactive film containing nanoemulsion of AF-2 and AF-1 showed significantly higher insecticidal properties, followed by bioactive PBAT-based and PLA-based nanocomposite films. Application of bioactive nanocomposite films along with γ -irradiation treatment increased the radiosensitivity of insects' ionizing radiation and showed an increased mortality of insects than the individual treatments. Hence, the incorporation of CNC as a reinforcing

agent was significant in lowering the release of active formulations from all tested polymeric matrices. Therefore, the application of bioactive nanocomposite films with γ -irradiation could be a promising way to control the insect population in packaged rice during long-term storage.

7.5. Acknowledgments

The authors are grateful to the Ministère de l'Économie, et de l'Innovation (MEI) du Québec (PSR SIIRI 985), Kerry Group, Biosecur Lab Inc., the Ministère de l'Agriculture, des Pêcheries, et de l'Agriculture du Québec (MAPAQ) for a chair on antimicrobial compounds (PPIA-12) and the U.S. Department of Agriculture, Agricultural Research Service (USDA ARS), U.S. Pacific Basin Agricultural Research Centre for supporting this research. The authors would like to acknowledge Dr. Shiv Shankar and Dr. Farah Hossain for their scientific and technical contributions.

7.6. References

- Abdelgaleil, S.A., Mohamed, M.I., Badawy, M.E., El-arami, S.A., 2009. Fumigant and contact toxicities of monoterpenes to *Sitophilus oryzae* (L.) and *Tribolium castaneum* (Herbst) and their inhibitory effects on acetylcholinesterase activity. *Journal of Chemical Ecology* 35, 518-525.
- Adak, T., Barik, N., Patil, N.B., Govindharaj, G.-P.-P., Gadratagi, B.G., Annamalai, M., Mukherjee, A.K., Rath, P.C., 2020. Nanoemulsion of eucalyptus oil: An alternative to synthetic pesticides against two major storage insects (*Sitophilus oryzae* (L.) and *Tribolium castaneum* (Herbst)) of rice. *Industrial Crops and Products* 143.
- Ahmadi, M., Abd-alla, A.M.M., Moharrampour, S., 2013. Combination of gamma radiation and essential oils from medicinal plants in managing *Tribolium castaneum* contamination of stored products. *Applied Radiation and Isotopes* 78, 16-20.
- Ali-Shtayeh, M.S., Jamous, R.M., Zaitoun, S.Y.A., Qasem, I.B., 2014. *In-vitro* screening of acetylcholinesterase inhibitory activity of extracts from Palestinian indigenous flora in relation to the treatment of Alzheimer's disease. *Functional Foods in Health and Disease* 4, 381-400.
- Anjali, C.H., Sharma, Y., Mukherjee, A., Chandrasekaran, N., 2012. Neem oil (*Azadirachta indica*) nanoemulsion--a potent larvicidal agent against *Culex quinquefasciatus*. *Pest Management Science* 68, 158-163.
- Asmawati, Mustapha, W.A.W., Yusop, S.M., Maskat, M.Y., Shamsuddin, A.F., 2014. Characteristics of cinnamaldehyde nanoemulsion prepared using APV-high pressure homogenizer and ultra turrax. *AIP Conference Proceedings. American Institute of Physics* 1614, 244-250.
- Ayari, S., Dussault, D., Jerbi, T., Hamdi, M., Lacroix, M., 2012. Radiosensitization of *Bacillus cereus* spores in minced meat treated with cinnamaldehyde. *Radiation Physics and Chemistry* 81, 1173-1176.
- Ayari, S., Shankar, S., Follett, P., Hossain, F., Lacroix, M., 2020. Potential synergistic antimicrobial efficiency of binary combinations of essential oils against *Bacillus cereus* and *Paenibacillus amylolyticus*-Part A. *Microbial Pathogenesis* 141, 104008.
- Badr, K., Ahmed, Z.S., El-Gamal, M., 2013. Assessment of antimicrobial activity of whey protein films incorporated with biocide plant-based essential oils. *Journal of Applied Sciences Research* 9, 2811-2818.
- Bakkali, F., Averbeck, S., Averbeck, D., Idaomar, M., 2008. Biological effects of essential oils—a review. *Food and Chemical Toxicology* 46, 446-475.

- Begum, T., Follett, P.A., Hossain, F., Christopher, L., Salmieri, S., Lacroix, M., 2020a. Microbicidal effectiveness of irradiation from Gamma and X-ray sources at different dose rates against the foodborne illness pathogens *Escherichia coli*, *Salmonella* Typhimurium and *Listeria monocytogenes* in rice. *LWT-Food Science and Technology* 132, 109841.
- Begum, T., Follett, P.A., Mahmud, J., Moskovchenko, L., Salmieri, S., Allahdad, Z., Lacroix, M., 2022a. Silver nanoparticles-essential oils combined treatments to enhance the antibacterial and antifungal properties against foodborne pathogens and spoilage microorganisms. *Microbial Pathogenesis* 164, 105411.
- Begum, T., Follett, P.A., Shankar, S., Mahmud, J., Salmieri, S., Lacroix, M., 2022b. Mixture design methodology and predictive modeling for developing active formulations using essential oils and citrus extract against foodborne pathogens and spoilage microorganisms in rice. *Journal of Food Science* 87, 353-369.
- Ben-Fadhel, Y., Maherani, B., Manus, J., Salmieri, S., Lacroix, M., 2020. Physicochemical and microbiological characterization of pectin-based gelled emulsions coating applied on pre-cut carrots. *Food Hydrocolloids* 101, 105573.
- Boumail, A., Salmieri, S., Klimas, E., Tawema, P.O., Bouchard, J., Lacroix, M., 2013. Characterization of trilayer antimicrobial diffusion films (ADFs) based on methylcellulose-polycaprolactone composites. *Journal of Agricultural and Food Chemistry* 61, 811-821.
- Caillet, S., Shareck, F., Lacroix, M., 2005. Effect of gamma radiation and oregano essential oil on murein and ATP concentration of *Escherichia coli* O157: H7. *Journal of Food Protection* 68, 2571-2579.
- Castillo-Morales, R.M., Serrano, S.O., Villamizar, A.L.R., Mendez-Sanchez, S.C., Duque, J.E., 2021. Impact of *Cymbopogon flexuosus* (Poaceae) essential oil and primary components on the eclosion and larval development of *Aedes aegypti*. *Scientific Reports* 11, 24291.
- Chang, Y., Lee, S.H., Na, J.H., Chang, P.S., Han, J., 2017. Protection of Grain Products from *Sitophilus oryzae* (L.) Contamination by Anti-Insect Pest Repellent Sachet Containing Allyl Mercaptan Microcapsule. *Journal of Food Science* 82, 2634-2642.
- Cheng, D., Wen, Y., An, X., Zhu, X., Cheng, X., Zheng, L., Nasrallah, J.E., 2016. Improving the colloidal stability of Cellulose nano-crystals by surface chemical grafting with polyacrylic acid. *Journal of Bioresources and Bioproducts* 1, 114-119.
- Choupanian, M., Omar, D., Basri, M., Asib, N., 2017. Preparation and characterization of neem oil nanoemulsion formulations against *Sitophilus oryzae* and *Tribolium castaneum* adults. *Journal of Pesticide Science* 42, 158-165.

- da Rosa, C.G., Sganzerla, W.G., de Oliveira Brisola Maciel, M.V., de Melo, A.P.Z., da Rosa Almeida, A., Ramos Nunes, M., Bertoldi, F.C., Manique Barreto, P.L., 2020. Development of poly (ethylene oxide) bioactive nanocomposite films functionalized with zein nanoparticles. *Colloids and Surfaces A: Physicochemical and Engineering Aspects* 586, 124268.
- Das, S., Singh, V.K., Dwivedy, A.K., Chaudhari, A.K., Dubey, N.K., 2021. *Anethum graveolens* Essential Oil Encapsulation in Chitosan Nanomatrix: Investigations on *In Vitro* Release Behavior, Organoleptic Attributes, and Efficacy as Potential Delivery Vehicles Against Biodeterioration of Rice (*Oryza sativa* L.). *Food and Bioprocess Technology* 14, 831-853.
- Demirel, N., Erdogan, C., 2017. Insecticidal effects of essential oils from Labiatae and Lauraceae families against cowpea weevil, *Callosobruchus maculatus* (F.) (Coleoptera: Bruchidae) in stored pea seeds. *Entomology and Applied Science Letters* 4, 13-19.
- Deng, Z., Jung, J., Simonsen, J., Wang, Y., Zhao, Y., 2017. Cellulose Nanocrystal Reinforced Chitosan Coatings for Improving the Storability of Postharvest Pears Under Both Ambient and Cold Storages. *Journal of Food Science* 82, 453-462.
- Fierascu, R.C., Fierascu, I.C., Dinu-Pirvu, C.E., Fierascu, I., Paunescu, A., 2020. The application of essential oils as a next-generation of pesticides: recent developments and future perspectives. *Zeitschrift fur Naturforschung. C, Journal of Biosciences* 75, 183-204.
- Follett, P.A., Snook, K., Janson, A., Antonio, B., Haruki, A., Okamura, M., Bisel, J., 2013. Irradiation quarantine treatment for control of *Sitophilus oryzae* (Coleoptera: Curculionidae) in rice. *Journal of Stored Products Research* 52, 63-67.
- Fortunati, E., Peltzer, M., Armentano, I., Jiménez, A., Kenny, J.M., 2013. Combined effects of cellulose nanocrystals and silver nanoparticles on the barrier and migration properties of PLA nano-biocomposites. *Journal of Food Engineering* 118, 117-124.
- Garrido-Miranda, K.A., Giraldo, J.D., Schoebitz, M., 2022. Essential Oils and Their Formulations for the Control of Curculionidae Pests. *Frontiers in Agronomy* 4, 876687.
- Hallman, G.J., 2013. Control of stored product pests by ionizing radiation. *Journal of Stored Products Research* 52, 36-41.
- Hategekimana, A., Erler, F., 2020. Comparative repellent activity of single, binary and ternary combinations of plant essential oils and their major components against *Sitophilus oryzae* L. (Coleoptera: Curculionidae). *Journal of Plant Diseases and Protection* 127, 873-881.
- Hossain, F., Follett, P., Salmieri, S., Vu, K.D., Frascini, C., Lacroix, M., 2019a. Antifungal activities of combined treatments of irradiation and essential oils (EOs) encapsulated

- chitosan nanocomposite films in *in vitro* and *in situ* conditions. International Journal of Food Microbiology 295, 33-40.
- Hossain, F., Follett, P., Salmieri, S., Vu, K.D., Harich, M., Lacroix, M., 2019b. Synergistic Effects of Nanocomposite Films Containing Essential Oil Nanoemulsions in Combination with Ionizing Radiation for Control of Rice Weevil *Sitophilus oryzae* in Stored Grains. Journal of Food Science 84, 1439-1446.
- Hossain, F., Follett, P., Salmieri, S., Vu, K.D., Jamshidian, M., Lacroix, M., 2016. Perspectives on essential oil-loaded nano-delivery packaging technology for controlling stored cereal and grain pests, CRC Press, In Green Pesticide Handbook, 487-508.
- Hossain, F., Follett, P., Shankar, S., Begum, T., Salmieri, S., Lacroix, M., 2021. Radiosensitization of rice weevil *Sitophilus oryzae* using combined treatments of essential oils and ionizing radiation with gamma-ray and X-Ray at different dose rates. Radiation Physics and Chemistry 180, 109286.
- Hossain, F., Follett, P., Vu, K.D., Salmieri, S., Fraschini, C., Jamshidian, M., Lacroix, M., 2018. Antifungal activity of combined treatments of active methylcellulose-based films containing encapsulated nanoemulsion of essential oils and γ -irradiation: *in vitro* and *in situ* evaluations. Cellulose 26, 1335-1354.
- Hossain, F., Follett, P., Vu, K.D., Salmieri, S., Senoussi, C., Lacroix, M., 2014a. Radiosensitization of *Aspergillus niger* and *Penicillium chrysogenum* using basil essential oil and ionizing radiation for food decontamination. Food Control 45, 156-162.
- Hossain, F., Lacroix, M., Salmieri, S., Vu, K., Follett, P.A., 2014b. Basil oil fumigation increases radiation sensitivity in adult *Sitophilus oryzae* (Coleoptera: Curculionidae). Journal of Stored Products Research 59, 108-112.
- Jankowska, M., Rogalska, J., Wyszowska, J., Stankiewicz, M., 2017. Molecular Targets for Components of Essential Oils in the Insect Nervous System-A Review. Molecules 23.
- Karabörklü, S., Ayvaz, A., Yilmaz, S., 2010. Bioactivities of different essential oils against the adults of two stored product insects. Pakistan Journal of Zoology 42.
- Khan, A., Khan, R.A., Salmieri, S., Le Tien, C., Riedl, B., Bouchard, J., Chauve, G., Tan, V., Kamal, M.R., Lacroix, M., 2012. Mechanical and barrier properties of nanocrystalline cellulose reinforced chitosan based nanocomposite films. Carbohydrate Polymers 90, 1601-1608.
- Khani, M., Marouf, A., Amini, S., Yazdani, D., Farashiani, M.E., Ahvazi, M., Khalighi-Sigaroodi, F., Hosseini-Gharalari, A., 2017. Efficacy of Three Herbal Essential Oils Against Rice Weevil, *Sitophilus oryzae* (Coleoptera: Curculionidae). Journal of Essential Oil Bearing Plants 20, 937-950.

- Kim, J., Park, N.h., Na, J.H., Han, J., 2016. Development of natural insect-repellent loaded halloysite nanotubes and their application to food packaging to prevent *Plodia interpunctella* infestation. *Journal of Food Science* 81, E1956-E1965.
- Kim, S.-W., Kang, J., Park, I.-K., 2013. Fumigant toxicity of Apiaceae essential oils and their constituents against *Sitophilus oryzae* and their acetylcholinesterase inhibitory activity. *Journal of Asia-Pacific Entomology* 16, 443-448.
- Lacroix, M., Follett, P., 2015. Combination irradiation treatments for food safety and phytosanitary uses. *Stewart Postharvest Review* 11, 1-10.
- Lee, B.-H., Annis, P.C., Tumaalii, F.a., Choi, W.-S., 2004. Fumigant toxicity of essential oils from the Myrtaceae family and 1,8-cineole against 3 major stored-grain insects. *Journal of Stored Products Research* 40, 553-564.
- Lee, S.E., Lee, B.H., Choi, W.S., Park, B.S., Kim, J.G., Campbell, B.C., 2001. Fumigant toxicity of volatile natural products from Korean spices and medicinal plants towards the rice weevil, *Sitophilus oryzae* (L). *Pest Management Science: formerly Pesticide Science* 57, 548-553.
- Llinares, R., Santos, J., Trujillo-Cayado, L.A., Ramírez, P., Muñoz, J., 2018. Enhancing rosemary oil-in-water microfluidized nanoemulsion properties through formulation optimization by response surface methodology. *LWT-Food Science and Technology* 97, 370-375.
- Lopez, M.D., Campoy, F.J., Pascual-Villalobos, M.J., Munoz-Delgado, E., Vidal, C.J., 2015. Acetylcholinesterase activity of electric eel is increased or decreased by selected monoterpenoids and phenylpropanoids in a concentration-dependent manner. *Chemico-biological Interactions* 229, 36-43.
- López, M.D., Jordán, M.J., Pascual-Villalobos, M.J., 2008. Toxic compounds in essential oils of coriander, caraway and basil active against stored rice pests. *Journal of Stored Products Research* 44, 273-278.
- López, M.D., Pascual-Villalobos, M.J., 2010. Mode of inhibition of acetylcholinesterase by monoterpenoids and implications for pest control. *Industrial Crops and Products* 31, 284-288.
- Malekjani, N., Jafari, S.M., 2021. Modeling the release of food bioactive ingredients from carriers/nanocarriers by the empirical, semiempirical, and mechanistic models. *Comprehensive Reviews in Food Science and Food Safety* 20, 3-47.
- Morelli, C.L., Belgacem, N., Bretas, R.E.S., Bras, J., 2016. Melt extruded nanocomposites of polybutylene adipate-co-terephthalate (PBAT) with phenylbutyl isocyanate modified cellulose nanocrystals. *Journal of Applied Polymer Science* 133, 43678.

- Ogendo, J.O., Kostyukovsky, M., Ravid, U., Matasyoh, J.C., Deng, A.L., Omolo, E.O., Kariuki, S.T., Shaaya, E., 2008. Bioactivity of *Ocimum gratissimum* L. oil and two of its constituents against five insect pests attacking stored food products. *Journal of Stored Products Research* 44, 328-334.
- Park, C.G., Jang, M., Yoon, K.A., Kim, J., 2016. Insecticidal and acetylcholinesterase inhibitory activities of Lamiaceae plant essential oils and their major components against *Drosophila suzukii* (Diptera: Drosophilidae). *Industrial Crops and Products* 89, 507-513.
- Patel, D.K., Dutta, S.D., Ganguly, K., Lim, K.T., 2021. Multifunctional bioactive chitosan/cellulose nanocrystal scaffolds eradicate bacterial growth and sustain drug delivery. *International Journal of Biological Macromolecules* 170, 178-188.
- Piccolo, M.I., Toloza, A.C., Mougabure Cueto, G., Zygadlo, J., Zerba, E., 2008. Anticholinesterase and pediculicidal activities of monoterpenoids. *Fitoterapia* 79, 271-278.
- Priestley, C.M., Burgess, I.F., Williamson, E.M., 2006. Lethality of essential oil constituents towards the human louse, *Pediculus humanus*, and its eggs. *Fitoterapia* 77, 303-309.
- Requena, R., Vargas, M., Chiralt, A., 2017. Release kinetics of carvacrol and eugenol from poly(hydroxybutyrate-co-hydroxyvalerate) (PHBV) films for food packaging applications. *European Polymer Journal* 92, 185-193.
- Salmieri, S., Islam, F., Khan, R.A., Hossain, F.M., Ibrahim, H.M.M., Miao, C., Hamad, W.Y., Lacroix, M., 2014a. Antimicrobial nanocomposite films made of poly(lactic acid)-cellulose nanocrystals (PLA-CNC) in food applications: part A—effect of nisin release on the inactivation of *Listeria monocytogenes* in ham. *Cellulose* 21, 1837-1850.
- Salmieri, S., Islam, F., Khan, R.A., Hossain, F.M., Ibrahim, H.M.M., Miao, C., Hamad, W.Y., Lacroix, M., 2014b. Antimicrobial nanocomposite films made of poly(lactic acid)-cellulose nanocrystals (PLA-CNC) in food applications—part B: effect of oregano essential oil release on the inactivation of *Listeria monocytogenes* in mixed vegetables. *Cellulose* 21, 4271-4285.
- Shankar, S., Rhim, J.W., 2018. Preparation of antibacterial poly(lactide)/poly(butylene adipate-co-terephthalate) composite films incorporated with grapefruit seed extract. *International Journal of Biological Macromolecules* 120, 846-852.
- Sharma, S., Barkauskaite, S., Jaiswal, A.K., Jaiswal, S., 2021. Essential oils as additives in active food packaging. *Food Chemistry* 343, 128403.
- Su, S., Duhme, M., Kopitzky, R., 2020. Uncompatibilized PBAT/PLA Blends: Manufacturability, Miscibility and Properties. *Materials (Basel)* 13, 4897.

- Suresh Kumar, R., Shiny, P., Anjali, C., Jerobin, J., Goshen, K.M., Magdassi, S., Mukherjee, A., Chandrasekaran, N., 2013. Distinctive effects of nano-sized permethrin in the environment. *Environmental Science and Pollution Research* 20, 2593-2602.
- Tandorost, R., Karimpour, Y., 2012. Evaluation of fumigant toxicity of orange peel *Citrus sinensis* (L.) essential oil against three stored product insects in laboratory condition. *Munis Entomology and Zoology* 7, 352-358.
- Trivedi, A., Nayak, N., Kumar, J., 2017. Fumigant toxicity study of different essential oils against stored grain pest *Callosobruchus chinensis*. *Journal of Pharmacognosy and Phytochemistry* 6, 1708-1711.
- Tunçbilek, A., 1995. Effect of ^{60}Co gamma radiation on the rice weevil, *Sitophilus oryzae* (L.). *Anzeiger für Schädlingskunde, Pflanzenschutz, Umweltschutz* 68, 37-38.
- Zarrad, K., Hamouda, A.B., Chaieb, I., Laarif, A., Jemâa, J.M.-B., 2015. Chemical composition, fumigant and anti-acetylcholinesterase activity of the Tunisian *Citrus aurantium* L. essential oils. *Industrial Crops and Products* 76, 121-127.

Chapter 8

Active polymers containing silver nanoparticles combined with active formulations based on essential oils: Quality effect on cereals and dairy products

This manuscript will be submitted to *Journal of Food Science*, Impact factor: 3.167, h-index: 160, Overall Ranking: 7454, SCImago Journal Rank: 0.653

Tofa Begum¹, Peter A. Follett², Lana Moskovchenko³, Stephane Salmieri¹, Monique Lacroix^{1*}

¹Research Laboratories in Sciences Applied to Food, Canadian Irradiation Center, INRS-Armand Frappier Health Biotechnology, 531, Boulevard des Prairies, Laval, Quebec, Canada, H7V 1B7

²United States Department of Agriculture, Agricultural Research Service, U.S. Pacific Basin Agricultural Research Center, 64 Nowelo Street, Hilo, HI 96720, USA

³NanoBrand (www.nanobrand.com), 230 Rue Bernard Belleau, Laval, Quebec, Canada, H7V 4A9

*Corresponding author. Dr. Monique Lacroix, Tel: 450-687-5010 # 4489, Fax: 450-686-5501, E-mail: Monique.Lacroix@inrs.ca

and Peter A. Follett, Ph.D., Email: peter.follett@usda.gov

Tel: (808) 959-4303, Fax: (808) 959-5470

Contribution of authors

Tofa Begum conducted the data curation, methodology, writing - original drafts, writing - review, and editing. Monique Lacroix and Peter A. Follett designed the methodology, conceptualization, and supervision. Stephane Salmieri and Lana Moskovchenko assisted with methodology, reviewing the methodology, editing the manuscript.

Résumé

Nous avons fabriqué plusieurs films nanocomposites bioactifs contenant des huiles essentielles végétales (EO) et des nanoparticules d'argent (AgNP) et les avons testés contre des agents pathogènes d'origine alimentaire, des organismes de détérioration et des insectes dans les aliments emballés. Les films étaient à base de chitosane (CH), de poly (butylène adipate-co-téréphtalate) (PBAT) ou d'acide polylactique (PLA) et contenaient des nanocristaux de cellulose (CNC), des plastifiants (Glycérol [Gly] ou polyéthylène glycol [PEG]), et l'un des trois mélanges actifs d'OE et d'AgNPs (AC-1, AC-2 ou AC-3). Les films nanocomposites bioactifs à base de CH et de PBAT ont montré de fortes propriétés antibactériennes, antifongiques et insecticides contre *Escherichia coli* O157:H7, *Salmonella* Typhimurium, *Aspergillus niger*, *Penicillium chrysogenum*, *Mucor circinelloides* et le charançon du riz *Sitophilus oryzae*. Les films à base de PLA ont montré moins de propriétés antibactériennes, antifongiques et insecticides que les films à base de CH et de PBAT. Des tests de provocation ont été menés avec du riz et du yogourt emballés inoculés avec des bactéries et des champignons sélectionnés et des films bioactifs. Le riz a été traité avec des films bioactifs à base de CH et de PBAT avec et sans traitement par irradiation γ (750 Gy) pendant 8 semaines à 28 °C pour contrôler la croissance des champignons et des bactéries, tandis que le yaourt a été traité avec des films bioactifs à base de PBAT et de PLA pendant 8 semaines à 4 °C. Pour contrôler la croissance des insectes dans le riz stocké, des films bioactifs combinés à une irradiation (100-300 Gy) ont contrôlé la croissance des insectes après 14 jours de stockage à 28 °C. La combinaison d'une irradiation γ de 300 Gy avec des films bioactifs a augmenté de manière significative l'augmentation de la mortalité par le charançon du riz à 96 à 100 % au jour 7 à 14 par rapport au traitement avec le film bioactif seul. Les films nanocomposites bioactifs à base de PLA et de PBAT ont considérablement réduit la croissance des bactéries pathogènes et des champignons de détérioration dans le yaourt stocké après 8 semaines à 4 °C.

Abstract

We fabricated several bioactive nanocomposite films containing plant essential oils (EOs) and silver nanoparticles (AgNPs) and tested them against food-borne pathogens and spoilage organisms and insects in packaged foods. The films were based on chitosan (CH), poly (butylene adipate-co-terephthalate) (PBAT) or polylactic acid (PLA) and contained cellulose nanocrystals (CNCs), plasticizers (Glycerol [Gly] or polyethylene glycol [PEG]), and one of three active mixtures of EOs and AgNPs (AC-1, AC-2, or AC-3). Bioactive CH-, PBAT-based nanocomposite films showed strong antibacterial, antifungal and insecticidal properties against *Escherichia coli* O157:H7, *Salmonella* Typhimurium, *Aspergillus niger*, *Penicillium chrysogenum*, *Mucor circinelloides* and rice weevil *Sitophilus oryzae*. PLA-based films showed less antibacterial, antifungal, and insecticidal properties than CH- and PBAT-based films. Challenge tests were conducted with packaged rice and yogurt inoculated with selected bacteria and fungi and bioactive films. Rice was treated with bioactive CH- and PBAT-based films with and without γ -irradiation treatment (750 Gy) for 8 weeks at 28 °C to control fungi and bacterial growth, while the yogurt was treated with bioactive PBAT- and PLA-based films for 8 weeks at 4 °C. To control the insect's growth in stored rice, bioactive films combined with irradiation (100-300 Gy) controlled the growth of insects after 14 days of storage at 28 °C. Combining 300Gy γ -irradiation with bioactive films significantly increased the rice weevil mortality to 96 to 100% at day 7 to 14 compared to treatment with the bioactive film alone. Bioactive PLA and PBAT-based nanocomposite films significantly reduced the growth of pathogenic bacteria and spoilage fungi in stored yogurt after 8 weeks at 4 °C.

8.1. Introduction

Dairy products including yogurt are consumed throughout the world because of their high nutritional value [Yangilar and Yildiz \(2018\)](#). Yogurt is typically acidic (pH = 4.4) which allows for extended shelf life, but may still be susceptible to spoilage from growth of fungi and yeasts that are able to grow under acidic conditions [\(Viljoen et al., 2003\)](#). The most common spoilage organisms in yogurt are *Aspergillus niger* and *Penicillium* sp., *Candida parapsilosis*, *C. maltosa*, *Debaryomyces castelli*, *D. hansenii*, *Saccharomyces cerevisiae*, *Kluyvermyces* [\(Moreira et al., 2001; Lee et al., 2014; Gougouli and Koutsoumanis, 2017\)](#). The fungus *Mucor circinelloides* is responsible for swelling and bloating in yogurt during storage [\(Snyder et al., 2016a\)](#). Yogurt is also susceptible to bacterial contamination by food-borne illness organisms including *Escherichia coli* O157:H7, *Salmonella* Typhimurium, *Listeria monocytogenes*, *Staphylococcus aureus*, etc. [\(Siddiqui and Nadeem, 2007; Lee et al., 2014\)](#).

Rice, *Oryza sativa* L., is an important staple food for more than half the world's population [\(Liu et al., 2020; Das et al., 2021b\)](#). Rice contains mainly carbohydrate and some protein, with practically no fat or sugar. Rice is sensitive to biodeterioration by pathogenic bacteria, spoilage fungi, and insect pests, which can cause discolored, off-flavor, unpleasant smell, reduced nutrition and also secreted mycotoxins and excretion of insects [\(Hossain et al., 2014a; Das et al., 2021a\)](#). The rice weevil, *Sitophilus oryzae* L. (Coleoptera: Curculionidae), is considered one of the most destructive pests of rice worldwide [\(Hossain et al., 2019b\)](#).

Plant derived essential oils (EOs) are getting increasing attention in the food industry because of their antibacterial, antifungal, antiviral, insecticidal, and antioxidant properties [\(Burt, 2004; Turgis et al., 2012\)](#). EOs are secondary metabolites of plants composed of monoterpenes, sesquiterpenes, and their oxygenated derivatives (alcohols, aldehydes, esters, ethers, ketones, phenols, and oxides) and they are generally recognized as safe (GRAS) by the US Food and Drug Administration (FDA) and the European Commission. [\(Turgis et al., 2012; Hossain et al., 2016b; Vishwakarma et al., 2016\)](#). Despite their strong bioactivity, their uses in food industry are limited because they may cause changes in the taste and aroma of foods at high concentrations. Therefore methods to reduce the concentration of EOs, such as combination treatments with other antimicrobial agents, could reduce the negative sensory impact on foods [\(Mohammadzadeh, 2017; Tardugno et al., 2019\)](#). Silver nanoparticles (AgNPs) are an important category of antimicrobial/antifungal agents widely used in packaging, pharmaceutical, food storage, and processing industries [\(Ghosh et al., 2013a; Weisany et al., 2019\)](#). The combined use of EOs and AgNP may improve the characteristics of both: (i) AgNP improves the stability of volatile EO by

inorganic core (core material is AgNP) , and (ii) EO improves the stability and compatibility of the AgNPs by conjugating EO compounds (Gherasim *et al.*, 2020). AgNPs showed bioactivities against a wide range of bacteria, fungi and insects at low concentrations, and the treated biological entities cannot become resistant because of their high surface area and multifaceted mode of action (Ghosh *et al.*, 2013a). However, the direct application of EOs and AgNPs in foods might affect the taste and other sensorial properties of the foods, and thus could reduce the market quality.

Encapsulation of active agents into biopolymeric matrices could reduce the limitation of application of active agents in food products. Biopolymers such as chitosan (CH), Poly (butylene adipate-co-terephthalate) (PBAT), and polylactic acid (PLA) are commercially available biodegradable polymeric materials (Khan *et al.*, 2012; Su *et al.*, 2020). Chemically, PBAT is an aliphatic-aromatic copolyester, flexible and compostable certified by the European Bioplastics (EN13432 standard criteria) and the Biodegradable Polymers Institute (ASTM D6400 standard specification) (Morelli *et al.*, 2016; Shankar and Rhim, 2018). PLA is biodegradable polymer having good mechanical properties, transparency and easy processibility prepared from renewable sources (Salmieri *et al.*, 2014a, b). CH is biodegradable polymer and used as a food ingredient approved by the FDA as biocompatible, non-toxic, and bio-functional (Khan *et al.*, 2012; Hossain *et al.*, 2019a). Cellulose nanocrystals (CNCs) are used as reinforcing agents in polymeric matrices for improving mechanical and barrier properties and also improving the controlled and extended release of active ingredients during storage (Khan *et al.*, 2013; Salmieri *et al.*, 2014b; Haafiz *et al.*, 2016). Combining bioactive packaging films with ionizing radiation (γ -rays) could result with lower doses for controlling foodborne pathogenic bacteria, spoilage fungi, and insect pests in stored cereal grains if the two act synergistically (Follett *et al.*, 2013; Hossain *et al.*, 2014b). The goals of the current studies were (i) to develop nanoemulsions of active combinations (EOs+AgNPs), (ii) to develop bioactive CH-, PBAT- and PLA-based nanocomposite films, (iii) to characterize the bioactive films by measuring mechanical properties, water solubility, water vapor permeability, *in vitro* release profile in food simulants and *in vitro* antibacterial, antifungal and insecticidal properties, (iv) to determine *in situ* antibacterial, antifungal and insecticidal properties of bioactive nanocomposite films to control foodborne pathogens in stored rice and yogurt, and (v) to evaluate the synergistic effect between γ -irradiation and bioactive nanocomposite packaging films.

8.2. Materials and Methods

8.2.1. Essential oils (EOs) and silver nanoparticles (AgNPs)

Essential oils (EOs) of cinnamon, lavang, citrus, Asian formulation and Mediterranean formulation, three types of silver nanoparticles (AgNPs) (AGPPH, AGPP and AGC0.5) were used as antibacterial, antifungal and insecticidal agents. Asian and Mediterranean formulation were bought from BSA (Montreal, Quebec, Canada), and citrus, lavang and cinnamon EO were purchased from Zayat Aroma (Bromont, QC, Canada). AgNPs containing samples (AGPPH, AGPP and AGC0.5) were provided by NanoBrand (www.nanobrand.com) and each sample had 1000 ppm silver concentration. Three active combinations (AC-1, AC-2 and AC-3) were prepared using AgNP and mixture of EOs followed by our previous study (Begum *et al.*, 2022a). The AC-1 was composed of AGPPH and cinnamon EO in the ratio of 0.1 : 6, AC-2 composed of AGC 0.5, Mediterranean formulation and citrus EO in the ratio of 0.1 : 12 : 6 and AC-3 composed of AGPP, cinnamon EO, Asian formulation and lavang EO in the ratio of 0.1 : 12 : 6 : 6.

8.2.2. Bacterial and fungal culture preparation

For the *in vitro* and *in situ* experiments, two pathogenic bacterial species (*Escherichia coli* O157:H7 NT 1931 and *Salmonella* Typhimurium SL 1344) and three food spoilage fungal species (*Aspergillus niger* ATCC 1015, *Penicillium chrysogenum* ATCC 10106, and *Mucor circinelloides* ATCC 56649) were selected. The bacterial and fungal species were preserved in tryptic soy broth (TSB) and in potato dextrose broth (PDB) with 10 % (v/v) glycerol at -80 °C, respectively (Ghabraie *et al.*, 2016). Prior to experiment, the cultures were passed through two consecutive cycles from -80 °C in TSB for 24 h at 37 °C and in PDB for at 48 h at 28 °C. Then the bacterial cultures were centrifuged and washed with saline water to obtain the bacterial concentration to 10⁵ CFU/mL for each experiment. Fungal culture concentrations were adjusted to 10⁵ spores/mL by collecting spores using saline water and filtered through sterile screens (40 µm nylon screen).

8.2.3. Insect (*S. oryzae*) culture

The Cereal Research Center, Agriculture and Agri-food Canada, Winnipeg, Manitoba provided the cultures of rice weevil (*S. oryzae* L.) and the adults (200 insects, sex ratio of male and female = 1 : 1) were reared in a well ventilated 2 L plastic container. The plastic container was previously filled with one-third quantity of sterile rice (Super quality basmati rice, Quebec, Canada). The

container was then incubated at 28 °C (65 % RH) for 12:12 h light : dark conditions. γ -radiation at 3 kGy was used to sterile the commercial rice for each experiment (Hossain *et al.*, 2021).

8.2.4. Development and characterization of nanoemulsion of active combinations

An oil-in-water (o/w) emulsion was prepared using a quantity of 2 % (w/w) active combination (AC-1, AC-2) with 1 % (w/w) Tween 80 (Sigma-Aldrich Ltd, St. Louis, Missouri, USA) and 2 % (w/w) AC-3 with 2 % (w/w) Tween 80 as emulsifier. Afterwards, the o/w emulsions were treated with an Ultra-Turax homogenizer (TP18/1059 homogenizer) at 15000 rpm for 1 min to obtain a homogenous mixture (coarse emulsion of active combinations). Afterwards, the coarse emulsions of AC-1, AC-2 and AC-3 were passed through a microfluidizer (Microfluidics Inc., Newton, MA, USA) at 8000 psi (2nd cycle), 10000 psi (3rd cycle) and 6000 psi (4th cycle), respectively, to get the stable nanoemulsion of AC-1, AC-2 and AC-3. The pressure and number of cycles of microfluidisation for each active combination were selected based on previous studies (Supplementary data table 8.1). The developed coarse and nanoemulsions of ACs were characterized by determining ζ -potential (zeta) (mV), average particle size (nm), and poly dispersity index-(PDI) using a photon correlation spectroscopy (Malvern Zetasizer Nano-ZS, Model ZEN3600, Westborough, MA, USA) at 25 °C as described by Ben-Fadhel *et al.* (2022). Briefly, the emulsions were diluted in deionized water in the ratio of 1 : 50 for preventing light scattering effect. Moreover, the encapsulation efficiency (EE) of nanoemulsion and coarse emulsion of AC-1, AC-2 and AC-3 was measured (Hossain *et al.*, 2019b). To measure EE, a volume of emulsion was centrifuged at 6000 rpm for 10 mins at 4 °C, thereafter, methanol (3 mL) was added to the pellet and passed through centrifugation treatment for 2nd time for further 30 min. Afterwards, the supernatant of ACs was measured a UV-VIS spectrophotometer at 360 nm wavelengths and calculated the EE using equation 8.1

$$EE = (\text{Total oil} - \text{Free oil}) / \text{Total oil} \times 100 \text{ Eq. 8.1}$$

Each experiment was performed in triplicate (n = 3).

8.2.5. Preparation of bioactive films

The active combinations (AC-1, AC-2 and AC-3) were encapsulated into PBAT+CNC-, PLA+CNC- and CH+CNC-based nanocomposite diffusion matrices to develop bioactive nanocomposite films. Bioactive CH-based nanocomposite films were fabricated using a solvent casting method. For CH-based film preparation, a quantity of 2 g chitosan (CH) was dissolved in 2 % (v/v) acetic acid

solution, followed by the addition of 0.12 g CNC and 0.5 % polyethylene glycol as a plasticizer. A volume of 1 % stable nanoemulsion of AC-1, AC-2 and AC-3 was added to the film forming solution and homogenized for 6 hours at least using an IKA RW-20 homogenizer at 1500 rpm. After mixing, a volume of 15 mL of film forming solution was poured onto a petri plate and let to dry for 24 h at room temperature. The concentration of CNC, active combinations and PEG were selected based on the results of initial tests.

PBAT and PLA-based nanocomposite films were fabricated using a compression molding method (hot-pressed). For PBAT-based film fabrication, 2 g of PBAT were mixed with 0.375 % CNC, 300 μ L of active combination (AC-1, AC-2 or AC-3), and 0.5 % glycerol and then hot pressed using a compression molding machine to a fabricate bioactive PBAT-based nanocomposite film loads with AC-1, AC-2 and AC-3. For PLA-based films, a quantity of 1 % CNC, 300 μ L active combination (either AC-1 or AC-2 or AC-3), and 1 % glycerol were incorporated into PLA (2 g) polymeric pellets and bioactive films were fabricated by hot-pressed.

8.2.6. Characterization of bioactive nanocomposite films

The mechanical properties (tensile strength [TS], tensile modulus [TM] and elongation at break [Eb]), water solubility (WS), water vapor permeability (WVP), *in vitro* release profile of active combinations from the optimized bioactive nanocomposite films (CH-, PBAT- and PLA-based) and *in vitro* antibacterial, antifungal and insecticidal properties were examined. The tested films were neat CH-film, CH+CNC+PEG+AC-1, CH+CNC+PEG+AC-2, CH+CNC+PEG+AC-3, neat PBAT-film, PBAT+CNC+Gly+AC-1, PBAT+CNC+Gly+AC-2, PBAT+CNC+Gly+AC-3, neat PLA-film, PLA+CNC+Gly+AC-1, PLA+CNC+Gly+AC-2, and PLA+CNC+Gly+AC-3 films. Each test is described briefly:

8.2.6.1. Mechanical properties

Mechanical properties (Tensile strength [TS], tensile modulus [TM], and elongation at break [Eb]) of the films were tested using a Universal Testing Machine (100 N-load cell; specimen grips: 1.5 kN) (Tinius Olsen Testing Machine Co., Inc., Horsham, PA, USA) a Traceable Carbon® Fiber Digital Caliper (Fisher Scientific) following a method described in [\(Khan *et al.*, 2014\)](#). The film thickness and width were recorded by using a Mitutoyo Digimatic Indicator (Type ID-110E; Mitutoyo Manufacturing Co. Ltd., Tokyo, Japan) and a Traceable Carbon® Fiber Digital Caliper (Fisher Scientific), respectively, at five different points.

8.2.6.2. Water solubility (WS)

Water solubility (WS) of the nanocomposite films were examined for measuring the water-resistant property of the films as described by [Khan et al. \(2014\)](#). Briefly, a 1.5 cm² film was cut and dried for 24 h at 105 °C to get the initial weight (W_i) of the dried film. Afterwards, the dried film was dipped in a volume for 100 mL water and left it for 24 h at room temperature in undisturbed condition. After 24 h, the film was taken from the water and dried for another 24 h at 105 °C, and then, determined the final weight (W_f) of the film was determined. The WS of the film was then calculated by the following equation 8.2

$$\text{Water solubility (WS)} = \frac{(W_i - W_f)}{W_f} \times 100 \text{ Eq. 8.2}$$

Where W_i = initial weight of the film and W_f = final weight of the film.

8.2.6.3. Water vapor permeability (WVP)

To measure WVP of the films, a film was placed onto a vapometer cell (model 68-1; Twining-Albert Instrument Co., West Berlin, NJ, USA) that was previously filled with anhydrous calcium chloride (30 g) (RH: 0 %). After sealing the cell, the initial weight of the cell was measured and kept in a humidity chamber (Shellab 9010L, Sheldon Manufacturing Inc., Cornelius, OR, USA) at 25 °C (RH: 60 %) for 24 h. The final weight of the cell was measured after 24 h and calculated the WVP of the film was calculated using equation 8.3:

$$\text{WVP (g mm m}^{-2} \text{ day}^{-1} \text{ kPa}^{-1}) = \Delta w \cdot x / A \cdot \Delta P \text{ Eq. 8.3}$$

Where Δw : Gained weight (g) of the cell after 24 h; x : Film thickness (mm); A : Area of exposed film ($31.67 \times 10^{-4} \text{ m}^2$); and ΔP : Differential vapor pressure of water through the film ($\Delta P = 3.282 \text{ kPa}$ at 25 °C).

8.2.6.4. *In vitro* antibacterial and antifungal properties

An inverted lid agar volatilization assay method was used to measure the antibacterial and antifungal properties of the films by calculating inhibitory capacity (IC, %) ([Begum et al., 2022a](#)). Briefly, the bacterial and fungal strains (approximately 10^5 CFU/mL) were inoculated on the surface of TSA or PDA media. Then, the plate was inverted, and a piece of film (1 cm²) was placed in the middle of the lid of the Petri plate, followed by sealing the plates with Parafilm®, incubating all plates at 37 °C for 24 h (bacteria) and at 27 °C for 48 h (fungi). The inhibitory capacity of the films was calculated using equation 8.4.

Inhibitory capacity (% , IC) = Diameter of the inhibition zone (mm) / Diameter of the petri plate (mm) × 100 Eq. 8.4

8.2.6.5. *In vitro* insecticidal properties

The fumigation toxicity tests of the fabricated bioactive nanocomposite films were tested against *S. oryzae* as described by [Hossain et al. \(2019b\)](#) with the following modifications. Briefly, a quantity of 10 g of rice was placed in a Petri dish. One piece of (2.5 cm²) bioactive CH-, PBAT- and PLA-based nanocomposite films were fixed onto the lid of the Petri dish (95 × 15 mm) and 25 adult rice weevils were inoculated. Each Petri dish was covered and sealed with laboratory Parafilm® and incubated at 28 °C (65 % RH) for 72 h. Each experiment was performed in triplicate (n = 3). The mortality (%) of insects was calculated at 24, 48, and 72 h using equation 8.5.

Mortality (%) = (Number of dead insect / Total number of insect) × 100 Eq. 8.5

8.2.6.6. *In vitro* release profiles of the active combinations from the bioactive films

The cumulative release of the active combinations from the bioactive films was tested in 3 % (v/v) acetic acid and 10 % (v/v) ethanol media as food simulants with different contact times ([Hossain et al., 2018](#); [Ben-Fadhel et al., 2020](#); [Felix da Silva Barbosa et al., 2021](#)). Briefly, 500 mg of film was kept in a volume of 200 mL of food simulant (ethanol or acetic acid) under constant magnetic stirring at room for 70 h of extraction time. A volume of 1 mL extracted sample was collected each hour until reach equilibrium and each time 1 mL of fresh acetic acid/ethanol was added to the film+food simulant bath to maintain the same volume. Then, the extracted sample was analysed using a UV-Vis spectrophotometer and calculated the cumulative release (%) of AC-1, AC-2 and AC-3 from the films using equation 8.6.

Cumulative release (%) = $\frac{\text{Volume of sample withdraw}}{\text{Bath volume}} \times P(t - 1) + P_t$ Eq. 8.6

Where, P_t is released (% , w/v) at time t; $P_{(t-1)}$ is released (% , w/v) at a time previous to “t”. All experiments were performed in triplicate. A total nine types of films were tested named PBAT+CNC+Gly+AC-1 film; PBAT+CNC+Gly+AC-2 film; PBAT+CNC+Gly+AC-3 film; PLA+CNC+Gly+AC-1 film; PLA+CNC+Gly+AC-2 film; PLA+CNC+Gly+AC-3 film; CH+CNC+PEG+AC-1 film; CH+CNC+PEG+AC-2 film; CH+CNC+PEG+AC-3 film. The blank sample consisted of the respective film without active combinations in the liquid phase. In addition, the obtained data were fitted into the Korsmeyer-Peppas model to understand the release mechanisms of active combinations through the polymeric matrices.

$$M_t/M_\infty = kt^n \text{ Eq. 8.7}$$

Where M_t/M_∞ : Fraction of the released active formulation at the time “t”; k: Rate constant of apparent release (related to the diffusion process); n: Release exponent (“n” values are given information associated with the release mechanism). Herein, an “n” value ≤ 0.45 : release through Fickian diffusion or quasi-Fickian diffusion, “n” value between 0.45 and 0.89: release through anomalous transportation (means the polymer relaxation and the diffusion rates are coupled), “n” value equal to 0.89: release follows a zero-order release mechanism (means through swelling processing), and “n” value > 0.89 : release through non-Fickian transportation mechanism (means deterioration of the polymeric chain and release occurs by both diffusion and relaxation processes) ([Requena et al., 2017](#); [Ben-Fadhel et al., 2020](#)).

8.2.7. Evaluate the antibacterial and antifungal properties of the films (for cereal grains)

The bioactive nanocomposite films with higher bactericidal and fungicidal properties along with satisfactory mechanical, WS, WVP, OTR, and release profiles were selected for an *in situ* challenging test in rice against two pathogenic bacteria (*E. coli* O157:H7 and *S. Typhimurium*) and two spoilage fungi (*A. niger* and *P. chrysogenum*) ([Begum et al., 2022a](#)). Furthermore, combining the bioactive nanocomposite with γ -irradiation (750 Gy) was applied to evaluate the possible synergistic effect for controlling the growth of bacteria and fungi in stored rice. Briefly, a quantity of sterile 500 g rice was poured into an inoculation bath of 10^5 CFU/mL of bacteria/fungi and mixed well for 30 sec. Then, the rice was filtered using a sterile screen to drain out the excess water and dried for 2 h under sterile conditions. After drying, 50 g of rice was taken out and placed into a sterile plastic bag containing the bioactive nanocomposite films (1 g/cm²). For irradiation treatment, the inoculated rice samples with and without bioactive nanocomposite films went under irradiation treatment (750 Gy) using a Cobalt-60 UC-15A γ -irradiator at a 7.1 kGy/h dose rate (Nordion, Laval, QC, Canada). The samples without bioactive nanocomposite films were considered as control (Rice+pathogenic bacteria/fungi) and γ -control (750 Gy irradiation alone). The microbiological analyses were carried out each week for 8 weeks ([Begum et al., 2022a](#)).

8.2.8. Evaluate the anti-insect properties of the films (for cereal grains)

The insecticidal properties of the nine nanocomposite films (CH+CNC+PEG+AC-1 film, CH+CNC+PEG+AC-2 film, CH+CNC+PEG+AC-3 film, PBAT+CNC+Gly+AC-1 film, PBAT+CNC+Gly+AC-2 film, PBAT+CNC+Gly+AC-3 film, PLA+CNC+Gly+AC-1 film, PLA+CNC+Gly+AC-2 film and PLA+CNC+Gly+AC-3 film) were tested against rice weevil (*S. oryzae*) (Hossain *et al.*, 2014b; Hossain *et al.*, 2019b). The samples without bioactive nanocomposite films were considered as control (rice+insects). A total of 15 adult rice weevils were added to a plastic bag containing 30 g of sterile rice. Two pieces of insecticidal films were inserted into the plastic bag and stored for 14 days. The samples were divided into two sets: one set of samples contained only insecticidal film and a 2nd set of the film was combined with 100-300 Gy of γ -irradiation using UC-15A γ -irradiator equipped with Cobalt-60 (Nordion, Laval, QC, Canada). Another set of samples underwent irradiation treatment alone at 100, 200, and 300 Gy to determine the insecticidal effect of irradiation during 14 days of storage. The rice weevils were considered as dead when their appendages were not moving even after probing with a fine camel brush. The experiments were performed in three replicates for each set of samples. The % mortality of insects were measured using equation 8.8.

$$\% \text{ mortality} = (\text{Number of dead insects} / \text{Number of total insects}) \times 100 \text{ Eq. 8.8}$$

8.2.9. Evaluate the antibacterial and antifungal properties of the film (for dairy products)

Six types of bioactive nanocomposite films (PBAT+CNC+Gly+AC-1, PBAT+CNC+Gly+AC-2, PBAT+CNC+Gly+AC-3, PLA+CNC+Gly+AC-1, PLA+CNC+Gly+AC-2 and PLA+CNC+Gly+AC-3 films) with higher bactericidal and fungicidal properties as well as with satisfactory physicochemical properties were tested against two pathogenic bacteria (*E. coli* O157:H7 and *S. Typhimurium*) and three spoilage fungi (*A. niger*, *P. chrysogenum* and *M. circinelloides*) in stored yogurt 4 °C as a food model of dairy products. Briefly, the films were cut in 7 cm in diameter and fixed in the inside lid of yogurt container. The yogurt was inoculated with 10⁵ CFU/mL of bacteria/fungi and the microbial analysis was performed for 8 weeks. The control sample consisted of the yogurt inoculated with pathogens without bioactive films.

8.3. Results and Discussion

8.3.1. Development and characterization of nanoemulsion of active combinations

The zeta potential, polydispersity index (PDI), size, and encapsulation efficiency (EE) of the nanoemulsion of active combinations (AC-1, AC-2 and AC-3) were tested and compared with their corresponding coarse emulsions (Table 8.1). Results showed that a microfluidization pressure of 8000 psi at the 2nd cycle reduced the droplet size of AC-1 from 162 to 76.2 nm ($P \leq 0.05$) (53 % reduction). The application of optimized microfluidization pressure of 10000 psi at the 3rd cycle on AC-2 and 6000 psi at the 4th cycle on AC-3 caused a significant reduction of droplet size by 26 % (from 122 to 90 nm) and 67 % (from 257.3 to 85 nm), respectively. High pressure microfluidizer treatment significantly ($P \leq 0.05$) increased the encapsulation efficiency (EE, %) of the nanoemulsions of AC-1, AC-2 and AC-3 as compared to the coarse emulsions of the corresponding active combinations. The EE of the coarse emulsion of AC-1, AC-2 and AC-3 was 32, 19 and 31.6 %, respectively, while the EE of the corresponding nanoemulsions were 85.6, 78 and 82 %. The microfluidization pressure had a significant effect on the zeta potential and PDI of the emulsions. The zeta potential was -33.7, -36.8 and -35.3 mV for the nanoemulsion of AC-1, AC-2 and AC-3, respectively, while zeta potential values for the corresponded coarse emulsions were -14.2, -18.7 and -21.5 mV. PDI values indicate the particle size distribution throughout the emulsion and higher the PDI values indicate broader size distribution and lower PDI values indicate smaller size distribution or homogeneity. The optimized microfluidization pressure significantly reduced the PDI values from 0.6 to 0.19 ($P \leq 0.05$), from 0.54 to 0.22 ($P \leq 0.05$) and from 0.67 to 0.19 ($P \leq 0.05$) for the nanoemulsions of AC-1, AC-2 and AC-3, respectively (Table 8.1).

The development of nanoemulsions using a microfluidizer is well known as a high energy emulsification method. The utilization of a microfluidizer has several advantages such as obtaining ultrafine nanoemulsions, maintaining the droplet size distributions, easy to scale up for industry. To get stable nanoemulsions, the function of the number of cycles and microfluidization pressures are important factors (Llinares *et al.*, 2018; Llinares *et al.*, 2021). Several studies have shown that the higher zeta potential values (around ± 30 mV), lower droplet size and PDI, and higher EE is an indication of stable and stronger nanoemulsion by preventing aggregation, creaming, and coalescence (Hossain *et al.*, 2019a; Hossain *et al.*, 2019b; Ben-Fadhel *et al.*, 2020). High-pressure microfluidisation treatment may play a significant role in the development of a stable nanoemulsion emulsion that is electrostatically stable because of its higher zeta potential values (ranges between

very high +30mV and very low -30 mV) (Asmawati *et al.*, 2014; Cheng *et al.*, 2016). In the current study, the obtained zeta potentials for nanoemulsions AC-1, AC-2 and AC-3 were between -33.7 and -36.8 mV which suggested that the obtained nanoemulsions were electrostatically stable. Furthermore, the stable nanoemulsions were encapsulated into polymeric matrices to develop biopolymeric films for controlling the growth of pathogenic bacteria, spoilage fungi and insect pests in stored rice.

Table 8.1. Effect of microfluidisation pressure and number of cycles on the zeta potential (mV), PDI (poly dispersity index), size (nm) and encapsulation efficiency (EE, %) of AC-, AC-2 and AC-3.

Active formulations (AF)	Zeta potential (mV)	PDI	Size (nm)	Encapsulation efficiency, EE (%)
Coarse emulsion AC-1	-14.2±0.8 ^a	0.6±0.17 ^b	162±10.7 ^a	32±5.3 ^a
Nanoemulsion AC-1	-33.7±6.7 ^b	0.19±0.0005 ^a	76.2±5.9 ^b	85.6±6.9 ^b
Coarse emulsion AC-2	-18.7±0.9 ^a	0.54±0.08 ^b	122±7.7 ^a	19.1±6.3 ^a
Nanoemulsion AC-2	-36.8±2.06 ^b	0.22 ± 0.02 ^a	90±16.48 ^b	78±5.75 ^b
Coarse emulsion AC-3	-21.5±2.3 ^a	0.67±0.15 ^b	257.3±7.1 ^a	31.6±3.5 ^a
Nanoemulsion AC-3	-35.3±4.04 ^b	0.19±0.005 ^a	85±5.2 ^b	82±11.2 ^b

Values means ± standard error. Within each column means with different lowercase letter are significantly different ($P \leq 0.05$).

8.3.2. Characterization of the bioactive nanocomposite films

CH-, PBAT- and PLA-based twelve films were fabricated and coded as: CH-film (no active combination); CH+CNC+PEG+AC-1 film; CH+CNC+PEG+AC-2 film; CH+CNC+PEG+AC-3 film; PBAT-film (no active combinations); PBAT+CNC+Gly+AC-1 film; PBAT+CNC+Gly+AC-2 film; PBAT+CNC+Gly+AC-3 film; PLA-film; PLA+CNC+Gly+AC-1 film; PLA+CNC+Gly+AC-2 film; PLA+CNC+Gly+AC-3 film. All fabricated films were characterized by their mechanical properties (TS, TM and Eb), water solubility (WS), water vapor permeability (WVP), oxygen transmission rate (OTR), *in vitro* bioassay (antibacterial, antifungal and insecticidal properties) and cumulative release of active combinations in food simulants for further application of the films in real foods. Each test was described below:

8.3.2.1. Mechanical properties

The effect of ACs (AC-1, AC-2 and AC-3) and CNC in polymeric matrices (CH-, PBAT- and PLA-based) on the mechanical properties (TS, TM and Eb) was tested and the results are shown in Table 8.2. To develop active packaging film for food preservation, the mechanical property of the fabricated film is an important parameter because TS, TM and Eb are associated with the mechanical strength, rigidity and flexibility of the fabricated films, respectively. The TS and TM of the bioactive CH-based nanocomposite films increased significantly ($P \leq 0.05$) with the incorporation of a 1 % nanoemulsion of ACs (AC-1, AC-2 and AC-3) and 0.12 g CNC compared to the CH-based film (without ACs and CNC). In this current study, TS values were found 83.7, 96.7 and 88.2 MPa in CH+CNC+PEG+AC-1, CH+CNC+PEG+AC-2 and CH+CNC+PEG+AC-3 film, respectively, which was significantly ($P \leq 0.05$) higher than CH-film (TS: 75.3 MPa) (Table 8.2). A significantly ($P \leq 0.05$) higher TM values were recorded for CH+CNC+PEG+AC-1 (TM: 1480 MPa), CH+CNC+PEG+AC-2 (TM: 1635 MPa) and CH+CNC+PEG+AC-3 film (TM: 1544 MPa) as compared to CH-film (TM: 1279 MPa). After incorporation of active combinations and CNC, the flexibility (Eb) of the bioactive CH-based nanocomposite films (CH+CNC+PEG+AC-1, CH+CNC+PEG+AC-2 and CH+CNC+PEG+AC-3 film) were significantly ($P \leq 0.05$) reduced than CH-film. The Eb values were obtained 61, 55, 48 and 43.9 % for the CH-film, CH+CNC+PEG+AC-1, CH+CNC+PEG+AC-2 and CH+CNC+PEG+AC-3 film, respectively. These values are in accordance with [Khan *et al.* \(2012\)](#); [Hossain *et al.* \(2019a\)](#) where the authors have delineated the enhancement of the TS and TM values of the CH-based nanocomposite films after incorporating CNC and EOs. [de Mesquita *et al.* \(2010\)](#) stated that the TS values of the CH-based nanocomposite films were increased due to the interaction between the cationic amine groups in CH polymer and the anionic sulfate groups in CNC that might increase the interface between the filler and the polymeric matrices and caused higher mechanical strength of the nanocomposite films. Moreover, the mean-field mechanical force may also be responsible for higher TS values because of the uniform distribution of the CNC throughout the CH-polymeric matrices without interactions ([Khan *et al.*, 2012](#)). It has been observed that the incorporation of CNC into CH-based polymer increased the brittleness of the films which is a very common phenomenon in filler-reinforced films observed by several authors ([Lee *et al.*, 2004a](#); [Khan *et al.*, 2012](#); [Hossain *et al.*, 2019a](#)). [Hossain *et al.* \(2018\)](#) reported a 15 % increment of TM values of the methylcellulose nanocomposite films when incorporated 7.5 % (w/w) CNC. The reduction of Eb of the nanocomposite films after loading CNC might be due to the strong interactions between polymeric matrices and CNCs that limited the movement of the polymeric matrices and thus lowered the Eb values of the CH-based nanocomposite films ([Samir *et al.*, 2004](#); [Hossain *et al.*, 2019a](#)).

Table 8.2. Effect on CNC content in the mechanical properties (TS, TM, Eb), water vapor permeability (WVP) and water solubility (WS) of the bioactive composite films.

Films	Mechanical properties			WVP (g.m.mm ⁻² . day ⁻¹ .kPa ⁻¹)	WS (%)
	TS (MPa)	TM(MPa)	Eb (%)		
CH-film	75.3±5.8 ^a	1279±120 ^a	61±7.1 ^c	10.2±1.1 ^c	32.2±4.9 ^b
CH+CNC+PEG+AC-1	83.7±6.9 ^b	1480±65 ^b	55±8.8 ^b	6.9±2.8 ^b	24.6±5.2 ^a
CH+CNC+PEG+AC-2	96.7±12.3 ^d	1635±45 ^d	48±6.8 ^a	7.2±3.4 ^b	26.8±4.6 ^a
CH+CNC+PEG+AC-3	88.2±9.5 ^c	1544±23 ^c	43.9±4.8 ^a	5.8±2.8 ^a	23.7±3.9 ^a
PBAT-film	24.4±2.9 ^c	76.8±5.8 ^c	627±11.3 ^c	2.35±0.59 ^b	0.74±0.03 ^a
PBAT+CNC+Gly+AC-1	19.1±4.6 ^b	75.7±4.5 ^c	669.7±13.8 ^d	2.07±0.51 ^a	0.87±0.05 ^a
PBAT+CNC+Gly+AC-2	12.5 ± 3.0 ^a	70 ± 10 ^b	584 ± 26.3 ^a	2.20 ± 0.17 ^a	0.69±0.04 ^a
PBAT+CNC+Gly+AC-3	13.2±2.04 ^a	63.7±6.52 ^a	619±21.7 ^b	2.16±0.35 ^a	0.76±0.07 ^a
PLA-film	66.7±7.6 ^d	1253±45 ^d	36.3±5.1 ^a	3.45±0.50 ^a	0.59±0.01 ^a
PLA+CNC+Gly+AC-1	51.3±9.7 ^c	896±42.3 ^b	68.7±8.9 ^b	3.74±0.85 ^c	0.79±0.04 ^a
PLA+CNC+Gly+AC-2	42.8±9.6 ^b	968±18.7 ^c	92.8±12.3 ^d	3.58±0.57 ^b	0.65±0.08 ^a
PLA+CNC+Gly+AC-3	36.8±5.4 ^a	788±21.2 ^a	82.9±14.8 ^c	3.65±0.85 ^b	0.69±0.06 ^a

Values means ± standard error. Within each column means with different lowercase letter are significantly different ($P \leq 0.05$).

It is well known that the PBAT film (TM: 76.8 MPa) is flexible plastic while the PLA film (TM: 1253 MPa) is rigid plastic (Table 8.2). Incorporation of CNC+Gly+ACs into PBAT polymeric matrices significantly ($P \leq 0.05$) reduced the TM of the films when compared to neat PBAT-film. The TM values were 75.7, 70 and 63.7 MPa for the PBAT+CNC+Gly+AC-1, PBAT+CNC+Gly+AC-2 and PBAT+CNC+Gly+AC-3 film, respectively, while this TM value for neat PBAT was 76.8 MPa. A similar phenomenon was observed with the TS values of the PBAT film. The TS value of the neat PBAT was 24.4 MPa, while the TS values were 19.1, 12.5 and 13.2 MPa for the PBAT+CNC+Gly+AC-1, PBAT+CNC+Gly+AC-2 and PBAT+CNC+Gly+AC-3 film nanocomposite films, respectively. On the other hand, an opposite tendency was observed in the case of the films' Eb values after incorporation of CNC+Gly+ACs into PBAT polymeric matrices, the Eb (significantly increased the flexibility of the nanocomposite films) of the films were increased compared to neat PBAT. The Eb values were 627, 669.7, 584 and 619 % for the neat PBAT-film,

PBAT+CNC+Gly+AC-1, PBAT+CNC+Gly+AC-2 and PBAT+CNC+Gly+AC-3 film, respectively (Table 8.2). The TS, TM, and Eb values of pure PBAT film were 22 MPa, 90.4 MPa, and 817.8 % found by [Li et al. \(2015a\)](#) which supported the results obtained in the current study. Moreover, the incorporation of CNC+Gly+ACs into the PBAT polymeric matrices acted as a plasticizer and reduced the intermolecular forces between polymeric chains, thus improving the flexibility and extensibility, and lessening the rigidity compared to the neat PBAT film.

The TS of the neat PLA film was 66.7 MPa, which was reduced significantly ($P \leq 0.05$) by 23 to 45 % after incorporation of CNC+Gly+ACs into the PLA matrices. The similar TS value of the neat PLA film (TS: 62 MPa) was found by [Wang et al. \(2016\)](#). Similarly, the TM values of the nanocomposite PLA films were also significantly ($P \leq 0.05$) reduced by 23 to 37 % after incorporation of CNC+Gly+ACs compared to neat PLA-film. After incorporation of CNC+Gly+ACs into PLA polymeric matrices, the Eb values tend to rise significantly ($P \leq 0.05$) than the Eb value of neat PLA-film. The Eb values were 36.3, 68.7, 92.8 and 82.9 % for the neat PLA-film, PLA+CNC+Gly+AC-1, PLA+CNC+Gly+AC-2 and PLA+CNC+Gly+AC-3 film, respectively. The plasticizer effect of CNC+active combinations could weaken the intermolecular interactions of the polymeric chains, thus, raising the mobility of the polymeric motion with lesser rigidity as well as higher flexibility and extensibility of the nanocomposite PLA and PBAT films ([Rhim et al., 2006](#); [Cardoso et al., 2017](#)). A similar trend has been observed by [Sharma et al. \(2020\)](#) where the authors prepared the bioactive PLA/PBAT composite polymeric film by incorporating clove oils (1-10 %). They found that the TS and Eb values of the PLA/PBAT composite film were 1.35 MPa and 5.63 %, respectively. However, after the incorporation of clove oil into the PLA/PBAT polymeric matrices, the clove acted as a plasticizer, and thus, the flexibility of the composite films was raised significantly (Eb: from 26 to 40 %) and reduced the TS values (TS: from 0.79 to 0.94 MPa) ([Sharma et al., 2020](#)).

8.3.2.2. Water solubility (WS)

The WS of twelve types of films (CH-, PBAT- and PLA-based) are presented in Table 8.2. The WS measurement of the film is very a important parameter in the context of food packaging as it is an index of the solubility to water or high moisture content food. Incorporation of CNC+ACs into the CH-based polymeric matrix significantly ($P \leq 0.05$) reduced WS by 24 % in CH+CNC+PEG+AC-1 film (WS: 24.6 %), by 17 % in CH+CNC+PEG+AC-2 film (WS: 26.8 %) and by 26 % in CH+CNC+PEG+AC-3 film (WS: 23.7 %) as compared to the neat CH-film (WS: 32.2 %). In the case of PBAT- and PLA-based films, the incorporation of CNC+ACs did not significantly affect the

WS of the bioactive nanocomposite films when compared to neat PLA- and PBAT-based films because of their insoluble nature in water. WS of the CH+CNC+PEG+AC-1, CH+CNC+PEG+AC-2 and CH+CNC+PEG+AC-3 film was significantly lower which might be due to chemical crosslinking among the hydrophilic polymeric matrices. The results are consistent with the findings of [Abdollahi *et al.* \(2012\)](#); [Sani *et al.* \(2019\)](#). [Sani *et al.* \(2019\)](#) fabricated chitosan-based active films by encapsulating melissa EO and ZnO nanoparticle, and they found a significant ($P \leq 0.05$) water solubility reduction of the chitosan films containing melissa EO and ZnO than pure chitosan film. In the current study, bioactive CH-based nanocomposite films significantly reduced the WS than neat CH films because of the incorporation of hydrophobic EOs which interrupt the binding of water molecules to the polymer by blocking free H-groups. Moreover, interactions between polymer matrices and nanoparticles could reduce the polymer solubility ([Sani *et al.*, 2019](#)). Herein, a transverse coupling reaction might have occurred between EOs and esters or amides group of CH and caused WS reduction of the bioactive CH-based nanocomposite film ([Abdollahi *et al.*, 2012](#)). Moreover, CNC could increase the cohesion of the film which reduced the free -OH groups to interact with water molecules and thus, reduce this WS in bioactive CH-based nanocomposite films when compared to neat CH-films ([Escamilla-García *et al.*, 2022](#)).

8.3.2.3. Water vapor permeability (WVP)

WVP is an important parameter of the packaging films because water from the atmosphere can play an important role in the degradation of films by accelerating the chemical and enzymatic reactions in the polymer, thus helping to increase the microbial growth in foods and deteriorate the food quality during storage ([Hossain *et al.*, 2019a](#)). WVP results of the films are presented in Table 8.2. WVP of the bioactive CH-based films (CH+CNC+PEG+AC-1, CH+CNC+PEG+AC-2 and CH+CNC+PEG+AC-3 film) was significantly ($P \leq 0.05$) reduced by 29.4 to 32 % after incorporating CNC+ACs (AC-1, AC-2 and AC-3) as compared to neat CH-film. Table 8.2 also shows the WVP of the neat PBAT and PLA films and bioactive PLA and PBAT-based nanocomposite films. The WVP of neat PBAT and neat PLA-film was 2.35 and 3.45 g.m.mm².day⁻¹.kPa⁻¹, respectively, and the values were in agreement with the previous studies by [Morelli *et al.* \(2016\)](#) and [Wang *et al.* \(2016\)](#). During the incorporation of CNC+ACs into PBAT matrices, the WVP was significantly ($P \leq 0.05$) reduced by 12 % (WVP: 2.07 g.m.mm².day⁻¹.kPa⁻¹), 6.4 % (WVP: 2.20 g.m.mm².day⁻¹.kPa⁻¹) and 8 % (WVP: 2.16 g.m.mm².day⁻¹.kPa⁻¹) in the PBAT+CNC+Gly+AC-1, PBAT+CNC+Gly+AC-2 and PBAT+CNC+Gly+AC-3 film, respectively, as compared to the neat PBAT-film. On the other hand, an opposite phenomenon was observed in the case of PLA films

when incorporating CNC+AC-1, CNC+AC-2 and CNC+AC-3. During the incorporation of CNC+ACs into PLA matrices, the WVP was significantly ($P \leq 0.05$) increased by 8 % (WVP: 3.74 g.m.mm².day⁻¹.kPa⁻¹), 4 % (WVP: 3.58 g.m.mm².day⁻¹.kPa⁻¹) and 6 % (WVP: 3.65 g.m.mm².day⁻¹.kPa⁻¹) in the PLA+CNC+Gly+AC-1, PLA+CNC+Gly+AC-2 and PLA+CNC+Gly+AC-3 film, respectively, as compared to the neat PLA-film. Similar observations have been obtained by several authors (Salmieri *et al.*, 2014a; Hossain *et al.*, 2018; Shankar and Rhim, 2018; Hossain *et al.*, 2019a). Salmieri *et al.* (2014a) developed bioactive PLA-CNC-nisin nanocomposite film for meat preservation and the authors found that the WVP values of bioactive PLA-CNC-nisin films (WVP: 3.8 g.m.mm².day⁻¹.kPa⁻¹) were comparatively higher than the PLA-CNC film (control film) (WVP: 3.2 g.m.mm².day⁻¹.kPa⁻¹) at day 0 (17 % increment).

However, several factors viz. vapor diffusion, adsorption, desorption, and polymeric affinity to water are affected by the WVP of the films (Srisa and Harnkarnsujarit, 2020). The presence of CNC throughout the bioactive PBAT- and CH-based nanocomposite films could create a tortuous path which might decrease the diffusion process and hence, lower the WVP of the bioactive PBAT- and CH-based nanocomposite films (Khan *et al.*, 2012; Khan *et al.*, 2013). Moreover, the presence of hydrophobic essential oils in active formulations might also effectively prevent the diffusion of vapor from the bioactive PBAT- and CH-based nanocomposite and result in improved WVP of the films (Srisa and Harnkarnsujarit, 2020). A percolated network might be created when CNC was incorporated into polymeric matrices by H-bonding which can reduce the molecular mobility and free volume of polymeric matrices and create more obstacles for water vapor diffusion, and thus reduce WVP (Pereda *et al.*, 2012). Khan *et al.* (2012) studied chitosan-based films by reinforcing cellulose nanocrystals (CNCs) for improving the mechanical and barrier properties. The authors found that the WVP of the CH-based nanocomposite films by incorporating 5 % CNC into the CH-polymeric matrix was decreased by 27 % than the control CH-based film (Khan *et al.*, 2012).

8.3.2.4. *In vitro* antibacterial and antifungal properties

The *in-vitro* antimicrobial and antifungal activities of twelve types of CH-, PBAT- and PLA-based films (CH-film [no active combinations], CH+CNC+PEG+AC-1, CH+CNC+PEG+AC-2, CH+CNC+PEG+AC-3, PBAT-film [no active combinations], PBAT+CNC+Gly+AC-1, PBAT+CNC+Gly+AC-2, PBAT+CNC+Gly+AC-3, PLA-film [no active combinations], PLA+CNC+Gly+AC-1, PLA+CNC+Gly+AC-2 and PLA+CNC+Gly+AC-3 film) were tested against two foodborne pathogenic bacteria (*E. coli* O157:H7 and *S. Typhimurium*) and three spoilage fungi (*A. niger*, *P. chrysogenum* and *M. circinelloides*) (Table 8.3). Three bioactive CH-based

nanocomposite films (CH+CNC+PEG+AC-1, CH+CNC+PEG+AC-2 and CH+CNC+PEG+AC-3 film) showed strong bactericidal and fungicidal properties against *E. coli* O157:H7, *S. Typhimurium*, *A. niger*, *P. chrysogenum* and *M. circinelloides* with the inhibitory capacity (IC) values ranges between 52.6 and 66.9 %, while the neat CH-film did not show any antibacterial and antifungal properties. Similarly, neat PBAT- and PLA-films did not show any antibacterial and antifungal properties against all tested bacteria and fungi. The bioactive PBAT-based nanocomposite films (PBAT+CNC+Gly+AC-1, PBAT+CNC+Gly+AC-2 and PBAT+CNC+Gly+AC-3) showed significantly ($P \leq 0.05$) higher IC values ranges from 62.9 to 88.3 % against all tested bacterial and fungal species as compared to the neat PBAT-film. Though bioactive PLA-based films (PLA+CNC+Gly+AC-1, PLA+CNC+Gly+AC-2 and PLA+CNC+Gly+AC-3) showed lower antibacterial and antifungal properties as compared to bioactive CH- and PBAT-based films, the bioactive PLA-based nanocomposite films showed significantly ($P \leq 0.05$) higher IC values ranges between 24.9 to 58.4 % against *E. coli* O157:H7, *S. Typhimurium*, *A. niger*, *P. chrysogenum* and *M. circinelloides* as compared to neat PLA-film (Table 8.3).

[Begum et al. \(2022a\)](#) developed three active combinations (AC-1, AC-2 and AC-3) using a mixture of silver nanoparticles (AGPPH, AGPP and AGC0.5) and EOs (cinnamon, Mediterranean formulation, citrus, Asian formulation and lavang EO) and the authors found strong antibacterial and antifungal properties against pathogenic bacteria (*E. coli* O157:H7 and *S. Typhimurium*) and spoilage fungi (*A. niger*, *P. chrysogenum* and *M. circinelloides*). The active combination released from the polymeric matrices (CH-, PBAT- and PLA-based nanocomposite films), acted on the bacterial and fungal species in a vapor state and inhibited their growth. AC-1 composed of cinnamon EO and AGPPH and cinnamaldehyde is the major chemical constituent in cinnamon EO. After releasing from the matrices, cinnamaldehyde and silver nanoparticles together could engage the surface of pathogenic bacteria and fungi and disrupt the cell membrane and energy balance and cause cell death ([Ghosh et al., 2013a](#)). Generally, oxygenated terpenoids, phenolic terpenes, phenyl-propanoids, and alcohols are present in the EOs used in this current study that are mainly responsible for antibacterial and antifungal properties ([Begum et al., 2022a](#)). It has been hypothesized that the EOs could encapsulate AgNPs and be released together which could increase the bioavailability as well as lead to increased stability from environmental influences ([Weisany et al., 2019](#)).

Table 8.3. Inhibitory capacity (IC, %) against pathogenic bacteria and spoilage fungi of bioactive nanocomposite films.

Films	Inhibitory capacity (IC, %)				
	<i>E. coli</i> O157:H7	<i>S.</i> Typhimurium	<i>A. niger</i>	<i>P.</i> <i>chrysogenum</i>	<i>M.</i> <i>circinelloides</i>
CH-film	0 ^{aA}	0 ^{aA}	0 ^{aA}	0 ^{aA}	0 ^{aA}
CH+CNC+PEG+ AC-1	52.6±8.3 ^{ba}	55.6±6.3 ^{ba}	65.3±9.3 ^{cc}	61.7±7.3 ^{bb}	66.9±8.8 ^{cc}
CH+CNC+PEG+ AC-2	57.3±5.9 ^{ca}	63.2±4.8 ^{cb}	58.4±5.7 ^{ba}	65.3±6.9 ^{bb}	59.9±6.6 ^{ba}
CH+CNC+PEG+ AC-3	59.6±9.3 ^{ca}	57.3±6.3 ^{ba}	60.5±6.1 ^{ba}	63.2±4.7 ^{bb}	58.2±6.4 ^{ba}
PBAT-film	0 ^{aA}	0 ^{aA}	0 ^{aA}	0 ^{aA}	0 ^{aA}
PBAT+CNC+Gly +AC-1	63.1±6.6 ^{ba}	62.9±7.4 ^{ba}	76.3±9.5 ^{bc}	72.9±7.1 ^{bb}	68.6±4.9 ^{bb}
PBAT+CNC+Gly +AC-2	66.9±7.4 ^{ba}	63.9±8.9 ^{ba}	78.3±8.6 ^{bb}	88.3±9.4 ^{dc}	75.6±8.5 ^{cb}
PBAT+CNC+Gly +AC-3	66.3±5.5 ^{ba}	63.3±4.9 ^{ba}	77.6±9.3 ^{bb}	81.3±6.7 ^{cc}	73.2±9.3 ^{cb}
PLA-film	0 ^{aA}	0 ^{aA}	0 ^{aA}	0 ^{aA}	0 ^{aA}
PLA+CNC+Gly+ AC-1	28.9±4.9 ^{ba}	32.4±3.9 ^{ca}	45.2±8.7 ^{bc}	41.9±11.1 ^{bb}	39.5±8.5 ^{bb}
PLA+CNC+Gly+ AC-2	29.7±6.7 ^{bb}	24.9±5.8 ^{ba}	47.6±6.5 ^{bc}	51.6±8.8 ^{cd}	43.6±8.2 ^{cc}
PLA+CNC+Gly+ AC-3	35.2±9.4 ^{cb}	32.6±8.7 ^{ca}	55.6±9.6 ^{cd}	58.4±7.4 ^{dd}	45.8±6.7 ^{cc}

Values means ± standard error. Within each column means with different lowercase letter are significantly different ($P \leq 0.05$), while the means with the different uppercase letter are significantly different ($P \leq 0.05$).

8.3.2.5. Insecticidal properties

The *in vitro* insecticidal properties of twelve fabricated films (CH-, PBAT- and PLA-based) were tested against rice weevil (*S. oryzae*) using a fumigation toxicity test for 24, 48 and 72 h of exposure time and results are presented in Table 8.4. Results showed that the mortality of insects increased with exposure time. The neat CH-film, PBAT-film and PLA-film showed 0 to 4 % mortality of insects from 24 to 72 h of incubation. The vapor effect of active combinations from the bioactive nanocomposite films showed significantly ($P \leq 0.05$) higher mortality (%) of insects as compared to the neat-polymeric films and increased the % mortality with incubation period. Bioactive CH-based films (CH+CNC+PEG+AC-1, CH+CNC+PEG+AC-2 and CH+CNC+PEG+AC-3 film) caused 2.6 to 6.5 % mortality at 24 h of incubation, the mortality increased from 23 to 40 % from 48 to 72 h of incubation when the insects were exposed to bioactive CH-based nanocomposite films (Table 8.4). The bioactive PBAT-based nanocomposite films caused of 0.5 to 38 % mortality

of insects at 24 to 72 h of incubation period with PBAT+CNC+Gly+AC-1, PBAT+CNC+Gly+AC-2 and PBAT+CNC+Gly+AC-3 film, while the bioactive PLA-based nanocomposite films caused 0 to 26 % insect mortality after at 24 to 72 h of incubation (Table 8.4).

Table 8.4. *In vitro* insecticidal properties of the bioactive nanocomposite films against rice weevil (*S. oryzae*).

Films	Mortality (%)		
	24 h	48 h	72 h
CH-film	0 ^{aA}	0 ^{aA}	2.6±0.6 ^{aB}
CH+CNC+PEG+AC-1	4±0.6 ^{bA}	23±6.8 ^{bB}	31±4.2 ^{bC}
CH+CNC+PEG+AC-2	2.6±3.2 ^{bA}	28±4.4 ^{cB}	39±6.3 ^{cC}
CH+CNC+PEG+AC-3	6.5±1.5 ^{bA}	26±7.8 ^{bB}	40±8.9 ^{cC}
PBAT-film	0 ^{aA}	2.6±0.6 ^{aB}	4 ^{aB}
PBAT+CNC+Gly+AC-1	8.1±2.9 ^{cA}	18±6.8 ^{bA}	29±8.7 ^{bC}
PBAT+CNC+Gly+AC-2	0.5±0.4 ^{bA}	15±4.8 ^{bB}	36±9.6 ^{cC}
PBAT+CNC+Gly+AC-3	2.6±0.5 ^{bA}	20±8.5 ^{cB}	38±10.2 ^{cC}
PLA-film	0 ^{aA}	0 ^{aA}	0 ^{aA}
PLA+CNC+Gly+AC-1	0±0 ^{aA}	1.5±0.6 ^{bB}	18±6.8 ^{bC}
PLA+CNC+Gly+AC-2	2.5±1.5 ^{bA}	4±0.5 ^{bA}	19±7.1 ^{bB}
PLA+CNC+Gly+AC-3	0±0 ^{aA}	5.8±2.5 ^{cB}	26±7.4 ^{cC}

Values means ± standard error. Within each column means with different lowercase letter are significantly different ($P \leq 0.05$), while the means with the different uppercase letter are significantly different ($P \leq 0.05$).

Several authors revealed that plant-derived EOs, their components and nanoparticles showed strong fumigation toxicity against several stored product insects (Abdelgaleil *et al.*, 2009; Hossain *et al.*, 2014b; Abdelgaleil *et al.*, 2016; Chand *et al.*, 2017; Khoobdel *et al.*, 2017; Benelli, 2018). The nanoemulsions with smaller droplet sizes have better insecticidal properties than coarse emulsions or EOs was shown by several authors and our current studies corroborated those findings (Anjali *et al.*, 2012; Suresh Kumar *et al.*, 2013; Choupanian *et al.*, 2017; Adak *et al.*, 2020). For example, Adak *et al.* (2020) worked with the eucalyptus EO and nanoemulsions of eucalyptus EO against *S. oryzae* and *Tribolium castaneum*. The authors found that the nanoemulsion of eucalyptus EO showed stronger insecticidal properties with the LC₅₀ values from 0.51-0.58 µL/cm² and 0.86-1.86 µL/cm² against *S. oryzae* and *T. castaneum*, respectively, while the eucalyptus EO

had higher concentration of LC₅₀ values of 0.83 and 4.17 µL/cm² for *S. oryzae* and *T. castaneum*, respectively (Adak *et al.*, 2020). In the current study we found that nanoemulsion containing CH-based films showed better insecticidal properties than PLA or PBAT-based films. El-Bakry *et al.* (2019) developed an insecticidal formulation using Ag-loaded 4A-zeolite (ZAg) along with *Rosmarinus officinalis* EO (RO) against *S. oryzae* (L.) and *Rhizopertha dominica* (F.). The authors observed that ZAg+RO EO accomplished a 100 % mortality of insects (*S. oryzae* and *R. dominica*) after 14 days, while the application of ZAg (1g/kg) alone took longest exposure time (21 days) to kill 100 and 96.7 % of *S. oryzae* and *R. dominica*, respectively (El-Bakry *et al.*, 2019). A repellent study of a single, binary, and ternary combination of EOs (anise EO, eucalyptus EO, and peppermint EO) and their major chemical components correspondingly (trans-anethole, 1,8-cineole, and L-menthol) on *S. oryzae* was studied by Hategekimana and Erler (2020). The authors found that the binary and ternary combinations required a lower concentration of EO to show RC₅₀ (Repellency concentration: the concentration required to show 50 % repellency) as compared to the single EO and their major chemical components (Hategekimana and Erler, 2020). The results obtained in the current study suggest that the mixture of EOs and AgNPs (AC-1, AC-2 and AC-3) have strong fumigation activities against *S. oryzae* when released from the bioactive polymeric matrices.

8.3.2.6. *In vitro* release profiles of the active combinations from the bioactive films

Controlled release behavior and release kinetics mechanism of the active combinations (AC-1, AC-2 and AC-3) from bioactive CH-, PBAT- and PLA-based nanocomposite films in acetic acid and ethanol were studied with optical absorbance measurement (UV-VIS spectrophotometer) as a function of time (Table 8.5-8.6, Figure 8.1-8.2. Figure 8.1a and Table 8.5 show the % cumulative release of AC-1, AC-2 and AC-3 from bioactive PBAT nanocomposite films (PBAT+CNC+Gly+AC-1, PBAT+CNC+Gly+AC-2 and PBAT+CNC+Gly+AC-3 film) for 70 h of extraction time in ethanol. Figure 8.1b shows the % cumulative release of AC-1, AC-2 and AC-3 from bioactive CH-based nanocomposite films (CH+CNC+PEG+AC-1, CH+CNC+PEG+AC-2 and CH+CNC+PEG+AC-3 film) for 70 h of extraction time in ethanol. Figure 8.2a and Table 8.6 show the % cumulative release of AC-1, AC-2 and AC-3 from bioactive PBAT nanocomposite films (PBAT+CNC+Gly+AC-1, PBAT+CNC+Gly+AC-2 and PBAT+CNC+Gly+AC-3 film) for 70 h of extraction time in 3 % acetic acid. Figure 8.2b shows the % cumulative release of AC-1, AC-2 and AC-3 from bioactive PLA-based nanocomposite films (PLA+CNC+Gly+AC-1, PLA+CNC+Gly+AC-2 and PLA+CNC+Gly+AC-3 film) for 70 h of extraction time in 3 % acetic acid.

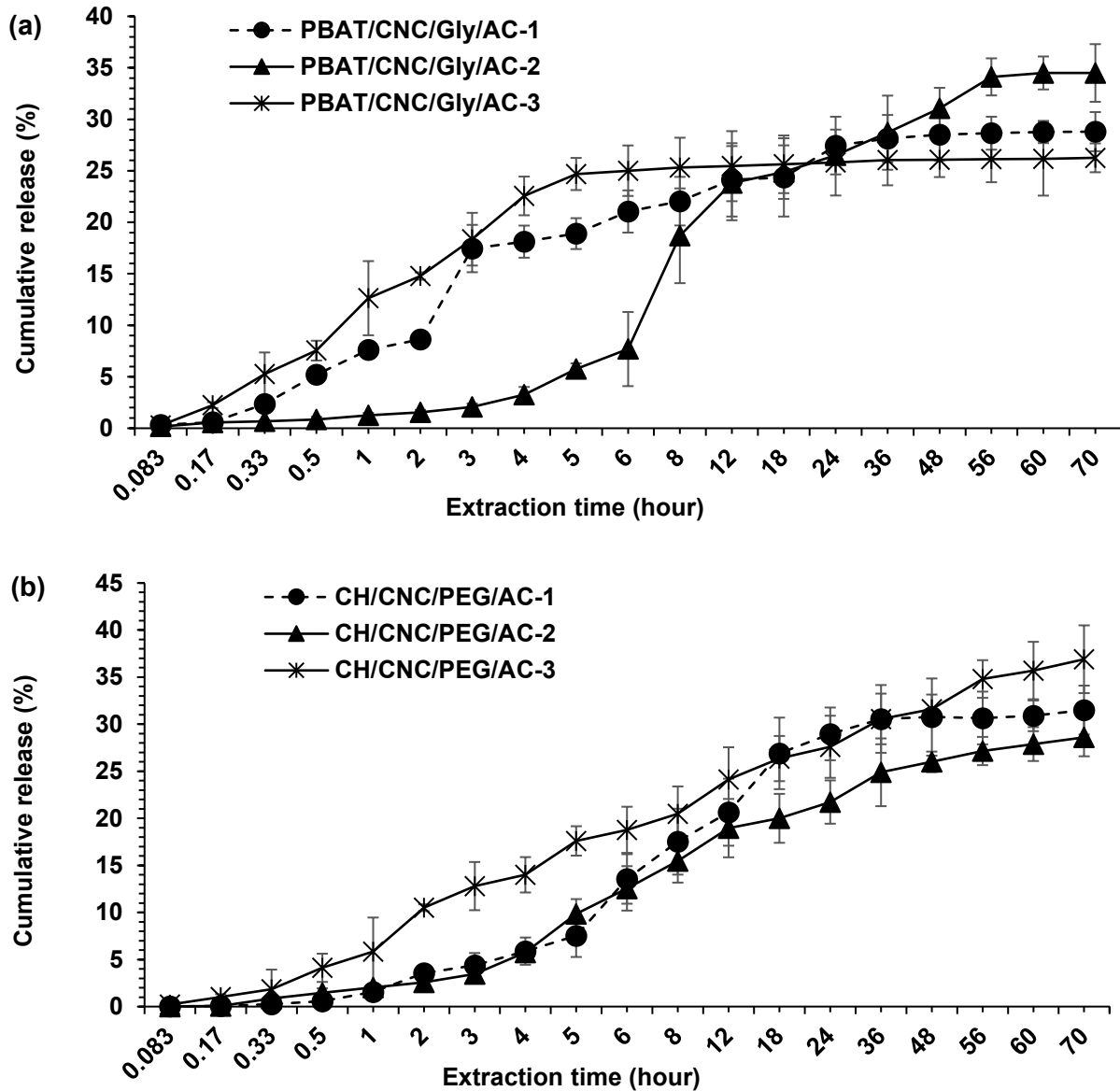


Figure 8.1. Cumulative release (%) of two active formulations in ethanol (food simulant) from PBAT (a) and CH (b) polymeric matrices during extraction time.

At the beginning of the extraction, the % release of AC-1, AC-2 and AC-3 was 5.21, 0.86 and 7.54 % at 0.5 h in ethanol from the PBAT+CNC+Gly+AC-1, PBAT+CNC+Gly+AC-2 and PBAT+CNC+Gly+AC-3 films, respectively. Afterward, the % release increased with extraction time and became stabilized after ~36, ~56 and ~24 h of extraction in ethanol for AC-1, AC-2 and AC-3 from PBAT-based nanocomposite films, respectively. A 28.8, 34.5 and 26.3 % release of the total retained active combinations (AC-1, AC-2 and AC-3) occurred from PBAT+CNC+Gly+AC-1,

PBAT+CNC+Gly+AC-2 and PBAT+CNC+Gly+AC-3 film, respectively, at 70 h contact with ethanol (Figure 8.1a). The release of AC-1, AC-2 and AC-3 from the bioactive CH-based nanocomposite films was very slow and the % release was gradually increased with contact time in ethanol solvent. The % release of active combinations was 0.58, 1.47 and 4.12 % from CH+CNC+PEG+AC-1, CH+CNC+PEG+AC-2 and CH+CNC+PEG+AC-3 films at 0.5 h, respectively. The release (%) of ACs from the bioactive CH-based nanocomposite was stabilized at 24-48 h of extraction in ethanol (% release: 26-31.6 %) and after 70 h of extraction, the % cumulative release of AC-1, AC-2 and AC-3 reached at 31.5, 26 and 36.9 % from CH+CNC+PEG+AC-1, CH+CNC+PEG+AC-2 and CH+CNC+PEG+AC-3 films, respectively (Figure 8.1b).

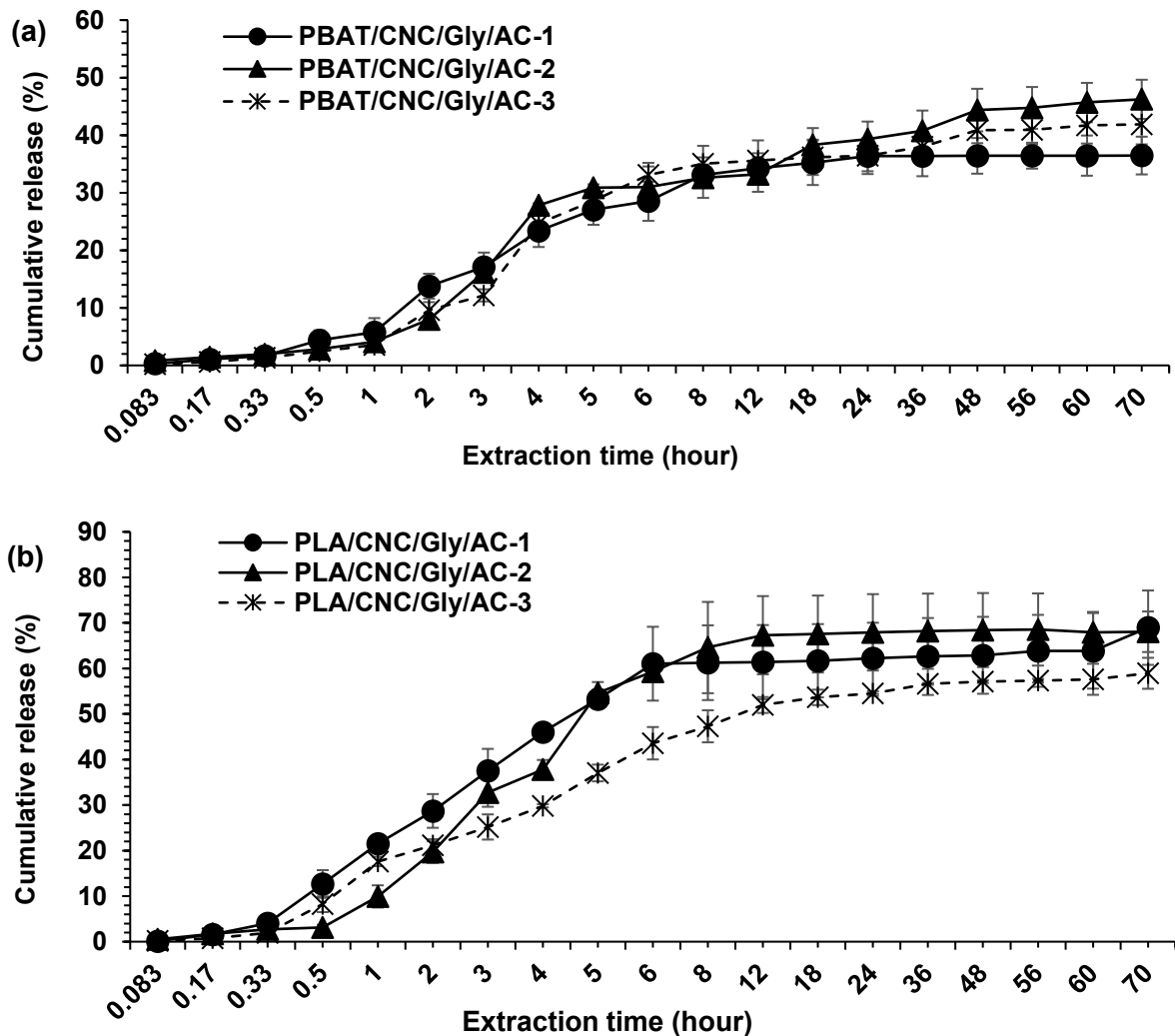


Figure 8.2. Cumulative release (%) of two active formulations in 3 % acetic acid (food simulant) from PBAT (a) and PLA (b) polymeric matrices during extraction time.

The cumulative release (%) of active combinations was higher in 3 % acetic acid than the release in ethanol. At the beginning of the extraction, the release (%) of AC-1, AC-2 and AC-3 was 4.4, 2.8 and 2.4 % at 0.5 h in 3 % acetic acid from the PBAT+CNC+Gly+AC-1, PBAT+CNC+Gly+AC-2 and PBAT+CNC+Gly+AC-3 film, respectively. Afterward, the release (%) increased with extraction time and became stabilized after 18, 24 and 48 h of extraction in 3 % acetic acid for AC-1, AC-2 and AC-3 from PBAT-based nanocomposite films, respectively. A 36.5, 46 and 42 % release of the total retained active combinations (AC-1, AC-2 and AC-3) occurred from PBAT+CNC+Gly+AC-1, PBAT+CNC+Gly+AC-2 and PBAT+CNC+Gly+AC-3 films, respectively, at 70 h contact with 3 % acetic acid (Figure 8.2a). The cumulative release (%) measurement of AC-1, AC-2 and AC-3 as a function of time from the bioactive PLA+CNC+Gly+AC-1, PLA+CNC+Gly+AC-2 and PLA+CNC+Gly+AC-3 films were tested and shown in Figure 8.2b. At the beginning of the extraction in 3 % acetic acid (at 0.5 h), the % release of the active combinations (AC-1, AC-2 and AC-3) was much less, and the values were 12.6, 3.15 and 8.21 %, respectively, from the three different types of bioactive PLA-based nanocomposite films. The release (%) of active combinations increased with time and the release from the PLA+CNC+Gly+AC-1, PLA+CNC+Gly+AC-2 and PLA+CNC+Gly+AC-3 films was reached at 69, 68 and 58.9 %, respectively, at 70 h of extraction time in 3 % acetic acid (Figure 8.2b).

The Korsmeyer-Peppas parameters viz. n , k , and R^2 were calculated for analyzing release kinetics and their mechanism of release of AC-1, AC-2 and AC-3 from bioactive CH, PLA and PBAT films in ethanol (Table 8.5) and 3 % acetic acid (Table 8.6). The higher R^2 values (≥ 78 %) for all tested films indicated that the Korsmeyer-Peppas model is fitted for the release of active combinations from the bioactive CH-, PLA- and PBAT-based nanocomposite films in both food simulants (3 % acetic acid and ethanol). The coefficient n values were obtained ranges between 0.26 to 0.32 for three different types of bioactive PBAT-based nanocomposite films (PBAT+CNC+Gly+AC-1, PBAT+CNC+Gly+AC-2 and PBAT+CNC+Gly+AC-3) in ethanol. It meant, the lower coefficient n values below 0.5 indicated that the release of active combinations occurred through Fickian or quasi-Fickian diffusion mechanism from the PBAT polymeric matrices in ethanol. The release from the bioactive CH-based nanocomposite films in ethanol (n : 0.54-0.63) occurred through polymer relaxation and diffusion (anomalous transportation). The release of AC-1, AC-2 and AC-3 in 3 % acetic acid from PBAT+CNC+Gly+AC-1, PBAT+CNC+Gly+AC-2, PBAT+CNC+Gly+AC-3, PLA+CNC+Gly+AC-1 and PLA+CNC+Gly+AC-3 occurred though anomalous transportation (n : 0.46-0.82), the release of AC-2 from the PLA+CNC+Gly+AC-2 film (n : 1.02) followed a non-Fickian transportation mechanism (means deterioration of the polymeric chain and release occurred in both diffusion and relaxation processes) (Requena *et al.*, 2017; Ben-Fadhel *et al.*, 2020). The

release of active compounds from polymeric matrices depends on several factors such as polymer morphology, polymer-active combination interactions, molecular weight distribution, polarity of the food simulants, temperature, solubility of the active compounds in food simulants, etc. (da Rosa *et al.*, 2020a). The current results were in line with the results obtained by several authors as they observed the release of active ingredients or essential oils from polymeric matrices that occurred by a diffusional mechanism (Petchwattana and Naknaen, 2015; Bustos *et al.*, 2016; Tawakkal *et al.*, 2016; Requena *et al.*, 2017; Ben-Fadhel *et al.*, 2020). Requena *et al.* (2017) studied the release kinetics mechanism of the eugenol and carvacrol from the poly (hydroxybutyrate-co-hydroxyvalerate) (PHBV) films in different food simulants (10 % ethanol, 50 % ethanol, 3 % acetic acid, and isooctane) and the authors found that the release of eugenol and carvacrol occurred through Fickian and quasi-Fickian diffusion in the PHBV matrix. This phenomenon suggested that the incorporation of CNC/Gly into polymeric matrices improved the interactions with active formulations which reduced their migration through the polymeric network by restriction of compound mobility (Requena *et al.*, 2017). After analyzing release kinetics results, it could be concluded that the bioactive PBAT-based films containing active combinations have a greater ability to retain the active combinations for a long time than bioactive CH-based nanocomposite films in ethanol. On the other hand, in 3 % acetic acid bioactive PBAT-based nanocomposite films containing active combinations have a greater ability to retain active agents for a long time as compared to the bioactive PLA-based nanocomposite films. Furthermore, a challenging test would be conducted with the bioactive PBAT, CH-based nanocomposite films in stored rice for controlling pathogenic bacteria, fungi and insects and while the bioactive PBAT- and PLA-based nanocomposite films were applied in stored yogurt to control the growth of bacteria and fungi.

Table 8.5. Parameters of the Korsmeyer-Peppas model as kinetic release parameters (rate constant (k) and diffusional exponent (n)) of the active formulations from polymeric matrices in ethanol.

Types of bioactive films	Korsmeyer-Peppas parameters		
	n	k	R ²
PBAT/CNC/Gly/AC-1	0.32	0.46	0.8374
PBAT/CNC/Gly/AC-2	0.27	0.44	0.8987
PBAT/CNC/Gly/AC-3	0.26	0.36	0.81456
CH/CNC/PEG/AC-1	0.63	0.28	0.8867
CH/CNC/PEG/AC-2	0.54	0.35	0.8392
CH/CNC/PEG/AC-3	0.58	0.32	0.9004

Table 8.6. Parameters of the Korsmeyer-Peppas model as kinetic release parameters (rate constant (k) and diffusional exponent (n)) of the active formulations from polymeric matrices in 3 % acetic acid.

Types of bioactive films	Korsmeyer-Peppas parameters		
	n	k	R ²
PBAT/CNC/Gly/AC-1	0.65	0.27	0.86
PBAT/CNC/Gly/AC-2	0.56	0.32	0.80
PBAT/CNC/Gly/AC-3	0.43	0.35	0.78
PLA/CNC/Gly/AC-1	0.67	0.34	0.8650
PLA/CNC/Gly/AC-2	1.02	0.34	0.9810
PLA/CNC/Gly/AC-3	0.82	0.30	0.83

8.3.3. Evaluation of the antibacterial and antifungal properties of the films (for cereal grains)

Six different types of bioactive nanocomposite films (PBAT- and CH-based film) were selected for the *in situ* tests in stored rice against *E. coli* O157:H7, *S. Typhimurium*, *A. niger* and *P. chrysogenum* with and without the presence of 750 Gy γ -irradiation (Figure 8.3a-d, Figure 8.4a-d, Figure 8.5a-b). The nanocomposite films were selected based on the results of mechanical properties, WS, WVP, *in vitro* antibacterial, antifungal properties and *in vitro* release kinetics tests. However, rice was treated under PBAT+CNC+Gly+AC-1, PBAT+CNC+Gly+AC-2, PBAT+CNC+Gly+AC-3, CH+CNC+PEG+AC-1, CH+CNC+PEG+AC-2 and CH+CNC+PEG+AC-3 film (Figure 8.3a-d, Figure 8.4a-d). The rice samples with inoculated fungi or bacteria were considered as Control (Rice+bacteria/fungi) and the rice samples with bacteria/fungi (Figure 8.3-8.4) and 750 Gy γ -irradiation alone were considered as γ -Control (Rice+bacteria/fungi+750 Gy radiation) (Figure 8.5a-b).

Figure 8.3a-b showed that the growth profiles of *E. coli* O157:H7 and *S. Typhimurium* in stored rice under bioactive PBAT-based nanocomposite films. The vapor effect of active combinations (AC-1, AC-2 and AC-3) from the PBAT-based matrices significantly reduced the growth of *E. coli* O157 and *S. Typhimurium* by 27-49.3 % and 22.5-52.3 %, respectively, with respect to the control sample after 8 weeks of storage. The growth of *E. coli* O157:H7 was 3.47, 2.13, 1.76 and 2.54 log CFU/g in the control sample, PBAT+CNC+Gly+AC-1, PBAT+CNC+Gly+AC-2, PBAT+CNC+Gly+AC-3, respectively, after 8 weeks (Figure 8.3a). A similar observation was found with the growth profile of *S. Typhimurium* in stored rice and the result was depicted in Figure 8.3b. PBAT+CNC+Gly+AC-1 showed the highest reduction of *S. Typhimurium* in stored rice by 52.3 %, followed by PBAT+CNC+Gly+AC-2 and PBAT+CNC+Gly+AC-3 film accomplished a reduction by

43 % and 22.5 % of *S. Typhimurium*, respectively (Figure 8.3b). The application of irradiation (750 Gy) with PBAT+CNC+Gly+AC-1, PBAT+CNC+Gly+AC-2, PBAT+CNC+Gly+AC-3 film caused 75.2, 86.2 and 77.8 % reduction of *E. coli* O157:H7 after 8 weeks of storage, while an 84.4, 89.8 and 86.9 % reduction of *S. Typhimurium* obtained in stored rice as compared to the control sample (Figure 8.5a).

Figure 8.4b shows the antibacterial properties of the bioactive CH-based nanocomposite films (CH+CNC+PEG+AC-1, CH+CNC+PEG+AC-2 and CH+CNC+PEG+AC-3 film) to control the growth of *E. coli* O157:H7 and *S. Typhimurium* in stored rice. The highest bacterial growth (*E. coli* O157:H7) reduced by CH+CNC+PEG+AC-2 film (49.3 %), followed by CH+CNC+PEG+AC-3 film (36 %) and by CH+CNC+PEG+AC-1 film (20.3 %) with respect to the control sample (growth count: 3.47 log CFU/g), and the corresponded bacterial count was 1.76, 2.23 and 2.77 log CFU/g of *E. coli* O157:H7 after 8 weeks in stored rice (Figure 8.4a). Similarly, CH+CNC+PEG+AC-2 film caused higher reduction of *S. Typhimurium* growth by 50.4 % (1.85 log CFU/g), CH+CNC+PEG+AC-3 and CH+CNC+PEG+AC-1 films caused 34.05 and 22.5 % reduction, respectively, as compared to the control samples (3.73 log CFU/g) after 8 weeks of stored rice (Figure 8.4b). Combining CH+CNC+PEG+AC-1, CH+CNC+PEG+AC-2 and CH+CNC+PEG+AC-3 film with γ -irradiation caused a reduction of 84.4, 92.2 and 81.8 % *E. coli* O157:H7, respectively, and 69.4, 85.5 and 79.6 % of *S. Typhimurium*, respectively, with respect with control samples after 8 weeks of storage (Figure 8.5b).

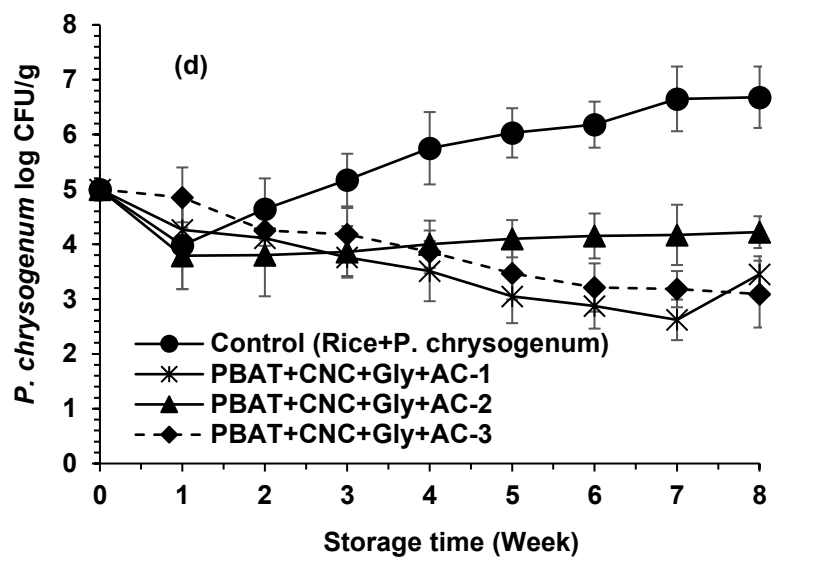
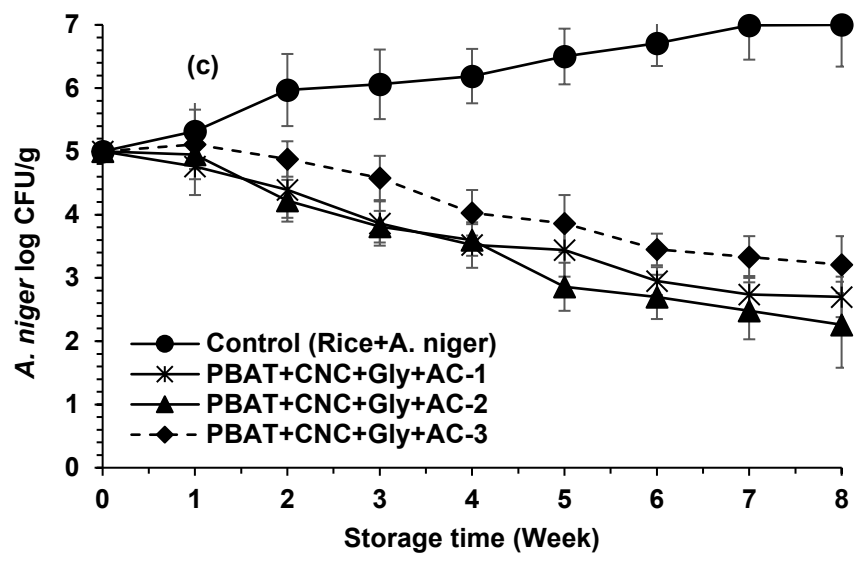
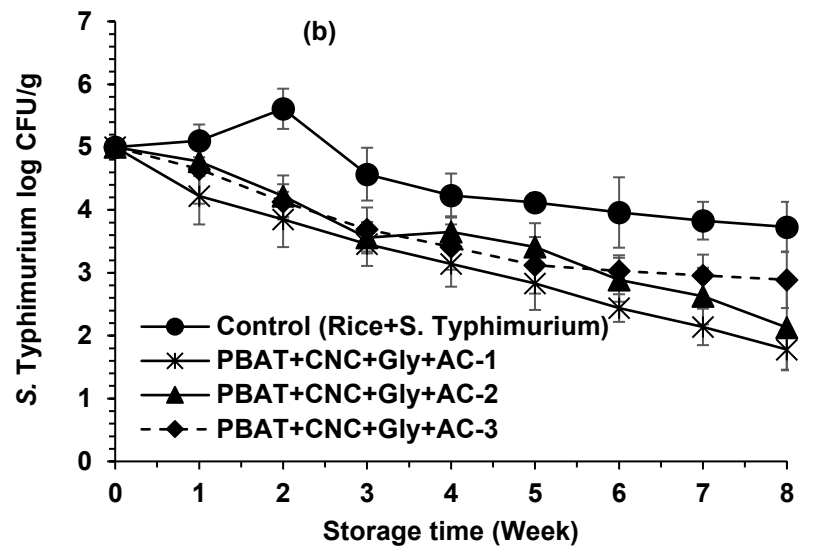
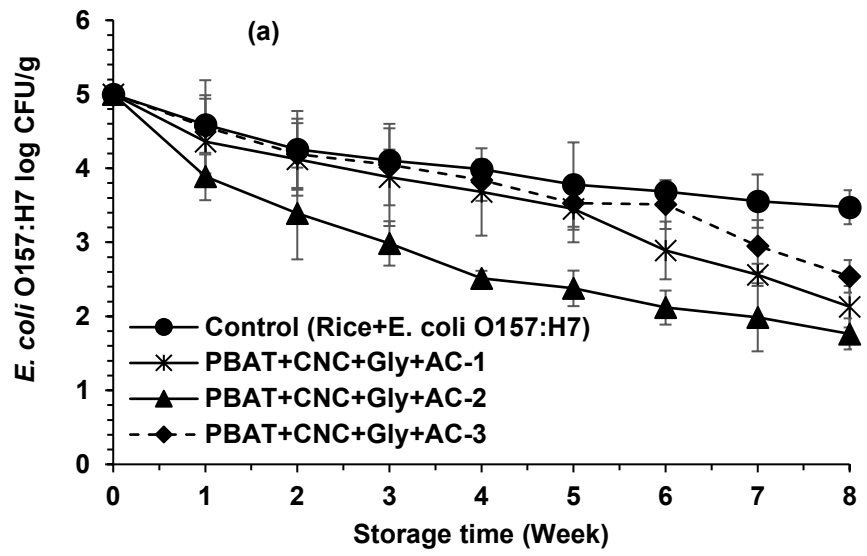


Figure 8.3. Bacterial (*E. coli* O157:H7 and *S. Typhimurium*) (a-b) and fungal (*A. niger* and *P. chrysogenum*) (c-d) growth profiles in storage rice under different bioactive films treatment for 8 weeks.

The antifungal activities of the fabricated bioactive PBAT and CH nanocomposite films were tested against *A. niger* and *P. chrysogenum* in stored rice for 8 weeks (Figure 8.3c-d and Figure 8.4c-d). The bioactive PBAT nanocomposite film having AC-2 (PBAT+CNC+Gly+AC-2 film) showed the strongest fungicidal effect than the bioactive PBAT-based films containing AC-1 (PBAT+CNC+Gly+AC-1) and AC-2 (PBAT+CNC+Gly+AC-3) against *A. niger*. In the case of *A. niger*, the fungal count increased from 5.32 to 7 log CFU/g during storage from week 1 to 8 in rice (Figure 8.3c). The samples treated with PBAT+CNC+Gly+AC-1 film, PBAT+CNC+Gly+AC-2 film and PBAT+CNC+Gly+AC-3 film showed reduced fungal (*A. niger*) growth by 61.4 % (2.7 log CFU/g), 67.7 % (2.26 log CFU/g) and 54.1 % (3.21 log CFU/g) with respect to the control sample after 8 weeks, respectively (Figure 8.3c). Figure 8.4c shows the fungicidal properties by bioactive CH-based films (CH+CNC+PEG+AC-1, CH+CNC+PEG+AC-2 and CH+CNC+PEG+AC-3 film) against *A. niger* in stored rice. CH+CNC+PEG+AC-1, CH+CNC+PEG+AC-2 and CH+CNC+PEG+AC-3 film caused the fungal (*A. niger*) reduction by 54.1 % (3.21 log CFU/g), 64.6 % (2.48 log CFU/g) and 50.9 % (3.44 log CFU/g) with respect to control sample (Figure 8.4c). The application of irradiation (750 Gy) with PBAT+CNC+Gly+AC-1, PBAT+CNC+Gly+AC-2, PBAT+CNC+Gly+AC-3 film caused an 86.3, 88.4 and 83.4 % reduction of *A. niger* growth, respectively, after 8 weeks of storage as compared to the control sample (5a). Combining CH+CNC+PEG+AC-1, CH+CNC+PEG+AC-2 and CH+CNC+PEG+AC-3 film with γ -irradiation caused a reduction of growth by 79.7, 85 and 82.6 % of *A. niger*, respectively, with respect to the control samples after 8 weeks of storage (Figure 8.5b).

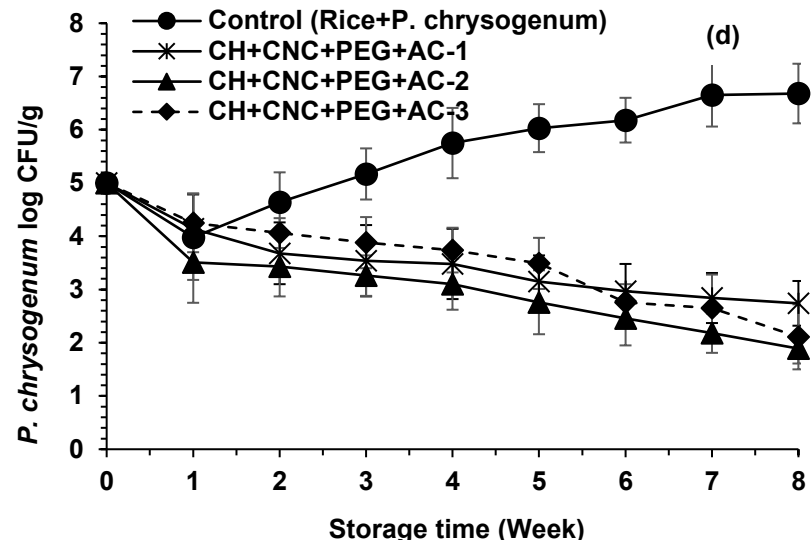
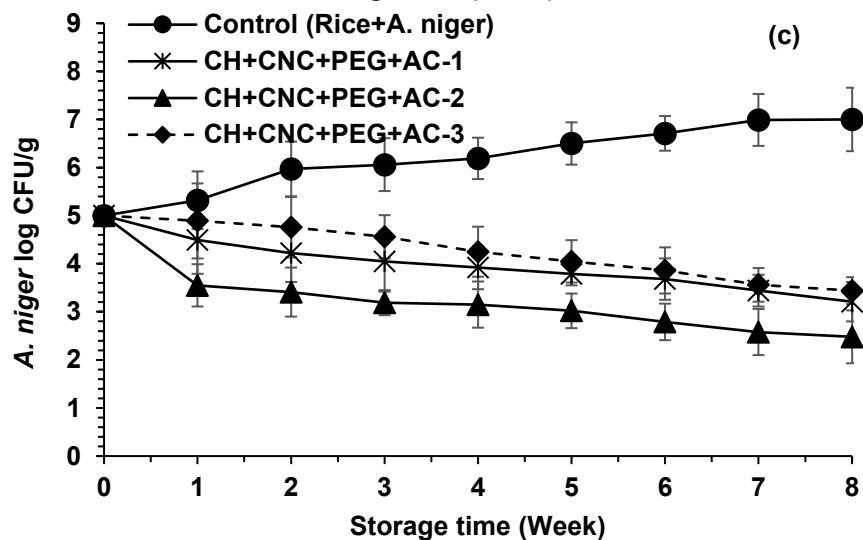
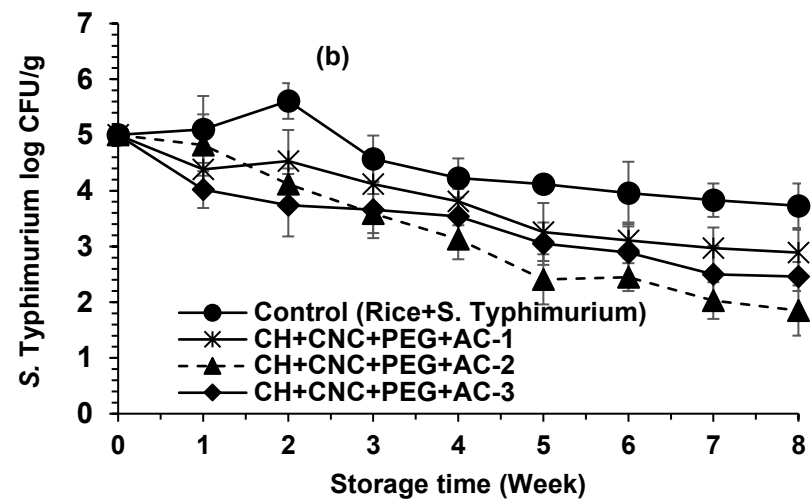
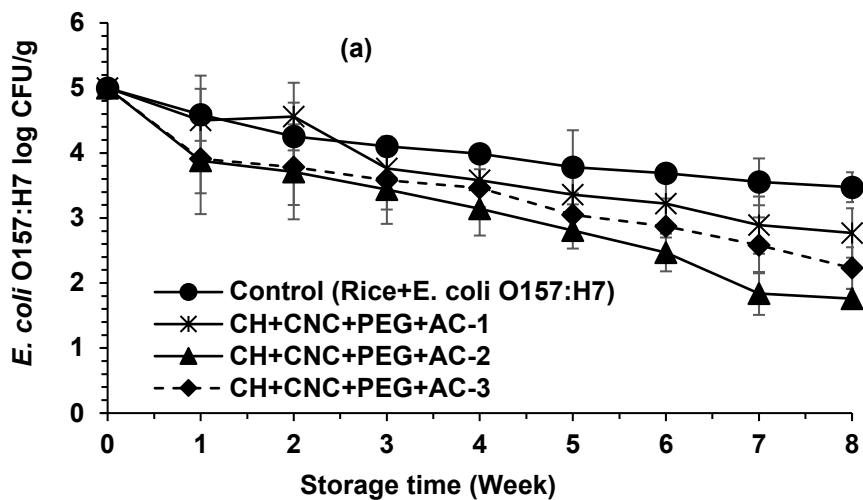


Figure 8.4. Bacterial (*E. coli* O157:H7 and *S. Typhimurium*) (a-b) and fungal (*A. niger* and *P. chrysogenum*) (c-d) growth profiles in storage rice under different bioactive films treatment for 8 weeks.

In case of *P. chrysogenum*, both bioactive PBAT and CH-based nanocomposite films significantly controlled the growth of *P. chrysogenum* in stored rice for 8 weeks as compared to the control samples, though bioactive CH-based nanocomposite films which were more effective than bioactive PBAT-based nanocomposite films (Figure 8.3d and Figure 8.4d). *P. chrysogenum* growth was increased from 3.98 to 6.68 log CFU/g in stored rice from week 1 to week 8. The samples treated with PBAT+CNC+Gly+AC-1 film, PBAT+CNC+Gly+AC-2 film and PBAT+CNC+Gly+AC-3 film reduced the fungal (*P. chrysogenum*) growth by 48.3 %, 37 % and 54 % with respect to the control sample after 8 weeks, respectively (Figure 8.3d). Figure 8.4d shows the fungicidal properties by bioactive CH-based films (CH+CNC+PEG+AC-1, CH+CNC+PEG+AC-2 and CH+CNC+PEG+AC-3 film) against *P. chrysogenum* in stored rice. CH+CNC+PEG+AC-1, CH+CNC+PEG+AC-2 and CH+CNC+PEG+AC-3 film caused the fungal (*P. chrysogenum*) growth reduction by 59 %, 71.7 % and 68.4 % with respect to control sample (Figure 8.4d). The application of irradiation (750 Gy) with PBAT+CNC+Gly+AC-1, PBAT+CNC+Gly+AC-2, PBAT+CNC+Gly+AC-3 film caused a 73.3, 65.4 and 77.9 % reduction of *P. chrysogenum* growth, respectively, after 8 weeks of storage as compared to the control sample (5a). Combining CH+CNC+PEG+AC-1, CH+CNC+PEG+AC-2 and CH+CNC+PEG+AC-3 film with γ -irradiation caused a reduction of 83.1, 88.9 and 87.7 % *P. chrysogenum* growth, respectively, with respect to the control samples after 8 weeks of storage (Figure 8.5b).

Begum *et al.* (2022a) found strong antibacterial and antifungal properties of active combinations (AC-1, AC-2 and AC-3) in a vapor state against food borne pathogenic bacteria (*E. coli* O157:H7 and *S. Typhimurium*) and spoilage fungi (*A. niger* and *P. chrysogenum*). In the current study, two types of bioactive PBAT- and CH-based nanocomposite films were used containing 300 μ L of ACs with CNC and plasticizer to control pathogenic bacteria (*E. coli* O157:H7 and *S. Typhimurium*) and spoilage fungi (*A. niger* and *P. chrysogenum*) in stored rice. The active combinations presented in AC-1, AC-2 and AC-3 were released from the bioactive CH- and PBAT-based nanocomposite films which prevented the growth of pathogenic bacteria and spoilage fungi in rice. Polymeric matrices loaded with the reinforcing agent CNC could control the release of active compounds and could retain the bioactivities of the polymeric films over the storage time and thus, prevented the microbial growth in stored foods (Boumail *et al.*, 2013; Salmieri *et al.*, 2014b; Deng *et al.*, 2017; Hossain *et al.*, 2018; Hossain *et al.*, 2019a). In accordance with our study, Hossain *et al.* (2018) fabricated bioactive methylcellulose-based films using oregano/thyme EO and CNC (MC/CNC/Oregano/thyme) and applied the films in stored rice for controlling the growth of spoilage fungi (*A. niger*, *A. flavus*, *A. parasiticus*, and *P. chrysogenum*). By applying MC / CNC / Oregano / thyme-based nanocomposite films, the authors reduced by 2 log CFU/g of fungal growth in rice

at 28 °C after 8 weeks. Moreover, the incorporation of CNC into a polymeric matrix reduced the release of active compounds by 35 % after 12 weeks in stored rice (Hossain *et al.*, 2018). A ternary bio-composite film composed of hydroxypropyl methylcellulose (HPMC), tragacanth and beeswax polymeric matrices loaded with AgNPs and the bioactive fabricated films inhibited the growth of pathogenic bacteria *Staphylococcus aureus*, *Listeria monocytogenes*, *E. coli*, *Bacillus cereus*, *Streptococcus pneumoniae*, *S. Typhimurium*, *Pseudomonas aeruginosa*, and *Klebsiella pneumoniae* (Bahrami *et al.*, 2019). de Souza *et al.* (2022) developed bioactive PBAT-based films using PLA-Cinnamon EO capsules and the film was fabricated by the solvent casting method for strawberry preservation, and the authors observed the bioactive PBAT/PLA/Cinnamon EO film potentially extended the shelf life of strawberries without compromising fruit quality and dehydration. Polyvinyl alcohol/chitosan-based nanocomposite films reinforced with CNC and carvacrol could modulate the mechanical properties and increase the antioxidant properties of the bioactive films, thus, controlling the microbial growth and preventing the oxidation of stored products (Luzi *et al.*, 2017).

Furthermore, combining ionizing radiation along with bioactive packaging films drastically reduced the bacterial and fungal growth in stored rice as compared to the treatment alone (either by bioactive film alone or γ -radiation alone). When ionizing radiation applied to the pathogenic bacteria and spoilage fungi, irradiation can damage the cellular DNA by breaking their chemical bonds, could alter the membrane permeability of the biological entities, and also could affect the cell's activity, and these mechanisms may increase the contact between the microbial cell and active components released from bioactive packaging and facilitate cell destruction (Caillet *et al.*, 2005; Caillet and Lacroix, 2006; Ayari *et al.*, 2012; Begum *et al.*, 2020a). The release of active components present in the active combinations (AC-1, AC-2 and AC-3) from the bioactive CH- and PBAT-based films and γ -irradiation might affect the cell integrity, accelerate the release of bacterial and fungal cell constituents and imbalance the internal pH and ATP synthesis (Caillet *et al.*, 2005; Oussalah *et al.*, 2006). Lined up with our current study, Shankar *et al.* (2021) worked with strawberry preservation using active chitosan-based nanocomposite films loaded with EO/Ag nanoparticles along with 1 kGy γ -irradiation and stated that the combination between active Chitosan nanocomposite film and irradiation significantly prolonged the shelf-life of strawberries by 4 days. Our current study is supported by several authors who obtained similar observations (Caillet *et al.*, 2005; Hossain *et al.*, 2014a; Lacroix and Follett, 2015; Hossain *et al.*, 2018; Hossain *et al.*, 2019a). The combined application of irradiation (either γ -ray or X-ray) and oregano/thyme EO drastically reduced the growth of *E. coli* O157:H7, *S. Typhimurium*, and *Listeria monocytogenes* in rice (Begum *et al.*, 2020b). Moreover, the authors found that the D₁₀ values

were 326, 266, and 236 Gy for the bacteria *E. coli* O157:H7, *S. Typhimurium*, and *L. monocytogenes*, respectively, when treated with a high dose rate of γ -irradiation alone (9.1 kGy/h), while the corresponded D_{10} values were significantly reduced ($P \leq 0.05$) to 274, 218, and 219 Gy in combined treatment between the vapor of EO and γ -irradiation (Begum *et al.*, 2020b). Therefore, it could be stated that the combined treatment between irradiation and bioactive CH- and PBAT-based nanocomposite films could be an effective strategy to control pathogenic bacteria and spoilage fungi in stored food products. Moreover, the current study could lead to a replacement of chemical preservatives and petroleum-based synthetic non-degradable polymer packaging, and could contribute to sustainable packaging goals.

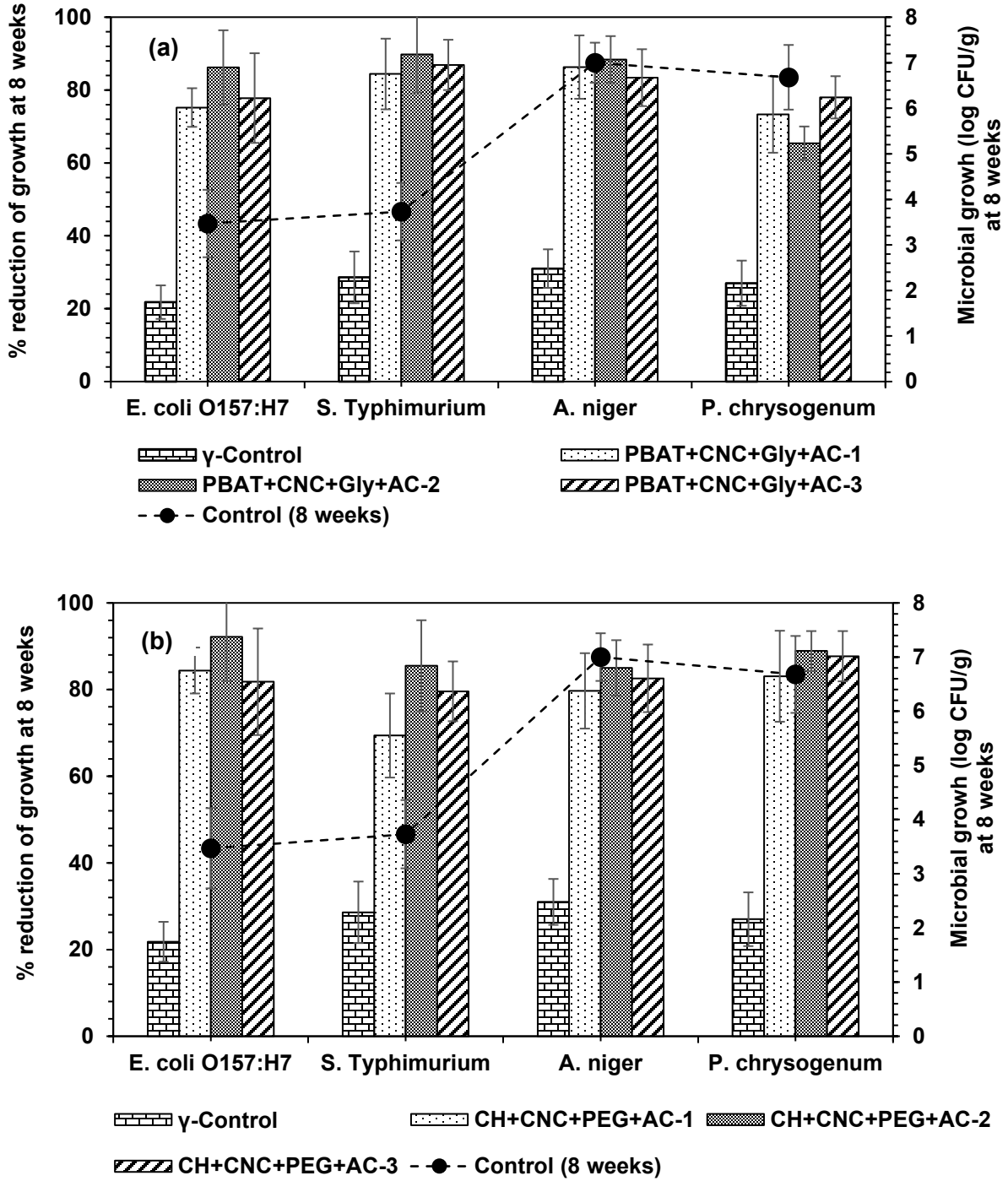


Figure 8.5. Effect of irradiation along with bioactive films against *E. coli* O157:H7, *S. Typhimurium*, *A. niger* and *P. chrysogenum* in stored rice after 8 weeks.

8.3.4. Evaluation of the anti-insect properties of the films (for cereal grains)

The nine nanocomposite films, named CH+CNC+PEG+AC-1 film, CH+CNC+PEG+AC-2 film, CH+CNC+PEG+AC-3 film, PBAT+CNC+Gly+AC-1 film, PBAT+CNC+Gly+AC-2 film, PBAT+CNC+Gly+AC-3 film, PLA+CNC+Gly+AC-1 film, PLA+CNC+Gly+AC-2 film and PLA+CNC+Gly+AC-3 film, were developed as diffusion matrices to control *S. oryzae* in stored rice as a model of cereal grains and results are depicted in Figure 8.6. The results showed that CH+CNC+PEG-, PBAT+CNC+Gly- and PLA+CNC+Gly-based polymeric matrices having either AC-1 or AC-2 or AC-3 showed a wide range (from lower to higher) of insecticidal properties against the rice weevil (*S. oryzae*) (Figure 8.6). The highest insecticidal properties were shown by the bioactive PBAT+CNC+Gly+AC-3 (mortality: 78 %) nanocomposite films against *S. oryzae* at 14 days of storage, followed by PBAT+CNC+Gly+AC-2 film (mortality: 73.3 %), CH+CNC+PEG+AC-1 film (mortality: 69 %), CH+CNC+PEG+AC-2 film (mortality: 64.4 %), CH+CNC+PEG+AC-3 film (mortality: 60 %), PBAT+CNC+Gly+AC-1 film (mortality: 58 %), PLA+CNC+Gly+AC-3 film (mortality: 44.4 %), PLA+CNC+Gly+AC-1/PLA+CNC+Gly+AC-2 film (mortality: 38 %). The mortality of insects under different bioactive nanocomposite film treatments increased with the incubation period. For example, PBAT+CNC+Gly+AC-3 film caused 13.3, 35.5, 49, 58 and 78 % mortality of insects on days 1, 3, 7, 10 and 14, respectively, whereas the control sample (no bioactive nanocomposite films) caused from 0-6 % mortality from 1 to 14 days of storage (Figure 8.6).

In the present study, the *in situ* insecticidal properties shown by nine different types of insecticidal nanocomposite films against rice weevil were different even though they contained different types of ACs as insecticidal agents. The significant difference in insect mortality depended on the diffusion rate of the insecticidal compounds which mostly relied on several factors such as the nature and chemical structure of the molecules, type of polymer, the binding affinity between the polymeric matrices and the active compounds, solubility, temperatures, storage time, as well as the degree of crystallinity (Hossain *et al.*, 2019b; Sharma *et al.*, 2021). Moreover, in the current study, the reinforcing agent CNC was incorporated into the polymeric matrices to improve the controlled release of active formulations over the storage period (Boumail *et al.*, 2013; Salmieri *et al.*, 2014b; Deng *et al.*, 2017; Hossain *et al.*, 2018; Hossain *et al.*, 2019a). In line with our current study, Hossain *et al.* (2019b) developed insecticidal chitosan (CH), methylcellulose (MC), and PLA-based nanocomposite films using a mixture of EOs (oregano:thyme) as insecticidal agents and CNC as a reinforcing agent to control the rice weevil in stored rice for 14 days. The authors observed that the CH/CNC-based film containing nanoemulsion of oregano:thyme EO had the highest insecticidal properties against *S. oryzae* with % a mortality of 43 % at 14 days, then

followed by MC/CNC-based film containing nanoemulsion of oregano:thyme EO (% mortality: 27 % at 14 days) and PLA/CNC-based film containing oregano:thyme EO with 20 % mortality of *S. oryzae* at 14 days, and these results were strongly supported our current findings (Hossain *et al.*, 2019b). The current findings suggest that the encapsulation of active combinations (mixture of EOs and AgNPs) within the polymeric matrices could control the release of active ingredients progressively from the bioactive films and thus, protect the stored product cereals from the infestation of insects for a longer storage time.

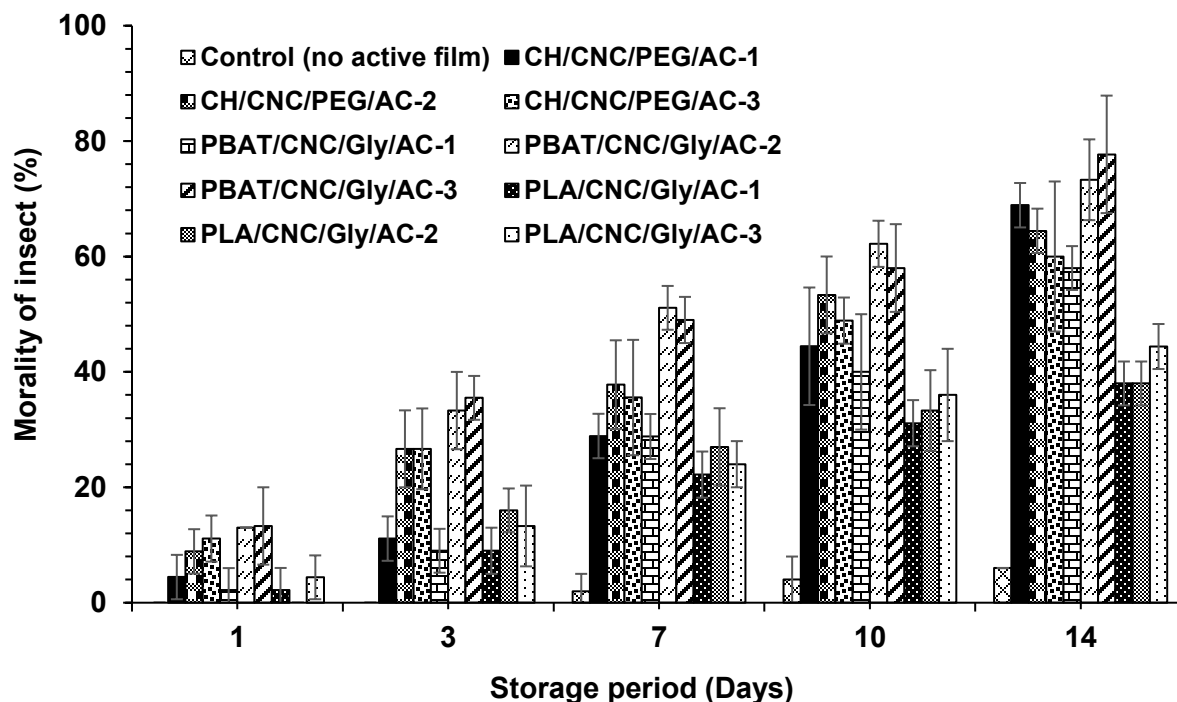


Figure 8.6. *In situ* fumigation toxicity of different insecticidal films in rice grains for 14 days against *S. oryzae*.

In the current study a new technology was introduced to prevent the insect infestation of stored rice by applying a hurdle technique where bioactive nanocomposite films were combined with γ -radiation. However, numerous experiments performed on the use of EOs or AgNPs to protect stored grains from insect infestation have been done but there were very few studies performed on the combination of ionizing radiation and insecticidal nanocomposite films (hurdle technique) against insect pests. In the current study, the effect of γ -irradiation at different doses on insect mortality was applied alone as well as in a combined treatment between nine different types of bioactive nanocomposite films and γ -irradiation doses (Table 8.7). We found that the mortality of

the rice weevil increased significantly ($P \leq 0.05$) with increased radiation dose as well as the incubation period. When the γ -irradiation was applied alone to control *S. oryzae* in stored rice for 14 days, the insect's mortality (%) increased from 7 days of incubation with higher doses (200-300 Gy) and mortality increased progressively. A 71 % insect mortality was evident when the sample was treated with 300 Gy γ -irradiation alone at day 14, whereas 51 and 62 % mortality was found when the samples were treated with 100 and 200 Gy γ -irradiation alone, respectively. The control sample (no bioactive film, no irradiation dose) showed only 6 % insect mortality at day 15 (Table 8.7). The mortality observed in this study was slightly lower than previously reported by [Hossain et al. \(2019b\)](#), who irradiated the rice weevil in presence of rice at 100-300 Gy and recorded the mortality 14 days after the irradiation; these authors reported 65, 79 and 100 % insect mortality at the corresponded irradiation doses. Moreover, [Tunçbilek \(1995\)](#) reported that 90 Gy γ -irradiation caused 100 % mortality of *S. oryzae* in 2nd week of incubation. So, insecticidal effectiveness shown by γ -irradiation alone may vary depending on several factors such as the dose rate of the radiation source, source-to-product distance, age of insects, and so on ([Begum et al., 2020a](#); [Hossain et al., 2021](#)).

In the combined treatment between γ -irradiation and CH-based nanocomposite films, the mortality (%) of insects was significantly higher ($P \leq 0.05$) as compared to the treatment alone (either by γ -irradiation alone or by bioactive CH-based nanocomposite film alone) (Figure 8.6 and Table 8.7). In the case of combined treatment between 100 Gy and CH+CNC+PEG matrix containing AC-1, AC-2 and AC-3, the % mortality of rice weevil increased from 27 to 100 % between 3 to 14 days of incubation. Higher irradiation doses of 200 and 300 Gy combined with CH+CNC+PEG- based matrix containing AC-1, AC-2 and AC-3 caused 91-100 % insect mortality on day 10. On day 3, the combined treatment between 300 Gy and CH+CNC+PEG+AC-3 film caused 63 % mortality, while the treated sample with 300 Gy irradiation alone caused significantly lower mortality of 9 %. Complete mortality of insects was observed in the combination treatment of 300 Gy with CH+CNC+PEG+AC-3 film at day 7, whereas the samples treated with 300 Gy alone caused only 22 % ($P \leq 0.05$) mortality at incubation day of 7, respectively (Table 8.7).

Table 8.7. Mortality (%) of rice weevil treated with γ -irradiation alone and in combination with bioactive CH-, PBAT- and PLA-based nanocomposite films.

Same of samples	Mortality (%)				
	Day 1	Day 3	Day 7	Day 10	Day 14
Control (no film, no radiation)	0±0	0±0	2±1.2	4±1.5	6±0.5
100 Gy	0±0	4±0	16±1.2	29±2.9	51±3.4
200 Gy	0±0	10±2.1	21±2.9	41±5.1	62±4.5
300 Gy	0±0	9±1.1	22±4.1	55±2.4	71±4.1
100 Gy+CH+CNC+PEG+AC-1	4.4±2.3	27±4.8	47±11	68±6.6	82±6.9
200 Gy+CH+CNC+PEG+AC-1	8±3.6	35±5.6	63±6.9	91±4.9	100±0
300 Gy+CH+CNC+PEG+AC-1	11±2.1	41±6.9	75±8.9	100±0	100±0
100 Gy+CH+CNC+PEG+AC-2	5±0.5	38±5.2	58±9.9	79±10.2	92±9.1
200 Gy+CH+CNC+PEG+AC-2	12±4.2	45±4.8	72±11	100±0	100±0
300 Gy+CH+CNC+PEG+AC-2	18±6.3	56±6.0	88±10.9	100±0	100±0
100 Gy+CH+CNC+PEG+AC-3	4.4±2.9	39±3.0	69±8.2	92±6.9	100±0
200 Gy+CH+CNC+PEG+AC-3	8.9±6	56±5.9	89±3.9	100±0	100±0
300 Gy+CH+CNC+PEG+AC-3	14±2.1	63±6.7	100±0	100±0	100±0
100 Gy+PBAT+CNC+Gly+AC-1	4.4±3.6	19±10	42±7.9	64±10.2	88±6.8
200 Gy+PBAT+CNC+Gly+AC-1	8±0.8	44±2.8	66±10.3	72±11.5	100±0
300 Gy+PBAT+CNC+Gly+AC-1	11±3.7	55±9.0	92±10.7	100±0	100±0
100 Gy+PBAT+CNC+Gly+AC-2	4.4±0.5	30±3.2	59±9.7	83±6.9	100±0
200 Gy+PBAT+CNC+Gly+AC-2	8±2.4	38±6.5	85±5.6	100±0	100±0
300 Gy+PBAT+CNC+Gly+AC-2	14±4.0	68±4.8	100±0	100±0	100±0
100 Gy+PBAT+CNC+Gly+AC-3	8±2.8	66±6.6	77±9.6	94±14.5	100±0
200 Gy+PBAT+CNC+Gly+AC-3	15±3.7	68±4.5	100±0	100±0	100±0

300 Gy+PBAT+CNC+Gly+AC-3	19±2.8	74±4.8	100±0	100±0	100±0
100 Gy+PLA+CNC+Gly+AC-1	4.4±0.6	25±6.7	32±4.2	46±5.9	66±8.9
200 Gy+PLA+CNC+Gly+AC-1	13±2.8	44±6.1	52±6.9	62±10.8	79±7.8
300 Gy+PLA+CNC+Gly+AC-1	12±3.2	55±5.8	62±6.7	79±11.2	96±5.9
100 Gy+PLA+CNC+Gly+AC-2	4.9±0.4	27±9.6	48±5.8	63±9.5	79±7.8
200 Gy+PLA+CNC+Gly+AC-2	8±1.8	37±5.7	52±11	74±9.6	100±0
300 Gy+PLA+CNC+Gly+AC-2	12±3.2	48±6.4	66±6.3	87±4.9	100±0
100 Gy+PLA+CNC+Gly+AC-3	6±0.9	35±7.8	44±8.9	56±6.5	88±8.9
200 Gy+PLA+CNC+Gly+AC-3	7±2.3	41±5.9	50±7.8	66±11.1	92±9.6
300 Gy+PLA+CNC+Gly+AC-3	14±3.4	56±4.9	71±10.7	87±9.0	100±0

Values means ± standard error. Within each column means with different lowercase letter are significantly different ($P \leq 0.05$), while the means with the different uppercase letter are significantly different ($P \leq 0.05$).

Similar observations were found in the case of the bioactive PBAT- and PLA-based nanocomposite films. The bioactive films (PBAT- and PLA-based nanocomposite films) along with 200 and 300 Gy of γ -irradiation were responsible for the complete mortality of experimental insects between 10-14 days of incubation. PBAT-based nanocomposite films containing AC-2 and AC-3 (PBAT+CNC+Gly+AF-2 and PBAT+CNC+Gly+AF-3) with 100 Gy γ -irradiation showed 100 % mortality after 14 days; the insect mortality increased when radiation doses were increased in the combined treatment. Upon assessing the results, the mortality of insects was significantly ($P \leq 0.05$) higher from 66-100 % at day 7-14 when the samples treated under PBAT-based film containing ACs (AC-1, AC-2 and AC-3) with the range of irradiation doses from 200 to 300 Gy (Table 8.7). The mortality of the rice weevil was significantly increased by applying bioactive PLA-based nanocomposite films with 100, 200, and 300 Gy γ -irradiation doses, and the mortality increased with higher doses of radiation and a longer incubation period. Bioactive PLA-based nanocomposite films having AC-2 (PLA+CNC+Gly+AC-2 film) in combination with 200 and 300 Gy irradiation doses caused 100 % mortality after 14 days of incubation (Table 8.7). The results of the combined treatment between irradiation and PLA-based nanocomposite film showed increased mortality, which is significantly higher as compared to the effect of each treatment as well as control samples. Bioactive PLA+CNC+Gly+AC-1 films in combination with 100, 200, and 300 Gy γ -irradiation caused 66, 79 and 96 % mortality at day 14 of incubation, respectively.

It has also been well-established and proven by several authors that the combined treatment between irradiation and bioactive films or plant-derived EOs could enhance the radiosensitization of foodborne pathogenic bacteria, spoilage fungi, and stored products insect pests (Caillet *et al.*, 2005; Ayari *et al.*, 2012; Hossain *et al.*, 2014b; Hossain *et al.*, 2019b; Ayari *et al.*, 2020; Begum *et al.*, 2020a; Hossain *et al.*, 2021). Hossain *et al.* (2021) worked with tea tree and eucalyptus EO along with γ -radiation and X-ray at different dose rates against *S. oryzae* and the authors stated that the application of EOs and irradiation treatment increased the mortality of rice weevil by 3-6 fold than the radiation treatment alone. In accordance, Ahmadi *et al.* (2013) reported a synergistic effect of the treatment between EOs (*Rosmarinus officinalis* EO and *Perovskia atriplicifolia* EO) and γ -irradiation on major stored product insect *Tribolium castaneum*. *R. officinalis* EO at 4.2 $\mu\text{L/mL}$ showed only 1 % *T. castaneum* mortality and 130-230 Gy γ -irradiation caused 1-5 % mortality of insects when applied alone, however, the insect mortality increased to 20 and 30.3 %, respectively when both treatments were combined (Ahmadi *et al.*, 2013). A study found that *S. oryzae* became 4.8 and 6.2 times more sensitive to γ -irradiation when they were exposed to basil EO at 0.2 and 0.4 $\mu\text{L/mL}$ concentration, respectively, compared to the rice weevils used in the control samples (120 Gy irradiation treatment alone) (Hossain *et al.*, 2014b). Moreover, the

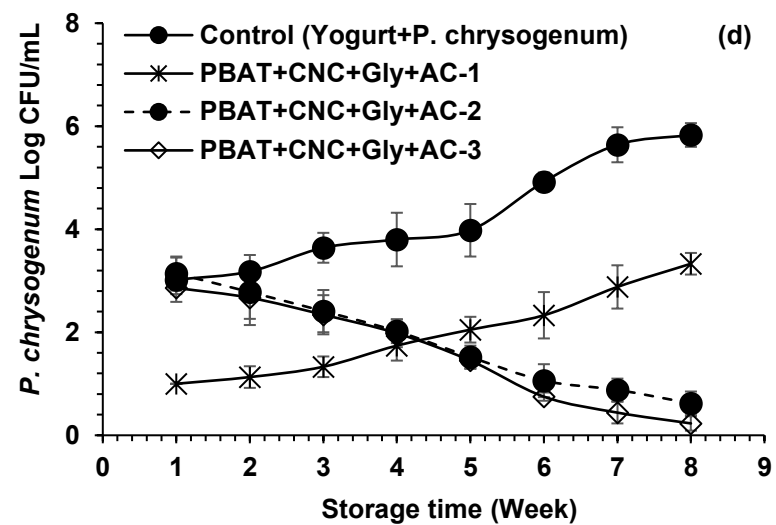
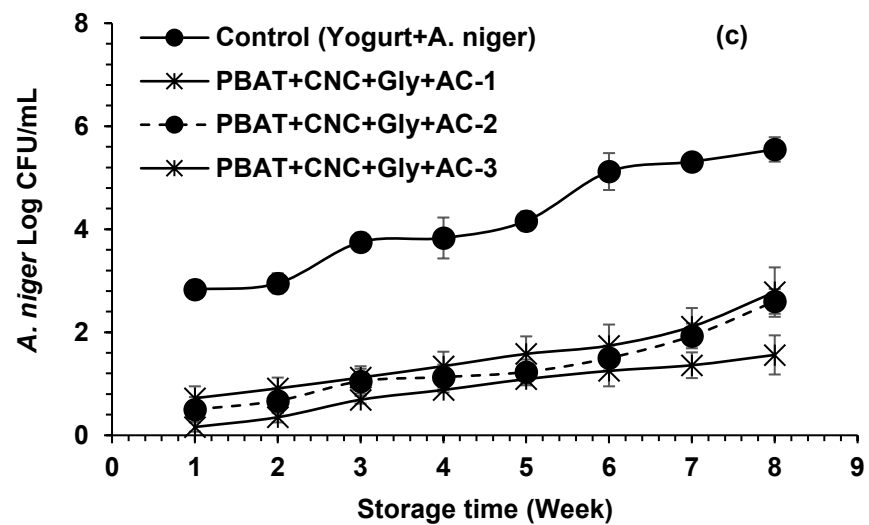
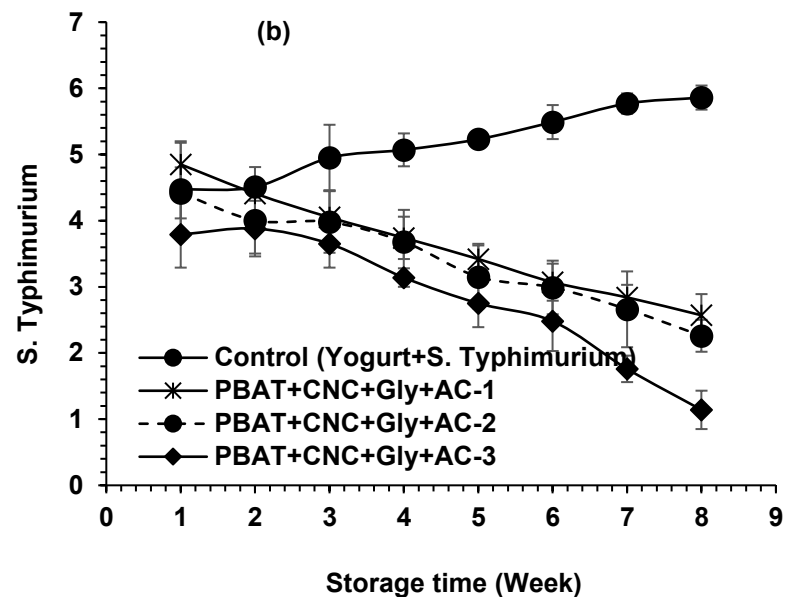
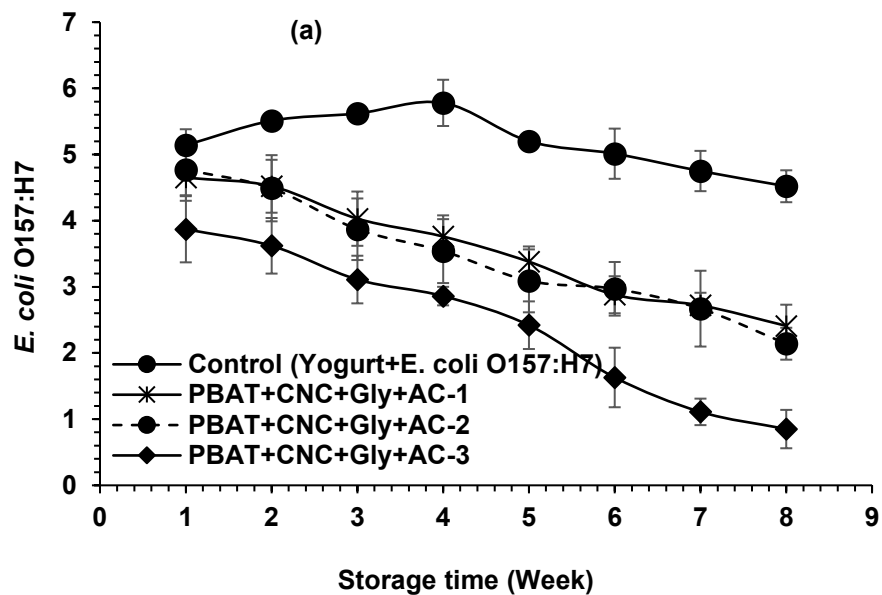
application of bioactive nanocomposite films in stored rice can release active ingredients slowly during the storage period and kill the adult rice weevils, although fumigation of EOs can not negatively affect their eggs and larvae because of their location inside the kernel. But application of low doses of γ -radiation could pass through the kernel and affect the development of insects at all stages. Thus, combining two treatments showed the synergistic effect to control insect pests in stored rice. Furthermore, the application of bioactive nanocomposite films and irradiation treatment separately to complete the elimination of the stored product insect pests required higher radiation doses and higher concentrations of EO which is expensive as well as time-consuming. The current study came up with an innovative solution to reduce the time, costs as well as pest infestation in stored cereal grains by combining γ -irradiation and bioactive nanocomposite films.

8.3.5. Evaluation of the antibacterial and antifungal properties of the film (for dairy products)

Six types of bioactive nanocomposite films (PBAT+CNC+Gly+AC-1, PBAT+CNC+Gly+AC-2, PBAT+CNC+Gly+AC-3, PLA+CNC+Gly+AC-1, PLA+CNC+Gly+AC-2 and PLA+CNC+Gly+AC-3) were selected for the *in situ* tests in stored yogurt to control the growth of *E. coli* O157:H7, *S. Typhimurium*, *A. niger*, *P. chrysogenum*, and *M. circinelloides* (Figure 8.7a-e and Figure 8.8a-e). The bioactive CH-based films (CH+CNC+PEG+AC-1, CH+CNC+PEG+AC-2 and CH+CNC+PEG+AC-3) were not selected because of their high-water solubility. Figure 8.7a-b shows the growth profile of *E. coli* O157:H7 and *S. Typhimurium* in stored yogurt for 8 weeks under different treatments. The tested bacterial growth profile was significantly affected in yogurt after 8 weeks stored with bioactive PBAT-based films. Briefly, yogurt was inoculated with 5 log CFU/g of *E. coli* O157:H7 and *S. Typhimurium*. The growth of *E. coli* O157:H7 was reached 4.52 log CFU/g in control sample after 8 weeks (Figure 8.7a). After 8 weeks of storage, *E. coli* O157:H7 growth was significantly reduced by 47 % (2.41 log CFU/g), 53 % (2.14 log CFU/g) and 81.2 % (0.85 log CFU/g) in yogurt stored with PBAT+CNC+Gly+AC-1, PBAT+CNC+Gly+AC-2 and PBAT+CNC+Gly+AC-3 film, respectively, as compared with control samples (no antimicrobial films) after 8 weeks (Figure 8.7a). A similar observation was found in the case of the growth profile of *S. Typhimurium* in stored yogurt and the result is shown in Figure 8.7b. *S. Typhimurium* growth in the control sample increased with storage time and reached 5.86 log CFU/g after 8 weeks. The highest bacterial growth (*S. Typhimurium*) reduction was observed by PBAT+CNC+Gly+AC-3 film (80.5 %), followed by PBAT+CNC+Gly+AC-2 film (61 %) and by PBAT+CNC+Gly+AC-1 film (56.1 %) with respect to the control sample, and the corresponding bacterial count was 1.14, 2.26 and

2.57 log CFU/g of *S. Typhimurium* after 8 weeks in stored yogurt. On the other hand, bioactive PLA-based nanocomposite films showed lower antibacterial properties when compared to the bioactive PBAT-based nanocomposite films. Figure 8.8a-b shows the antibacterial properties of the bioactive PLA-based nanocomposite films (PLA+CNC+Gly+AC-1, PLA+CNC+Gly+AC-2 and PLA+CNC+Gly+AC-3 film) to control the growth of *E. coli* O157:H7 and *S. Typhimurium* in stored yogurt. The highest bacterial growth (*E. coli* O157:H7) reduction was observed by PLA+CNC+Gly+AC-3 film (42.2 %), followed by PLA+CNC+Gly+AC-2 film (36.5 %) and by PLA+CNC+Gly+AC-1 film (25.6 %) with respect to the control sample (4.52 log CFU/g), and the corresponded bacterial count was 2.61, 2.87 and 3.36 log CFU/g of *E. coli* O157:H7 after 8 weeks in stored yogurt. Similarly, PLA+CNC+Gly+AC-3 film caused a higher reduction of *S. Typhimurium* growth by 53.2 % (2.74 log CFU/g), PLA+CNC+Gly+AC-1 and PLA+CNC+Gly+AC-2 films caused 43 and 48.5 % reduction, respectively, as compared to the control samples (5.86 log CFU/g) after 8 weeks in stored yogurt (Figure 8.8b).

The antifungal activities of the fabricated bioactive PBAT and PLA nanocomposite films were tested against three spoilage fungi *A. niger*, *P. chrysogenum*, and *M. circinelloides* in stored yogurt for 8 weeks (Figure 8.7c-e and Figure 8.8c-e). The bioactive PBAT nanocomposite film containing AC-3 (PBAT+CNC+Gly+AC-3 film) showed the strongest fungicidal effect compared to the bioactive PBAT-based films containing either AC-1 or AC-2. Moreover, bioactive PBAT-based films were more efficient to control the growth of fungi in yogurt than bioactive PLA-based films. In the case of *A. niger*, the fungal count reached from 2.83 to 5.55 log CFU/g during storage from week 1 to 8 in yogurt (Figure 8.7c). The samples treated with PBAT+CNC+Gly+AC-1 film, PBAT+CNC+Gly+AC-2 film and PBAT+CNC+Gly+AC-3 film showed reduced fungal level (*A. niger*) by 50 % (2.78 log CFU/g), 53 % (2.6 log CFU/g) and 72 % (1.56 log CFU/g) with respect to the control sample after 8 weeks, respectively (Figure 8.7c). Figure 8.7c shows the fungicidal properties by bioactive PLA-based films (PLA+CNC+Gly+AC-1, PLA+CNC+Gly+AC-2 and PLA+CNC+Gly+AC-3 film) against *A. niger* in stored yogurt. PLA+CNC+Gly+AC-1, PLA+CNC+Gly+AC-2 and PLA+CNC+Gly+AC-3 film caused the fungal (*A. niger*) growth reduction by 32.4 % (3.75 log CFU/g), 39.1 % (3.38 log CFU/g) and 49.2 % (2.82 log CFU/g) with respect to control sample (Figure 8.8c).



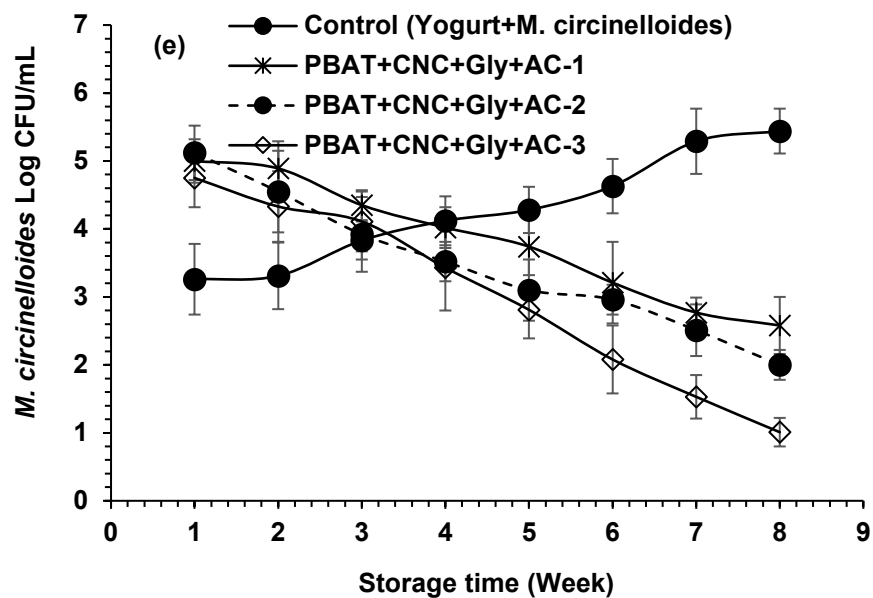
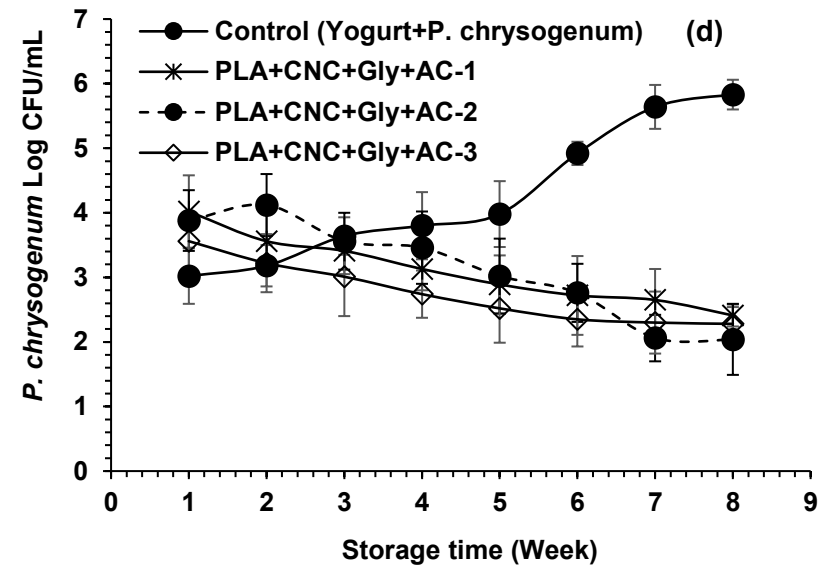
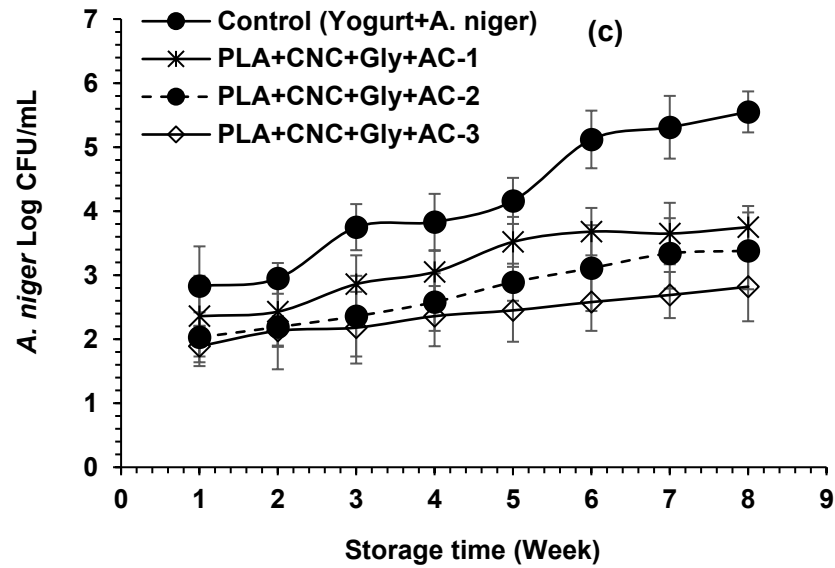
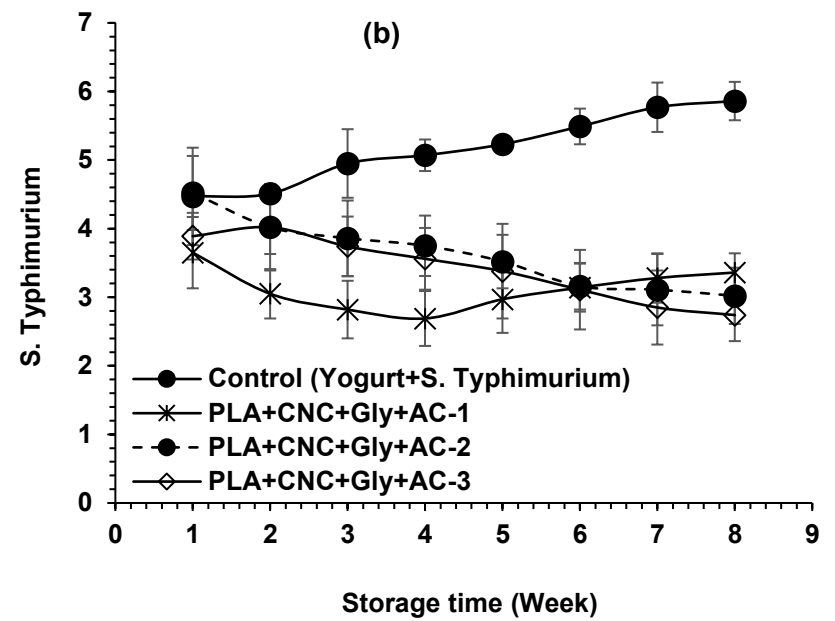
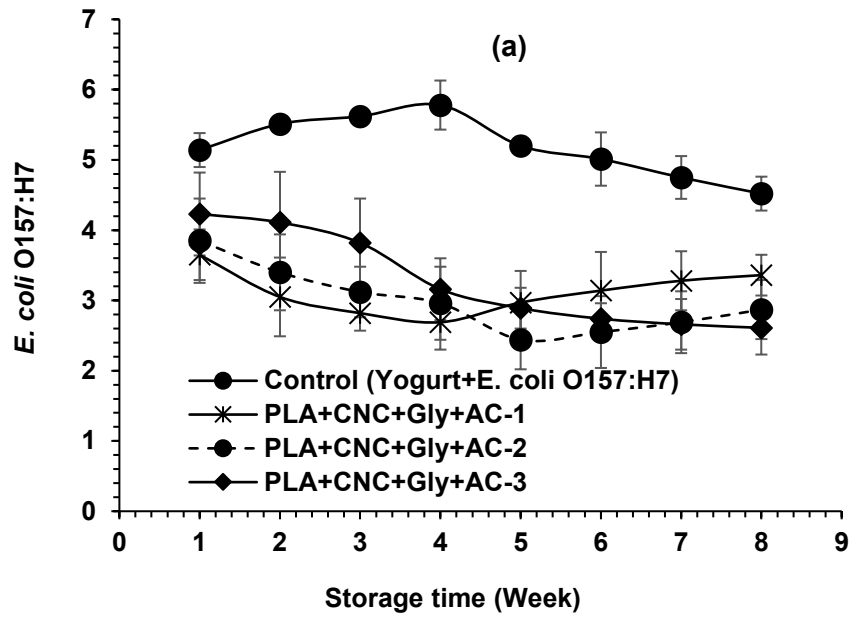


Figure 8.7. Bacterial (*E. coli* O157:H7 and *S. Typhimurium*) (a-b) and fungal (*A. niger*, *P. chrysogenum*, and *M. circinelloides*) (c-e) growth profiles in storage yogurt under different bioactive films treatment for 8 weeks.

For *P. chrysogenum*, both bioactive PBAT and PLA-based nanocomposite films significantly controlled the growth of *P. chrysogenum* in stored yogurt for 8 weeks as compared to the control samples, though bioactive PBAT-based nanocomposite films were more effective than bioactive PLA-based nanocomposite films (Figure 8.7d and Figure 8.7d). *P. chrysogenum* growth increased from 3.02 to 5.83 log CFU/g in stored yogurt from week 1 to week 8. The samples treated with PBAT+CNC+Gly+AC-1 film, PBAT+CNC+Gly+AC-2 film and PBAT+CNC+Gly+AC-3 film reduced the fungal level (*P. chrysogenum*) by 81.4 % (0.62 log CFU/g), 93 % (0.23 log CFU/g) and 93 % (0.23 log CFU/g) with respect to the control sample after 8 weeks, respectively (Figure 8.7d). Figure 8.7d shows the fungicidal properties by bioactive PLA-based films (PLA+CNC+Gly+AC-1, PLA+CNC+Gly+AC-2 and PLA+CNC+Gly+AC-3 film) against *P. chrysogenum* in stored yogurt. PLA+CNC+Gly+AC-1, PLA+CNC+Gly+AC-2 and PLA+CNC+Gly+AC-3 film reduced the fungal (*P. chrysogenum*) growth by 58.6 % (2.41 log CFU/g), 65 % (2.04 log CFU/g) and 61 % (2.28 log CFU/g) with respect to control sample (Figure 8.8d).

Figure 8.7e shows the fungicidal effectiveness given by the bioactive PBAT-based nanocomposite films to control *M. circinelloides* in stored yogurt for 8 weeks. The growth of *M. circinelloides* in control samples was 5.44 log CFU/g after 8 weeks of storage at 4 °C. The fungal (*M. circinelloides*) growth was 2.58, 2 and 1.01 log CFU/g while the samples treated with PBAT+CNC+Gly+AC-1 film, PBAT+CNC+Gly+AC-2 film and PBAT+CNC+Gly+AC-3 film, respectively, which represents the corresponded reduction by 52.6, 63.2 and 81.4 % of *M. circinelloides* after 8 weeks of stored yogurt as compared to the control sample. The application of PLA+CNC+Gly+AC-1, PLA+CNC+Gly+AC-2 and PLA+CNC+Gly+AC-3 films in stored yogurt reduced the fungal (*M. circinelloides*) growth by 43 % (3.11 log CFU/g), 50.4 % (2.7 log CFU/g) and 54.9 % (2.45 log CFU/g), respectively, at the end of the incubation period with respect to the control ($P \leq 0.05$) (Figure 8.8e).



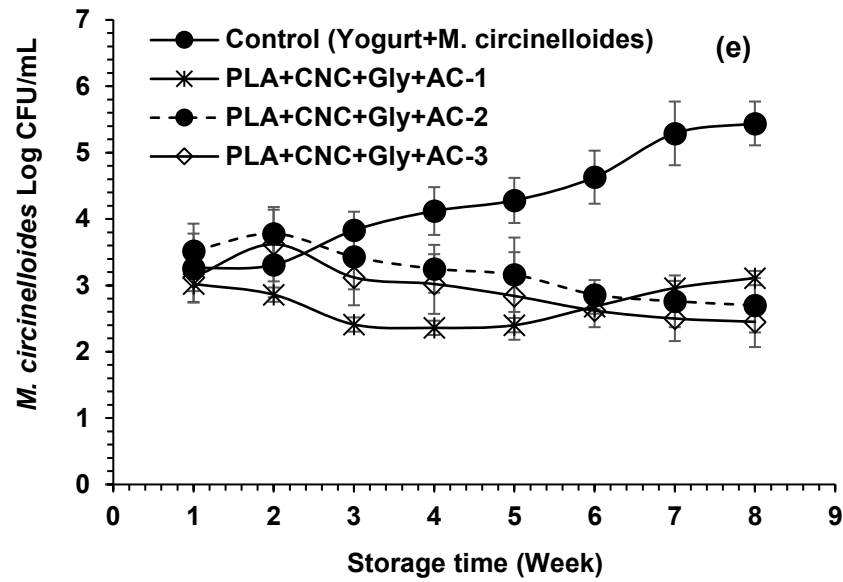


Figure 8.8. Bacterial (*E. coli* O157:H7 and *S. Typhimurium*) (a-b) and fungal (*A. niger*, *P. chrysogenum*, and *M. circinelloides*) (c-e) growth profiles in storage yogurt under different bioactive films treatment for 8 weeks.

Several authors have used EOs to extend the shelf-life of yogurt by adding EOs directly into the yogurt (Singh *et al.*, 2011; Yangilar and Yildiz, 2018; El Omari *et al.*, 2020), but to our knowledge no studies were performed where bioactive films released active compounds during storage from the lid of the yogurt container. El Omari *et al.* (2020) extended the shelf-life of Lebanese yogurt using *Micromeria barbata* EO (0.125 and 0.25 $\mu\text{L}/100\text{ mL}$). *M. barbata* EO (0.125 $\mu\text{L}/100\text{ mL}$) could significantly reduce the growth of fungi as compared to fat free yogurt without compromising the growth of starter lactic acid bacteria (LAB) and organoleptic properties. Vazquez *et al.* (2001) used eugenol and thymol in Spanish cheeses to control the production of citrinin from *P. citrinum*. The authors found that 200 $\mu\text{g}/\text{mL}$ eugenol could completely inhibit the fungal growth on cheese. A study found that low-density polyethylene (LDPE) film containing bimetallic nanoparticles (4 % Ag-Au NPs) with cinnamon EO showed strong antibacterial activities against *Salmonella* Typhimurium, *Listeria monocytogenes*, and *Campylobacter jejuni* at 4 °C for 21 days storage in meat. It was also observed that combined Ag-Au/cinnamon EO was capable of a 100 % reduction of *S. Typhimurium* and *C. jejuni* from meat during the storage (Ahmed *et al.*, 2018). Another study was conducted by Dehkordi *et al.* (2019) to evaluate the antibacterial properties of the AgNPs and eugenol, alone and in combination, against *Staphylococcus aureus* and *S. Typhimurium* in meat and milk. The authors found combined (AgNPs/eugenol) treatment achieved 6 log reduction of *S. Typhimurium* and *S. aureus* from meat and milk samples in 3 and 24 h, respectively, while the single antimicrobial treatment took a long time to reach 6 log reduction of those bacteria (Dehkordi *et al.*, 2019).

8.4. Conclusion

Nine different types of bioactive nanocomposite films were fabricated using CH-, PBAT- and PLA-based polymeric matrices. The films were PBAT+CNC+Gly+AC-1, PBAT+CNC+Gly+AC-2, PBAT+CNC+Gly+AC-3, CH+CNC+PEG+AC-1, CH+CNC+PEG+AC-2, CH+CNC+PEG+AC-3, PLA+CNC+Gly+AC-1, PLA+CNC+Gly+AC-2 and PLA+CNC+Gly+AC-3 films. Three active combinations (ACs) were developed using mixtures of EOs and AgNPs to increase the efficiency of active agents. Nanoemulsions of ACs were developed using microfluidization techniques and incorporated into a CH-based polymeric matrix. CH-based films were developed using solvent casting, while the PBAT- and PLA-based films were developed by compression molding. Microfluidization pressure and thus number of cycles could significantly reduce the size of the droplet and significantly increased the encapsulation efficiency of the nanoemulsion of ACs as compared to the coarse emulsions. The films were characterized by measuring mechanical

properties, water solubility (WS), water vapor permeability (WVP), *in vitro* antibacterial, antifungal and insecticidal properties, and *in vitro* release profile in food simulants (ethanol and 3 % acetic acid) before applying to real foods. Fabricated films significantly improved the mechanical WS, WVP properties and release kinetics of the active combinations from the bioactive nanocomposite films. Application of bioactive films in stored rice could significantly control the growth of foodborne pathogenic bacteria, spoilage fungi and insect (*S. oryzae*) along with irradiation treatment. The current study proved that the combination between bioactive nanocomposite films and irradiation could work synergistically and increase the microbicidal and insecticidal effectiveness more significantly than the treatment alone (either by bioactive film or by irradiation alone). Thereafter, the application of bioactive PBAT- and PLA-based nanocomposite films in stored yogurt was able to eliminate the growth of *E. coli* O157:H7, *S. Typhimurium*, *A. niger*, *P. chrysogenum* and *M. circinelloides* at 4 °C, after 8 weeks of storage. Finally, it could be concluded that the application of bioactive CH- and PBAT-based films and irradiation together could be an effective and safe way to protect cereal grains during long-term storage as well as contribute to “Green Consumerism” and “Sustainable Packaging” in the agriculture sector and food industry. In addition, the application of bioactive PLA- and PBAT-based nanocomposite films could significantly control the growth of pathogenic bacteria and spoilage fungi in stored dairy products such as yogurt without changing their quality and organoleptic properties.

8.5. Acknowledgments

The authors are grateful for the financial support from Natural Sciences and Engineering Research Council of Canada (NSERC) no: RDCPJ 534563 - 18, Biosecur Lab. (A Kerry division), NanoBrand Lab, the Ministry of Economy and Innovation (MEI) of the province of Quebec no: 2019-PSO-I-2, the U.S. Department of Agriculture, Agricultural Research Service (USDA ARS), U.S. Pacific Basin Agricultural Research Centre and by a chair granted by Quebec Ministry of Agriculture, Fishery and Food (MAPAQ) no: PPIA12.

8.6. References

- Abdelgaleil, S.A., Mohamed, M.I., Badawy, M.E., El-arami, S.A., 2009. Fumigant and contact toxicities of monoterpenes to *Sitophilus oryzae* (L.) and *Tribolium castaneum* (Herbst) and their inhibitory effects on acetylcholinesterase activity. *Journal of Chemical Ecology* 35, 518-525.
- Abdelgaleil, S.A.M., Mohamed, M.I.E., Shawir, M.S., Abou-Taleb, H.K., 2016. Chemical composition, insecticidal and biochemical effects of essential oils of different plant species from Northern Egypt on the rice weevil, *Sitophilus oryzae* L. *Journal of Pest Science* 89, 219-229.
- Abdollahi, M., Rezaei, M., Farzi, G., 2012. A novel active bionanocomposite film incorporating rosemary essential oil and nanoclay into chitosan. *Journal of Food Engineering* 111, 343-350.
- Adak, T., Barik, N., Patil, N.B., Govindharaj, G.-P.-P., Gadratagi, B.G., Annamalai, M., Mukherjee, A.K., Rath, P.C., 2020. Nanoemulsion of eucalyptus oil: An alternative to synthetic pesticides against two major storage insects (*Sitophilus oryzae* (L.) and *Tribolium castaneum* (Herbst)) of rice. *Industrial Crops and Products* 143.
- Ahmadi, M., Abd-alla, A.M.M., Moharramipour, S., 2013. Combination of gamma radiation and essential oils from medicinal plants in managing *Tribolium castaneum* contamination of stored products. *Applied Radiation and Isotopes* 78, 16-20.
- Ahmed, J., Mulla, M., Arfat, Y.A., Bher, A., Jacob, H., Auras, R., 2018. Compression molded LLDPE films loaded with bimetallic (Ag-Cu) nanoparticles and cinnamon essential oil for chicken meat packaging applications. *LWT-Food Science and Technology* 93, 329-338.
- Anjali, C.H., Sharma, Y., Mukherjee, A., Chandrasekaran, N., 2012. Neem oil (*Azadirachta indica*) nanoemulsion--a potent larvicidal agent against *Culex quinquefasciatus*. *Pest Management Science* 68, 158-163.
- Asmawati, Mustapha, W.A.W., Yusop, S.M., Maskat, M.Y., Shamsuddin, A.F., 2014. Characteristics of cinnamaldehyde nanoemulsion prepared using APV-high pressure homogenizer and ultra turrax. *AIP Conference Proceedings*. American Institute of Physics, 1614, 244-250.
- Ayari, S., Dussault, D., Jerbi, T., Hamdi, M., Lacroix, M., 2012. Radiosensitization of *Bacillus cereus* spores in minced meat treated with cinnamaldehyde. *Radiation Physics and Chemistry* 81, 1173-1176.

- Ayari, S., Shankar, S., Follett, P., Hossain, F., Lacroix, M., 2020. Potential synergistic antimicrobial efficiency of binary combinations of essential oils against *Bacillus cereus* and *Paenibacillus amylolyticus*-Part A. *Microbial Pathogenesis* 141, 104008.
- Bahrami, A., Mokarram, R.R., Khiabani, M.S., Ghanbarzadeh, B., Salehi, R., 2019. Physico-mechanical and antimicrobial properties of tragacanth/hydroxypropyl methylcellulose/beeswax edible films reinforced with silver nanoparticles. *International Journal of Biological Macromolecules* 129, 1103-1112.
- Begum, T., Follett, P.A., Hossain, F., Christopher, L., Salmieri, S., Lacroix, M., 2020a. Microbicidal effectiveness of irradiation from Gamma and X-ray sources at different dose rates against the foodborne illness pathogens *Escherichia coli*, *Salmonella* Typhimurium and *Listeria monocytogenes* in rice. *LWT-Journal of Food Science and Technology* 132, 109841.
- Begum, T., Follett, P.A., Mahmud, J., Moskovchenko, L., Salmieri, S., Allahdad, Z., Lacroix, M., 2022a. Silver nanoparticles-essential oils combined treatments to enhance the antibacterial and antifungal properties against foodborne pathogens and spoilage microorganisms. *Microbial Pathogenesis* 164, 105411.
- Begum, T., Follett, P.A., Shankar, S., Mahmud, J., Salmieri, S., Lacroix, M., 2022b. Mixture design methodology and predictive modeling for developing active formulations using essential oils and citrus extract against foodborne pathogens and spoilage microorganisms in rice. *Journal of Food Science* 87, 353-369.
- Ben-Fadhel, Y., Maherani, B., Manus, J., Salmieri, S., Lacroix, M., 2020. Physicochemical and microbiological characterization of pectin-based gelled emulsions coating applied on pre-cut carrots. *Food Hydrocolloids* 101, 105573.
- Ben-Fadhel, Y., Maherani, B., Salmieri, S., Lacroix, M., 2022. Preparation and characterization of natural extracts-loaded food grade nanoliposomes. *LWT-Journal of Food Science and Technology* 154, 112781.
- Benelli, G., 2018. Mode of action of nanoparticles against insects. *Environmental Science and Pollution Research International* 25, 12329-12341.
- Boumail, A., Salmieri, S., Klimas, E., Tawema, P.O., Bouchard, J., Lacroix, M., 2013. Characterization of trilayer antimicrobial diffusion films (ADFs) based on methylcellulose-polycaprolactone composites. *Journal of Agricultural and Food Chemistry* 61, 811-821.
- Burt, S., 2004. Essential oils: their antibacterial properties and potential applications in foods—a review. *International Journal of Food Microbiology* 94, 223-253.
- Bustos, C.R., Alberti, R.F., Matiacevich, S.B., 2016. Edible antimicrobial films based on microencapsulated lemongrass oil. *Journal of Food Science and Technology* 53, 832-839.

- Caillet, S., Lacroix, M., 2006. Effect of gamma radiation and oregano essential oil on murein and ATP concentration of *Listeria monocytogenes*. *Journal of Food Protection* 69, 2961-2969.
- Caillet, S., Shareck, F., Lacroix, M., 2005. Effect of gamma radiation and oregano essential oil on murein and ATP concentration of *Escherichia coli* O157: H7. *Journal of Food Protection* 68, 2571-2579.
- Cardoso, L.G., Pereira Santos, J.C., Camilloto, G.P., Miranda, A.L., Druzian, J.I., Guimarães, A.G., 2017. Development of active films poly (butylene adipate co-terephthalate) – PBAT incorporated with oregano essential oil and application in fish fillet preservation. *Industrial Crops and Products* 108, 388-397.
- Chand, R., Jokhan, A., Gopalan, R., 2017. A mini-review of essential oils in the South Pacific and their insecticidal properties. *Advances in Horticultural Science* 31, 295-310.
- Cheng, D., Wen, Y., An, X., Zhu, X., Cheng, X., Zheng, L., Nasrallah, J.E., 2016. Improving the colloidal stability of Cellulose nano-crystals by surface chemical grafting with polyacrylic acid. *Journal of Bioresources and Bioproducts* 1, 114-119.
- Choupanian, M., Omar, D., Basri, M., Asib, N., 2017. Preparation and characterization of neem oil nanoemulsion formulations against *Sitophilus oryzae* and *Tribolium castaneum* adults. *Journal of Pesticide Science* 42, 158-165.
- da Rosa, C.G., Sganzerla, W.G., de Oliveira Brisola Maciel, M.V., de Melo, A.P.Z., da Rosa Almeida, A., Ramos Nunes, M., Bertoldi, F.C., Manique Barreto, P.L., 2020. Development of poly (ethylene oxide) bioactive nanocomposite films functionalized with zein nanoparticles. *Colloids and Surfaces A: Physicochemical and Engineering Aspects* 586, 124268.
- Das, S., Kumar Singh, V., Kumar Dwivedy, A., Kumar Chaudhari, A., Deepika, Kishore Dubey, N., 2021a. Nanostructured Pimpinella anisum essential oil as novel green food preservative against fungal infestation, aflatoxin B1 contamination and deterioration of nutritional qualities. *Food Chemistry* 344, 128574.
- Das, S., Singh, V.K., Dwivedy, A.K., Chaudhari, A.K., Dubey, N.K., 2021b. *Anethum graveolens* Essential Oil Encapsulation in Chitosan Nanomatrix: Investigations on *In Vitro* Release Behavior, Organoleptic Attributes, and Efficacy as Potential Delivery Vehicles Against Biodeterioration of Rice (*Oryza sativa* L.). *Food and Bioprocess Technology* 14, 831-853.
- de Mesquita, J.P., Donnici, C.L., Pereira, F.V., 2010. Biobased nanocomposites from layer-by-layer assembly of cellulose nanowhiskers with chitosan. *Biomacromolecules* 11, 473-480.

- de Souza, A.G., Barbosa, R.F.d.S., Quispe, Y.M., Rosa, D.d.S., 2022. Essential oil microencapsulation with biodegradable polymer for food packaging application. *Journal of Polymers and the Environment* 30, 3307-3315.
- Dehkordi, N.H., Tajik, H., Moradi, M., Kousheh, S.A., Molaei, R., 2019. Antibacterial Interactions of Colloid Nanosilver with Eugenol and Food Ingredients. *Journal of Food Protection* 82, 1783-1792.
- Delavenne, E., Ismail, R., Pawtowski, A., Mounier, J., Barbier, G., Le Blay, G., 2013. Assessment of lactobacilli strains as yogurt bioprotective cultures. *Food Control* 30, 206-213.
- Deng, Z., Jung, J., Simonsen, J., Wang, Y., Zhao, Y., 2017. Cellulose Nanocrystal Reinforced Chitosan Coatings for Improving the Storability of Postharvest Pears Under Both Ambient and Cold Storages. *Journal of Food Science* 82, 453-462.
- El-Bakry, A.M., Youssef, H.F., Abdel-Aziz, N.F., Sammour, E.A., 2019. Insecticidal potential of Ag-loaded 4A-zeolite and its formulations with *Rosmarinus officinalis* essential oil against rice weevil (*Sitophilus oryzae*) and lesser grain borer (*Rhyzopertha dominica*). *Journal of Plant Protection Research* 59.
- El Omari, K., Al Kassaa, I., Farraa, R., Najib, R., Alwane, S., Chihib, N., Hamze, M., 2020. Using the essential oil of *Micromeria barbata* plant as natural preservative to extend the shelf life of lebanese YogurtPak. *Journal of Biological Sciences* 23, 848-855.
- Escamilla-García, M., García-García, M.C., Gracida, J., Hernández-Hernández, H.M., Granados-Arvizu, J.Á., Di Pierro, P., Regalado-González, C., 2022. Properties and Biodegradability of Films Based on Cellulose and Cellulose Nanocrystals from Corn Cob in Mixture with Chitosan. *International Journal of Molecular Sciences* 23, 10560.
- Felix da Silva Barbosa, R., Gabrieli de Souza, A., Rangari, V., Rosa, D.D.S., 2021. The influence of PBAT content in the nanocapsules preparation and its effect in essential oils release. *Food Chemistry* 344, 128611.
- Follett, P.A., Snook, K., Janson, A., Antonio, B., Haruki, A., Okamura, M., Bisel, J., 2013. Irradiation quarantine treatment for control of *Sitophilus oryzae* (Coleoptera: Curculionidae) in rice. *Journal of Stored Products Research* 52, 63-67.
- Ghabraie, M., Vu, K.D., Tata, L., Salmieri, S., Lacroix, M., 2016. Antimicrobial effect of essential oils in combinations against five bacteria and their effect on sensorial quality of ground meat. *LWT-Food Science and Technology* 66, 332-339.
- Gherasim, O., Grumezescu, A.M., Mogosanu, G.D., Vasile, B.S., Bejenaru, C., Bejenaru, L.E., Andronesu, E., Mogoanta, L., 2020. Biodistribution of essential oil-conjugated silver

- nanoparticles. Romanian journal of morphology and embryology = Revue roumaine de Morphologie et Embryologie 61, 1099-1109.
- Ghosh, I.N., Patil, S.D., Sharma, T.K., Srivastava, S.K., Pathania, R., Navani, N.K., 2013. Synergistic action of cinnamaldehyde with silver nanoparticles against spore-forming bacteria: a case for judicious use of silver nanoparticles for antibacterial applications. International Journal of Nanomedicine 8, 4721-4731.
- Gougouli, M., Koutsoumanis, K.P., 2017. Risk assessment of fungal spoilage: A case study of *Aspergillus niger* on yogurt. Food Microbiology 65, 264-273.
- Haafiz, M.K., Hassan, A., Khalil, H.P., Fazita, M.R., Islam, M.S., Inuwa, I.M., Marliana, M.M., Hussin, M.H., 2016. Exploring the effect of cellulose nanowhiskers isolated from oil palm biomass on polylactic acid properties. International Journal of Biological Macromolecules 85, 370-378.
- Hategekimana, A., Eler, F., 2020. Comparative repellent activity of single, binary and ternary combinations of plant essential oils and their major components against *Sitophilus oryzae* L. (Coleoptera: Curculionidae). Journal of Plant Diseases and Protection 127, 873-881.
- Hossain, F., Follett, P., Salmieri, S., Vu, K.D., Frascini, C., Lacroix, M., 2019a. Antifungal activities of combined treatments of irradiation and essential oils (EOs) encapsulated chitosan nanocomposite films in *in vitro* and *in situ* conditions. International Journal of Food Microbiology 295, 33-40.
- Hossain, F., Follett, P., Salmieri, S., Vu, K.D., Harich, M., Lacroix, M., 2019b. Synergistic Effects of Nanocomposite Films Containing Essential Oil Nanoemulsions in Combination with Ionizing Radiation for Control of Rice Weevil *Sitophilus oryzae* in Stored Grains. Journal of Food Science 84, 1439-1446.
- Hossain, F., Follett, P., Salmieri, S., Vu, K.D., Jamshidian, M., Lacroix, M., 2016. Perspectives on essential oil-loaded nano-delivery packaging technology for controlling stored cereal and grain pests. In Green Pesticides Handbook, 487-508.
- Hossain, F., Follett, P., Shankar, S., Begum, T., Salmieri, S., Lacroix, M., 2021. Radiosensitization of rice weevil *Sitophilus oryzae* using combined treatments of essential oils and ionizing radiation with gamma-ray and X-Ray at different dose rates. Radiation Physics and Chemistry 180, 109286.
- Hossain, F., Follett, P., Vu, K.D., Salmieri, S., Frascini, C., Jamshidian, M., Lacroix, M., 2018. Antifungal activity of combined treatments of active methylcellulose-based films containing encapsulated nanoemulsion of essential oils and γ -irradiation: *in vitro* and *in situ* evaluations. Cellulose 26, 1335-1354.

- Hossain, F., Follett, P., Vu, K.D., Salmieri, S., Senoussi, C., Lacroix, M., 2014a. Radiosensitization of *Aspergillus niger* and *Penicillium chrysogenum* using basil essential oil and ionizing radiation for food decontamination. *Food Control* 45, 156-162.
- Hossain, F., Lacroix, M., Salmieri, S., Vu, K., Follett, P.A., 2014b. Basil oil fumigation increases radiation sensitivity in adult *Sitophilus oryzae* (Coleoptera: Curculionidae). *Journal of Stored Products Research* 59, 108-112.
- Khan, A., Khan, R.A., Salmieri, S., Le Tien, C., Riedl, B., Bouchard, J., Chauve, G., Tan, V., Kamal, M.R., Lacroix, M., 2012. Mechanical and barrier properties of nanocrystalline cellulose reinforced chitosan based nanocomposite films. *Carbohydrate polymers* 90, 1601-1608.
- Khan, A., Salmieri, S., Fraschini, C., Bouchard, J., Riedl, B., Lacroix, M., 2014. Genipin cross-linked nanocomposite films for the immobilization of antimicrobial agent. *ACS Applied Materials and Interfaces* 6, 15232-15242.
- Khan, R.A., Beck, S., Dussault, D., Salmieri, S., Bouchard, J., Lacroix, M., 2013. Mechanical and barrier properties of nanocrystalline cellulose reinforced poly(caprolactone) composites: Effect of gamma radiation. *Journal of Applied Polymer Science* 129, 3038-3046.
- Khoobdel, M., Ahsaei, S.M., Farzaneh, M., 2017. Insecticidal activity of polycaprolactone nanocapsules loaded with *Rosmarinus officinalis* essential oil in *Tribolium castaneum* (Herbst). *Entomological Research* 47, 175-184.
- Lacroix, M., Follett, P., 2015. Combination irradiation treatments for food safety and phytosanitary uses. *Stewart Postharvest Review* 11, 1-10.
- Lee, B.-H., Annis, P.C., Tumaalii, F.a., Choi, W.-S., 2004. Fumigant toxicity of essential oils from the Myrtaceae family and 1,8-cineole against 3 major stored-grain insects. *Journal of Stored Products Research* 40, 553-564.
- Lee, S.C., Billmyre, R.B., Li, A., Carson, S., Sykes, S.M., Huh, E.Y., Mieczkowski, P., Ko, D.C., Cuomo, C.A., Heitman, J., 2014. Analysis of a food-borne fungal pathogen outbreak: virulence and genome of a *Mucor circinelloides* isolate from yogurt. *Microbiology* 5, 10-1128.
- Li, G., Shankar, S., Rhim, J.-W., Oh, B.-Y., 2015. Effects of preparation method on properties of poly(butylene adipate-co-terephthalate) films. *Food Science and Biotechnology*, pp. 1679-1685.
- Llinares, R., Ramirez, P., Carmona, J.A., Trujillo-Cayado, L.A., Munoz, J., 2021. Assessment of Fennel Oil Microfluidized Nanoemulsions Stabilization by Advanced Performance Xanthan Gum. *Foods* 10, 693.

- Llinares, R., Santos, J., Trujillo-Cayado, L.A., Ramírez, P., Muñoz, J., 2018. Enhancing rosemary oil-in-water microfluidized nanoemulsion properties through formulation optimization by response surface methodology. *LWT-Journal of Food Science and Technology* 97, 370-375.
- Luzi, F., Fortunati, E., Giovanale, G., Mazzaglia, A., Torre, L., Balestra, G.M., 2017. Cellulose nanocrystals from *Actinidia deliciosa* pruning residues combined with carvacrol in PVA-CH films with antioxidant/antimicrobial properties for packaging applications. *International Journal of Biological Macromolecules* 104, 43-55.
- Mohammadzadeh, A., 2017. In vitro antibacterial activity of essential oil and ethanolic extract of *Ajowan (Carum copticum)* against some food-borne pathogens. *Journal of Global Pharma Technology* 9, 20-25.
- Moreira, S.R., Schwan, R.F., Carvalho, E.P.d., Wheals, A.E., 2001. Isolation and identification of yeasts and filamentous fungi from yoghurts in Brazil. *Brazilian Journal of Microbiology* 32, 117-122.
- Morelli, C.L., Belgacem, N., Bretas, R.E.S., Bras, J., 2016. Melt extruded nanocomposites of polybutylene adipate-co-terephthalate (PBAT) with phenylbutyl isocyanate modified cellulose nanocrystals. *Journal of Applied Polymer Science* 133, 43678.
- Oussalah, M., Caillet, S., Lacroix, M., 2006. Mechanism of action of Spanish oregano, Chinese cinnamon, and savory essential oils against cell membranes and walls of *Escherichia coli* O157: H7 and *Listeria monocytogenes*. *Journal of Food Protection* 69, 1046-1055.
- Pereda, M., Amica, G., Marcovich, N.E., 2012. Development and characterization of edible chitosan/olive oil emulsion films. *Carbohydrate Polymers* 87, 1318-1325.
- Petchwattana, N., Naknaen, P., 2015. Utilization of thymol as an antimicrobial agent for biodegradable poly(butylene succinate). *Materials Chemistry and Physics* 163, 369-375.
- Requena, R., Vargas, M., Chiralt, A., 2017. Release kinetics of carvacrol and eugenol from poly(hydroxybutyrate-co-hydroxyvalerate) (PHBV) films for food packaging applications. *European Polymer Journal* 92, 185-193.
- Rhim, J.-W., Mohanty, A.K., Singh, S.P., Ng, P.K.W., 2006. Effect of the processing methods on the performance of polylactide films: Thermocompression versus solvent casting. *Journal of Applied Polymer Science* 101, 3736-3742.
- Salmieri, S., Islam, F., Khan, R.A., Hossain, F.M., Ibrahim, H.M.M., Miao, C., Hamad, W.Y., Lacroix, M., 2014a. Antimicrobial nanocomposite films made of poly(lactic acid)-cellulose nanocrystals (PLA-CNC) in food applications: part A—effect of nisin release on the inactivation of *Listeria monocytogenes* in ham. *Cellulose* 21, 1837-1850.

- Salmieri, S., Islam, F., Khan, R.A., Hossain, F.M., Ibrahim, H.M.M., Miao, C., Hamad, W.Y., Lacroix, M., 2014b. Antimicrobial nanocomposite films made of poly(lactic acid)–cellulose nanocrystals (PLA–CNC) in food applications—part B: effect of oregano essential oil release on the inactivation of *Listeria monocytogenes* in mixed vegetables. *Cellulose* 21, 4271-4285.
- Samir, M.A.S.A., Alloin, F., Sanchez, J.-Y., Dufresne, A., 2004. Cellulose nanocrystals reinforced poly (oxyethylene). *Polymer* 45, 4149-4157.
- Sani, I.K., Pirsá, S., Tađı, Ő., 2019. Preparation of chitosan/zinc oxide/Melissa officinalis essential oil nano-composite film and evaluation of physical, mechanical and antimicrobial properties by response surface method. *Polymer Testing* 79, 106004.
- Shankar, S., Khodaei, D., Lacroix, M., 2021. Effect of chitosan/essential oils/silver nanoparticles composite films packaging and gamma irradiation on shelf life of strawberries. *Food Hydrocolloids* 117, 106750.
- Shankar, S., Rhim, J.W., 2018. Preparation of antibacterial poly(lactide)/poly(butylene adipate-co-terephthalate) composite films incorporated with grapefruit seed extract. *International Journal of Biological Macromolecules* 120, 846-852.
- Sharma, S., Barkauskaite, S., Duffy, B., Jaiswal, A.K., Jaiswal, S., 2020. Characterization and Antimicrobial Activity of Biodegradable Active Packaging Enriched with Clove and Thyme Essential Oil for Food Packaging Application. *Foods* 9, 1117.
- Sharma, S., Barkauskaite, S., Jaiswal, A.K., Jaiswal, S., 2021. Essential oils as additives in active food packaging. *Food Chemistry* 343, 128403.
- Siddiqui, M.S., Nadeem, S.F., 2007. Epidemiological investigation of an outbreak of food poisoning traced to yogurt among personnel of a Military training center. *Pakistan Armed Forces Medical Journal* 57, 194-200.
- Singh, G., Kapoor, I.P.S., Singh, P., 2011. Effect of volatile oil and oleoresin of anise on the shelf life of yogurt. *Journal of Food Processing and Preservation* 35, 778-783.
- Snyder, A.B., Churey, J.J., Worobo, R.W., 2016. Characterization and control of *Mucor circinelloides* spoilage in yogurt. *International Journal of Food Microbiology* 228, 14-21.
- Srisa, A., Harnkarnsujarit, N., 2020. Antifungal films from trans-cinnamaldehyde incorporated poly(lactic acid) and poly(butylene adipate-co-terephthalate) for bread packaging. *Food Chemistry* 333, 127537.
- Su, S., Duhme, M., Kopitzky, R., 2020. Uncompatibilized PBAT/PLA Blends: Manufacturability, Miscibility and Properties. *Materials (Basel)* 13, 4897.

- Suresh Kumar, R., Shiny, P., Anjali, C., Jerobin, J., Goshen, K.M., Magdassi, S., Mukherjee, A., Chandrasekaran, N., 2013. Distinctive effects of nano-sized permethrin in the environment. *Environmental Science and Pollution Research* 20, 2593-2602.
- Swanson, K., 2011. International Commission on Microbiological Specifications for Foods (ICMSF). *Milk and Dairy Products* 2, 305-327.
- Tardugno, R., Serio, A., Pellati, F., D'Amato, S., Chaves López, C., Bellardi, M.G., Di Vito, M., Savini, V., Paparella, A., Benvenuti, S., 2019. *Lavandula x intermedia* and *Lavandula angustifolia* essential oils: phytochemical composition and antimicrobial activity against foodborne pathogens. *Natural product research* 33, 3330-3335.
- Tawakkal, I.S.M.A., Cran, M.J., Bigger, S.W., 2016. Release of thymol from poly(lactic acid)-based antimicrobial films containing kenaf fibres as natural filler. *LWT - Food Science and Technology* 66, 629-637.
- Tunçbilek, A., 1995. Effect of ⁶⁰Co gamma radiation on the rice weevil, *Sitophilus oryzae* (L.). *Anzeiger für Schädlingskunde, Pflanzenschutz, Umweltschutz* 68, 37-38.
- Turgis, M., Vu, K.D., Dupont, C., Lacroix, M., 2012. Combined antimicrobial effect of essential oils and bacteriocins against foodborne pathogens and food spoilage bacteria. *Food Research International* 48, 696-702.
- Vazquez, B.I., Fente, C., Franco, C., Vazquez, M., Cepeda, A., 2001. Inhibitory effects of eugenol and thymol on *Penicillium citrinum* strains in culture media and cheese. *International Journal of Food Microbiology* 67, 157-163.
- Viljoen, B.C., Lourens-Hattingh, A., Ikalafeng, B., Peter, G., 2003. Temperature abuse initiating yeast growth in yoghurt. *Food Research International* 36, 193-197.
- Vishwakarma, G.S., Gautam, N., Babu, J.N., Mittal, S., Jaitak, V., 2016. Polymeric encapsulates of essential oils and their constituents: A review of preparation techniques, characterization, and sustainable release mechanisms. *Polymer Reviews* 56, 668-701.
- Wang, L.-F., Rhim, J.-W., Hong, S.-I., 2016. Preparation of poly(lactide)/poly(butylene adipate-co-terephthalate) blend films using a solvent casting method and their food packaging application. *LWT - Food Science and Technology* 68, 454-461.
- Weisany, W., Amini, J., Samadi, S., Hossaini, S., Yousefi, S., Struik, P.C., 2019. Nano silver-encapsulation of *Thymus daenensis* and *Anethum graveolens* essential oils enhances antifungal potential against strawberry anthracnose. *Industrial Crops and Products* 141, 111808.
- Yangilar, F., Yildiz, P.O., 2018. Effects of using combined essential oils on quality parameters of bio-yogurt. *Journal of Food Processing and Preservation* 42, 13332.

Chapter 9

Evaluation of bioactive low-density polyethylene (LDPE) nanocomposite films in combined treatment with irradiation on strawberry shelf-life extension

This article has been published in *Journal of Food Science*, 2023, 1-21, Impact factor: 3.167, h-index: 160, Overall Ranking: 7454, SCImago Journal Rank: 0.653

<https://doi.org/10.1111/1750-3841.16551>

Tofa Begum¹, Peter A. Follett², Shiv Shankar¹, Lana Moskovchenko³, Stephane Salmieri¹, Monique Lacroix^{1,*}

¹INRS-Armand Frappier Health Biotechnology Research Centre, Research Laboratories in Sciences, Applied to Food (RESALA), MAPAQ Research Chair in food safety and quality, Canadian Irradiation Center (CIC), Institute of Nutrition and Functional Foods (INAF), 531 des Prairies Blvd, Laval, QC, H7V 1B7, Canada

²United States Department of Agriculture, Agricultural Research Service, U.S. Pacific Basin Agricultural Research Center, 64 Nowelo Street, Hilo, HI 96720, USA

³NanoBrand (www.nanobrand.com), 230 Rue Bernard Belleau, Laval, Quebec, Canada, H7V 4A9

*Corresponding author: Monique Lacroix, Ph.D., Email: Monique.Lacroix@inrs.ca

Tel: 450-687-5010 # 4489, Fax: 450-686-5501

Contribution of authors

Tofa Begum conducted the data curation, methodology, writing - original drafts, writing - review, and editing. Monique Lacroix and Peter A. Follett designed the methodology, conceptualization, supervision, and software. Stephane Salmieri, Lana Moskovchenko, and Shiv Shankar assisted with methodology, reviewing the methodology, editing the manuscript.

Résumé

Un film de polyéthylène basse densité (LDPE) renforcé de nanocristaux de cellulose (CNC) avec une formulation bioactive encapsulée (huile essentielle de cannelle + nanoparticules d'argent) a été développé pour la conservation des fraises fraîches. L'activité antimicrobienne des films de LDPE actifs a été testée contre *Escherichia coli* O157:H7, *Salmonella typhimurium*, *Aspergillus niger* et *Penicillium chrysogenum* par un test de volatilisation sur gélose. L'état optimal des films a montré une capacité inhibitrice $\geq 75\%$ contre les microbes testés. Les fraises ont été stockées avec différents types de films: Groupe 1 (témoin) : (LDPE + CNC + Glycérol), Groupe 2 : (LDPE + CNC + Glycérol + AGPPH nanoparticules d'argent), Groupe 3 : (LDPE + CNC + Glycérol + cannelle) , Groupe 4 : (PEBD + CNC + Glycérol + formulation active) et Groupe 5 : (PEBD + CNC + Glycérol + formulation active + 0,5 kGy de rayonnement γ) à 4 °C pendant 12 jours. La perte de poids (WL) (%), la décomposition (%), la fermeté (N), la couleur et la teneur totale en composés phénoliques et en anthocyanes des fraises ont été mesurées. Les résultats ont montré que le film LDPE-nanocomposite le plus efficace pour réduire la croissance microbienne était le film LDPE + CNC + Glycérol + formulation active (Groupe 4). Lorsqu'elle est combinée avec l'irradiation γ (0,5 kGy), la formulation LDPE + CNC + Glycérol + active (Groupe 5) a réduit de manière significative à la fois la décomposition et la WL de 94 %, par rapport aux échantillons témoins après 12 jours de stockage. Les teneurs en phénols totaux (de 952 à 1711 mg/kg) et en anthocyanes (de 185 à 287 mg/kg) ont augmenté avec la durée de stockage sous les différents traitements. Les propriétés mécaniques, la perméabilité à la vapeur d'eau (WVP) et la couleur de surface des films ont également été testées. Bien que la WVP des films n'ait pas été influencée par les types d'agents antimicrobiens, ils ont modifié de manière significative ($p \leq 0,05$) la couleur et les propriétés mécaniques des films. Par conséquent, le traitement combiné du film actif et de l'irradiation γ a un potentiel en tant que méthode alternative pour prolonger la durée de conservation des fraises de stockage tout en maintenant la qualité des fruits.

Application pratique

Un film nanocomposite bioactif en polyéthylène basse densité (LDPE) a été développé dans l'étude en incorporant une formulation active (huile essentielle et nanoparticule d'argent) pour prolonger la durée de conservation des fraises stockées. Le film nanocomposite bioactif à base de LDPE ainsi que l'irradiation γ pourraient être utilisés pour conserver les fruits pour un stockage à long terme en contrôlant la croissance des bactéries pathogènes d'origine alimentaire et des champignons de détérioration.

Mots-clés: emballage actif; bactéries; champignons; traitement par irradiation; durée de conservation; fraise

Abstract

A low-density polyethylene (LDPE) film reinforced with cellulose nanocrystals (CNCs) with an encapsulated bioactive formulation (cinnamon essential oil + silver nanoparticles) was developed for preservation of fresh strawberries. Antimicrobial activity of the active LDPE films was tested against *Escherichia coli* O157:H7, *Salmonella typhimurium*, *Aspergillus niger*, and *Penicillium chrysogenum* by agar volatilization assay. The optimal condition of the films showed $\geq 75\%$ inhibitory capacity against the tested microbes. Strawberries were stored with different types of films: Group 1 (control): (LDPE + CNCs + Glycerol), Group 2: (LDPE + CNCs + Glycerol + AGPPH silver nanoparticles), Group 3: (LDPE + CNCs + Glycerol + cinnamon), Group 4: (LDPE + CNCs + Glycerol + active formulation), and Group 5: (LDPE + CNCs + Glycerol + active formulation + 0.5 kGy γ -radiation) at 4 °C for 12 days. Weight loss (WL) (%), decay (%), firmness (N), color, and total phenolics and anthocyanin content of the strawberries were measured. Results showed that the most effective LDPE-nanocomposite film for reducing the microbial growth was LDPE + CNCs + Glycerol + active formulation film (Group 4). When combined with γ -irradiation (0.5 kGy), the LDPE + CNCs + Glycerol + active formulation (Group 5) significantly reduced both decay and WL by 94 %, as compared to the control samples after 12 days of storage. Total phenols (from 952 to 1711 mg/kg) and anthocyanins content (from 185 to 287 mg/kg) increased with storage time under the different treatments. The mechanical properties, water vapor permeability (WVP), and surface color of the films were also tested. Though the WVP of the films were not influenced by the types of antimicrobial agents, they did significantly ($p \leq 0.05$) change color and mechanical properties of the films. Therefore, combined treatment of active film and γ -irradiation has potential as an alternative method for extending the shelf-life of storage strawberries while maintaining fruit quality.

Practical Application

Bioactive Low-density polyethylene (LDPE) nanocomposite film was developed in the study by incorporating active formulation (essential oil and silver nanoparticle) to extend the shelf life of stored strawberries. The bioactive LDPE-based nanocomposite film along with γ -irradiation could be used to preserve fruits for long-term storage by controlling the growth of foodborne pathogenic bacteria and spoilage fungi.

Keywords: active packaging; bacteria; fungi; irradiation treatment; shelf-life; strawberry

9.1. Introduction

Strawberry, *Fragaria ananassa* (Rosaceae), is a highly perishable fruit with a limited shelf-life with a rapid moisture loss, a susceptibility to physical and mechanical injury, and sensitivity to bacterial and fungal infections (Treviño-Garza *et al.*, 2015; Zhang *et al.*, 2018). Losses of strawberries due to microbial decay can be >40 % annually, and fruit may also become contaminated with food-borne illness organisms. The main microorganisms responsible of the strawberries spoilage and food safety concerns are fungi (*Botrytis cinerea*, *Penicillium* sp., *Aspergillus* sp., *Rhizopus* sp., *Mucor* sp.), bacteria (*Escherichia coli*, *Salmonella* sp., *Pseudomonas* sp., *Bacillus* sp., *Enterobacter* sp., *Arthrobacter* sp.) and viruses (Norovirus, Hepatitis A virus) (Lafarga *et al.*, 2019). In 2011, an *E. coli* O157:H7 outbreak occurred in strawberries in the United States and 15 people were hospitalized including two deaths (Laidler *et al.*, 2013). Delbeke *et al.* (2014) showed that *E. coli* O157:H7 and *Salmonella* sp. can survive on the surface of strawberries during one week of storage at room temperature and refrigerated conditions.

Control of postharvest losses in strawberries depends on cool storage, limiting moisture loss, and the packaging systems. Usually, cooling immediately after harvesting and then storing at 0-4 °C can extend the shelf life of strawberries for a maximum of five days without any packaging treatment (Han, 2014; Shankar *et al.*, 2021). Other methods such as irradiation treatment (UV-C or γ -radiation) and chemical treatments are used to reduce fruit decay (Sallato *et al.*, 2007). Majeed *et al.* (2014) demonstrated that treatment with γ -irradiation at 1 and 1.5 kGy extended the shelf life of strawberries on an average to 5.75 and 7.75 days, respectively, whereas the shelf life of non-irradiated fruits averaged 3.25 days. The International Atomic Energy Agency (IAEA) recommends treatment up to 2 kGy for the disinfection of strawberries at low temperatures (0-5 °C) (WHO, 1994).

The use of bioactive films are innovative technologies that reduce microbial growth and moisture loss (Vu *et al.*, 2011). Low-density polyethylene (LDPE) is a material widely used for food packaging and storage to prevent moisture loss and extend shelf-life. The production of LDPE films with active ingredients and other biodegradable polymers is an innovative way to preserve foods (Li *et al.*, 2020; Radfar *et al.*, 2020). Bioactive packaging involves the incorporation of controlled-release bioactive or functional substances within the walls of the packaging to prevent microbial decay. Cellulose nanocrystals (CNCs) are potential nanofillers extracted from plants, bacteria, and algae that can improve the mechanical and barrier properties of LDPE films and provide a better-controlled release of active ingredients (Salmieri *et al.*, 2014a; Hossain *et al.*, 2018; Hossain *et al.*, 2019a).

Many plant-derived essential oils (EOs) have strong antibacterial, antifungal, insecticidal, and antiviral properties. EOs contain secondary metabolites of plants and a mixture of volatile bioactive components (e.g., monoterpenes, phenolic compounds) (Turgis *et al.*, 2012; Hossain *et al.*, 2016a). The incorporation of EOs into polymeric matrices can make active packaging films that can control foodborne microbes and preserve the quality of storage products (Salmieri and Lacroix, 2006). For example, *Cinnamomum verum* (cinnamon EO), which contains predominantly cinnamaldehyde (73 %), has strong bioactivity because it can covalently link with bacterial DNA and proteins via amine groups, thus interrupting their function and causing microbial cell death (Hyldgaard *et al.*, 2012a); also, cinnamon EO can significantly induce the depletion of intracellular pH and ATP concentration of the bacterial cell and increase the release of cellular constituents (Oussalah *et al.*, 2006). EOs including cinnamon encapsulated in silver nanoparticles (AgNPs) have been shown to act synergistically in controlling fungal growth in strawberries (Weisany *et al.*, 2019). AgNP is a novel category of antibacterial and antifungal agents which is widely used in the pharmaceutical and food industries (Ghosh *et al.*, 2013a; Weisany *et al.*, 2019). Ionizing radiation is another technology for reducing foodborne pathogens and spoilage fungi in food (Maherani *et al.*, 2016). Combining active LDPE films with ionizing radiation could lead to synergistic effects which may allow a reduction in the concentration of active compounds and irradiation dose compared with a single treatment (Lacroix and Follett, 2015). The objectives of the present study were to (1) Optimize the antibacterial and antifungal LDPE+CNCs nanocomposite films containing active formulation (EOs+AgNPs) and glycerol, (2) study the effect of strawberries preservation when packed in the presence of active LDPE+CNCs films combined with irradiation, and (3) evaluate some physicochemical properties of the films and the fruits packed with the bioactive film and treated with γ -irradiation during post-treatment cold storage.

9.2. Materials and methods

9.2.1. Materials

A film-grade low-density polyethylene (LDPE) (LDPE2427) was purchased from Hanwha Chemical Co. (Seoul, South Korea) with a density of 0.924 g/cm³, melt flow index (MFI) of 4.0 g/10 min, and a melting point of 111 °C. Cellulose nanocrystals (CNCs) (100×5 nm) were provided by FP Innovations (Pointe-Claire, Quebec, Canada). The cinnamon essential oil (EO) was purchased from Zayat Aroma (Bromont, QC, Canada). Silver nanoparticles (AgNPs) containing sample “AGPPH” (a mixture of two fractions of nanospheres: the larger one contains the nanoparticles of 20-35 nm and the smaller one contains the nanoparticles of 3-7 nm) was provided by NanoBrand

(www.nanobrand.com) (Bernard-Belleau, Laval, Quebec, Canada). Folin-Ciocalteu reagent, sodium carbonate monohydrate, gallic acid, and glycerol were procured from Sigma-Aldrich Ltd. (St. Louis, Missouri, United States). The nutrient media for fungal culture was potato dextrose broth (PDB) and for bacterial culture was tryptic soy broth (TSB) purchased from Alpha Biosciences Inc. (Baltimore, MD, USA).

9.2.2. Preparation of active LDPE films

All ingredients, including 2 g of LDPE granules, CNCs (wt % of polymer), glycerol (wt % of polymer) and active formulation (cinnamon EO:AGPPH = 6:0.1) (wt % of polymer), were mixed at different concentrations, and the blended formulations are shown in Table 9.1. The film formulation blends were hot-pressed by a compression molding machine (Carver Inc., Indiana, USA, Model-3912) to prepare the desired active nanocomposite films. The active formulation (cinnamon EO:AGPPH = 6:0.1) was selected based on our previous antibacterial and antifungal tests ([Begum et al., 2022a](#)).

Table 9.1. Experimental design using central composite design (CCD) for developing active LDPE films.

Number of formulation blends	LDPE (g)	Active formulation (μL)	CNCs (% wt)	Glycerol (% wt)
1	2	200	0.375	0.625
2	2	300	0.75	1
3	2	200	0.75	0.625
4	2	200	0.375	0.625
5	2	100	0.375	0.625
6	2	200	0.375	0.25
7	2	300	0	1
8	2	200	0	0.625
9	2	300	0.75	0.25
10	2	200	0.375	0.625
11	2	100	0.75	1
12	2	200	0.375	1
13	2	300	0	0.25
14	2	100	0.75	0.25
15	2	100	0	0.25
16	2	300	0.375	0.625
17	2	100	0	1

9.2.3. Optimisation of the active ingredients in LDPE films

To obtain the best antibacterial and antifungal properties of the active LDPE films, the levels and proportions of all ingredients (independent variables) were determined by central composite design (CCD) using Design-Expert software (version 11, Stat-Ease, Inc.) (Radfar *et al.*, 2020; Begum *et al.*, 2022b). A total of 17 experimental runs were performed with three replications each (Table 9.1). A list of film components with their maximum and minimum levels which were used in the experimental CCD are shown in Table 9.2. The antibacterial and antifungal properties of the LDPE films for each run against two pathogenic bacteria (*E. coli* O157:H7 NT 1931 and *S. typhimurium* SL 1344) and two spoilage fungi (*A. niger* ATCC 1015 and *P. chrysogenum* ATCC 10106) were tested as dependent variables (Table 9.3).

Table 9.2. Film ingredients and their constraints for the central composite design.

Symbol	Film ingredient	Units	Low actual	High actual
A	Active formulation	μL	100	300
B	CNCs	%	0	0.75
C	Glycerol	%	0.25	1.0

9.2.4. *In vitro* antibacterial and antifungal properties of the films

An inverted lid agar volatilization test was performed to measure the antibacterial and antifungal properties of the active LDPE films (Cardiet *et al.*, 2012; Hossain *et al.*, 2019a; Begum *et al.*, 2022a). Briefly, the bacterial and fungal species (approximately 10⁵ CFU/mL or 10⁵ spores/mL) were inoculated on the surface of nutrient media (TSA for bacteria and PDA for fungi). The plates were inverted and 1 cm² of the film pieces were placed in the middle of the lid of the Petri plates. All plates were sealed with Parafilm® to prevent vapor escape and incubated at 37 °C for 24 h for bacteria (27 °C for 48 h for fungi). The antibacterial and antifungal properties of the films were measured as inhibitory capacity (IC, %) following Eq 9.1.

Inhibitory capacity (%), IC) = $D_i/D_p \times 100$ Eq. 9.1

Where, D_i = Diameter of the inhibition zone (mm); D_p = diameter of the petri plate (mm).

9.2.5. Optimization of the active ingredients in LDPE films

Each independent variable was fitted into the design expert software to obtain the final film with the highest antibacterial and antifungal properties, and each of the measured independent variables was fitted into linear and quadratic models in Eq. 9.2 and Eq. 9.3.

$$Y = B_0 + \sum_{i=1}^q B_i X_i + \sum_{i=1}^q B_j X_j \quad \text{Eq. 9.2}$$

$$Y = B_0 + \sum_{i=1}^q B_i X_i + \sum_{1 \leq i < j}^q B_{ij} X_i X_j + \sum_{1 \leq i < j < k}^q B_{ijk} X_i X_j X_k \quad \text{Eq. 9.3}$$

Where, Y = dependent variables (Inhibitory Capacity [IC] against each bacterium and fungus); B₀ = constant-coefficient; B_i = linear coefficient; B_{ij} = interactive coefficient; X₁...X_j...X_k = independent variables; q = number of variables. The experiments were performed three times. The models' level of significance was assessed by the analysis of the variance (ANOVA) with alpha = 0.05 (Falleh *et al.*, 2019; Begum *et al.*, 2022b).

9.2.6. *In vitro* release profiles of the active formulation from the active film

The cumulative release of the active formulation (cinnamon EO + AGPPH) from the active LDPE-based nanocomposite film (LDPE + CNCs + Glycerol + active formulation) was tested in 10 % (v/v) ethanol media as food simulants for fruits and vegetables with different contact times (Hossain *et al.*, 2018; Ben-Fadhel *et al.*, 2020; Felix da Silva Barbosa *et al.*, 2021). Briefly, a 500 mg of active LDPE-nanocomposite film was kept in a volume of 200 mL of food simulant (ethanol) under constant magnetic stirring at room for 36 h of extraction time. A volume of 1 mL extracted sample was collected each hour until reach equilibrium and each time 1 mL of fresh ethanol was added to the film + food simulant bath for respecting same volume. Then, the extracted sample was analysed using a UV-Vis spectrophotometer for calculating the cumulative release (%) of active formulation from the films as following Eq 9.4.

$$\text{Cumulative release (\%)} = \frac{\text{Volume of sample withdraw}}{\text{Bath volume}} \times P(t-1) + P_t \quad \text{Eq 9.4}$$

Where, P_t is released (% w/v) at time t; P_(t-1) is released (% w/v) at a time previous to "t". All experiments were performed in triplicate. The blank sample was considered the respective film without active formulation in the liquid phase.

9.2.7. *In situ* application of the active LDPE films for strawberry preservation

Methods followed those described in Shankar *et al.* (2021) with some modifications. Strawberry fruits (L'île d'Orleans Inc.) were purchased from Walmart (Laval, Quebec, Canada) and the test fruits were undamaged and selected for similar size and color. Fruits were soaked in sodium

hypochlorite (NaClO) (1 %, v/v) for 1 min, then rinsed with distilled water and dried on sterile aluminium foil for 2 h at room temperature. The strawberries were categorized into five groups: (1) Group-1/Control: strawberries were packaged in clamshells with LDPE nanocomposite films (LDPE + CNCs + Glycerol), (2) Group-2: strawberries with active LDPE + CNCs + Glycerol + AGPPH nanocomposite film, (3) Group-3: strawberries with active LDPE + CNCs + Glycerol + cinnamon EO nanocomposite film, (4) Group-4: strawberries with LDPE + CNCs + Glycerol + active formulation (AGPPH + cinnamon EO) film and (5) Group-5: strawberries with LDPE + CNCs + Glycerol + active formulation + 500 Gy γ -irradiation. For each group, approximately 300 g of fruits (25-30 fruits) were placed into a polyethylene terephthalate (PET) clamshell box (15 × 20 × 10 cm) with a hole at the lid and bottom for air exchange. The digital image of LDPE films from each group is presented in Figure 9.2. The γ -irradiation was performed using an underwater calibrator UC-15A equipped with Cobalt-60 (Nordion, Laval, Quebec, Canada) having a dose rate of 7.1 kGy/h (Dosimeter: Alanine Pellet Dosimeter, mass 66.0±0.5 mg, Far West Technology and Harwell Gammachrome YR® Perspex Dosimeter [range 0.1–3.0 kGy]; temperature: 25 °C).

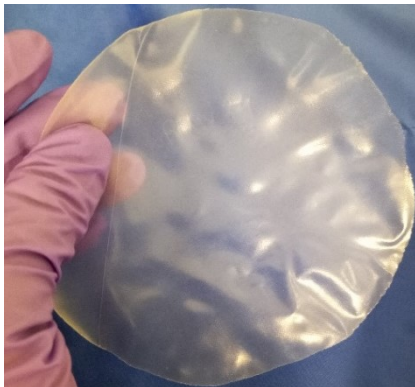
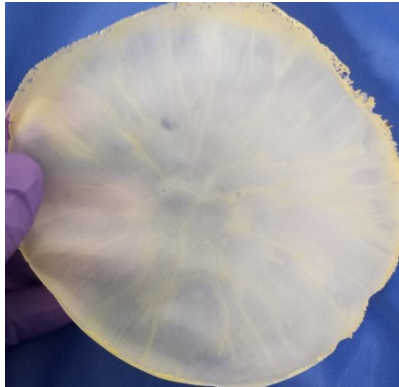
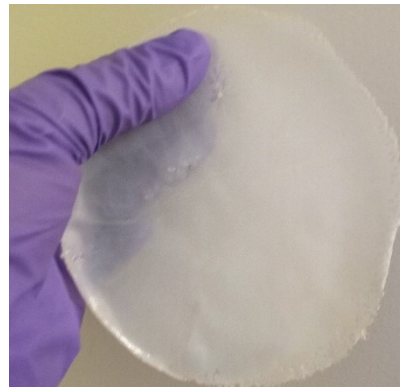
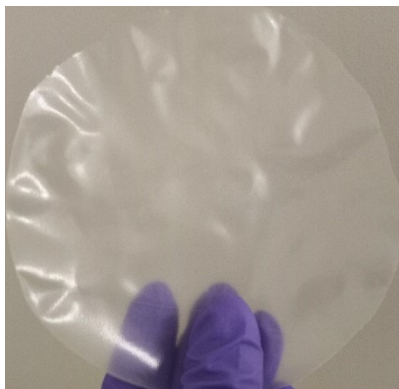
Control (Group-1)**(Group-2)****(Group-3)****(Group-4)****(Group-5)**

Figure 9.2. Digital images of the nanocomposite LDPE film from different Groups. Group-1: LDPE + CNCs + Glycerol (Control); Group-2: LDPE + CNCs + Glycerol + AGPPH; Group-3: LDPE + CNCs + Glycerol + cinnamon EO; Group-4: LDPE + CNCs + Glycerol + active formulation (AGPPH + cinnamon EO); and Group-5: LDPE + CNCs + Glycerol + active formulation + γ -irradiation. LDPE nanocomposite film composed of LDPE polymer (2 g), CNCs (0.375 %), glycerol (0.625 %).

The active nanocomposite film was also placed at a different position inside the PET clamshell to evaluate the effect of film position, shown schematically in Figure 3. The film positions were named as film position-1, film position-2, and film position-3. Briefly, film position-1: a 1.5 piece bioactive nanocomposite film was placed on the bottom and a 1.5 piece film was attached to the inner surface of the lid of the clamshell; film position-2: three films (9 cm diameter) were kept only on the bottom; and film position-3: three films (9 cm diameter) were attached at the inner surface of the lid, and fruits were stored at 4 °C for 12 days (Figure 9.3). The film position effect on the weight loss (%), decay (%), and the color of stored fruits was tested (Supplementary data Table 9.2, 9.4 and 9.5, respectively). All experiments were performed in triplicate.

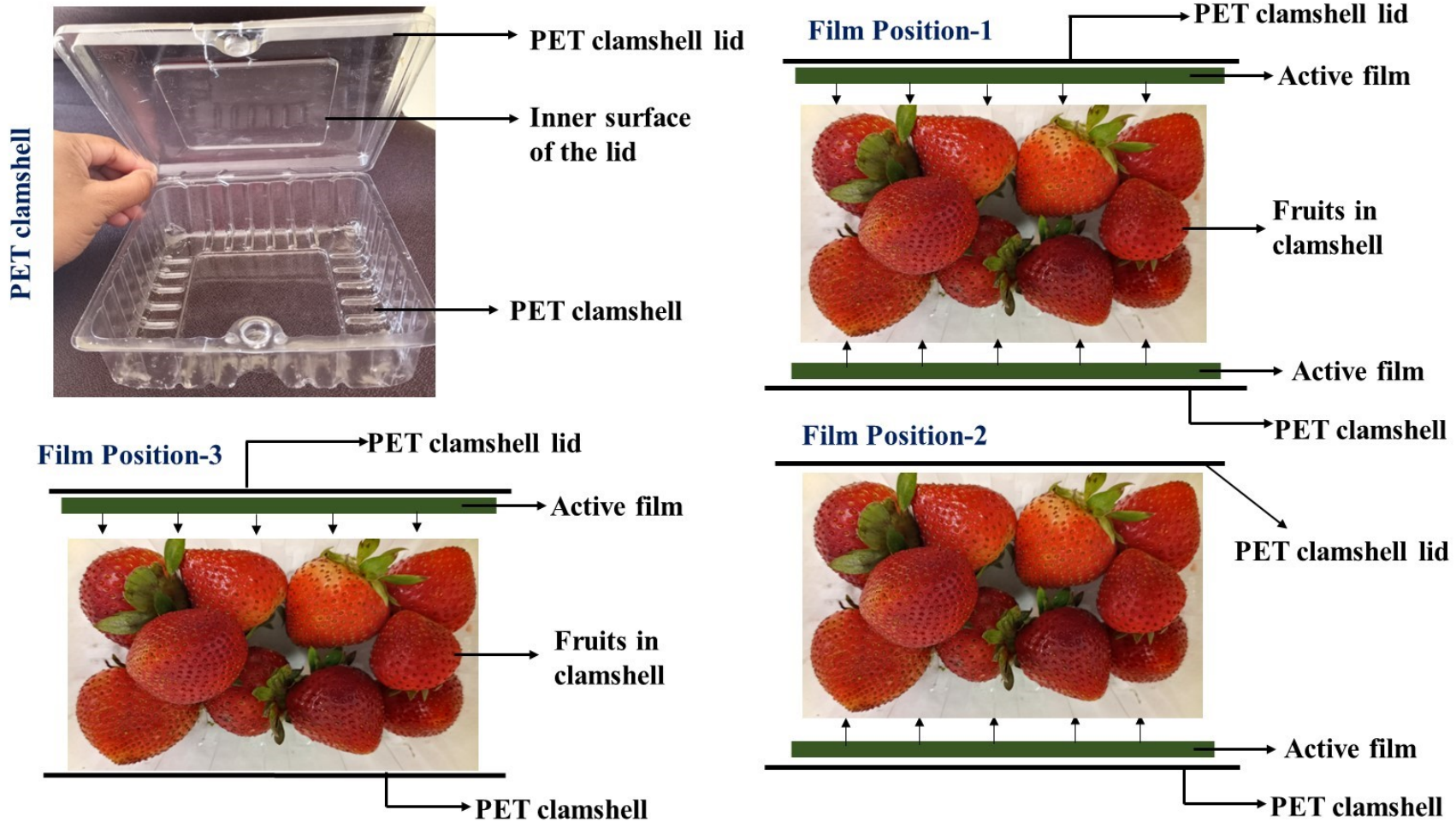


Figure 9.3. A schematic diagram of the film position-1, position-2, and position-3 inside the PET clamshell during strawberry preservation.

9.2.8. Physicochemical characterization of the packaged strawberries

The physicochemical analyses such as weight loss (%), decay (%), the surface color of the strawberries, the firmness, the total soluble solids (TSS), the total phenols, and the total anthocyanins content of the strawberries during storage were measured at a different time intervals (days 0, 1, 2, 5, 7, 9 and 12).

9.2.8.1. Weight loss and decay (%) of the packaged strawberries

The weight loss (%) of strawberries during storage was measured by weighing the samples at different time intervals using a digital balance (TE15025, Sartorius, Canada). The percent weight loss of strawberry at different time intervals were determined as follows-

$$\text{Weight loss (\%)} = (W_i - W_t / W_i) \times 100 \text{ Eq. 9.4}$$

Where W_i = initial weight of fruits (g); W_t = weight of fruits at a different time (g).

The percent decay of the fruits during storage was determined by visual checking's such as grey mold growth, any brown spots, soft skin, or any wounded area on the surface of strawberries were considered as decay. The results were expressed as % decay followed by Eq. 9.5.

$$\text{Decay (\%)} = (\text{Number of decay fruit} / \text{Total number of fruit}) \times 100 \text{ Eq. 9.5}$$

9.2.8.2. Surface color of the packaged strawberries

The surface color (L^* , a^* , b^*) and total soluble solids (TSS) of the strawberries were measured at different time intervals (Yoshida *et al.*, 2002). Briefly, a Chroma meter Model CR-400 (Konica Minolta Sensing, Inc., Osaka) was used to measure L^* , a^* , and b^* values on the skin color of fruits. Where, L^* : lightness; a^* : redness ($-a^*$: greenness); b^* : yellowness ($-b^*$: blueness), and a white color plate was used as a standard background for color measurement where lightness (L^*): 97.75, redness (a^*): -0.49 and yellowness (b^*): 1.96 (Shankar *et al.*, 2021). The color was measured using 5 readings for each fruit and from each group, 3 fruits were considered.

9.2.8.3. Firmness and total soluble solid of the packaged strawberries

The firmness of the storage strawberries was analyzed by puncture test (Khodaei and Hamidi-Esfahani, 2019) to determine maximum force needed to penetrate the strawberry by a Texture Analyzer (Texture Technologies Corp., Scarsdale, NY, USA) (Table 9.8). A stainless-steel cylindrical probe with a 2 mm diameter flat head was penetrated 6 mm into each strawberry analysed with 1 mm/s speed. The results were expressed as the peak force in Newton (N), and the experiments were performed for four strawberries in each group.

A 5 mm thick piece of strawberries was cut for total soluble solids (TSS) measurement (Figure 5). The samples were homogenized and filtered through a cheesecloth. Then, the filtrated samples were analyzed for TSS measurement (%) using a hand refractometer (PAL-1, Atago, Japan) at room temperature. The TSS was measured using 5 readings for each fruit and from each group, 3 fruits were considered.

9.2.8.4. Total phenols (TP) and total anthocyanins content measurement

The Folin-Ciocalteu method was used to measure the total phenols (TP) content in strawberries at different storage times (Ben-Fadhel *et al.*, 2020). Briefly, a volume of homogenized sample (1 mL) (filtered through cheesecloth) was added into a test tube containing 6 mL of water, then a 1 mL of Folin-Ciocalteu reagent was added into the mixture, the mixture was stirred well, then held for 6 min. After 6 min, a 2 mL of 20 % (w/v) sodium carbonate monohydrate ($\text{Na}_2\text{CO}_3 \cdot \text{H}_2\text{O}$) was added to the mixture and heated at 40 °C for 20 min in a water bath. The absorbance of the mixture sample and blank (water + reagent) was measured at 760 nm using UV-visible spectrophotometer model Cary-8454 (Agilent Technologies, Santa Clara, CA, USA) and measured the TP using Gallic acid as standard (Caillet and Lacroix, 2006). The results were expressed as Gallic acid equivalent (GAE) in gram/kg of fruit weight (g/kg FW).

Total anthocyanins content in strawberries were measured according to Shankar *et al.* (2021). A volume of 40 mL ethanol containing 1.5 M HCl acid solution was prepared, then added to 5 g of strawberries. After homogenization for 1 min, the mixture was filtered, and the filtrate was transferred into a 100 mL volumetric flask and distilled water added up to 100 mL. The absorbance of the mixture was measured using a spectrophotometer at 535 nm and total anthocyanins content was measured as GAE in g/kg FW.

9.2.9. Characterization of irradiated and non-irradiated LDPE films

The thickness, mechanical, water vapor permeability (WVP), oxygen transmission rate and water solubility (WS) and surface color of the films were evaluated for five types of irradiated and non-irradiated LDPE films to evaluate the effect of the active agents (either AGPPH or cinnamon EO alone or in combination) on the prepared films used in the strawberry preservation experiments. The five types of films were named Group 1-5 as previously mentioned in section 2.3 for each active agent treatment.

9.2.9.1. Thickness and mechanical properties of the LDPE films

The thickness and mechanical properties (tensile strength-TS and elongation at break-Eb) of the LDPE films for each group (Groups 1-5), were measured ([Salmieri *et al.*, 2014a](#)). In studying polymeric films, the TS and Eb measurements are important factors because those values indicate the film's ability to retain integrity under different stress conditions. Briefly, the thickness of the film was measured at five random positions using a Mitutoyo Digimatic Indicator Model ID-110E with a resolution of 1 μm ; (Mitutoyo MFG Co. Ltd, Tokyo, Japan) and the width of the film was measured via a Traceable Carbon Fiber Digital Caliper (Fisher Scientific). A Universal Testing Machine Model-H5KT (Tinius Olsen Testing Machine Co., Inc., Horsham, PA, USA) equipped with a 100 N-load cell and 1.5 kN-specimen grips was used for measuring the mechanical properties of the films ([ASTM, 1995](#)). The position of the machine was controlled as initial grip separation: 30 mm, crosshead speed: 50 mm/min, and a load cell: 100 N. Five measurements were carried out for each film, and average values were presented with standard error.

9.2.9.2. Oxygen permeability rate (OTR) of the LDPE films

The oxygen transmission rate (OTR) of the film from each Group was measured using an OX-TRAN Model 1/50 (Minneapolis, MN, USA) machine following the method adopted by [Criado *et al.* \(2020\)](#) and [Kang *et al.* \(2021\)](#). Briefly, a 5 cm^2 film area was adjusted to an aluminum foil mask, and a test was performed at 0 % relative humidity at 23 °C. Prior to the experiment, the thickness of each film was measured at five random points using a Mitutoyo micrometer (BDI Canada Inc., Laval, QC, Canada). The measured thickness was each film between 91-110 μm . The results were expressed as $\text{cm}^3 \cdot \text{m}^{-2} \cdot \text{day}^{-1}$. The test cells were divided into two chambers separated by the film samples and the gas (N_2 and O_2) pressure ranges were stabilized at 33 PSIG. An oxy-dot sensor measured the O_2 absorption over time at 20 min intervals to get OTR for 24 h. The tests were performed in triplicate for each film.

9.2.9.3. Water vapor permeability (WVP) of the LDPE films

The WVP tests of the films from each Group were performed [Hossain *et al.* \(2018\)](#). Films were sealed onto Vapometer cells (model 68-1; Twining-Albert Instrument Co., West Berlin, NJ, USA) with 30 g of anhydrous CaCl_2 . The initial weight of the cell was recorded and kept in a controlled humidity chamber (Shellab-9010L, Sheldon Manufacturing Inc., Cornelius, OR, USA) at 25 °C and 60 % relative humidity (RH) for 24 h. After 24 h, the weight of the Vapometer cell was recorded again. The weight gained after 24 h indicated the amount of H_2O vapor absorbed by anhydrous CaCl_2 through the LDPE films which were calculated using the following equation.

$$\text{WVP (g mm m}^{-2}\text{day}^{-1}\text{kPa}^{-1}) = \Delta w \cdot x / A \cdot \Delta P \text{ Eq. 9.6}$$

Where Δw = Vapometer cell weight (g) gain after 24 h; x = Film thickness (mm); A = Area of exposed film ($31.67 \times 10^{-4} \text{ m}^2$); ΔP = Differential vapor pressure of water through the film ($\Delta P = 3.282 \text{ kPa}$ at $25 \text{ }^\circ\text{C}$).

9.2.9.4. Water solubility (WS) of the LDPE films

Water solubility (WS) of the LDPE-based nanocomposite films were tested for measuring the water-resistant property of the films followed by [Khan et al. \(2014\)](#). Briefly, a 1.5 cm^2 film was cut and dried for 24 h at $105 \text{ }^\circ\text{C}$ to get the initial weight (W_i) of the dried film. Afterwards, the dried film was dipped in a volume for 100 mL water and left it for 24 h at room temperature in undisturbed condition. After 24 h, the film was taken from the water and dried for another 24 h at $105 \text{ }^\circ\text{C}$, and then, determined the final weight (W_f) of the film. The WS of the film was then calculated by the following equation:

$$\text{Water solubility (WS)} = \frac{(W_i - W_f)}{W_f} \times 100 \text{ Eq. 9.7}$$

Where W_i = initial weight of the film and W_f = final weight of the film.

9.2.9.5. Color properties of the LDPE films

Color (L^* , a^* , and b^*) of the film was measured using a Chroma meter Model CR-400 (Konica Minolta Sensing, Inc., Osaka). The L^* (lightness), a^* (redness) and b^* (yellowness) values were calculated using the average values from five readings for each film. The ΔL^* , Δa^* , and Δb^* values were calculated from a difference between the standard color plate value ($L^* = 97.75$, $a^* = -0.49$, and $b^* = 1.96$) and film color value ([Shankar et al., 2014](#)). The color difference (ΔE) of the film was measured using the following Eq. 9.8.

$$\text{Color difference } (\Delta E) = [(\Delta L^*)^2 + (\Delta a^*)^2 + (\Delta b^*)^2]^{0.5} \text{ Eq. 9.8}$$

9.2.10. Statistical analyses

All experiments were performed in triplicate and values were presented as mean \pm standard error. All data were analyzed by one-way analysis of variance (ANOVA) and for significant effects means separations were performed using Duncan's multiple range test ($\alpha = 0.05$) via SPSS software (SPSS Inc., Chicago, IL, USA).

9.3. Results and discussions

9.3.1. Optimization of active LDPE/CNCs nanocomposite film

The result of antibacterial and antifungal properties against *E. coli* O157:H7, *S. typhimurium*, *A. niger*, and *P. chrysogenum* of the LDPE films are shown in Table 9.3. The ANOVA analyses of the central composite design (CCD) for each response are presented in Table 9.4. The film ingredients and their constraints for CCD are shown in Table 9.2. ANOVA analyses and statistical models obtained from experimental design were described and predicted the effect of independent variables (cellulose nanocrystal [CNCs], active formulation [cinnamon EO+AGPPH], and plasticizer [glycerol]) on antimicrobial properties of films by measuring inhibitory capacity (IC, %). A linear and quadratic model was significant for *E. coli* O157:H7 and *S. typhimurium*, respectively (Table 9.4). The F-values for *E. coli* O157:H7 and *S. typhimurium* were 83.47 ($P \leq 0.0001$) and 74.59 ($P \leq 0.0001$; $df = 3$), respectively, which showed the model was statistically significant ($P \leq 0.05$; $df = 9$). The higher R^2 values (coefficient of determination) for *E. coli* O157:H7 and *S. typhimurium* were 94 and 99 %, respectively, indicating that corresponding linear and quadratic models have a good agreement between the experimental and the predicted values. A quadratic model was significant for spoilage fungi *A. niger* and *P. chrysogenum* having the respected F-values were 23.07 ($P = 0.0002$; $df = 9$) and 29.89 ($P \leq 0.0001$; $df = 9$) (Table 9.4). There was a good agreement between the experimental and predictive values which was proved by getting higher R^2 values (coefficient of determination) of the quadratic model for *A. niger* (97 %) and *P. chrysogenum* (97 %). The mathematical models for representing dependent variables (responses) were expressed as inhibitory capacity (IC, %) against two foodborne pathogenic bacteria (*E. coli* O157:H7 and *S. typhimurium*) and two spoilage fungi (*A. niger* and *P. chrysogenum*) responsible for strawberries contamination and spoilage in the terms of three independent variables (A: active formulation, B: CNCs and C: Glycerol) is as follows equation 9.9, 9.10, 9.11 and 9.12, respectively:

$$E. coli \text{ O157:H7 (IC, \%)} = + 54.8 + 14.6A + 0.6B - 0.2C \text{ Eq. 9.9}$$

$$S. typhimurium \text{ (IC, \%)} = + 55.15 + 14.5A + 0.0B - 0.7C + 0.0AB - 2.25AC - 0.25BC + 2.98A^2 - 3.52B^2 - 0.021C^2 \text{ Eq. 9.10}$$

$$A. niger \text{ (IC, \%)} = + 61.45 + 13.5A + 3.6B + 1.2C + 1.12AB - 1.88AC + 0.62BC - 1.29A^2 - 4.79B^2 - 1.79C^2 \text{ Eq. 9.11}$$

$$P. chrysogenum \text{ (IC, \%)} = + 66.21 + 16.5A + 2.9B + 0.0C + 1.88AB - 3.63AC + 1.62BC - 0.21A^2 - 5.12B^2 - 2.62C^2 \text{ Eq. 9.12}$$

The mixture of LDPE (2 g), CNCs (0.375 % wt), active formulation (cinnamon EO+AGPPH) (300 μ L), and glycerol (0.625 % wt) (Formulation blend number 16) showed the highest antibacterial

and antifungal properties among seventeen blended formulations (Table 9.3). The LDPE films containing 300 µL of active formulation, 0.375 % of CNCs, and 0.625 % of glycerol showed the significantly highest ($P \leq 0.05$) inhibitory capacity of *E. coli* O157:H7, *S. typhimurium*, *A. niger*, and *P. chrysogenum*, and their IC values were 75, 75, 78 and 84 %, respectively. It has been found that the higher the concentration of active formulation, the higher the inhibitory capacity (Table 9.3). However, the addition of CNCs and glycerol improved significantly the microbicidal effectiveness. For example, in formulation blend number 7 (LDPE + 300 µL active formulation + 0 % CNCs + 1 % Glycerol) had significantly lower antibacterial and antifungal effects as compared to formulation blend number 16 (LDPE + 300 µL active formulation + 0.375 % CNC + 0.625 % glycerol) while the IC values were 69, 66, 60, and 64 % for *E. coli* O157:H7, *S. typhimurium*, *A. niger* and *P. chrysogenum* ($P \leq 0.05$). According to the data in Table 9.3, the central composite design optimized (based on the highest microbicidal effectiveness) that the mixture of LDPE, active formulation, CNCs, and glycerol at the corresponded amount of 2 g, 300 µL, 0.375 %, and 0.625 % expressed the highest IC (%) against all tested bacteria and fungi.

Table 9.3. Experimental results of the inhibitory capacity (IC, %) of the active LDPE films against two pathogenic bacteria and two spoilage fungi.

No. formulation blend	Inhibitory capacity (IC, %)			
	<i>E. coli</i> O157:H7	<i>S. Typhimurium</i>	<i>A. niger</i>	<i>P. chrysogenum</i>
1	58±1.2 ^d	56±1.1 ^c	62±5.1 ^g	72±0.3 ^h
2	68±0.9 ^e	65±1.6 ^d	72±4.3 ^h	79±2.5 ^j
3	50±1.4 ^b	52±2.4 ^b	59±2.1 ^{ef}	62±1.5 ^{ef}
4	57±0.3 ^{cd}	56±2.2 ^c	61±0.9 ^{fg}	66±4.2 ^g
5	40±0.5 ^a	42±2.0 ^a	42±0.5 ^b	46±2.3 ^b
6	52±0.3 ^{bc}	56±1.2 ^c	61±0.6 ^{fg}	65±2.5 ^{fg}
7	69±0.1 ^e	66±0.5 ^d	60±1.7 ^{efg}	64±4.1 ^{fg}
8	51±2.1 ^b	52±0.4 ^b	54±1.5 ^d	58±0.8 ^d
9	70±3.1 ^e	72±3.2 ^e	70±2.3 ^h	80±5.1 ^j

10	55±2.4 ^{bcd}	52±2.5 ^b	62±3.2 ^g	65±1.6 ^{fg}
11	43±2.5 ^a	42±4.2 ^a	48±2.2 ^c	49±2.9 ^c
12	53±1.2 ^{bcd}	55±2.8 ^{bc}	58±2.1 ^e	60±2.1 ^{de}
13	69±1.8 ^e	71±4.2 ^e	62±2.0 ^g	75±0.9 ⁱ
14	43±0.5 ^a	39±4.1 ^a	40±2.6 ^b	39±2.8 ^a
15	40±0.1 ^a	39±2.3 ^a	35±1.6 ^a	38±2.6 ^a
16	75±0.6 ^f	75±2.0 ^f	78±4.5 ⁱ	84±2.3 ^k
17	39±0.4 ^a	42±0.8 ^a	42±2.3 ^b	45±2.2 ^b

Values are means±standard error. Within each column means with the same lowercase letter are not significantly different (P > 0.05).

Table 9.4. ANOVA results for antibacterial and antifungal properties.

Bacteria/fungi	Model	F-Value	P-value	df	R ²	Predicted equation
<i>E. coli</i> O157:H7	Linear	83.47	≤ 0.0001	3	0.9393	+ 54.8 + 14.6A + 0.6B - 0.2C
<i>S. Typhimurium</i>	Quadratic	74.59	≤ 0.0001	9	0.9897	+ 55.15 + 14.5A + 0.0B - 0.7C + 0.0AB - 2.25AC - 0.25BC + 2.98A ² - 3.52B ² - 0.021C ²
<i>A. niger</i>	Quadratic	23.07	≤ 0.0002	9	0.9674	+ 61.45 + 13.5A + 3.6B + 1.2C + 1.12AB - 1.88AC + 0.62BC - 1.29A ² - 4.79B ² - 1.79C ²
<i>P. chrysogenum</i>	Quadratic	29.89	≤ 0.0001	9	0.9746	+ 66.21 + 16.5A + 2.9B + 0.0C + 1.88AB - 3.63AC + 1.62BC - 0.12A ² - 5.12B ² - 2.62C ²

Active formulations containing plant-derived cinnamon essential oil (EO) and silver nanoparticles (AGPPH) in combination showed strong antibacterial and antifungal properties, because the cinnamaldehyde (73 %) present as the main chemical component in cinnamon EO has strong bioactivity (Bouhdid *et al.*, 2010). As was found in our study, according to Mith *et al.* (2014), cinnamon EO has strong antimicrobial activities against *E. coli* O157:H7, *S. typhimurium*, and *Listeria monocytogenes*. Silver nanoparticles (AgNPs) are another type of metallic active agent having strong antibacterial and antifungal properties (Emamifar *et al.*, 2010; Metak *et al.*, 2015; Bocate *et al.*, 2019). When cinnamon EO and silver nanoparticles (AgNPs) are combined, they

engaged in the surface of bacteria and fungi and disrupt the membrane and energy balance leading to the death of microorganisms (Ghosh *et al.*, 2013a). Weisany *et al.* (2019) hypothesized that the combination of AgNPs and EOs can increase the microbicidal effectiveness by encapsulation of AgNPs by EOs, which can increase the physical stability of both EOs and AgNPs. Studies found that the incorporation of CNCs into polymeric matrices could improve the control release of active compounds from films and improve the mechanical properties (Khan *et al.*, 2012; Radfar *et al.*, 2020). The current approach to develop active LDPE nanocomposite films using CNCs, glycerol, active formulation by central composite design method could be an efficient and innovative way to develop active packaging for extending the shelf life of storage fruits.

9.3.2. *In vitro* release profiles of the active formulation from the active film

Controlled release behavior of the active formulation (cinnamon EO + AGPPH) from active LDPE-based nanocomposite film in ethanol was studied with optical absorbance measurement as a function of time. Figure 9.1 shows the % cumulative release of active formulation (AF) from active LDPE-based nanocomposite film (LDPE + CNCs + Glycerol + active formulation) for 36 h of extraction time in ethanol. Beginning of the extraction, the % release of AF was obtained of 1.68 % at 0.5 h in ethanol from the LDPE + CNCs + Glycerol + active formulation film. Afterward, the % release of AF increased with extraction time and became stabilized after ~6 h of extraction in ethanol from the active nanocomposite film. A 42.3 % release of the total retained AF occurred from active LDPE-nanocomposite film at 36 h contact with the ethanol (Figure 9.1). Release of AF from the polymeric matrix depends on several factors such as polymer morphology, polymer-active formulation interactions, molecular weight distribution, polarity of the food simulants, temperature, solubility of the active formulations in food simulants, etc. (da Rosa *et al.*, 2020a). The current results were in line with the results obtained by several authors as they observed the release of active ingredients or essential oils from polymeric matrices (Petchwattana and Naknaen, 2015; Bustos *et al.*, 2016; Tawakkal *et al.*, 2016; Requena *et al.*, 2017; Ben-Fadhel *et al.*, 2020). Requena *et al.* (2017) studied the release kinetics mechanism of the eugenol and carvacrol from the poly (hydroxybutyrate-co-hydroxyvalerate) (PHBV) films in different food simulants (10 % ethanol, 50 % ethanol, 3 % acetic acid, and isooctane) and the authors found that the release of eugenol and carvacrol occurred through Fickian and quasi-Fickian diffusion in the PHBV matrix. Moreover, the incorporation of CNC/Glycerol into polymeric matrices improved the interactions with active formulations which reduced their migration through the polymeric network by the restriction of compound mobility (Requena *et al.*, 2017). It could be concluded that the active LDPE-based nanocomposite film containing active formulation have a greater ability to retain the

active formulation for a long time. Further, the fabricated active LDPE-based nanocomposite film was applied for strawberry preservation as a challenging test.

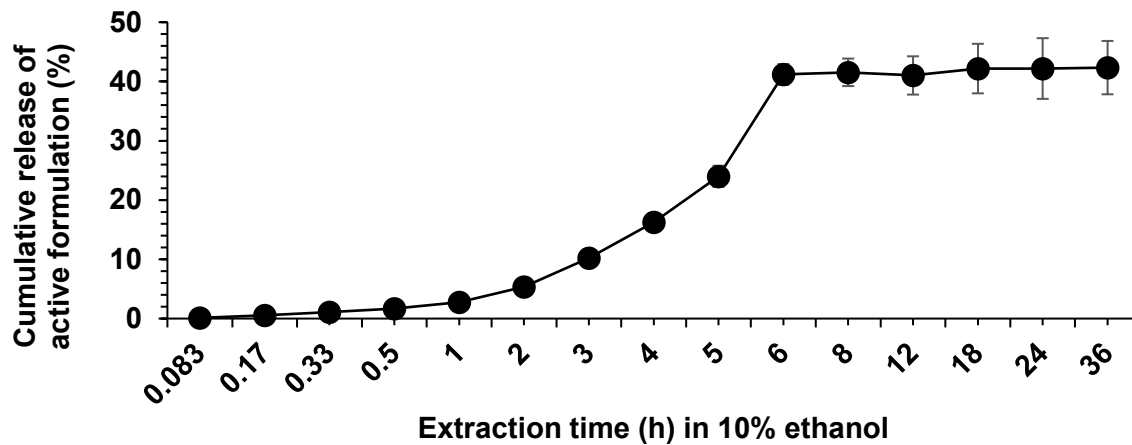


Figure 9.1. Cumulative release (%) of active formulation in ethanol (food simulant) from active LDPE-based nanocomposite film during extraction time.

9.3.3. Physicochemical characterization of the packaged strawberries

9.3.3.1. Weight loss of the packaged strawberries

The weight loss (WL) and percent decay (%) of stored strawberries in Group-1 (control) to Group-5 evaluated during 12 days of storage at 4 °C are depicted in Figures 9.4a and 9.4b, respectively. The fruits in Group-1/control were preserved in PET clamshell with LDPE nanocomposite films without active formulation (LDPE + CNCs + Glycerol). Group-2 contained strawberries with LDPE + CNCs + Glycerol + AGPPH, Group-3 contained strawberries with LDPE + CNCs + Glycerol + cinnamon EO, Group-4 contained strawberries with LDPE+CNCs+Glycerol+active formulation (cinnamon EO + AGPPHs), and Group-5 contained strawberries with LDPE + CNCs + Glycerol + active formulation + γ -irradiation. The WL of the strawberries in each Group was significantly ($P \leq 0.05$) increased with storage time and different treatment conditions (Supplementary data Table 9.1). The WL of the control samples (Group-1) was 41 % at 12 days of storage at 4 °C, while the WL was 23.1, 21.6, 8.1, and 4.5 % during 12 days of storage in Group-2, Group-3, Group-4, and Group-5, respectively, (Figure 9.4a, Supplementary data Table 9.1).

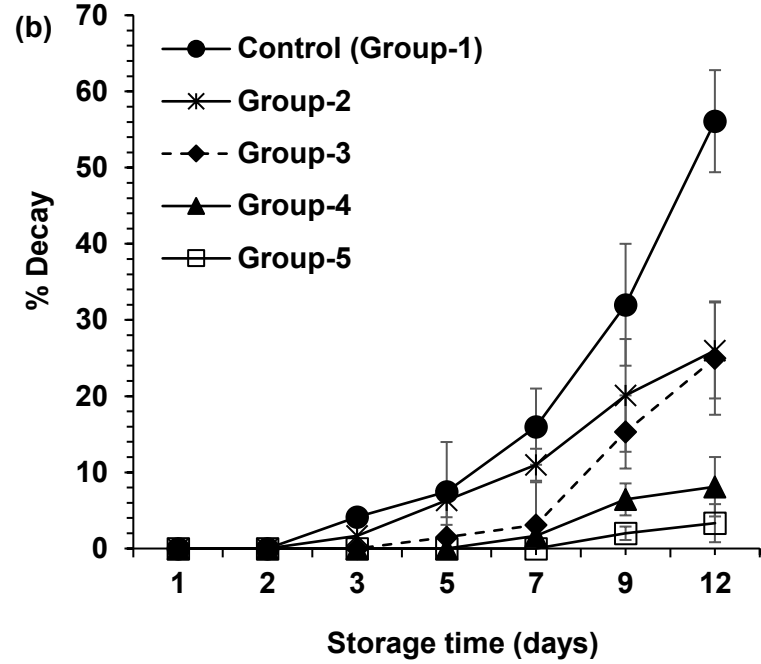
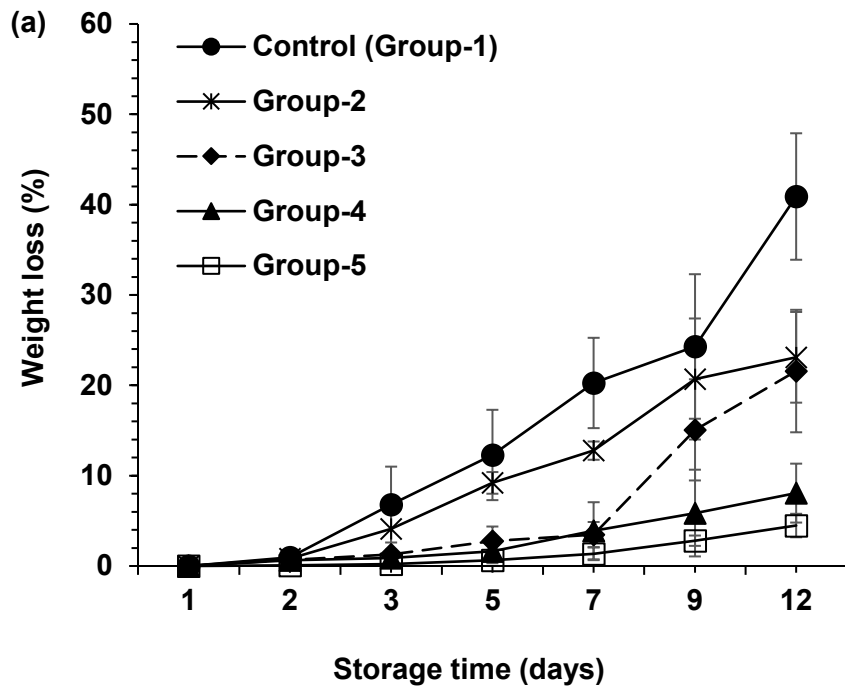


Figure 9.4. Weight loss (%) (a) and % decay (b) of strawberries under different active film packaging treatments during storage.

LDPE + CNCs + Glycerol + active formulation + γ -irradiation (Group-5) reduced WL of fruits by 89 % compared to Group-1 (control) ($P \leq 0.05$), while LDPE + CNCs + Glycerol + active formulation film (Group-4) without irradiation reduced WL by 80 % than control sample during storage at day 12 ($P \leq 0.05$) (Supplementary data Table 9.1). To evaluate the effect of the active LDPE nanocomposite films from Group-4 at a different position (either on the bottom of the PET clamshell or on the top of the fruits, and both on the bottom and on top), the weight loss (%) (WL) of stored strawberries were performed at 4 °C for 2, 3, 5, 7, 9, and 12 days (Supplementary data Table 9.2). Different positions of the films did not show any significant effect ($P > 0.05$) on the weight loss of the fruits at 12 days of storage. The WL (%) of the fruits stored at LDPE nanocomposite films at different positions inside the clamshell varied from 8.07 to 8.32 % among all positions (Supplementary data Table 9.2).

Polymeric matrix loaded with nanoparticles can create an indirect and longer path for passing the air, gas, and moisture that are the key factors for influencing the growth of microorganisms, and thus, preserved the fruits under an internal atmosphere and low-moisture environment (Yang *et al.*, 2010; Motlagh *et al.*, 2020). In our study, active LDPE nanocomposite films containing AGPPHs, cinnamon EO, and active formulation (cinnamon EO + AGPPH) significantly reduced the WL of stored fruits by preventing water loss from the fruit's thin skins and thus reducing the shrinking of skin and keeping them fresh compared to control samples. Hernández-Muñoz *et al.* (2006) stated that strawberries lost water from the fruit to the environment and become shrink rapidly which influences the decay of fruits. In our study showed that combined treatment of active LDPE nanocomposite films and irradiation treatment (Group-5) reduced the WL of fruits synergistically. Because irradiation treatment can reduce the metabolic activity of the fruits which can decrease the respiration rate and thus improve the WL properties of the stored fruits (Maraei and Elsawy, 2017).

9.3.3.2. Percent decay (%) of the packaged strawberries

The decay (%) of the fruits in each Group (1-5) was studied for 12 days of storage at 4 °C as shown in Figure 9.4b, supplementary data Table 9.3. The decay (%) significantly increased with time in the control sample (Group-1). The % decay of the samples packed in presence of the active films was significantly lower compared to the control ($P \leq 0.05$) (Supplementary data Table 9.3). A higher level of decay (%) was observed in the control sample (56 %) (Group-1) after 12 days of storage ($P \leq 0.05$) at 4 °C, while a 26, 25, 8.1, and 3.3 % decay was observed in Group-2, Group-3, Group-4, and Group-5, respectively, after 12 days (Figure 9.4b and Supplementary data Table 9.3). Consequently, it could be stated that the combined treatment of γ -irradiation and active

LDPE-nanocomposite films (Group-5) was the best at controlling decay during the storage of strawberries. The most effective active LDPE nanocomposite film (LDPE + CNCs + Glycerol + active formulation film) was placed at different positions inside the PET clamshell (either on the bottom of the PET clamshell alone or on the top of the fruits alone) for evaluating the position effect of the active films on % decay of fruits during storage (Supplementary data Table 9.4). After 12 days, the level of decay (%) was 8.11 and 8.63 % ($P > 0.05$) when the films were placed on the clamshell at the top and both positions (top and bottom), respectively, and a 9.62 % decay of fruits was observed when the film was placed on the bottom alone (Supplementary data Table 9.4).

Partly because of the high sugar content, strawberries were very susceptible to bacterial and fungal contamination (Ayala-Zavala *et al.*, 2004). The antimicrobial activity of LDPE, EO / AgNPs (AGPPH), and irradiation worked synergistically to reduce the microbial load and the decay (%) of strawberries by restricting the pathogenic and spoilage bacteria and fungi from surroundings and inhibiting the growth of microorganisms as well as a slow release of active components throughout storage time (Carbone *et al.*, 2016; Shankar *et al.*, 2021). The γ -irradiation can penetrate fruit tissue and destroy the indigenous spoilage microorganisms present in tissues and wounds, thus preventing the decay (%) of stored fruits (Barkai-Golan, 2001). Shankar *et al.* (2021) reported that using the essential oil and AgNPs-loaded chitosan films reduced the decay in strawberries by up to 7 % compared with control samples after 12 days of storage. Montero *et al.* (2021b) developed bioactive polybutylene adipate terephthalate (PBAT) films containing cinnamon EO and cellulose nanofibers (CNF) for extending the shelf life of strawberries during storage, and found that PABT / CNF films reduced weight loss and % decay of strawberries and antibacterial activity against *Salmonella* sp. and *Listeria monocytogenes* (Montero *et al.*, 2021b).

9.3.3.3. Surface color of the packaged strawberries

The surface color of the strawberries under different film treatments with and without γ -irradiation was evaluated by measuring lightness (L^*), redness (a^*), and yellowness (b^*) and which is shown in Tables 9.5, 9.6, and 9.7, respectively, for various days of storage. The color measurement of packed fruits is an important factor because it is directly related to appearance and the consumer's perception of quality (Khodaei and Hamidi-Esfahani, 2019). The position of the films inside the clamshell (either on the bottom of the PET clamshell or on the top of the fruits and both on the bottom and top) did not have a significant effect ($P > 0.05$) on the color of the stored fruits (Supplementary data Table 9.5). The results showed that different packaging treatments with and without γ -irradiation did not have any significant ($P > 0.05$) effect on the lightness of stored

strawberries (Table 9.5). Storage time do not significantly affect the lightness (L^*) of strawberries in Group-3 (from 41 to 37.1), in Group-4 (from 38.2 to 34.2), and in Group-5 (from 38.3 to 36.2) during the storage from day 0 to 12 ($P > 0.05$). However, storage time (day 0-12) significantly ($P \leq 0.05$) reduced lightness (L^*) of strawberries in Group-1 (from 38 to 33.4) and Group-2 (from 36.7 to 28.6) (Table 9.5) which corresponded 12 % and 22 % of L^* value reduction, respectively. Similarly, [Shankar et al. \(2021\)](#) observed that the L^* values of strawberries with chitosan film + AgNP film and chitosan + AGNP + EOs + 1 kGy γ -radiation film was affected and a 23 and 30 % of lightness reduction was respectively observed after 12 days of storage strawberries at 4 °C.

Table 9.5. Hunter L^* values of strawberries under different packaging treatments during storage.

Storage time (Day)	Hunter L^* value (lightness)				
	Control (Group-1)	Group-2	Group-3	Group-4	Group-5
0	38.0±2.5 ^{ba}	36.7±5.6 ^{ba}	41.0±4.5 ^{aA}	38.2±3.5 ^{aA}	38.3±3.2 ^{aA}
1	38.2±3.1 ^{ba}	34.3±2.8 ^{ba}	40.3±2.3 ^{aB}	38.1±2.9 ^{aB}	38.0±2.8 ^{aA}
5	36.5±4.3 ^{ba}	33.3±4.1 ^{ba}	39.5±5.2 ^{aB}	36.2±3.8 ^{aA}	37.2±6.3 ^{aA}
7	35.9±3.5 ^{aB}	29.2±3.6 ^{aA}	37.6±6.3 ^{aB}	35.8±3.6 ^{aB}	38.7±6.8 ^{aB}
10	34.5±2.8 ^{aB}	29.5±0.9 ^{aA}	38.3±2.9 ^{aB}	35.2±5.1 ^{aB}	37.6±5.1 ^{aB}
12	33.4±6.1 ^{aB}	28.6±2.5 ^{aA}	37.1±5.6 ^{aB}	34.2±1.5 ^{aB}	36.2±1.9 ^{aB}

Values are means±standard error. Within each column means with the same lowercase letter are not significantly different ($P > 0.05$) and within each row means with same uppercase letter are not significantly different ($P > 0.05$).

The redness (a^*) and yellowness (b^*) of the packed strawberries under the treatment of different packaging films with or without radiation was evaluated and the results are shown in Table 9.6 and Table 9.7, respectively. The a^* and b^* values in packed strawberries were relatively stable during the storage. The storage time did not significantly affect the a^* values ($P > 0.05$) under the same treatment conditions from 0 to 12 days of storage, and the a^* values varied between 29.5 to 38.2. But a significant reduction ($P \leq 0.05$) of redness (Hunter a^*) was observed in strawberries treated with LDPE + CNCs + Glycerol + AGPPH film (Group-2) and LDPE + CNCs + Glycerol +

cinnamon EO film (Group-3) after 12 days of storage and the corresponded redness reduction was 15 and 17 % compared to the control sample (Group-1) (Table 9.6). The redness is reduced due to excess respiration rate and enzymatic degradation of anthocyanins by hydrolytic enzymes of fruits which affect the color and increase the browning of the stored fruits (Peretto *et al.*, 2014). However, the samples in Group-4 and Group-5 showed 3.9 and 3.6 % a^* value reduction ($P > 0.05$), respectively, compared to the control sample on day 12. The storage time and different packaging treatments with or without irradiation did not significantly affect the b^* yellowness (Hunter b^*) values of stored strawberries ($P > 0.05$) (Table 9.7). The b^* (yellowness) values of the fruits in each group varied between 15.4 to 21.1 from 0-12 days of storage. The reduction of color might be occurred during storage due to enhance respiration and enzymatic browning reactions in strawberries (Del-Valle *et al.*, 2005). The results obtained from the study showed that the radiation and active LDPE + CNCs nanocomposite did not have any significant influence on the redness of packed strawberries.

Table 9.6. Hunter a^* values of strawberries under different packaging treatments during storage.

Storage time (Day)	Hunter a^* value (redness)				
	Control (Group-1)	Group-2	Group-3	Group-4	Group-5
0	36.3±3.2 ^{ab}	33.2±3.3 ^{aA}	30.8±2.9 ^{aA}	36.2±6.9 ^{ab}	35.8±4.1 ^{ab}
1	38.2±5.1 ^{ab}	31.3±1.8 ^{aA}	31.3±2.3 ^{aA}	35.9±5.4 ^{ab}	36.5±5.8 ^{ab}
5	37.2±0.9 ^{ab}	33.9±3.9 ^{aA}	30.5±4.2 ^{aA}	35.5±6.3 ^{ab}	35.6±2.8 ^{ab}
7	36.5±5.5 ^{ab}	31.5±4.4 ^{aA}	29.6±3.9 ^{aA}	34.8±6.0 ^{ab}	34.9±6.5 ^{ab}
10	36.1±3.6 ^{ab}	30.2±2.3 ^{aA}	28.9±5.7 ^{aA}	34.6±2.9 ^{ab}	34.2±3.9 ^{ab}
12	35.6±3.8 ^{ab}	30.0±6.1 ^{aA}	29.5±2.5 ^{aA}	34.2±6.1 ^{ab}	34.3±2.6 ^{ab}

Values are means±standard error. Within each column means with the same lowercase letter are not significantly different ($P > 0.05$) and within each row means with same uppercase letter are not significantly different ($P > 0.05$).

Table 9.7. Hunter b^* values of strawberries under different packaging treatments during storage.

Storage time (Day)	Hunter b^* value (yellowness)				
	Control (Group-1)	Group-2	Group-3	Group-4	Group-5
0	17.3±0.9 ^{aA}	21.1±3.3 ^{bA}	17.6±2.9 ^{aA}	18.2±2.1 ^{aA}	17.6±1.4 ^{aA}
1	15.4±2.8 ^{aA}	18.9±6.1 ^{aB}	16.8±5.2 ^{aA}	18.0±3.1 ^{aA}	16.2±2.9 ^{aA}
5	16.3±3.1 ^{aA}	18.5±3.9 ^{aA}	16.2±2.8 ^{aA}	17.5±2.8 ^{aA}	15.6±3.9 ^{aA}
7	14.6±3.8 ^{aA}	16.8±6.1 ^{aA}	15.6±1.9 ^{aA}	17.2±6.1 ^{aA}	16.2±2.2 ^{aA}
10	16.5±2.9 ^{aA}	17.6±5.1 ^{aA}	16.8±2.3 ^{aA}	17.9±1.4 ^{aA}	16.5±2.8 ^{aA}
12	16.9±2.8 ^{aA}	17.8±3.9 ^{aA}	16.1±3.1 ^{aA}	16.8±2.4 ^{aA}	16.8±3.3 ^{aA}

Values are means±standard error. Within each column means with the same lowercase letter are not significantly different ($P > 0.05$) and within each row means with same uppercase letter are not significantly different ($P > 0.05$).

9.3.3.4. Firmness and total soluble solid of the packaged strawberries

The firmness (N) and total soluble solids (TSS) (%) of strawberries after storage under different packaging film treatments with and without irradiation are presented in Table 9.8 and Figure 9.5, respectively. The firmness (N) of the strawberries showed no significant differences under the different treatment conditions such as LDPE nanocomposite film (LDPE + CNCs + Glycerol) (control/Group-1), LDPE + CNCs + Glycerol + AGPPH film (Group-2), LDPE + CNCs + Glycerol + cinnamon EO film (Group-3), LDPE + CNCs + Glycerol + active formulation film (Group-4), and LDPE + CNCs + Glycerol + active formulation + 500 Gy γ -irradiation (Group-5) on the same day of storage ($P > 0.05$) (Table 9.8). However, the firmness of fruits decreased significantly with storage time ($P \leq 0.05$) in each Group of strawberries. The highest reduction of firmness was found in control samples/Group-1 where the firmness values were reduced from 0.76 N to 0.46 N from day 0-12 of stored fruits ($P \leq 0.05$). [Khodaei and Hamidi-Esfahani \(2019\)](#) found the hardness of strawberries naturally declines with storage time. The reduction of firmness or hardness of strawberries depends on the hydrolysis and depolymerization of pectin, cell wall degradation, and breakdown, and fruit skin-softening might be continued during postharvest storage because of ripening ([Paniagua et al., 2014](#); [Peretto et al., 2014](#)). The radiation effect on strawberry preservation was studied previously by several authors ([Kader, 1986](#); [Majeed et al., 2014](#); [Maraei and Elsawy, 2017](#)). According to [Kader \(1986\)](#) γ -irradiation treatment of fruits with higher doses (>2 kGy) may reduced the firmness of fruits which may have occurred because of the proteolytic

enzyme activation and degradation of the polysaccharides that can solubilize pectin and cell wall of fruits (Kader, 1986; Ayala-Zavala *et al.*, 2004).

Table 9.8. The firmness of strawberries under different packaging treatments.

Storage time (Day)	Firmness (N)				
	Control (Group-1)	Group-2	Group-3	Group-4	Group-5
0	0.76±0.08 ^{eA}	0.71±0.02 ^{eA}	0.75±0.02 ^{dA}	0.78±0.02 ^{eA}	0.71±0.05 ^{dA}
1	0.75±0.10 ^{eA}	0.65±0.01 ^{dB}	0.73±0.01 ^{dA}	0.75±0.01 ^{dA}	0.68±0.02 ^{dA}
5	0.62±0.10 ^{dA}	0.60±0.01 ^{cA}	0.67±0.01 ^{cA}	0.70±0.02 ^{cA}	0.63±0.02 ^{cA}
7	0.58±0.04 ^{cA}	0.52±0.02 ^{bA}	0.65±0.01 ^{cA}	0.64±0.02 ^{bA}	0.57±0.03 ^{bA}
10	0.51±0.03 ^{bA}	0.50±0.01 ^{abA}	0.55±0.02 ^{bA}	0.58±0.01 ^{aA}	0.50±0.03 ^{aA}
12	0.46±0.10 ^{aA}	0.48±0.01 ^{aA}	0.50±0.01 ^{aA}	0.56±0.02 ^{aA}	0.48±0.01 ^{aA}

Values are means±standard error. Within each column means with the same lowercase letter are not significantly different ($P > 0.05$) and within each row means with same uppercase letter are not significantly different ($P > 0.05$).

Total soluble solids (TSS) (%) of packaged strawberries under different treatments at 4 °C for 12 days are shown in Figure 9.5. The results showed that the TSS content of fruits in each Group (Group-1/Control: LDPE + CNCs + Glycerol; Group-2: LDPE + CNCs + Glycerol + AGPPH; Group-3: LDPE + CNCs + Glycerol + cinnamon EO; Group-4: LDPE + CNCs + Glycerol + active formulation; Group-5: LDPE + CNCs + Glycerol + active formulation + γ -irradiation) was not significantly different ($P > 0.05$) and that the TSS values were not affected by storage time ($P > 0.05$). The TSS values were ~14.2 % for each Group at day 0 and remained unchanged after 12 days of storage. In this study, irradiation did not affect the TSS content of strawberries compared to control samples/Group-1 ($P > 0.05$). Similar to our study, Shankar *et al.* (2021) found that irradiation and active chitosan films (with essential oils and AgNPs) treatment did not affect the TSS content in strawberries during storage of 12 days, with average values of ~13.5 %. TSS measurement generally indicates the degree of maturity and metabolic reactions of fruits under different treatments which may increase in sugar level (Treviño-Garza *et al.*, 2015). In contrast, several studies have reported that the TSS content in strawberries increased during storage time which may reflect water loss or the solubilization of polyuronides and hemicellulose in the cell wall of mature strawberries (Mitcham, 2007; Peretto *et al.*, 2014; Treviño-Garza *et al.*, 2015).

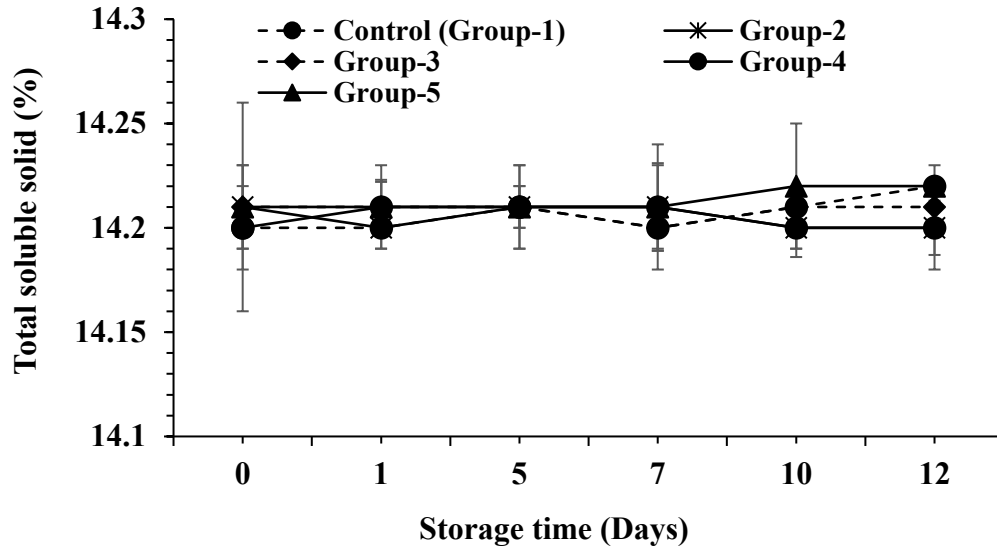


Figure 9.5. Total soluble solid (TSS) of strawberries under different packaging treatments during storage. Group-1: LDPE + CNCs + Glycerol (Control); Group-2: LDPE + CNCs + Glycerol + AGPPH; Group-3: LDPE + CNCs + Glycerol + cinnamon EO; Group-4: LDPE + CNCs + Glycerol + active formulation (AGPPH + cinnamon EO); and Group-5: LDPE + CNCs + Glycerol + active formulation + γ -irradiation.

9.3.3.5. Total phenols (TP) and total anthocyanins content measurement

The total phenols (TP) and anthocyanins content of strawberries in each Group is depicted in Figure 9.6a and Figure 9.6b, respectively. Storage time significantly influenced ($P \leq 0.05$) the TP content in strawberries. The TP content in strawberries were found 1521, 1452, 1235, 1325, and 1156 g/kg FW (fruit weight) at day 0 in Group-1 (Control: LDPE + CNCs + Glycerol), Group-2: (LDPE + CNCs + Glycerol + AGPPH), Group-3: (LDPE + CNCs + Glycerol + cinnamon EO), Group-4: (LDPE + CNCs + Glycerol + active formulation), and Group-5: (LDPE + CNCs + Glycerol + active formulation + γ -irradiation), respectively. The highest TP content was observed in the control sample/Group-1 (TP: 1521 g/kg FW) on day 0 which was significantly ($P \leq 0.05$) reduced (TP: 925 g/kg FW) at day 12. The TP values in Group-3 (TP: 1536 g/kg FW), Group-4 (TP: 1652 g/kg FW), and Group-5 (TP: 1711 g/kg FW) significantly ($P \leq 0.05$) increased at day 12. However, the combined treatment between active film and γ -irradiation (Group-5) showed the highest TP content in fruits after 12 days of storage (from 1156 g/kg FW to 1711 g/kg FW). Previous studies showed that strawberries stored in clamshells containing active LDPE nanocomposite film increased the TP content which might be because phenylalanine ammonia-lyase (PAL) enzyme activation (Oufedjikh *et al.*, 2000; Jiang and Joyce, 2003). Irradiation treatment is known to activate

the PAL enzyme which is important for the biosynthesis of phenolic contents in fruits (Oufedjikh *et al.*, 2000; Maraei and Elsayy, 2017). Oufedjikh *et al.* (2000) studied the influence of γ -irradiation (0.3 kGy) on the phenolics content and PAL of Citrus clementina (Moroccan citrus fruits) at 3 °C for 49 days. The authors found that the irradiation treatment was significantly ($P \leq 0.05$) increased the total phenolics and PAL in stored citrus fruits than the control samples (fruits without irradiation) (Oufedjikh *et al.*, 2000). Thus, in this study, results showed that irradiation and LDPE + CNCs + Glycerol + active formulation synergistically increased the TP content in the stored strawberries at day 12. γ -irradiation along with active packaging films helped to increase or retain the phenolic content in stored strawberries. Several other studies have observed the same trend (Hussain *et al.*, 2012; Maraei and Elsayy, 2017).

Anthocyanins in strawberries are responsible for the red color which indicates maturity. Pelargonidin-3-glucoside and cyanidin-3-glucoside are two types of anthocyanins found in strawberries that are mostly responsible for the red color (Kalt *et al.*, 1993). The content of anthocyanins in strawberries for each Group are presented in Figure 9.6b. The anthocyanins content is gradually increasing in strawberries in Group-1/control until storage day 7 (from 153-243 g/kg FW) but decreased from 243-185 g/kg FW at 7-12 days. The anthocyanins content in Group-2, Group-3, Group-4, and Group-5 was significantly ($P \leq 0.05$) increased with storage time. The anthocyanins content in Group-2, Group-3, Group-4, and Group-5 was 152, 142, 153, and 135 g/kg FW at day 0, respectively, while the corresponding anthocyanins content was 225, 261, 271, and 287 g/kg FW ($P \leq 0.05$) on day 7 (Figure 9.6b). The reduction in anthocyanins content in the control sample/Group-1 after storage day 7 might be due to natural ripening, senescence, and decay (Khodaei and Hamidi-Esfahani, 2019). The highest anthocyanins content (287 g/kg FW at day 12) was observed in the strawberries under the combined treatment of LDPE+CNCs+Glycerol+active formulation film and γ -radiation (500 Gy) (Group-5) which might have occurred because of the activation two key enzymes (phenylalanine ammonia lyase-PAL and glucosyltransferase-GT) (Tezotto-Uliana *et al.*, 2013).

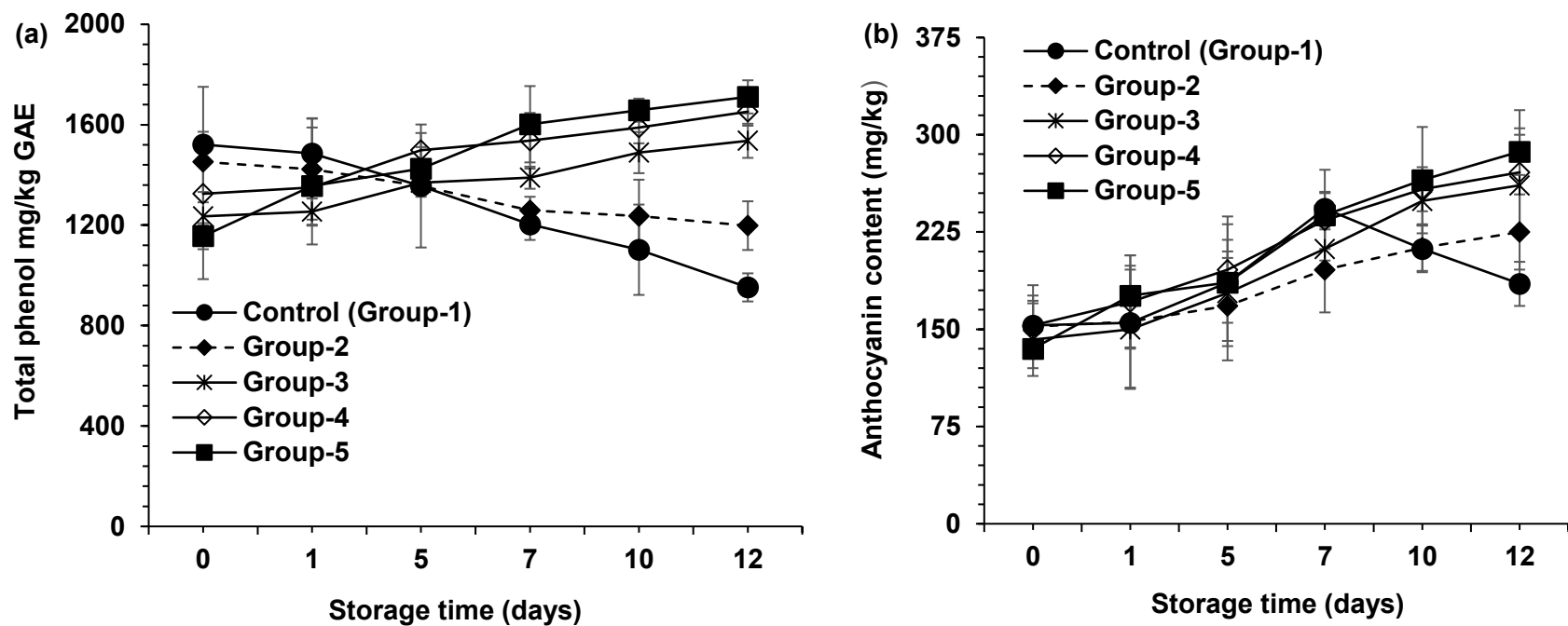


Figure 9.6. Total phenol (a) and anthocyanins content (b) of strawberries under different active film packaging treatments during storage. Group-1: LDPE + CNCs + Glycerol (Control); Group-2: LDPE + CNCs + Glycerol + AGPPH; Group-3: LDPE + CNCs + Glycerol + cinnamon EO; Group-4: LDPE + CNCs + Glycerol + active formulation (AGPPH + cinnamon EO); and Group-5: LDPE + CNCs + Glycerol + active formulation + γ -irradiation.

9.3.4. Characterization of irradiated and non-irradiated LDPE films

The characterization of the films (thickness, mechanical, WVP, oxygen transmission rate [OTR], water solubility [WS], surface color) was performed for five different types of irradiated and non-irradiated LDPE films (Table 9.9). The five different types of films were control (Group-1: LDPE + CNCs + Glycerol), Group-2: (LDPE + CNCs + Glycerol + AGPPH), Group-3: (LDPE + CNCs + Glycerol + cinnamon EO), Group-4: (LDPE + CNCs + Glycerol + active formulation) and Group-5: (LDPE + CNCs + Glycerol + active formulation + irradiation). The thickness of the control film in Group-1 (LDPE + CNCs + Glycerol film) was 91.8 μm which increased significantly ($P \leq 0.05$) after incorporating AGPPH (Group-2) (thickness: 102 μm), cinnamon EO (Group-3) (thickness: 110 μm), active formulation (EO + AGPPH) (Group-4) (thickness: 107 μm) and active formulation + radiation (Group-5) (thickness: 108 μm) (Table 9.9). The thickness of the active LDPE-based nanocomposite films increased as compared to the control film. This might be due to the addition of total soluble content. Similar observations were found by [Arfat *et al.* \(2017\)](#); [Shankar *et al.* \(2021\)](#). [Shankar *et al.* \(2021\)](#) found for the thickness of neat chitosan film a value of 96.8 μm which increased significantly to 132.4 μm after adding EO + AgNPs. The tensile strength (TS) of the film in Group-1 was 16 MPa which decreased significantly in Group-2 (12 MPa) ($P \leq 0.05$). However, the TS values in Group-4 and 5 were not significantly ($P > 0.05$) different, showing values of 17.6 and 17.2 MPa, respectively, compared to the control film (TS: 16 MPa). A significant reduction of TS value for the LDPE + CNCs + Glycerol + AGPPH film was observed compared to the control film. The agglomeration and uneven distribution of hydrophilic AgNPs into the polymeric matrix created cracks, micro-voids, and stress concentration areas in the polymeric matrices ([Radfar *et al.*, 2020](#)). The TS values obtained in this study showed that the values were increased for the films in presence of the active compounds i.e. Group-3, Group-4 and Group-5 which may have resulted from a reduction of intermolecular force among the polymeric chain after the incorporation of active ingredients which acted as a plasticizer and helped to improve the flexibility of the LDPE nanocomposite films ([Mousavian *et al.*, 2021](#)).

The elongation at break (E_b) of the composite films in Group-2, Group-3, Group-4, and Group-5 significantly ($P \leq 0.05$) decreased as compared to Group-1/control film (Table 9.9). The E_b of LDPE composite film in Group-1 was 674 %, while the E_b values were 580, 646, 652, and 645 % for Group-2, Group-3, Group-4, and Group-5, respectively. The E_b of active LDPE composite films was decreased when incorporated AGPPH, but the E_b value was increased when cinnamon EO was incorporated (Table 9.9). [Shankar *et al.* \(2021\)](#) found that the E_b was increased in chitosan film when EOs were incorporated, however, it was decreased when AgNPs were incorporated, which is like in the current study. γ -irradiation treatment did not have any significant effect on either

TS or Eb ($P > 0.05$). Moreover, when active ingredients (AGPPH, cinnamon EO, active formulation) were incorporated into nanocomposite LDPE film (LDPE + CNCs + Glycerol), the Eb was reduced compared to control film (LDPE + CNCs + Glycerol) which might be occurred because of the reinforcing and stiffing effect of active agents into the polymeric network, causing reduced mobility of polymeric chain (Hajiabdolrasouli and Babaei, 2018; Radfar *et al.*, 2020).

The oxygen transmission rate (OTR) test of the active packaging film is one of the important parameter because food's quality and shelf life are greatly affected by O_2 (Sharmin *et al.*, 2012).

The OTR of each LDPE-based nanocomposite film was characterized and summarized in Table 9.9. The OTR value of the control film (Group-1: LDPE + CNCs + Glycerol film) was obtained of $172 \text{ cm}^3 \cdot \text{m}^{-2} \cdot \text{day}^{-1}$ which was significantly ($P \leq 0.05$) reduced in Group-4 (OTR: $162 \text{ cm}^3 \cdot \text{m}^{-2} \cdot \text{day}^{-1}$) and Group-5 (OTR: $160 \text{ cm}^3 \cdot \text{m}^{-2} \cdot \text{day}^{-1}$). After applying either active formulation (cinnamon EO + AGPPH) or active formulation + radiation into LDPE-nanocomposite films, a tortuous path might be created in the presence of CNC and active formulation into the polymeric matrix which created a longer diffusion path for oxygen gas and increased the film's impermeability, reducing the OTR values in Group-4 and Group-5. Vatansever *et al.* (2020) developed the poly butylene adipate terephthalate (PBAT)-based nanocomposite films loaded with CNC nanoparticles at different contents (1-5 %) and the authors found that the incorporation of 5 % CNC into the PBAT matrix was significantly reduced the OTR of PBAT nanocomposite film by 41 % which is the similar phenomenon of the current study. Criado *et al.* (2020) found that after incorporation of CNC into the alginate matrix reduced the OTR values from 125 to 92 of the neat alginate and alginate-CNC films, respectively. However, a reverse phenomenon was observed when AGPPH was incorporated into LDPE-nanocomposite film (Group-2), the OTR value of LDPE + CNCs + Glycerol + AGPPH film (Group-2) was significantly ($P \leq 0.05$) increased (OTR: $196 \text{ cm}^3 \cdot \text{m}^{-2} \cdot \text{day}^{-1}$) as compared to the control sample (Table 9.9). Similar observation was found by Srisa and Harnkarnsujarit (2020), the authors developed PBAT/PLA film (poly butylene adipate terephthalate/poly lactic acid) at a ratio of 60/40 by incorporating *trans*-cinnamaldehyde (2-10 %). Incorporation of *trans*-cinnamaldehyde upto 5 % significantly increased the oxygen permeability (OP) of the PBAT/PLA film due to the plasticization effect, a reduction in the orientation and non-homogeneity of the polymeric network, and a creation of the micropore in the films which allowed oxygen dissolved into the matrices and augmented the oxygen transportation (Srisa and Harnkarnsujarit, 2020).

Table 9.9. Color measurement, mechanical properties, thickness, oxygen transmission rate (OTR), and water vapor permeabilities (WVP) of the active LDPE films.

Films' Groups	Color measurement				Mechanical properties		Thickness (μm)	Oxygen transmission rate (OTR) $\text{cm}^3 \cdot \text{m}^{-2} \cdot \text{day}^{-1}$	Water solubility (WS)	WVP $\text{g m mm}^{-2} \text{ day}^{-1} \text{ kPa}^{-1}$
	L^*	a^*	b^*	ΔE	TS (Mpa)	Eb (%)				
Control (Group-1)	62 \pm 5.7 ^b	4.2 \pm 0.4 ^a	22 \pm 3.2 ^a	42 \pm 3.7 ^a	16 \pm 1.7 ^b	674 \pm 8 ^b	91.8 \pm 6.8 ^a	172 \pm 9.1 ^b	0.65 \pm 0.05 ^a	1.35 \pm 0.24 ^a
Group-2	35 \pm 4.2 ^a	30 \pm 6.1 ^c	32 \pm 3.0 ^b	76 \pm 1.1 ^c	12 \pm 3.0 ^a	580 \pm 11 ^a	102 \pm 5.7 ^b	196 \pm 8.5 ^c	0.70 \pm 0.04 ^a	1.45 \pm 0.92 ^a
Group-3	48 \pm 4.0 ^a	17 \pm 1.0 ^b	31 \pm 5.1 ^b	60 \pm 3.2 ^b	15.6 \pm 2.6 _{ab}	646 \pm 11 ^{ab}	110 \pm 7.5 ^b	178 \pm 7.8 ^b	0.72 \pm 0.07 ^a	1.98 \pm 0.6 ^a
Group-4	47 \pm 9.4 ^a	19 \pm 3.0 ^b	29 \pm 4.0 ^{ab}	60 \pm 9.4 ^b	17.6 \pm 0.6 _b	652 \pm 7 ^{ab}	107 \pm 5.9 ^b	162 \pm 5.6 ^a	0.67 \pm 0.03 ^a	1.89 \pm 0.8 ^a
Group-5	42 \pm 9.1 ^a	22 \pm 3.5 ^b	27 \pm 3.05 ^a _b	65 \pm 9.0 ^b _c	17.2 \pm 1.04 ^b	645 \pm 12 ^{ab}	108 \pm 6.3 ^b	160 \pm 7.2 ^a	0.71 \pm 0.08 ^a	1.78 \pm 0.86 ^a

Values were means \pm standard error. The same lowercase letter in each column was not significantly different ($P > 0.05$).

The water vapor permeability (WVP) values of the LDPE composite films in Group-1/control, Group-2, Group-3, Group-4, and Group-5 were 1.35, 1.45, 1.98, 1.89, and 1.78 g m mm⁻²day⁻¹kPa⁻¹, respectively, (Table 9.9). The WVP values were insignificantly higher ($P > 0.05$) in Group-2, Group-3, Group-4, and Group-5 than the control film (Group-1: LDPE + CNCs + Glycerol) which might be occurred due to the incorporation of active agents that increased the hydrophilic portion and created micro-voids into the polymeric matrices and increased the diffusion of water vapor and thus promoted higher WVP (Salmieri *et al.*, 2014a). The WS of the LDPE-based nanocomposite film from each Group was evaluated and the results are presented in Table 9.9. Incorporation of AGPPH (Group-2), cinnamon EO (Group-3), active formulation (cinnamon EO + AGPPH) (Group-4) and active formulation irradiation (Group-5) in the LDPE-based nanocomposite film did not significantly ($P > 0.05$) affect the WS of the bioactive LDPE-nanocomposite films while comparing with the control film (Group-1) because of their insoluble nature in water.

The surface color of the LDPE composite films in each Group is presented in Table 9.9 and Figure 9.2. The lightness (L^*) of the control film (Group-1) showed the highest value (62), however, and the L^* values were significantly decreased when incorporating AGPPH, cinnamon EO, and the active compound, and after irradiation treatment ($P \leq 0.05$). The L^* values were 35, 48, 47, and 42 ($P > 0.05$) for the films in Group-2, Group-3, Group-4, and Group-5, respectively. However, the redness (a^*) and yellowness (b^*) of the films were significantly increased in Group-2, Group-3, Group-4, and Group-5 films compared to the control film ($P \leq 0.05$). The LDPE + CNCs + Glycerol + AGPPH film (Group-2) showed significantly ($P \leq 0.05$) higher color difference ($\Delta E = 76$) as compared to the control film ($\Delta E = 42$). The composite films in Group-3, Group-4, and Group-5 showed ΔE values around ~60. In Figure 9.2, the visible color of the LDPE nanocomposite films from each Group (Control/Group-1: LDPE + CNCs + Glycerol; Group-2: LDPE + CNCs + Glycerol + AGPPH; Group-3: LDPE + CNCs + Glycerol + cinnamon EO; Group-4: LDPE + CNCs + Glycerol + active formulation; Group-5: LDPE + CNCs + Glycerol + active formulation + γ -radiation) were presented though it was hard to see the color difference with the naked eye. However, the yellowness (b^*) and redness (a^*) were more pronounced in the films in Group-2 because of the color of AGPPH agents. The control sample was more transparent compared to the samples treated with different active components in Group-2, Group-3, Group-4, and Group-5. The color difference may have occurred because of the interactions between the polymer and active components, as the redness and yellowness in the composite films were increased. For appearance and consumer acceptance, the surface color of the composite biofilms may be important (Srinivasa *et al.*, 2002).

9.4. Conclusion

The combined treatment between active LDPE-nanocomposite film and irradiation showed synergistic activity and significantly ($P \leq 0.05$) reduced fruit weight loss and decay (%) during storage as compared to the control. The combined treatment of active film and γ -irradiation helped to retain the phenolics and anthocyanins content significantly ($P \leq 0.05$) during storage (12 days) as compared to the control samples. The application of active LDPE-nanocomposite film and γ -irradiation did not significantly ($P > 0.05$) affect on the total soluble solids, firmness, and color of stored strawberries as compared to the control samples. The color and mechanical properties of the active LDPE films were dependent on the type of active agents incorporated into the polymeric matrices. The lightness (L^*) of the control film was significantly affected by the addition of the antimicrobial formulation. However, the incorporation of active agents with or without irradiation into LDPE polymeric matrices did not have any effect on the WVP of the films as compared to the control film. The results obtained in this study suggest an innovative way to design active nanocomposite film having enhanced antibacterial and antifungal properties which could extend the shelf-life of perishable fruits, and the use of combined treatment of biofilms with irradiation can act synergistically and further increase the shelf-life and quality of fruits.

9.5. Acknowledgment

The authors are grateful for the financial support from the Natural Sciences and Engineering Research Council of Canada (NSERC) no: RDCPJ 534563-18, the Natural Sciences and Engineering Research Council of Canada (NSERC) discovery program project number: RGPIN-2017-05947 and no RDCPJ 534563-18 Partnership Program with Nanobrand; Chair of the Ministry of Agricultural Fishery Food of Quebec (Ministère de l'Agriculture, des Pêcheries et de l'Alimentation du Québec: MAPAQ-Chair) PPIA-12, NanoBrand, the U.S. Department of Agriculture, Agricultural Research Service (USDA ARS), U.S. Pacific Basin Agricultural Research Centre.

9.6. References

- Arfat, Y.A., Ahmed, J., Hiremath, N., Auras, R., Joseph, A., 2017. Thermo-mechanical, rheological, structural and antimicrobial properties of bionanocomposite films based on fish skin gelatin and silver-copper nanoparticles. *Food Hydrocolloids* 62, 191-202.
- ASTM, D., 1995. Standard test method for tensile properties of thin plastic sheeting. Annual book of ASTM standards 8, 182-190.
- Ayala-Zavala, J.F., Wang, S.Y., Wang, C.Y., González-Aguilar, G.A., 2004. Effect of storage temperatures on antioxidant capacity and aroma compounds in strawberry fruit. *LWT-Food Science and Technology* 37, 687-695.
- Barkai-Golan, R., 2001. Postharvest diseases of fruits and vegetables: development and control. Elsevier
- Begum, T., Follett, P.A., Mahmud, J., Moskovchenko, L., Salmieri, S., Allahdad, Z., Lacroix, M., 2022a. Silver nanoparticles-essential oils combined treatments to enhance the antibacterial and antifungal properties against foodborne pathogens and spoilage microorganisms. *Microbial Pathogenesis* 164, 105411.
- Begum, T., Follett, P.A., Shankar, S., Mahmud, J., Salmieri, S., Lacroix, M., 2022b. Mixture design methodology and predictive modeling for developing active formulations using essential oils and citrus extract against foodborne pathogens and spoilage microorganisms in rice. *Journal of Food Science* 87, 353-369.
- Ben-Fadhel, Y., Maherani, B., Manus, J., Salmieri, S., Lacroix, M., 2020. Physicochemical and microbiological characterization of pectin-based gelled emulsions coating applied on pre-cut carrots. *Food Hydrocolloids* 101, 105573.
- Bocate, K.P., Reis, G.F., de Souza, P.C., Oliveira Junior, A.G., Duran, N., Nakazato, G., Furlaneto, M.C., de Almeida, R.S., Panagio, L.A., 2019. Antifungal activity of silver nanoparticles and simvastatin against toxigenic species of *Aspergillus*. *International Journal Food Microbiology* 291, 79-86.
- Bouhdid, S., Abrini, J., Amensour, M., Zhiri, A., Espuny, M., Manresa, A., 2010. Functional and ultrastructural changes in *Pseudomonas aeruginosa* and *Staphylococcus aureus* cells induced by *Cinnamomum verum* essential oil. *Journal of Applied Microbiology* 109, 1139-1149.
- Bustos, C.R., Alberti, R.F., Matiacevich, S.B., 2016. Edible antimicrobial films based on microencapsulated lemongrass oil. *Journal of Food Science and Technology* 53, 832-839.
- Caillet, S., Lacroix, M., 2006. Effect of gamma radiation and oregano essential oil on murein and ATP concentration of *Listeria monocytogenes*. *Journal of Food Protection* 69, 2961-2969.

- Carbone, M., Donia, D.T., Sabbatella, G., Antiochia, R., 2016. Silver nanoparticles in polymeric matrices for fresh food packaging. *Journal of King Saud University - Science* 28, 273-279.
- Cardiet, G., Fuzeau, B., Barreau, C., Fleurat-Lessard, F., 2012. Contact and fumigant toxicity of some essential oil constituents against a grain insect pest *Sitophilus oryzae* and two fungi, *Aspergillus westerdijkiae* and *Fusarium graminearum*. *Journal of Pest Science* 85, 351-358.
- Criado, P., Frascini, C., Salmieri, S., Lacroix, M., 2020. Cellulose nanocrystals (CNCs) loaded alginate films against lipid oxidation of chicken breast. *Food Research International* 132, 109110.
- da Rosa, C.G., Sganzerla, W.G., de Oliveira Brisola Maciel, M.V., de Melo, A.P.Z., da Rosa Almeida, A., Ramos Nunes, M., Bertoldi, F.C., Manique Barreto, P.L., 2020. Development of poly (ethylene oxide) bioactive nanocomposite films functionalized with zein nanoparticles. *Colloids and Surfaces A: Physicochemical and Engineering Aspects* 586, 124268.
- Del-Valle, V., Hernández-Muñoz, P., Guarda, A., Galotto, M., 2005. Development of a cactus-mucilage edible coating (*Opuntia ficus indica*) and its application to extend strawberry (*Fragaria ananassa*) shelf-life. *Food Chemistry* 91, 751-756.
- Delbeke, S., Hessel, C., Verguldt, E., De Beleyer, A., Clicque, T., Boussemaere, J., Jacxsens, L., Uyttendaele, M., 2014. Survival of *Salmonella* and *E. coli* O157 on strawberries and basil during storage at different temperatures. 19th Conference on Food Microbiology. Belgian Society for Food Microbiology (BSFM), 13-113.
- Emamifar, A., Kadivar, M., Shahedi, M., Soleimani-Zad, S., 2010. Evaluation of nanocomposite packaging containing Ag and ZnO on shelf life of fresh orange juice. *Innovative Food Science and Emerging Technologies* 11, 742-748.
- Falleh, H., Ben Jemaa, M., Djebali, K., Abid, S., Saada, M., Ksouri, R., 2019. Application of the mixture design for optimum antimicrobial activity: Combined treatment of *Syzygium aromaticum*, *Cinnamomum zeylanicum*, *Myrtus communis*, and *Lavandula stoechas* essential oils against *Escherichia coli*. *Journal of Food Processing and Preservation* 43, 14257.
- Felix da Silva Barbosa, R., Gabrieli de Souza, A., Rangari, V., Rosa, D.D.S., 2021. The influence of PBAT content in the nanocapsules preparation and its effect in essential oils release. *Food Chemistry* 344, 128611.
- Ghosh, I.N., Patil, S.D., Sharma, T.K., Srivastava, S.K., Pathania, R., Navani, N.K., 2013. Synergistic action of cinnamaldehyde with silver nanoparticles against spore-forming

- bacteria: a case for judicious use of silver nanoparticles for antibacterial applications. *International Journal of Nanomedicine* 8, 4721-4731.
- Hajjabdolrasouli, M., Babaei, A., 2018. Rheological, thermal and tensile properties of PE/nanoclay nanocomposites and PE/nanoclay nanocomposite cast films. *Polyolefins Journal* 5, 47-58.
- Han, J.H., 2014. Edible films and coatings: a review. *Innovations in Food Packaging*, 213-255.
- Hernández-Muñoz, P., Almenar, E., Ocio, M.J., Gavara, R., 2006. Effect of calcium dips and chitosan coatings on postharvest life of strawberries (*Fragaria x ananassa*). *Postharvest Biology and Technology* 39, 247-253.
- Hossain, F., Follett, P., Dang Vu, K., Harich, M., Salmieri, S., Lacroix, M., 2016. Evidence for synergistic activity of plant-derived essential oils against fungal pathogens of food. *Food Microbiology* 53, 24-30.
- Hossain, F., Follett, P., Salmieri, S., Vu, K.D., Fraschini, C., Lacroix, M., 2019. Antifungal activities of combined treatments of irradiation and essential oils (EOs) encapsulated chitosan nanocomposite films in *in vitro* and *in situ* conditions. *International Journal of Food Microbiology* 295, 33-40.
- Hossain, F., Follett, P., Vu, K.D., Salmieri, S., Fraschini, C., Jamshidian, M., Lacroix, M., 2018. Antifungal activity of combined treatments of active methylcellulose-based films containing encapsulated nanoemulsion of essential oils and γ -irradiation: *in vitro* and *in situ* evaluations. *Cellulose* 26, 1335-1354.
- Hussain, P.R., Dar, M.A., Wani, A.M., 2012. Effect of edible coating and gamma irradiation on inhibition of mould growth and quality retention of strawberry during refrigerated storage. *International Journal of Food Science and Technology* 47, 2318-2324.
- Hyldgaard, M., Mygind, T., Meyer, R.L., 2012. Essential oils in food preservation: mode of action, synergies, and interactions with food matrix components. *Frontiers in Microbiology* 3, 12.
- Jiang, Y., Joyce, D.C., 2003. ABA effects on ethylene production, PAL activity, anthocyanin and phenolic contents of strawberry fruit. *Plant Growth Regulation* 39, 171-174.
- Kader, A.A., 1986. Potential applications of ionizing radiation in postharvest handling of fresh fruits and vegetables. *Food Technology* 40, 117-121.
- Kalt, W., Prange, R., Lidster, P., 1993. Postharvest color development of strawberries: Influence of maturity, temperature and light. *Canadian Journal of Plant Science* 73, 541-548.
- Kang, J.H., Jeon, Y.J., Min, S.C., 2021. Effects of packaging parameters on the microbial decontamination of Korean steamed rice cakes using in-package atmospheric cold plasma treatment. *Food Science and Biotechnology* 30, 1535-1542.

- Khan, A., Khan, R.A., Salmieri, S., Le Tien, C., Riedl, B., Bouchard, J., Chauve, G., Tan, V., Kamal, M.R., Lacroix, M., 2012. Mechanical and barrier properties of nanocrystalline cellulose reinforced chitosan based nanocomposite films. *Carbohydrate Polymers* 90, 1601-1608.
- Khan, A., Salmieri, S., Frascini, C., Bouchard, J., Riedl, B., Lacroix, M., 2014. Genipin cross-linked nanocomposite films for the immobilization of antimicrobial agent. *ACS Applied Materials and Interfaces* 6, 15232-15242.
- Khodaei, D., Hamidi-Esfahani, Z., 2019. Influence of bioactive edible coatings loaded with *Lactobacillus plantarum* on physicochemical properties of fresh strawberries. *Postharvest Biology and Technology* 156, 110944.
- Lacroix, M., Follett, P., 2015. Combination irradiation treatments for food safety and phytosanitary uses. *Stewart Postharvest Review* 11, 1-10.
- Lafarga, T., Colás-Medà, P., Abadías, M., Aguiló-Aguayo, I., Bobo, G., Viñas, I., 2019. Strategies to reduce microbial risk and improve quality of fresh and processed strawberries: A review. *Innovative Food Science and Emerging Technologies* 52, 197-212.
- Laidler, M.R., Tourdjman, M., Buser, G.L., Hostetler, T., Repp, K.K., Leman, R., Samadpour, M., Keene, W.E., 2013. *Escherichia coli* O157: H7 infections associated with consumption of locally grown strawberries contaminated by deer. *Clinical Infectious Diseases* 57, 1129-1134.
- Li, L., Song, W., Shen, C., Dong, Q., Wang, Y., Zuo, S., 2020. Active packaging film containing oregano essential oil microcapsules and their application for strawberry preservation. *Journal of Food Processing and Preservation* 44, 14799.
- Maherani, B., Hossain, F., Criado, P., Ben-Fadhel, Y., Salmieri, S., Lacroix, M., 2016. World market development and consumer acceptance of irradiation technology. *Foods* 5, 79.
- Majeed, A., Muhammad, Z., Majid, A., Shah, A., Hussain, M., 2014. Impact of low doses of gamma irradiation on shelf life and chemical quality of strawberry (*Fragaria x ananassa*) CV.'CORONA'. *JAPS: Journal of Animal and Plant Sciences* 24.
- Maraei, R.W., Elsayy, K.M., 2017. Chemical quality and nutrient composition of strawberry fruits treated by γ -irradiation. *Journal of Radiation Research and Applied Sciences* 10, 80-87.
- Metak, A.M., Nabhani, F., Connolly, S.N., 2015. Migration of engineered nanoparticles from packaging into food products. *LWT - Food Science and Technology* 64, 781-787.
- Mitcham, E., 2007. Quality of berries associated with preharvest and postharvest conditions. *Food Science and Technology-New York-Marcel Dekker-* 168, 207.

- Mith, H., Dure, R., Delcenserie, V., Zhiri, A., Daube, G., Clinquart, A., 2014. Antimicrobial activities of commercial essential oils and their components against food-borne pathogens and food spoilage bacteria. *Food Science and Nutrition* 2, 403-416.
- Montero, Y., Souza, A.G., Oliveira, É.R., Rosa, D.d.S., 2021. Nanocellulose functionalized with cinnamon essential oil: A potential application in active biodegradable packaging for strawberry. *Sustainable Materials and Technologies* 29, 00289.
- Motlagh, N.V., Aliabadi, M., Rahmani, E., Ghorbanpour, S., 2020. The Effect of Nano-Silver Packaging on Quality Maintenance of Fresh Strawberry. *International Journal of Nutrition and Food Engineering* 14, 123-128.
- Mousavian, D., Mohammadi Nafchi, A., Nouri, L., Abedinia, A., 2021. Physicomechanical properties, release kinetics, and antimicrobial activity of activated low-density polyethylene and orientated polypropylene films by Thyme essential oil active component. *Journal of Food Measurement and Characterization* 15, 883-891.
- Oufedjikh, H., Mahrouz, M., Amiot, M.J., Lacroix, M., 2000. Effect of γ -irradiation on phenolic compounds and phenylalanine ammonia-lyase activity during storage in relation to peel injury from peel of *Citrus clementina* Hort. Ex. Tanaka. *Journal of Agricultural and Food Chemistry* 48, 559-565.
- Oussalah, M., Caillet, S., Lacroix, M., 2006. Mechanism of action of Spanish oregano, Chinese cinnamon, and savory essential oils against cell membranes and walls of *Escherichia coli* O157: H7 and *Listeria monocytogenes*. *Journal of Food Protection* 69, 1046-1055.
- Paniagua, C., Posé, S., Morris, V.J., Kirby, A.R., Quesada, M.A., Mercado, J.A., 2014. Fruit softening and pectin disassembly: an overview of nanostructural pectin modifications assessed by atomic force microscopy. *Annals of botany* 114, 1375-1383.
- Peretto, G., Du, W.-X., Avena-Bustillos, R.J., Sarreal, S.B.L., Hua, S.S.T., Sambo, P., McHugh, T.H., 2014. Increasing strawberry shelf-life with carvacrol and methyl cinnamate antimicrobial vapors released from edible films. *Postharvest Biology and Technology* 89, 11-18.
- Petchwattana, N., Naknaen, P., 2015. Utilization of thymol as an antimicrobial agent for biodegradable poly(butylene succinate). *Materials Chemistry and Physics* 163, 369-375.
- Radfar, R., Hosseini, H., Farhodi, M., Ghasemi, I., Srednicka-Tober, D., Shamloo, E., Khaneghah, A.M., 2020. Optimization of antibacterial and mechanical properties of an active LDPE/starch/nanoclay nanocomposite film incorporated with date palm seed extract using D-optimal mixture design approach. *International Journal of Biological Macromolecules* 158, 790-799.

- Requena, R., Vargas, M., Chiralt, A., 2017. Release kinetics of carvacrol and eugenol from poly(hydroxybutyrate-co-hydroxyvalerate) (PHBV) films for food packaging applications. *European Polymer Journal* 92, 185-193.
- Sallato, B., Torres, R., Zóffoli, J.P., Latorre, B., 2007. Effect of boscalid on postharvest decay of strawberry caused by *Botrytis cinerea* and *Rhizopus stolonifer*. *Spanish Journal of Agricultural Research* 5, 67-78.
- Salmieri, S., Islam, F., Khan, R.A., Hossain, F.M., Ibrahim, H.M.M., Miao, C., Hamad, W.Y., Lacroix, M., 2014. Antimicrobial nanocomposite films made of poly(lactic acid)-cellulose nanocrystals (PLA-CNC) in food applications: part A—effect of nisin release on the inactivation of *Listeria monocytogenes* in ham. *Cellulose* 21, 1837-1850.
- Salmieri, S., Lacroix, M., 2006. Physicochemical properties of alginate/polycaprolactone-based films containing essential oils. *Journal of Agricultural and Food Chemistry* 54, 10205-10214.
- Shankar, S., Khodaei, D., Lacroix, M., 2021. Effect of chitosan/essential oils/silver nanoparticles composite films packaging and gamma irradiation on shelf life of strawberries. *Food Hydrocolloids* 117, 106750.
- Shankar, S., Teng, X., Rhim, J.-W., 2014. Properties and characterization of agar/CuNP bionanocomposite films prepared with different copper salts and reducing agents. *Carbohydrate Polymers* 114, 484-492.
- Sharmin, N., Khan, R.A., Salmieri, S., Dussault, D., Lacroix, M., 2012. Fabrication and Characterization of Biodegradable Composite Films Made of Using Poly(caprolactone) Reinforced with Chitosan. *Journal of Polymers and the Environment* 20, 698-705.
- Srinivasa, P., Baskaran, R., Ramesh, M., Harish Prashanth, K., Tharanathan, R., 2002. Storage studies of mango packed using biodegradable chitosan film. *European Food Research and Technology* 215, 504-508.
- Srisa, A., Harnkarnsujarit, N., 2020. Antifungal films from trans-cinnamaldehyde incorporated poly(lactic acid) and poly(butylene adipate-co-terephthalate) for bread packaging. *Food Chemistry* 333, 127537.
- Tawakkal, I.S.M.A., Cran, M.J., Bigger, S.W., 2016. Release of thymol from poly(lactic acid)-based antimicrobial films containing kenaf fibres as natural filler. *LWT - Food Science and Technology* 66, 629-637.
- Tezotto-Uliana, J.V., Berno, N.D., Saji, F.R.Q., Kluge, R.A., 2013. Gamma radiation: An efficient technology to conserve the quality of fresh raspberries. *Scientia Horticulturae* 164, 348-352.

- Treviño-Garza, M.Z., García, S., del Socorro Flores-González, M., Arévalo-Niño, K., 2015. Edible active coatings based on pectin, pullulan, and chitosan increase quality and shelf life of strawberries (*Fragaria ananassa*). *Journal of Food Science* 80, 1823-1830.
- Turgis, M., Vu, K.D., Dupont, C., Lacroix, M., 2012. Combined antimicrobial effect of essential oils and bacteriocins against foodborne pathogens and food spoilage bacteria. *Food Research International* 48, 696-702.
- Vatansever, E., Arslan, D., Sarul, D.S., Kahraman, Y., Gunes, G., Durmus, A., Nofar, M., 2020. Development of CNC-reinforced PBAT nanocomposites with reduced percolation threshold: a comparative study on the preparation method. *Journal of Materials Science* 55, 15523-15537.
- Vu, K.D., Hollingsworth, R.G., Leroux, E., Salmieri, S., Lacroix, M., 2011. Development of edible bioactive coating based on modified chitosan for increasing the shelf life of strawberries. *Food Research International* 44, 198-203.
- Weisany, W., Amini, J., Samadi, S., Hossaini, S., Yousefi, S., Struik, P.C., 2019. Nano silver-encapsulation of *Thymus daenensis* and *Anethum graveolens* essential oils enhances antifungal potential against strawberry anthracnose. *Industrial Crops and Products* 141, 111808.
- WHO, 1994. Irradiation of strawberries. A compilation of technical data for its authorization and control. Food and Agriculture Organization of the United Nations.
- Yang, F.M., Li, H.M., Li, F., Xin, Z.H., Zhao, L.Y., Zheng, Y.H., Hu, Q.H., 2010. Effect of nano-packing on preservation quality of fresh strawberry (*Fragaria ananassa* Duch. cv Fengxiang) during storage at 4 degrees C. *Journal of Food Science* 75, 236-240.
- Yoshida, Y., Koyama, N., Tamura, H., 2002. Color and anthocyanin composition of strawberry fruit: Changes during fruit development and differences among cultivars, with special reference to the occurrence of pelargonidin 3-malonylglucoside. *Journal of the Japanese Society for Horticultural Science* 71, 355-361.
- Zhang, C., Li, W., Zhu, B., Chen, H., Chi, H., Li, L., Qin, Y., Xue, J., 2018. The Quality Evaluation of Postharvest Strawberries Stored in Nano-Ag Packages at Refrigeration Temperature. *Polymers* 10, 894.

Supplementary data Table 9.1. Weight loss (%) of strawberries under different active film packaging treatments during storage.

Storage day	Weight loss (%)				
	Control (Group-1)	Group-2	Group-3	Group-4	Group-5
1	0±0 ^{aA}	0±0 ^{aA}	0±0 ^{aA}	0±0 ^{aA}	0±0 ^{aA}
2	0.96±0.1 ^{bB}	0.80±0.1 ^{bB}	0.68±0.1 ^{bB}	0.62±0.1 ^{bB}	0.06±0.05 ^{bA}
3	6.80±4.2 ^{cD}	4.10±2.3 ^{cC}	1.28±0.2 ^{cB}	0.90±0.1 ^{bA}	0.20±0.08 ^{bA}
5	12.3±5.0 ^{dE}	9.20±1.2 ^d _D	2.78±1.6 ^{dC}	1.62±0.2 ^{bB}	0.62±0.31 ^{bA}
7	20.3±5.0 ^{eF}	12.8±1.0 ^e _D	3.48±1.4 ^{dC}	3.90±3.2 ^{cB}	1.35±0.70 ^{cA}
9	24.3±8.0 ^{fE}	20.7±6.7 ^{fD}	15.1±5.6 ^{eC}	5.86±4.8 ^{dB}	2.80±0.57 ^{dA}
12	40.9±7.0 ^{gE}	23.1±5.0 ^g _D	21.6±6.8 ^{fC}	8.07±3.3 ^{eB}	4.48±1.30 ^{eA}

Values are means±standard error. Within each column means with the same lowercase letter are not significantly different ($P > 0.05$) and within each row means with same uppercase letter are not significantly different ($P > 0.05$).

Supplementary data Table 9.2. Weight loss (%) of strawberries by placing the optimized LDPE nanocomposite films at different position inside the PET clamshell.

Storage day	Weight loss (%)		
	Film on the bottom (alone)	Film on the top (alone)	Film both on the bottom and on the top
2	0.70±0.32 ^{aA}	0.69±0.21 ^{aA}	0.62±0.10 ^{aA}
3	0.93±0.29 ^{bA}	1.00±0.18 ^{aA}	0.90±0.13 ^{bA}
5	1.70±0.33 ^{cA}	2.21±0.56 ^{bA}	1.62±0.16 ^{cA}
7	3.66±1.22 ^{dA}	3.75±1.30 ^{cA}	3.90±2.10 ^{dA}
9	5.8±1.58 ^{eA}	5.96±1.25 ^{dB}	5.86±3.80 ^{eA}
12	8.31±2.55 ^{fA}	8.28±2.33 ^{eA}	8.07±3.20 ^{fA}

Values are means±standard error. Within each column means with the same lowercase letter are not significantly different ($P > 0.05$) and within each row means with same uppercase letter are not significantly different ($P > 0.05$).

Supplementary data Table 9.3. Decay (%) of strawberries under different active film packaging treatments during storage.

Storage day	Decay of fruits (%)				
	Control (Group-1)	Group-2	Group-3	Group-4	Group-5
1	0±0 ^{aA}	0±0 ^{aA}	0±0 ^{aA}	0±0 ^{aA}	0±0 ^{aA}
2	0±0 ^{aA}	0±0 ^{aA}	0±0 ^{aA}	0±0 ^{aA}	0±0 ^{aA}
3	4.15±0.8 ^{bC}	1.67±2.9 ^{bB}	0±0 ^{aA}	0±0 ^{aA}	0±0 ^{aA}
5	7.48±6.5 ^{cD}	6.31±2.2 ^{cC}	1.51±1.6 ^{bB}	0±0 ^{aA}	0±0 ^{aA}
7	16.0±5.0 ^{dE}	11.0±2.1 ^{dD}	3.10±5.6 ^{cC}	1.66±0.8 ^{bB}	0±0 ^{aA}
9	32.0±8.0 ^{eE}	20.1±7.4 ^{eD}	15.3±4.8 ^{dC}	6.45±2.1 ^{cB}	2.00±0.9 ^{aA}
12	56.1±6.7 ^{fD}	26.0±6.3 ^{fC}	25.0±7.4 ^{eC}	8.11±3.9 ^{dB}	3.33±2.5 ^{bA}

Values are means±standard error. Within each column means with the same lowercase letter are not significantly different ($P > 0.05$) and within each row means with same uppercase letter are not significantly different ($P > 0.05$).

Supplementary data Table 9.4. Decay (%) of strawberries after placing the optimized LDPE nanocomposite films at different positions inside the PET clamshell.

Storage day	Decay of fruits (%)		
	Film on the bottom (alone)	Film on the top (alone)	Film both on the bottom and on the top
2	0.56±0.3 ^{aB}	0.55±0.2 ^{aB}	0.00±0.0 ^{aA}
3	1.3±0.4 ^{bB}	2.10±0.6 ^{bC}	0.00±0.0 ^{aA}
5	2.9±0.6 ^{cB}	3.20±1.5 ^{cB}	0.00±0.0 ^{aA}
7	5.8±1.9 ^{dC}	4.60±2.6 ^{dB}	1.66±0.8 ^{bA}
9	7.3±3.4 ^{eB}	6.90±2.3 ^{eA}	6.45±2.1 ^{cA}
12	9.62±3.1 ^{fB}	8.63±3.3 ^{fA}	8.11±3.9 ^{dA}

Values are means±standard error. Within each column means with the same lowercase letter are not significantly different ($P > 0.05$) and within each row means with same uppercase letter are not significantly different ($P > 0.05$).

Supplementary data Table 9.5. Color measurement (Hunter L*, a*, b* values) of the strawberries when placing the optimized LDPE nanocomposite films at different positions inside the PET clamshell.

Storage day	Color measurement								
	Film on the bottom (alone)			Film on the top (alone)			Film both on the bottom and on the top		
	L* (lightness)	a* (redness)	b* (yellowness)	L* (lightness)	a* (redness)	b* (yellowness)	L* (lightness)	a* (redness)	b* (yellowness)
0	40.3±3.6 ^{dB}	36.1±2.6 ^{cA}	19.6±1.9 ^{dB}	39.6±5.2 ^{cB}	37.5±6.1 ^{dB}	18.6±5.1 ^{cA}	38.2±3.5 ^{dA}	36.2±6.9 ^{cA}	18.2±2.1 ^{cA}
1	38.6±3.3 ^{cA}	36.5±6.3 ^{bA}	18.9±2.4 ^{cA}	39.2±2.9 ^{cA}	36.6±5.2 ^{cA}	18.9±2.1 ^{cA}	38.5±2.9 ^{dA}	35.9±5.4 ^{bA}	18.0±3.1 ^{cA}
5	39.1±2.9 ^{dB}	35.4±2.3 ^{bA}	17.6±4.1 ^{bA}	36.9±2.8 ^{bA}	34.6±2.8 ^{bA}	17.7±2.0 ^{bA}	36.2±3.8 ^{cA}	35.5±6.3 ^{bA}	17.5±2.8 ^{bA}
7	36.6±6.2 ^{bA}	35.1±3.2 ^{bA}	17.1±2.3 ^{bA}	36.1±6.3 ^{bA}	34.1±1.8 ^{bA}	16.3±0.9 ^{aA}	35.8±3.6 ^{bA}	34.8±6.0 ^{aA}	17.2±6.1 ^{bA}
10	35.2±2.8 ^{bA}	34.1±1.9 ^{aA}	16.8±2.7 ^{aA}	35.9±4.2 ^{aA}	33.6±7.1 ^{aA}	16.8±3.2 ^{aA}	35.2±5.1 ^{bA}	34.6±2.9 ^{aA}	17.9±1.4 ^{bB}
12	34.3±5.1 ^{aA}	33.2±2.8 ^{aA}	16.7±1.8 ^{aA}	35.1±2.9 ^{aA}	33.2±3.9 ^{aA}	16.1±1.1 ^{aA}	34.2±1.5 ^{aA}	34.2±6.1 ^{aA}	16.8±2.4 ^{aA}

Values are means±standard error. Within each column means with the same lowercase letter are not significantly different (P > 0.05) and within each row means of same group (Lightness L*, redness a* and yellowness b*) with same uppercase letter are not significantly different (P > 0.05).

Chapter 10

General discussion and conclusion

General discussion

In the current study, we developed five active formulations (mixture of essential oils [EOs] either with citrus extract [CE] or with silver nanoparticles [AgNPs]). Based on the literature survey, seven EOs, two citrus extract and four silver nanoparticles (AgNPs) were selected for evaluating the most efficient antimicrobial, antifungal and insecticidal agents against two most common foodborne pathogenic bacteria *E. coli* O157:H7, *S. Typhimurium*, three spoilage fungi *A. niger*, *P. chrysogenum* and *M. circinelloides*, and one major stored product insect pest *S. oryzae* (rice weevil). In chapter 3, the antibacterial and antifungal effects of six plant-derived (EOs) (cinnamon EO, Savory thyme EO, Asian formulation, Mediterranean EO, Southern formulation and citrus EO) and two types of citrus extracts (CEs) (organic citrus extract [OCE] and natural citrus extract [NCE]) were tested to control the growth of pathogenic bacteria (*Salmonella* Typhimurium and *Escherichia coli* O157:H7) and three spoilage fungi (*A. niger*, *P. chrysogenum*, and *M. circinelloides*) in stored rice. A broth microdilution assay was performed to determine the minimal inhibitory concentration (MIC) of tested EOs and CEs, and the results showed that cinnamon EO, Mediterranean EO, Southern formulation, citrus EO, OCE, and NCE had the highest antimicrobial and antifungal activity (MIC ranges between 312.5 ppm to 2500 ppm). The interactions between fourteen different combinations (between EO and CE) were performed using the checkerboard method. Binary combination of Mediterranean EO and OCE showed synergistic activity against tested pathogenic bacteria and spoilage fungi. In addition, a centroid mixture design was used to develop active formulations by predicting optimal concentrations of combining more than two EO/CEs for increased antibacterial/antifungal activity. A mixture of four formulations (625 ppm OCE, 313 ppm Mediterranean EO, 625 ppm citrus EO, and 313 ppm cinnamon EO) named as active formulation 1, and the mixture from five formulations (625 ppm NCE, 625 ppm Asian formulation, 313 ppm Southern formulation, 625 ppm cinnamon EO, and 313 ppm savory thyme EO) named as active formulation 2, were formulated and tested for their microbicidal effectiveness. *In situ* tests with rice showed a significant reduction ($P \leq 0.05$) of all tested pathogenic bacteria and fungi from the vapor of active formulations 1 and 2 after 28 days of storage (Begum *et al.*, 2022b).

In chapter 4, the MIC of silver nanoparticles (AgNPs), named AGC 1, AGC 0.5, AGPP and AGPPH, was measured using the broth microdilution assay against all tested bacteria and spoilage fungi. All AgNPs showed strong antibacterial and antifungal properties and the MIC values ranged between 7.8 to 62.5 ppm against *E. coli* O157:H7, *S. Typhimurium*, *A. niger*, *P. chrysogenum* and *M. circinelloides* (Begum *et al.*, 2022a). AgNPs showed strong antibacterial and

antifungal properties because of their small size that can create pits on the cell surface and damage the microbial cell, moreover, they can react with microbial proteins and enzymes in ribosome thus disrupting their functions (Emamifar *et al.*, 2010; Bocate *et al.*, 2019). Using the checkerboard method, the possible interaction between the EOs and the AgNPs was determined by calculating fractional inhibitory concentration (FIC) values. The combination of two or more EOs and AgNPs (Active combination 1: AGPPH+cinnamon EO, Active combination 2: AGC 0.5+Mediterranean formulation+citrus EO, Active combination 3: AGPP+cinnamon EO+Asian formulation+lavang EO) showed synergistic effects (FIC < 1.0) against all tested bacteria and fungi. The vapor of these active combinations (ACs) (AC-1, AC-2 and AC-3) significantly ($P \leq 0.05$) reduced colony diameter (A), maximum growth rate (V_m) and extended the lag phase (λ) from 1 to 5 days for all tested bacteria and fungi. The vapor effect of three ACs (AC-1, AC-2 and AC-3) significantly ($P \leq 0.05$) reduced the bacterial and fungal growth in stored rice for 28 days at 27 °C (Begum *et al.*, 2022a).

Though EOs have strong antibacterial, antifungal and insecticidal properties, the application of EOs or mixture of EOs in the food industry is still limited because of their highly volatile nature, low water solubility, their chemical instability due to environmental factors such as temperature, moisture, pH, oxidation, light, and isomerization (Das *et al.*, 2021b). These drawbacks of EOs or mixture of EOs can be reduced by developing an oil-in-water nanoemulsion (droplet size from 2 to 200 nm) with improved properties such as transparency, physical stability, increased bioactivity, and enhanced encapsulation efficiency (Hossain *et al.*, 2018; Llinares *et al.*, 2018). To do so, our two previously developed active formulations (AF-1: OCE+Mediterranean EO+citrus EO+cinnamon EO; and AF-2: NCE+Asian formulation+Southern formulation+cinnamon EO+savory thyme EO) (Publication 2) and three active combinations (AC-1: AGPPH+cinnamon EO, AC-2: AGC 0.5+Mediterranean formulation+citrus EO, AC-3: AGPP+cinnamon EO+Asian formulation+lavang EO) (Chapter 4) were passed through high pressure microfluidisation at different pressures and numbers of cycles to obtain a stable oil-in-water nanoemulsion. In chapter 5, a central composite design (CCD) was applied with three independent variables (microfluidisation pressure, number of cycles and concentration of emulsifier) and their responses (ζ -potential, polydispersity index [PDI], droplet size and encapsulation efficiency [EE]) to optimize the microfluidisation, pressure, number of cycles and emulsifier concentration for stable nanoemulsion of AF-1 and AF-2. AF-1 was optimized at 8000 PSI pressure, 2 cycles and 2 % Tween 80 having the highest EE (77 %) and ζ -potential (49 mV), lowest size (116 nm), and PDI (0.17) values, while the AF-2 optimized at 15,000 PSI at 3rd cycle with 2 % emulsifier (Tween 80)

having the highest EE (79 %) and ζ -potential (32.3 mV), and lowest size (40 nm) and lowest PDI (0.2) values. In chapter 8, the nanoemulsions of AC-1, AC-2 and AC-3 were optimized at 8000 PSI pressure (2nd cycle), 10,000 PSI (3 cycle) and 6000 PSI (4 cycle), respectively. The stable nanoemulsion of ACs significantly increased the encapsulation efficiency (EE) ranges between 78 to 85 % as compared to the coarse emulsions (ranges between 19 to 32 %). It is well known that the higher the ζ -potential value, the greater the chance for obtaining an electrostatically stable nanoemulsion (Asmawati *et al.*, 2014; Cheng *et al.*, 2016; Hossain *et al.*, 2018). Nanoemulsions with very high (+30 mV) or very low (-30 mV) ζ -potential values are considered electrostatically stable emulsions (Asmawati *et al.*, 2014). Moreover, the non-ionic emulsifier Tween 80 has a strong interaction with AFs (mixture of EOs and CEs) or ACs (mixture of EOs and AgNPs) by adsorbing quickly at the oil/water interface, thus producing small particles with better stability in the dispersion system (Hossain *et al.*, 2018).

The aim of the current study was to develop active packing films using biodegradable polymers. To do so, we developed three different types of active packaging films (PBAT-, CH- and PLA-based) by impregnating active formulations (mixture of essential oils [EOs] with citrus extracts or mixture of EOs with silver nanoparticles [AgNPs]) for application in stored yogurt and bagged cereal grains for preservation during storage against foodborne pathogenic bacteria, spoilage fungi and insect pests. Moreover, cellulose nanocrystals (CNCs) were used as reinforcing agents with biopolymers. Moreover, CNCs have some interesting properties such as abundance in nature, biodegradability, low cost, non-toxic nature and renewability that make them good potential reinforcing agents. The addition of CNCs as reinforcing agents into PBAT-, CH- and PLA-based films improved the mechanical and barrier properties of the films as well as improved the release properties of the active ingredients (either active formulations or active combinations) during storage (Azeredo *et al.*, 2010; Hossain *et al.*, 2018; Hossain *et al.*, 2019a). CNC is one of the abundant biopolymers extracted from wood, cotton, plant-based sources, bacteria, algae, etc. (Khan *et al.*, 2012). The addition of CNCs improved the tensile strength (TS), tensile modulus (TM) and reduced the WVP of the CH-based composite films by 24 %, 76 % and 41 %, respectively, as compared to the neat CH-based film (chapter 5). The increase in TS might be due to interactions between the cationic amine groups present in the CH polymer and the anionic sulfate groups in the CNC, which effectively increased the interface between the filler and the matrix and thus leading to higher TS values (de Mesquita *et al.*, 2010). A percolated network might be created when CNC incorporated into polymeric matrices by H-bonding which can reduce the molecular mobility and free volume of polymeric matrices and create more obstacles for water vapor

diffusion, and thus reduced WVP (Pereda *et al.*, 2012). The incorporation of CNCs showed a significantly slower release (from 20 to 50 %) of the active formulations from the CH-, PBAT- and PLA-based composite films compared to the film without CNCs (chapters 5 and 7) ($P \leq 0.05$). Similarly, incorporation of CNCs greatly reduced the release of active combinations (AC-1, AC-2 and AC-3) from the CH-, PBAT- and PLA-based nanocomposite films (chapter 8). CNCs improve and slow the release of active formulations from nanocomposite matrices by forming a percolation network connected by H-bonds and helping in the homogenous distribution of the nanoemulsion of active formulations within the polymeric matrices (Boumail *et al.*, 2013). Incorporation of CNCs into the polymeric matrices is a promising way to develop bioactive packaging films for food preservation because CNCs can preserve the active ingredients for long storage times as well as their bioavailability, biocompatibility and biodegradability. Moreover, CNCs do not have any negative impact on human health and the environment (Endes *et al.*, 2016).

In chapter 5 and chapter 8, optimized nanoemulsions of AFs and ACs were encapsulated into chitosan-based (CH) biopolymeric matrices and fabricated bioactive CH-based nanocomposite films reinforced with CNCs. The fabricated bioactive CH-based nanocomposite films were applied to control two pathogenic bacteria (*E. coli* O15:H7, *S. Typhimurium*), three spoilage fungi (*A. niger*, *P. chrysogenum* and *M. circinelloides*) and one stored product insect pest (*S. oryzae*) in stored rice for 2 months. *In situ* tests rice with bioactive CH-based nanocomposite films containing the nanoemulsion of AF-1 and AF-2 (mixture of EOs and CEs) reduced bacterial growth by 50 to 58.4 % bacterial and fungal growth by 58 to 71.4 % as compared to the control samples in stored rice after 8 weeks (chapter 5), while the bioactive CH-based nanocomposite films incorporated with ACs reduced the bacterial growth by 20 to 50 % and fungal growth by 51 to 72 % in accordance with control samples in stored rice after 8 weeks at 28 °C (chapter 8). Two active formulations (AF-1 and AF-2) and three active combinations (AC-1, AC-2 and AC-3) were also encapsulated into poly (butylene adipate-co-terephthalate) (PBAT) and poly lactic acid (PLA) to fabricate bioactive PBAT- and PLA-based nanocomposite films for food preservation (chapters 6 and 8). PBAT and PLA-based nanocomposite films were developed using either AFs or ACs, CNCs as reinforcing agents and plasticizers (glycerol). *In situ* application of fabricated PBAT- and PLA-based nanocomposite films were applied in stored rice for 8 weeks to control the growth of foodborne pathogenic bacteria (*E. coli* O157:H7 and *S. Typhimurium*) and three spoilage fungi (*A. niger*, *P. chrysogenum* and *M. circinelloides*) at 28 °C. Bioactive PBAT-based nanocomposite films containing AFs showed stronger antibacterial and antifungal activities in *in situ* tests in rice and reduced the bacterial and fungal growth by 43 to 66 % and 53 to 71 % as compared to the control

samples, respectively (chapter 6). The bioactive PLA-based nanocomposite films containing either AFs or ACs showed less effective antibacterial and antifungal properties as compared to the bioactive PBAT-based nanocomposite films. The bioactive PBAT-based nanocomposite films containing ACs (AC-1, AC-2 and AC-3) reduced the bacterial growth by 23 to 52 % and fungal growth by 37 to 68 % as compared to control samples in stored rice after 8 weeks at 28 °C. When the vapor of active formulations or active combinations was released from the CH-, PBAT- and PLA-based nanocomposite films and exposed to the bacterial and fungal growth, it might interact with the inner and outer membrane proteins, intracellular targets, affecting the energy-generating process, disrupting the lipopolysaccharides and outer membrane, thus leading to cell death (Hyldgaard *et al.*, 2012b; Mith *et al.*, 2014). Moreover, the encapsulation of active agents into polymeric matrices allowed a sustained release of active ingredients from the nanoemulsions of AFs or ACs by prolonging the efficacy of bioactive nanocomposite films during 8 weeks of storage in rice. Combining bioactive nanocomposite films (CH- and PBAT-based) with γ -irradiation treatment at 750 Gy significantly ($P \leq 0.05$) increased the microbial (both bacterial and fungal growth) reduction by 58 to 93 % as compared to control samples. When irradiation is applied along with active packaging, irradiation could increase contact between the microbial cell and active components released from the bioactive packaging and facilitate cell destruction by damaging the chemical bonds between microbial DNA and this could alter the membrane permeability and could affect cell's activity (Caillet *et al.*, 2005; Caillet and Lacroix, 2006; Ayari *et al.*, 2012; Begum *et al.*, 2020a). Moreover, application of bioactive films with irradiation could lower the radiation dose for controlling the growth of foodborne pathogenic bacteria and spoilage fungi in stored cereal grains.

Based on the findings from Chapter 3, six EOs (cinnamon EO, savory thyme EO, Asian formulation, Mediterranean EO, Southern formulation and citrus EO), two citrus extract (CEs) (OCE, NCE) and two active formulations (AF-1 and AF-2) were tested against *S. oryzae* (rice weevil) (Chapter 7). The study showed the insecticidal activity of six EOs, two CEs and two AFs against *S. oryzae* using fumigant toxicity tests. While two AFs and some EOs showed strong toxicities against *S. oryzae*, like AF-1 and AF-2, others showed moderate to lower toxicity (e.g., NCE and OCE) after 24 h of exposure. At the lowest contact time (24 h), the AF-1 displayed the highest % mortality of 12 and 31 % against *S. oryzae* when exposed to 0.2 and 0.4 $\mu\text{L/mL}$ of AF-1 ($P \leq 0.05$), respectively. A quantity of 0.6, 0.8, and 1.6 $\mu\text{L/mL}$ AF-2 showed 32, 38, and 52 % of insect mortality ($P \leq 0.05$), respectively, at the shortest exposure time of 24 h. A 32, 39, and 43 % ($P \leq 0.05$) insect mortality was found when *S. oryzae* was exposed to 0.6, 0.8, and 1.6 $\mu\text{L/mL}$ AF-1, respectively, at 24 h. Cinnamon and Mediterranean EOs showed 41 and 30 % mortality ($P \leq 0.05$)

of insects, respectively, at 1.6 $\mu\text{L}/\text{mL}$ after 24 h. It is noticeable that the % mortality of insects was higher when treated with a higher concentration of insecticidal agents (Chapter 7). The presence of monoterpenoids in individual and mixture of EOs/CEs are responsible for insecticidal efficiency because the lipophilic volatile nature of monoterpenoids can penetrate insects and disrupt their physiological functions (Khani *et al.*, 2017). Because active formulations contain several major and minor chemical ingredients, they showed multiple ways to control insect growth with less chance of the insect becoming resistant. For example, some minor chemical ingredients may not have strong insecticidal activity when applied alone, but they may show an increased activity when exposed to other chemical ingredients (Bakkali *et al.*, 2008; Hossain *et al.*, 2019b). Hence, mixtures of EOs and CEs (active formulations) displayed higher fumigant and acetylcholinesterase (AChE) inhibitory activity than individual EO or CE.

The bioactive PBAT- and PLA-based nanocomposite films showed strong antibacterial and antifungal properties in stored yogurt for 8 weeks at 4 °C against *E. coli* O157:H7, *S. Typhimurium*, *A. niger*, *P. chrysogenum* and *M. circinelloides*. Bioactive PBAT-based nanocomposite films containing ACs (AC-1, AC-2 and AC-3) showed the strongest antibacterial and antifungal properties compared to the bioactive PLA-based nanocomposite films (chapter 8). The bioactive PBAT-based nanocomposite films were able to reduce the bacterial load in stored yogurt by 47 to 81.2 % by the end of the storage as compared to the control samples, while the bioactive PLA-based nanocomposite films were able to reduce the bacterial load by 25.6 to 53.2 % as compared to the control samples after 8 weeks of storage at 4 °C. In case of fungi, the bioactive PBAT-based nanocomposite films showed significantly higher reduction of all tested fungal growth by 50 to 93 % as compared to control samples in stored yogurt after 8 weeks, while the bioactive PLA-based nanocomposite films reduced the fungal growth by 32.4 to 65 % as compared to the control samples in stored yogurt after 8 weeks. Bioactive PLA-based nanocomposite films showed less antibacterial and antifungal properties because of the fast release of active ingredients from the PLA-based matrix as compared to the PBAT-based matrix. Release of active ingredients from polymeric matrices depends on several factors such as polymer morphology, polymer-active combination interactions, molecular weight distribution, polarity of the food simulants, temperature, solubility of the active compounds in food simulants, etc. (da Rosa *et al.*, 2020a). CNCs as reinforcing agents have greatly influenced the release of active ingredients from the bioactive polymeric matrices and prolonged the release of active ingredients (Hossain *et al.*, 2018; Hossain *et al.*, 2019a).

Based on the above results of the insecticidal and antimicrobial effectiveness of AFs (mixture of EOs and CEs) and ACs (mixture of EOs and AgNPs), three types of insecticidal films (CH-, PBAT- and PLA-based nanocomposite films) were developed to control the growth of the rice weevil (*S. oryzae*) in stored rice for 14 days at 28 °C. CNCs were reinforced into the three types of polymeric matrices as reinforcing agents (chapter 7 and chapter 8). The bioactive CH-, PBAT- and PLA-based nanocomposite films containing AFs (AF-1 and AF-2) caused 49 to 83 % insect mortality after 14 days of storage, while the control samples (without bioactive nanocomposite films) caused only 6 % mortality of insects after 14 days (chapter 7). Herein, the bioactive CH-based nanocomposite film containing a nanoemulsion of AF-2 showed the highest insecticidal properties (83 %) due to the smaller droplet size of the nanoemulsion (40 nm) as they have better insecticidal properties than the larger droplet size and this phenomenon was proven by several authors and current studies corroborated those findings (Anjali *et al.*, 2012; Suresh Kumar *et al.*, 2013; Choupanian *et al.*, 2017; Adak *et al.*, 2020). Combining γ -irradiation at 300 Gy with bioactive nanocomposite films containing AFs increased the mortality of insects between 92 to 100 % from day 7 to day 14 and the mortality was significantly ($P \leq 0.05$) higher as compared to the treatment alone (either by irradiation alone or by bioactive nanocomposite film alone). Similarly, bioactive CH-, PBAT- and PLA-based nanocomposite films containing ACs (AC-1, AC-2 and AC-3) showed strong insecticidal properties against *S. oryzae* from 44.4 to 78 % mortality in stored rice after 14 days (chapter 8). The significant difference in insect mortality depended on several factors such as the diffusion rate of the insecticidal compounds which mostly relied on several factors such as the nature and chemical structure of the molecules, type of polymer, the binding affinity between the polymeric matrices and the active compounds, solubility, temperatures, storage time, as well as the degree of crystallinity (Hossain *et al.*, 2019b; Sharma *et al.*, 2021). Application of γ -irradiation along with bioactive nanocomposite films containing ACs significantly increased the insects mortality in stored rice ($p \leq 0.05$). The application of bioactive nanocomposite films in stored rice can release active ingredients slowly during the storage period and kill the adult rice weevils, although fumigation of EOs has no effect on their eggs and larvae because of their location inside the kernel. Moreover, the application of low doses of γ -radiation could pass through the kernel and affect the development of insects in all stages. Thus, combining two treatments shows a synergistic effect to control insect pests in stored rice.

The high volatile nature and strong odor EOs have limited in their application as natural food preservatives. Combining two or more treatments that may permit a synergistic effect might be a possible way to overcome these limitations of the utilization of EOs. The vapor effect of EOs with

radiation treatments from different sources (X-ray and γ -ray) against foodborne pathogenic bacteria were studied to evaluate the effectiveness of a combined treatment of either X-rays or γ -rays with EOs to increase the radiosensitivity of pathogenic bacteria. In chapter 2, the microbicidal effectiveness of three foodborne illness pathogenic bacteria (*Escherichia coli*, *Salmonella* Typhimurium and *Listeria monocytogenes*) was tested for irradiation with low energy X-ray and cobalt-60 γ radiation at different dose rates with and without the presence of oregano/thyme EO in rice. The target doses were 0 (control), 250, 500, 750, 1000 and 1500 Gy with either γ irradiation (dose rates: 9.1, 3.9 and 0.22 kGy/h) or X-ray radiation (dose rate: 0.76 kGy/h). The study found that the different dose rate of γ radiation did not significantly affect ($P \leq 0.05$) D_{10} values (dose required to reduce 90 % of the pathogens) for tested γ -irradiated pathogens, however, X-ray irradiated pathogens required higher doses to achieve 90 % reduction in rice (Higher D_{10} values or lower microbicidal effectiveness). For example, when *E. coli* O157:H7, *S. Typhimurium* and *L. monocytogenes* were irradiated with high dose rate γ -radiation alone (9.1 kGy/h), the D_{10} values were 326, 266 and 236 Gy, respectively, while the samples were irradiated with oregano/thyme EO the D_{10} values were significantly ($P \leq 0.05$) reduced for the corresponding bacteria at 274, 218 and 219 Gy. When the irradiation is applied with the mixture of oregano/thyme EO fumigation, the radiosensitivity (RS) of bacteria (microbicidal effectiveness) significantly increased as compared to the irradiation treatment alone. When ionizing radiation is applied alone, it can break the chemical bonds in DNA in microbial cells, can alter the membrane permeability and other cellular functions (Caillet *et al.*, 2005; Caillet and Lacroix, 2006). Application of irradiation with EOs can affect the bacterial membrane integrity, murein composition, induce the release of cellular constituents, decrease internal pH and ATP (Caillet *et al.*, 2005; Caillet and Lacroix, 2006; Oussalah *et al.*, 2006). Moreover, combined treatments may facilitate contact between cell membrane and antimicrobial compounds, thus, leading to cell damage (Ayari *et al.*, 2012). Based on the results, further experiments were performed at 750 Gy irradiation with high dose rate γ -radiation to eliminate the bacterial and fungal contamination in stored bagged cereal grains.

In chapter 9, a commercial non-biodegradable but recyclable polymer, LDPE, was used to develop active LDPE-nanocomposite film by incorporating CNCs, active compound 1 (AC-1) [details in chapter 4] and glycerol as plasticizer for preservation of strawberries with and without the presence of γ -irradiation (Publication 4). The antibacterial and antifungal properties of active LDPE-based nanocomposite film (LDPE+CNCs+AC-1+Glycerol) tested against *E. coli* O157:H7, *S. Typhimurium*, *A. niger* and *P. chrysogenum* and the active LDPE-based nanocomposite film showed strong inhibitory capacity against all tested bacteria and fungi (IC, ≥ 75 %). Fresh

strawberries were preserved with different types of active LDPE-based nanocomposite films (Group 1 [control]: (LDPE+CNCs+Glycerol), Group 2: [LDPE + CNCs + Glycerol + AGPPH silver nanoparticles], Group 3: [LDPE + CNCs + Glycerol + cinnamon], Group 4: [LDPE + CNCs + Glycerol + active formulation], and Group 5: [LDPE + CNCs + Glycerol + active formulation + 0.5 kGy γ -radiation]) for 12 days at 4 °C. The weight loss (WL), % decay, firmness (N), color, and total phenolics and anthocyanins content of stored strawberries were tested in each group. The active LDPE-nanocomposite film with γ -irradiation (Group-5) significantly ($P \leq 0.05$) reduced the WL and % decay by 94 % of stored strawberries as compared to the control samples (Group-1) after 12 days. The active LDPE-based nanocomposite film with γ -irradiation acted synergistically to reduce the WL and % decay of fruits. Because nanoparticles presented in the AC-1 can create an indirect and longer path for passing the air, gas and moisture that are the key growth factors for microorganisms as well as EO is releasing the active ingredients during over the storage and preventing the microbial growth (Yang *et al.*, 2010; Motlagh *et al.*, 2020). The active nanocomposite film prevented water loss from the fruit's skin and reduced the shrinking of skin and kept them fresh as compared to the control samples. Moreover, the application of irradiation treatment could reduce the metabolic activity of the fruits and decrease the respiration rate and thus improve the WL properties of the stored fruits (Maraei and Elsayy, 2017). Also, γ -irradiation can penetrate fruit tissue and destroy the indigenous spoilage microorganisms present in tissues and wounds, thus preventing the decay (%) of stored fruits (Barkai-Golan, 2001). Total phenols (TP) (from 952 to 1711 mg/kg) and anthocyanins content (from 185 to 287 mg/kg) were significantly increased in Group-5 samples after 12 days of storage as compared to the control samples. Our study proved that the application of γ -irradiation combined with active films retained the phenolic content in stored strawberries. Because active LDPE-based nanocomposite film along with irradiation increased TP synergistically due to the activation of phenylalanine ammonia-lyase (PAL) enzyme which is important for the biosynthesis of phenolic contents in fruits (Oufedjikh *et al.*, 2000; Jiang and Joyce, 2003). Though the WVP of the films were not influenced by the types of antimicrobial agents, they did significantly ($P \leq 0.05$) change color and mechanical properties of the films. Therefore, the active LDPE-based nanocomposite film along with γ -irradiation could be an alternative method for preserving the strawberries without compromising their quality.

Sensory evaluation of the treated food with bioactive films is an important aspect to introduce new active packaging films in food industries because this test offers insights into consumers appreciation, acceptance of the products and quality assurance. Hence sensory properties of the

packed rice with bioactive CH-, PBAT-based nanocomposite films loaded with AFs (mixture of EOs and CEs) were assessed for 2 months of storage. There was no significant ($P > 0.05$) difference in color, odor, taste and global appreciation between treated and untreated cooked rice. In the food industry, sensory attributes (color, odor, taste) are important key parameters because the product marketing uses these attributes as their key features of the products, comparing the brand to other company' products and ensuring the products' quality and extended shelf-life. Hence the fabricated bioactive nanocomposite films containing active formulations for rice preservation could be an alternative way to develop green shelf-life enhancers by replacing synthetic preservatives.

Conclusion

Considering consumers' demand for high quality food products and preserving with natural antimicrobials or minimally processed foods, the food industries and food scientists are trying to develop new technologies for food preservation without changing their nutritional quality and safety. To do so, the current research of our team has developed four different types of bioactive nanocomposite films impregnating either with plant-derived EOs with citrus extract (CE) or EOs with silver nanoparticles (AgNPs) for application in stored yogurt, bagged cereal grain (rice) and strawberry to control the harmful effect of foodborne bacteria, spoilage fungi and stored product insect pests. Three bioactive nanocomposite films were chitosan (CH-), poly (butylene adipate-co-terephthalate) (PBAT), poly lactic acid (PLA) and low-density polyethylene (LDPE)-based polymeric matrices. Cellulose nanocrystals (CNCs) were reinforced in the polymeric matrices to develop novel bioactive nanocomposite films that significantly improved the mechanical and barrier properties of the films and significantly helped to retain the active formulations in nanocomposite films for longer times. Prolonging the retaining time of active formulations in bioactive nanocomposite films significantly controlled the growth of bacteria, fungi and insects by slowly releasing the active ingredients over the storage period and ensured the food safety and quality. Combining bioactive nanocomposite films with γ -irradiation at either 500 Gy or 750 Gy increased the radiosensitivity of the treated bacteria, fungi and insects and acted synergistically by lowering the radiation doses. The sensorial properties of the packed rice covered with bioactive nanocomposite films for two months, was highly acceptable by consumers and there were no significant difference between the treated and untreated cooked rice. The current commercial food preservatives to control foodborne pathogenic bacteria, spoilage fungi and insects in stored foods are very specific and pathogens and insects become resistant after long term exposure, unlike our

bioactive nanocomposite films which control a wide range of pathogenic bacteria and fungi as well as harmful insect pests, which do not become resistant due to the multifaceted mode of action. Therefore, the developed technology in the current study for food preservation has a great opportunity to control the bacteria, fungi and insects in stored cereal grains, fruits and dairy products.

Bibliography

- Abbas, S., Karangwa, E., Bashari, M., Hayat, K., Hong, X., Sharif, H.R., Zhang, X., 2015. Fabrication of polymeric nanocapsules from curcumin-loaded nanoemulsion templates by self-assembly. *Ultrasonics Sonochemistry* 23, 81-92.
- Abd-Alla, M., Haggag, W.M., 2013. Use of some plant essential oils as post-harvest botanical fungicides in the management of anthracnose disease of Mango fruits (*Mangi feraindica* L.) caused by *Colletotrichum gloeosporioides* (Penz). *International Journal of Agriculture and Forestry* 3, 1-6.
- Abdelgaleil, S.A., Mohamed, M.I., Badawy, M.E., El-arami, S.A., 2009. Fumigant and contact toxicities of monoterpenes to *Sitophilus oryzae* (L.) and *Tribolium castaneum* (Herbst) and their inhibitory effects on acetylcholinesterase activity. *Journal of Chemical Ecology* 35, 518-525.
- Abdelgaleil, S.A.M., Mohamed, M.I.E., Shawir, M.S., Abou-Taleb, H.K., 2016. Chemical composition, insecticidal and biochemical effects of essential oils of different plant species from Northern Egypt on the rice weevil, *Sitophilus oryzae* L. *Journal of Pest Science* 89, 219-229.
- Abdollahi, M., Rezaei, M., Farzi, G., 2012. A novel active bionanocomposite film incorporating rosemary essential oil and nanoclay into chitosan. *Journal of Food Engineering* 111, 343-350.
- Adak, T., Barik, N., Patil, N.B., Govindharaj, G.-P.-P., Gadratagi, B.G., Annamalai, M., Mukherjee, A.K., Rath, P.C., 2020. Nanoemulsion of eucalyptus oil: An alternative to synthetic pesticides against two major storage insects (*Sitophilus oryzae* (L.) and *Tribolium castaneum* (Herbst)) of rice. *Industrial Crops and Products* 143.
- Ahebwa, A., Mongkol, R., Sawangsri, P., Kanjanamaneesathian, M., 2020. Vapour-phase efficacy of selected essential oils individually and in combination against *Aspergillus flavus*, *A. niger*, *Fusarium proliferatum*, and *Curvularia lunata*. *New Zealand Plant Protection* 73, 40-48.
- Ahmadi, M., Abd-alla, A.M.M., Moharrampour, S., 2013. Combination of gamma radiation and essential oils from medicinal plants in managing *Tribolium castaneum* contamination of stored products. *Applied Radiation and Isotopes* 78, 16-20.
- Ahmed, J., Mulla, M., Arfat, Y.A., Bher, A., Jacob, H., Auras, R., 2018. Compression molded LLDPE films loaded with bimetallic (Ag-Cu) nanoparticles and cinnamon essential oil for chicken meat packaging applications. *LWT-Food Science and Technology* 93, 329-338.

- Ahmed, S., Ahmad, M., Ikram, S., 2014. Chitosan: a natural antimicrobial agent-a review. *Journal of Applicable Chemistry* 3, 493-503.
- Ali-Shtayeh, M.S., Jamous, R.M., Zaitoun, S.Y.A., Qasem, I.B., 2014. *In-vitro* screening of acetylcholinesterase inhibitory activity of extracts from Palestinian indigenous flora in relation to the treatment of Alzheimer's disease. *Functional Foods in Health and Disease* 4, 381-400.
- Almasi, H., Jahanbakhsh Oskouie, M., Saleh, A., 2021. A review on techniques utilized for design of controlled release food active packaging. *Critical Reviews in Food Science and Nutrition* 61, 2601-2621.
- Anjali, C.H., Sharma, Y., Mukherjee, A., Chandrasekaran, N., 2012. Neem oil (*Azadirachta indica*) nanoemulsion--a potent larvicidal agent against *Culex quinquefasciatus*. *Pest Management Science* 68, 158-163.
- Arfat, Y.A., Ahmed, J., Hiremath, N., Auras, R., Joseph, A., 2017. Thermo-mechanical, rheological, structural and antimicrobial properties of bionanocomposite films based on fish skin gelatin and silver-copper nanoparticles. *Food Hydrocolloids* 62, 191-202.
- Arrieta, M.P., López, J., Hernández, A., Rayón, E., 2014. Ternary PLA-PHB-Limonene blends intended for biodegradable food packaging applications. *European Polymer Journal* 50, 255-270.
- Asghar Heydari, M., Mobini, M., Salehi, M., 2017. The Synergic Activity of Eucalyptus Leaf Oil and Silver Nanoparticles Against Some Pathogenic Bacteria. *Archives of Pediatric Infectious Diseases* 5.
- Asmawati, Mustapha, W.A.W., Yusop, S.M., Maskat, M.Y., Shamsuddin, A.F., 2014. Characteristics of cinnamaldehyde nanoemulsion prepared using APV-high pressure homogenizer and ultra turrax. *AIP Conference Proceedings. American Institute of Physics* 1614, 244-250.
- ASTM, D., 1995. Standard test method for tensile properties of thin plastic sheeting. *Annual book of ASTM standards* 8, 182-190.
- Avila-Sosa, R., Palou, E., Munguía, M.T.J., Nevárez-Moorillón, G.V., Cruz, A.R.N., López-Malo, A., 2012. Antifungal activity by vapor contact of essential oils added to amaranth, chitosan, or starch edible films. *International Journal of Food Microbiology* 153, 66-72.
- Avinc, O., Khoddami, A., 2009. Overview of Poly (lactic acid)(PLA) Fibre. *Fibre Chemistry* 41, 391-401.

- Ayala-Zavala, J.F., Wang, S.Y., Wang, C.Y., González-Aguilar, G.A., 2004. Effect of storage temperatures on antioxidant capacity and aroma compounds in strawberry fruit. *LWT-Food Science and Technology* 37, 687-695.
- Ayari, S., Dussault, D., Jerbi, T., Hamdi, M., Lacroix, M., 2012. Radiosensitization of *Bacillus cereus* spores in minced meat treated with cinnamaldehyde. *Radiation Physics and Chemistry* 81, 1173-1176.
- Ayari, S., Shankar, S., Follett, P., Hossain, F., Lacroix, M., 2020. Potential synergistic antimicrobial efficiency of binary combinations of essential oils against *Bacillus cereus* and *Paenibacillus amylolyticus*-Part A. *Microbial Pathogenesis* 141, 104008.
- Azeredo, H.M.C., Mattoso, L.H.C., Avena-Bustillos, R.J., Filho, G.C., Munford, M.L., Wood, D., McHugh, T.H., 2010. Nanocellulose Reinforced Chitosan Composite Films as Affected by Nanofiller Loading and Plasticizer Content. *Journal of Food Science* 75, N1-N7.
- Aziz, M., Karboune, S., 2018. Natural antimicrobial/antioxidant agents in meat and poultry products as well as fruits and vegetables: A review. *Critical Reviews in Food Science and Nutrition* 58, 486-511.
- Badr, K., Ahmed, Z.S., El-Gamal, M., 2013. Assessment of antimicrobial activity of whey protein films incorporated with biocide plant-based essential oils. *Journal of Applied Sciences Research* 9, 2811-2818.
- Bahrami, A., Delshadi, R., Assadpour, E., Jafari, S.M., Williams, L., 2020. Antimicrobial-loaded nanocarriers for food packaging applications. *Advances in Colloid and Interface Science* 278, 102140.
- Bahrami, A., Mokarram, R.R., Khiabani, M.S., Ghanbarzadeh, B., Salehi, R., 2019. Physico-mechanical and antimicrobial properties of tragacanth/hydroxypropyl methylcellulose/beeswax edible films reinforced with silver nanoparticles. *International Journal of Biological Macromolecules* 129, 1103-1112.
- Bakkali, F., Averbeck, S., Averbeck, D., Idaomar, M., 2008. Biological effects of essential oils—a review. *Food and Chemical Toxicology* 46, 446-475.
- Balan, G.C., Paulo, A.F.S., Correa, L.G., Alvim, I.D., Ueno, C.T., Coelho, A.R., Ströher, G.R., Yamashita, F., Sakanaka, L.S., Shirai, M.A., 2021. Production of wheat flour/PBAT active films incorporated with oregano oil microparticles and its application in fresh pastry conservation. *Food and Bioprocess Technology* 14, 1587-1599.
- Barkai-Golan, R., 2001. *Postharvest diseases of fruits and vegetables: development and control*. Elsevier.

- Barkai-Golan, R., Follett, P.A., 2017. Irradiation for quality improvement, microbial safety and phytosanitation of fresh produce. Academic Press.
- Bassolé, I., Lamien-Meda, A., Bayala, B., Obame, L., Ilboudo, A., Franz, C., Novak, J., Nebié, R., Dicko, M., 2011. Chemical composition and antimicrobial activity of *Cymbopogon citratus* and *Cymbopogon giganteus* essential oils alone and in combination. *Phytomedicine* 18, 1070-1074.
- Beck-Candanedo, S., Roman, M., Gray, D.G., 2005. Effect of reaction conditions on the properties and behavior of wood cellulose nanocrystal suspensions. *Biomacromolecules* 6, 1048-1054.
- Begum, T., Follett, P.A., Hossain, F., Christopher, L., Salmieri, S., Lacroix, M., 2020a. Microbicidal effectiveness of irradiation from Gamma and X-ray sources at different dose rates against the foodborne illness pathogens *Escherichia coli*, *Salmonella* Typhimurium and *Listeria monocytogenes* in rice. *LWT-Food Science and Technology* 132, 109841.
- Begum, T., Follett, P.A., Mahmud, J., Moskovchenko, L., Salmieri, S., Allahdad, Z., Lacroix, M., 2022a. Silver nanoparticles-essential oils combined treatments to enhance the antibacterial and antifungal properties against foodborne pathogens and spoilage microorganisms. *Microbial Pathogenesis* 164, 105411.
- Begum, T., Follett, P.A., Shankar, S., Mahmud, J., Salmieri, S., Lacroix, M., 2022b. Mixture design methodology and predictive modeling for developing active formulations using essential oils and citrus extract against foodborne pathogens and spoilage microorganisms in rice. *Journal of Food Science* 87, 353-369.
- Ben-Fadhel, Y., Maherani, B., Manus, J., Salmieri, S., Lacroix, M., 2020. Physicochemical and microbiological characterization of pectin-based gelled emulsions coating applied on pre-cut carrots. *Food Hydrocolloids* 101, 105573.
- Ben-Fadhel, Y., Maherani, B., Salmieri, S., Lacroix, M., 2022. Preparation and characterization of natural extracts-loaded food grade nanoliposomes. *LWT-Food Science and Technology* 154, 112781.
- Benelli, G., 2018. Mode of action of nanoparticles against insects. *Environmental Science and Pollution Research international* 25, 12329-12341.
- Betts, G., Linton, P., Betteridge, R., 1999. Food spoilage yeasts: effects of pH, NaCl and temperature on growth. *Food Control* 10, 27-33.
- Bianchini, A., Wood, C.M., 2003. Mechanism of acute silver toxicity in *Daphnia magna*. *Environmental Toxicology and Chemistry: An International Journal* 22, 1361-1367.

- Bilbao, M.d.L.M., Andrés-Lacueva, C., Jáuregui, O., Lamuela-Raventos, R.M., 2007. Determination of flavonoids in a Citrus fruit extract by LC–DAD and LC–MS. *Food Chemistry* 101, 1742-1747.
- Bocate, K.P., Reis, G.F., de Souza, P.C., Oliveira Junior, A.G., Duran, N., Nakazato, G., Furlaneto, M.C., de Almeida, R.S., Panagio, L.A., 2019. Antifungal activity of silver nanoparticles and simvastatin against toxigenic species of *Aspergillus*. *International Journal of Food Microbiology* 291, 79-86.
- Bordes, P., Pollet, E., Avérous, L., 2009. Nano-biocomposites: biodegradable polyester/nanoclay systems. *Progress in Polymer Science* 34, 125-155.
- Bouhdid, S., Abrini, J., Amensour, M., Zhiri, A., Espuny, M., Manresa, A., 2010. Functional and ultrastructural changes in *Pseudomonas aeruginosa* and *Staphylococcus aureus* cells induced by *Cinnamomum verum* essential oil. *Journal of Applied Microbiology* 109, 1139-1149.
- Boumail, A., Salmieri, S., Klimas, E., Tawema, P.O., Bouchard, J., Lacroix, M., 2013. Characterization of trilayer antimicrobial diffusion films (ADFs) based on methylcellulose-polycaprolactone composites. *Journal of Agricultural and Food Chemistry* 61, 811-821.
- Braide, W., Nwaoguikpe, R., Oranusi, S., Udegbonam, L., Akobondu, C., Okorondu, S., 2011. The effect of biodeterioration on the nutritional composition and microbiology of an edible long-winged reproductive termite, *Macrotermes bellicosus*. *International Journal of Food Safety* 13, 107-114.
- Bruschi, M.L., 2015. Strategies to modify the drug release from pharmaceutical systems. Woodhead Publishing.
- Bullerman, L.B., 1983. Effects of potassium sorbate on growth and aflatoxin production by *Aspergillus parasiticus* and *Aspergillus flavus*. *Journal of Food Protection* 46, 940-942.
- Burt, S., 2004. Essential oils: their antibacterial properties and potential applications in foods—a review. *International Journal of Food Microbiology* 94, 223-253.
- Bustos, C.R., Alberti, R.F., Matiacevich, S.B., 2016. Edible antimicrobial films based on microencapsulated lemongrass oil. *Journal of Food Science and Technology* 53, 832-839.
- Buteler, M., Sofie, S., Weaver, D., Driscoll, D., Muretta, J., Stadler, T., 2015. Development of nanoalumina dust as insecticide against *Sitophilus oryzae* and *Rhyzopertha dominica*. *International Journal of Pest Management* 61, 80-89.
- Caggiano, G., De Giglio, O., Lovero, G., Rutigliano, S., Diella, G., Balbino, S., Napoli, C., Montagna, M.T., 2015. Detection of *Listeria monocytogenes* in ready-to-eat foods sampled

- from a catering service in Apulia, Italy. *Annali Di Igiene Medicina Preventiva E Di Comunita* 27, 590-594.
- Caillet, S., Lacroix, M., 2006. Effect of gamma radiation and oregano essential oil on murein and ATP concentration of *Listeria monocytogenes*. *Journal of Food Protection* 69, 2961-2969.
- Caillet, S., Millette, M., Turgis, M., Salmieri, S., Lacroix, M., 2006. Influence of antimicrobial compounds and modified atmosphere packaging on radiation sensitivity of *Listeria monocytogenes* present in ready-to-use carrots (*Daucus carota*). *Journal of Food Protection* 69, 221-227.
- Caillet, S., Shareck, F., Lacroix, M., 2005. Effect of gamma radiation and oregano essential oil on murein and ATP concentration of *Escherichia coli* O157: H7. *Journal of Food Protection* 68, 2571-2579.
- Carbone, M., Donia, D.T., Sabbatella, G., Antiochia, R., 2016. Silver nanoparticles in polymeric matrices for fresh food packaging. *Journal of King Saud University - Science* 28, 273-279.
- Cardiet, G., Fuzeau, B., Barreau, C., Fleurat-Lessard, F., 2012. Contact and fumigant toxicity of some essential oil constituents against a grain insect pest *Sitophilus oryzae* and two fungi, *Aspergillus westerdijkiae* and *Fusarium graminearum*. *Journal of Pest Science* 85, 351-358.
- Cardoso, L.G., Pereira Santos, J.C., Camilloto, G.P., Miranda, A.L., Druzian, J.I., Guimarães, A.G., 2017. Development of active films poly (butylene adipate co-terephthalate) – PBAT incorporated with oregano essential oil and application in fish fillet preservation. *Industrial Crops and Products* 108, 388-397.
- Castillo-Morales, R.M., Serrano, S.O., Villamizar, A.L.R., Mendez-Sanchez, S.C., Duque, J.E., 2021. Impact of *Cymbopogon flexuosus* (Poaceae) essential oil and primary components on the eclosion and larval development of *Aedes aegypti*. *Scientific Reports* 11, 24291.
- Chand, R., Jokhan, A., Gopalan, R., 2017. A mini-review of essential oils in the South Pacific and their insecticidal properties. *Advances in Horticultural Science* 31, 295-310.
- Chang, Y., Lee, S.H., Na, J.H., Chang, P.S., Han, J., 2017. Protection of Grain Products from *Sitophilus oryzae* (L.) Contamination by Anti-Insect Pest Repellent Sachet Containing Allyl Mercaptan Microcapsule. *Journal of Food Science* 82, 2634-2642.
- Char, C.D., Guerrero, S.N., Alzamora, S.M., 2007. Growth of *Eurotium chevalieri* in milk jam: influence of pH, potassium sorbate and water activity. *Journal of Food Safety* 27, 1-16.
- Chen, L., Remondetto, G.E., Subirade, M., 2006. Food protein-based materials as nutraceutical delivery systems. *Trends in Food Science and Technology* 17, 272-283.

- Chen, X., Li, C., Chen, Y., Ni, C., Chen, X., Zhang, L., Xu, X., Chen, M., Ma, X., Zhan, H., 2019. Aflatoxin B1 impairs leydig cells through inhibiting AMPK/mTOR-mediated autophagy flux pathway. *Chemosphere* 233, 261-272.
- Cheng, D., Wen, Y., An, X., Zhu, X., Cheng, X., Zheng, L., Nasrallah, J.E., 2016. Improving the colloidal stability of Cellulose nano-crystals by surface chemical grafting with polyacrylic acid. *Journal of Bioresources and Bioproducts* 1, 114-119.
- Choupanian, M., Omar, D., Basri, M., Asib, N., 2017. Preparation and characterization of neem oil nanoemulsion formulations against *Sitophilus oryzae* and *Tribolium castaneum* adults. *Journal of Pesticide Science* 42, 158-165.
- Codex, C.A., 2003. General standard for irradiated foods: CODEX STAN 106–1983, REV. 1–2003. Food and Agriculture Organization of the United Nations, Rome.
- Commission, C.A., 2000. Report of the 32nd Session of the Codex Committee on Food Additives and Contaminants.
- Costard, S., Espejo, L., Groenendaal, H., Zgmutt, F.J., 2017. Outbreak-related disease burden associated with consumption of unpasteurized cow's milk and cheese, United States, 2009–2014. *Emerging Infectious Diseases* 23, 957.
- Criado, P., Frascini, C., Salmieri, S., Lacroix, M., 2020. Cellulose nanocrystals (CNCs) loaded alginate films against lipid oxidation of chicken breast. *Food Research International* 132, 109110.
- Criado, P., Hossain, F.M., Salmieri, S., Lacroix, M., 2018. Nanocellulose in food packaging. *Composites Materials for Food Packaging*, 297-329.
- Crini, G., 2019. Historical review on chitin and chitosan biopolymers. *Environmental Chemistry Letters* 17, 1623-1643.
- da Rosa, C.G., Sganzerla, W.G., de Oliveira Brisola Maciel, M.V., de Melo, A.P.Z., da Rosa Almeida, A., Ramos Nunes, M., Bertoldi, F.C., Manique Barreto, P.L., 2020. Development of poly (ethylene oxide) bioactive nanocomposite films functionalized with zein nanoparticles. *Colloids and Surfaces A: Physicochemical and Engineering Aspects* 586, 124268.
- Dambolena, J.S., Zunino, M.P., Herrera, J.M., Pizzolitto, R.P., Areco, V.A., Zygadlo, J.A., 2016. Terpenes: Natural products for controlling insects of importance to human health—A structure-activity relationship study. *Journal of Entomology* 2016, 1-17.
- Das, S., Kumar Singh, V., Kumar Dwivedy, A., Kumar Chaudhari, A., Deepika, Kishore Dubey, N., 2021a. Nanostructured *Pimpinella anisum* essential oil as novel green food preservative

- against fungal infestation, aflatoxin B1 contamination and deterioration of nutritional qualities. *Food Chemistry* 344, 128574.
- Das, S., Singh, V.K., Dwivedy, A.K., Chaudhari, A.K., Dubey, N.K., 2021b. *Anethum graveolens* Essential Oil Encapsulation in Chitosan Nanomatrix: Investigations on *In Vitro* Release Behavior, Organoleptic Attributes, and Efficacy as Potential Delivery Vehicles Against Biodeterioration of Rice (*Oryza sativa* L.). *Food and Bioprocess Technology* 14, 831-853.
- de Azeredo, G.A., Stamford, T.L.M., Nunes, P.C., Gomes Neto, N.J., de Oliveira, M.E.G., de Souza, E.L., 2011. Combined application of essential oils from *Origanum vulgare* L. and *Rosmarinus officinalis* L. to inhibit bacteria and autochthonous microflora associated with minimally processed vegetables. *Food Research International* 44, 1541-1548.
- de Mesquita, J.P., Donnici, C.L., Pereira, F.V., 2010. Biobased nanocomposites from layer-by-layer assembly of cellulose nanowhiskers with chitosan. *Biomacromolecules* 11, 473-480.
- de Souza, A.G., Barbosa, R.F.d.S., Quispe, Y.M., Rosa, D.d.S., 2022. Essential oil microencapsulation with biodegradable polymer for food packaging application. *Journal of Polymers and the Environment* 30, 3307-3315.
- Deepika, Singh, A., Chaudhari, A.K., Das, S., Dubey, N.K., 2021. *Zingiber zerumbet* L. essential oil-based chitosan nanoemulsion as an efficient green preservative against fungi and aflatoxin B1 contamination. *Journal of Food Science* 86, 149-160.
- Dehkordi, N.H., Tajik, H., Moradi, M., Kousheh, S.A., Molaei, R., 2019. Antibacterial Interactions of Colloid Nanosilver with Eugenol and Food Ingredients. *Journal of Food Protection* 82, 1783-1792.
- Del-Valle, V., Hernández-Muñoz, P., Guarda, A., Galotto, M., 2005. Development of a cactus-mucilage edible coating (*Opuntia ficus indica*) and its application to extend strawberry (*Fragaria ananassa*) shelf-life. *Food Chemistry* 91, 751-756.
- Delavenne, E., Ismail, R., Pawtowski, A., Mounier, J., Barbier, G., Le Blay, G., 2013. Assessment of lactobacilli strains as yogurt bioprotective cultures. *Food Control* 30, 206-213.
- Delbeke, S., Hessel, C., Verguldt, E., De Beleyer, A., Clicque, T., Boussemaere, J., Jacxsens, L., Uyttendaele, M., 2014. Survival of *Salmonella* and *E. coli* O157 on strawberries and basil during storage at different temperatures. 19th Conference on Food Microbiology. Belgian Society for Food Microbiology (BSFM), 113-113.
- Demirel, N., Erdogan, C., 2017. Insecticidal effects of essential oils from Labiatae and Lauraceae families against cowpea weevil, *Callosobruchus maculatus* (F.)(Coleoptera: Bruchidae) in stored pea seeds. *Entomology and Applied Science Letters* 4, 13-19.

- Deng, Z., Jung, J., Simonsen, J., Wang, Y., Zhao, Y., 2017. Cellulose Nanocrystal Reinforced Chitosan Coatings for Improving the Storability of Postharvest Pears Under Both Ambient and Cold Storages. *Journal of Food Science* 82, 453-462.
- Dhar, P., Tarafder, D., Kumar, A., Katiyar, V., 2015. Effect of cellulose nanocrystal polymorphs on mechanical, barrier and thermal properties of poly (lactic acid) based bionanocomposites. *Rsc Advances* 5, 60426-60440.
- Dong, L.M., Quyen, N.T.T., Thuy, D.T.K., 2020. Effect of edible coating and antifungal emulsion system on *Colletotrichum acutatum* and shelf life of strawberries. *Vietnam Journal of Chemistry* 58, 237-244.
- Donsì, F., Annunziata, M., Sessa, M., Ferrari, G., 2011. Nanoencapsulation of essential oils to enhance their antimicrobial activity in foods. *LWT-Food Science and Technology* 44, 1908-1914.
- Donsì, F., Annunziata, M., Vincenzi, M., Ferrari, G., 2012. Design of nanoemulsion-based delivery systems of natural antimicrobials: effect of the emulsifier. *Journal of Biotechnology* 159, 342-350.
- Donsi, F., Ferrari, G., 2016. Essential oil nanoemulsions as antimicrobial agents in food. *Journal of Biotechnology* 233, 106-120.
- Durán, N., Durán, M., Souza, C.E.d., 2017. Silver and silver chloride nanoparticles and their anti-tick activity: a mini review. *Journal of the Brazilian Chemical Society* 28, 927-932.
- Dussault, D., Vu, K.D., Lacroix, M., 2014. *In vitro* evaluation of antimicrobial activities of various commercial essential oils, oleoresin and pure compounds against food pathogens and application in ham. *Meat Science* 96, 514-520.
- Dzamic, A., Sokovic, M., Ristic, M., Grujic-Jovanovic, S., Vukojevic, J., Marin, P., 2008. Chemical composition and antifungal activity of *Origanum heracleoticum* essential oil. *Chemistry of Natural Compounds* 44, 659-660.
- Eghbalifam, N., Frouchi, M., Dadbin, S., 2015. Antibacterial silver nanoparticles in polyvinyl alcohol/sodium alginate blend produced by gamma irradiation. *International Journal of Biological Macromolecules* 80, 170-176.
- El-Bakry, A.M., Youssef, H.F., Abdel-Aziz, N.F., Sammour, E.A., 2019. Insecticidal potential of Ag-loaded 4A-zeolite and its formulations with *Rosmarinus officinalis* essential oil against rice weevil (*Sitophilus oryzae*) and lesser grain borer (*Rhyzopertha dominica*). *Journal of Plant Protection Research* 59.

- El Omari, K., Al Kassaa, I., Farraa, R., Najib, R., Alwane, S., Chihib, N., Hamze, M., 2020. Using the essential oil of *Micromeria barbata* plant as natural preservative to extend the shelf life of lebanese YogurtPak. *Journal of Biological Sciences* 23, 848-855.
- Emamifar, A., Kadivar, M., Shahedi, M., Soleimani-Zad, S., 2010. Evaluation of nanocomposite packaging containing Ag and ZnO on shelf life of fresh orange juice. *Innovative Food Science and Emerging Technologies* 11, 742-748.
- Emamifar, A., Kadivar, M., Shahedi, M., SOLIMANIAN-ZAD, S., 2012. Effect of nanocomposite packaging containing Ag and ZnO on reducing pasteurization temperature of orange juice. *Journal of Food Processing and Preservation* 36, 104-112.
- Enan, E., 2001. Insecticidal activity of essential oils: octopaminergic sites of action. *Comparative Biochemistry and Physiology Part C: Toxicology and Pharmacology* 130, 325-337.
- Endes, C., Camarero-Espinosa, S., Mueller, S., Foster, E.J., Petri-Fink, A., Rothen-Rutishauser, B., Weder, C., Clift, M.J.D., 2016. A critical review of the current knowledge regarding the biological impact of nanocellulose. *Journal of Nanobiotechnology* 14, 1-14.
- Escamilla-García, M., García-García, M.C., Gracida, J., Hernández-Hernández, H.M., Granados-Arvizu, J.Á., Di Pierro, P., Regalado-González, C., 2022. Properties and Biodegradability of Films Based on Cellulose and Cellulose Nanocrystals from Corn Cob in Mixture with Chitosan. *International Journal of Molecular Sciences* 23 10560.
- Eustice, R.F., 2015. Using irradiation to make safe food safer. *Stewart Postharvest Review* 11, 1-5.
- Fadhel, Y.B., Leroy, V., Dussault, D., St-Yves, F., Lauzon, M., Salmieri, S., Jamshidian, M., Vu, D.K., Lacroix, M., 2016. Combined effects of marinating and γ -irradiation in ensuring safety, protection of nutritional value and increase in shelf-life of ready-to-cook meat for immunocompromised patients. *Meat science* 118, 43-51.
- Fadil, M., Fikri-Benbrahim, K., Rachiq, S., Ihssane, B., Lebrazi, S., Chraïbi, M., Haloui, T., Farah, A., 2018. Combined treatment of *Thymus vulgaris* L., *Rosmarinus officinalis* L. and *Myrtus communis* L. essential oils against *Salmonella typhimurium*: Optimization of antibacterial activity by mixture design methodology. *European Journal of Pharmaceutics and Biopharmaceutics* 126, 211-220.
- Falleh, H., Ben Jemaa, M., Djebali, K., Abid, S., Saada, M., Ksouri, R., 2019. Application of the mixture design for optimum antimicrobial activity: Combined treatment of *Syzygium aromaticum*, *Cinnamomum zeylanicum*, *Myrtus communis*, and *Lavandula stoechas*

- essential oils against *Escherichia coli*. Journal of Food Processing and Preservation 43, 14257.
- FAO, G., 2011. Global food losses and food waste—Extent, causes and prevention. SAVE FOOD: An Initiative on Food Loss and Waste Reduction.
- Farah, S., Anderson, D.G., Langer, R., 2016. Physical and mechanical properties of PLA, and their functions in widespread applications—A comprehensive review. Advanced Drug Delivery Reviews 107, 367-392.
- Farkas, J., Ehlermann, D., Mohacsi-Farkas, C., 2004. Charged particle and photon interactions with matter. Food irradiation, 785-812.
- Felix da Silva Barbosa, R., Gabrieli de Souza, A., Rangari, V., Rosa, D.D.S., 2021. The influence of PBAT content in the nanocapsules preparation and its effect in essential oils release. Food Chemistry 344, 128611.
- Feron, V., Til, H., De Vrijer, F., Woutersen, R., Cassee, F., Van Bladeren, P., 1991. Aldehydes: occurrence, carcinogenic potential, mechanism of action and risk assessment. Mutation Research/Genetic Toxicology 259, 363-385.
- Ferreira, F.V., Mariano, M., Pinheiro, I.F., Cazalini, E.M., Souza, D.H.S., Lepesqueur, L.S.S., Koga-Ito, C.Y., Gouveia, R.F., Lona, L.M.F., 2019. Cellulose nanocrystal-based poly(butylene adipate-co-terephthalate) nanocomposites covered with antimicrobial silver thin films. Polymer Engineering and Science 59, 356-365.
- Fierascu, R.C., Fierascu, I.C., Dinu-Pirvu, C.E., Fierascu, I., Paunescu, A., 2020. The application of essential oils as a next-generation of pesticides: recent developments and future perspectives. Journal of Biosciences 75, 183-204.
- Filtenborg, O., Frisvad, J.C., Thrane, U., 1996. Moulds in food spoilage. International Journal of Food Microbiology 33, 85-102.
- Fleet, G., 1990. Yeasts in dairy products. Journal of Applied Bacteriology 68, 199-211.
- Foldbjerg, R., Jiang, X., Miclăuş, T., Chen, C., Autrup, H., Beer, C., 2015. Silver nanoparticles—wolves in sheep's clothing? Toxicology Research 4, 563-575.
- Follett, P.A., Snook, K., Janson, A., Antonio, B., Haruki, A., Okamura, M., Bisel, J., 2013. Irradiation quarantine treatment for control of *Sitophilus oryzae* (Coleoptera: Curculionidae) in rice. Journal of Stored Products Research 52, 63-67.
- FOOD, S., 2016. Global initiative on food loss and waste reduction. Key facts on food loss and waste you should know.

- Fortunati, E., Armentano, I., Zhou, Q., Iannoni, A., Saino, E., Visai, L., Berglund, L.A., Kenny, J., 2012a. Multifunctional bionanocomposite films of poly (lactic acid), cellulose nanocrystals and silver nanoparticles. *Carbohydrate Polymers* 87, 1596-1605.
- Fortunati, E., Armentano, I., Zhou, Q., Iannoni, A., Saino, E., Visai, L., Berglund, L.A., Kenny, J.M., 2012b. Multifunctional bionanocomposite films of poly(lactic acid), cellulose nanocrystals and silver nanoparticles. *Carbohydrate Polymers* 87, 1596-1605.
- Fortunati, E., Peltzer, M., Armentano, I., Jiménez, A., Kenny, J.M., 2013. Combined effects of cellulose nanocrystals and silver nanoparticles on the barrier and migration properties of PLA nano-biocomposites. *Journal of Food Engineering* 118, 117-124.
- Fortunati, E., Rinaldi, S., Peltzer, M., Bloise, N., Visai, L., Armentano, I., Jiménez, A., Latterini, L., Kenny, J.M., 2014. Nano-biocomposite films with modified cellulose nanocrystals and synthesized silver nanoparticles. *Carbohydrate Polymers* 101, 1122-1133.
- Fournier, L., Rivera Mirabal, D.M., Hillmyer, M.A., 2022. Toward Sustainable Elastomers from the Grafting-Through Polymerization of Lactone-Containing Polyester Macromonomers. *Macromolecules* 55, 1003-1014.
- Fukushima, K., Wu, M.H., Bocchini, S., Rasyida, A., Yang, M.C., 2012. PBAT based nanocomposites for medical and industrial applications. *Materials science and engineering* 32, 1331-1351.
- Garavand, F., Cacciotti, I., Vahedikia, N., Rehman, A., Tarhan, Ö., Akbari-Alavijeh, S., Shaddel, R., Rashidinejad, A., Nejatian, M., Jafarzadeh, S., 2022. A comprehensive review on the nanocomposites loaded with chitosan nanoparticles for food packaging. *Critical Reviews in Food Science and Nutrition* 62, 1383-1416.
- Garrido-Miranda, K.A., Giraldo, J.D., Schoebitz, M., 2022. Essential Oils and Their Formulations for the Control of Curculionidae Pests. *Frontiers in Agronomy* 4, 876687.
- Ghabraie, M., Vu, K.D., Tata, L., Salmieri, S., Lacroix, M., 2016. Antimicrobial effect of essential oils in combinations against five bacteria and their effect on sensorial quality of ground meat. *LWT-Food Science and Technology* 66, 332-339.
- Gherasim, O., Grumezescu, A.M., Mogosanu, G.D., Vasile, B.S., Bejenaru, C., Bejenaru, L.E., Andronescu, E., Mogoanta, L., 2020. Biodistribution of essential oil-conjugated silver nanoparticles. *Romanian Journal of Morphology and Embryology* 61, 1099-1109.
- Ghosh, I.N., Patil, S.D., Sharma, T.K., Srivastava, S.K., Pathania, R., Navani, N.K., 2013a. Synergistic action of cinnamaldehyde with silver nanoparticles against spore-forming

- bacteria: a case for judicious use of silver nanoparticles for antibacterial applications. *International Journal of Nanomedicine* 8, 4721-4731.
- Ghosh, V., Mukherjee, A., Chandrasekaran, N., 2013b. Formulation and characterization of plant essential oil based nanoemulsion: evaluation of its larvicidal activity against *Aedes aegypti*. *Asian Journal of Chemistry* 25, 321.
- Gibaldi, M., Feldman, S., 1967. Establishment of sink conditions in dissolution rate determinations. Theoretical considerations and application to nondisintegrating dosage forms. *Journal of Pharmaceutical Sciences* 56, 1238-1242.
- Gómez-Estaca, J., De Lacey, A.L., López-Caballero, M., Gómez-Guillén, M., Montero, P., 2010. Biodegradable gelatin–chitosan films incorporated with essential oils as antimicrobial agents for fish preservation. *Food Microbiology* 27, 889-896.
- Gougouli, M., Koutsoumanis, K.P., 2017. Risk assessment of fungal spoilage: A case study of *Aspergillus niger* on yogurt. *Food Microbiology* 65, 264-273.
- Ha, T.V.A., Kim, S., Choi, Y., Kwak, H.-S., Lee, S.J., Wen, J., Oey, I., Ko, S., 2015. Antioxidant activity and bioaccessibility of size-different nanoemulsions for lycopene-enriched tomato extract. *Food Chemistry* 178, 115-121.
- Haafiz, M.K., Hassan, A., Khalil, H.P., Fazita, M.R., Islam, M.S., Inuwa, I.M., Marliana, M.M., Hussin, M.H., 2016. Exploring the effect of cellulose nanowhiskers isolated from oil palm biomass on polylactic acid properties. *International Journal of Biological Macromolecules* 85, 370-378.
- Hajjabdolrasouli, M., Babaei, A., 2018. Rheological, thermal and tensile properties of PE/nanoclay nanocomposites and PE/nanoclay nanocomposite cast films. *Polyolefins Journal* 5, 47-58.
- Hallman, G.J., 2013. Control of stored product pests by ionizing radiation. *Journal of Stored Products Research* 52, 36-41.
- Han, J.H., 2014. Edible films and coatings: a review. *Innovations in Food Packaging*, 213-255.
- Han, J.W., Ruiz-Garcia, L., Qian, J.P., Yang, X.T., 2018. Food packaging: A comprehensive review and future trends. *Comprehensive Reviews in Food Science and Food Safety* 17, 860-877.
- Hategekimana, A., Erler, F., 2020. Comparative repellent activity of single, binary and ternary combinations of plant essential oils and their major components against *Sitophilus oryzae* L. (Coleoptera: Curculionidae). *Journal of Plant Diseases and Protection* 127, 873-881.

- Helmlinger, J., Sengstock, C., Groß-Heitfeld, C., Mayer, C., Schildhauer, T.A., Köller, M., Epple, M., 2016. Silver nanoparticles with different size and shape: equal cytotoxicity, but different antibacterial effects. *RSC Advances* 6, 18490-18501.
- Hernández-Muñoz, P., Almenar, E., Ocio, M.J., Gavara, R., 2006. Effect of calcium dips and chitosan coatings on postharvest life of strawberries (*Fragaria x ananassa*). *Postharvest Biology and Technology* 39, 247-253.
- Heydari-Majd, M., Ghanbarzadeh, B., Shahidi-Noghabi, M., Najafi, M.A., Hosseini, M., 2019. A new active nanocomposite film based on PLA/ZnO nanoparticle/essential oils for the preservation of refrigerated *Otolithes ruber* fillets. *Food Packaging and Shelf Life* 19, 94-103.
- Hossain, F., Follett, P., Dang Vu, K., Harich, M., Salmieri, S., Lacroix, M., 2016a. Evidence for synergistic activity of plant-derived essential oils against fungal pathogens of food. *Food Microbiology* 53, 24-30.
- Hossain, F., Follett, P., Salmieri, S., Vu, K.D., Fraschini, C., Lacroix, M., 2019a. Antifungal activities of combined treatments of irradiation and essential oils (EOs) encapsulated chitosan nanocomposite films in *in vitro* and *in situ* conditions. *International Journal of Food Microbiology* 295, 33-40.
- Hossain, F., Follett, P., Salmieri, S., Vu, K.D., Harich, M., Lacroix, M., 2019b. Synergistic Effects of Nanocomposite Films Containing Essential Oil Nanoemulsions in Combination with Ionizing Radiation for Control of Rice Weevil *Sitophilus oryzae* in Stored Grains. *Journal of Food Science* 84, 1439-1446.
- Hossain, F., Follett, P., Salmieri, S., Vu, K.D., Jamshidian, M., Lacroix, M., 2016b. Perspectives on essential oil-loaded nano-delivery packaging technology for controlling stored cereal and grain pests. In *Green Pesticides Handbook*, 487-508.
- Hossain, F., Follett, P., Shankar, S., Begum, T., Salmieri, S., Lacroix, M., 2021. Radiosensitization of rice weevil *Sitophilus oryzae* using combined treatments of essential oils and ionizing radiation with gamma-ray and X-Ray at different dose rates. *Radiation Physics and Chemistry* 180, 109286.
- Hossain, F., Follett, P., Vu, K.D., Salmieri, S., Fraschini, C., Jamshidian, M., Lacroix, M., 2018. Antifungal activity of combined treatments of active methylcellulose-based films containing encapsulated nanoemulsion of essential oils and γ -irradiation: *in vitro* and *in situ* evaluations. *Cellulose* 26, 1335-1354.

- Hossain, F., Follett, P., Vu, K.D., Salmieri, S., Senoussi, C., Lacroix, M., 2014a. Radiosensitization of *Aspergillus niger* and *Penicillium chrysogenum* using basil essential oil and ionizing radiation for food decontamination. *Food Control* 45, 156-162.
- Hossain, F., Lacroix, M., Salmieri, S., Vu, K., Follett, P.A., 2014b. Basil oil fumigation increases radiation sensitivity in adult *Sitophilus oryzae* (Coleoptera: Curculionidae). *Journal of Stored Products Research* 59, 108-112.
- Hosseini, M., Razavi, S., Mousavi, M., 2009. Antimicrobial, physical and mechanical properties of chitosan-based films incorporated with thyme, clove and cinnamon essential oils. *Journal of Food Processing and Preservation* 33, 727-743.
- Hughes, J., Thomas, R., Byun, Y., Whiteside, S., 2012. Improved flexibility of thermally stable poly-lactic acid (PLA). *Carbohydrate Polymers* 88, 165-172.
- Hussain, P.R., Dar, M.A., Wani, A.M., 2012. Effect of edible coating and gamma irradiation on inhibition of mould growth and quality retention of strawberry during refrigerated storage. *International Journal of Food Science and Technology* 47, 2318-2324.
- Hyltdgaard, M., Mygind, T., Meyer, R.L., 2012a. Essential oils in food preservation: mode of action, synergies, and interactions with food matrix components. *Frontiers in Microbiology* 3, 12.
- Irradiation, I.C.G.o.F., 1991. Facts about food irradiation. International Consultative Group on Food Irradiation.
- Jafari, S.M., Assadpoor, E., He, Y., Bhandari, B., 2008. Re-coalescence of emulsion droplets during high-energy emulsification. *Food Hydrocolloids* 22, 1191-1202.
- Jamróz, E., Kulawik, P., Kopel, P., 2019. The effect of nanofillers on the functional properties of biopolymer-based films: A review. *Polymers* 11, 675.
- Jankowska, M., Rogalska, J., Wyszowska, J., Stankiewicz, M., 2017. Molecular Targets for Components of Essential Oils in the Insect Nervous System-A Review. *Molecules* 23, 34.
- Jasmani, L., Eyley, S., Schütz, C., Van Gorp, H., De Feyter, S., Thielemans, W., 2016. One-pot functionalization of cellulose nanocrystals with various cationic groups. *Cellulose* 23, 3569-3576.
- Jiang, L., Wolcott, M.P., Zhang, J., 2006. Study of biodegradable polylactide/poly (butylene adipate-co-terephthalate) blends. *Biomacromolecules* 7, 199-207.
- Jiang, Y., Joyce, D.C., 2003. ABA effects on ethylene production, PAL activity, anthocyanin and phenolic contents of strawberry fruit. *Plant Growth Regulation* 39, 171-174.

- Jo, Y.-K., Cromwell, W., Jeong, H.-K., Thorkelson, J., Roh, J.-H., Shin, D.-B., 2015. Use of silver nanoparticles for managing *Gibberella fujikuroi* on rice seedlings. *Crop Protection* 74, 65-69.
- Ju, J., Xie, Y., Guo, Y., Cheng, Y., Qian, H., Yao, W., 2019. The inhibitory effect of plant essential oils on foodborne pathogenic bacteria in food. *Critical Reviews in Food Science and Nutrition* 59, 3281-3292.
- Jung, K., Song, B.-S., Kim, M.J., Moon, B.-G., Go, S.-M., Kim, J.-K., Lee, Y.-J., Park, J.-H., 2015. Effect of X-ray, gamma ray, and electron beam irradiation on the hygienic and physicochemical qualities of red pepper powder. *LWT-Food Science and Technology* 63, 846-851.
- Kader, A.A., 1986. Potential applications of ionizing radiation in postharvest handling of fresh fruits and vegetables. *Food Technology* 40, 117-121.
- Kalt, W., Prange, R., Lidster, P., 1993. Postharvest color development of strawberries: Influence of maturity, temperature and light. *Canadian Journal of Plant Science* 73, 541-548.
- Kang, J.H., Jeon, Y.J., Min, S.C., 2021. Effects of packaging parameters on the microbial decontamination of Korean steamed rice cakes using in-package atmospheric cold plasma treatment. *Food Science and Biotechnology* 30, 1535-1542.
- Karabörklü, S., Ayvaz, A., Yilmaz, S., 2010. Bioactivities of different essential oils against the adults of two stored product insects. *Pakistan Journal of Zoology* 42.
- Karthik, P., Ezhilarasi, P., Anandharamakrishnan, C., 2017. Challenges associated in stability of food grade nanoemulsions. *Critical Reviews in Food Science and Nutrition* 57, 1435-1450.
- Keykhosravy, K., Khanzadi, S., Hashemi, M., Azizzadeh, M., 2020. Chitosan-loaded nanoemulsion containing *Zataria Multiflora* Boiss and *Bunium persicum* Boiss essential oils as edible coatings: Its impact on microbial quality of turkey meat and fate of inoculated pathogens. *International Journal of Biological Macromolecules* 150, 904-913.
- Khan, A., Khan, R.A., Salmieri, S., Le Tien, C., Riedl, B., Bouchard, J., Chauve, G., Tan, V., Kamal, M.R., Lacroix, M., 2012. Mechanical and barrier properties of nanocrystalline cellulose reinforced chitosan based nanocomposite films. *Carbohydrate Polymers* 90, 1601-1608.
- Khan, A., Salmieri, S., Frascini, C., Bouchard, J., Riedl, B., Lacroix, M., 2014. Genipin cross-linked nanocomposite films for the immobilization of antimicrobial agent. *ACS Applied Materials and Interfaces* 6, 15232-15242.
- Khan, I., Tango, C.N., Miskeen, S., Lee, B.H., Oh, D.-H., 2017a. Hurdle technology: A novel approach for enhanced food quality and safety—A review. *Food Control* 73, 1426-1444.

- Khan, R.A., Beck, S., Dussault, D., Salmieri, S., Bouchard, J., Lacroix, M., 2013. Mechanical and barrier properties of nanocrystalline cellulose reinforced poly(caprolactone) composites: Effect of gamma radiation. *Journal of Applied Polymer Science* 129, 3038-3046.
- Khani, M., Marouf, A., Amini, S., Yazdani, D., Farashiani, M.E., Ahvazi, M., Khalighi-Sigaroodi, F., Hosseini-Gharalari, A., 2017. Efficacy of Three Herbal Essential Oils Against Rice Weevil, *Sitophilus oryzae* (Coleoptera: Curculionidae). *Journal of Essential Oil Bearing Plants* 20, 937-950.
- Khodaei, D., Hamidi-Esfahani, Z., 2019. Influence of bioactive edible coatings loaded with *Lactobacillus plantarum* on physicochemical properties of fresh strawberries. *Postharvest Biology and Technology* 156, 110944.
- Khoobdel, M., Ahsaei, S.M., Farzaneh, M., 2017. Insecticidal activity of polycaprolactone nanocapsules loaded with *Rosmarinus officinalis* essential oil in *Tribolium castaneum* (Herbst). *Entomological Research* 47, 175-184.
- Kim, J., Park, N.h., Na, J.H., Han, J., 2016. Development of natural insect-repellent loaded halloysite nanotubes and their application to food packaging to prevent *Plodia interpunctella* infestation. *Journal of Food Science* 81, 1956-1965.
- Kim, S.-W., Kang, J., Park, I.-K., 2013. Fumigant toxicity of Apiaceae essential oils and their constituents against *Sitophilus oryzae* and their acetylcholinesterase inhibitory activity. *Journal of Asia-Pacific Entomology* 16, 443-448.
- Kostyukovsky, M., Rafaei, A., Gileadi, C., Demchenko, N., Shaaya, E., 2002. Activation of octopaminergic receptors by essential oil constituents isolated from aromatic plants: possible mode of action against insect pests. *Pest Management Science: formerly Pesticide Science* 58, 1101-1106.
- Krishnamachari, P., Zhang, J., Lou, J., Yan, J., Uitenham, L., 2009. Biodegradable poly (lactic acid)/clay nanocomposites by melt intercalation: a study of morphological, thermal, and mechanical properties. *International Journal of Polymer Analysis and Characterization* 14, 336-350.
- Kumar, S., Shukla, A., Baul, P.P., Mitra, A., Halder, D., 2018. Biodegradable hybrid nanocomposites of chitosan/gelatin and silver nanoparticles for active food packaging applications. *Food Packaging and Shelf Life* 16, 178-184.
- Kumar, S., Sinha, R., Prasad, T., 1993. Propionic acid as a preservative of maize grains in traditional storage in India. *Journal of Stored Products Research* 29, 89-93.

- Kuorwel, K.K., Cran, M.J., Orbell, J.D., Buddhadasa, S., Bigger, S.W., 2015. Review of mechanical properties, migration, and potential applications in active food packaging systems containing nanoclays and nanosilver. *Comprehensive Reviews in Food Science and Food Safety* 14, 411-430.
- Kusmono, Wildan, M.W., Lubis, F.I., 2021. Fabrication and Characterization of Chitosan/Cellulose Nanocrystal/Glycerol Bio-Composite Films. *Polymers* 13, 1096.
- Kyung, H.K., Ramakrishnan, S.R., Kwon, J.H., 2019. Dose rates of electron beam and gamma ray irradiation affect microbial decontamination and quality changes in dried red pepper (*Capsicum annuum* L.) powder. *Journal of the Science of Food and Agriculture* 99, 632-638.
- Lacroix, M., Follett, P., 2015. Combination irradiation treatments for food safety and phytosanitary uses. *Stewart Postharvest Review* 11, 1-10.
- Lafarga, T., Colás-Medà, P., Abadías, M., Aguiló-Aguayo, I., Bobo, G., Viñas, I., 2019. Strategies to reduce microbial risk and improve quality of fresh and processed strawberries: A review. *Innovative Food Science and Emerging Technologies* 52, 197-212.
- Laidler, M.R., Tourdjman, M., Buser, G.L., Hostetler, T., Repp, K.K., Leman, R., Samadpour, M., Keene, W.E., 2013. *Escherichia coli* O157: H7 infections associated with consumption of locally grown strawberries contaminated by deer. *Clinical Infectious Diseases* 57, 1129-1134.
- Lee, B.-H., Annis, P.C., Tumaalii, F.a., Choi, W.-S., 2004a. Fumigant toxicity of essential oils from the Myrtaceae family and 1,8-cineole against 3 major stored-grain insects. *Journal of Stored Products Research* 40, 553-564.
- Lee, S.-Y., Chung, H.-J., Shin, J.-H., Dougherty, R.H., Kang, D.-H., 2006. Survival and growth of foodborne pathogens during cooking and storage of oriental-style rice cakes. *Journal of Food Protection* 69, 3037-3042.
- Lee, S.-Y., Yang, H.-S., Kim, H.-J., Jeong, C.-S., Lim, B.-S., Lee, J.-N., 2004b. Creep behavior and manufacturing parameters of wood flour filled polypropylene composites. *Composite Structures* 65, 459-469.
- Lee, S.C., Billmyre, R.B., Li, A., Carson, S., Sykes, S.M., Huh, E.Y., Mieczkowski, P., Ko, D.C., Cuomo, C.A., Heitman, J., 2014. Analysis of a food-borne fungal pathogen outbreak: virulence and genome of a *Mucor circinelloides* isolate from yogurt. *Microbiology* 5, 10-1128.

- Lee, S.E., Lee, B.H., Choi, W.S., Park, B.S., Kim, J.G., Campbell, B.C., 2001. Fumigant toxicity of volatile natural products from Korean spices and medicinal plants towards the rice weevil, *Sitophilus oryzae* (L). *Pest Management Science: formerly Pesticide Science* 57, 548-553.
- Leyva Salas, M., Mounier, J., Valence, F., Coton, M., Thierry, A., Coton, E., 2017. Antifungal Microbial Agents for Food Biopreservation-A Review. *Microorganisms* 5, 37.
- Li, F., Xu, X., Yu, J., Cao, A., 2007. The morphological effects upon enzymatic degradation of poly (butylene succinate-co-butylene terephthalate) s (PBST). *Polymer Degradation and Stability* 92, 1053-1060.
- Li, G., Shankar, S., Rhim, J.-W., Oh, B.-Y., 2015a. Effects of preparation method on properties of poly(butylene adipate-co-terephthalate) films. *Food Science and Biotechnology*, 24, 1679-1685.
- Li, L., Song, W., Shen, C., Dong, Q., Wang, Y., Zuo, S., 2020. Active packaging film containing oregano essential oil microcapsules and their application for strawberry preservation. *Journal of Food Processing and Preservation* 44, 14799.
- Li, P.-H., Chiang, B.-H., 2012. Process optimization and stability of D-limonene-in-water nanoemulsions prepared by ultrasonic emulsification using response surface methodology. *Ultrasonics Sonochemistry* 19, 192-197.
- Li, Q., Zhou, J., Zhang, L., 2009. Structure and properties of the nanocomposite films of chitosan reinforced with cellulose whiskers. *Journal of Polymer Science Part B: Polymer Physics* 47, 1069-1077.
- Li, W., Bai, L., Fu, P., Han, H., Liu, J., Guo, Y., 2018. The epidemiology of *Listeria monocytogenes* in China. *Foodborne Pathogens and Disease* 15, 459-466.
- Li, W., Chen, H., He, Z., Han, C., Liu, S., Li, Y., 2015b. Influence of surfactant and oil composition on the stability and antibacterial activity of eugenol nanoemulsions. *LWT-Food Science and Technology* 62, 39-47.
- Lim, L.T., Vanyo, T., Randall, J., Cink, K., Agrawal, A.K., 2022. Processing of poly (lactic acid). *Poly (Lactic Acid) Synthesis, Structures, Properties, Processing, Applications, and End of Life*, 231-270.
- Lima, F., Vieira, K., Santos, M., de Souza, P.M., 2018. Effects of radiation technologies on food nutritional quality. *Descriptive Food Science* 1, 17.
- Liu, Y., Tang, T., Duan, S., Qin, Z., Zhao, H., Wang, M., Li, C., Zhang, Z., Liu, A., Han, G., 2020. Applicability of rice doughs as promising food materials in extrusion-based 3D printing. *Food and Bioprocess Technology* 13, 548-563.

- Llana-Ruiz-Cabello, M., Pichardo, S., Bermúdez, J., Baños, A., Núñez, C., Guillamón, E., Aucejo, S., Cameán, A., 2016. Development of PLA films containing oregano essential oil (*Origanum vulgare* L. *virens*) intended for use in food packaging. *Food Additives and Contaminants: Part A* 33, 1374-1386.
- Llinares, R., Ramirez, P., Carmona, J.A., Trujillo-Cayado, L.A., Munoz, J., 2021. Assessment of fennel oil microfluidized nanoemulsions stabilization by advanced performance xanthan gum. *Foods* 10, 693.
- Llinares, R., Santos, J., Trujillo-Cayado, L.A., Ramirez, P., Muñoz, J., 2018. Enhancing rosemary oil-in-water microfluidized nanoemulsion properties through formulation optimization by response surface methodology. *LWT-Food Science and Technology* 97, 370-375.
- Lopez, M.D., Campoy, F.J., Pascual-Villalobos, M.J., Munoz-Delgado, E., Vidal, C.J., 2015. Acetylcholinesterase activity of electric eel is increased or decreased by selected monoterpenoids and phenylpropanoids in a concentration-dependent manner. *Chemico-Biological Interactions* 229, 36-43.
- López, M.D., Jordán, M.J., Pascual-Villalobos, M.J., 2008. Toxic compounds in essential oils of coriander, caraway and basil active against stored rice pests. *Journal of Stored Products Research* 44, 273-278.
- López, M.D., Pascual-Villalobos, M.J., 2010. Mode of inhibition of acetylcholinesterase by monoterpenoids and implications for pest control. *Industrial Crops and Products* 31, 284-288.
- López, V., Avendaño V, S., Romero R, J., Garrido, S., Espinoza, J., Vargas, M., 2005. Effect of gamma irradiation on the microbiological quality of minimally processed vegetables. *L. Archivos latinoamericanos de Nutricion* 55, 287-292.
- Luzi, F., Fortunati, E., Giovanale, G., Mazzaglia, A., Torre, L., Balestra, G.M., 2017. Cellulose nanocrystals from *Actinidia deliciosa* pruning residues combined with carvacrol in PVA_CH films with antioxidant/antimicrobial properties for packaging applications. *International Journal of Biological Macromolecules* 104, 43-55.
- Machado-Moreira, B., Richards, K., Brennan, F., Abram, F., Burgess, C.M., 2019. Microbial Contamination of Fresh Produce: What, Where, and How? *Comprehensive Reviews in Food Science and Food Safety* 18, 1727-1750.
- Maherani, B., Harich, M., Salmieri, S., Lacroix, M., 2018. Comparative evaluation of antimicrobial efficiency of FOODGARD F410B citrus extract and sodium benzoate against foodborne pathogens in strawberry filling. *Journal of Food Processing and Preservation* 42, e13549.

- Maherani, B., Hossain, F., Criado, P., Ben-Fadhel, Y., Salmieri, S., Lacroix, M., 2016. World market development and consumer acceptance of irradiation technology. *Foods* 5, 79.
- Mahmud, J., Sarmast, E., Shankar, S., Lacroix, M., 2022. Advantages of nanotechnology developments in active food packaging. *Food Research International* 154, 111023.
- Maity, J.P., Kar, S., Banerjee, S., Sudershan, M., Chakraborty, A., Santra, S.C., 2011. Effects of gamma radiation on fungi infected rice (*in vitro*). *International Journal of Radiation Biology* 87, 1097-1102.
- Majeed, A., Muhammad, Z., Majid, A., Shah, A., Hussain, M., 2014. Impact of low doses of gamma irradiation on shelf life and chemical quality of strawberry (*Fragaria x ananassa*) CV.'CORONA'. *JAPS: Journal of Animal and Plant Sciences* 24.
- Malekjani, N., Jafari, S.M., 2021. Modeling the release of food bioactive ingredients from carriers/nanocarriers by the empirical, semiempirical, and mechanistic models. *Comprehensive Reviews in Food Science and Food Safety* 20, 3-47.
- Mannaa, M., Kim, K.D., 2018. Biocontrol activity of volatile-producing *Bacillus megaterium* and *Pseudomonas protegens* against *Aspergillus* and *Penicillium* spp. predominant in stored rice grains: study II. *Mycobiology* 46, 52-63.
- Maraei, R.W., Elsayy, K.M., 2017. Chemical quality and nutrient composition of strawberry fruits treated by γ -irradiation. *Journal of Radiation Research and Applied Sciences* 10, 80-87.
- Martínez-Castañón, G.A., Niño-Martínez, N., Martínez-Gutierrez, F., Martínez-Mendoza, J.R., Ruiz, F., 2008. Synthesis and antibacterial activity of silver nanoparticles with different sizes. *Journal of Nanoparticle Research* 10, 1343-1348.
- Martínez-Hernández, G.B., Amodio, M.L., Colelli, G., 2017. Carvacrol-loaded chitosan nanoparticles maintain quality of fresh-cut carrots. *Innovative Food Science and Emerging Technologies* 41, 56-63.
- McClements, D.J., 2002. Theoretical prediction of emulsion color. *Advances in Colloid and Interface Science* 97, 63-89.
- Metak, A.M., Nabhani, F., Connolly, S.N., 2015. Migration of engineered nanoparticles from packaging into food products. *LWT - Food Science and Technology* 64, 781-787.
- Milanović, V., Sabbatini, R., Garofalo, C., Cardinali, F., Pasquini, M., Aquilanti, L., Osimani, A., 2021. Evaluation of the inhibitory activity of essential oils against spoilage yeasts and their potential application in yogurt. *International Journal of Food Microbiology* 341, 109048.
- Mitcham, E., 2007. Quality of berries associated with preharvest and postharvest conditions. *Food Science and Technology-New York-Marcel Dekker-* 168, 207.

- Mith, H., Dure, R., Delcenserie, V., Zhiri, A., Daube, G., Clinquart, A., 2014. Antimicrobial activities of commercial essential oils and their components against food-borne pathogens and food spoilage bacteria. *Food Science and Nutrition* 2, 403-416.
- Moghimi, R., Ghaderi, L., Rafati, H., Aliahmadi, A., McClements, D.J., 2016. Superior antibacterial activity of nanoemulsion of *Thymus daenensis* essential oil against *E. coli*. *Food Chemistry* 194, 410-415.
- Mohammadzadeh, A., 2017. *In vitro* antibacterial activity of essential oil and ethanolic extract of Ajowan (*Carum copticum*) against some food-borne pathogens. *Journal of Global Pharma Technology* 9, 20-25.
- Montero, Y., Souza, A.G., Oliveira, É.R., dos Santos Rosa, D., 2021a. Nanocellulose functionalized with cinnamon essential oil: A potential application in active biodegradable packaging for strawberry. *Sustainable Materials and Technologies* 29, e00289.
- Moraes Filho, L.E.P.T., Andrade, M.F., Freitas, L.F., Palha, M.d.L.A.P.F., Vinhas, G.M., 2022. Development and characterization of poly(butylene adipate-co-terephthalate) (PBAT) antimicrobial films with clove and cinnamon essential oils. *Journal of Food Processing and Preservation* 46, 16489.
- Moreira, S.R., Schwan, R.F., Carvalho, E.P.d., Wheals, A.E., 2001. Isolation and identification of yeasts and filamentous fungi from yoghurts in Brazil. *Brazilian Journal of Microbiology* 32, 117-122.
- Morelli, C.L., Belgacem, N., Bretas, R.E.S., Bras, J., 2016. Melt extruded nanocomposites of polybutylene adipate-co-terephthalate (PBAT) with phenylbutyl isocyanate modified cellulose nanocrystals. *Journal of Applied Polymer Science* 133, 43678.
- Morones, J.R., Elechiguerra, J.L., Camacho, A., Holt, K., Kouri, J.B., Ramirez, J.T., Yacaman, M.J., 2005. The bactericidal effect of silver nanoparticles. *Nanotechnology* 16, 2346-2353.
- Motlagh, N.V., Aliabadi, M., Rahmani, E., Ghorbanpour, S., 2020. The Effect of Nano-Silver Packaging on Quality Maintenance of Fresh Strawberry. *International Journal of Nutrition and Food Engineering* 14, 123-128.
- Mousavian, D., Mohammadi Nafchi, A., Nouri, L., Abedinia, A., 2021. Physicomechanical properties, release kinetics, and antimicrobial activity of activated low-density polyethylene and orientated polypropylene films by Thyme essential oil active component. *Journal of Food Measurement and Characterization* 15, 883-891.

- Mujtaba, M., Lipponen, J., Ojanen, M., Puttonen, S., Vaittinen, H., 2022. Trends and challenges in the development of bio-based barrier coating materials for paper/cardboard food packaging; a review. *The Science of the Total Environment* 851, 158328.
- Mujtaba, M., Morsi, R.E., Kerch, G., Elsabee, M.Z., Kaya, M., Labidi, J., Khawar, K.M., 2019. Current advancements in chitosan-based film production for food technology; A review. *International Journal of Biological Macromolecules* 121, 889-904.
- Nagarajan, V., Misra, M., Mohanty, A.K., 2013. New engineered biocomposites from poly (3-hydroxybutyrate-co-3-hydroxyvalerate)(PHBV)/poly (butylene adipate-co-terephthalate)(PBAT) blends and switchgrass: Fabrication and performance evaluation. *Industrial Crops and Products* 42, 461-468.
- Nazarzadeh, E., Anthonypillai, T., Sajjadi, S., 2013. On the growth mechanisms of nanoemulsions. *Journal of Colloid and Interface Science* 397, 154-162.
- Nazzaro, F., Fratianni, F., De Martino, L., Coppola, R., De Feo, V., 2013. Effect of essential oils on pathogenic bacteria. *Pharmaceuticals* 6, 1451-1474.
- Nesci, A.V., Etcheverry, M.G., 2006. Control of *Aspergillus* growth and aflatoxin production using natural maize phytochemicals under different conditions of water activity. *Pest Management Science: formerly Pesticide Science* 62, 775-784.
- Nguefack, J., Leth, V., Dongmo, J.L., Torp, J., Zollo, P.A., Nyasse, S., 2008. Use of three essential oils as seed treatments against seed-borne fungi of rice (*Oryza sativa* L.). *American-Eurasian Journal of Agricultural and Environmental Science*, New work 4, 554-560.
- Nguefack, J., Somda, I., Mortensen, C., Amvam Zollo, P., 2005. Evaluation of five essential oils from aromatic plants of Cameroon for controlling seed-borne bacteria of rice (*Oryza sativa* L.). *Seed Science and Technology* 33, 397-407.
- Nikkhah, M., Hashemi, M., Habibi Najafi, M.B., Farhoosh, R., 2017a. Synergistic effects of some essential oils against fungal spoilage on pear fruit. *International Journal of Food Microbiology* 257, 285-294.
- Nirmal, N.P., Mereddy, R., Li, L., Sultanbawa, Y., 2018. Formulation, characterisation and antibacterial activity of lemon myrtle and anise myrtle essential oil in water nanoemulsion. *Food Chemistry* 254, 1-7.
- Njoroge, S.M., Phi, N.T.L., Sawamura, M., 2009. Chemical composition of peel essential oils of sweet oranges (*Citrus sinensis*) from Uganda and Rwanda. *Journal of Essential Oil Bearing Plants* 12, 26-33.

- Nyenje, M.E., Odadjare, C.E., Tanih, N.F., Green, E., Ndip, R.N., 2012. Foodborne pathogens recovered from ready-to-eat foods from roadside cafeterias and retail outlets in Alice, Eastern Cape Province, South Africa: public health implications. *International Journal of Environmental Research and Public Health* 9, 2608-2619.
- Ogendo, J.O., Kostyukovsky, M., Ravid, U., Matasyoh, J.C., Deng, A.L., Omolo, E.O., Kariuki, S.T., Shaaya, E., 2008. Bioactivity of *Ocimum gratissimum* L. oil and two of its constituents against five insect pests attacking stored food products. *Journal of Stored Products Research* 44, 328-334.
- Oladzadabbasabadi, N., Nafchi, A.M., Ariffin, F., Wijekoon, M.J.O., Al-Hassan, A., Dheyab, M.A., Ghasemlou, M., 2022. Recent advances in extraction, modification, and application of chitosan in packaging industry. *Carbohydrate Polymers* 277, 118876.
- Oufedjikh, H., Mahrouz, M., Amiot, M.J., Lacroix, M., 2000. Effect of γ -irradiation on phenolic compounds and phenylalanine ammonia-lyase activity during storage in relation to peel injury from peel of Citrus clementina Hort. Ex. Tanaka. *Journal of Agricultural and Food Chemistry* 48, 559-565.
- Oussalah, M., Caillet, S., Lacroix, M., 2006. Mechanism of action of Spanish oregano, Chinese cinnamon, and savory essential oils against cell membranes and walls of *Escherichia coli* O157: H7 and *Listeria monocytogenes*. *Journal of Food Protection* 69, 1046-1055.
- Oussalah, M., Caillet, S., Saucier, L., Lacroix, M., 2007. Inhibitory effects of selected plant essential oils on the growth of four pathogenic bacteria: *E. coli* O157: H7, *Salmonella typhimurium*, *Staphylococcus aureus* and *Listeria monocytogenes*. *Food Control* 18, 414-420.
- Paniagua, C., Posé, S., Morris, V.J., Kirby, A.R., Quesada, M.A., Mercado, J.A., 2014. Fruit softening and pectin disassembly: an overview of nanostructural pectin modifications assessed by atomic force microscopy. *Annals of Botany* 114, 1375-1383.
- Park, C.G., Jang, M., Yoon, K.A., Kim, J., 2016. Insecticidal and acetylcholinesterase inhibitory activities of Lamiaceae plant essential oils and their major components against *Drosophila suzukii* (Diptera: Drosophilidae). *Industrial Crops and Products* 89, 507-513.
- Park, J.S., Ha, J.W., 2019. X-ray irradiation inactivation of *Escherichia coli* O157:H7, *Salmonella enterica* Serovar Typhimurium, and *Listeria monocytogenes* on sliced cheese and its bactericidal mechanisms. *International Journal of Food Microbiology* 289, 127-133.

- Paster, N., Droby, S., Chalutz, E., Menasherov, M., Nitzan, R., Wilson, C., 1993. Evaluation of the potential of the yeast *Pichia guilliermondii* as a biocontrol agent against *Aspergillus flavus* and fungi of stored soya beans. *Mycological Research* 97, 1201-1206.
- Patel, D.K., Dutta, S.D., Ganguly, K., Lim, K.T., 2021. Multifunctional bioactive chitosan/cellulose nanocrystal scaffolds eradicate bacterial growth and sustain drug delivery. *International Journal of Biological Macromolecules* 170, 178-188.
- Patil, D.K., Agrawal, D.S., Mahire, R.R., More, D.H., 2016. Synthesis, characterization and controlled release studies of ethyl cellulose microcapsules incorporating essential oil using an emulsion solvent evaporation method. *American Journal of Essential Oils and Natural Products* 4, 23-31.
- Pereda, M., Amica, G., Marcovich, N.E., 2012. Development and characterization of edible chitosan/olive oil emulsion films. *Carbohydrate Polymers* 87, 1318-1325.
- Peretto, G., Du, W.-X., Avena-Bustillos, R.J., Sarreal, S.B.L., Hua, S.S.T., Sambo, P., McHugh, T.H., 2014. Increasing strawberry shelf-life with carvacrol and methyl cinnamate antimicrobial vapors released from edible films. *Postharvest Biology and Technology* 89, 11-18.
- Petchwattana, N., Naknaen, P., 2015. Utilization of thymol as an antimicrobial agent for biodegradable poly(butylene succinate). *Materials Chemistry and Physics* 163, 369-375.
- Piccolo, M.I., Toloza, A.C., Mougabure Cueto, G., Zygadlo, J., Zerba, E., 2008. Anticholinesterase and pediculicidal activities of monoterpenoids. *Fitoterapia* 79, 271-278.
- Pinheiro, I., Ferreira, F., Souza, D., Gouveia, R., Lona, L., Morales, A., Mei, L., 2017. Mechanical, rheological and degradation properties of PBAT nanocomposites reinforced by functionalized cellulose nanocrystals. *European Polymer Journal* 97, 356-365.
- Pitt, J.I., Hocking, A.D., 2009. *Fungi and food spoilage*. New York Springer 519, 388.
- Poimenidou, S.V., Bikouli, V.C., Gardeli, C., Mitsi, C., Tarantilis, P.A., Nychas, G.-J., Skandamis, P.N., 2016a. Effect of single or combined chemical and natural antimicrobial interventions on *Escherichia coli* O157: H7, total microbiota and color of packaged spinach and lettuce. *International Journal of Food Microbiology* 220, 6-18.
- Poimenidou, S.V., Bikouli, V.C., Gardeli, C., Mitsi, C., Tarantilis, P.A., Nychas, G.J., Skandamis, P.N., 2016b. Effect of single or combined chemical and natural antimicrobial interventions on *Escherichia coli* O157:H7, total microbiota and color of packaged spinach and lettuce. *International Journal of Food Microbiology* 220, 6-18.

- Prakash, A., Baskaran, R., Paramasivam, N., Vadivel, V., 2018. Essential oil based nanoemulsions to improve the microbial quality of minimally processed fruits and vegetables: A review. *Food Research International* 111, 509-523.
- Priestley, C.M., Burgess, I.F., Williamson, E.M., 2006. Lethality of essential oil constituents towards the human louse, *Pediculus humanus*, and its eggs. *Fitoterapia* 77, 303-309.
- Qian, C., McClements, D.J., 2011. Formation of nanoemulsions stabilized by model food-grade emulsifiers using high-pressure homogenization: Factors affecting particle size. *Food Hydrocolloids* 25, 1000-1008.
- Radfar, R., Hosseini, H., Farhodi, M., Ghasemi, I., Srednicka-Tober, D., Shamloo, E., Khaneghah, A.M., 2020. Optimization of antibacterial and mechanical properties of an active LDPE/starch/nanoclay nanocomposite film incorporated with date palm seed extract using D-optimal mixture design approach. *International Journal of Biological Macromolecules* 158, 790-799.
- Rajeshkumar, G., Seshadri, S.A., Devnani, G., Sanjay, M., Siengchin, S., Maran, J.P., Al-Dhabi, N.A., Karuppiah, P., Mariadhas, V.A., Sivarajasekar, N., 2021. Environment friendly, renewable and sustainable poly lactic acid (PLA) based natural fiber reinforced composites—A comprehensive review. *Journal of Cleaner Production* 310, 127483.
- Rangel, J.M., Sparling, P.H., Crowe, C., Griffin, P.M., Swerdlow, D.L., 2005. Epidemiology of *Escherichia coli* O157: H7 outbreaks, united states, 1982–2002. *Emerging Infectious Diseases* 11, 603.
- Raquez, J.M., Nabar, Y., Narayan, R., Dubois, P., 2008. *In situ* compatibilization of maleated thermoplastic starch/polyester melt-blends by reactive extrusion. *Polymer Engineering and Science* 48, 1747-1754.
- Rawat, S., 2015. Food Spoilage: Microorganisms and their prevention. *Asian Journal of Plant Science and Research* 5, 47-56.
- Reichert, C.L., Bugnicourt, E., Coltelli, M.-B., Cinelli, P., Lazzeri, A., Canesi, I., Braca, F., Martínez, B.M., Alonso, R., Agostinis, L., 2020. Bio-based packaging: Materials, modifications, industrial applications and sustainability. *Polymers* 12, 1558.
- Requena, R., Vargas, M., Chiralt, A., 2017. Release kinetics of carvacrol and eugenol from poly(hydroxybutyrate-co-hydroxyvalerate) (PHBV) films for food packaging applications. *European Polymer Journal* 92, 185-193.

- Requena, R., Vargas, M., Chiralt, A., 2019. Study of the potential synergistic antibacterial activity of essential oil components using the thiazolyl blue tetrazolium bromide (MTT) assay. *LWT-Food Science and Technology* 101, 183-190.
- Revol, J.-F., Bradford, H., Giasson, J., Marchessault, R., Gray, D., 1992. Helicoidal self-ordering of cellulose microfibrils in aqueous suspension. *International Journal of Biological Macromolecules* 14, 170-172.
- Rezaeigolestani, M., Misaghi, A., Khanjari, A., Basti, A.A., Abdulkhani, A., Fayazfar, S., 2017. Antimicrobial evaluation of novel poly-lactic acid based nanocomposites incorporated with bioactive compounds *in-vitro* and in refrigerated vacuum-packed cooked sausages. *International Journal of Food Microbiology* 260, 1-10.
- Rhim, J.-W., 2011. Effect of clay contents on mechanical and water vapor barrier properties of agar-based nanocomposite films. *Carbohydrate Polymers* 86, 691-699.
- Rhim, J.-W., 2013. Effect of PLA lamination on performance characteristics of agar/k-carrageenan/clay bio-nanocomposite film. *Food Research International* 51, 714-722.
- Rhim, J.-W., Mohanty, A.K., Singh, S.P., Ng, P.K.W., 2006. Effect of the processing methods on the performance of polylactide films: Thermocompression versus solvent casting. *Journal of Applied Polymer Science* 101, 3736-3742.
- Sabbour, M., 2012. Entomotoxicity assay of two nanoparticle materials 1-(Al₂O₃ and TiO₂) against *Sitophilus oryzae* under laboratory and store conditions in Egypt. *Journal of Applied Sciences* 1, 103-108.
- Salgado, V., 2013. Insecticide mode of action: technical training manual. BASF Corporation, Ludwigshafen, Germany.
- Sallato, B., Torres, R., Zóffoli, J.P., Latorre, B., 2007. Effect of boscalid on postharvest decay of strawberry caused by *Botrytis cinerea* and *Rhizopus stolonifer*. *Spanish Journal of Agricultural Research* 5, 67-78.
- Salmieri, S., Islam, F., Khan, R.A., Hossain, F.M., Ibrahim, H.M.M., Miao, C., Hamad, W.Y., Lacroix, M., 2014a. Antimicrobial nanocomposite films made of poly(lactic acid)-cellulose nanocrystals (PLA-CNC) in food applications: part A—effect of nisin release on the inactivation of *Listeria monocytogenes* in ham. *Cellulose* 21, 1837-1850.
- Salmieri, S., Islam, F., Khan, R.A., Hossain, F.M., Ibrahim, H.M.M., Miao, C., Hamad, W.Y., Lacroix, M., 2014b. Antimicrobial nanocomposite films made of poly(lactic acid)-cellulose nanocrystals (PLA-CNC) in food applications—part B: effect of oregano essential oil

- release on the inactivation of *Listeria monocytogenes* in mixed vegetables. *Cellulose* 21, 4271-4285.
- Salmieri, S., Lacroix, M., 2006. Physicochemical properties of alginate/polycaprolactone-based films containing essential oils. *Journal of Agricultural and Food Chemistry* 54, 10205-10214.
- Samir, M.A.S.A., Alloin, F., Sanchez, J.-Y., Dufresne, A., 2004. Cellulose nanocrystals reinforced poly (oxyethylene). *Polymer* 45, 4149-4157.
- Sani, I.K., Pirsä, S., Tağı, Ş., 2019. Preparation of chitosan/zinc oxide/Melissa officinalis essential oil nano-composite film and evaluation of physical, mechanical and antimicrobial properties by response surface method. *Polymer Testing* 79, 106004.
- Santana-Melo, G.F., Rodrigues, B.V., da Silva, E., Ricci, R., Marciano, F.R., Webster, T.J., Vasconcellos, L.M., Lobo, A.O., 2017. Electrospun ultrathin PBAT/nHAp fibers influenced the *in vitro* and *in vivo* osteogenesis and improved the mechanical properties of neoformed bone. *Colloids and Surfaces B: Biointerfaces* 155, 544-552.
- SAS, I., 2013. JMP 11 basic analysis. SAS Institute.
- Sassi, G., Salmieri, S., Allahdad, Z., Karboune, S., Lacroix, M., 2022. Development of a natural antifungal formulation for grated cheese and a microencapsulation approach using whey protein isolate and maltodextrin blend. *Journal of Food Science* 87, 3822-3840.
- Scallan, E., Hoekstra, R.M., Angulo, F.J., Tauxe, R.V., Widdowson, M.-A., Roy, S.L., Jones, J.L., Griffin, P.M., 2011. Foodborne illness acquired in the United States—major pathogens. *Emerging Infectious Diseases* 17, 7.
- Scandorieiro, S., de Camargo, L.C., Lancheros, C.A., Yamada-Ogatta, S.F., Nakamura, C.V., de Oliveira, A.G., Andrade, C.G., Duran, N., Nakazato, G., Kobayashi, R.K., 2016. Synergistic and Additive Effect of Oregano Essential Oil and Biological Silver Nanoparticles against Multidrug-Resistant Bacterial Strains. *Frontiers in Microbiology* 7, 760.
- Sessa, M., Ferrari, G., Donsi, F., 2015. Novel edible coating containing essential oil nanoemulsions to prolong the shelf life of vegetable products. *Chemical Engineering Transactions* 43, 55-60.
- Severino, R., Vu, K.D., Donsi, F., Salmieri, S., Ferrari, G., Lacroix, M., 2014. Antibacterial and physical effects of modified chitosan based-coating containing nanoemulsion of mandarin essential oil and three non-thermal treatments against *Listeria innocua* in green beans. *International Journal of Food Microbiology* 191, 82-88.

- Shaaya, E., Kostjukovski, M., Eilberg, J.e., Sukprakarn, C., 1997. Plant oils as fumigants and contact insecticides for the control of stored-product insects. *Journal of Stored Products Research* 33, 7-15.
- Shahlari, M., Lee, S., 2012. Mechanical and morphological properties of poly (butylene adipate-co-terephthalate) and poly (lactic acid) blended with organically modified silicate layers. *Polymer Engineering and Science* 52, 1420-1428.
- Shankar, S., Follett, P., Ayari, S., Hossain, F., Salmieri, S., Lacroix, M., 2020. Microbial radiosensitization using combined treatments of essential oils and irradiation-part B: Comparison between gamma-ray and X-ray at different dose rates. *Microbial Pathogenesis* 143, 104118.
- Shankar, S., Khodaei, D., Lacroix, M., 2021. Effect of chitosan/essential oils/silver nanoparticles composite films packaging and gamma irradiation on shelf life of strawberries. *Food Hydrocolloids* 117, 106750.
- Shankar, S., Rhim, J.-W., 2016. Tocopherol-mediated synthesis of silver nanoparticles and preparation of antimicrobial PBAT/silver nanoparticles composite films. *LWT - Food Science and Technology* 72, 149-156.
- Shankar, S., Rhim, J.W., 2018. Preparation of antibacterial poly(lactide)/poly(butylene adipate-co-terephthalate) composite films incorporated with grapefruit seed extract. *International Journal of Biological Macromolecules* 120, 846-852.
- Shankar, S., Teng, X., Rhim, J.-W., 2014. Properties and characterization of agar/CuNP bionanocomposite films prepared with different copper salts and reducing agents. *Carbohydrate Polymers* 114, 484-492.
- Sharma, S., Barkauskaite, S., Duffy, B., Jaiswal, A.K., Jaiswal, S., 2020. Characterization and Antimicrobial Activity of Biodegradable Active Packaging Enriched with Clove and Thyme Essential Oil for Food Packaging Application. *Foods* 9, 1117.
- Sharma, S., Barkauskaite, S., Jaiswal, A.K., Jaiswal, S., 2021. Essential oils as additives in active food packaging. *Food Chemistry* 343, 128403.
- Sharma, S., Mulrey, L., Byrne, M., Jaiswal, A.K., Jaiswal, S., 2022. Encapsulation of Essential Oils in Nanocarriers for Active Food Packaging. *Foods* 11, 2337.
- Sharmin, N., Khan, R.A., Salmieri, S., Dussault, D., Lacroix, M., 2012. Fabrication and Characterization of Biodegradable Composite Films Made of Using Poly(caprolactone) Reinforced with Chitosan. *Journal of Polymers and the Environment* 20, 698-705.

- Shavisi, N., Khanjari, A., Basti, A.A., Misaghi, A., Shahbazi, Y., 2017. Effect of PLA films containing propolis ethanolic extract, cellulose nanoparticle and Ziziphora clinopodioides essential oil on chemical, microbial and sensory properties of minced beef. *Meat Science* 124, 95-104.
- Sheikholeslami, S., Mousavi, S.E., Ahmadi Ashtiani, H.R., Hosseini Doust, S.R., Mahdi Rezayat, S., 2016. Antibacterial Activity of Silver Nanoparticles and Their Combination with *Zataria multiflora* Essential Oil and Methanol Extract. *Jundishapur Journal of Microbiology* 9, e36070.
- Siddiqui, M.S., Nadeem, S.F., 2007. Epidemiological investigation of an outbreak of food poisoning traced to yogurt among personnel of a Military training center. *Pakistan Armed Forces Medical Journal* 57, 194-200.
- Simbine, E.O., Rodrigues, L.d.C., Lapa-GuimarÃEs, J., Kamimura, E.S., Corassin, C.H., Oliveira, C.A.F.d., 2019. Application of silver nanoparticles in food packages: a review. *Food Science and Technology* 39, 793-802.
- Singh, G., Kapoor, I.P.S., Singh, P., 2011. Effect of volatile oil and oleoresin of anise on the shelf life of yogurt. *Journal of Food Processing and Preservation* 35, 778-783.
- Siracusa, V., Rocculi, P., Romani, S., Dalla Rosa, M., 2008. Biodegradable polymers for food packaging: a review. *Trends in Food Science and Technology* 19, 634-643.
- Snyder, A.B., Churey, J.J., Worobo, R.W., 2016a. Characterization and control of *Mucor circinelloides* spoilage in yogurt. *International Journal of Food Microbiology* 228, 14-21.
- Sotiriou, G.A., Pratsinis, S.E., 2011. Engineering nanosilver as an antibacterial, biosensor and bioimaging material. *Current Opinion in Chemical Engineering* 1, 3-10.
- Srinivasa, P., Baskaran, R., Ramesh, M., Harish Prashanth, K., Tharanathan, R., 2002. Storage studies of mango packed using biodegradable chitosan film. *European Food Research and Technology* 215, 504-508.
- Srisa, A., Harnkarnsujarit, N., 2020. Antifungal films from trans-cinnamaldehyde incorporated poly(lactic acid) and poly(butylene adipate-co-terephthalate) for bread packaging. *Food Chemistry* 333, 127537.
- Stadler, T., Buteler, M., Weaver, D.K., Sofie, S., 2012. Comparative toxicity of nanostructured alumina and a commercial inert dust for *Sitophilus oryzae* (L.) and *Rhizopertha dominica* (F.) at varying ambient humidity levels. *Journal of Stored Products Research* 48, 81-90.
- Su, S., Duhme, M., Kopitzky, R., 2020. Uncompatibilized PBAT/PLA Blends: Manufacturability, Miscibility and Properties. *Materials (Basel)* 13, 4897.

- Subbuvel, M., Kavan, P., 2021. Development and investigation of antibacterial and antioxidant characteristics of poly lactic acid films blended with neem oil and curcumin. *Journal of Applied Polymer Science* 139, 51891.
- Sung, S.H., Chang, Y., Han, J., 2017. Development of polylactic acid nanocomposite films reinforced with cellulose nanocrystals derived from coffee silverskin. *Carbohydrate Polymers* 169, 495-503.
- Suppakul, P., Miltz, J., Sonneveld, K., Bigger, S.W., 2003. Active packaging technologies with an emphasis on antimicrobial packaging and its applications. *Journal of Food Science* 68, 408-420.
- Suresh Kumar, R., Shiny, P., Anjali, C., Jerobin, J., Goshen, K.M., Magdassi, S., Mukherjee, A., Chandrasekaran, N., 2013. Distinctive effects of nano-sized permethrin in the environment. *Environmental Science and Pollution Research* 20, 2593-2602.
- Tajkarimi, M., Ibrahim, S.A., Cliver, D., 2010. Antimicrobial herb and spice compounds in food. *Food Control* 21, 1199-1218.
- Tallentire, A., Miller, A., 2015. Microbicidal effectiveness of X-rays used for sterilization purposes. *Radiation Physics and Chemistry* 107, 128-130.
- Tallentire, A., Miller, A., Helt-Hansen, J., 2010. A comparison of the microbicidal effectiveness of gamma rays and high and low energy electron radiations. *Radiation Physics and Chemistry* 79, 701-704.
- Tančinová, D., Mašková, Z., Mendelová, A., Foltinová, D., Barboráková, Z., Medo, J., 2022. Antifungal Activities of Essential Oils in Vapor Phase against *Botrytis cinerea* and Their Potential to Control Postharvest Strawberry Gray Mold. *Foods* 11, 2945.
- Tandorost, R., Karimpour, Y., 2012. Evaluation of fumigant toxicity of orange peel *Citrus sinensis* (L.) essential oil against three stored product insects in laboratory condition. *Munis Entomology and Zoology* 7, 352-358.
- Tang, S., Zheng, J., 2018. Antibacterial Activity of Silver Nanoparticles: Structural Effects. *Advanced Healthcare Materials* 7, e1701503.
- Tardugno, R., Serio, A., Pellati, F., D'Amato, S., Chaves López, C., Bellardi, M.G., Di Vito, M., Savini, V., Paparella, A., Benvenuti, S., 2019. *Lavandula x intermedia* and *Lavandula angustifolia* essential oils: phytochemical composition and antimicrobial activity against foodborne pathogens. *Natural Product Research* 33, 3330-3335.

- Tassou, C., Drosinos, E., Nychas, G., 1995. Effects of essential oil from mint (*Mentha piperita*) on *Salmonella enteritidis* and *Listeria monocytogenes* in model food systems at 4 and 10 C. *Journal of Applied Bacteriology* 78, 593-600.
- Tauxe, R.V., 2001. Food safety and irradiation: protecting the public from foodborne infections. *Emerging Infectious Diseases* 7, 516.
- Tawakkal, I.S.M.A., Cran, M.J., Bigger, S.W., 2016. Release of thymol from poly(lactic acid)-based antimicrobial films containing kenaf fibres as natural filler. *LWT - Food Science and Technology* 66, 629-637.
- Tezotto-Uliana, J.V., Berno, N.D., Saji, F.R.Q., Kluge, R.A., 2013. Gamma radiation: An efficient technology to conserve the quality of fresh raspberries. *Scientia Horticulturae* 164, 348-352.
- Thomas, P., 2001a. Irradiation of fruits and vegetables. *Food Irradiation Principles and Applications*. Wiley Interscience, New York, 213-240.
- Thomas, P., 2001b. Irradiation of tuber and bulb crops. *Food irradiation: Principles and applications*, 241-271.
- Threepopnatkul, P., Charoendee, N., Wiriyamontree, N., Phodaeng, A., 2022. Effect of essential oil on properties of PBAT/PBS for bio-packaging films. *Journal of Physics: Conference Series*. IOP Publishing, p. 012023.
- Tongnuanchan, P., Benjakul, S., 2014. Essential oils: extraction, bioactivities, and their uses for food preservation. *Journal of Food Science* 79, R1231-R1249.
- Treviño-Garza, M.Z., García, S., del Socorro Flores-González, M., Arévalo-Niño, K., 2015. Edible active coatings based on pectin, pullulan, and chitosan increase quality and shelf life of strawberries (*Fragaria ananassa*). *Journal of Food Science* 80, M1823-M1830.
- Trivedi, A., Nayak, N., Kumar, J., 2017. Fumigant toxicity study of different essential oils against stored grain pest *Callosobruchus chinensis*. *Journal of Pharmacognosy and Phytochemistry* 6, 1708-1711.
- Tunçbilek, A., 1995. Effect of ⁶⁰Co gamma radiation on the rice weevil, *Sitophilus oryzae* (L.). *Anzeiger für Schädlingskunde, Pflanzenschutz, Umweltschutz* 68, 37-38.
- Turgis, M., Borsa, J., Millette, M., Salmieri, S., Lacroix, M., 2008. Effect of selected plant essential oils or their constituents and modified atmosphere packaging on the radiosensitivity of *Escherichia coli* O157: H7 and *Salmonella* Typhi in ground beef. *Journal of Food Protection* 71, 516-521.

- Turgis, M., Vu, K.D., Dupont, C., Lacroix, M., 2012. Combined antimicrobial effect of essential oils and bacteriocins against foodborne pathogens and food spoilage bacteria. *Food Research International* 48, 696-702.
- Ultee, A., Bennik, M.H., Moezelaar, R., 2002. The phenolic hydroxyl group of carvacrol is essential for action against the food-borne pathogen *Bacillus cereus*. *Applied and Environmental Microbiology* 68, 1561-1568.
- Upadhyay, N., Singh, V.K., Dwivedy, A.K., Chaudhari, A.K., Dubey, N.K., 2021. Assessment of nanoencapsulated *Cananga odorata* essential oil in chitosan nanopolymer as a green approach to boost the antifungal, antioxidant and *in situ* efficacy. *International Journal of Biological Macromolecules* 171, 480-490.
- Upadhyay, R., 2016. Botanicals; its safe use in pest control and environmental management. *International Journal of Zoological Investigations* 2, 58-102.
- Ureña-Benavides, E.E., Brown, P.J., Kitchens, C.L., 2010. Effect of jet stretch and particle load on cellulose nanocrystal– alginate nanocomposite fibers. *Langmuir* 26, 14263-14270.
- USDHS, U.S.D.o.H.S., 2019. CISA (cybersecurity and infrastructure security agency) (p. 155). Non-radioisotopic Alternative Technologies White Paper.
- Uz, M., Altinkaya, S.A., 2011. Development of mono and multilayer antimicrobial food packaging materials for controlled release of potassium sorbate. *LWT-Food Science and Technology* 44, 2302-2309.
- Van Calenberg, S., Vanhaelewyn, G., Van Cleemput, O., Callens, F., Mondelaers, W., Huyghebaert, A., 1998. Comparison of the effect of X-ray and electron beam irradiation on some selected spices. *LWT-Food Science and Technology* 31, 252-258.
- Vatansever, E., Arslan, D., Sarul, D.S., Kahraman, Y., Gunes, G., Durmus, A., Nofar, M., 2020. Development of CNC-reinforced PBAT nanocomposites with reduced percolation threshold: a comparative study on the preparation method. *Journal of Materials Science* 55, 15523-15537.
- Vazquez, B.I., Fente, C., Franco, C., Vazquez, M., Cepeda, A., 2001. Inhibitory effects of eugenol and thymol on *Penicillium citrinum* strains in culture media and cheese. *International Journal of Food Microbiology* 67, 157-163.
- Vieira, M.G.A., Da Silva, M.A., Dos Santos, L.O., Beppu, M.M., 2011. Natural-based plasticizers and biopolymer films: A review. *European Polymer Journal* 47, 254-263.
- Vilarinho, F., Sanches Silva, A., Vaz, M.F., Farinha, J.P., 2018a. Nanocellulose in green food packaging. *Critical Reviews in Food Science and Nutrition* 58, 1526-1537.

- Viljoen, B.C., Lourens-Hattingh, A., Ikalafeng, B., Peter, G., 2003. Temperature abuse initiating yeast growth in yoghurt. *Food Research International* 36, 193-197.
- Vishwakarma, G.S., Gautam, N., Babu, J.N., Mittal, S., Jaitak, V., 2016. Polymeric encapsulates of essential oils and their constituents: A review of preparation techniques, characterization, and sustainable release mechanisms. *Polymer Reviews* 56, 668-701.
- Viuda-Martos, M., Ruiz-Navajas, Y., Fernández-López, J., Pérez-Álvarez, J., 2007. Antifungal activities of thyme, clove and oregano essential oils. *Journal of Food Safety* 27, 91-101.
- Vu, K.D., Hollingsworth, R.G., Leroux, E., Salmieri, S., Lacroix, M., 2011. Development of edible bioactive coating based on modified chitosan for increasing the shelf life of strawberries. *Food Research International* 44, 198-203.
- Wang, H., Qian, J., Ding, F., 2018. Emerging chitosan-based films for food packaging applications. *Journal of Agricultural and Food Chemistry* 66, 395-413.
- Wang, L.-F., Rhim, J.-W., Hong, S.-I., 2016. Preparation of poly(lactide)/poly(butylene adipate-co-terephthalate) blend films using a solvent casting method and their food packaging application. *LWT - Food Science and Technology* 68, 454-461.
- Wang, L., Xu, J., Zhang, M., Zheng, H., Li, L., 2022. Preservation of soy protein-based meat analogues by using PLA/PBAT antimicrobial packaging film. *Food Chemistry* 380, 132022.
- Weisany, W., Amini, J., Samadi, S., Hossaini, S., Yousefi, S., Struik, P.C., 2019. Nano silver-encapsulation of *Thymus daenensis* and *Anethum graveolens* essential oils enhances antifungal potential against strawberry anthracnose. *Industrial Crops and Products* 141.
- WHO, 1994. Irradiation of strawberries. A compilation of technical data for its authorization and control. Food and Agriculture Organization of the United Nations.
- WHO, 1999. High-dose irradiation: wholesomeness of food irradiated with doses above 10 kGy. World Health Organization.
- Won, G., Lee, J.H., 2017. *Salmonella* Typhimurium, the major causative agent of foodborne illness inactivated by a phage lysis system provides effective protection against lethal challenge by induction of robust cell-mediated immune responses and activation of dendritic cells. *Veterinary Research* 48, 1-12.
- Xanthos, D., Walker, T.R., 2017. International policies to reduce plastic marine pollution from single-use plastics (plastic bags and microbeads): A review. *Marine Pollution Bulletin* 118, 17-26.
- Yahyaraeyat, R., Khosravi, A., Shahbazzadeh, D., Khalaj, V., 2013. The potential effects of *Zataria multiflora* Boiss essential oil on growth, aflatoxin production and transcription of aflatoxin

- biosynthesis pathway genes of toxigenic *Aspergillus parasiticus*. Brazilian Journal of Microbiology 44, 649-655.
- Yang, F.M., Li, H.M., Li, F., Xin, Z.H., Zhao, L.Y., Zheng, Y.H., Hu, Q.H., 2010. Effect of nano-packing on preservation quality of fresh strawberry (*Fragaria ananassa* Duch. cv Fengxiang) during storage at 4 degrees C. Journal of Food Science 75, C236-240.
- Yangilar, F., Yildiz, P.O., 2018. Effects of using combined essential oils on quality parameters of bio-yogurt. Journal of Food Processing and Preservation 42.
- Yemiş, G.P., Candoğan, K., 2017. Antibacterial activity of soy edible coatings incorporated with thyme and oregano essential oils on beef against pathogenic bacteria. Food Science and Biotechnology 26, 1113-1121.
- Yoshida, Y., Koyama, N., Tamura, H., 2002. Color and anthocyanin composition of strawberry fruit: Changes during fruit development and differences among cultivars, with special reference to the occurrence of pelargonidin 3-malonylglucoside. Journal of the Japanese Society for Horticultural Science 71, 355-361.
- Yousefi, M.R., Razdari, A.M., 2015. Irradiation and its potential to food preservation. International Journal of Advanced Biological and Biomedical Research 3, 51-54.
- Zachariah, T.J., Leela, N.K., 2006. Volatiles from herbs and spices. Handbook of Herbs and Spices, pp. 177-218.
- Zarrad, K., Hamouda, A.B., Chaieb, I., Laarif, A., Jemâa, J.M.-B., 2015. Chemical composition, fumigant and anti-acetylcholinesterase activity of the Tunisian *Citrus aurantium* L. essential oils. Industrial Crops and Products 76, 121-127.
- Zhang, C., Li, W., Zhu, B., Chen, H., Chi, H., Li, L., Qin, Y., Xue, J., 2018. The Quality Evaluation of Postharvest Strawberries Stored in Nano-Ag Packages at Refrigeration Temperature. Polymers 10, 894.
- Zhang, X., Liu, D., Jin, T.Z., Chen, W., He, Q., Zou, Z., Zhao, H., Ye, X., Guo, M., 2021. Preparation and characterization of gellan gum-chitosan polyelectrolyte complex films with the incorporation of thyme essential oil nanoemulsion. Food Hydrocolloids 114, 106570.
- Zhang, Z., Vriesekoop, F., Yuan, Q., Liang, H., 2014. Effects of nisin on the antimicrobial activity of D-limonene and its nanoemulsion. Food Chemistry 150, 307-312.

Annexe A

List of publications

- (1) Begum, T., Follett, P. A., Shankar, S., Moskovchenko, L., Salmieri, S., & Lacroix, M. (2023). Evaluation of bioactive low-density polyethylene (LDPE) nanocomposite films in combined treatment with irradiation on strawberry shelf-life extension. *Journal of Food Science*.
- (2) Begum, T., Follett, P. A., Shankar, S., Mahmud, J., Salmieri, S., & Lacroix, M. (2022). Mixture design methodology and predictive modeling for developing active formulations using essential oils and citrus extract against foodborne pathogens and spoilage microorganisms in rice. *Journal of Food Science*, 87(1), 353-369.
- (3) Begum, T., Follett, P. A., Mahmud, J., Moskovchenko, L., Salmieri, S., Allahdad, Z., & Lacroix, M. (2022). Silver nanoparticles-essential oils combined treatments to enhance the antibacterial and antifungal properties against foodborne pathogens and spoilage microorganisms. *Microbial Pathogenesis*, 164, 105411.
- (4) Hossain, F., Follett, P., Shankar, S., Begum, T., Salmieri, S., & Lacroix, M. (2021). Radiosensitization of rice weevil *Sitophilus oryzae* using combined treatments of essential oils and ionizing radiation with gamma-ray and X-Ray at different dose rates. *Radiation Physics and Chemistry*, 180, 109286.
- (5) Begum, T., Follett, P. A., Hossain, F., Christopher, L., Salmieri, S., & Lacroix, M. (2020). Microbicidal effectiveness of irradiation from Gamma and X-ray sources at different dose rates against the foodborne illness pathogens *Escherichia coli*, *Salmonella Typhimurium* and *Listeria monocytogenes* in rice. *LWT*, 132, 109841.

List of conference presentations

(1) Nanotechnological breakthroughs in the development of nanoemulsions of natural compounds-based formulations for improved bioactivity.

Tofa Begum, Peter Follett, Shiv Shankar, Monique Lacroix*

Poster Presentation: Pacifichem 2021 Congress, Honolulu, Hawaii, USA

Poster ID: 3405324

Presentation date: 19 December 2021

(2) Design of bioactive chitosan nanocomposite films containing natural antimicrobials as a new active nanomaterial to control biological hazards.

Tofa Begum, Peter A. Follett, Monique Lacroix*

Oral presentation: 2021 5th International Conference on Composite Material, Polymer Science and Engineering (CMPSE2021).

Presentation ID: 05

Presentation date: 15 November 2021